University of KwaZulu-Natal

A Simple Yet Novel Strategies for the Synthesis of Pharmacologically Versatile Benzoxazole and Benzothiazole Scaffolds *via* Transamidation

By

Vishal Kumar

219095362

2022

A Simple Yet Novel Strategies for the Synthesis of Pharmacologically Versatile Benzoxazole and Benzothiazole Scaffolds via Transamidation

A Thesis

Submitted in fulfilment for the requirements

for the award of the degree of

Doctor of Philosophy

in the

Department of Pharmaceutical Chemistry

Discipline of Pharmaceutical Science

College of Health Science,

By

Vishal Kumar

2022

Supervisor: Prof. Rajshekhar Karpoormath

Co-supervisor: Prof. Parvesh Singh

A Simple Yet Novel Strategies for the Synthesis of Pharmacologically Versatile Benzoxazole and Benzothiazole Scaffolds via Transamidation by

Vishal Kumar

219095362

2022

A thesis submitted to the School of Health Science, Discipline of Pharmaceutical science, Department of Pharmaceutical Chemistry, University of KwaZulu-Natal, Westville, for the degree of Doctor of Philosophy.

This thesis has been prepared according to **Format 4** (Thesis by publications) as outlined in the guidelines of College of Health Sciences, University of KwaZulu-Natal. The chapters consist of an overall introduction, chapters in discrete research papers and a final discussion. Two chapters have been published and the remaining chapters revision have been submitted in peer-reviewed internationally accepted journals.

As the candidate's supervisor, I have approved this thesis for examination/submission.

Supervisor: Prof Rajshekhar Karpoormath

Signed:……

Date: 30-Oct-2022

Co-Supervisior: Prof Parvesh Singh

Signed:……..

Date: 30-Oct-2022

// Shree Ganeshaya Namah: //

Vakratunda Mahakaya Suryakoti Samaprabha /

Nirvighnam Kuru Mey Deva Sarva Karyeshu Sarvada //

Preface

I hereby declare that the thesis entitled "**A Simple Yet Novel Strategies for the Synthesis of Pharmacologically Versatile Benzoxazole and Benzothiazole Scaffolds via Transamidation**" submitted to the University of KwaZulu-Natal for the award of the degree of Doctor of Philosophy in Pharmaceutical Chemistry under the supervision of Prof. R. Karpoormath and Prof. P. Singh represents original work by the author and has not been submitted in full or part for any degree or diploma at this or any other University.

Where use was made of the work of others it has been duly acknowledged in the text. This work was carried out in the School of Health Science, Discipline of Pharmaceutical science, Department of Pharmaceutical Chemistry, University of KwaZulu-Natal, Westville Campus, Durban, South Africa.

Signed: 

Date: 30-Oct-2022

Vishal Kumar

As the candidate's supervisors, we have approved this dissertation for submission

Signed:

Dated: 30-Oct-2022

Prof. Rajshekhar Karpoormath

(**Supervisor**)

Signed:

Dated: 30-Oct-2022

Prof. Parvesh Singh

(**Co-supervisor**)

Abstract

Transamidation is a popular way for amide transformation from another amide despite conventional amide bond formation methods. Acid and acid chloride were utilised as starting ingredients in previous procedures. Transamidation has shifted the perspective of researchers on amide synthesis. Nowadays, many methodologies have recently come to light for amide transformation, using non-metal and metal-mediated techniques. On the other hand, a few approaches involving amide bond activators have been reported. Moreover, N-Boc, Tosyl, and Mesyl groups are commonly utilised as amide bond activators. As a result, many amides transformations have been synthesised and published in the literature over the last few decades. Based on previous research, we have attempted to develop cost-effective and novel techniques of transamidation for unactivated amides, which could serve as a potential alternative to synthesising amide bond containing compounds from lab to plant scale. We also demonstrated a novel approach for synthesising 2-substituted benzoxazole/benzothiazole compounds using this transformation.

The history and development of unactivated amides transformation are briefly described in **Chapter 2**. This chapter also discusses different transamidation methods for primary, secondary, and tertiary unactivated amides that are transformed into other amides without the need for an amide bond activator.

The development of a novel green, efficient catalyst-free, one-pot synthetic methodology to synthesise amides is described in **Chapter 3**. Under the optimisation investigations, the effects of various acids, solvents, temperatures, and time intervals were also described. The reaction was catalysed by hydrochloride, which activated the carbonyl bond, and then attacked the carbonyl carbon with an additive amine as a nucleophile. Finally, the amine as a byproduct is removed, resulting in the desired converted amide. Furthermore, this new transamidation process allows for a wide range of amide types, including primary, secondary, and tertiary. This approach also works with a variety of primary and secondary amines, including aliphatic and bulky, hetero-aromatic substituted amines.

To continue the work begun in **Chapter 4**, we develop a new solvent-free and metal-free method for synthesising 2-substituted benzoxazole and benzothiazole in **Chapter 4**. In this approach, we increase

the temperature and employ substituted 2-aminophenols or 2-aminothiophenols instead of amines. To lead the annulation product, the oxygen or sulphur atom of phenol or thiophenol attacks the carbonyl carbon of the transformed amide group. Furthermore, this technique works well with a variety of substituted 2-aminophenols. Additionally, the amide scope for this reaction is quite broad.

Chapter 5 describes the development of a new method for the transamidation of aliphatic amides using $CuCl_2$ as a catalyst. The effects of various catalysts and Lewis acids and the effect of different solvents were explained. Moreover, the annulated substituted 2-benzoxazole and 2-benzothiazole derivatives obtain in the case of 2-aminophenol and 2-aminothiophenol. Besides, this new versatile methodology provides a wide substrate scope for the synthesis of different functionally substituted amides and 1,3-benzoxazole scaffolds. It can be further exploited as building blocks for the synthesis of pharmaceutical drugs.

Declaration 1: plagiarism

I, **Vishal Kumar**, declare that

i. The research reported in this dissertation, except where otherwise indicated, is my original work.

ii. This dissertation has not been submitted for any degree or examination at any other university.

iii. This dissertation does not contain other persons' data, pictures, graphs or other information, unless specifically acknowledged as being sourced from other persons.

iv. This dissertation does not contain other persons' writing, unless specifically acknowledged as being sourced from other researchers. Where other written sources have been quoted, then:

a. their words have been re-written but the general information attributed to them has been referenced;

b. where their exact words have been used, their writing has been placed inside quotation marks, and referenced.

v. Where I have reproduced a publication of which I am an author, co-author or editor, I have indicated in detail which part of the publication was actually written by myself alone and have fully referenced such publications.

vi. This dissertation does not contain text, graphics or tables copied and pasted from the Internet, unless specifically acknowledged, and the source being detailed in the dissertation and in the References sections.

Signed [redacted] **Date**: 30-Oct-2022

Declaration 2: publications

DETAILS OF CONTRIBUTION TO PUBLICATIONS that form part and/or include research presented in this thesis (include publications in preparation, submitted, *in the press* and published and give details of the contributions of each author to the experimental work and writing of each publication).

First Author Publications

1. **Vishal Kumar**, Sanjeev Dhawan, Pankaj Sanjay Girase, Paul Awolade, Suraj Raosaheb Shinde, Rajshekhar Karpoormath, and Parvesh Singh; **Recent Advances in Chalcone-based Anticancer Heterocycles: A Structural and Molecular Target Perspective**. *Current Medicinal Chemistry*, ***2021, 28, 1-40.***

Contributions: I did the literature review and wrote the manuscript under the supervision of Prof. Rajshekhar Karpoormath and Prof. Parvesh Singh. Rest all the co-authors assisted me in improvisation, writing up and summarizing the literature review (conclusion).

2. **Vishal Kumar**, Sanjeev Dhawan, Pankaj Sanjay Girase, Parvesh Singh, and Rajshekhar Karpoormath; **An Environmentally Benign, Catalyst-Free N-C Bond Cleavage/Formation of Primary, Secondary, and Tertiary Unactivated Amides**. *European Journal of Organic Chemistry*, ***2021, 5627–5639.***

Contributions: I generated the rationale and did all the experimental and characterization as well as writing up of the manuscript under the guidance of Prof. Rajshekhar Karpoormath and Prof. Parvesh Singh. The co-authors assisted me in writing up results and discussing and designing the target molecules.

3. **Vishal Kumar**, Sanjeev Dhawan, Renu Bala, Pankaj Sanjay Girase, Parvesh Singh and Rajshekhar Karpoormath; **Metal-free direct annulation of 2-aminophenols and 2-aminothiophenols with unactivated amides through transamidation: Access to polysubstituted benzoxazole and benzothiazole derivatives**. *Tetrahedron*, 2022.

Contributions: I developed the new method, optimized the condition and did the experimental and characterization, and wrote up the manuscript under the guidance of Prof. Rajshekhar Karpoormath and Prof. Parvesh Singh. The co-authors assisted me in writing up results and discussing and designing the target molecules.

4. **Vishal Kumar**, Sanjeev Dhawan, Renu Bala, Sachin Balaso Mohite, Parvesh Singh and Rajshekhar Karpoormath; **Cu-Catalysed Transamidation of Unactivated Aliphatic Amides**. Under review in *Organic & Biomolecular Chemistry Journal*.

Contributions: I developed the new method, optimized the condition and did the experimental and characterization, and wrote up the manuscript under the guidance of Prof. Rajshekhar Karpoormath and Prof. Parvesh Singh. The co-authors assisted me in writing up results and discussing and designing the target molecules.

5. **Vishal Kumar**, Sanjeev Dhawan, Renu Bala, Pankaj S. Girase, Parvesh Singh, Rajshekhar Karpoormath; **Recent Advances in Transamidation of Unactivated Amides**. *Manuscript*.

Contributions: I did the literature review and wrote the manuscript under the supervision of Prof. Rajshekhar Karpoormath and Prof. Parvesh Singh. Rest all the co-authors assisted me in improvisation, writing up and summarizing the literature review.

6. **Vishal Kumar**, Renu Bala, Sanjeev Dhawan, Parvesh Singh and Rajshekhar Karpoormath; **Focus on the multi-biological targeted role of DZG and its analogues: A mini-review**. *Manuscript*.

Contributions: I did the literature review and wrote the manuscript under the supervision of Prof. Rajshekhar Karpoormath and Prof. Parvesh Singh. Rest all the co-authors assisted me in improvisation, writing up and summarizing the literature review.

7. **Vishal Kumar**, Sanjeev Dhawan, Renu Bala, Karolína Kozlanská, Veronika Vojáčková, Vladimír Kryštof, Parvesh Singh and Rajshekhar Karpoormath; **Design, synthesis and characterisation of novel Dehydrozingerone (DZG)-2-Azetidinone hybrids as an anticancer agents**. *Manuscript*.

Contributions: I designed the scheme and did the experimental work, characterization as well as writing up of the manuscript under supervision of Prof. Rajshekhar Karpoormath and Prof. Parvesh Singh. Sanjeev Dhawan assisted me in experimental, characterization of the target molecules as well as writing up of manuscript. Renu Bala assisted me in experimental and writing up of results and discussion. Karolína Kozlanská, Veronika Vojáčková, Vladimír Kryštof, carried out singlepoint evaluation of compounds efficacy against Cancer cell lines.

8. **Vishal Kumar**, Sanjeev Dhawan, Renu Bala, Parvesh Singh and Rajshekhar Karpoormath; **Design, synthesis and characterisation of novel mono-carbonyl analogues of curcumin (MACs)- 2-Azetidinone hybrids as an anticancer agents**. *Manuscript*.

Contributions: My role in all the publications mentioned above included carrying out all the experimental work and writing of the publications. My supervisors guided me and assisted me with writing the results for publication. The other co-author's contribution was mainly in the bioactivity and checking whether the results were correctly interpreted.

9. **Vishal Kumar**, Sanjeev Dhawan, Renu Bala, Parvesh Singh and Rajshekhar Karpoormath; **Design, synthesis and characterisation of novel Dehydrozingerone (DZG)-Triazole hybrids as an anticancer agents**. *Manuscript*.

Contributions: My role in all the publications mentioned above included carrying out all the experimental work and writing of the publications. My supervisors guided me and assisted me with writing the results for publication. The other co-author's contribution was mainly in the bioactivity and checking whether the results were correctly interpreted.

Other publications

1. Pankaj Sanjay Girase, Sanjeev Dhawan, **Vishal Kumar**, Suraj Raosaheb Shinde, Mahesh B. Palkar, Rajshekhar Karpoormath; **An appraisal of anti-mycobacterial activity with structure-activity relationship of Piperazine and its analogues: A review**. *European Journal of Medicinal Chemistry*. ***2021***, *210, 112967*.

2. Sanjeev Dhawan, **Vishal Kumar**, Pankaj S. Girase, Sithabile Mokoena, and Rajshekhar Karpoormath; **Recent Progress in Iodine-Catalysed C-O/C-N Bond Formation of 1,3-Oxazoles: A Comprehensive Review**. *ChemistrySelect*, ***2021***, *6, 754-787*.

3. Sivanandhan Karunanidhi, Balakumar Chandrasekaran, Rajshekhar Karpoormath, Harun M. Patel, Francis Kayamba, Srinivas Reddy Merugu, **Vishal Kumar**, Sanjeev Dhawan, Babita Kushwaha, Mavela Cleopus Mahlalela; **Novel thiomorpholine tethered isatin hydrazones as potential inhibitors of resistant *Mycobacterium tuberculosis***. *Bioorganic Chemistry, **2021**, 115, 105133.*

4. Sanjeev Dhawan, Pankaj Sanjay Girase, **Vishal Kumar** & Rajshekhar Karpoormath; **HCl-mediated transamidation of unactivated formamides using aromatic amines in aqueous media**. *Synthetic Communications, **2021**, 51(24), 3729-3739.*

5. Suraj R. Shinde, Pankaj Girase, Sanjeev Dhawan, Shaukatali N. Inamdar, **Vishal Kumar**, Chandrakant Pawar, Mahesh B. Palkar, Mahadev Shinde & Rajshekhar Karpoormath; **A systematic appraisal on catalytic synthesis of 1,3-oxazole derivatives: A mechanistic review on metal dependent synthesis**. *Synthetic Communications, **2022**, 52(1), 1-36.*

6. Pankaj Sanjay Girase, **Vishal Kumar**, Sanjeev Dhawan, and Rajshekhar Karpoormath; **The facile synthesis of amides through transamidation with iodine under neat conditions.** *ChemistrySelect, **2022**, 7(6), e202103237.*

7. Rajeshwar Reddy Aleti, Srinivasulu Cherukupalli, Sanjeev Dhawan, **Vishal Kumar**, Pankaj S Girase, Sachin Mohite, Rajshekhar Karpoormath; **A Metal-free Approach for in-situ Regioselective**

Synthesis of Isoxazoles *via* 1,3 Dipolar Cycloaddition Reaction of Nitrile Oxide with Propargyl bromide. *Chemical papers, **2022**, 76, 3005-3010.*

8. Shaik Baji Baba, Naresh Kumar Katari, Pule Seboletswe, Gundla Rambabu, Narva Deshwar Kushwaha, **Vishal Kumar**, Parvesh Singh, Rajshekhar Karpoormath, Muhammad D Bala; **Recent literature review on Coumarin hybrids as potential anti-cancer agents**. *Anti-Cancer Agents in Medicinal Chemistry*, **2022**.

Signed [redacted] **Date**: 30-Oct-2022

Dedicated

to

My Mother, a strong and gentle soul, who has taught me value of education and never stop learning,

My Father for his unconditional support, who has taught me to work hard and carry your own burdens,

My beloved better half for her support and loves the way, without whom none of my success would be possible,

My Younger sister for her support and encouragement, who have raised me to be the person I am today.

Acknowledgements

This dissertation would not have been possible without the guidance and the help of several individuals who, in one way or another, contributed and extended their valuable assistance in the preparation and completion of this study.

First and foremost, I bow to almighty and my Family, to whom I owe the successful completion of my thesis. I would also like to express my deepest gratitude and heartfelt thanks to all those who helped me directly or indirectly in the completion of my research work.

I would like to express my deepest gratitude to the Almighty God for a source of life and His Grace to see the end of the PhD work and my supervisor and mentor, ***Prof. Rajshekhar Karpoormath*** *for his excellent guidance, caring, patience, support and providing me with an excellent atmosphere throughout my years of study on both an academic and a personal level. His passion and humility have always encouraged me to give my best to my studies. His guidance helped me in all the time of research and writing of this thesis. I could not have imagined having a better advisor and mentor for my PhD study.*

I express my sincere gratitude to my co-supervisor ***Prof. Parvesh Singh,*** *who has provided academic support for this research and encouragement to fulfil my research work. For this, I am extremely grateful.*

A very special thank you to my best friend and my better half, Mrs. ***Renu Bala****. She was always stood by me, without her love, encouragement, and assistance, I would not have finished this thesis.*

I would like to take a moment to thank my brothers ***Dr. Sanjeev Dhawan*** *and* ***Mr. Ram Chaudhary*** *for his constant support and encouragement.*

Especially to all the colleagues of the laboratory, ***Narva Deshwar kushwaha****,* ***Pankaj Girase****,* ***Babita kushwaha****,* ***Ruchika Chauhan****,* ***Ashish Sharma****,* ***Anamika Sharma*** *and all lab mates with whom I've had the pleasure to work with during all these years, for all the good times we've had together in and outside the lab and for every wonderful day we've spent together. Also, to all the visitors who have been*

*at our lab. My time at UKZN was made enjoyable in large part due to the many friends and "**SMCRG** group" that became a part of my life.*

I am grateful to my research group's past and present members (SMCRG) for their support and encouragement throughout my studies.

*I would like to thank the technical staff, Mr **Vuyisa Mzozoyana** and Ms **Caryl Janse van Rensburg**, Mass Spectrometry Laboratory, School of Chemistry, UKZN-Pietermaritzburg, for their assistance in spectroscopic experiments. My special thanks to all the past and present group members of Synthetic and Medicinal Chemistry Research Group for their support and contributions. The blissful days spent with you all will be cherished forever.*

My humble gratitude to the University of KwaZulu-Natal, South Africa, for granting approval for my research proposal and providing all the necessary facilities to carry it out successfully. My sincere thanks and appreciation for all the supporting staff at Discipline of Pharmaceutical Sciences College of Health Sciences.

My special thanks go to the Indian community at the University of KwaZulu-Natal. I am also indebted to all my friends for their invaluable support, day in and day out, during all these years.

*I would again like to thank my family for mentioning the name of each; my parents, Mr **Ramesh Sharma** and Mrs **Kamal Sharma** and sibling's elder sister Mrs. **Pooja Sharma** and her husband Mr. **Sushil Dutt** and sibling's elder sister Mrs. **Rajnish Sharma** and her husband Mr. **Gaurav Sharma** and my younger sister **Neha Sharma**. They have given me their unequivocal support throughout, as always, for which my mere expression of thanks likewise does not suffice.*

I extend my gratitude to my previous teachers, lecturers and professors who shaped me to reach this position

Lastly, I thank all those who have helped me directly or indirectly in the successful completion of my thesis. Anyone missed in this acknowledgement is also appreciated.

Ethical Clearance Certificate

UNIVERSITY OF KWAZULU-NATAL
INYUVESI YAKWAZULU-NATALI

Mr Vishal Kumar (219095362)
School Of Health Sciences
Westville

Dear Mr Vishal Kumar,

Original application number: 00013685
Project title: Design, Synthesis and biological evaluation of dehydrozingerone conjugates
Amended title:

Exemption from Ethics Review

In response to your **amendment** application received on the 6 July 2022, your school has indicated that the amendment has been granted **EXEMPTION FROM ETHICS REVIEW.**

Any alteration/s to the exempted research protocol, e.g., Title of the Project, Location of the Study, Research Approach and Methods must be reviewed and approved through an amendment/modification prior to its implementation. The original exemption number must be cited.

For any changes that could result in potential risk, an ethics application including the proposed amendments must be submitted to the relevant UKZN Research Ethics Committee. The original exemption number must be cited.

In case you have further queries, please quote the above reference number.

PLEASE NOTE:
Research data should be securely stored in the discipline/department for a period of 5 years.

I take this opportunity of wishing you everything of the best with your study.

Yours sincerely,

[redacted]

Prof Khathutshelo Percy Mashige
Academic Leader Research
School Of Health Sciences

UKZN Research Ethics Office
Westville Campus, Govan Mbeki Building
Postal Address: Private Bag X54001, Durban 4000
Website: http://research.ukzn.ac.za/Research-Ethics/

Founding Campuses: Edgewood Howard College Medical School Pietermaritzburg Westville

INSPIRING GREATNESS

List of abbreviations

^{13}C-NMR:	Carbon (C-13) nuclear magnetic resonance spectroscopy
^{1}H-NMR:	proton (H-1) nuclear magnetic resonance spectroscopy
^{19}F-NMR:	fluorine-19 (F-19) nuclear magnetic resonance spectroscopy
Ac:	acetate
EtOH:	ethanol
MeOH:	methanol
Aq:	aqueous
Br:	broad
Cc:	column chromatography
$CDCl_3$:	deuterated chloroform
DMSO-d_6:	deuterated dimethyl sulfoxide
d:	doublet
dd:	double of doublets
DEPT:	distortionless enhancement by polarization transfer
EIMS:	electron impact mass spectroscopy
Hz:	hertz
Me:	methyl
MS:	mass spectroscopy
m:	multiplet
s:	singlet
d:	doublet
t:	triplet
td:	triplet of doublets
TLC:	thin layer chromatography
UV:	ultraviolet
DMF:	dimethylformamide
HCl:	hydrochloride
HRMS:	High-resolution mass spectrometry
ND:	Not determined
ppm:	Parts per million
RT:	Room temperature

Table of Contents

List of Figures

Chapter 1:

Chapter 2:

Chapter 3:

Nil

Chapter 4:

List of Tables

Chapter 1:

Nil

Chapter 3:

Chapter 4:

Chapter 5:

List of Schemes

Chapter 2:

Chapter 3:

Chapter 4:

Chapter 5:

Chapter 1

1.0 General Introduction

Amide

A nitrogen (N) atom is joined to an acyl group (R-C=O) to form an amide. The presence of two highly electronegative atoms i.e. N and O in close proximity to each other makes amides capable of forming strong H-bond. The amide bond functionality plays is a key role in biological systems as it constitutes an important part of peptides and proteins essential for survival of living beings and in organic chemistry. As a result, the amide bond serves as an essential linkage in many industries, including natural products, pharmaceuticals, polymers, lubricants, agrochemicals, and others[1]. A number of amide based drugs are known for binding to their receptor site through amide functional group to exert their therapeutic action. A 2006 study found that 25% of all pharmaceutical drugs currently on the market and about 70% of drug contenders contained amide bonds[2,3]. Several amide-containing medicines are illustrated in **Figure 1**.

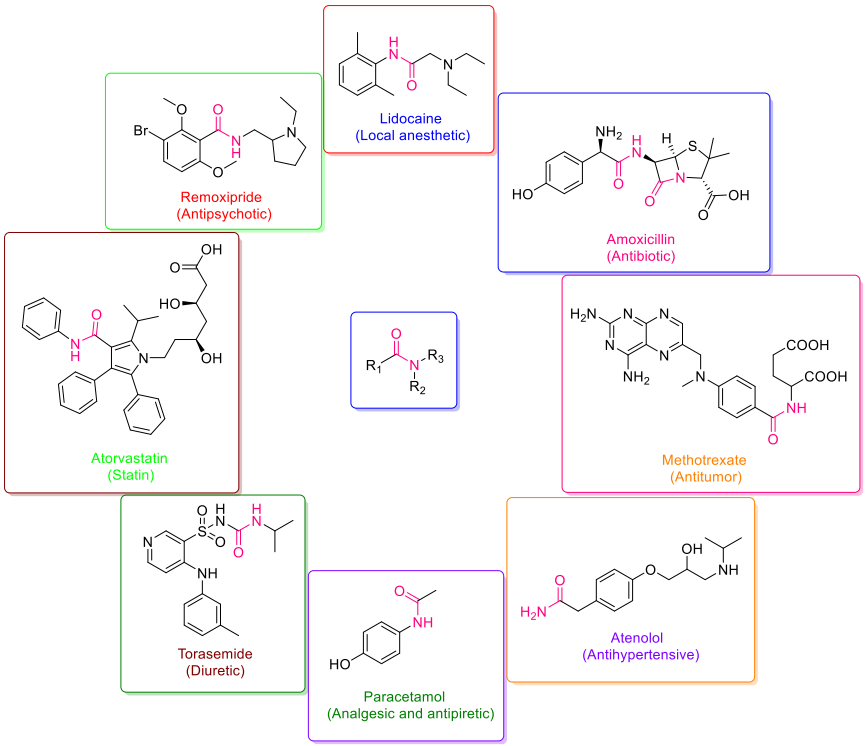

Fig 1: Examples of drugs carrying an amide bond functionality.

Methods for amide synthesis

Conventionally, amide synthesis is carried out by reacting activated carboxylic acid derivatives like acid chlorides, anhydrides and esters with amines, including ammonia (**Scheme 1**). Most of these methods employ stoichiometric amounts of coupling reagents, making them expensive and wasteful by-products.

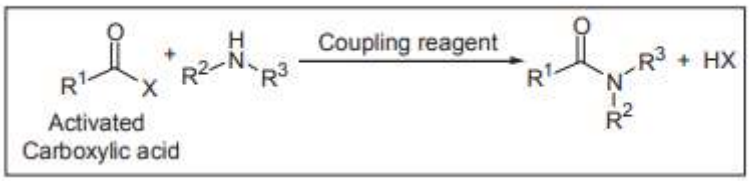

Scheme 1: Conventional method of amide synthesis

Presently, a major area of interest for researchers in the development of new techniques that are practical and affordable, have a wide substrate scope, produce the desired product in maximum yield with the least amount of waste generation, and avoid using a stoichiometric amount of coupling reagents leading to high atom economy. In this respect, numerous atom-efficient catalytic techniques have been developed in the last few years for synthesising amides from alcohols, aldehydes, nitriles, oximes, imines, esters, etc., resulting in a significant amount of publications in this field. The oxidative amidation process is used in the majority of these techniques, but very few efforts have been made to develop transamidation processes.

Amines as precursors for amide synthesis

Amines are the most significant precursors for amide production and are found in many natural and pharmaceutical products. As a result, modern organic synthesis and medicinal chemistry both actively pursue the synthesis of amines. While C-N bond formation techniques are the most extensively used method for the synthesis of substituted amines, methods such as nitro reduction, nitrile reduction, and amide reduction are among the most popular procedures for the synthesis of primary amines.

Methods for C-N bond formation

For C-N bond formation reactions leading to substituted amines, a number of approaches are available such as N-alkylation of amines with alkyl halides, N-alkylation of amines with alcohols, reductive amination of carbonyl compounds and reductive hydroamination of terminal alkynes. Moreover, the naming reaction and non-classical routes[4] for amide synthesis from various functionalities[5] include well-known synthetic approaches such as the acid-catalysed Schmidt reaction[6,7], Ritter reaction[8,9], Schotten-Baumann reaction[10], Passerini[11], Ugi reaction[12] and Beckmann rearrangement[13,14] (**Fig. 2)** are well known for the synthesis of substituted amines via C-N bond formation. Despite having numerous methods for C-N bond formation, sustainable approaches utilising environment-friendly catalysts and solvents are highly demanded.

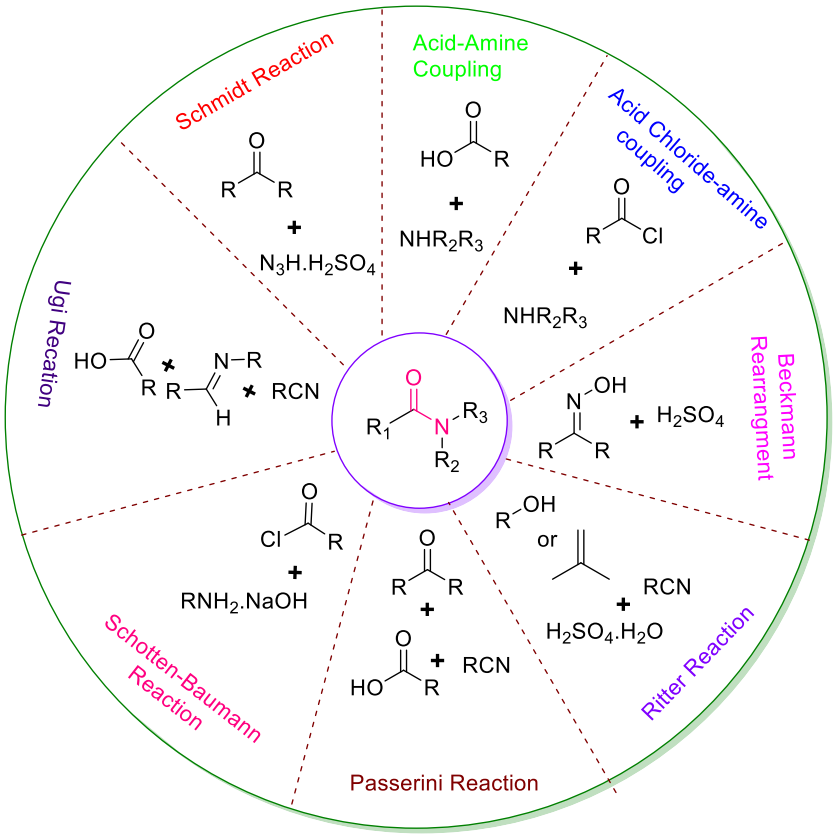

Fig 2: Name Reactions for amide bond synthesis.

Without a doubt, amide linkages are a privileged bond in organic chemistry; hence, reactions for forming these bonds are among the most often employed conversions in organic and medicinal chemistry. In addition, the innovative ways to synthesise amide bonds from various functionalities have

attracted the scientific community's attention; consequently, the synthetic methods for obtaining these structural moieties continue to progress. Traditional methods for forming amide bonds involve the condensation of a carboxylic acid and an amine with a pre-activation of the acid moiety[4,5].

Transamidation

The direct conversion of amides, commonly known as transamidation (**Scheme 2**), is a typical reaction that is gaining importance rapidly because it offers an alternative method for preparing amides that would exchange the constituents of two different amide groups. The reactivity of amide is based on the reaction conditions, activating agent, and amide structure. However, due to their resonance structure and reactivity, amides are extremely inert under normal conditions[15] (**Figure 3**). Despite the fact that amides are usually weak electrophiles, they can be activated in the presence of metal[16,17] or non-metal additives to undergo transformation reactions[18,19].

Since many simple amides are readily available, this strategy could become a valuable tool in protein engineering or preparing complicated bio-inspired derivatives. In the next chapter, we are describing the literature on the transamidation of unactivated amides.

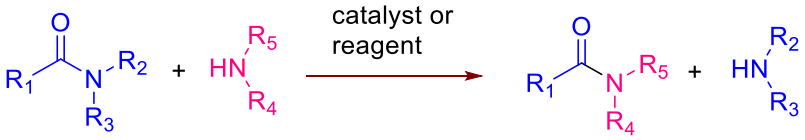

Scheme 2: General representation of transamidation reaction.

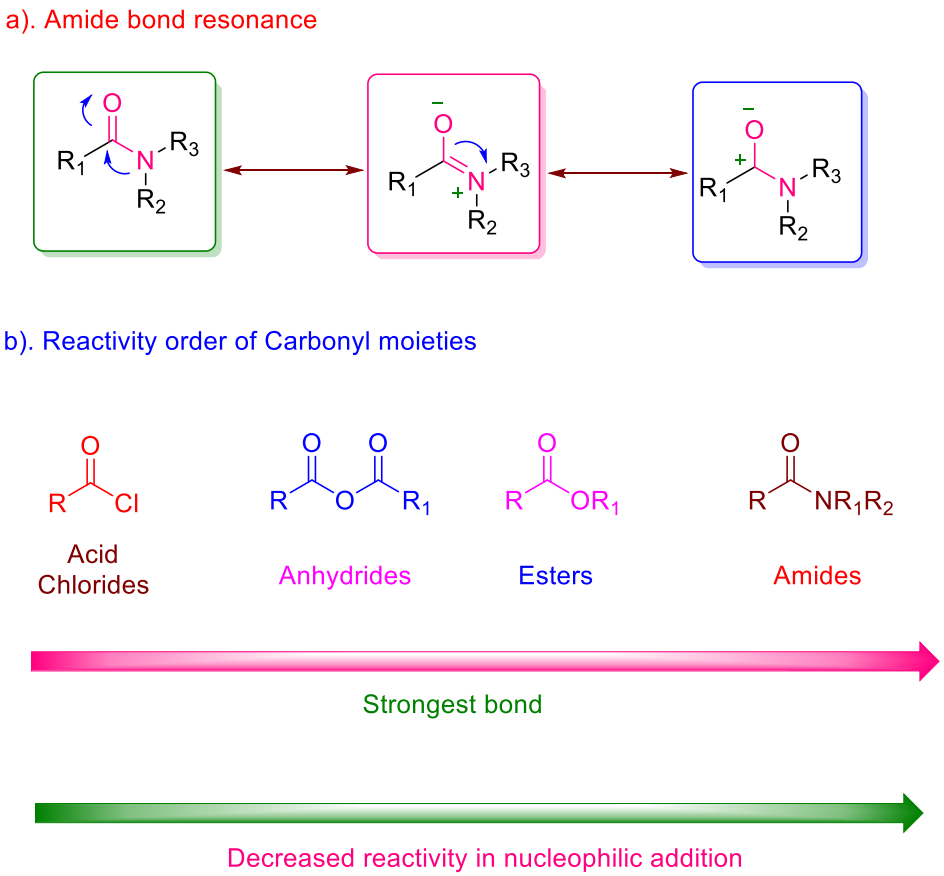

Fig 3: Amide bond resonance structures, amide bond strength and reactivity.

Objective of the Present Research Work

The aims and objective of the present research work are:-

1. To carryout a through literature survey on transamidation of unactiviated amides.
2. To develop a convenient and efficient method for the transamidation of HCl salt amines with unactiviated amides.
3. To establish a new green method for the synthesis of 2-subsitututed benzoxazole and benzothiazole through 2-aminophenol HCl salt transamidation with amides.
4. To develop a Cu-catalyzed chemo selective transamidation method of unactiviated aliphatic amides and its application to synthesize 2-subsitututed benzoxazole and benzothiazole.

References

1 V. R. Pattabiraman and J. W. Bode, *Nature*, **2011**, 480, 471-479.

2 J. S. Carey, D. Laffan, C. Thomson and M. T. Williams, *Organic and Biomolecular Chemistry*, **2010**, 68, 228-237.

3 A. K. Ghose, V. N. Viswanadhan and J. J. Wendoloski, *Journal of Combinatorial Chemistry*, **2021**, 14, 655.

4 R. M. De Figueiredo, J. S. Suppo and J. M. Campagne, *Chemical Reviews*, **2016**, 116, 12029-12122.

5 A. Ojeda-Porras and D. Gamba-Sánchez, *Journal of Organic Chemistry*, **2016**, 81, 11548-11555.

6 P. A. S. Smith, *Journal of the American Chemical Society*, **1948**, 70, 320-323.

7 E. H. Huntress, *Journal of the American Chemical Society*, **1949**, 71, 2233-2237.

8 J. J. Ritter and P. Paul Minieri, *Journal of the American Chemical Society*, **1948**, 70, 4045-4048.

9 C. Feng, B. Yan, G. Yin, J. Chen and M. Ji, *Synlett*, **2018**, 29, 2257-2264.

10 Z. Wang, in *Comprehensive Organic Name Reactions and Reagents*, 2010.

11 T. Soeta, Y. Kojima, Y. Ukaji and K. Inomata, *Organic Letters*, **2010**, 12, 4341-4343.

12 I. Ugi, *Angewandte Chemie International Edition in English*, **1961**, 94, 2229-2233.

13 J. Zhang, Y. Liu, W. Feng and Y. Wu, *Chinese Journal of Organic Chemistry*, 2019.

14 K. Kaur and S. Srivastava, *New Journal of Chemistry*, **2020**, 44, 18530-18572.

15 E. Kovács, B. Rózsa, A. Csomos, I. G. Csizmadia and Z. Mucsi, *Molecules*, 2018, 23, 2859.

16 M. B. Chaudhari and B. Gnanaprakasam, *Chemistry - An Asian Journal*, **2019**, 14, 76-93.

17 M. Kolympadi Marković, D. Marković and S. Laclef, *Synthesis (Germany)*, **2020**, 52, 3231-3242.

18 E. Massolo, M. Pirola and M. Benaglia, *European Journal of Organic Chemistry*, **2020**, 30, 4641-4651.

19 D. Procopio, C. Siciliano, S. Trombino, D. E. Dumitrescu, F. Suciu and M. L. Di Gioia, *Organic and Biomolecular Chemistry*, **2022**, 20, 1137-1149.

Chapter 2

Recent Advances in Transamidation of Unactivated Amides

Under review: Chemical Papers Journal.

Graphical Abstract

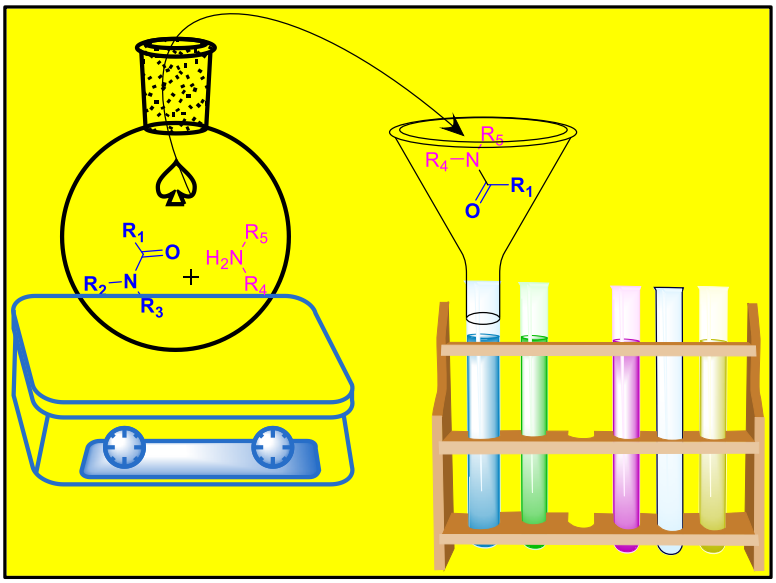

Abstract

In recent years, transamidation has been an essential topic in the formation of amide bonds over the conventional route due to chemoselectivity and greenside products. So many groups have disclosed new amide transformation techniques. Transamidation is typically classified into two categories based on amide activation: activated amide and unactivated amide. We conducted a review of the pertinent literature that discusses the cross amidation reactions of unactivated amides employing a variety of reagents, enabling contemporary research professionals to overcome synthetic barriers.

Keywords: *N*-Formylation, *N*-Acetylation, Transamidation, Unactivated amides.

Table of content

Introduction

Amides are also known as carboxamides, an organic functional group in which amine is directly linked to the carbonyl carbon having the general structure "R^1-CO-NR^2R^3", whereby the variables R^1, R^2 and R^3 can be any organic groups or a hydrogen atom[1,2]. Amides and their analogues are widely present in biomolecules[3], natural products[4], pharmaceuticals[5,6], drugs[7], polymers[8]. The amide unit contains drugs that display anthelmintic, antitumor, antifungal, antispasmodic, herbicide, insecticide, and antibacterial activity[9–11]. In biomolecules such as proteins, amides are the key components used to connect two amino acids known as peptide linkages[12].

Based on the substituents on the nitrogen atom of amide, they are categorised as primary, secondary and tertiary amides (**Fig-2-1a**). Because of its intermolecular hydrogen bonding[13,14], the order of amides' boiling point and melting point is primary > secondary > tertiary. The amide resonance structure shows the C-N double bond character with its plane geometry[15], which reveals its stability and inner strength in the presence of other chemical substances (**Fig-2-1b**).

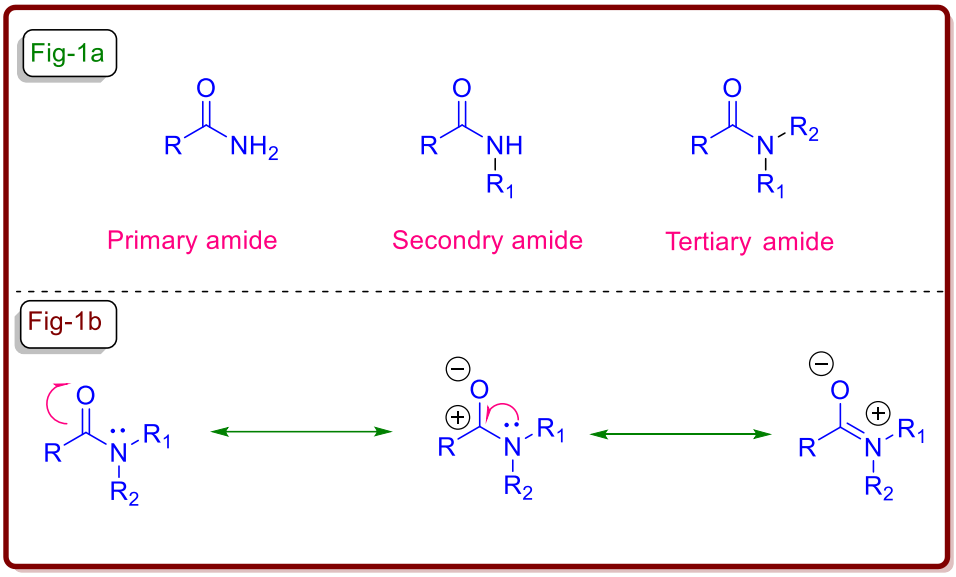

Figure 2- 1: Category and Resonance structures of amides

Due to amides' low reactivity, transamidation reactions have been challenging for researchers over the years. Many researchers have activated amides by N-substitution of an activated group on the nitrogen atom of amide to boost its reactivity. N-tosyl, N-Boc, N-acetyl, and N-triflyl are commonly used as activated groups to activate the unactivated amides. However, this step has disadvantages because it is a two-step reaction, and only primary and secondary amides have predominantly been explored because an activating group can replace the one proton of amide.

On the other hand, multiple groups have published a variety of unactivated amide transamidation approaches utilising various reagents. The main advantage of these approaches is that no activation group is required for the amide transformation. Furthermore, these methods do not produce any side products that may be employed as activating groups. The only byproduct of this coversion is the elimination of amide's amine (**Fig-2-2**). In a single step, these procedures can convert amides into other amides. These methodologies are mostly chemoselective reactions.

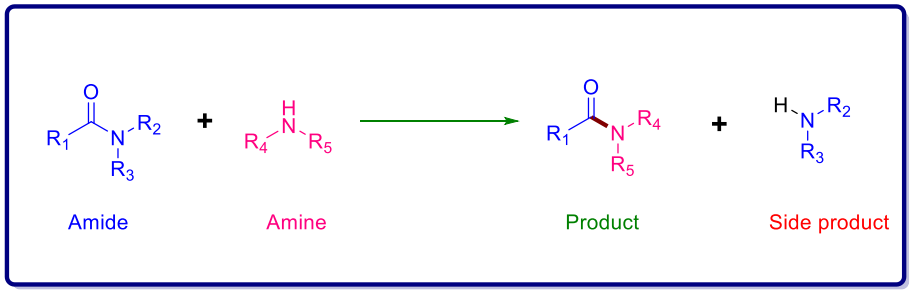

Figure 2- 2: Unactivated amide reaction

Transamidation reagents list

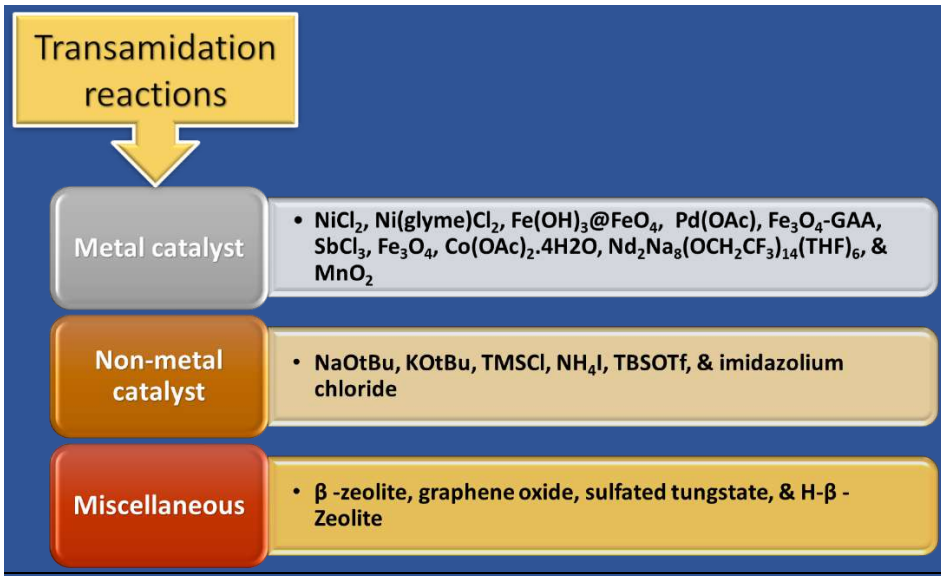

The preceding chart summarises the metal, non-metal, and miscellaneous reagents used to carry out the transamidation reactions discussed in this article.

Literature study

Following that, we discussed a summary of the literature that reported trans amidation reactions, categorising them as metal, non-metal, and miscellaneous catalysts, in which we systematically summarised optimisation studies and reaction scope of all previously covered articles.

Metal Catalysed

In the metal catalysed transamidation, the metal activates the amides due to its poor electrophilic nature. We proposed a general metal catalyst mechanism to explain the transformation based on previous mechanistic experiments and research, as shown in **Fig-2-3**. Initially, metal (**M**) activates the amide bond of amide **2** to generate amidate complex **T1**, which can be synthesised from free metal. When the complex **T1** is treated with amine **1**, the Cu-N bond of **T1** is cleaved, resulting in the unstable species **T2**. Usually, basic ligand amines exchange with the amide, resulting in protonated free ligands; it has been proposed in other similar mechanisms. **T2** annulates occur due to intramolecular interactions

between the amine nitrogen atom and the carbonyl carbon atom, leading to intermediate **T3**, which is in equilibrium with its isomer **T4**. **T3** can regenerate **T2** in the same way that **T4** can produce **T5** (an isomer of **T2**). As a result, the removal of amine generates the **M** complex species **T6**. Eventually, **T6** splits to give the transamidated product **3,** and the **M** catalyst is used for the next cycle.

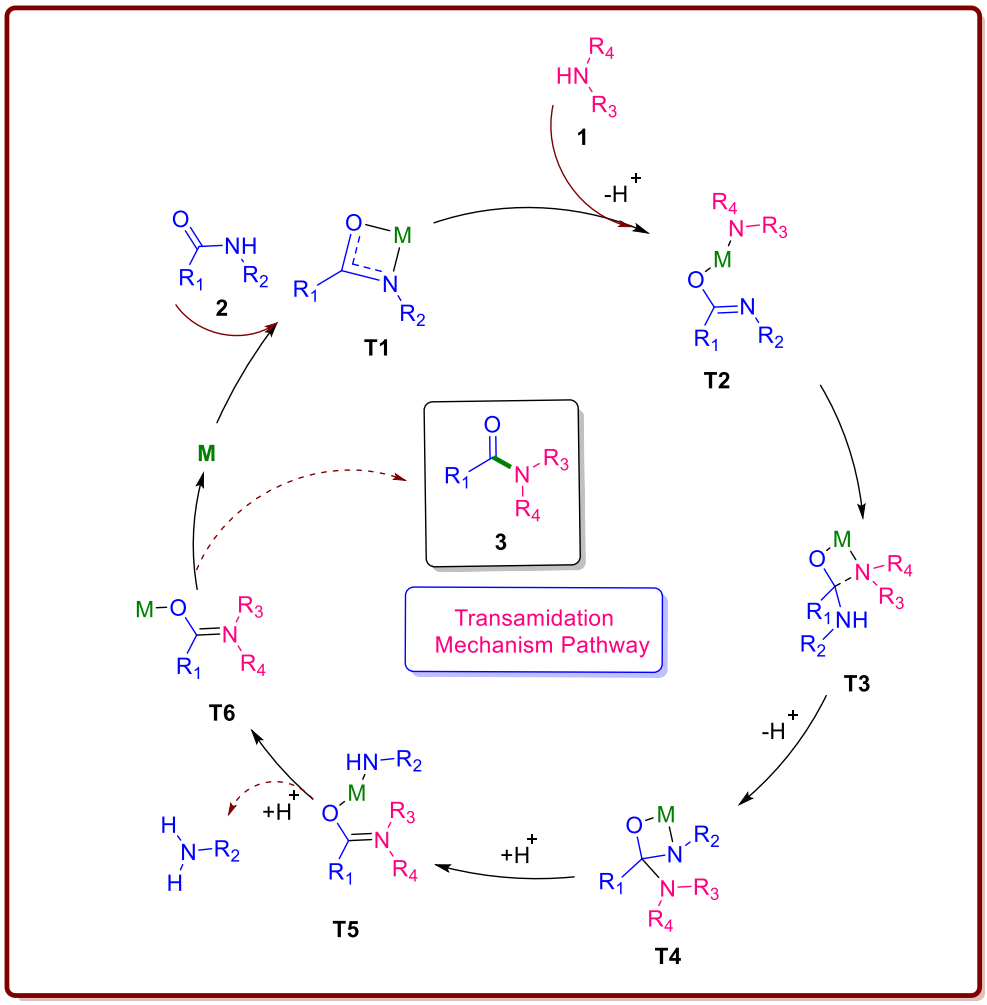

Figure 2- 3: Proposed metal-catalysed transamidation mechanism pathway between primary or secondary amides with secondary amines.

Yu et al.[16] developed a metal-catalysed transamidation reaction between N-Phenyl-substituted 2° benzamide and 1° amines (**Scheme 2-1**). The researcher examined different nickel catalysts during the optimisation study, but Ni(glyme)Cl_2 showed better conversion. The authors observed that the highest yield of transamidated products was obtained when Briphos-Ni(glyme)Cl_2 was used as the ligand-catalyst combination and NMP as the solvent. They performed reactions of numerous amines with amide under optimised conditions and found that the *para*-substituted anilines showed a much better

yield than *ortho* substitutes. However, the reaction had failed with 2,6-diisopropylaniline due to steric hindrance. They reported that hetero-aromatic, bulky anilines and aliphatic amines performed well in this procedure. Moreover, the authors studied the scope of amide by bringing the different substitutions on the phenyl ring and found them compatible under standard conditions. They also tried reaction with 2^{o} amines, which showed a poor yield of the desired product (**1h** and **1i**). Finally, the author concluded by the control experiment that the electron-donating amine and the electron-withdrawing benzamide have been triggering the reaction.

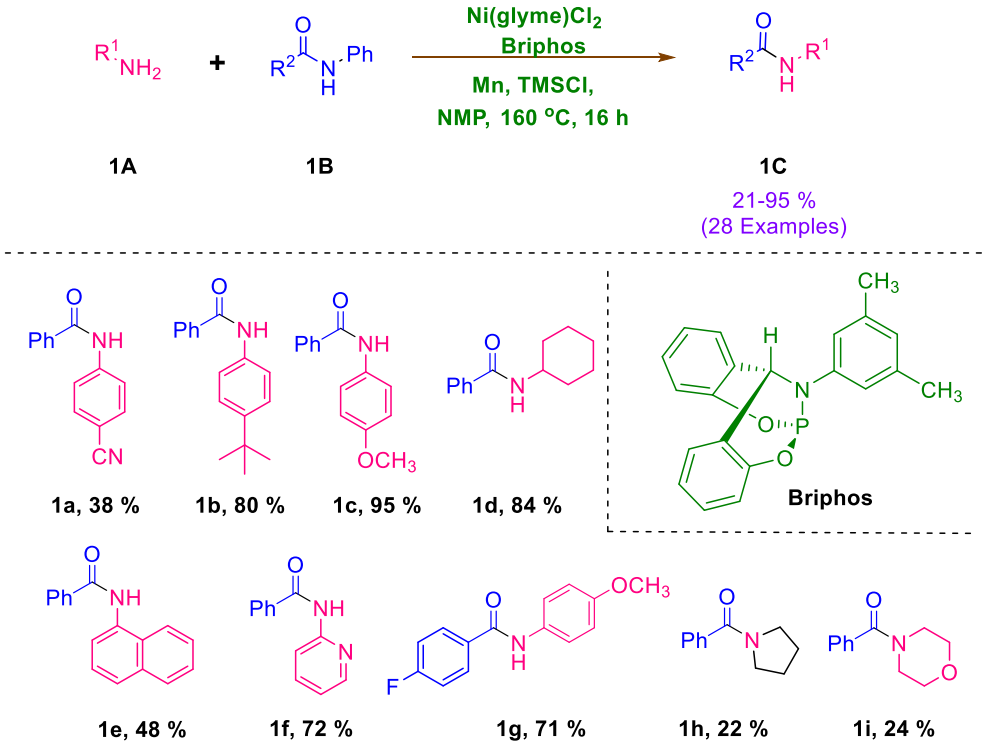

Scheme 2- 1. Ni-catalysed transamidation of 2^{o} benzamide derivatives with amines.

The same group also reported a transamidation of N-methyl-N-phenylbenzamide derivatives and primary amines using a similar condition (**Scheme 2-2**)[17]. The authors used trimethylsilyl chloride as an activator to investigate several nickel (II) species in the presence of manganese. They concluded from optimisation studies that $NiCl_2$ delivered the best yield with the help of methoxy substituted *t*-Bu-briphos. This method worked well with electron-withdrawing and donating groups substituted aniline. Heterocyclic and aliphatic amines also had yielded a good yield of transamidation products. However, the bulky group substituted aliphatic amines (**2f**) had generated a moderate yield due to steric hindrance.

Furthermore, the diversity of amides used in this reaction resulted in moderate to good desired products. The researchers conducted some experiments to demonstrate the relevance of N-methyl and N-benzyl in activating the amide for this transamidation.

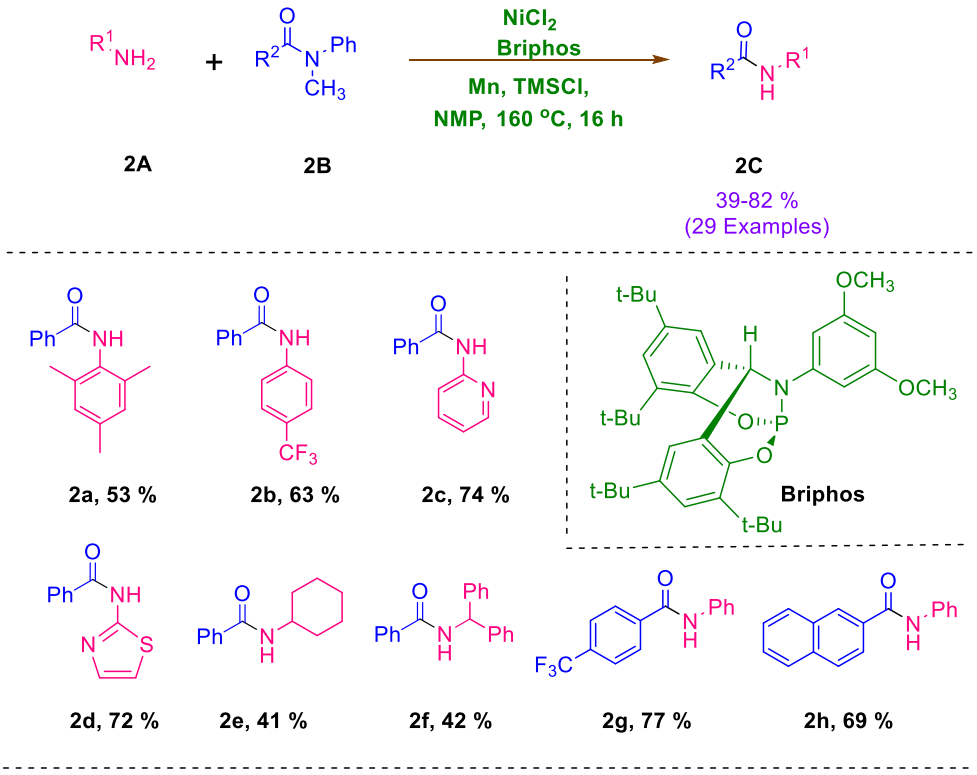

Scheme 2- 2. Ni-catalysed transamidation of 3° benzamide derivatives with amines.

Arefi et al.[18] established a methodology in which unactivated amides can be converted to another amide (**Scheme 2-3**). The researchers observed that a recyclable magnetic nanocatalyst $Fe(OH)_3@Fe_3O_4$ had enhanced the amide scope during this transformation. In catalyst preparation, they used 90.6% vibrating sample magnetometry of Fe_3O_4 and 9.4% of $Fe(OH)_3$. Additionally, the nano size of the catalyst was confirmed by SEM and TEM images. However, several catalyst concentrations and organic solvent studies were carried out during the process optimisation. Furthermore, their analysis of the reaction scope concluded that arylamines with electron reach groups yielded more product than electron-deficient groups. Additionally, this process has been shown to be consistent with phthalimide, urea, and thiourea.

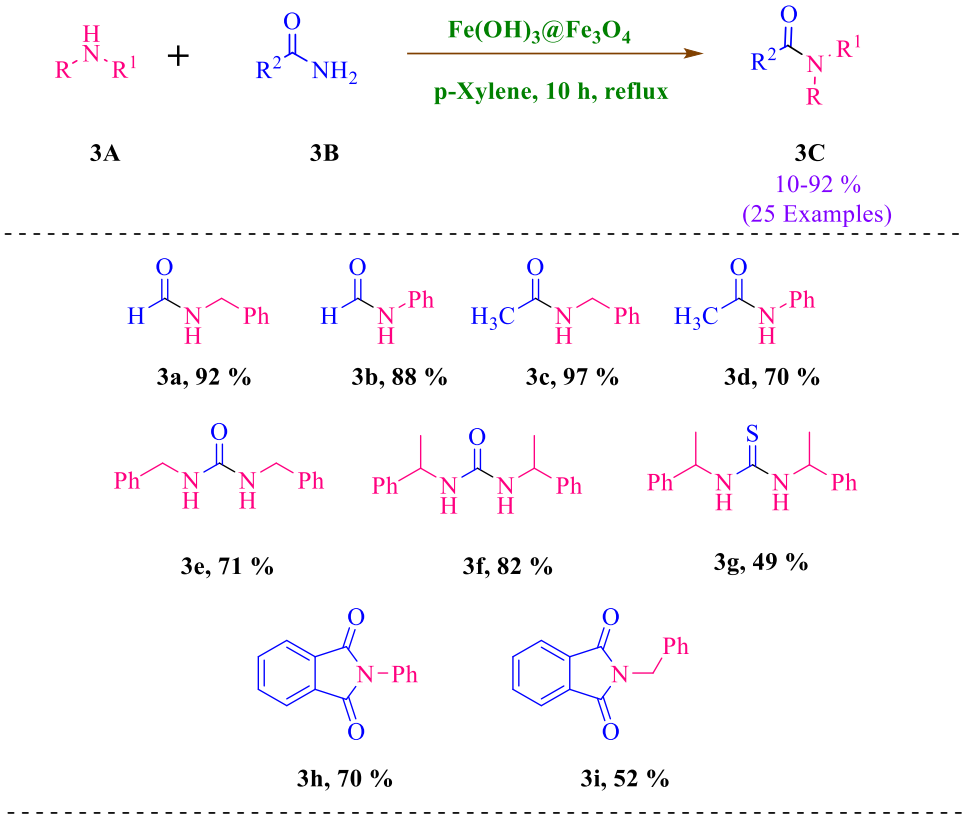

Scheme 2- 3. Fe-catalyzed transamidation of carboxamides, phthalimide, urea and thiourea.

One more methodology of recyclable magnetic nanoparticle of Fe_3O_4-Guanidine acetic Acid (Fe_3O_4-GAA) catalysed transamidation reported by same group[19] (**Scheme 2-4**). They attached -COOH of guanidine acetic on magnetic nanoparticle during catalyst preparation. In addition, the resultant Fe_3O_4-GAA-immobilised magnetic particle was also confirmed by FT-IR spectra, SEM image, vibrating sample magnetometer, and X-ray diffraction. Catalysts performed effectively in the absence of solvent, according to the researchers. Indeed, they reported that the reaction of electron-donating (OCH_3 and CH_3) and withdrawing (Cl and Br) substituted anilines with acetamide, urea, and thiourea formed targeted amides in good to excellent yields. However, benzamide produced a moderate to a good yield of amide transformation. It's also worth mentioning that this organocatalyst can be re-used up to six times without losing its catalytic activity.

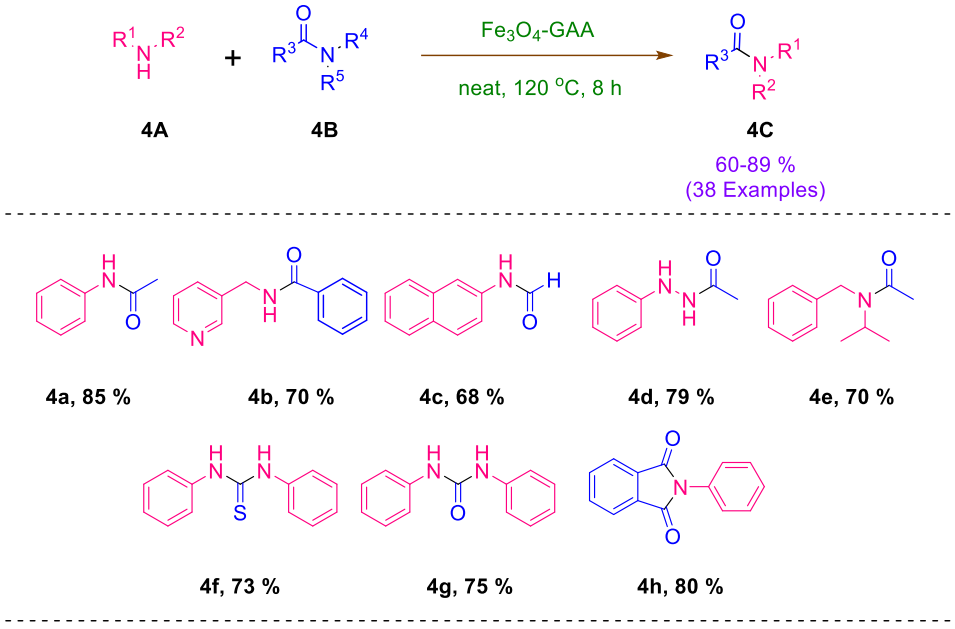

Scheme 2- 4. Fe-catalysed transamidation of carboxamides, phthalimide, urea and thiourea.

In 2016, another example of unactivated amides being transamidation by iron-mediated was disclosed. Shankarling and colleagues[20] synthesized transamide products with the Fe_3O4 nanocatalyst, which they re-used six times without decreasing its efficiency (**Scheme 2-5**). The researchers noted that Fe_3O_4 catalysts performed effectively in the absence of a solvent and produced the desired product in a high yield. However, the outputs of those processes that took place in the presence of solvents were almost useless. Indeed, the additional catalysts Al_2O_3, MgO, and ZnO were also examined, but none of them could compete with Fe_3O_4. They obtained a converted amides yield between 68 to 98 % by reacting benzamide with aromatic and aliphatic amines. Interestingly, the yield observation revealed that aliphatic amines produced more yield than aromatic amines. It's important to note that they had good results with benzylamine derivatives after transamidation with acetamide, formamide, and phthalimide.

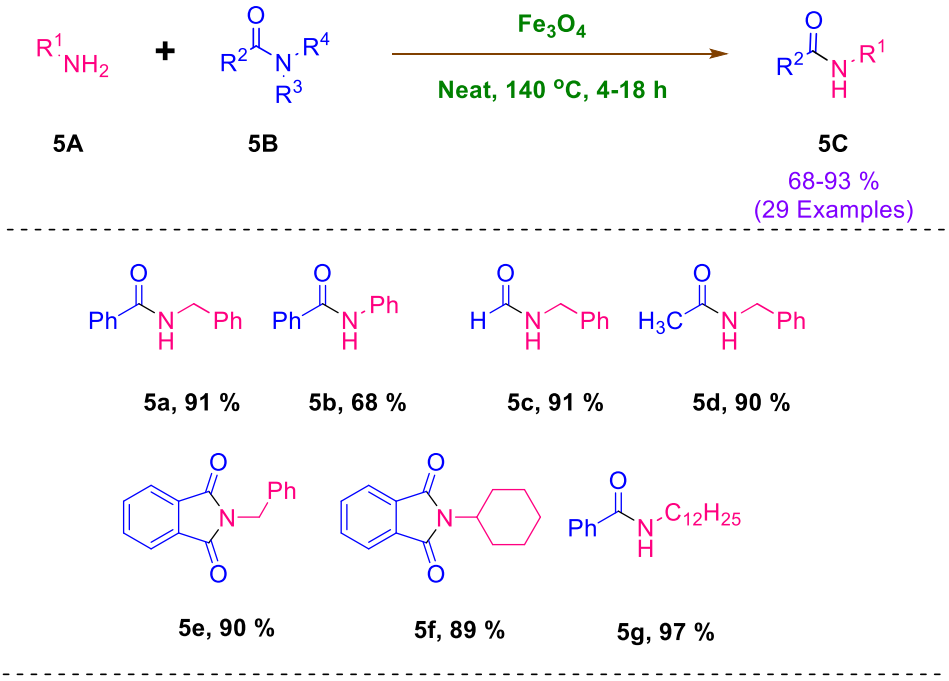

Scheme 2- 5. Fe-catalysed transamidation of carboxamides, phthalimide, urea and thiourea.

Porras et al.[21] published their work on cross-amidation between thioacetamide and amines using $SbCl_3$ catalyst (**Scheme 2-6**). Thioacetamide was shown to be compatible with both aliphatic and aromatic amines in this study. Furthermore, secondary aliphatic amines were yielded less yield in more time than primary aliphatic amines. However, in the case of aromatic amines, the transamidation results were obtained a moderate to good range. Additionally, aromatic amine conversion takes longer than aliphatic amine conversion. The authors also attempted to broaden the thioamide scope from aliphatic to aromatic, but no changes occurred. They also reported a phthalimide and benzylamine reaction, but the yield was substantially lower after more time was spent on it.

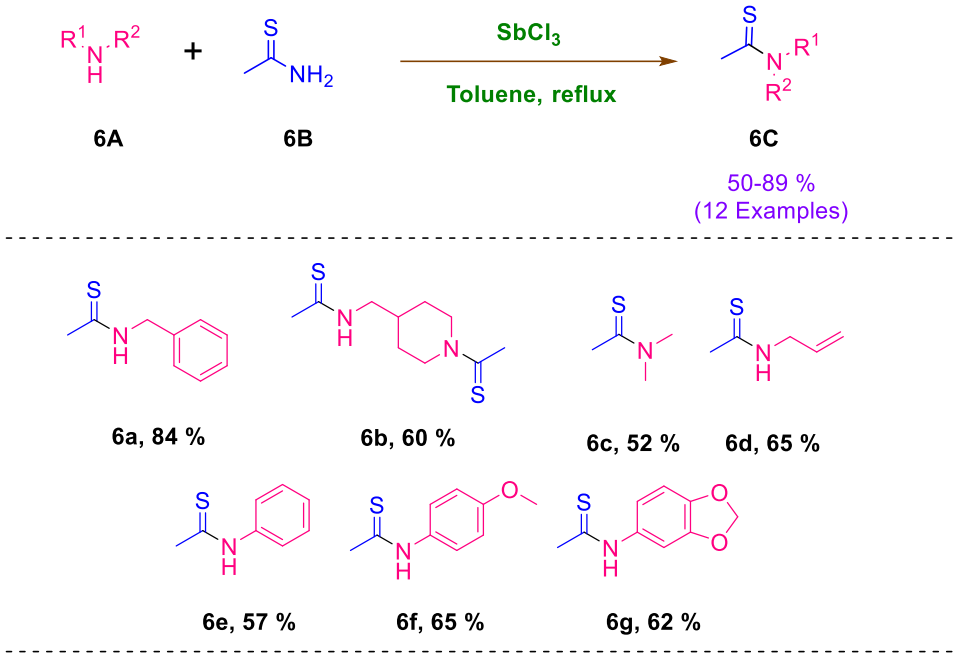

Scheme 2- 6. Sb-catalysed transamidation of thioacetamide.

Sheng et al.[22] got the idea to perform the multimetallic catalysed transamidation reaction after investigating the previous literature[23–26] (**Scheme 2-7**). Researchers examined different lanthanoids catalysts while standardising reaction conditions and found that $Nd_2Na_8(OCH_2CF_3)_{14}(THF)_6$ was the most effective catalyst. They also observed that heterobimetallic lanthanide/sodium alkoxide complexes performed better during transamidation than monometallic lanthanide complexes. Furthermore, this approach helped researchers to obtain a satisfactory yield of transamidated products from 1° and 2° aromatic, aliphatic, and heterocyclic amines on treatment with a benzamide. Notably, the reported protocol showed that benzylamine and long-chain aliphatic amine were compatible with the reaction of aromatic and heteroaromatic carboxamides.

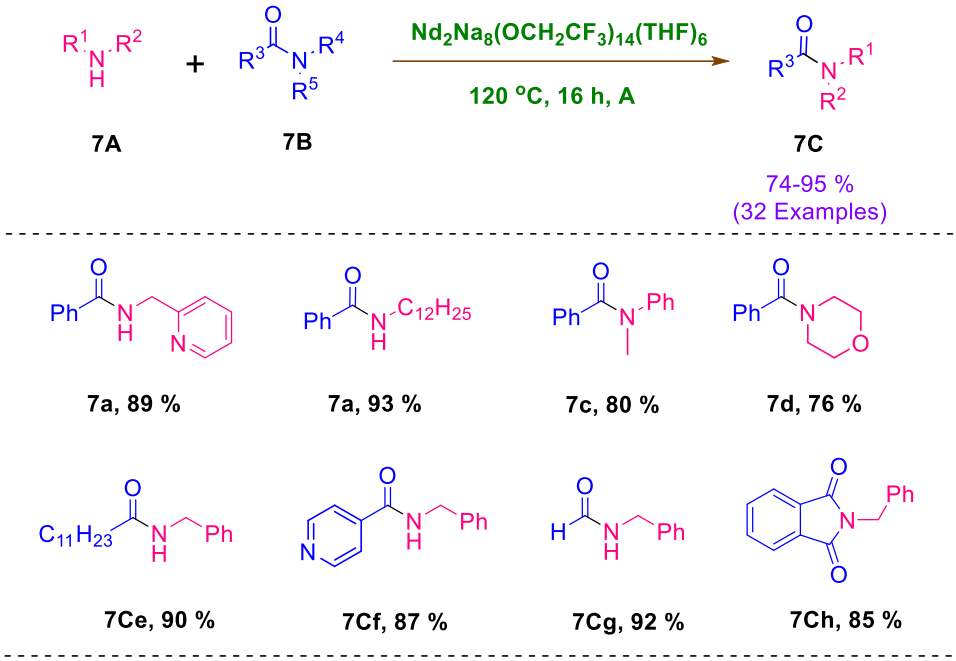

Scheme 2- 7. Multimetallic catalysed transamidation reaction between benzamide and amine.

Gu et al.[27] developed a novel method of palladium catalysed reaction among DMF derivatives and substituted 1° anilines (**Scheme 2-8**). The study utilises several ligands and also organic acids and Lewis acids as additives at different temperatures to standardise the reaction. In addition, the optimisation study revealed that the addition of additives has a significant effect on product yield. The electron-donating substituted aniline yielded a higher yield than electron-deficient substituted anilines. Moreover, para-substituted anilines were more comfortable with this transformation than ortho- and meta-substituted. Additionally, the bulky group produced a moderate yield of the desired product due to steric hindrance. Furthermore, formamide derivatives produced moderate to good results in this conversion. The researcher observed that the transamidation yield was lowered due to the bulky replacement on the nitrogen atom of amides. In a subsequent analysis, they tried different amide derivatives with aniline, and the study concluded that formyl derivatives were more compatible than acetyl derivatives.

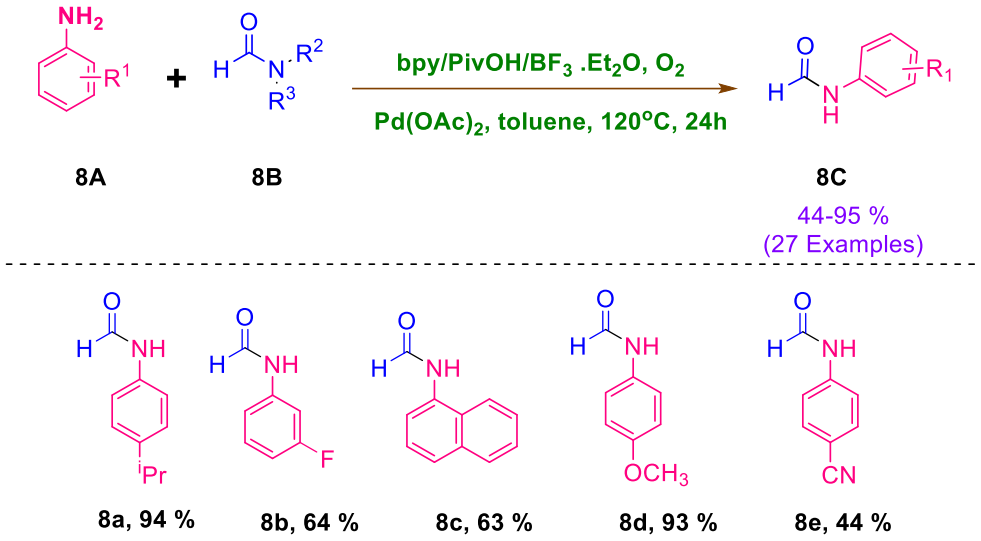

Scheme 2- 8. Pd-catalysed transamidation between carboxamide of DMF and anilines.

Bhanage and his colleagues reviewed the literature on manganese oxide applications and found that it is a good oxidant as well as an excellent catalyst in organic reactions[28–30]. They established a transamidation method of a broad range of primary amides and amines utilising MnO_2 as a catalyst, based on the previous research[31] (**Scheme 2-9**). This process showed excellent tolerance to aromatic amines that were substituted with electron-donating and withdrawing groups during the treatment with formamide. However, ortho-substituted anilines had produced a lower yield than meta- and para-substituted anilines. Similarly, meta and para substitutions were found to be more efficient than ortho substituents during the transformation of substituted benzamides. Furthermore, the protocol showed the compatibility of phthalimides with aromatic and aliphatic amines. As a consequence, the authors were able to scale up their technique to the grams scale and obtain a good yield of transamide product.

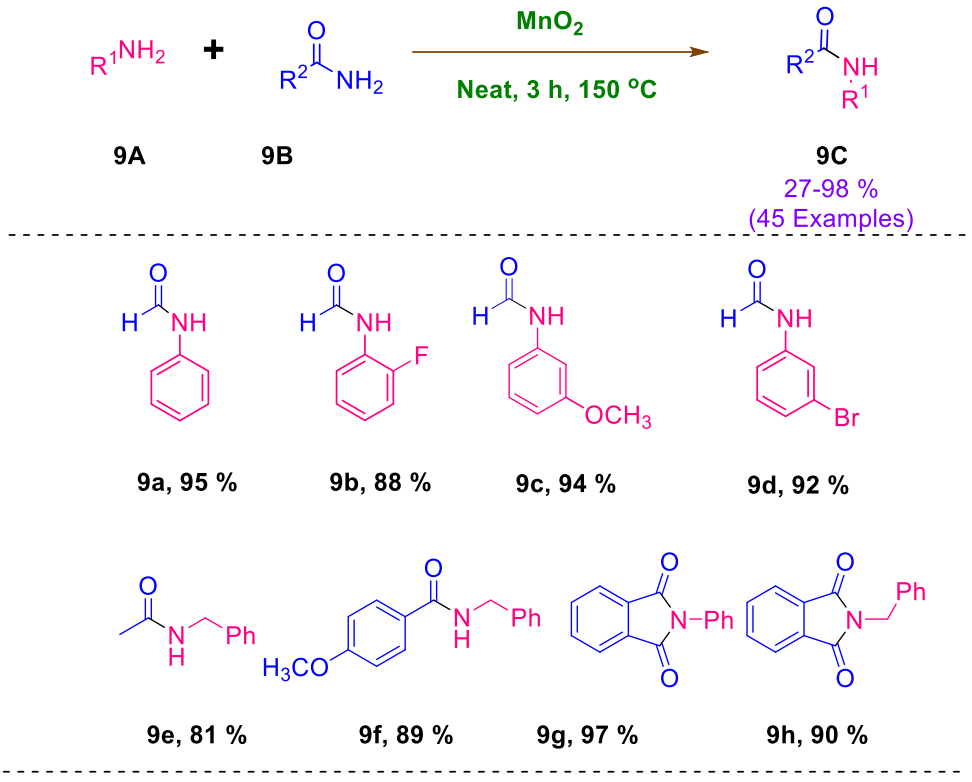

Scheme 2- 9. Mn-catalysed transamidation of primary carboxamides and phthalimide.

Recently, *Feng et al*. reported a tungsten-catalyzed conversion of tertiary alkyl amides to another amide in the presence of NMP utilising phenanthroline as a ligand (**Scheme 2-10**). Compared to other metal catalysts such as Al, Fe, Zr, and Mo, the tungsten catalyst produced the best results during the process optimization study. In addition, the yield was decreased when they performed the experiments in each absence of ligand, catalyst and TMSCl. This approach had a wide scope of anilines containing electron-donating groups (CH_3, OCH_3, SCH_3, CO_2CH_3, *i*-Pr and *t*-Bu), halogen (F, Cl and Br), electron-withdrawing groups (CF_3, CN, NO_2, CO_2H and $COCH_3$) and bulky ring (Naphthyl). Moreover, the aliphatic amines (benzyl, cyclohexyl and cyclopentyl) and heterocyclic amines (indole, pyridine, thiazole and benzothiazole) had also familiar with reaction conditions. Similarly, the various substituted amides had generated transamide products in good to excellent yields. Finally, they concluded from competition studies of primary, secondary, and tertiary amides transamidation that tertiary amides produced more yield than primary and secondary amides.

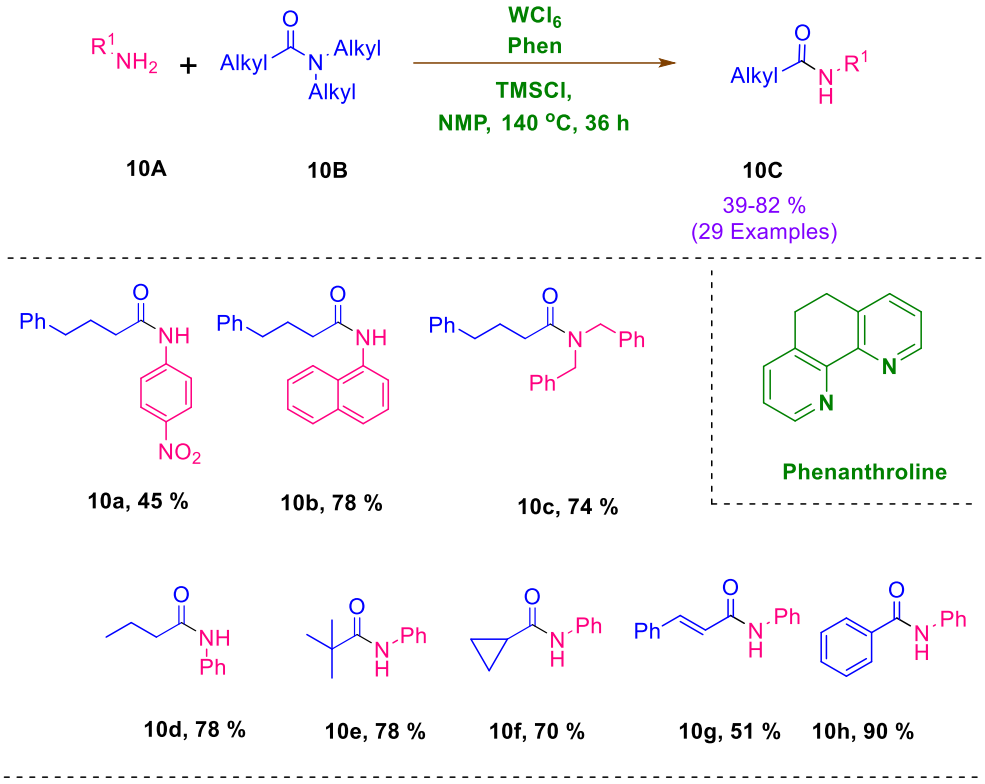

Scheme 2- 10. W-catalysed transamidation of tertiary alkyl amides with amines.

Singh and his group reported a binuclear Mn-catalysed transamidation of acetamide and formamide with amines under solvent-free conditions[30] (**Scheme 2-11**). The observation indicated that lowering the temperature below 120 °C had an effect on the yield of the transformation. The approach uses a wide range of amine substrates, including both electron-withdrawing and electron-donating groups.

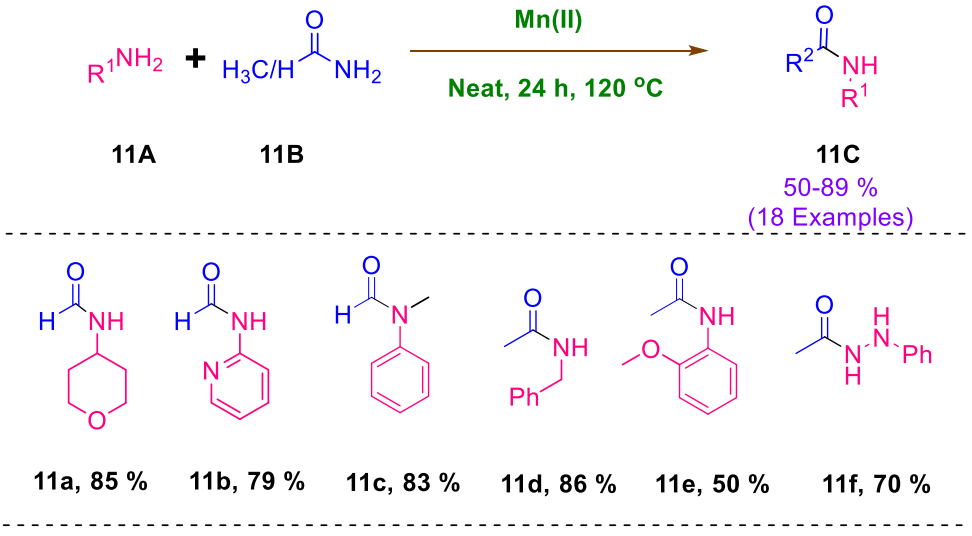

Scheme 2- 11. Mn-catalysed transamidation of acetamide and formamide with amines.

In April 2017, another example of Ni-catalyzed transamidation conversion of DMF and DMA came to light. *Sonawane et al.* found that a Ni (II)-metal complex with 8-hydroquinoline [Ni(quin)$_2$] was an excellent catalyst for the N-formaylation and N-acylation of various amines with DMF and DMA[32] (**Scheme 2-12**). The catalyst is efficiently transformed into another amide in the presence of imidazole. Interestingly, the reaction conditions were found to be feasible and did not necessitate the use of an inert atmosphere. The technique is quite versatile since it may be used to N-formylate and N-acylate of electron-withdrawing (F, Cl, Br, and NO_2) and electron-donating (CH_3 and OCH_3) substituted anilines. Notably, both amide transformations are compatible with linear, cyclic, and heterocyclic aliphatic amines. It has been noted that when electron-withdrawing groups substituted anilines are utilized as coupling partners, the yield is often lowered.

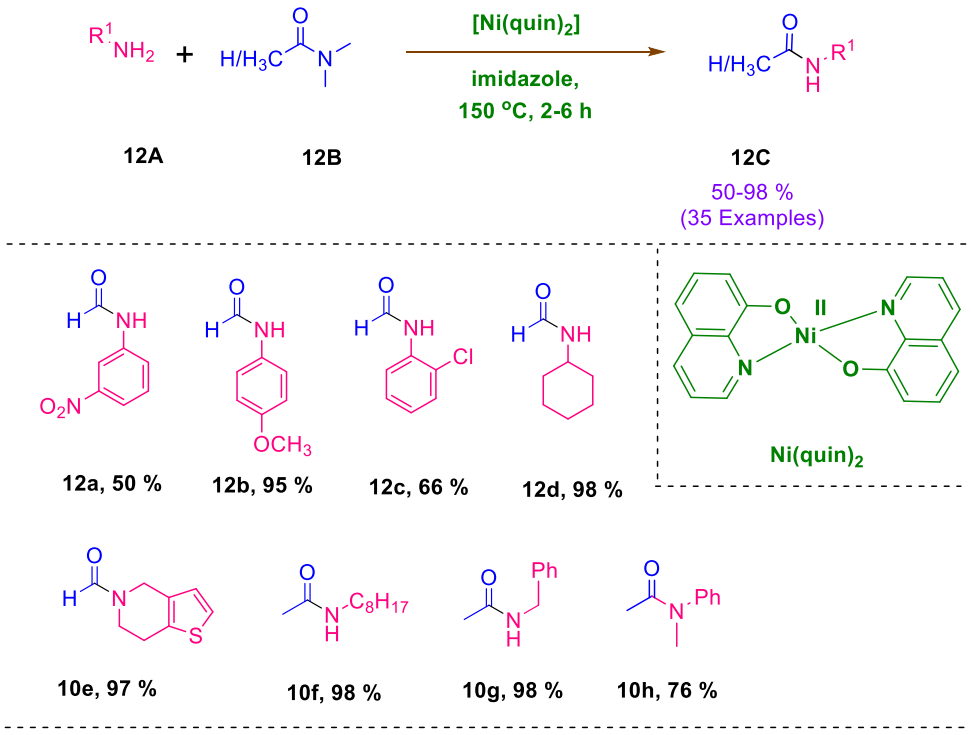

Scheme 2- 12. Ni-catalysed transamidation of DMA and DMF with amines.

Wagh et al.[33] promoted a transamination of urea and thiourea in the presence of heterogeneous catalyst sulfated tungstate; they recycled and re-used the catalyst 4-5 times without losing efficiency **(Scheme 2-13)**. After the optimisation study, they obtained 98% of desired urea on the neat reaction between aniline and urea in the presence of 10 wt % of sulfated tungstate at 90 °C within 1.5 hr. The method produced transamide symmetrical and unsymmetrical ureas and thioureas from unsubstituted and

monosubstituted ureas and thioureas. The researcher obtained an excellent yield of symmetrical and unsymmetrical ureas under the set condition from reacting aniline, aliphatic amines, hetero amines and aryl hydrazides with unsubstituted and monosubstituted ureas. They also confirmed the similar kind of reactivity of thioureas against different amines.

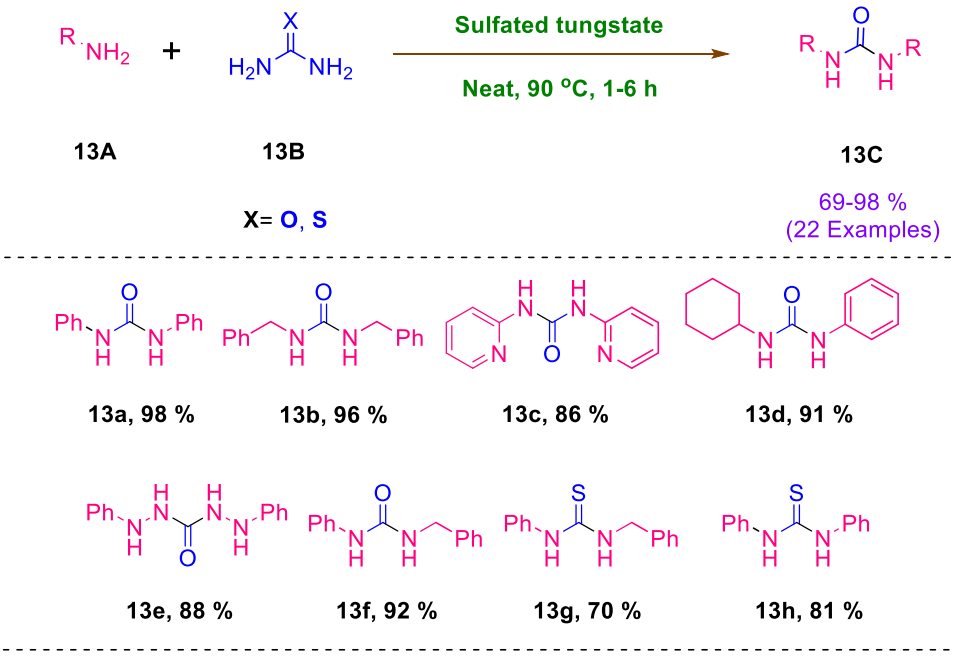

Scheme 1- 13. Sulfated tungstate catalysed transamidation of N-substituted urea and thiourea.

Ma et al.[34] used cobalt catalyst to perform *N*-formylation and *N*-acetylation of a variety of amines and carboxamides **(Scheme 2-14**). Prior to selecting cobalt catalysts, they screened a variety of transition metal catalysts, including Ni, Cu, Mn, and Fe, of which Co catalyst was found to be the most prevalent for obtaining the best results. This study systematically examined the scope of amines and carboxamides. They formylated 1° and 2° aliphatic amines, and the results indicated that 1° aliphatic amines produced an excellent yield of product. They observed that aromatic amines have no reactivity. Further, the amide scope revealed a predominance of formylation over acetylation; benzamide and thiophen amide exhibited significantly lower reactivity.

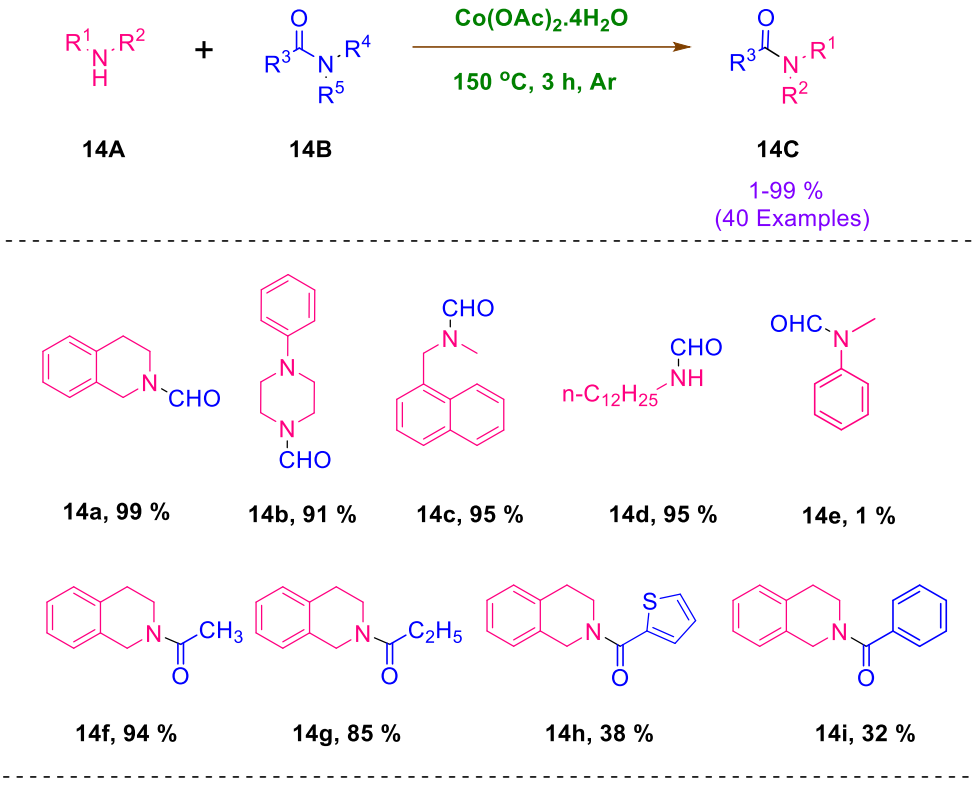

Scheme 2- 14. Co-catalysed N-formylation and N-acetylation reaction.

Non-metal Catalysed

Ghosh et al.[35] reported a strong base potassium *tert*-butoxide mediated transamidation of primary and tertiary amides. Initially, they tried readily available inorganic bases *viz* KOH, K_2CO_3, Cs_2CO_3, KO^{t}Bu, DBU, and NaOH. Among them, KO^{t}Bu showed the best-desired product yield. They claimed that this method supported amines including aryl, heteroaryl and aliphatic amines, transamidation with amides such as DMF and DMA (**Scheme 2-15**). Moreover, the yield observation concluded that the electron-withdrawing group substituted aniline took place more time with less yield as the comparatively electron-donating group substituted aniline. Furthermore, the method features broad substrate scope of amides, including DMA, DMF, trifluoroactamide and benzamide. Finally, they concluded from mechanistic studies that the transmaidtion proceeded through a free-radical pathway.

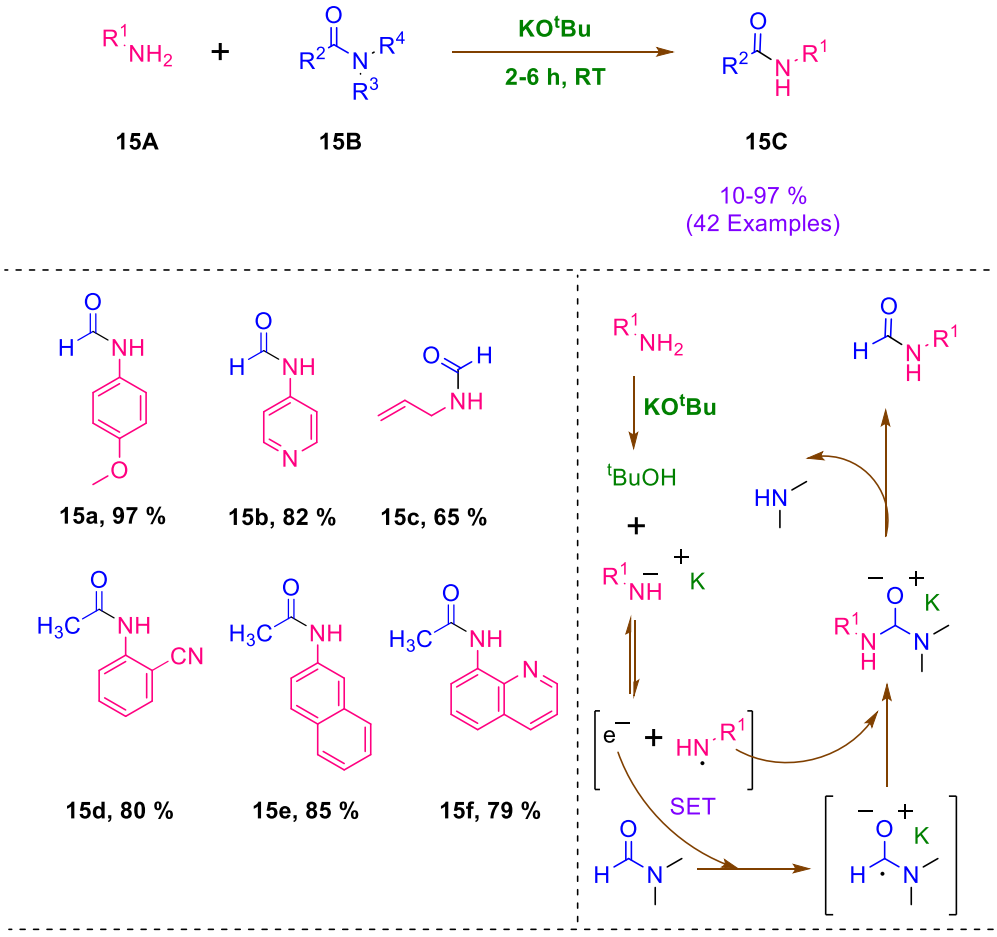

Scheme 2- 15. KO^{t}Bu mediated transamidation reaction of primary and secondary amide.

Tan et al. reported one more t-BuOK-mediated methodology for transamidation of tertiary amide in the same year[36] (**Scheme 2-16**). The transamidation of DMF proceeds smoothly in the presence of t-BuOK as a base (4.0 equiv) and DMF as solvent at 25°C for 2 hours in an inert environment. However, when DMA and dimethylbenzamide (DMB) are used for transformation, this reaction acts differently because it occurs at 110-130 °C in the microwave for 30-50 minutes while utilising its diglyme as a solvent and in the presence of t-BuOK. The transamidation of DMF produces excellent yields of amide compounds. Additionally, the approach utilizes a broad range of amines during the treatment with DMF and DMA, including anilines substituted with electron-withdrawing and electron-donating groups, heteroaromatic, and aliphatic amines. Notably, the procedure's main flaw is that ortho-substituted anilines produced lower yields than other positions. This method follows the same mechanism as **Scheme 2-15**.

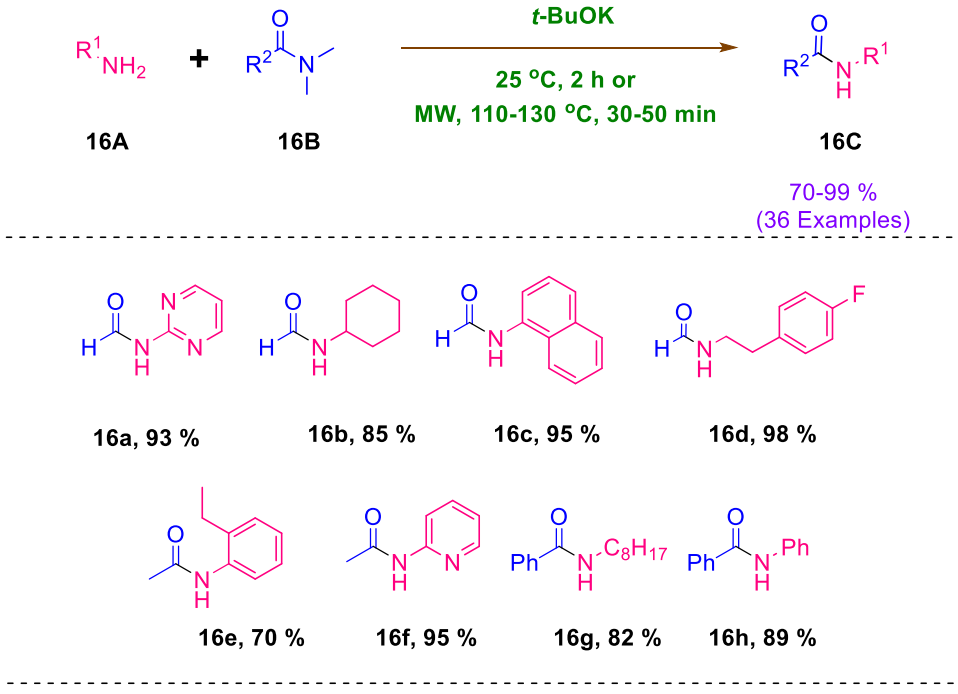

Scheme 2- 16. KO^{t}Bu mediated transamidation reaction of tertiary amide.

One methodology reported by our group was the use of amine salt instead of an additional salt additive[37] (**Scheme 2-17**). Notably, the simplicity of processing and the moisture and air reliability provided are significant advantages of this technique. In particular, this approach allowed the development of functionalised transamide products from amides, including sterically hindered, aliphatic, heteroaromatic, and aromatic amides. The method is also efficient with primary, secondary, and tertiary amides, yielding good to exceptional converted amide yields. Furthermore, various cyclic and linear aliphatic, heteroaromatic, and aromatic amines are substituted with electron-rich and deficient groups that were compatible as nucleophiles for this amide conversion in the substrate scope. This methodology has additional advantages if it raises the temperature in the case of substituted 2-aminophenols as nucleophiles reacting with amides to produce 2-substituted benzoxazole as a final product. The hydrogen ion activates the amide, followed by amines attack as a nucleophile and eliminating the amine as a side product, leading to the final amide product.

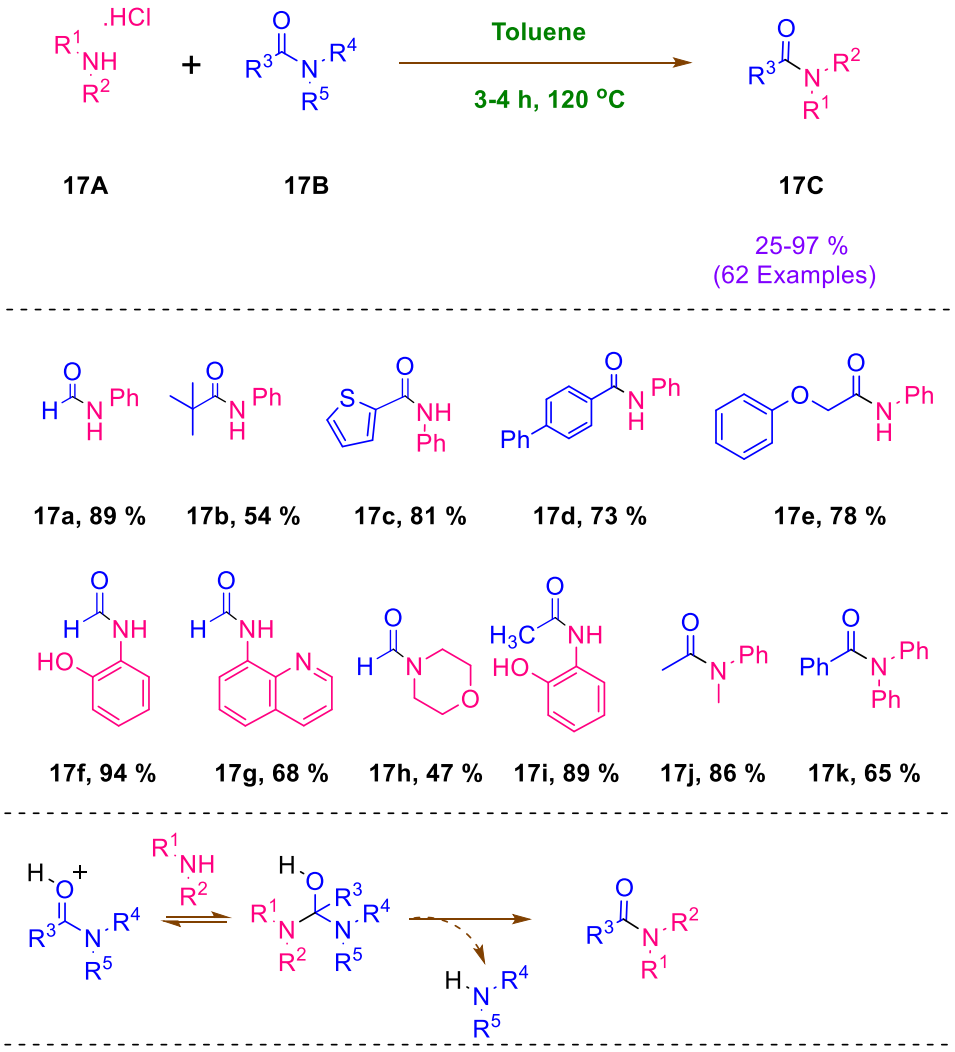

Scheme 2- 17. HCl-mediated transamidation of unactivated amides.

One more example of transmaidation conversion of DMF and DMA using metal free conditions, published by Zhang and Xie's[38] team. Authors found that NH_4I is the best salt to use as a reagent among the other salts evaluated, such as KI, CuI, NH4F, NH_4Cl, and NH_4Br (**Scheme 2-18**). They also tried DMSO and *o*-Xylene as solvents but observed low transamidation conversion. Researchers demonstrated an excellent to a good yield of transamidation from a wide range of substituted anilines and DMF. The procedure was less compatible with ortho-substituted anilines when used. Furthermore, the scope of amine with DMA yielded a transamide product with a conversion range of 33 to 52 % utilising 2 equiv of NH_4I. Nevertheless, the range of the reaction is narrow; this approach can only use DMF and DMA.

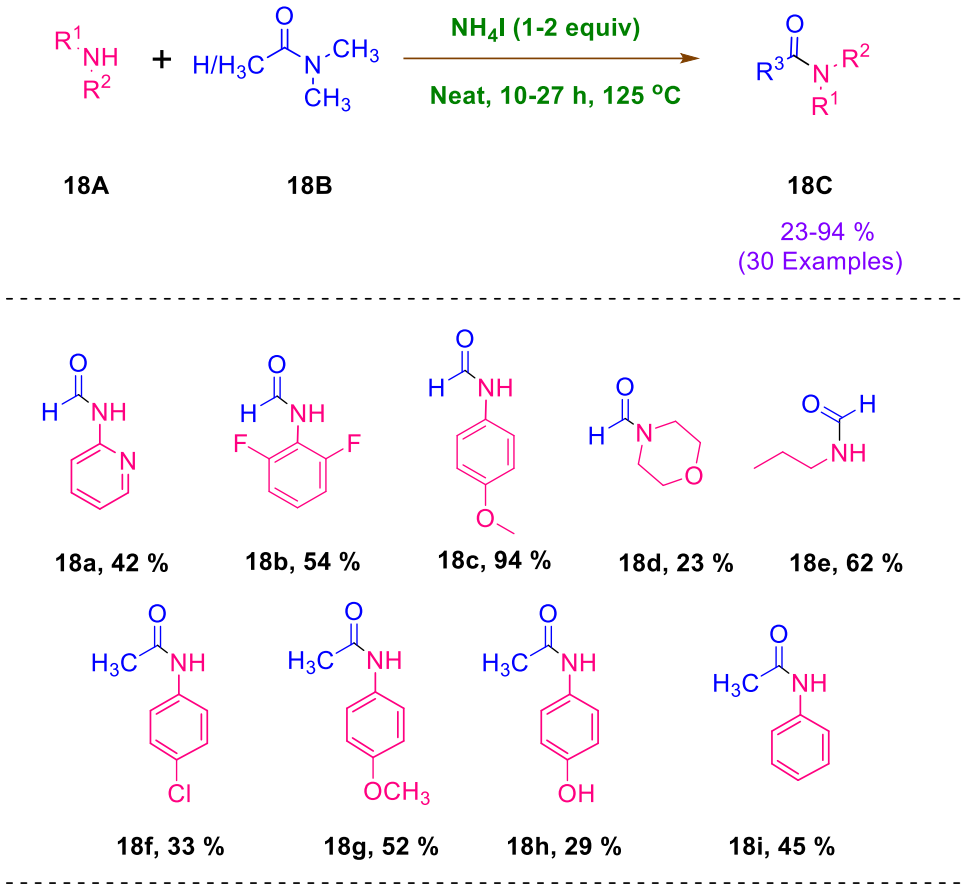

Scheme 2- 18. NH_4I catalysed transamidation reactions of unactivated amides.

The transamidation of *N*,*N*-dimethyl amides with various primary amines was also accomplished using the sodium-*tert*-butoxide (NaO^tBu)[39] (**Scheme 2-19**). They studied various bases during reaction optimisation and found that NaO^tBu provided the highest yield of transamide product under an inert atmosphere. In addition, the procedure standardisation studies show that base equivalent plays a critical role in the success of conversion. A good to an excellent yield of amides was obtained from aromatic, heteroaromatic, and aliphatic primary amines. The primary disadvantage of this approach is that the base is incompatible with aromatic substitution on the α-position of amide. The mechanistic studies reveal that transamidation does not include a radical pathway in the reaction mechanism like KO^tBu-mediated methodologies.

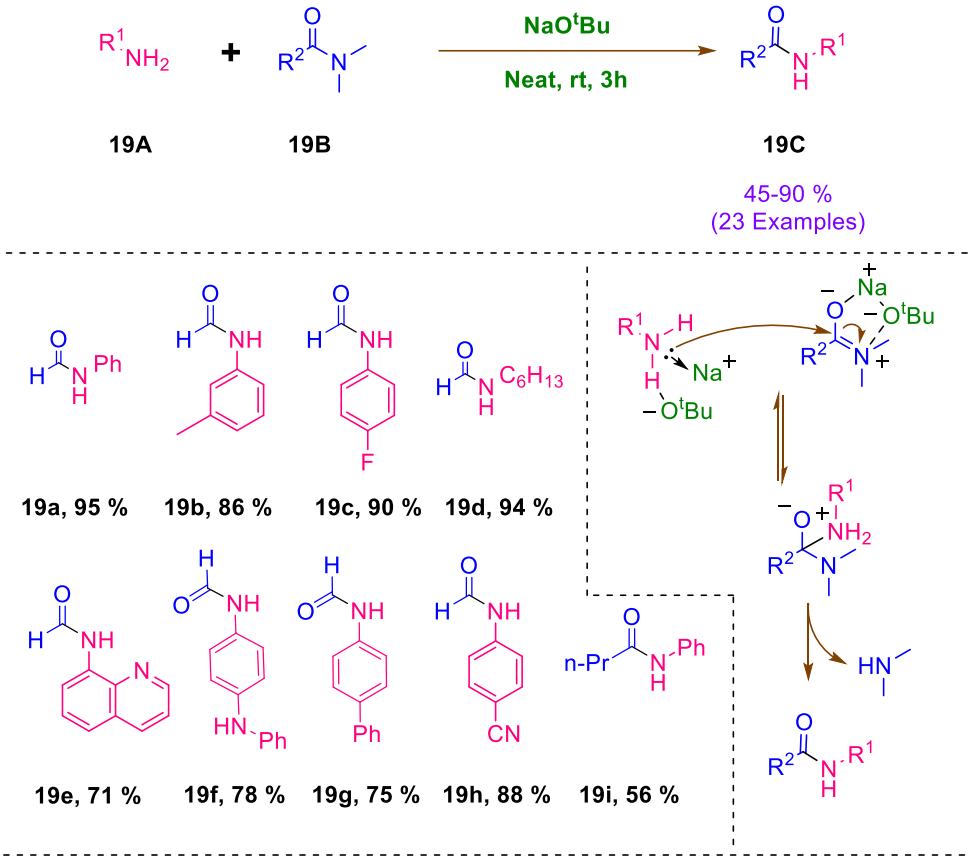

Scheme 2- 19. NaO^{t}Bu-mediated transamidation of amides with a variety of 1^o amines.

Srinivas et al.[40] developed a simple route to achieve transamidation without involving any hazardous metal catalyst (**Scheme 2-20**). The reaction was carried out by utilising $K_2S_2O_8$ as an additive and water as the solvent. However, the transformation greatly relies on the reaction temperature. Additionally, the reaction carries out using both conventional and microwave methods. The comparative studies demonstrate that the microwave process is more effective and efficient than the conventional method, producing more than 95% of the desired product. The reaction scope revealed that this reaction produced an excellent yield of amides from halo, alkoxy, carboxyl and alkyl groups substituted anilines using both procedures. Notably, the reaction is compatible with aromatic, aliphatic, cyclic amines as well as N-substituted formamides and phthalimide, which yielded the desired transamide products in sound yields. According to a mechanistic analysis that $K_2S_2O_8$ may activate the amide, followed by an amine approach as a nucleophile, to produce the required transamide product.

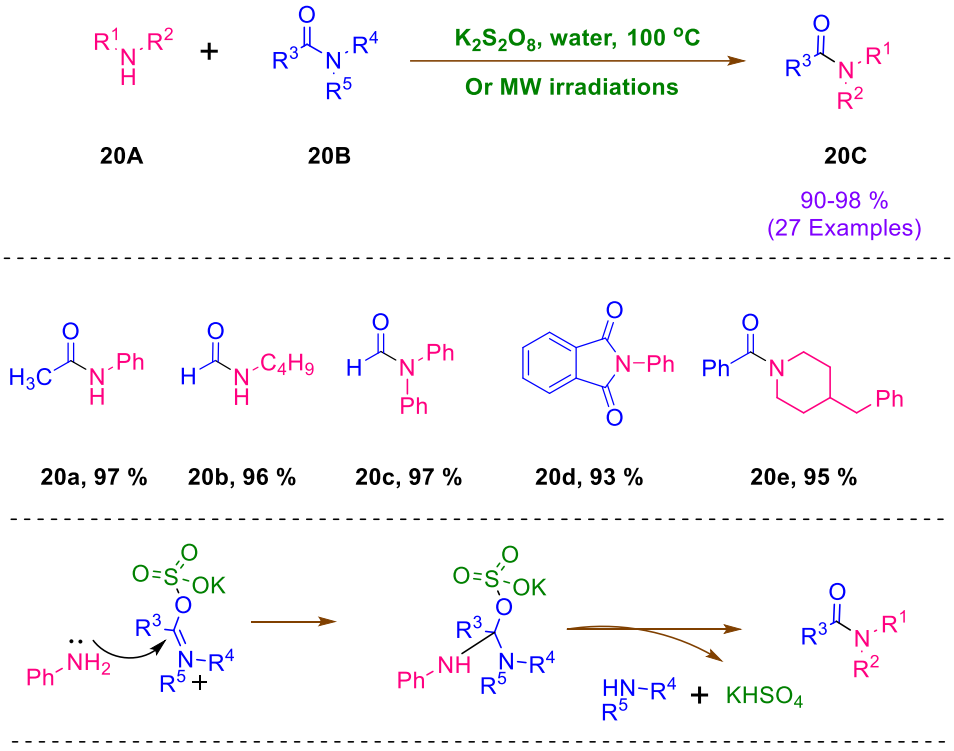

Scheme 2- 20. $K_2S_2O_8$-mediated transamidation of amide derivatives with anilines.

In 2019, Lee and co-workers[41] developed a TMSCl mediated transamidation reaction to synthesise transamide products from primary amides (**Scheme 2-21**). This protocol demonstrated that TMSCl activates 1° amide, which triggers the transamidation reaction in the presence of NMP as a solvent. Except for TMSCl, no suitable results were obtained during optimisation studies when other silyl lewis acids were used as the additive. Some primary amides bearing phenyl, cyclohexyl, benzyl or even sterical hindered (tert-butyl) groups can be successfully converted under standard conditions. Moreover, aliphatic, heterocyclic, electron-deficient and donating group substituted and even steric hindered aromatic amines can be reacted efficiently with a benzamide. However, when 2,5-disubstituted aniline derivatives were utilised, the intended product was not produced, indicating that electronic and steric factors play a significant role in the success of this reaction. In addition, alkyl-substituted on the *para* position of aniline produced excellent results for transamide products. It was also noteworthy that the aliphatic secondary amine and amides were reacted using NMP/$CHCl_3$ solvent mixture. Further, the control experiment revealed that *N*,*N*-disilyated amides and amines are not active intermediates for transamidation reaction.

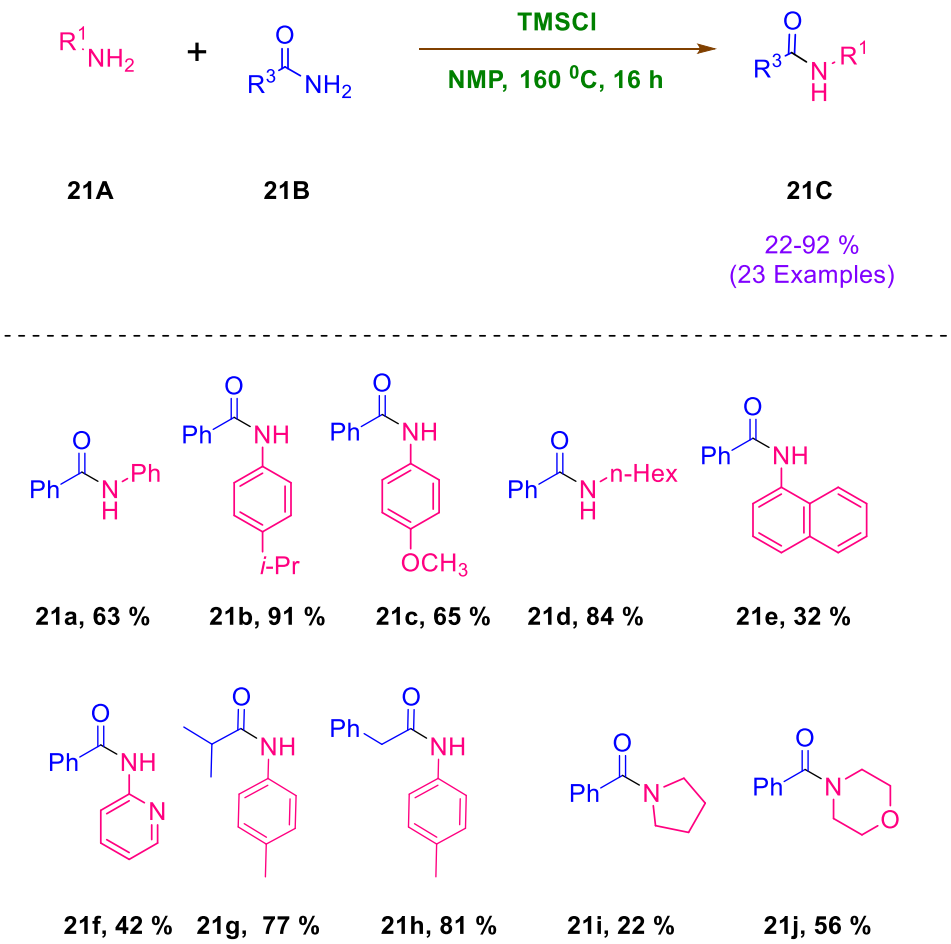

Scheme 2- 21. TMSCl mediated transamidation to synthesise 2° amides.

Jiang et al. recently reported that phosphoric acid can be employed as a promotor in the transformation of DMF and DMA to transamide compounds[42] (**Scheme 2-22**). In neat circumstances at 110-150 °C, they used an organophosphoric acid-mediated amide to amide conversion. Several anilines, including electron-donating and withdrawing group substitution and linear and cyclic aliphatic amines, provide good to exceptional yields of amide products. Interestingly, bromo, nitro, hydroxy, and bulky group substituted aniline and linear and cyclohexyl amines require more time and temperature to react with amides under these acidic circumstances. Furthermore, DMA transamidation occurred around 140-150 °C. This metal-free reaction occurs when an acid activates the amide, followed by a nucleophilic attack on the amine, which results in the amine being eliminated as a side product and the formation of the desired transamide product.

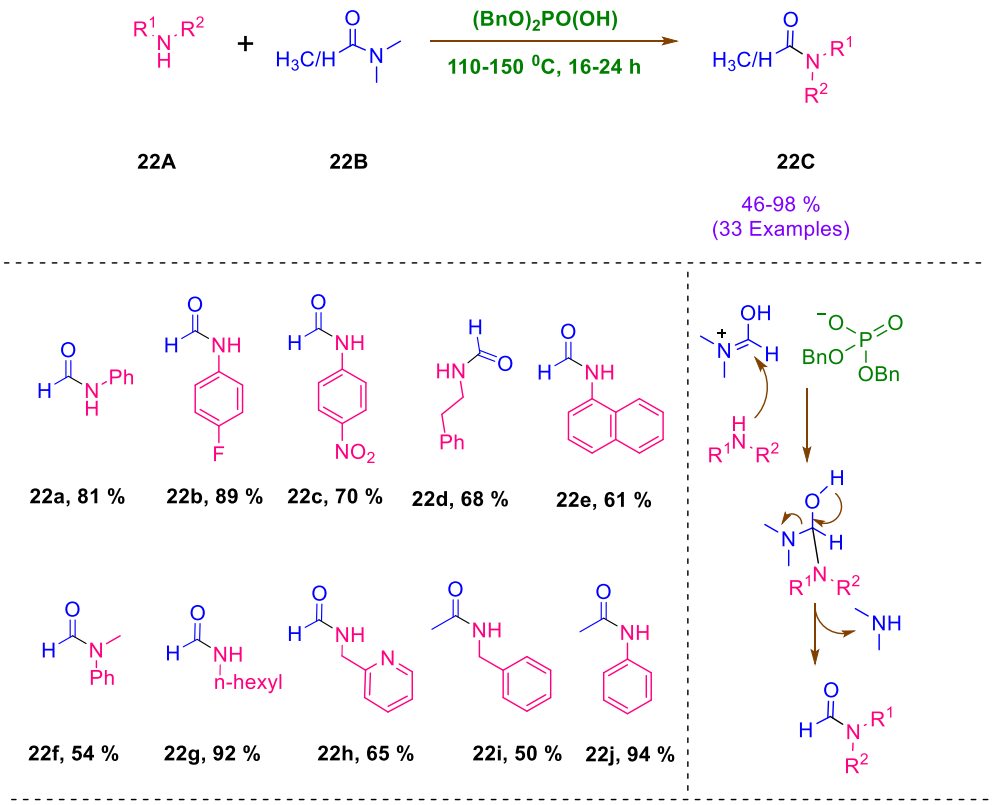

Scheme 2- 22. organophosphoric acid-mediated transamidation of DMF and DMA.

The use of tert-butyl nitrite as a promoter facilitated in situ conversion of the N-nitrosamide, which can be held in various amines to generate the final transamide product[43] (**Scheme 2-23**). The transamidation reaction was carried out at room temperature in DCM solvent utilising N-substituted benzamide amides as the precursor and amines, including linear, cyclic, and secondary aliphatic amines, gave the corresponding transamide product. Surprisingly, transamidation of aniline with N-methyl benzamide was unable to complete the transformation. However, secondary amines yielded a lower yield of amide products than primary amines. Additionally, the approach is compatible with the N-substitution of benzamide with aliphatic groups such as methyl, ethyl, n-propyl, n-butyl, cyclohexyl, and benzyl. Furthermore, benzamide substituted with 4-methoxy, nitro, or 2-fluoro effectively converts to other amides. Mechanistically, the tert-butyl nitrite attached with the nitrogen atom of amide to make N-nitrosamide as a labile group followed by amine attack as a nucleophile affords the unstable intermediate, which provides transamide product with the release of alkyl N-nitrosamine.

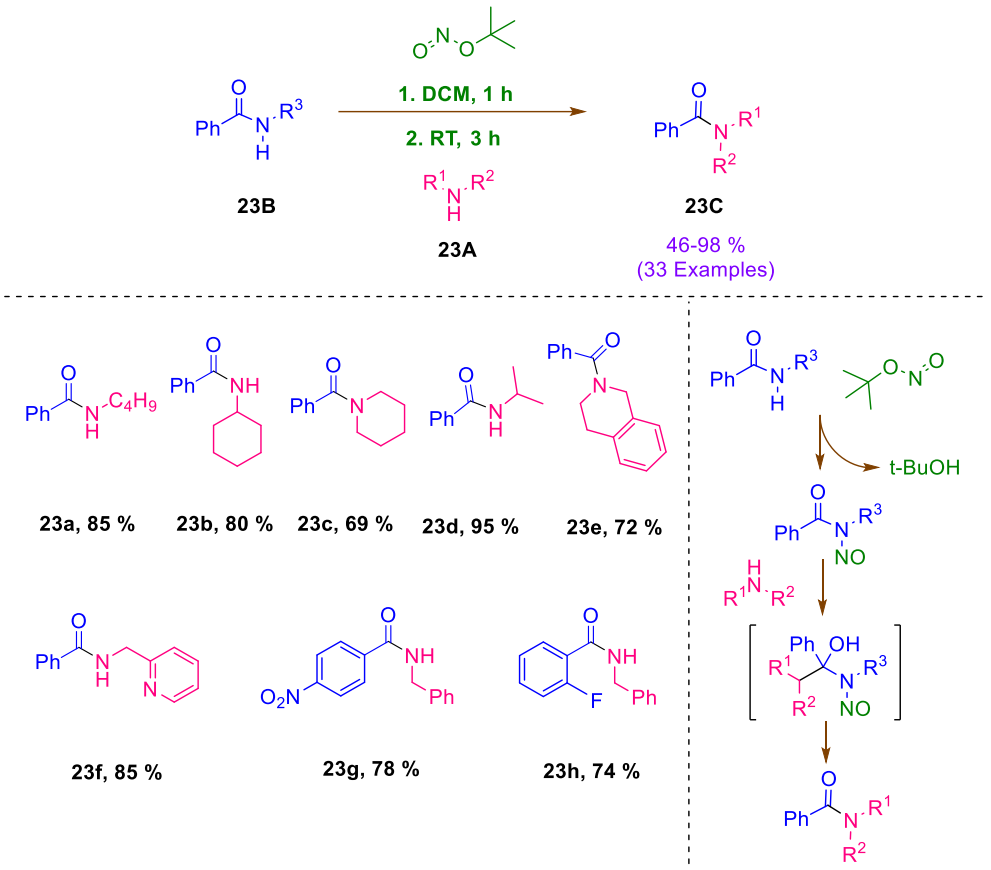

Scheme 2- 23. Tert-butyl nitrite-mediated transamidation of N-alkyl benzamide.

Transamidation of amides using iodine and hydroxylamine hydrochloride was recently reported by our group[44] (**Scheme 2-24**). Both conventional and microwave methods carried out this reaction under neat conditions at 120 °C. The reaction has a wide range of amides, including aliphatic and aromatic, with different N-substitutions on amides. Furthermore, aryl, heteroaryl, and aliphatic amines can be easily converted to their amides. The proposed mechanism is quite similar to acid-catalysed transamidation. Initially, the amide is activated by a hydrogen ion and then attacked by hydroxylamine as a nucleophile, resulting in hydroxamic acid and amine elimination as a side product. Iodine then promotes the conversion of the acid intermediate to the nitroso moiety, resulting in the formation of a transamide product with the liberation of nitrosyl hydride.

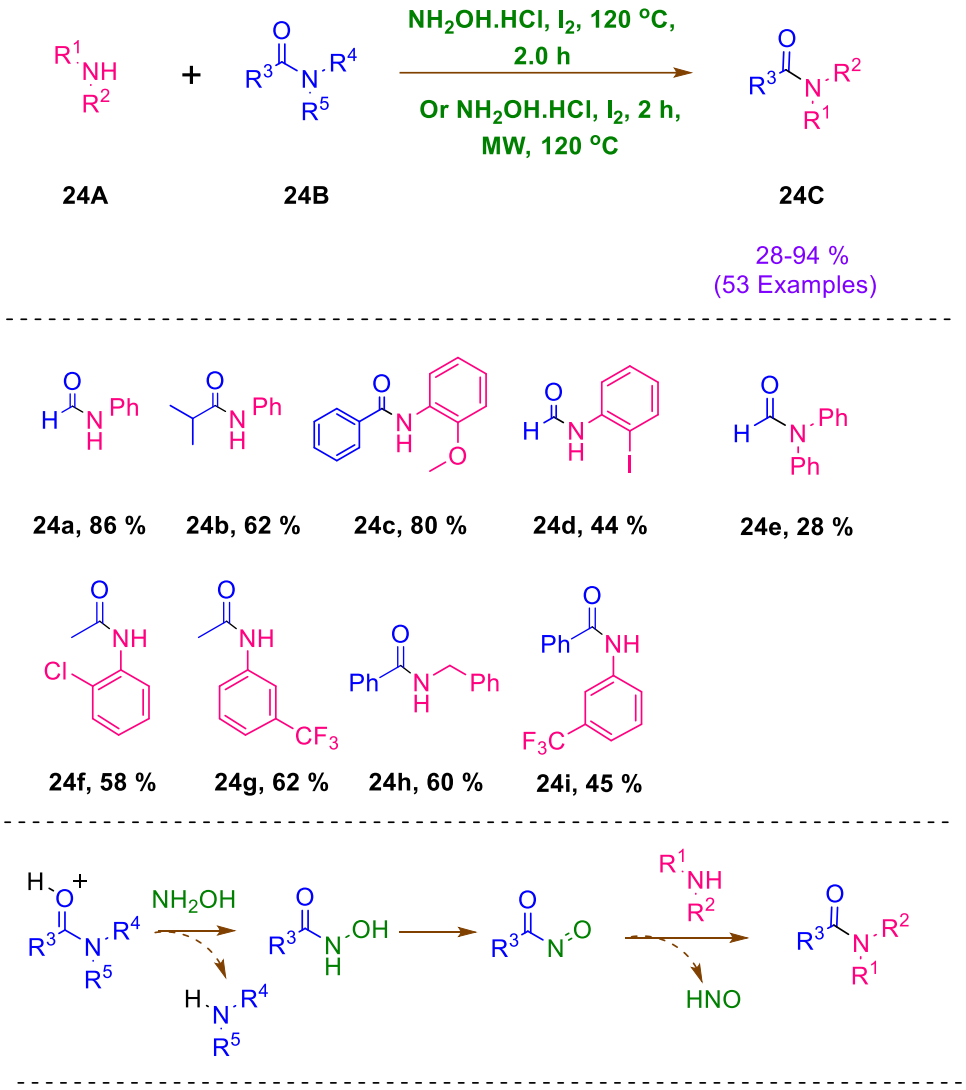

Scheme 2- 24. I_2-mediated transamidation of unactivated amides.

Lewis acids were shown to be involved in the transamidation in metal literature. *Sakurai et al.*[45]. developed an efficient method to perform the formylation of various amines and hydrazides with the help of *tert*-butyldimethylsilyl triflate (TBSOTf) as an activator (**Scheme 2-25**). The optimisation study revealed that silane-based Lewis acids (TMSCl, TMSOTf and TBSOTf) showed better results than other Lewis acids such as $BF_3.OEt_2$, $AlCl_3$, $TiCl_4$ and $SnCl_4$. The amide products had good to excellent yields and a high tolerance for aliphatic, aromatic, and heteroaromatic hydrazides. Moreover, the same conditions worked for amines, including aliphatic, aromatic, and heterocyclic amines. However, the yield statistics demonstrated that 2° amines had a higher yield than 1° amines. Notably, the additional equivalent of TBSOTf and imidazole were used in the reaction with amines/hydrazines bearing a

hydroxy group. According to the proposed mechanism, the amide is activated via lewis acid and then reacts with an amine to form the transamide product.

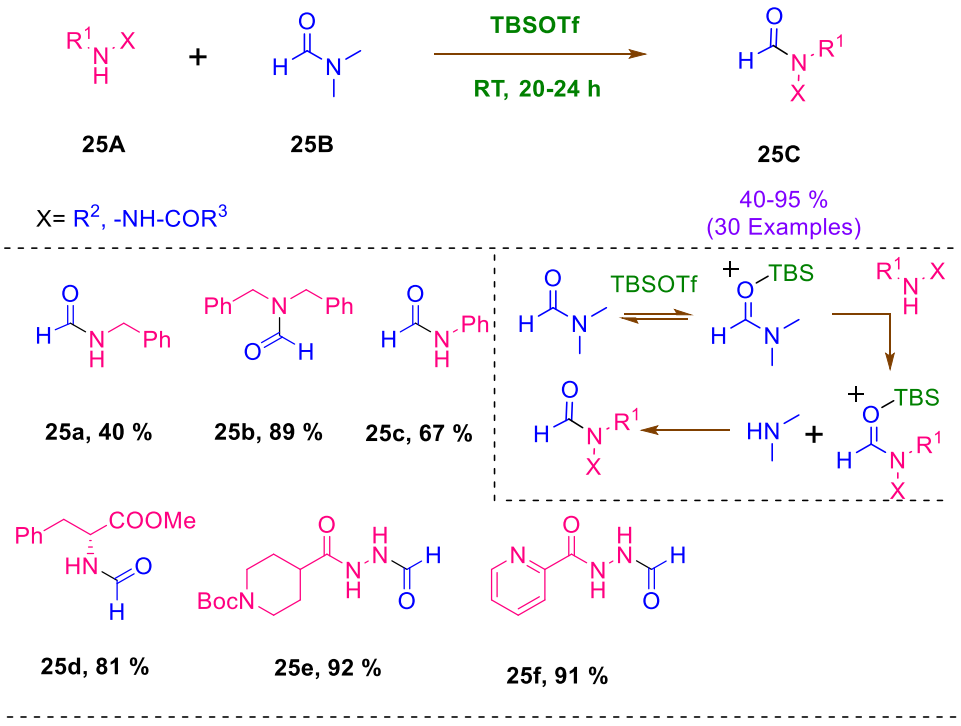

Scheme 2- 25. Tert-butyldimethylsilyl triflate (TBSOTf) catalysed transamidation reaction.

Compared to metal-mediated transamidation, the salt-mediated conversion reaction has been regarded as a cost-effective approach. Imidazolium chloride had received much attention when *Tian et al*. disclosed a method for the transformation of 1° amines with tertiary amides utilizing imidazolium chloride salt as an additive[46] (**Scheme 2-26**). Anilines with electron-rich and electron-deficient substituents, aliphatic and heteroaromatic amines all reacted to DMA admirably during the reaction scope evaluation. In particular, the nitro substituted anilines yielded less transamide product. Moreover, the study showed that the process is tolerant to amides such as DMF and benzamide. A mechanistic investigation was conducted to clarify the role of imidazolium chloride. The acidic proton of salt activates the amide, and the imidazole serves as a good leaving group to introduce the amine to the amide to obtain the other amide.

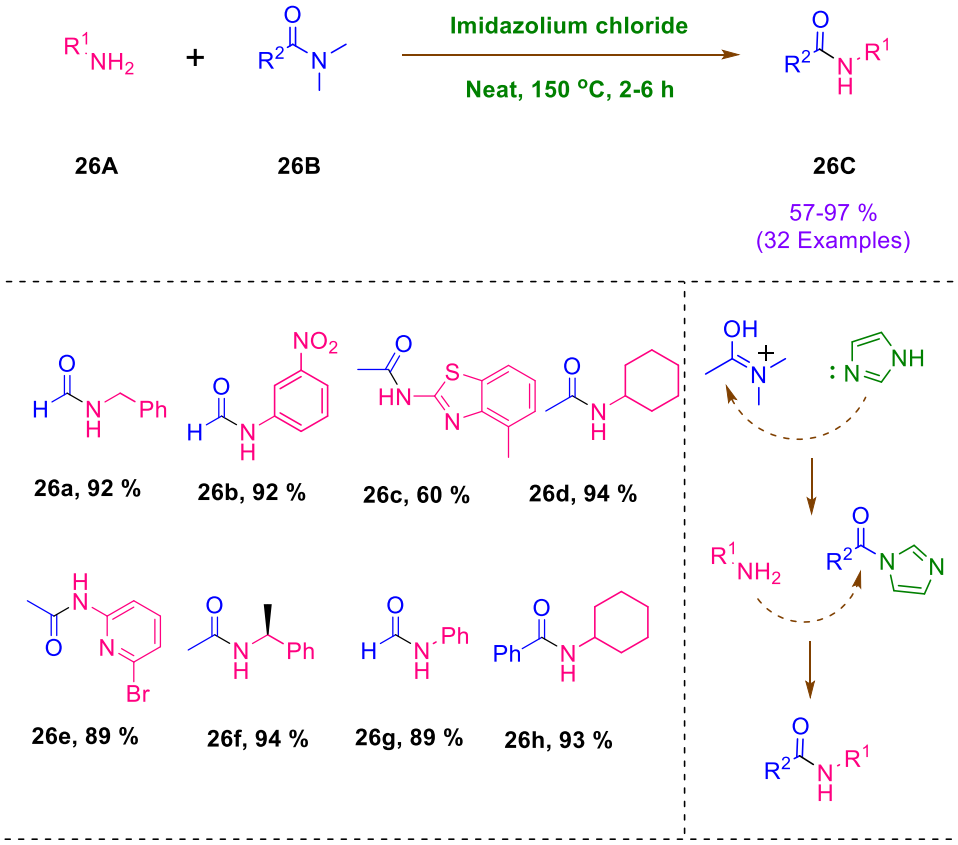

Scheme 2- 26. Imidazolium chloride mediated transamidation reaction of tertiary amides.

Miscellaneous

Hang Gong's[47] group have developed a reagent and solvent-free method for the cross amidation reaction between amides and amines (**Scheme 2-27**) and proved it on the gram scale. In the initial phase, they found the best result with simple formamide compared to *N*-substituted ones. The optimisation study revealed that the 10 equivalent of formamide at 150 °C within 24 h produced an excellent yield of formylation on *p*-toluidine. Using this standard condition, they performed formylation on aryl and heteroaryl amines with 60-98% range of yield of the corresponding products. The anilines with various electron-deficient groups such as (NO_2, CN, CF_3, CO_2CH_3), and bulky and heteroaryl amines showed a poor yield of transamide products. The formylation of aliphatic amines was more compatible with DMF at the same temperature for 24-96 h. Further, the competition analysis revealed that the formylation with DMF on aliphatic amine is more preferred over aromatic amine.

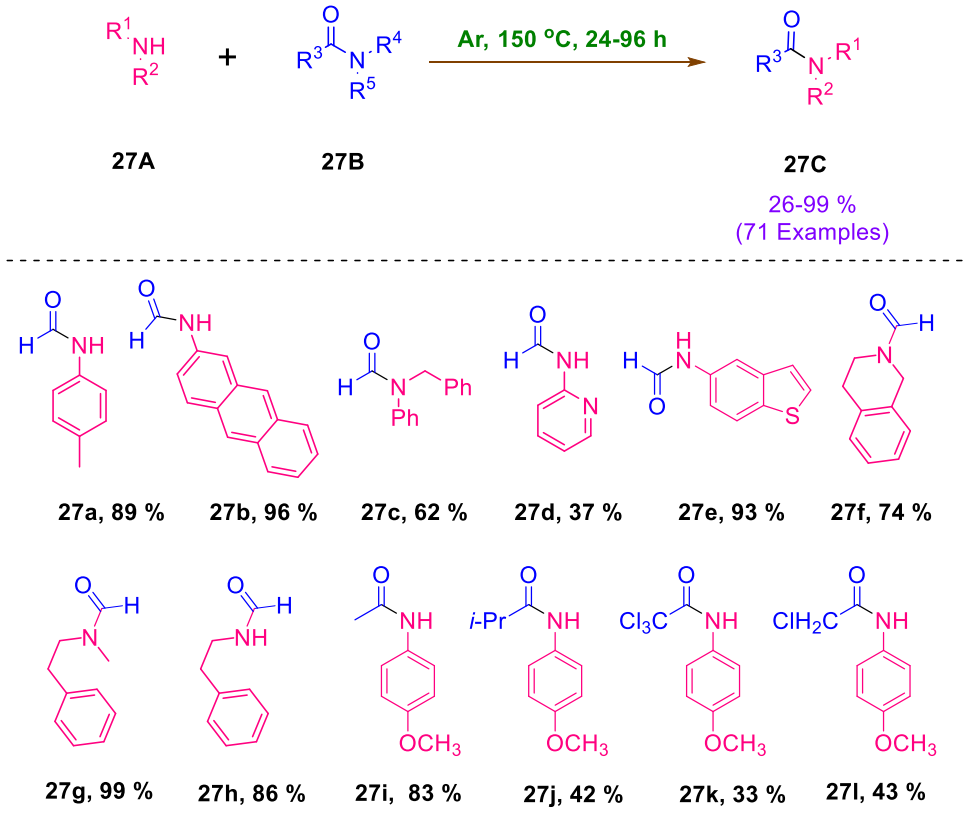

Scheme 2- 27. Solvent-free method for the cross amidation reaction.

Bensalah et al.[48] and their teammates developed a green approach to achieve selective transamidation on glycosyl carboxamide derivatives without disturbing any other hydroxy group. They were able to obtain an outstanding yield of the final product without the use of any solvent, reagent, or catalyst, despite the fact that they had tried catalysts such as L-Proline, D-Proline, and hydroxylamine hydrochloride, as well as solvents such as H_2O and DMF. They investigated various aromatic, aliphatic, and cyclic amines and established their compatibility by demonstrating a satisfactory yield (60–94%) of final products **(Scheme 2-28)**. Primary amines showed a better yield than secondary anilines. On the other hand, they showed well tolerance of glycosyl carboxamide derivatives with different amine reactions.

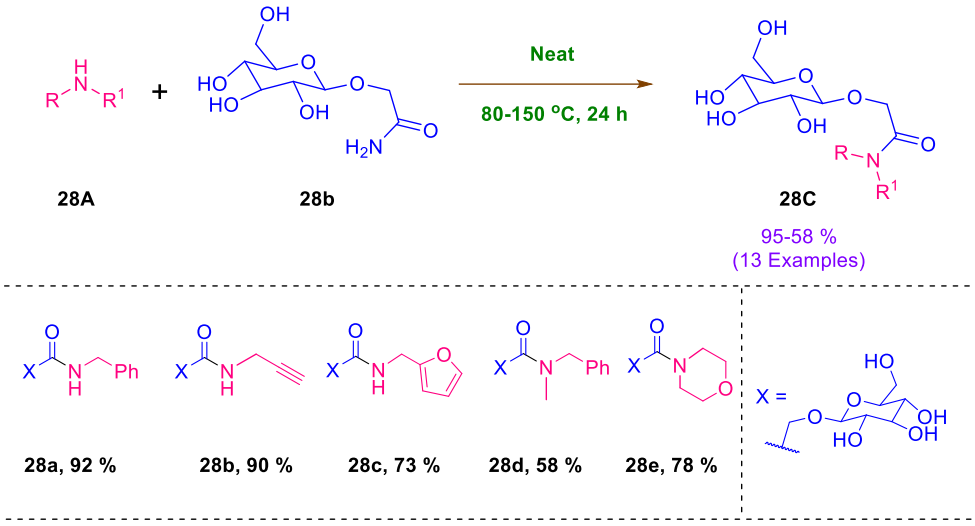

Scheme 2- 28. Green approach to achieving selective transamidation on glycosyl carboxamide.

Chevella et al.[49] developed a novel method to the obtained cross-amidation reaction of unactivated primary amides without using a solvent **(Scheme 2-29)**. This method used nano zeolite beta as a catalyst that provides large micro-pore volume, a large-pore channel system used for facelifted acid catalysed reactions. In the reaction optimisation study, they used benzamide and benzylamine as ideal starting materials and treated them in the presence of zeolites, MCM-41 and Montmorillonite. Among them, nanosized zeolite beta provided 93% of respective amide in the 1:2 ratio of benzamide and benzylamine. The study of reaction scope confirmed that this method tolerated different substituted benzylamines and aliphatic amines *viz* cyclic and acyclic. It also demonstrated that a wide range of benzamide has been compatible under this method with good to an excellent yield of the final product.

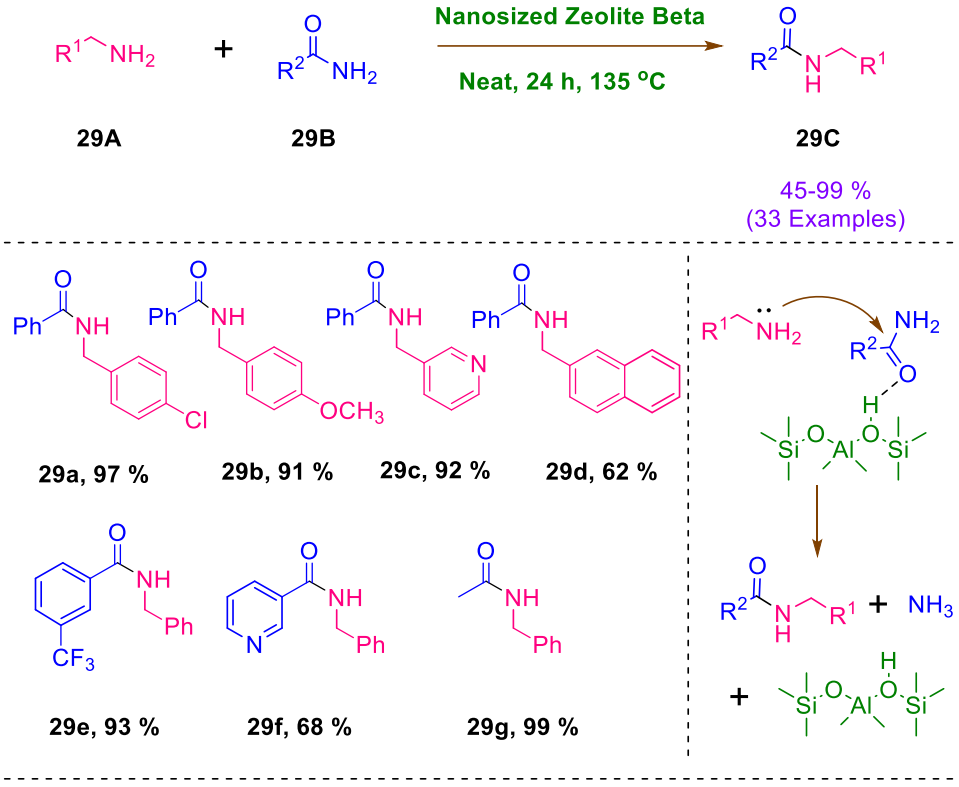

Scheme 2- 29. Nano zeolite beta catalysed transamidation of amides.

Researchers have recently drawn their attention to carbon nanomaterials because of their exceptional thermal, optical, mechanical, and electronic properties. They kept in that mind *Patel et al.*[50] explored graphene oxide as a heterogeneous catalyst to conduct transamidation reactions. Researchers have systematically first fixed catalyst amount during reaction optimisation, followed by solvent choice and temperature adjustment. Additionally, other carbon nanomaterials were also tried, and the best results were obtained using 20% of graphene oxide at 130°C. The reaction obtained 97-76% yield of the desired compound from aryl-substituted benzylamine and unsubstituted benzamides, wherein substituted benzamides showed comparatively lower transformation **(Scheme 2-30)**. The method is also compatible with the reactivity of branched-chain and cyclic aliphatic amines. Further, the reaction scope of formamides and the results confirmed the compatibility of aryl, heteroaryl, aliphatic and cyclic amines are suitable for conversion. Interestingly, researchers also showed the tolerance of phthalimide and thioamides with amines. Notably, the dimer transamide product obtains in the treatment of urea. The advantage of this mode is more selective toward aliphatic amines over aromatic and heterocyclic amines at the end of the study.

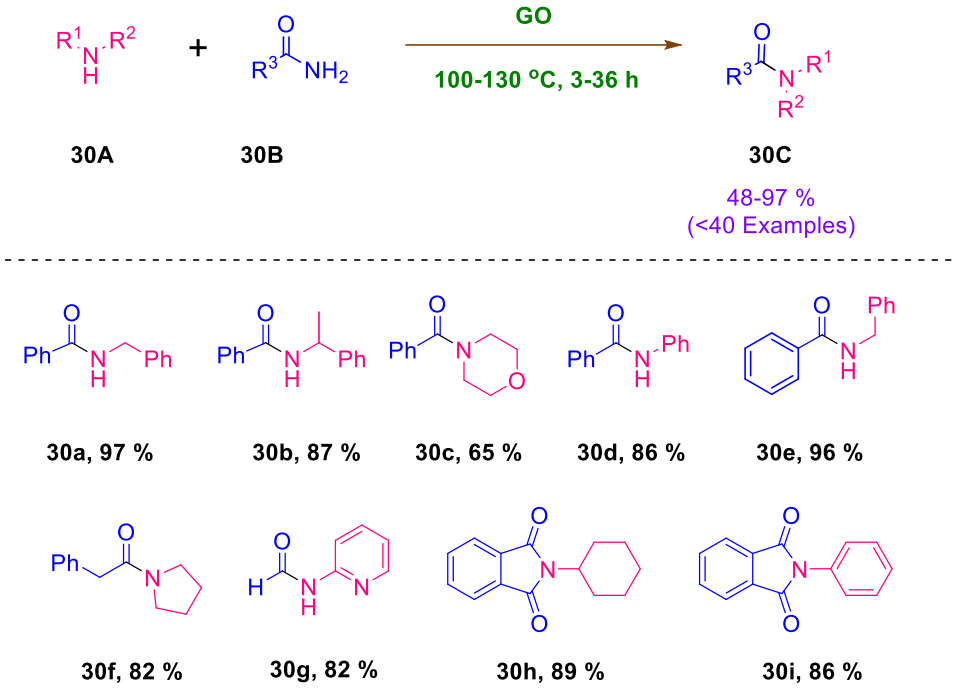

Scheme 2- 30. Graphene oxide assisted transamidation of unactivated amides.

Rao et al.[51] used H-β-Zeolite to assist the transamidation reaction of unactivated primary amides with amines under solvent-free conditions **(Scheme 2-31**). The optimisation experiments confirmed that solvent-free condition is more effective than the presence of solvent at 130 °C. The method generated a significant yield of the respective desired products from various substituted benzylamine/aniline. This study concludes that aliphatic amines showed a better result than aryl amines in reaction with acetamide. The yield of transamide product was less when a long chain substituted amide on the alpha position was used for conversion. Afterwards, they showed the compatibility of phthalimide and heteroaryl amide on treatment with a wide range of amines. Similarly, they also tried this method on thioamides and results shown its transformation into the desired product in good to excellent yields.

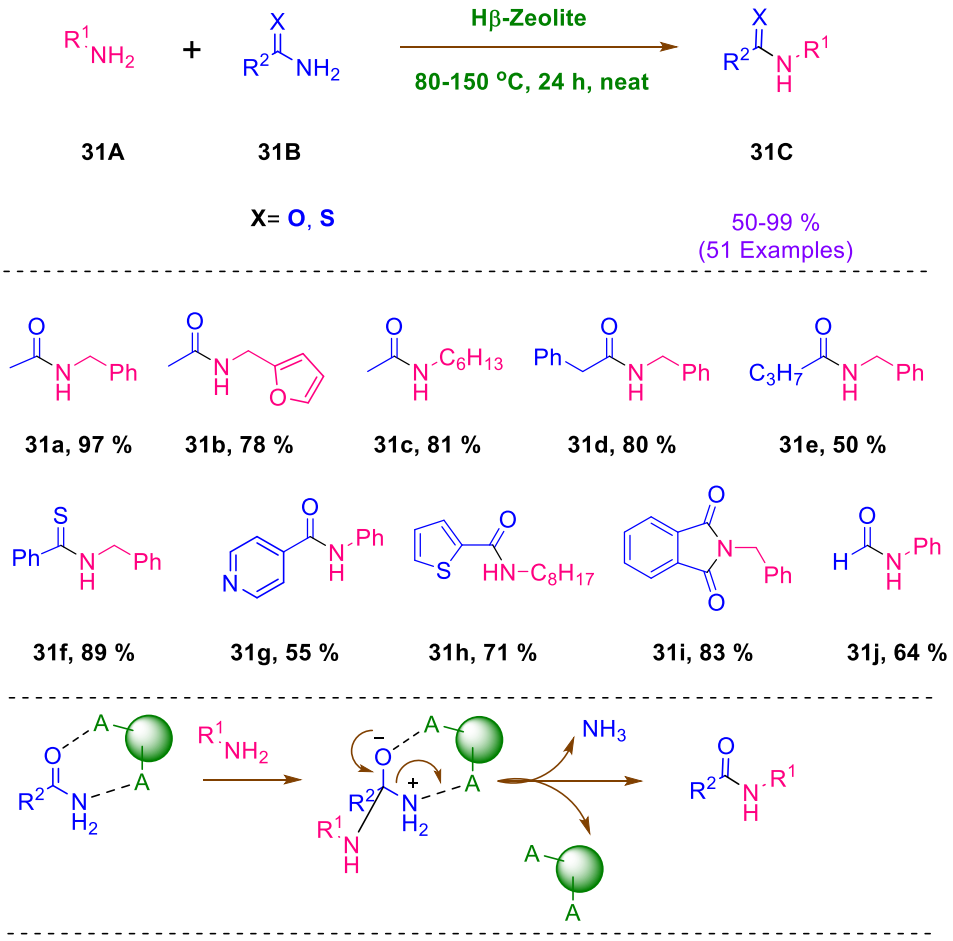

Scheme 2- 31. H-β-Zeolite, assisted transamidation of amides and thioamides.

Bhattacharya et al.[52] developed a metal-free and environmentally safe approach for transamidation. The researchers utilised a heterogeneous catalyst, graphene oxide (GO), that efficiently absorbs reactive molecules and accelerates the reaction **(Scheme 2-32)**. During the optimisation of the process, they performed a reaction in the presence of organic and inorganic solvents at various temperatures using GO catalysts, but the results did not meet the predicted yield. Notably, the neat condition with the same amount of catalyst at 150°C produced a high yield of the target product. The method generated a range of converted formamides and acetamides products from the reaction of aromatic anilines with various aliphatic carboxamides. In contrast, the reaction of an aliphatic amine with carboxamides failed to produce the respective transamide product. Additionally, this approach is selective for aromatic amines.

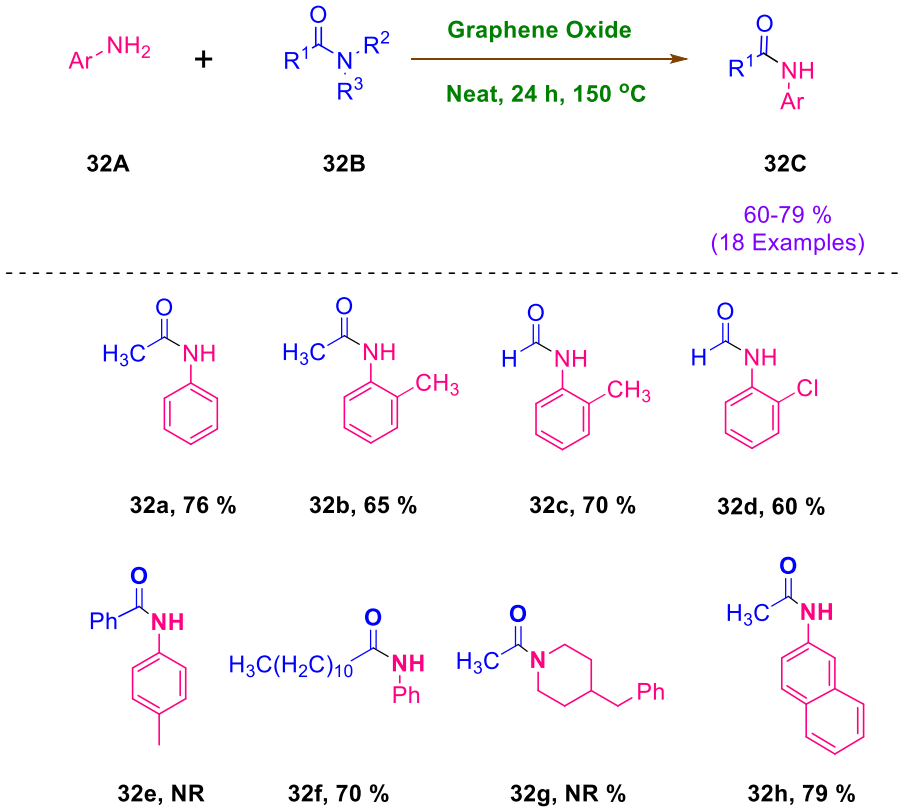

Scheme 2- 32. Graphene oxide-catalysed N-formylation and N-acetylation transamidations.

Conclusion

The amide moiety is an important functional group in chemical, pharmacological, and biological chemistry. Several researchers have focused on its synthesis; alternative methods for amide synthesis remain elusive. While novel and recent methods for amide activation are available, simple activation of the C–N bond in amides *via* coordination with metals or interaction with small molecules remains a crucial alternative in amide bond synthesis. Herein, we examined unactivated amides in transamidation processes and explored many examples in this article. We believe that this review will assist researchers, provide motivation for future work, and help in their knowledge of several recently described transamidation mechanisms.

References

(1) Acosta-Guzmán, P.; Mateus-Gómez, A.; Gamba-Sánchez, D. Molecules **2018**, 23, 2382.

(2) Kolympadi Marković, M.; Marković, D.; Laclef, S. Synth. **2020**, 52, 3231-3242.

(3) Mahesh, S.; Tang, K. C.; Raj, M. Molecules **2018**, 23, 2615.

(4) Marchetti, P. M.; Richardson, S. M.; Kariem, N. M.; Campopiano, D. J. Medchemcomm **2019**,

10, 1192-1196.

(5) Santos, A. S.; Silva, A. M. S.; Marques, M. M. B. European J. Org. Chem. **2020**, 2501-2516.

(6) Viveiros, R.; Bonifácio, V. D. B.; Heggie, W.; Casimiro, T. In *ACS Sustainable Chemistry and Engineering*; **2019**, 7, 15445-15451.

(7) Dorr, B. M.; Fuerst, D. E. Curr. Opin. Chem. Biol. **2018**, 43, 127-133.

(8) Papadopoulos, L.; Kluge, M.; Bikiaris, D. N.; Robert, T. Polymers (Basel). **2020**, 12, 980.

(9) Petchey, M. R.; Grogan, G. Adv. Synth. Catal. **2019**, 361, 3895-3914.

(10) Szostak, R.; Szostak, M. Molecules **2019**, 24, 274.

(11) Chaudhari, M. B.; Gnanaprakasam, B. Chem. - An Asian J. **2019**, 14, 76-93.

(12) Miyanaga, A.; Kudo, F.; Eguchi, T. Nat. Prod. Rep. **2018**, 35, 1185-1209.

(13) Abraham, M. H.; Abraham, R. J. New J. Chem. **2017**, 41, 6064-6066.

(14) Han, L.; Zhang, K.; Ishida, H.; Froimowicz, P. Macromol. Chem. Phys. **2017**, 218.

(15) Kemnitz, C. R.; Loewen, M. J. J. Am. Chem. Soc. **2007**, 129, 2521-2528.

(16) Yu, S.; Shin, T.; Zhang, M.; Xia, Y.; Kim, H.; Lee, S. Org. Lett. **2018**, 20, 7563-7566.

(17) Yang, D.; Shin, T.; Kim, H.; Lee, S. Org. Biomol. Chem. **2020**, 18, 6053-6057.

(18) Arefi, M.; Heydari, A. RSC Adv. **2016**, *6*, 24684.

(19) Kazemi Miraki, M.; Arefi, M.; Yazdani, E.; Abbasi, S.; Karimi, M.; Azizi, K.; Heydari, A. ChemistrySelect **2016**, *1*, 6328.

(20) Thale, P. B.; Borase, P. N.; Shankarling, G. S. RSC Adv. **2016**, *6*, 52724.

(21) Ojeda-Porras, A.; Gamba-Sánchez, D. Tetrahedron Lett. **2015**, *56*, 4308.

(22) Sheng, H.; Zeng, R.; Wang, W.; Luo, S.; Feng, Y.; Liu, J.; Chen, W.; Zhu, M.; Guo, Q. Adv. Synth. Catal. **2017**, *359*, 302.

(23) Serrano-Plana, J.; Garcia-Bosch, I.; Company, A.; Costas, M. Acc. Chem. Res. **2015**, 48, 2397-2406.

(24) Valdez, C. E.; Smith, Q. A.; Nechay, M. R.; Alexandrova, A. N. Acc. Chem. Res. **2014**, 47, 3110.

(25) Haak, R. M.; Wezenberg, S. J.; Kleij, A. W. Chem. Commun. **2010**, 46, 2713-2723.

(26) Delferro, M.; Marks, T. J. Chem. Rev. **2011**, 111, 2450-2485.

(27) Gu, D. W.; Guo, X. X. Tetrahedron **2015**, *71*, 9117.

(28) Che, C. M.; Lo, V. K. Y.; Zhou, C. Y.; Huang, J. S. Chem. Soc. Rev. **2011**, 40, 1950-1975.

(29) Vanjari, R.; Guntreddi, T.; Singh, K. N. Org. Lett. **2013**, 15, 4908-4911.

(30) Singh, D. P.; Allam, B. K.; Singh, K. N.; Singh, V. P. RSC Adv. **2014**, 4, 1155-1158.

(31) Yedage, S. L.; D'Silva, D. S.; Bhanage, B. M. RSC Adv. **2015**, *5*, 80441.

(32) Sonawane, R. B.; Rasal, N. K.; Jagtap, S. V. Org. Lett. **2017**, 19, 2078-2081.

(33) Wagh, G. D.; Pathare, S. P.; Akamanchi, K. G. ChemistrySelect **2018**, *3*, 7049.

(34) Ma, J.; Zhang, F.; Zhang, J.; Gong, H. European J. Org. Chem. **2018**, *2018*, 4940.

(35) Ghosh, T.; Jana, S.; Dash, J. Org. Lett. **2019**, *21*, 6690.

(36) Tan, Z.; Li, Z.; Ma, Y.; Qin, J.; Yu, C. European J. Org. Chem. **2019**, *2019*, 4538.

(37) Kumar, V.; Dhawan, S.; Girase, P. S.; Singh, P.; Karpoormath, R. European J. Org. Chem. **2021**, 5627-5639.

(38) Chen, J.; Jia, J.; Guo, Z.; Zhang, J.; Xie, M. Tetrahedron Lett. **2019**, *60*, 1426.

(39) Zhang, R.; Zhang, J. C.; Zhang, W. Y.; He, Y. Q.; Cheng, H.; Chen, C.; Gu, Y. C. Synth. **2020**, *52*, 3286.

(40) Srinivas, M.; Hudwekar, A. D.; Venkateswarlu, V.; Reddy, G. L.; Kumar, K. A. A.; Vishwakarma, R. A.; Sawant, S. D. Tetrahedron Lett. **2015**, 56, 4775-4779.

(41) Yu, S.; Ho Song, K.; Lee, S. Asian J. Org. Chem. **2019**, 8, 1613-1616.

(42) Jiang, J.; Li, L.; Zhang, L.; Chen, Q.; Sun, H.; Liao, S.; Li, C.; Zhang, L. ChemistrySelect **2021**, *6*, 12834.

(43) Sureshbabu, P.; Azeez, S.; Chaudhary, P.; Kandasamy, J. Org. Biomol. Chem. **2019**, 17, 845-850.

(44) Girase, P. S.; Kumar, V.; Dhawan, S.; Karpoormath, R. ChemistrySelect **2022**, *7*, e202103237.

(45) Sakurai, M.; Kawakami, R.; Kihara, N. Tetrahedron Lett. **2019**, *60*, 1291.

(46) Tian, Q.; Gan, Z.; Wang, X.; Li, D.; Luo, W.; Wang, H.; Dai, Z.; Yuan, J. Molecules **2018**, 23, 2234.

(47) Yin, J.; Zhang, J.; Cai, C.; Deng, G. J.; Gong, H. Org. Lett. **2019**, 21, 387-392.

(48) Bensalah, F. O.; Bil, A.; Wittine, K.; Bellahouel, S.; Lesur, D.; Markovic, D.; Laclef, S. Org.

Biomol. Chem. **2019**, *17*, 9425.

(49) Durgaiah, C.; Naresh, M.; Swamy, P.; Srujana, K.; Rammurthy, B.; Narender, N. Catal. Commun. **2016**, *81*, 29.

(50) Patel, K. P.; Gayakwad, E. M.; Patil, V. V.; Shankarling, G. S. Adv. Synth. Catal. **2019**, *361*, 2107.

(51) Rao, S. N.; Chandra Mohan, D.; Adimurthy, S. RSC Adv. **2015**, *5*, 95313.

(52) Bhattacharya, S.; Ghosh, P.; Basu, B. Tetrahedron Lett. **2018**, *59*, 899.

Chapter 3

An Environmentally Benign, Catalyst-Free N-C bond cleavage/formation of Primary, Secondary and Tertiary Unactivated Amides

Published: European Journal of Organic Chemistry Journal (DOI: 10.1002/ejoc.202101114)

Graphical Abstract

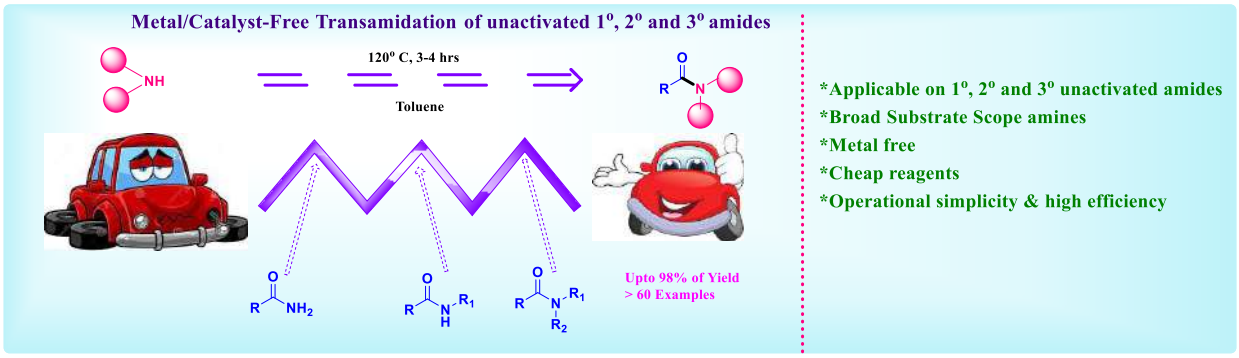

Abstract

Herein, we report an operationally simple, cheap, and catalyst-free method for the transamidation of a diverse range of unactivated amides furnishing the desired products in excellent yields. This protocol is environmentally friendly and operates under extremely mild conditions without using any promoter or additives. Significantly, this strategy has been implied in the chemoselective synthesis of a pharmaceutical molecule, paracetamol, on a gram-scale with excellent yield. We anticipate that this universally applicable strategy will be of great interest in drug discovery, biochemistry, and organic synthesis.

Keywords

Amine, Amide, Hydrochloride salt, Metal-free chemistry, Transamidation.

Introduction

In chemistry and biology, the amide bond is the most fundamental functional group[1]. The amide linkages are widely used in the organic synthesis of pharmaceuticals[2], natural products[3], pesticides[4], polymers[5] and biologically relevant molecules[6]. Recent studies signify that the amide bond is prevalent in 25% of pharmaceuticals[7], whereas amidation reactions depict the most common reaction conducted to synthesise new drugs[8]. In particular, amide bonds are the most prevalent form of bond found in various drugs, such as formoterol, tetrahydrolipstatin, leucovorin, penicillin G, lacosamide, and paracetamol (**Figure 3-1**). As a consequence of the prevalence of amide bonds, novel methods for the synthesis of amides significantly impact every branch of organic chemistry[8].

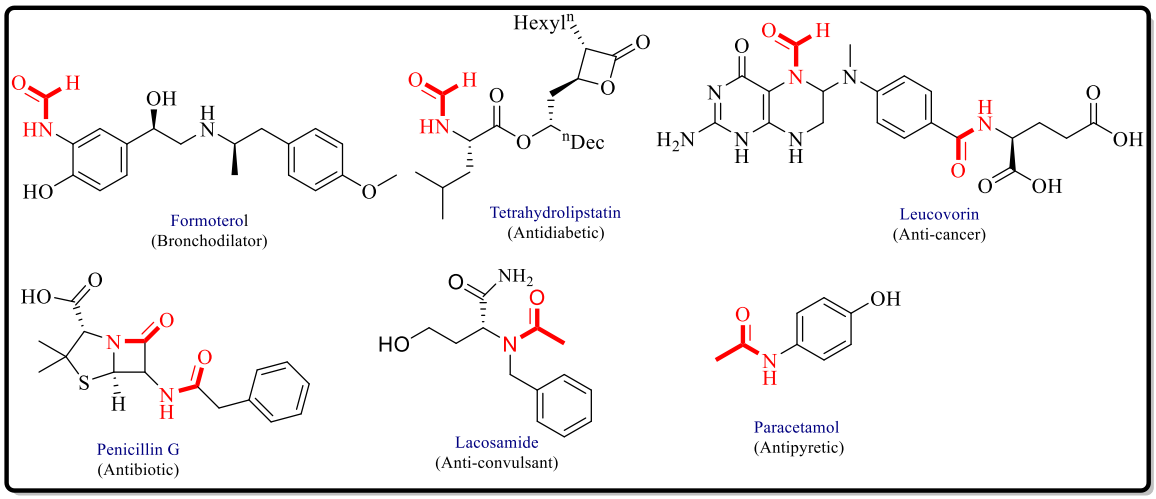

Figure 3- 1: Marketed bioactive compounds with amide framework.

Transamidation has recently garnered significant interest from a variety of research groups[9]. However, due to the amide bond's stability, various catalysts or activating agents are used for the transamidation of amines[10]. Several transition-metal based catalytic systems employed in the transamidation reactions *viz*: Pd[11], Ni[12] (**Scheme 3-1B**), Fe[13], Cu[14], Mn[15], lanthanides[16], Ti[17], Zr[18], Al[19], and sulfated tungstate[20] are widely used in academia and industry for the preparation of amides[21]. Additionally, metal-catalysed reactions are undesirable due to waste metal and increasing synthetic costs. Despite these challenges, numerous discoveries in metal-free approaches have been reported, including the use of benzotriazole, boric acid derivatives[22], chitosan[23], *N*, *N* di-alkyl formamide[24], hypervalent iodine[25], L-proline[26], hydroxylamine hydrochloride[27] (**Scheme 3-1A'**) and imidazole derivatives[28],

as well as microwave irradiation processes. The Szostak group recently reported a LiHMDS promoted chemo-selective transamidation of amides at room temperature through N-C (acyl) cleavage[29] (**Scheme 3-1A**). While these metal-free protocols have several benefits, some pitfalls remain, including the need for stoichiometric catalysts, low selectivity, and challenges with catalysts separation. Despite these breakthroughs, a realistic solution to the transamidation is only restricted to active 1° amides, while the challenging aliphatic 2° and 3° amides remained less exploited[30]. Recent advances, as reported, are incompatible with highly valuable less-nucleophilic amines and low reactive, secondary and tertiary amides under metal- or catalyst-free conditions.

In thinking through the consequences noted earlier, in this paper, we describe the successful realisation of a high-yielding transition metal-free strategy for transamidation reactions using amine hydrochloride salts and unactivated amide derivatives as carbonyl sources (**Scheme 3-1C**) *via* highly selective N–C bond cleavage. The protocol is extremely versatile across a wide variety of structurally diverse substrates (> 60 examples) and operationally easy and cost-effective due to the absence of an acid, bases, catalyst, ligands, or other additives with prolonged reaction time. We believe that this straightforward N–C cleavage/formation will be of great interest, offers a robust approach to the classic problem of 2° and 3° unactivated aliphatic/aromatic amide transamidation, and it is expected that this work will influence future efforts to synthesise pharmaceuticals, natural products, and polymers.

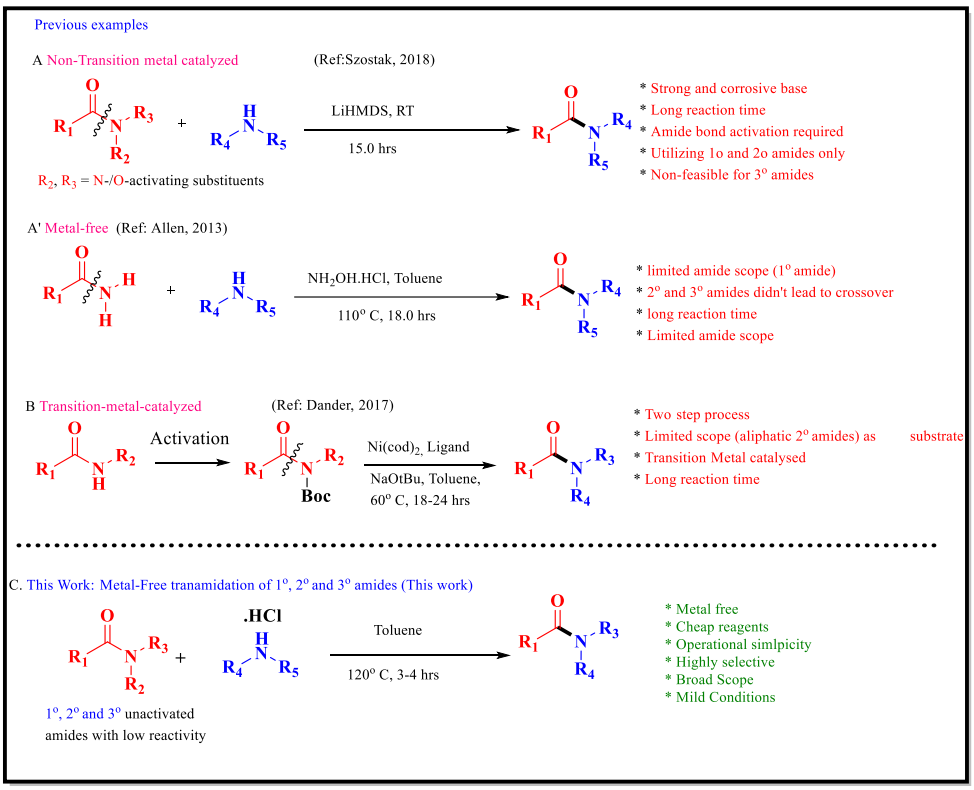

*Scheme 3- 1: LiHMDS, $NH_2OH.HCl$ and Nickel-catalyzed transamidation reactions of amides with amines: previously reported protocols (**A**−**B**) and (**C**) This work, depicting transamidation using 1°, 2° and 3° unactivated amides.*

Results and Discussion

We selected readily available formamide (**2o**) as a formyl source and *p*-anisidine (**1e**) as the reaction partners to initiate our studies. The outcomes are illustrated in **Table 3-1**. As previously shown in classical nucleophilic substitution reactions, solvent selection, temperature, acids, and time significantly impact yield. So initially, various commercially available acids such as trifluoroacetic acid, hydrochloric acid, sulphuric acid, acetic acid, and nitric acid (entries 1-5) were investigated but revealed a decrease in yield when compared to HCl. Subsequently, we investigated transamidation in various organic solvents (entries 6-10); however, toluene emerged as the most optimal solvent and provided the desired product **3e** in 97% yield (entry 6). Moreover, an increase in the reaction time to 4.0 hrs does not affect the outcome of corresponding products (entry 14). To increase the yield of **3e**, we analysed other parameters such as formamide equivalents and temperature. Further, it was observed that when 1.0 to 5.0 eq. of **2o** was used as the formylating agent in toluene, the amide **3e** was obtained in moderate to an excellent yield of 56-98% (entries 15-19). The utilisation of **2o** to 4.0 and 5.0 eq. had no discernible impact on the yield of **3e** (entries 18 and 19). Notably, the reduction of reaction temperature to 80 and 100 ^{o}C afforded the poor result of the desired product (5-30%), emphasising the importance of temperature in facilitating the net transamidation reaction (entries 20 and 21). Thus, the optimum result was obtained when 3.0 eq of **2o** was used as the formyl source, using toluene as a solvent and extending the reaction time to 3.0 h at 120 ^{o}C (entries 13, 17 and 22).

Table 3- 1. Reaction conditions optimisation for N-Formylation of p-anisidine with formamide.

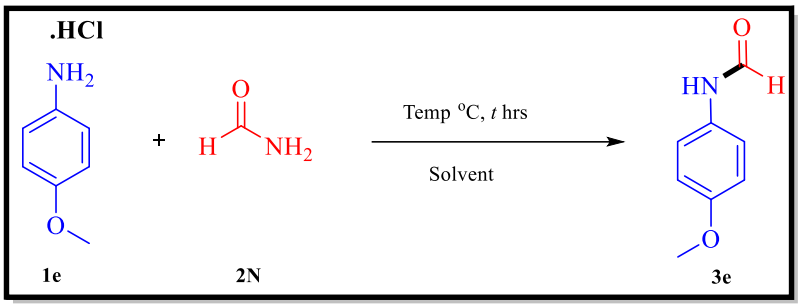

Acid Study					
S.No.	**Acid**	**Solvent (5.0 Vol)**	**Temp (°C)**	**Time (hr)**	**% Yield[c]**
1[a]	CF_3COOH	Toluene	120	4	**20**
2[a]	**HCl**	**Toluene**	**120**	**4**	**97**
3[a]	H_2SO_4	Toluene	120	4	**5**
4[a]	CH_3COOH	Toluene	120	4	**30**
5[a]	HNO_3	Toluene	120	4	**10**

Solvent Study					Formamide Equivalents Study				
S.No.	**Solvent (5.0 Vol)**	**Temp (°C)**	**Time (hr)**	**Yield[c]**	**S.NO.**	**Eq (2o)**	**Temp (°C)**	**Time (hr)**	**Yield[c]**
6[a]	**Toluene**	**120**	**4**	**97**	**15[b]**	1	120	3	56
7[a]	DMSO	120	4	20	**16[b]**	2	120	3	86
8[a]	Xylene	120	4	88	**17[b]**	**3**	**120**	**3**	**98**
9[a]	NMP	120	4	52	**18[b]**	4	120	3	97
10[a]	Water	120	4	81	**19[b]**	5	120	3	98
Time Study					**Temperature Study**				
S.No.	**Solvent (5.0 Vol)**	**Temp (°C)**	**Time (hr)**	**Yield[c]**	**S.NO.**	**Solvent (5.0 Vol)**	**Temp (°C)**	**Time (hr)**	**Yield[c]**
11[a]	Toluene	120	1	72	**20[a]**	Toluene	80	3	5
12[a]	Toluene	120	2	83	**21[a]**	Toluene	100	3	30
13[a]	**Toluene**	**120**	**3**	**98**	**22[a]**	**Toluene**	**120**	**3**	**98**
14[a]	Toluene	120	4	97					

[a]Conditions: *p*-anisidine **1e** (1.0 mmol), formamide **2N** (3.0 mmol). [b]Conditions: *p*-anisidine **1e** (1.0 mmol), Solvent: Toluene (5.0 Vol), all the reactions were conducted under air. [c]Isolated yields.

With the optimised reaction conditions, we examined the scope of carbonyl sources (**2A**-Y) for the transamidation of aniline **1**[5]**a** (**Scheme 3-2**). From **2A-M** are tertiary amides (*N*,*N*-dimethyl), while **2N-Y** are amides with various nitrogen substitutions. Fortunately, the aliphatic amides like the *N*-formylation (**2A**), and *N*-acylation (**2B**) reactions proceeded smoothly when 3,3-dimethylbutanamide (**2I**) was used as carbonyl sources, provided a good yield of 78%, respectively. However, Due to the hindrance of branched/cyclo alkyl groups, the resultant *tert*-butylate (**2C**), isobutyramide (**2D**) and cyclohexanecarboxamide (**3G**) products were obtained in the moderate yields. Tri-chloroacetamide (**2E**), 2-phenylacetamide (**2J**) and 2-phenoxyacetamide (**2M**) were also employed effectively as an acyl source yielding the desired products (**3E, 3J** and **3M**) in moderate to good yields of 64-78%. Further, multiple benzamide derivatives were used as benzoyl sources. The results indicate that the nitro substituted benzamide provided less yield comparable to other benzamides. We got moderate results when N,N-diethyl amides (**2P, 2T**, and **2X**) were utilised for their respective compounds due to steric hindrance.

Scheme 3- 2. The substrate scope of 1°, 2° and 3° unactivated amides.

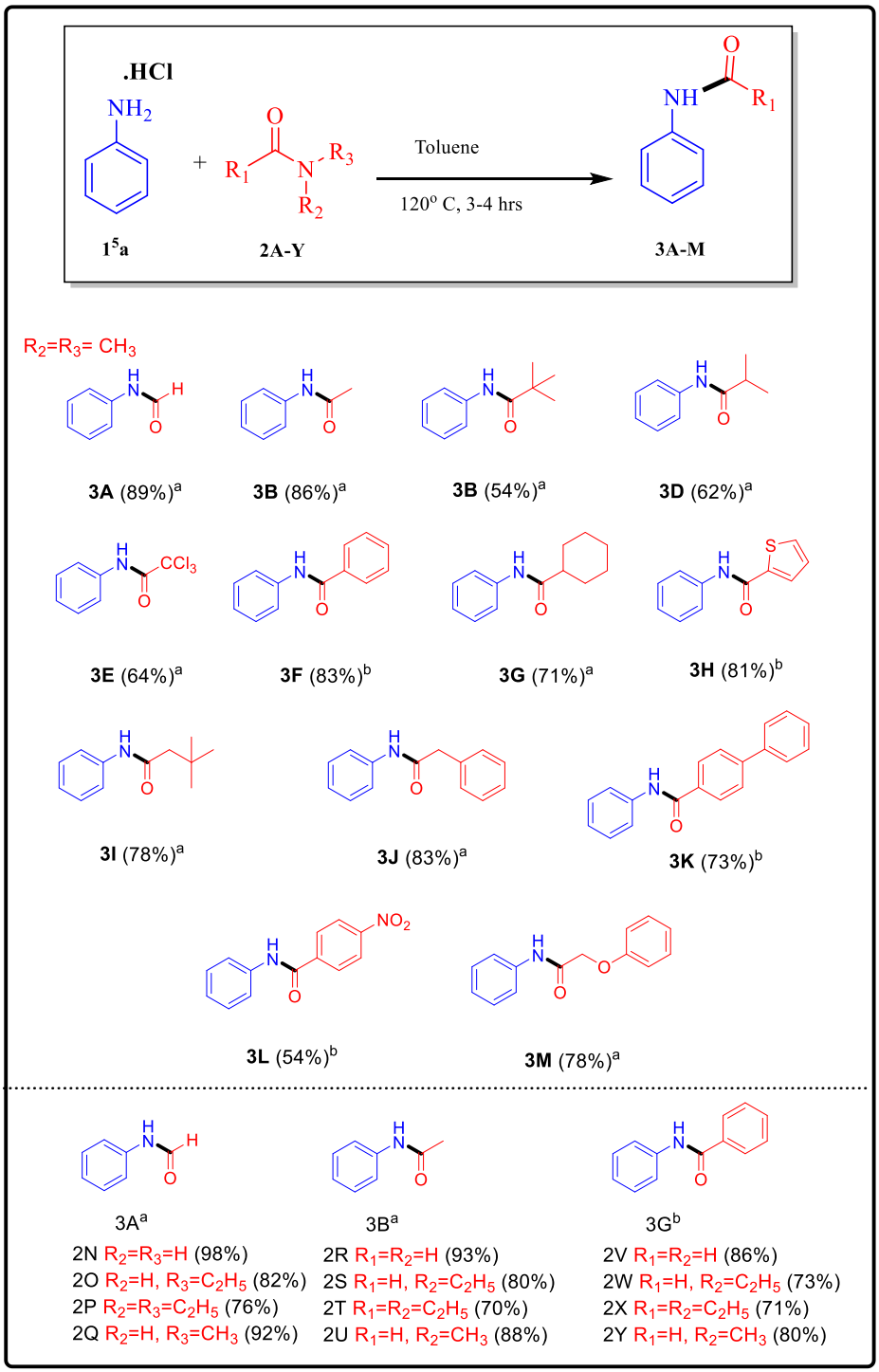

[a]All the reactions were conducted on a 1.0 mmol scale, 3.0 mmol of amide, under air for 3.0 hrs, using toluene (5.0 vol). [b]time=4.0 hrs.

The universality of the transamidation was explored using a wide variety of amines (**Scheme 3-3)**. We performed the *N*-formylation, *N*-acetylation and *N*-benzoylation of multiple amines, including 1°, 2°, electron-donating and withdrawing substitutions aromatic, heterocyclic, and aliphatic amines (**Scheme 3-3**). The current protocol is compatible with a wide range of anilines substituted with functional groups such as alkyl (**3h**, **3p** and **3r**), alkoxyl (**3e, 5e** and **5f**), hydroxyl (**3a, 3r,** and **4b-d**), nitro (**3q** and **4e**), halo (**3f-g, 3i-3o, 4d,** and **5b-c**), keto (**3s-t**), and ester (**3u**), heteroaromatic (**3b** and **3d**), quinoline (**3c**), secondary amines (**3w, 4a, 4h, 5c** and **5g**), and aliphatic amines (**3d, 3w, 4a, 5c** and **5h**), respectively. We also analysed various aromatic amines with different substituents and obtained the resulting *N*-formylated products in good to excellent yields (**Scheme 3-3**). Pleasingly, the heterocyclic aromatic anilines rapidly converted to the corresponding products (**3b-d**) in the range of 68-85% yield, whereas **3c** had a lower yield, possibly due to steric hindrance, as we observed when synthesising the **5g** product. Interestingly, substrates containing a hydroxyl group have afforded excellent yields (89-97%) without any difficulty (**3a, 3r** and **4b-d**). Furthermore, methoxy substituted anilines also performed well in the synthesis of *N*-formylation (**3e**) and *N*-benzoylation (**5e-f**) products at all substituent positions. When aniline contained strong electron-withdrawing nitro groups, only low to moderate yields (25 and 62%) of the corresponding products were obtained (**3q** and **4e**). In this study, we found that *meta*-nitro aniline, 4-(trifluoromethoxy)-aniline and 3-trifluoromethyl aniline converted into their corresponding products (**4f-g**) with good yields (71-79%). Additionally, the halogenated anilines tested afforded the corresponding *N*-formylated/benzoylated products (**3f-g**, **3m-o** and **5b-c**) in moderate to excellent yields (50-90%). *Ortho* halogen-substituted anilines were also shown to be less reactive than *meta* and *para*-substituted anilines in these experiments. On the other hand, di-substituted anilines produced a good product yield, whether both were electron-donating groups (EWG) or electron-donating groups (EDG). To our delight, amines with acid-sensitive functionalities, such as an ester, were well tolerated, yielding formamide (**3u)** in 72% yields. Similarly, when aniline substituted acetophenone, and carboxylic acid analogues (**3s-t** and **3zn**) were used as substrates, the reaction proceeded well and yielded the expected products in moderate to excellent yields (78-91%). Finally, the transamidation reaction of aliphatic 1° and 2° amines were investigated, and the corresponding products (**3d**, and **5a**) were obtained in good yields.

Scheme 3- 3[a]. The substrate scope of diversified amines with formamide.

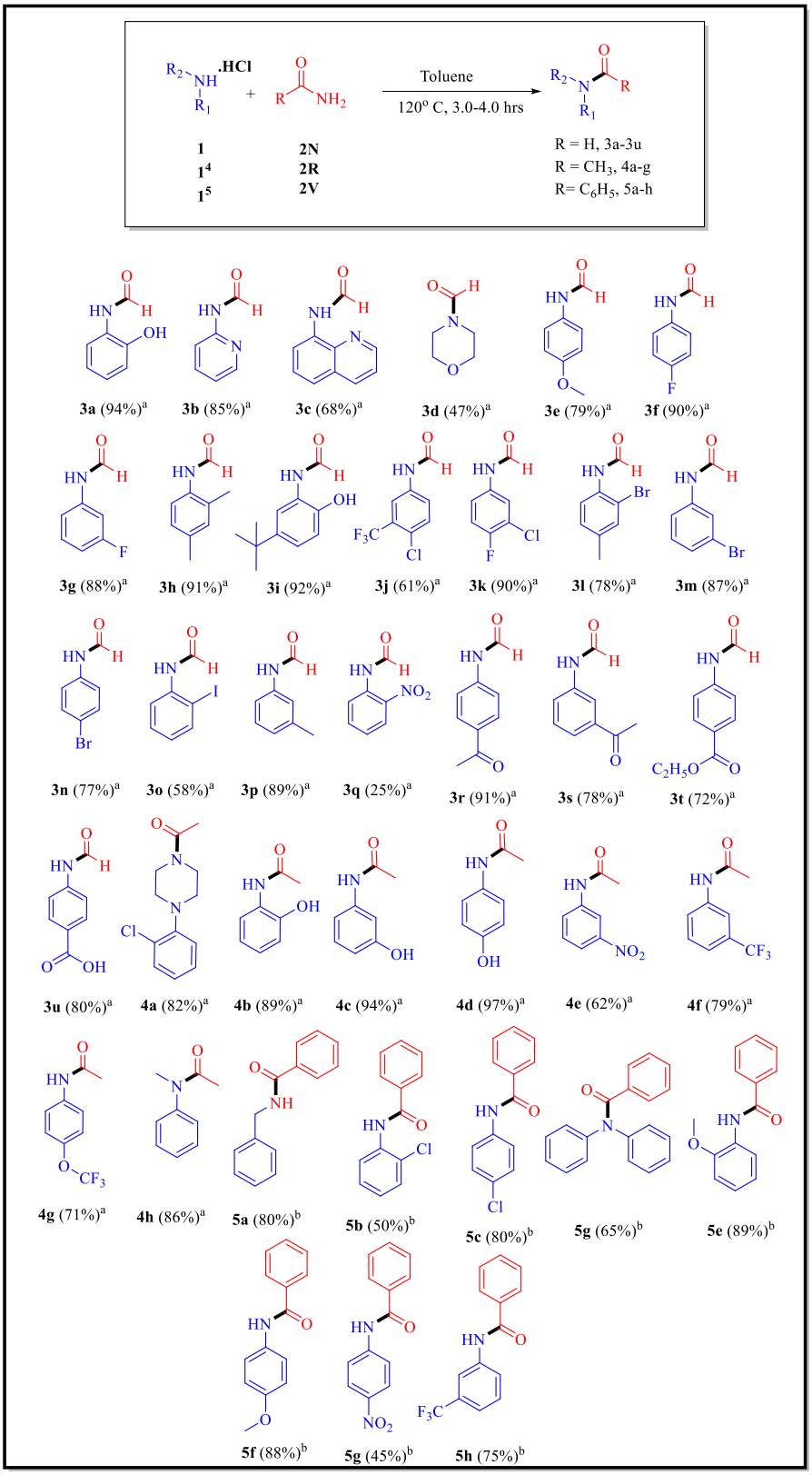

[a]Isolated yields were reported. [a]t=3 hr and [b]t=4 hr

Further, only *N*-formylation reaction occurred in the presence of water (**Scheme 3-4A**); the other reactions, such as *N*-acylation and *N*-benzoylation, did not produce the desired products. Likewise, similar results were obtained in the presence of in conc HCl (**Scheme 3-4B**). Subsequently, the same reaction was attempted under NET conditions utilising various amides, namely formamide, acetamide, and benzamide derivatives. Under standard reaction conditions, the corresponding products were obtained in moderate to excellent yields (**Scheme 3-4C**).

Scheme 3- 4. The road map for transamidation under different reactions conditions.

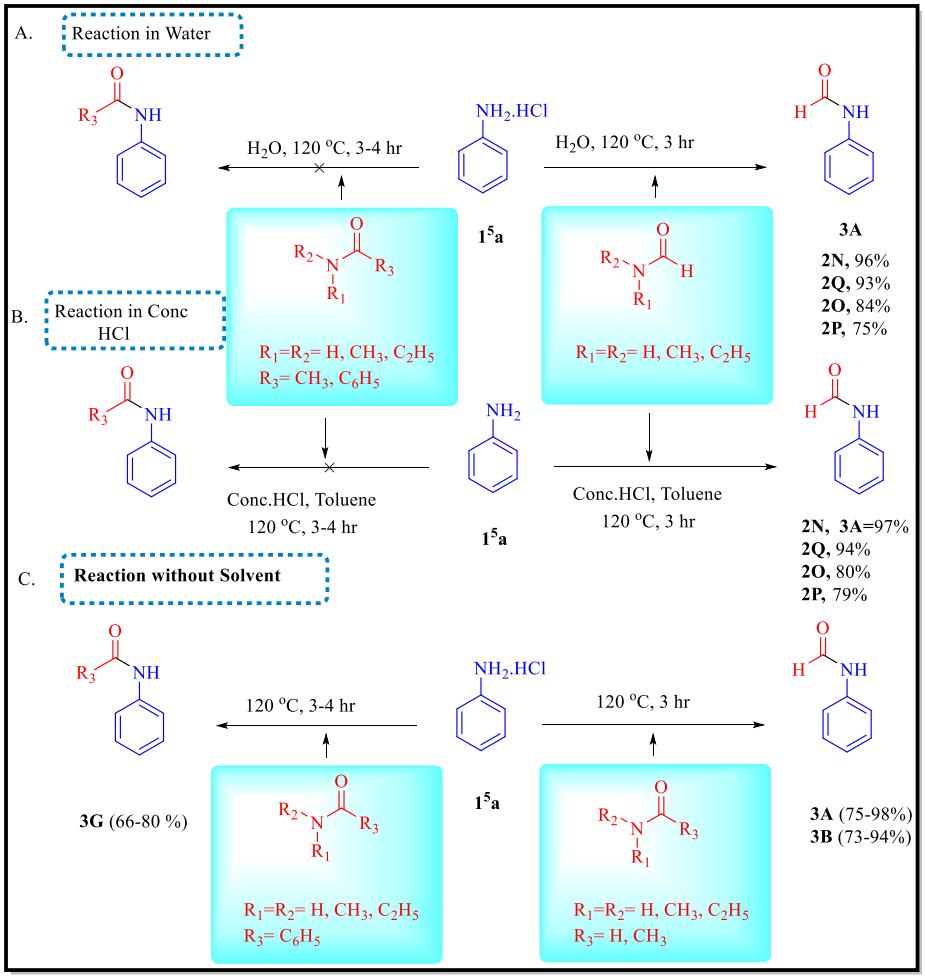

Mechanistic Study

To depict the current protocol's reaction mechanism, four control experiments were carried out, and the results are illustrated in **Scheme 3-5**. First, transamidation of acetamide (**2R**) showed that the free amine **1[4]d** exerted an indicative impact, producing the target product (**4d**) in traces. Second, the yield of acylated product (**1[4]d**) remained the same when HCl gas purged through reaction mass containing free amine (**1[4]d**) in toluene (**Scheme 3-5A**). Lastly, the yield of *N*-acetylated product (**4d**) remained the same using TEMPO as a radical trap. It was found that TEMPO did not suppress the yield of the transamidation product as a radical scavenger (**Scheme 3-5B**). The results indicated that no radical intermediates were formed during the transamidation process.

Scheme 3- 5. Some control experiments and the reaction in radical scavenger conditions.

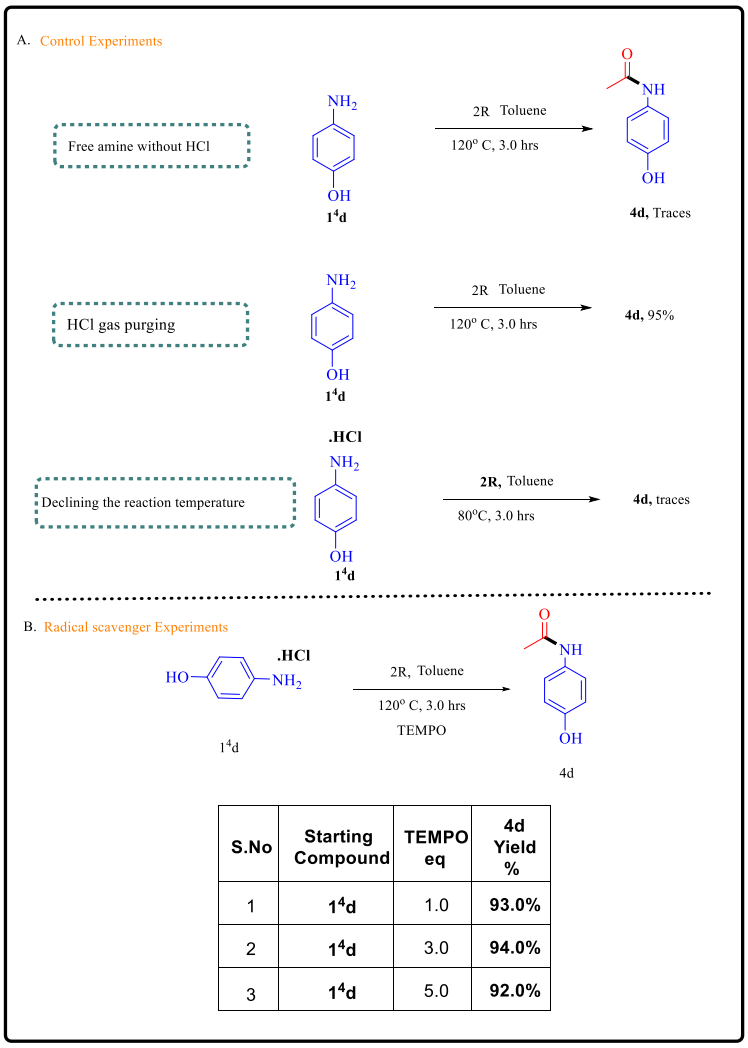

S.No	Starting Compound	TEMPO eq	4d Yield %
1	**1[4]d**	1.0	**93.0%**
2	**1[4]d**	3.0	**94.0%**
3	**1[4]d**	5.0	**92.0%**

Based on the experimental results, the plausible reaction mechanism is presented in **Scheme 3-6**. Initially, the carbonyl group of **2** is activated with HCl followed by a nucleophilic attack of amine (**1**) on **A** (**A** and **B** are in resonance) and resulted in the formation of intermediate **C**. Then, **C** could transform into **D** through tautomerisation. In the next step, intermediate **E** is formed through the elimination of amine (**D1**). Finally, the deprotonation step results in the formation of the final product **3**.

Scheme 2- 6. The plausible reaction mechanism.

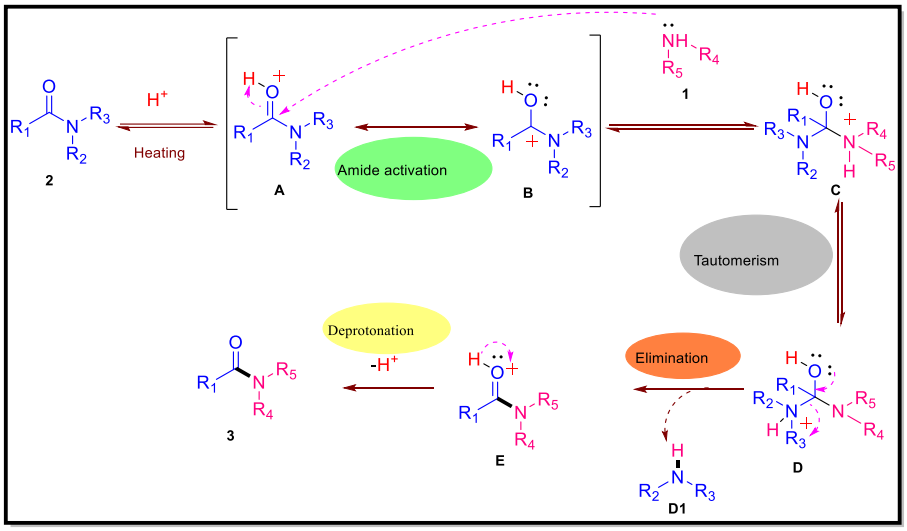

Ultimately, the viability of the pharmaceutical of this metal-free protocol for the synthesis of the marketed drug acetaminophen (Antipyretic drug) was demonstrated on a grams-scale (**Scheme 3-7**). In contrast to conventional methods, the current protocol is beneficial for API (Active pharmaceutical ingredients) products and intermediates as it does not include the utilisation of metal residues. Subsequently, we examined the chemo-selectivity between amino and hydroxyl groups present in the same substrate. Pleasantly, we got selective *N*-formylated and *N*-acetylated products, demonstrating the selectivity of the current transamidation process.

Scheme 3- 7. Commercial application of protocol on Gram-Scale and chemo-selectivity experiments[31–33].

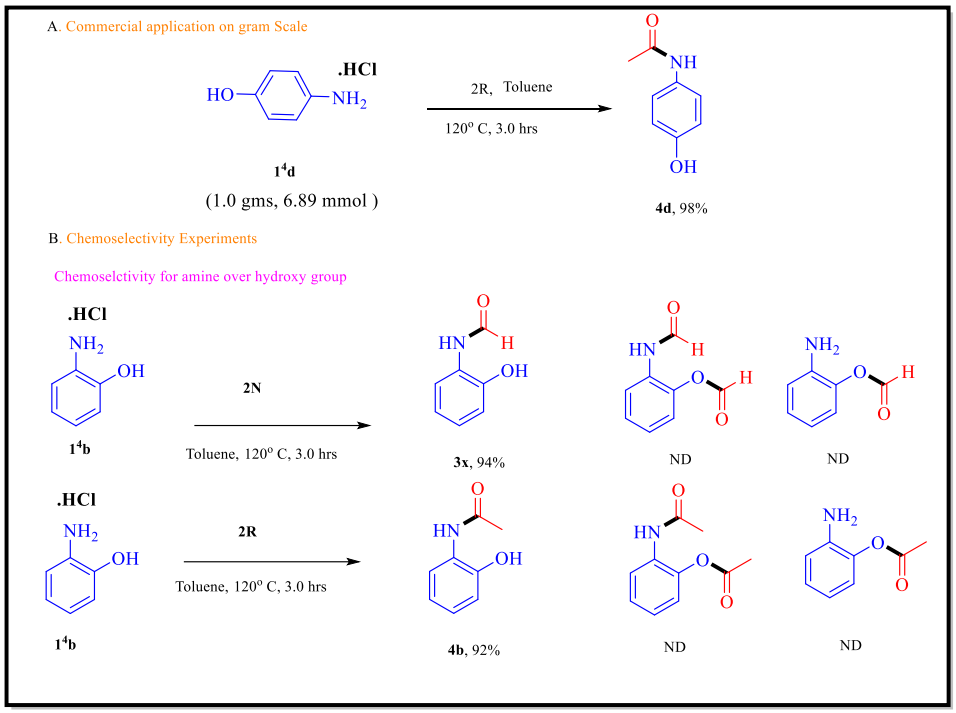

*ND= Not developed.

Conclusion

A highly efficient, catalyst-free, and convenient protocol for the synthesis of amides *via* transamidation of diverse amines has been reported using amine hydrochloride salt as a reactant as well as the catalyst. This amidation reaction is well tolerated for a wide variety of amines with diverse functionalities *viz*: acids, ester, and ketones. The environmental compatibility, mild reaction conditions, adaptability, and accessible and easily accessible starting materials are all strengths of this strategy. It is noteworthy that amides have the potential to be highly efficient transamidation agents.

Experimental Section

General Information: All reactions were conducted under standard operating conditions without the use of any stringent conditions. All chemicals were obtained from Aldrich Chemical Co., Alfa Aesar, used as received without additional purification. Lab reagent (LR) grade solvents were used for extraction and column chromatography purchased from Roma-chem. The reaction progress was monitored on Merck TLC Silica gel 60 F254 plates, and the spots were visualized under ultraviolet (UV) light, followed by iodine or ninhydrin staining solution followed by heating. ^{1}H, ^{13}C and ^{19}F NMR spectra were recorded on 400, 100, 377 MHz NMR spectrometer using $CDCl_3$ and DMSO-d_6 as solvents unless otherwise stated. Chemical shifts are expressed in parts per million (ppm) relative to TMS is used as an internal standard. Unless otherwise specified, all reagents were weighed and handled in air.

Experimental Procedure for N-formylation of amines (EP-1): A mixture of amine salt **1** (1.0 eq), amide **2** (3.0 eq), and Toluene (5.0 Vol) was stirred in a vial under atmospheric air at 120 °C for 3.0 hrs. After bringing the mixture to room temperature, 10 mL water was added and the mixture was extracted with ethyl acetate (3 X 20 mL). The EtOAc layer was washed with 3 x 5 mL of 1M sodium bicarbonate solution. The combined organic layers were dried with anhydrous Na_2SO_4. Under vacuum, the solvent was evaporated, and the crude product was purified using column chromatography (silica gel, EtOAc/Hexane) in order to obtain a pure product.

Experimental Procedure for N-Benzoylation of amines (EP-2): A mixture of amine salt **1** (1.0 eq), amide **2** (3.0 eq), and Toluene (5.0 Vol) was stirred in vial under atmospheric air at 120 °C for 4.0 hrs. After bringing the mixture to room temperature, 10 mL water was added and the mixture was extracted with ethyl acetate (3 X 20 mL). The EtOAc layer was washed with 3 x 5 mL of 1M sodium bicarbonate solution. The combined organic layers were dried with anhydrous Na_2SO_4. Under vacuum, the solvent was evaporated, and the crude product was purified using column chromatography (silica gel, EtOAc/Hexane) in order to obtain a pure product.

Experimental Procedure for gram scale preparation of Paracetamol (PCM): A solution of 4-aminophenol (1 g, 6.89 mmol) and acetamide (1.22 g, 20.66 mmol) was stirred in a round bottom flask (25 mL) under atmosphere of air at 120 °C for 3.0 hrs. After bringing the mixture to room temperature, 20 mL water was added and the mixture was extracted with ethyl acetate (3 X 20 mL). The EtOAc layer was washed with 3 x 5 mL of 1M sodium bicarbonate solution. The combined organic layers were dried with anhydrous Na_2SO_4. Under vacuum, the solvent was evaporated, and the crude product was purified using column chromatography (silica gel, EtOAc/Hexane 6:4) in order to obtain a pure product in a yield of 98% (1.03 g).

Analytical data of compounds

N-phenylformamide[15a] **(3A):** Using the experimental procedure **EP-1**, the product was obtained as yellow solid in 94% yield; A mixture of rotamers is observed; **^{1}H NMR** (400 MHz, $CDCl_3$) δ 9.22 (Minor rotamer, s, 0.44H), 8.71 (Major rotamer, d, *J* = 11.3 Hz, 0.48H), 8.60 (Minor rotamer, s, 0.42H), 8.34 (Major rotamer, s, 0.50H), 7.58 (d, *J* = 8.2 Hz, 1.0H), δ 7.36 – 7.29 (m, 2.0H), 7.19 (t, *J* = 7.4 Hz, 0.47H), 7.13 (t, *J* = 7.1 Hz, 1.42H); **^{13}C NMR** (100 MHz, $CDCl_3$) δ major rotamer 163.23, 136.84, 129.41, 125.24, 118.78, minor rotamer 159.90, 137.09, 129.69, 124.74, 120.23.

N-phenylacetamide[15b] **(3B)**: Using the experimental procedure **EP-1**, the product was obtained as colourless oil in 93%; **^{1}H NMR** (400 MHz, $CDCl_3$) δ 7.91 (s, 1H), 7.43 (d, *J* = 8.0 Hz, 2H), 7.21 (t, *J* = 7.7 Hz, 2H), 7.02 (t, *J* = 7.4 Hz, 1H), 2.08 (s, 3H). **^{13}C NMR** (100 MHz, $CDCl_3$) δ 169.05, 138.03, 129.03, 124.47, 120.25, 24.47.

N-phenylpivalamide[15c] **(3C):** Using the experimental procedure **EP-1**, the product was obtained as white solid in 54%; **^{1}H NMR** (400 MHz, $CDCl_3$) δ 7.52 (d, *J* = 8.3 Hz, 2H), 7.31 (t, *J* = 7.7 Hz, 3H), 7.10 (t, *J* = 7.4 Hz, 1H), 1.32 (s, 9H). ^{13}C NMR (100 MHz, $CDCl_3$) δ 176.73, 138.16, 129.02, 124.29, 120.17, 39.68, 27.72.

N-phenylisobutyramide[15d] **(3D):** Using the experimental procedure **EP-1**, the product was obtained as white solid in 62%; **^{1}H NMR** (400 MHz, $CDCl_3$) δ 7.53 (d, *J* = 8.0 Hz, 2H), 7.43 (s, 1H), 7.30 (t, *J* =

7.7 Hz, 2H), 7.09 (t, *J* = 7.3 Hz, 1H), 2.57 – 2.47 (m, 1H), 1.24 (d, *J* = 6.8 Hz, 6H). **^{13}C NMR** (100 MHz, $CDCl_3$) δ 176.72, 138.24, 128.99, 124.23, 120.11, 77.47, 77.15, 76.84, 36.64, 19.69.

2,2,2-trichloro-N-phenylacetamide[15e] **(3E):** Using the experimental procedure **EP-1**, the product was obtained as white solid in 64%; **^{1}H NMR** (400 MHz, $CDCl_3$) δ 8.26 (s, 1H), 7.50 (d, *J* = 8.3 Hz, 2H), 7.33 (t, *J* = 7.7 Hz, 2H), 7.16 (t, *J* = 7.6 Hz, 1H). **^{13}C NMR** (100 MHz, $CDCl_3$) δ 136.05, 129.45, 126.18, 120.52.

N-phenylbenzamide[15e] **(3F):** Using the experimental procedure **EP-2**, the product was obtained as white solid in 83%; **^{1}H NMR** (400 MHz, DMSO-d_6) δ 10.26 (s, 1H), 7.97 (d, *J* = 7.2 Hz, 2H), 7.81 (d, *J* = 8 Hz, 2H), 7.59 (t, *J* = 8.3 Hz, 1H), 7.53 (t, *J* = 8.3 Hz, 2H), 7.36 (t, *J* = 7.7 Hz, 2H), 7.10 (t, *J* = 7.6 Hz, 1H). **^{13}C NMR** (100 MHz, DMSO-d_6) δ 165.57, 139.19, 135.01, 131.52, 128.85, 128.59, 128.36, 127.65, 123.64, 120.38.

N-phenylcyclohexanecarboxamide[16a] (**3G**): Using the experimental procedure **EP-1**, the product was obtained as light white solid in 71% yield; **^{1}H NMR** (400 MHz, DMSO-d_6) δ 9.78 (s, 1H), 7.60 (d, *J* = 8.4 Hz, 2H), 7.27 (t, 2H), 7.01 (t, 1H), 2.32 (m, 1.0H), 1.77 (t, 4.0H), 1.65 (d, *J* = 10.4 Hz, 1H), 1.41 (m, 2H), 1.27 (m, 3H); **^{13}C NMR** (100 MHz, DMSO-d_6) δ 174.27, 139.51, 128.58, 122.81, 119.00, 44.85, 29.13, 25.40, 25.24.

N-phenylthiophene-2-carboxamide[16b] (**3H**): Using the experimental procedure **EP-2**, the product was obtained as light white solid in 81% yield; **^{1}H NMR** (400 MHz, DMSO-d_6) δ 10.22 (s, 1H), 8.03 (d, *J* = 2.8 Hz, 1H), 7.85 (d, *J* = 5.2 Hz, 1H), 7.72 (d, *J* = 7.6 Hz, 2H), 7.35 (t, 2H), 7.22 (t, 1H), 7.10 (t, 1H); **^{13}C NMR** (100 MHz, DMSO-d_6) δ 159.88, 138.71, 131.86, 129.10, 128.68, 128.07, 123.75, 120.39.

3,3-dimethyl-N-phenylbutanamide[16c] (**3I**): Using the experimental procedure **EP-1**, the product was obtained as light brown solid in 78% yield; **^{1}H NMR** (400 MHz, DMSO-d_6) δ 9.77 (s, 1H), 7.59 (d, *J* = 8 Hz, 2H), 7.27 (t, 2H), 7.01 (t, 1H), 2.18 (s, 2H), 1.02 (s, 9H); **^{13}C NMR** (100 MHz, DMSO-d_6) δ 169.96, 139.28, 128.58, 122.94, 119.18, 49.60, 30.83, 29.62.

N,2-diphenylacetamide[16d] (**3J**): Using the experimental procedure **EP-1**, the product was obtained as light brown solid in 83% yield; **^{1}H NMR** (400 MHz, DMSO-d_6) δ 10.19 (s, 1H), 7.61 (d, *J* = 8 Hz, 2H),

7.29 (m, 7H), 7.03 (t, 1H), 3.64 (s, 2H); **^{13}C NMR** (100 MHz, DMSO-d_6) δ 169.10, 139.24, 136.03, 129.11, 128.71, 128.30, 126.52, 123.20, 119.10, 43.35.

N-phenyl-[1,1'-biphenyl]-4-carboxamide[16e] (**3K**): Using the experimental procedure **EP-2**, the product was obtained as light white solid in 73% yield; **^{1}H NMR** (400 MHz, DMSO-d_6) δ 10.30 (s, 1H), 8.06 (d, *J* = 8 Hz, 2H), 7.82 (dd, *J* = 14.4, 8 Hz, 4H), 7.76 (d, *J* = 8 Hz, 2H), 7.51 (t, 2H), 7.43 (t, 1H), 7.36 (t, 2H), 7.11 (t, 1H); **^{13}C NMR** (100 MHz, DMSO-d_6) δ 165.17, 143.10, 139.21, 139.12, 133.73, 129.09, 128.64, 128.39, 128.18, 126.94, 126.60, 123.68, 120.37.

4-nitro-N-phenylbenzamide[16d] (**3L**)**:** Using the experimental procedure **EP-2**, the product was obtained as light white solid in 54% yield; **^{1}H NMR** (400 MHz, DMSO-d_6) δ 10.58 (s, 1H), 8.37 (d, *J* = 8.4 Hz, 2H), 8.19 (d, *J* = 8.4 Hz, 2H), 7.78 (d, *J* = 8.4 Hz, 2H), 7.38 (t, 2H), 7.14 (t, 1H); **^{13}C NMR** (100 MHz, DMSO-d_6) δ 163.90, 149.15, 140.64, 138.72, 129.24, 128.74, 124.19, 123.57, 120.49.

2-phenoxy-N-phenylacetamide[17a] (**3M**): Using the experimental procedure **EP-1**, the product was obtained as light white solid in 78% yield; **^{1}H NMR** (400 MHz, DMSO-d_6) δ 10.11 (s, 1H), 7.65 (d, *J* = 8.0 Hz, 2H), 7.32 (t, 4H), 7.01 (t, 1H), 6.98 (m, 3H); **^{13}C NMR** (100 MHz, DMSO-d_6) δ 166.59, 157.83, 138.41, 129.53, 128.74, 123.70, 121.19, 119.71, 114.66, 67.10.

N-(2-Hydroxy-4-methylphenyl)formamide[17b] **(3a):** Using the experimental procedure **EP-1**, the product was obtained as brown solid in 94% yield; **^{1}H NMR** (400 MHz, DMSO) δ 9.92 (s, 1H), 9.55 (s, 1H), 8.28 (s, 1H), 8.02 (d, *J* = 7.9 Hz, 1H), 6.94 – 6.82 (m, 2H), 6.75 (*t*, *J* = 7.4 Hz, 1H); **^{13}C NMR** (100 MHz, DMSO): δ 163.47, 160.03, 148.97, 146.73, 126.00, 125.48, 125.34, 124.19, 121.76, 120.83, 119.53, 119.00, 116.10, 115.10.

N-(pyridin-2-yl)formamide[17c] (**3b**): Using the experimental procedure **EP-1**, the product was obtained as brown solid in 85%; **^{1}H NMR** (400 MHz, $CDCl_3$) δ 10.58 (s, 1H), 9.28 (d, *J* = 10.0 Hz, 0.57H), 8.33 (s, 1H), 8.24 (s, 0.60H), 8.06 (d, *J* = 7.9 Hz, 0.45H), 7.78 – 7.771 (m, 1H), 7.08 (d, *J* = 5.6 Hz, 1H), 6.92 (d, *J* = 7.9 Hz, 0.59H). **^{13}C NMR** (100 MHz, $CDCl_3$) δ 162.13, 160.31, 151.65, 148.06, 138.70, 138.31, 119.76, 119.22, 113.78, 111.12.

N-(quinolin-8-yl)formamide[17d] (**3c**): Using the experimental procedure **EP-1**, the product was obtained as brown solid in 68% yield. A mixture of rotamers is observed; **^{1}H NMR** (400 MHz, $CDCl_3$) δ 9.61 (br, s, 0.80H), 9.20 (br, s, 0.11H), 8.84 (t, *J* = 18.7 Hz, 0.12H), 8.56 (d, *J* = 4.1 Hz, 0.98H), 8.49 (dd, *J* = 11.5, 7.0 Hz, 0.89H), 8.44 (s, 0.88H), 7.93 (d, *J* = 8.3 Hz, 1.0H), 7.29-7.01 (m, 3.19H); **^{13}C NMR** (100 MHz, $CDCl_3$) δ Major rotamer: 159.98, 144.41, 141.25, 125.41, 120.81, 117.92, 114.64, minor rotamer: 163.63, 146.67, 141.89, 124.54, 122.03, 119.06, 115.62.

piperidine-1-carbaldehyde[17e] **(3d):** Using the experimental procedure **EP-1**, the product was obtained as yellow oil in 52%; **^{1}H NMR** (400 MHz, $CDCl_3$) δ 7.78 (s, 1H), 3.26 (t, *J* = 4.8 Hz, 2H), 3.10 (t, *J* = 4.8 Hz, 2H), 1.47 (d, *J* = 4.2 Hz, 2H), 1.37 – 1.31 (m, 4H).**^{13}C NMR** (100 MHz, $CDCl_3$) δ 160.34, 46.34, 40.11, 26.31, 26.14, 24.66, 24.23.

N-(4-methoxyphenyl) formamide[18a] (**3e**): Using the experimental procedure **EP-1**, the product was obtained as reddish brown solid in 98% yield. A mixture of rotamers is observed; **^{1}H NMR** (400 MHz, $CDCl_3$) δ 8.52 (t, *J* = 13.2 Hz, 0.84H), 8.28 (Major rotamer, s, 0.52H), 7.88 (Minor rotamer, s, 0.43H), 7.43 (d, *J* = 8.8 Hz, 1.03H), 7.03 (d, *J* = 8.7 Hz, 0.92H), 6.85 (dd, *J* = 14.3, 8.8 Hz, 1.98H), 3.77 (d, *J* = 7.5 Hz, 3H). **^{13}C NMR** (100 MHz, $CDCl_3$) δ Major rotamer: 159.33, 157.68, 129.74, 121.74, 114.97, 55.55, minor rotamer: 163.42, 156.77, 130.13, 121.61, 114.28, 55.63.

N-(4-fluorophenyl) formamide[18b] (**3f**): Using the experimental procedure **EP-1**, the product was obtained as off-white solid in 90% yield. A mixture of rotamers is observed; **^{1}H NMR** (400 MHz, $CDCl_3$) δ 8.63 (Minor rotamer, s, 0.33H), 8.57 (Major rotamer, d, *J* = 11.0 Hz, 0.50H), 8.33 (Major rotamer, s, 0.60H), 7.76 (Minor rotamer, s, 0.47H), 7.50 (dd, *J* = 8.7, 4.8 Hz, 1.17H), 7.11 – 6.96 (m, 3H); **^{13}C NMR** (100 MHz, $CDCl_3$) δ Major rotamer: 159.36, 160.94, 158.52, 122.03, 115.99, minor rotamer: 163.19, 161.79, 159.30, 121.95, 115.77; **^{19}F NMR** (377 MHz, $CDCl_3$) δ -116.84, -116.85, -116.86, -116.87, -116.89, -116.89, -116.91, -117.06, -117.07, -117.08, -117.09, -117.10, -117.11, -117.12.

N-(3-fluorophenyl)formamide[18c] (**3g**): Using the experimental procedure **EP-1**, the product was obtained as yellow solid in 88% yield. A mixture of rotamers is observed; **^{1}H NMR** (400 MHz, $CDCl_3$)

δ 8.98 (Minor rotamer, s, 042H), 8.73 (Minor rotamer, d, *J* = 11.2 Hz, 0.47H), 8.39 (Major rotamer, s, 0.60H), 8.11 (Major rotamer, d, *J* = 4.0 Hz, 0.53H), 7.50 (d, *J* = 10.7 Hz, 0.57H), 7.39 – 6.81 (m, 1.71H), 6.95 – 6.82 (m, 2H); **^{13}C NMR** (100 MHz, $CDCl_3$) δ Major rotamer: 159.59, 130.3 (d, *J* = 9.3 Hz), 115.39 (*d*, J = 2.9 Hz), 107.88, 107.88, 107.62, Minor rotamer: 162.82, 131.2 (d, *J* = 9.3 Hz), 114.16 (d, *J* = 2.9 Hz), 106.15, 105.9; **^{19}F NMR** (377 MHz, $CDCl_3$) δ -110.46, -110.48, -110.50, -110.52, -111.18, -111.21, -111.22, -111.23, -111.24.

N-(2,4-dimethylphenyl)formamide[18d] (**3h**): Using the experimental procedure **EP-1**, the product was obtained as off-white solid in 91% yield. A mixture of rotamers is observed; **^{1}H NMR** (400 MHz, $CDCl_3$) δ 8.45 (d, *J* = 11.2 Hz, 0.62H), 8.39 (s, 0.37H), 8.17 (br, s, 0.58H), 7.66 (d, *J* = 8.6 Hz, 0.36H), 7.35 (br, s, 0.28H), 7.00 (t, *J* = 7.2 Hz, 2.69H), 2.29 (d, *J* = 10.3 Hz, 3H), 2.24 (d, *J* = 15.6 Hz, 3H). **^{13}C NMR** (100 MHz, $CDCl_3$) δ Major rotamer: 159.50, 136.08, 132.53, 130.23, 127.63, 121.46, minor rotamer: 163.82, 135.45, 131.96, 129.26, 127.26, 127.36, 123.52.

N-(5-(tert-butyl)-2-hydroxyphenyl)formamide[18e] (**3i**): Using the experimental procedure **EP-1**, the product was obtained as brown solid in 92% yield. A mixture of rotamers is observed; **^{1}H NMR** (400 MHz, DMSO) δ 9.67 (s, 0.81H), 9.53 (s, 0.99H), 9.18 (Minor rotamer, d, *J* = 11.0 Hz, 0.17H), 8.52 (Minor rotamer, d, *J* = 11.2 Hz, 0.17H), 8.27 (Major rotamer, s, 0.82H), 8.07 (Major rotamer, d, *J* = 1.4 Hz, 0.82H), 7.10 (s, 0.16H), 6.99 (d, *J* = 8.4 Hz, 0.18H), 6.93 (dd, *J* = 8.4, 1.8 Hz, 0.80H), 6.79 (t, *J* = 10.1 Hz, 0.98H), 1.22 (s, 9H). **^{13}C NMR** (100 MHz, DMSO) δ Major: 159.98, 144.41, 141.25, 125.41, 120.81, 117.92, 115.62, minor rotamer; 163.63, 146.67, 141.89, 124.54, 122.03, 122.03, 119.06, 114.64.

N-(4-chloro-3-(trifluoromethyl)phenyl)formamide (**3j**): Using the experimental procedure **EP-1**, the product was obtained as yellow solid in 61% yield. A mixture of rotamers is observed; **^{1}H NMR** (400 MHz, $CDCl_3$) δ 8.70 (s, 0.77H), 8.41 (s, 1H), 7.85 (d, *J* = 15.4 Hz, 1.18H), 7.75 (d, *J* = 8.6 Hz, 0.61H), 7.50 (d, *J* = 8.5 Hz, 1.11H), 7.47 – 7.40 (m, 0.42H), 7.24 (d, *J* = 8.5 Hz, 0.41H); **^{13}C NMR** (100 MHz, $CDCl_3$) δ Major rotamer: 159.36, 132.29, 121.19, 11.94, minor rotamer: 162.35, 133.03, 119.08, 117.89; **^{19}F NMR** (377 MHz, $CDCl_3$) δ -62.91 (minor, s), -63.05 (minor, s).

N-(3-chloro-4-fluorophenyl)formamide[19a] (**3k**): Using the experimental procedure **EP-1**, the product was obtained as off-white solid in 65% yield. A mixture of rotamers is observed; **^{1}H NMR** (400 MHz, $CDCl_3$) δ 8.64 (d, *J* = 19.6 Hz, 0.34H), 8.58 (d, *J* = 11.0 Hz, 0.45H), 8.35 (s, 0.77H), 7.72 (dd, *J* = 6.4, 2.1 Hz, 0.48H), 7.39 – 7.32 (m, 0.87H), 7.20 – 7.04 (m, 0.76H), 7.02 – 6.95 (m, 2H). **^{13}C NMR** (100 MHz, $CDCl_3$) δ Major rotamer: 159.30, 156.42, 153.96, 122.46, 116.77, minor rotamer: 162.88, 157.26, 154.80, 121.61, 116.99; **^{19}F NMR** (377 MHz, $CDCl_3$) δ -119.23, -119.25, -119.27, -119.48, -119.50, -119.51, -119.51, -119.52, -119.53.

N-(2-bromo-4-methylphenyl)formamide[19b] (**3l**): Using the experimental procedure **EP-1**, the product was obtained as off-white solid in 78% yield. A mixture of rotamers is observed; **^{1}H NMR** (400 MHz, $CDCl_3$) δ 8.62 (d, *J* = 11.2 Hz, 0.35H), 8.45 (s, 0.66H), 8.22 (d, *J* = 8.3 Hz, 0.66H), 7.62 (br, s, 0.82H), 7.42 (s, 0.48H), 7.36 (s, 0.49H), 7.12 (t, *J* = 8.8 Hz, 1.32H), 2.30 (d, *J* = 7.8 Hz, 3H). **^{13}C NMR** (100 MHz, CDCl3) δ Major rotamer: 158.88, 133.88, 132.72, 129.42, 122.24, 114.78, minor rotamers: 161.90, 135.93, 132.88, 129.17, 119.17, 119.46, 113.04.

N-(3-chlorophenyl)formamide[17b] (**3m**): Using the experimental procedure **EP-1**, the product was obtained as yellow solid in 87% yield. A mixture of rotamers is observed; **^{1}H NMR** (400 MHz, $CDCl_3$) δ 8.72 (t, *J* = 11.9 Hz, 0.83H), 8.38 (s, 0.55H), 7.82 (s, 1.0H), 7.47 (d, *J* = 8.0 Hz, 0.56H), 7.36 – 7.17 (m, 2.4H), 7.06 (d, *J* = 8.0 Hz, 0.44H), **^{13}C NMR** (100 MHz, $CDCl_3$) δ Major rotamer: 159.36, 130.52, 127.97, 123.08, 122.78, 118.58, minor rotamers: 162.68, 131.18, 128.41, 123.46, 121.78, 117.32.

N-(4-bromophenyl)formamide[19c] (**3n**): Using the experimental procedure **EP-1**, the product was obtained as yellow solid in 77% yield. A mixture of rotamers is observed; **^{1}H NMR** (400 MHz, $CDCl_3$) δ 8.66 (Major rotamer, d, *J* = 11.1 Hz, 0.51H), 8.61 (Minor rotamer, s, 0.35H), 8.37 (Major rotamer, s, 0.62H), 7.62 (minor rotamer, s, 0.47H), 7.48 (s, 0.99H), 7.44 (d, *J* = 8.2 Hz, 2.20H), 6.98 (d, *J* = 8.6 Hz, 0.92H); **^{13}C NMR** (100 MHz, $CDCl_3$) δ Major rotamer: 159.20, 132.21, 121.21, 117.63, minor rotamer: 162.63, 132.92, 120.45, 118.42.

N-(2-iodophenyl)formamide[17b] (**3o**): Using the experimental procedure **EP-1**, the product was obtained as brown solid in 58% yield; A mixture of rotamers is observed; **^{1}H NMR** (400 MHz, $CDCl_3$)

δ 8.73 (Minor rotamer, s, 0.33H), 8.69 (Major rotamer, d, *J* = 11.0 Hz, 0.62H), 8.36 (Major rotamer, s, 0.44H), 7.85 (Minor rotamer, s, 0.38H), 7.55 (d, *J* = 7.9 Hz, 0.86H), 7.37-7.30 (m, 1.92H), 7.21 – 7.07 (m, 1.44H). **^{13}C NMR** (100 MHz, $CDCl_3$) δ major rotamer: 163.03, 137.04, 129.99, 125.40, 118.93, minor rotamer: 159.44, 136.84, 129.84, 124.90, 120.17.

N-m-tolylformamide[19d] (**3p**): Using the experimental procedure **EP-1**, the product was obtained as brown oil in 89% yield; A mixture of rotamers is observed; **^{1}H NMR** (400 MHz, $CDCl_3$) δ 8.98 (Major rotamer, br s, 0.51H), 8.71 (Major rotamer, d, *J* = 11.4 Hz, 0.56H), 8.35 (Minor rotamer, s, 0.45H), 8.11 (Minor rotamer, br d, *J* = 5.0 Hz, 0.42H), 7.39 (s, 0.44H), 7.33 (d, *J* = 8.1 Hz, 0.44H), 7.20 (dt, *J* = 12.0, 7.9 Hz, 1.0H), 6.99 (d, *J* = 7.6 Hz, 0.55H), 6.93 (d, *J* = 10.8 Hz, 1.52H), 2.32 (d, *J* = 10.8 Hz, 3H). **^{13}C NMR** (100 MHz, $CDCl_3$) δ Major rotamer: 163.16, 139.87, 136.81, 129.56, 125.60, 119.54, 115.80, 21.41, minor rotamer: 159.57, 139.05, 137.01, 128.91, 126.09, 120.79, 117.24, 21.47.

N-(2-nitrophenyl)formamide[19e] (**3q**): Using the experimental procedure **EP-1**, the product was obtained as yellow oil in 25% yield; A mixture of rotamers is observed; **^{1}H NMR** (400 MHz, $CDCl_3$) δ 8.73 (Minor rotamer, d, *J* = 11.1 Hz, 0.32H), 8.52 (Major rotamer, s, 0.69H), 8.41 (d, *J* = 8.2 Hz, 0.67H), 7.81 (s, 0.89), 7.43 (d, *J* = 8.0 Hz, 0.33H), 7.37 (d, *J* = 8.0 Hz, 0.67H), 7.27 (dd, *J* = 8.9, 5.8 Hz, 1.38H), 7.15 – 7.11 (m, 0.31H), 7.06 (t, *J* = 7.7 Hz, 0.70H). **^{13}C NMR** (100 MHz, CDCl3) δ Major rotamer: 159.03, 129.23, 127.92, 125.26, 122.70, 161.73, 130.43, 128.13, 126.09, 122.14.

N-(4-acetylphenyl)formamide[20a] (**3r**): Using the experimental procedure **EP-1**, the product was obtained as white solid in 91% yield. A mixture of rotamers is observed; **^{1}H NMR** (400 MHz, $CDCl_3$) δ 8.93 (Minor rotamer, d, *J* = 10.8 Hz, 0.36H), 8.75 (Minor rotamer, d, *J* = 11.2 Hz, 0.38H), 8.47 (Major rotamer, s, 0.53H), 8.42 (Major rotamer, s, 0.69H), 8.07 (s, 0.67H), 7.92 (d, *J* = 8.1 Hz, 0.68H), 7.73 (d, *J* = 7.5 Hz, 0.76H), 7.67 (d, *J* = 7.7 Hz, 0.65H), 7.46-7.38 (m, 1.05H), 7.32 (d, *J* = 8.3 Hz, 0.38H), 2.58 (d, *J* = 9.2 Hz, 3H), **^{13}C NMR** (100 MHz, $CDCl_3$) δ Major rotamer: 198.34, 159.83, 137.83, 129.53, 124.85, 119.42, minor rotamer: 197.66, 162.74, 138.53, 130.18, 123.20, 117.84.

N-(3-acetylphenyl)formamide[20b] (**3s**): Using the experimental procedure **EP-1**, the product was obtained as white solid in 78% yield. A mixture of rotamers is observed; **^{1}H NMR** (400 MHz, $CDCl_3$)

δ 9.00 (d, *J* = 10.5 Hz, 0.36H), 8.86 (Minor rotamer, d, *J* = 11.1 Hz, 0.39H), 8.42 (Major rotamer, s, 0.65H), 8.38 (br, s, 0.73H), 7.93 (dd, *J* = 13.4, 8.5 Hz, 0.2.02H), 7.67 (d, *J* = 8.5 Hz, 1.24H), 7.18 (d, *J* = 8.4 Hz, 0.80H), 2.57 (d, *J* = 4.4 Hz, 3H); **^{13}C NMR** (100 MHz, $CDCl_3$) δ Major rotamer: 159.27, 133.30, 129.87, 119.40, minor rotamer: 162.27, 133.75, 130.52, 117.35.

Ethyl 4-formamidobenzoate[20c] (**3t**): Using the experimental procedure **EP-1**, the product was obtained as white solid in 72% yield. A mixture of rotamers is observed; **^{1}H NMR** (400 MHz, DMSO-d_6) δ 10.53 (Major rotamer, s, 0.73H), 10.46 (Minor rotamer, d, *J* = 10.7 Hz, 0.25H), 8.96 (Minor rotamer, d, *J* = 10.7 Hz, 0.24H), 8.35 (Major rotamer, s, 0.75H), 7.91 (t, *J* = 10.5 Hz, 2.01H), 7.71 (d, *J* = 8.5 Hz, 1.53H), 7.31 (t, *J* = 7.6 Hz, 0.61H), 4.28 (q, *J* = 7.1 Hz, 2H), 1.30 (t, *J* = 7.1 Hz, 3H); **^{13}C NMR** (100 MHz, DMSO-d_6) δ Major rotamer: 160.11, 142.43, 130.32, 118.62, minor rotamer: 162.53, 142.90, 121.19, 116.43.

4-formamidobenzoic acid[20d] (**3u**): Using the experimental procedure **EP-1**, the product was obtained as brown oil in 80% yield. A mixture of rotamers is observed; **^{1}H NMR** (400 MHz, $CDCl_3$) δ 8.85 (s, 0.48H), 8.69 (d, *J* = 11.3 Hz, 0.55H), 8.35 (s, 0.47H), 8.00 (s, 0.45H), 7.55 (d, *J* = 8.1 Hz, 0.93H), 7.39 – 7.27 (m, 2H), 7.18 (t, *J* = 7.4 Hz, 0.53H), 7.11 (dd, *J* = 10.9, 8.0 Hz, 1.47H); **^{13}C NMR** (100 MHz, $CDCl_3$) δ Major rotamer: 163.09, 136.87, 129.97, 125.37, 118.90, minor rotamer: 159.55, 137.06, 129.15, 124.87, 120.19.

1-(4-(2-chlorophenyl)piperazin-1-yl)ethan-1-one **(4a):** Using the experimental procedure **EP-1**, the product was obtained as light yellow solid in 82%; **^{1}H NMR** (400 MHz, DMSO-d_6) δ 7.43 (d, *J* = 7.9 Hz, 1H), 7.31 (t, *J* = 7.7 Hz, 1H), 7.15 (d, *J* = 8.0 Hz, 1H), 7.07 (t, *J* = 7.6 Hz, 1H), 3.58 (t, *J* = 4.4 Hz, 4H), 2.97 (t, *J* = 4.4 Hz, 2H), 2.90 (t, *J* = 4.4 Hz, 2H), 2.05 (s, 3H). **^{13}C NMR** (100 MHz, DMSO-d_6) δ 168.32, 148.64, 130.30, 128.08, 127.72, 124.22, 121.09, 51.15, 50.73, 45.90, 45.47, 41.02, 21.18, 8.45.

N-(2-hydroxyphenyl)acetamide[21a] **(4b)**: Using the experimental procedure **EP-1**, the product was obtained as white solid in 89%; **^{1}H NMR** (400 MHz, DMSO-d_6) δ 9.73 (s, 1H), 9.30 (s, 1H), 7.67 (d, *J* = 7.9 Hz, 1H), 6.93 (t, *J* = 7.5 Hz, 1H), 6.85 (d, *J* = 7.7 Hz, 1H), 6.75 (t, *J* = 7.6 Hz, 1H), 2.09 (s, 3H). **^{13}C NMR** (100 MHz, DMSO-d_6) δ 169.02, 147.89, 126.42, 124.65, 122.37, 118.98, 115.95, 23.59.

N-(3-hydroxyphenyl)acetamide[21b] **(4c):** Using the experimental procedure **EP-1**, the product was obtained as colourless semisolid in 94%; **^{1}H NMR** (400 MHz, DMSO-d_6) δ 9.78 (s, 1H), 9.33 (s, 1H), 7.19 (s, 1H), 7.05 (t, *J* = 8.0 Hz, 1H), 6.92 (d, *J* = 8.1 Hz, 1H), 6.43 (dd, *J* = 8.0, 1.7 Hz, 1H), 2.02 (s, 3H). **^{13}C NMR** (100 MHz, DMSO-d_6) δ 168.18, 157.56, 140.36, 129.27, 110.12, 109.77, 106.19, 24.05.

N-(4-hydroxyphenyl)acetamide[21c] **(4d)** Using the experimental procedure **EP-1**, the product was obtained as light yellow solid in 97%; **^{1}H NMR** (400 MHz, DMSO-d_6) δ 9.64 (s, 1H), 9.13 (s, 1H), 7.34 (d, *J* = 8.5 Hz, 2H), 6.68 (d, *J* = 8.5 Hz, 2H), 1.98 (s, 3H). **^{13}C NMR** (100 MHz, DMSO-d_6) δ 167.50, 153.11, 131.02, 120.81, 114.98, 23.72.

N-(3-nitrophenyl)acetamide[18c] **(4e):** Using the experimental procedure **EP-1**, the product was obtained as yellow solid in 62%; **^{1}H NMR** (400 MHz, DMSO-d_6) δ 10.44 (s, 1H), 8.60 (t, *J* = 2.0 Hz, 1H), 7.87 (dd, *J* = 8.2, 2.1 Hz, 2H), 7.57 (t, *J* = 8.2 Hz, 1H), 2.09 (s, 3H). **^{13}C NMR** (100 MHz, DMSO-d_6) δ 166.08, 144.94, 137.39, 127.07, 121.86, 114.49, 110.03, 109.93, 21.01.

N-(3-(trifluoromethyl)phenyl)acetamide[21d] **(4f):** Using the experimental procedure **EP-1**, the product was obtained as white solid in 79%; **^{1}H NMR** (400 MHz, DMSO-d_6) δ 10.27 (s, 1H), 8.08 (s, 1H), 7.75 (d, *J* = 8.2 Hz, 1H), 7.53 (t, *J* = 8.0 Hz, 1H), 7.36 (t, *J* = 11.5 Hz, 1H), 2.08 (s, 3H). **^{13}C NMR** (100 MHz, DMSO-d_6) δ 168.91, 151.00, 140.03, 130.32, 129.90, 122.44, 119.31, 119.27, 117.78, 114.98, 114.94, 111.27, 110.71, 24.00, 20.55.

N-(4-(trifluoromethoxy)phenyl)acetamide[21e] **(4g):** Using the experimental procedure **EP-1**, the product was obtained as Colourless Solid in 71%; **^{1}H NMR** (400 MHz, $CDCl_3$) δ 7.95 (s, 1H), 7.53 (d, *J* = 8.8 Hz, 2H), 7.14 (d, *J* = 8.5 Hz, 2H), 2.16 (s, 3H). **^{13}C NMR** (100 MHz, $CDCl_3$) δ 169.00, 145.43, 136.71, 128.95, 127.92, 127.80, 121.87, 121.77, 121.32, 119.32, 24.46.

N-methyl-N-phenylacetamide[17c] **(4h)**: Using the experimental procedure **EP-1**, the product was obtained as light brown solid in 86%; **^{1}H NMR** (400 MHz, DMSO-d_6) δ 7.44 (t, *J* = 7.0 Hz, 2H), 7.32 (d, *J* = 7.5 Hz, 3H), 3.14 (s, 3H), 1.75 (s, 3H). **^{13}C NMR** (100 MHz, DMSO-d_6) δ 144.39, 129.56, 127.38, 127.06, 36.52, 22.17.

N-benzylbenzamide[22a] **(5a):** Using the experimental procedure **EP-2**, the product was obtained as white solid in 80%; **^{1}H NMR** (400 MHz, DMSO-d_6) δ 9.08 (s, 1H), 7.92 (d, *J* = 7.2 Hz, 2H), 7.55 – 7.50 (m, 1H), 7.47 (t, *J* = 7.5 Hz, 2H), 7.33 (d, *J* = 4.1 Hz, 4H), 7.26 – 7.21 (m, 1H). **^{13}C NMR** (100 MHz, DMSO-d_6) δ 166.17, 139.70, 134.32, 131.19, 128.28, 128.24, 127.23, 127.17, 126.68.

N-(2-chlorophenyl)benzamide[22b] **(5b):** Using the experimental procedure **EP-2**, the product was obtained as white solid in 50%; **^{1}H NMR** (400 MHz, DMSO-d_6) δ 10.06 (s, 1H), 8.02 (d, *J* = 7.8 Hz, 2H), 7.66 – 7.58 (m, 2H), 7.55 (dd, *J* = 12.4, 5.4 Hz, 3H), 7.39 (t, *J* = 7.6 Hz, 1H), 7.30 (t, *J* = 7.7 Hz, 1H). **^{13}C NMR** (100 MHz, DMSO-d_6) δ 165.35, 135.08, 133.95, 131.78, 129.48, 129.44, 128.43, 128.33, 127.65, 127.39, 127.36.

N-(4-chlorophenyl)benzamide[20c] **(5c)**: Using the experimental procedure **EP-2**, the product was obtained as white solid in 80%; **^{1}H NMR** (400 MHz, DMSO-d_6) δ 10.41 (s, 1H), 7.98 (d, *J* = 7.5 Hz, 2H), 7.85 (d, *J* = 8.8 Hz, 2H), 7.61 – 7.50 (m, 3H), 7.40 (d, *J* = 8.8 Hz, 2H). **^{13}C NMR** (100 MHz, DMSO-d_6) δ 165.60, 138.14, 134.64, 131.61, 128.42, 128.33, 127.65, 127.22, 121.85, 121.76.

N,N-diphenylbenzamide[23a] **(5d):** Using the experimental procedure **EP-2**, the product was obtained as yellow solid in 65%; **^{1}H NMR** (400 MHz, DMSO-d_6) δ 7.73-7.64 (m, 7H), 7.32 – 7.14 (m, 4H), 7.00 (t, *J* = 8.4 Hz, 4H). **^{13}C NMR** (100 MHz, DMSO-d_6) δ 188.20, 169.86, 159.63, 149.42, 149.08, 142.53, 142.05, 141.96, 130.18, 128.24, 127.86, 124.21, 123.83, 123.71, 122.71, 114.98, 112.94, 111.25.

N-(2-methoxyphenyl)benzamide[23b] **(5e):** Using the experimental procedure **EP-2**, the product was obtained as white solid in 89%; **^{1}H NMR** (400 MHz, DMSO-d_6) δ 9.39 (s, 1H), 7.98 (d, *J* = 7.4 Hz, 2H), 7.84 (d, *J* = 7.9 Hz, 1H), 7.59 (t, *J* = 7.3 Hz, 3H), 7.18 (t, *J* = 7.8 Hz, 1H), 7.09 (d, *J* = 7.5 Hz, 1H), 6.98 (t, *J* = 7.6 Hz, 1H), 3.84 (s, 3H). **^{13}C NMR** (100 MHz, DMSO-d_6) δ 164.90, 151.30, 134.51, 131.53, 128.44, 127.38, 126.87, 125.55, 123.99, 120.17, 111.34, 55.69.

N-(4-methoxyphenyl)benzamide[15c] **(5f)**: Using the experimental procedure **EP-2**, the product was obtained as white solid in 88%; **^{1}H NMR** (400 MHz, DMSO-d_6) δ 10.12 (s, 1H), 7.96 (d, *J* = 7.8 Hz, 2H), 7.69 (d, *J* = 8.8 Hz, 2H), 7.61 – 7.47 (m, 3H), 6.94 (d, *J* = 8.8 Hz, 2H), 3.75 (s, 3H). **^{13}C NMR** (100 MHz, DMSO-d_6) δ 165.06, 155.53, 135.02, 132.20, 131.29, 128.27, 127.48, 121.96, 113.69.

N-(4-nitrophenyl)benzamide[23c] **(5g):** Using the experimental procedure **EP-1**, the product was obtained as brown solid in 75%; **^{1}H NMR** (400 MHz, DMSO-d_6) δ 10.84 (s, 1H), 8.26 (d, *J* = 9.0 Hz, 2H), 8.08 (d, *J* = 9.0 Hz, 2H), 8.00 (d, *J* = 7.9 Hz, 2H), 7.63 (t, *J* = 6.9 Hz, 1H), 7.56 (t, *J* = 7.6 Hz, 2H). **^{13}C NMR** (100 MHz, DMSO-d_6) δ 166.27, 145.52, 142.44, 134.20, 132.14, 128.48, 127.93, 124.74, 119.83, 119.75.

N-(3-(trifluoromethyl)phenyl)benzamide[22c] **(5h):** Using the experimental procedure **EP-1**, the product was obtained as white solid in 45%; **^{1}H NMR** (400 MHz, DMSO-d_6) δ 10.68 (s, 1H), 8.30 (s, 1H), 8.10 (d, *J* = 8.0 Hz, 1H), 8.02 (d, *J* = 7.9 Hz, 1H), 7.65 – 7.51 (m, 2H), 7.45 (d, *J* = 7.8 Hz, 1H). **^{13}C NMR** (101 MHz, DMSO-d_6) δ 140.00, 131.87, 129.79, 128.41, 127.77, 123.82.

References

[1] Y. L. Zheng, S. G. Newman, *ACS Catal.* **2019**, 9, 5, 4426–4433.

[2] a) M. R. Petchey, G. Grogan, *Adv. Synth. Catal.* **2019**, 361, 17, 3895-3914; b) D. Kaiser, A. Bauer, M. Lemmerer, N. Maulide, *Chem. Soc. Rev.* **2018**, 47, 7899-7925; c) M. B. Chaudhari, B. Gnanaprakasam, *Chem. - An Asian J.* **2019**, 14, 1, 76-93; d) A. C. Fonseca, M. H. Gil, P. N. Simões, *Prog. Polym. Sci.* **2014**, 39, 7, 1291-1311; e) M. Todorovic, D. M. Perrin, *Pept. Sci.* **2020**, 112, 6, e24210.

[3] T. Narendar Reddy, A. Beatriz, V. Jayathirtha Rao, D. P. de Lima, *Chem. - An Asian J.* **2019**, 14, 3, 344-388.

[4] S. Mahesh, K. C. Tang, M. Raj, *Molecules* **2018**, 23, 10, 2615.

[5] P. Acosta-Guzmán, A. Mateus-Gómez, D. Gamba-Sánchez, *Molecules* **2018**, 23, 9, 2382.

[6] R. Sanichar, J. C. Vederas, *Org. Lett.* **2017**, 19, 1950-1953.

[7] a) I. S. Young, A. L. Glass, T. Cravillion, C. Han, H. Zhang, F. Gosselin, *Org. Lett.* **2018**, 20, 3902-3906; b) J. E. Dander, E. L. Baker, N. K. Garg, *Chem. Sci.* **2017**, *8*, 6433–6438; c) Y. Li, F. Jia, Z. Li, *Chem. - A Eur. J.* **2013**, 19, 1, 82-86; d) G. Pelletier,

D. A. Powell, *Org. Lett.* **2006**, 8, 26, 6031-6034; e) X. Kong, B. Xu, *Org. Lett.* **2018**, 20, 15, 4495-4498.

[8] a) Z. Li, C. Guo, J. Chen, Y. Yao, Y. Luo, *Appl. Organomet. Chem.* **2020**, 34, 4, 5517; b) H. Jiang, Z. Hu, C. Gan, B. Sun, S. Kong, F. Bian, *Mol. Catal.* **2021**, 504, 111490; c) D. C. Lenstra, D. T. Nguyen, J. Mecinović, *Tetrahedron* **2015**, 71, 34, 5547-5553; d) E. Bon, D. C. H. Bigg, G. Bertrand, *J. Org. Chem.* **1994**, 59, 15, 4035-4036; e) S. P. Pathare, A. K. H. Jain, K. G. Akamanchi, *RSC Adv.* **2013**, 21, 3, 7697-7703.

[9] J. Briffa, E. Sinagra, R. Blundell, *Heliyon* **2020**, 6, 9, e04691.

[10] a) T. B. Nguyen, J. Sorres, M. Q. Tran, L. Ermolenko, A. Al-Mourabit, *Org. Lett.* **2012**, 14, 12, 3202-3205; b) S. Nageswara Rao, D. Chandra Mohan, S. Adimurthy, *Green Chem.* **2014**, 16, 9, 4122-4126; c) J. Yin, J. Zhang, C. Cai, G. J. Deng, H. Gong, *Org. Lett.* **2019**, *21*, 387–392.

[11] a) R. Vanjari, B. Kumar Allam, K. Nand Singh, *RSC Adv.* **2013**, 3, 6, 1691-1694; b) S. Adimurthy, *J. Biomol. Res. Ther.* **2016**, 5, 2; c) C. L. Allen, B. N. Atkinson, J. M. J. Williams, *Angew. Chemie - Int. Ed.* **2012**, 51, 1383-1386; d) A. K. Brel, S. V. Lisina, S. S. Popov, Y. N. Budaeva, *Russ. J. Gen. Chem.* **2016**, 86, 3, 549-551.

[12] G. Li, M. Szostak, *Nat. Commun.* **2018**, *9*, 1–8.

[13] E. L. Baker, M. M. Yamano, Y. Zhou, S. M. Anthony, N. K. Garg, *Nat. Commun.* **2016**, *7*, 1–5.

[14] a) R. Chutia, B. Chetia, *New J. Chem.* **2018**, 42, 18, 15200-15206; b) C. Chen, Y. Pan, H. Zhao, X. Xu, J. Xu, Z. Zhang, S. Xi, L. Xu, H. Li, *Org. Chem. Front.* **2018**, 5, 3, 415-422; c)U. V. Mallavadhani, L. Sahoo, S. Roy, *Indian J. Chem. - Sect. B Org. Med. Chem.* **2004**, 43B, 10, 2175-2177.

[15] a) W. D. Li, D. Y. Zhu, G. Li, J. Chen, J. B. Xia, *Adv. Synth. Catal.* **2019**, 361, 22, 5098-5104; b) P. V. Ramachandran, H. J. Hamann, *Org. Lett.* **2021**, 23, 8, 2938–2942; c) Z.

Fu, X. Wang, S. Tao, Q. Bu, D. Wei, N. Liu, *J. Org. Chem.* **2021**, 86, 3, 2339–2358; d) J. S. Li, X. Y. Xie, S. Jiang, P. P. Yang, Z. W. Li, C. H. Lu, W. D. Liu, *Org. Chem. Front.* **2021**, 8, 4, 697-701; e) T. Imanishi, Y. Fujiwara, Y. Sawama, Y. Monguchi, H. Sajiki, *Adv. Synth. Catal.* **2012**, 354, 5, 771-776.

[16] a) F. F. Feng, X. Y. Liu, C. W. Cheung, J. A. Ma, *ACS Catal.* **2021**, 11, 12, 7070–7079; b) K. Wang, J. Hou, T. Wei, C. Zhang, R. Bai, Y. Xie, *Tetrahedron Lett.* **2021**, 62, 152623; c) X. Yi, X. Yi, S. Lei, W. Liu, F. Che, C. Yu, X. Liu, Z. Wang, X. Zhou, Y. Zhang, *Org. Lett.* **2020**, 22, 12, 4583–4587; d) Y. J. Wang, G. Y. Zhang, A. Shoberu, J. P. Zou, *Tetrahedron Lett.* **2021**, 80, 153316; e) D. Joseph, M. S. Park, S. Lee, *Org. Biomol. Chem.* **2021**, 19, 28, 6227-6232.

[17] a) R. Sallio, P. A. Payard, P. Pakulski, I. Diachenko, I. Fabre, S. Berteina-Raboin, C. Colas, I. Ciofini, L. Grimaud, I. Gillaizeau, *RSC Adv.* **2021**, 11, 15885-15889; b) T. Ghosh, S. Jana, J. Dash, *Org. Lett.* **2019**, *21*, 6690–6694; c) C. Li, M. Wang, X. Lu, L. Zhang, J. Jiang, L. Zhang, *ACS Sustain. Chem. Eng.* **2020**, 8, 11, 4353-4361; d) M. C. Pichardo, G. Tavakoli, J. E. Armstrong, T. Wilczek, B. E. Thomas, M. H. G. Prechtl, *ChemSusChem* **2020**, 13, 5, 882-887; e) K. Zhang, L. Zong, X. Jia, *Adv. Synth. Catal.* **2021**, 363, 5, 1335-1340.

[18] a) S. Wu, Z. Huang, X. Jiang, F. Yan, Y. Li, C. X. Du, *ChemSusChem* **2021**, 14, 7, 1763-1766; b) M. Amirsoleimani, M. A. Khalilzadeh, D. Zareyee, *J. Mol. Struct.* **2021**, 1225, 129076; c) R. B. Sonawane, N. K. Rasal, D. S. Bhange, S. V. Jagtap, *ChemCatChem* **2018**, 10, 17, 3907-3913; d) M. R. Mutra, G. K. Dhandabani, J. J. Wang, *Adv. Synth. Catal.* **2018**, 360, 20, 3960-3968; e) Y. Yang, Y. Li, Z. Zhang, Y. Zhao, W. Feng, *Synth. Commun.* **2019**, 49, 8, 1040-1046.

[19] a) B. Kaboudin, M. Khodamorady, *Synlett* **2010**, 19, 2905-2907; b) W. Mazumdar, N. Jana, B. T. Thurman, D. J. Wink, T. G. Driver, *J. Am. Chem. Soc.* **2017**, 139, 14, 5031–

5034; c) R. Zhang, J. C. Zhang, W. Y. Zhang, Y. Q. He, H. Cheng, C. Chen, Y. C. Gu, *Synth.* **2020**, *52*, 3286–3294; d) L. S. R. Yadav, R. Venkatesh, M. Raghavendra, T. Ramakrishnappa, N. Dhananjaya, G. Nagaraju, *Curr. Nanomater.* **2020**, 5, 1, 66-78(13); e) N. Vodnala, R. Gujjarappa, S. Polina, V. Satheesh, D. Kaldhi, A. K. Kabi, C. C. Malakar, *New J. Chem.* **2020**, 44, 48, 20940-20944.

[20] a) J. Li, D. huai Tu, J. Zhang, J. Li, Y. Xue, Q. Xu, Y. Du, C. Li, J. Lu, *Catal. Commun.* **2020**, 147, 106138; b) B. Karimi, F. Mansouri, H. Vali, *Chempluschem* **2015**, 80, 12, 1750-1759; c) K. Škoch, I. Císařová, P. Štěpnička, *Chem. - A Eur. J.* **2018**, 24, 52, 13788-13791; d) M. Tajbakhsh, R. Hosseinzadeh, Heshmatollah, Alinezhad, Parizad, Rezaee, M. Tajbakhsh, *Lett. Org. Chem.* **2013**, 10, 657-663.

[21] a) X. Wang, T. Gensch, A. Lerchen, C. G. Daniliuc, F. Glorius, *J. Am. Chem. Soc.* **2017**, 139, 18, 6506–6512; b) G. Lu, Y. Ren, B. Dong, B. Zhou, J. Ren, Y. Ke, B. B. Zeng, *Tetrahedron Lett.* **2019**, 60, 39, 150859; c) R. Ma, X. Chen, Z. Xiao, M. Natarajan, C. Lu, X. Jiang, W. Zhong, X. Liu, *Tetrahedron Lett.* **2021**, 63, 19, 152707; d) S. M. Mali, R. D. Bhaisare, H. N. Gopi, *J. Org. Chem.* **2013**, 78, 11, 5550–5555; e) K. N. Lee, Z. Lei, C. A. Morales-Rivera, P. Liu, M. Y. Ngai, *Org. Biomol. Chem.* **2016**, 14, 24, 5599-5605.

[22] a) Z. Wang, A. Matsumoto, K. Maruoka, *Chem. Sci.* **2020**, *11*, 12323–12328; b) Y. X. Liang, M. Yang, B. W. He, Y. L. Zhao, *Org. Lett.* **2020**, 22, 19, 7640–7644; c) A. Sen, R. N. Dhital, T. Sato, A. Ohno, Y. M. A. Yamada, *ACS Catal.* **2020**, 10, 14410-14418.

[23] a) M. Fairley, L. J. Bole, F. F. Mulks, L. Main, A. R. Kennedy, C. T. O'Hara, J. García-Alvarez, E. Hevia, *Chem. Sci.* **2020**, 11, 6500-6509; b) B. A. Mair, M. H. Fouad, U. S. Ismailani, M. Munch, B. H. Rotstein, *Org. Lett.* **2020**, 22, 7, 2746–2750; c) D. S. Barak, D. J. Dahatonde, S. U. Dighe, R. Kant, S. Batra, *Org. Lett.* **2020**, 22, 23, 9381–9385.

Chapter 4

Metal-free direct annulation of 2-aminophenols and 2-aminothiophenols with unactivated amides through transamidation: Access to polysubstituted benzoxazole and benzothiazole derivatives

Published: Tetrahedron. DOI: 10.1016/j.tet.2022.132794

Graphical Abstract

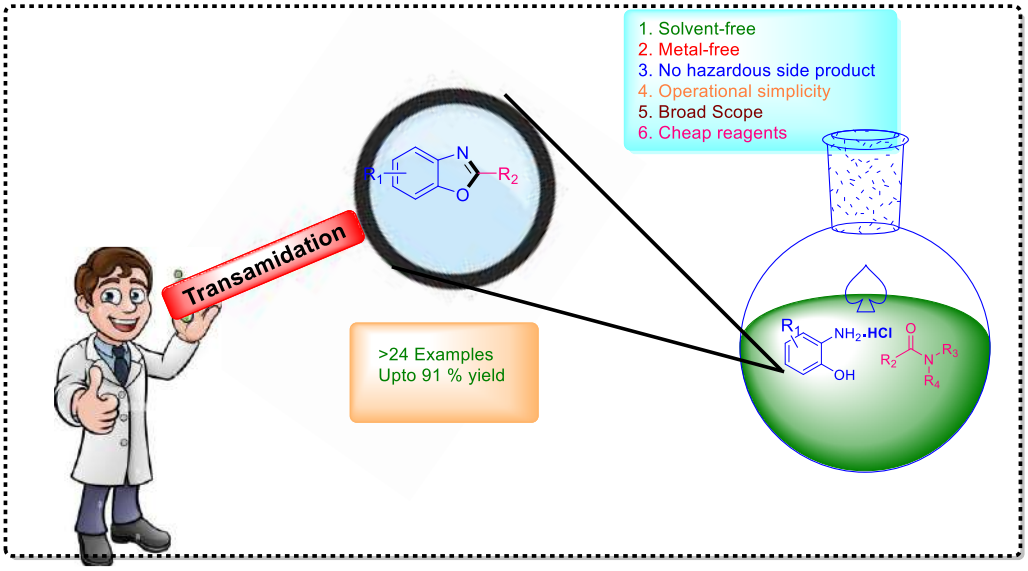

Abstract

We herein report a simple yet novel oxidant, metal and solvent-free green protocol for synthesising differently 2-substituted 1,3-benzoxazoles and benzothiazoles from 2-aminophenol hydrochloride salt unactivated amide as *in situ* carbon source. Further, the hydrogen ion of hydrochloride initially activates the amide, and then the key compound amine attacks as a nucleophile in the reaction. After that, the elimination of side product amine and de-hydrolysis lead to the final annulated product. This versatile strategy is applicable to a wide variety of differently substituted *o*-aminophenols, unactivated aliphatic and aromatic amides, yielding the corresponding product in good to excellent yields in a single step.

Keywords

2-Aminophenol, Amide, Hydrochloride salt, Metal-free chemistry, Annulation.

Introduction

The development of convenient, economical and effective greener methods for benzoxazole synthesis is gaining significant interest. Benzoxazole is an important precursor or building block for the synthesis of more complex chemical structures[1], including pharmaceuticals[2], agrochemicals[3], and natural products[4]. Among these, the 2-substituted 1,3-benzoxazoles scaffold is of particular interest due to its wide range of applications[5]. Despite the usefulness of previously reported benzoxazole synthetic methods, they suffered from disadvantages such as expensive starting materials and reagents, specific or transition metal catalysts[6], environmentally hazardous chemicals[7] and solvents. As a result, there has been an ever-increasing demand for exploring new economical and greener methods for the synthesis of 2-substituted benzoxazole[8].

Recently, our research group reported on the reaction of diverse unactivated amides with widely substituted anilines to produce transamidation products[9] (**Scheme 4-1**). This protocol proceeds without any difficulty utilising hydrochloric acid in toluene under metal-free, radiation-free, and oxidant-free conditions.

Scheme 4- 1. Previously explored transamidation reaction of unactivated amide.

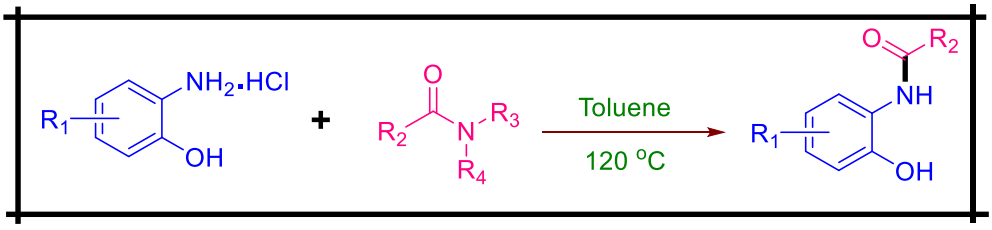

Our success in transamidation reactions[10] of 2-aminothiophenols with a variety of amides encouraged us to explore the cyclisation reactions of 2-aminothiophenols with a variety of amides under similar reaction conditions except for solvent (**Scheme 4-2**). Thus, in our present work, we report the synthesis of benzoxazoles *via* cyclisation of 2-aminophenols with unactivated amides under neat conditions. Further, the hydrogen ion of hydrochloride initially activates the amide, and then the key compound amine attacks as a nucleophile in the reaction. After that, the elimination of side product amine and de-hydrolysis lead to the final annulated product.

Scheme 4- 2. 2-substituted benzoxazole synthesis from substituted 2-aminophenols.

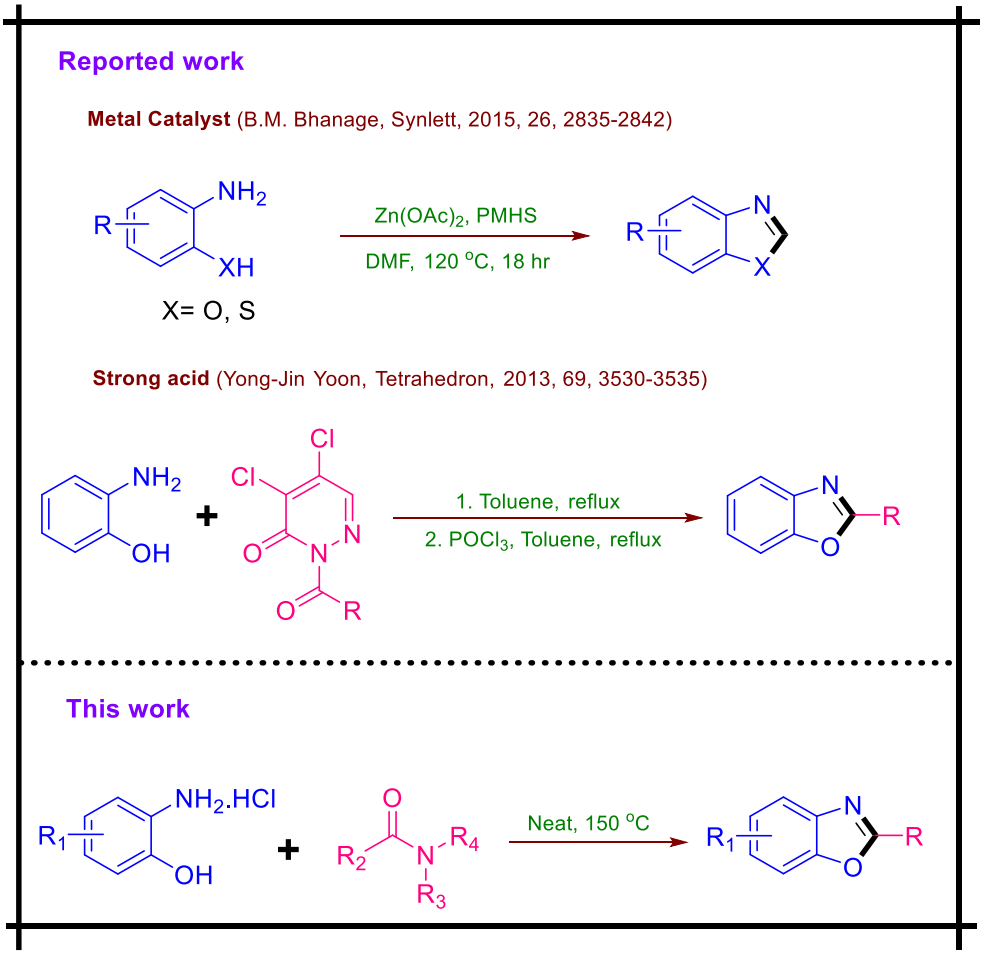

Result and Discussion

To optimise the reaction conditions of benzoxazole synthesis (**Table 4-1**), we studied the effect of HCl salt mediated benzoxazole synthesis using 5-methyl-2-aminophenol **1a** as a model substrate and N,N-dimethylacetamide **2a,** in the presence of toluene at 150 ^{o}C for 15 hrs. This reaction yielded good results. Subsequently, we screened different solvents such as DMSO, xylene, and NMP (**entries 2-4**), but no improvement in the yield was observed. However, solvent-free reaction (**entry 5**) afforded a slightly improved yield as compared to that obtained in NMP solvent (**entry 1)**. Further, the use of 4.0 equivalent (equiv.) of **2a** provided the best yield in the optimisation studies (**entries 6-9**). However, it was noted that excess of **2a** and longer duration of stirring resulted in no improvement in the yield, while shorter reaction time significantly decreased the reaction yield (**entries 11-13**). Subsequently, we investigated the effect of temperature on the reaction rate (**entries 15-17**) and observed that lower temperatures (**entries 15-16**) resulted in no formation of the desired product, whereas heating at 150 ^{o}C, resulted in excellent yields (**entry 17**). Finally, in terms of output, the optimal reaction condition was achieved when the reaction was carried out at 150 ^{o}C for 15.0 hours with 5-methyl-2-aminophenol (**1a**) and N,N-dimethylacetamide (**2a**), both as a reactant and solvent (**entries 9, 14** and **17**).

Table 4- 1. Optimisation studies for 2,5-dimethyl-1,3-benzoxazole from 5-methyl-2-aminophenol hydrochloride and acetamide.

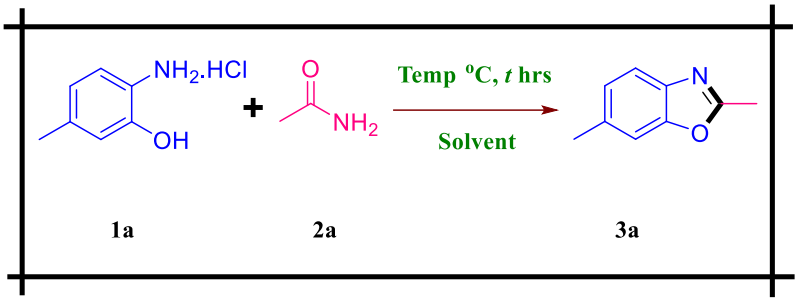

Solvent study				
S.NO.	**Solvent (5.0 Vol)**	**Temp (°C)**	**Time (hr)**	**% Yield[b]**
1[a]	Toluene	150	15	85
2[a]	DMSO	150	15	15
3[a]	Xylene	150	15	80
4[a]	NMP	150	15	60
5	**2a**	**150**	**15**	**91**
Eq. study of acetamide				
S.NO.	**Eq (2a)**	**Temp (°C)**	**Time (hr)**	**Yield[b]**
6	1	150	15	45
7	2	150	15	72
8	3	150	15	85
9	**4**	**150**	**15**	**90**
10	5	150	15	91
Time study				
S.NO.	**2a (4.0 eq)**	**Temp (°C)**	**Time (hr)**	**Yield[b]**
11[a]	2a	150	4	10
12[a]	2a	150	8	60
13[a]	2a	150	12	80
14[a]	**2a**	**150**	**15**	**90**
Temperature study				
S.NO.	**2a (4.0 eq)**	**Temp (°C)**	**Time (hr)**	**Yield[b]**
15[a]	2a	100	15	0
16[a]	2a	120	15	0
17[a]	**2a**	**150**	**15**	**90**

[a]Conditions: 5-methyl-2-aminophenol **1a** (1.0 mmol), N,N-dimethylacetamide **2a** (4.0 mmol). All the reactions were conducted under air. [b]Isolated yields.

Next, we explored the scope of different 2-aminophenols **1** with differently substituted tertiary amides **2** (**Table 4-2**). Initially, N,N-dimethylacetamide **2a** was reacted with several substituted 2-aminophenols (**1a-h**) (**entries 1-8**). Compounds **3a** and **3b** synthesised from 5-methyl (**1a**) and 4-methyl-2-aminophenol (**1b**) produced excellent yields (90 and 87% respectively), and when the reaction was carried out with 4-tertbutyl-2-aminophenol (**1c**), a similar result (91%) was obtained **3c**. To see the effect of electron-withdrawing groups, we included the chloro and nitro analogues (**entries 4-6**), which revealed that the yield of the desired product (**3d**) was higher for 4-chloro-2-aminophenol (**1d**) than those obtained from its 5-chloro-2-aminophenol (**1e**) and 5-nitro-2-aminophenol (**1f**) analogues. As a result of the electronic effect, the chloro on the meta position with respect to the amine of the 2-aminophenol produced an excellent yield. In addition, the heterocyclic compound (3-aminopyridin-3-ol, **1g**) provided a good yield of 2-methyloxazolo[5,4-b]pyridine (**3g**).

With the exception of N,N-dimethylacetamide (**2a**), a variety of derivatives of N,N-dimethylamide **2** bearing different R_1 groups such as butyramide (**2b**), valeramide (**2c**), 3,3-dimethylbutanamide (**2d**), isobutyramide (**2e**), pivalamide (**2f**), cyclopropanecarboxamide (**2g**), cyclohexanecarboxamide (**2h**), 2-phenylacetamide (**2i**), benzamide (**2j**), 2-phenoxyacetamide (**2k**), 2,2,2-trichloroacetamide (**2l**) and thiophene-2-carboxamide (**2m**) were reacted with 2-aminophenol (**1h**) employing optimised conditions (**entries 9-20**, **Table 4-2**). The steric hindrance of R_1 had a noticeable effect on this reaction, with the yield of **3** gradually reducing as the bulkiness of R_1 increased. (**entries 8-13**). The yields of benzoxazoles (**3n** and **3o**) obtained from the aliphatic cyclic amide (**2g** and **2h**) presented a similar trend suggesting steric hindrance affecting the product yields. Furthermore, aromatic amide derivatives (**entries 16-18**) resulted in a good yield (76-81%) of the desired products (**3p-3s**), respectively. Finally, trichloro substituted amide yielded the least of the corresponding product (**3t**), whereas heterocyclic amide (**2m**) yielded well under Standard conditions.

Table 4- 2. The HCl-promoted direct cyclisation of 2-aminophenols with amides: scope of amines and tertiary amides[a].

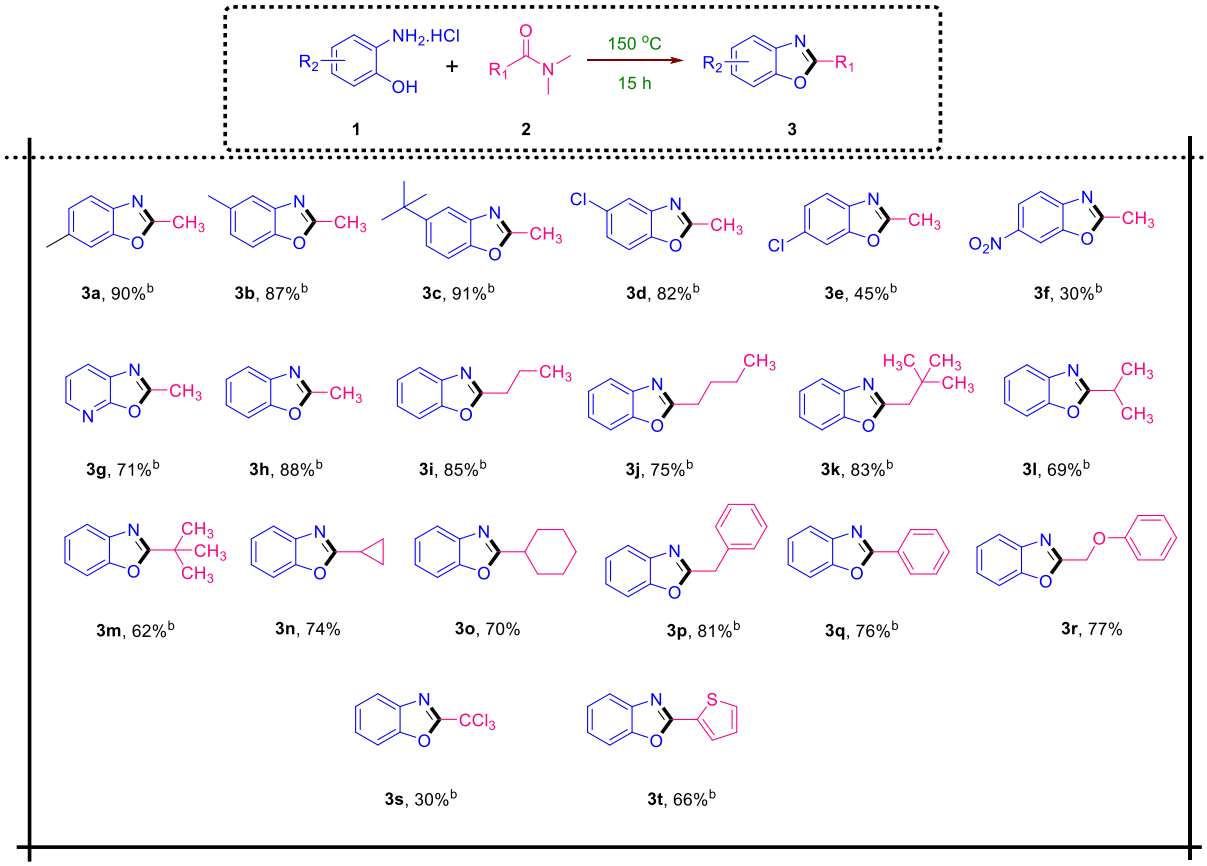

[a] Reaction conditions: A mixture of substituted 2-aminophenol hydrochloride salt **1** (1 mmol), amide **2** (4.0 mmol), 150 °C, 15 hr. [b] isolated yield.

Subsequently explored the synthesis of 1,3-benzoxazoles from primary, secondary and tertiary amides as shown in **Table 4-3**. First, experiments were carried out using 5-methyl-2-aminophenol with various substitutions at nitrogen atoms in acetamide (**Table 4-3**, **entries 1-4**). It was observed that increasing the carbon chain length and the number of nitrogen atom substitutions reduced the yield of the corresponding oxazole compounds. Similar results were obtained when benzamides were reacted with the aminophenol **1h** (**entries 5-8**).

Table 4- 3. HCl-promoted 2-substituted 1,3-benzoxazole synthesis from 2-aminophenols and amides: scope of primary, secondary and tertiary amides[a].

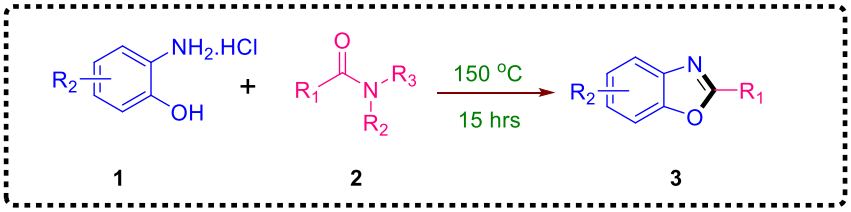

1 2 3

Entry	1	Amide 2	Benzoxzole 3	Yield[b]
1	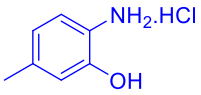	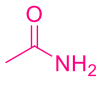	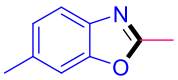	93%
	1a	2n	3a	
2	1a		3a	90%
		2o		
3	1a	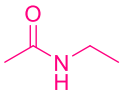	3a	79%
		2p		
4	1a	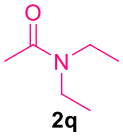	3a	68%
		2q		
5	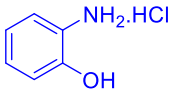	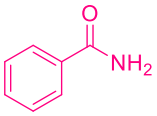	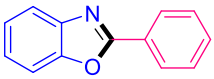	87%
	1h	2r	3o	
6	1h	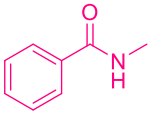	3o	81%
		2s		
7	1h	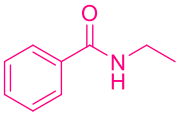	3o	64%
		2t		
8	1h	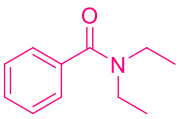	3o	53%
		2u		

[a] Reaction conditions: A mixture of substituted 2-aminophenol hydrochloride salt **1** (1 mmol), amide **2** (4.0 mmol), 150 °C, 15 hr.
[b] isolated yield.

After establishing a suitable novel method for 2-substituted benzoxazole synthesis from o-aminophenol, we further explored the possibility of synthesising benzothiazole by replacing o-aminophenol with o-aminothiophenol. To our delight, it was observed that the two aminothiophenol presented a good yield of corresponding benzothiazoles (**5a** and **5b**) (**scheme 4-3**).

Scheme 4- 3. Synthesis of 2-substituted benzothiazoles.

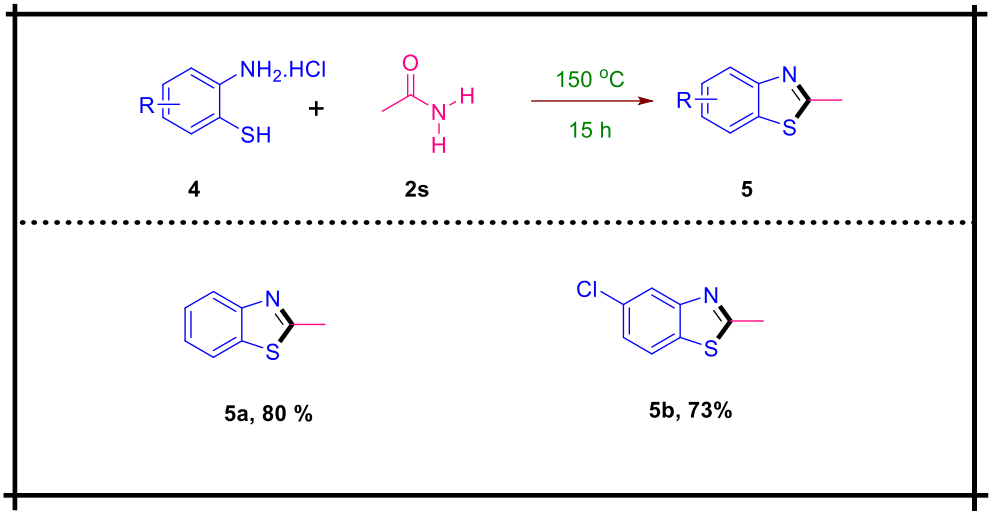

However, the reaction of 2-aminophenol (**1h**) with formamide (**2v**) did not yield the desired product **3v** (**Scheme 4-4**) and only resulted in the formation of intermediate transamidation product **6a**.

Scheme 4- 4. The reaction between 2-aminophenol hydrochloride salt with formamide under optimised conditions.

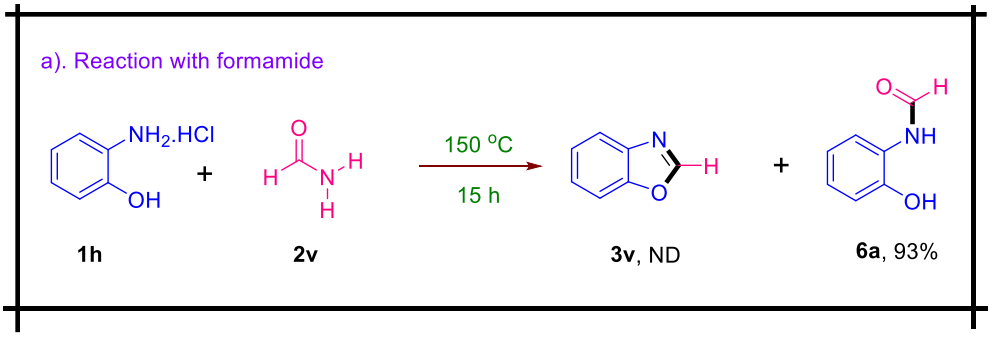

Mechanistic Study

Additionally, reactions performed at low temperatures did not result in the formation of the cyclised products, irrespective of the duration of stirring for 3 or 15 hrs (**Scheme 4-5a**), yielding only respective transamidation intermediate products. Thus, the annulation of the benzoxazole ring at a high temperature may correspond to the dehydration required temperature[9]. Subsequently, we examined the importance of hydrochloride salt based on the cyclisation reaction of 5-methyl-2-aminophenol (**1a**) with acetamide (**2a**) in the absence of hydrochloride (**Scheme 4-5b)**; however, no desired cyclised product[11] was obtained. Further, to determine whether a radical pathway was responsible for the annulation, an equivalent of TEMPO was introduced to the reaction mixture as a radical trap (**Scheme 4-5c**). The corresponding product, **3c**, was formed in 88 % yield. As a result, no discernible difference in the outcome occurred, indicating that the reaction did not occur *via* a radical process. In continuation, we investigated the reactivity of the intermediate species **6d** in the presence or absence of hydrochloride under the annulation condition (**Scheme 4-5d**). To begin, we observed that **6d** cyclised independently and generated around 10% of **3c**. Subsequently, we performed an experiment in which the intermediate was annulated in the presence of hydrochloride, noting that hydrochloride boosted the production of the product to over 90%. Thus, we concluded that hydrochloride was a critical activator of the amide and intermediate in the reaction[12]. Finally, to verify whether the amide's oxygen participates in the cyclisation, we performed an annulation reaction between amine **7** and amide **2a** (**Scheme 4-5e**), resulting in no cyclised product **3h,** but only the formation of transamidation product **8**, confirming that the amide's oxygen did not participate in the annulation.

Scheme 4- 5. Mechanistic Investigation Experiments.

a). Probing the Temperature effect

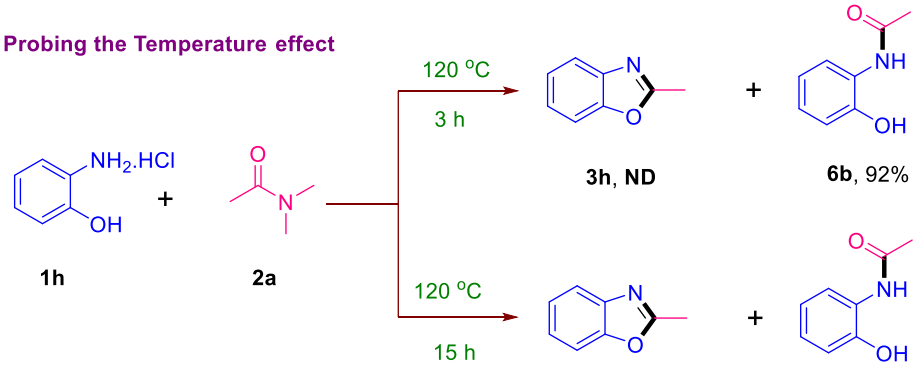

b). Probing the importance of HCl

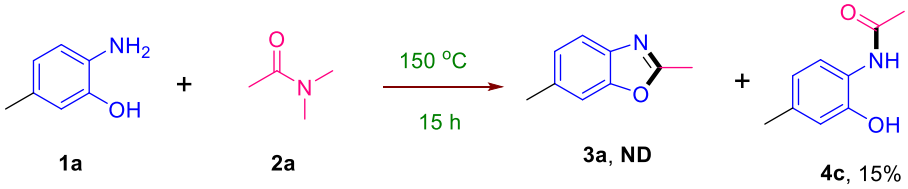

c). Probing the radical mechanism

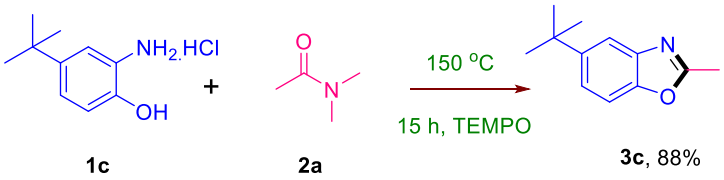

d). Probing the effect of HCl

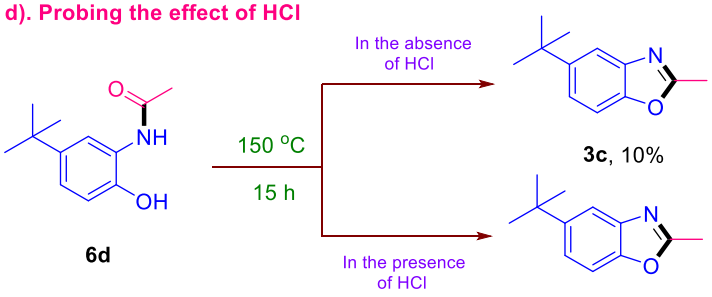

e). Probing the intermediacy of amide

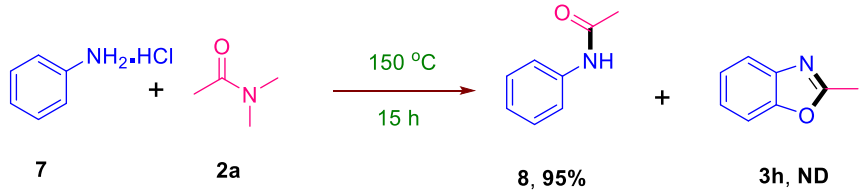

We proposed a probable mechanism based on the experimental data and published results[9] (**Scheme 4-6**). First, H ion activates the C-O bond of amide **2** to form cationic (highly electron-deficient centre) intermediate **a**, thereby promoting the nucleophilic attack of 2-aminophenol **1**, leading to a tetrahedral species **b**. The formation of transamidated compound **c** *via* elimination of the more basic amine of the amide with proton extraction from intermediate **b**. Eventually, an acidic proton activates the C-O bond (carbonyl) of compound **c**, creating an electron-deficient carbon again and in this instance, leading to intramolecular nucleophilic attack by phenol's oxygen resulting in a tetrahedral moiety **d**. Lastly, elimination of water from intermediate **e** to give the target compound **3**.

Scheme 4- 6. The plausible mechanism.

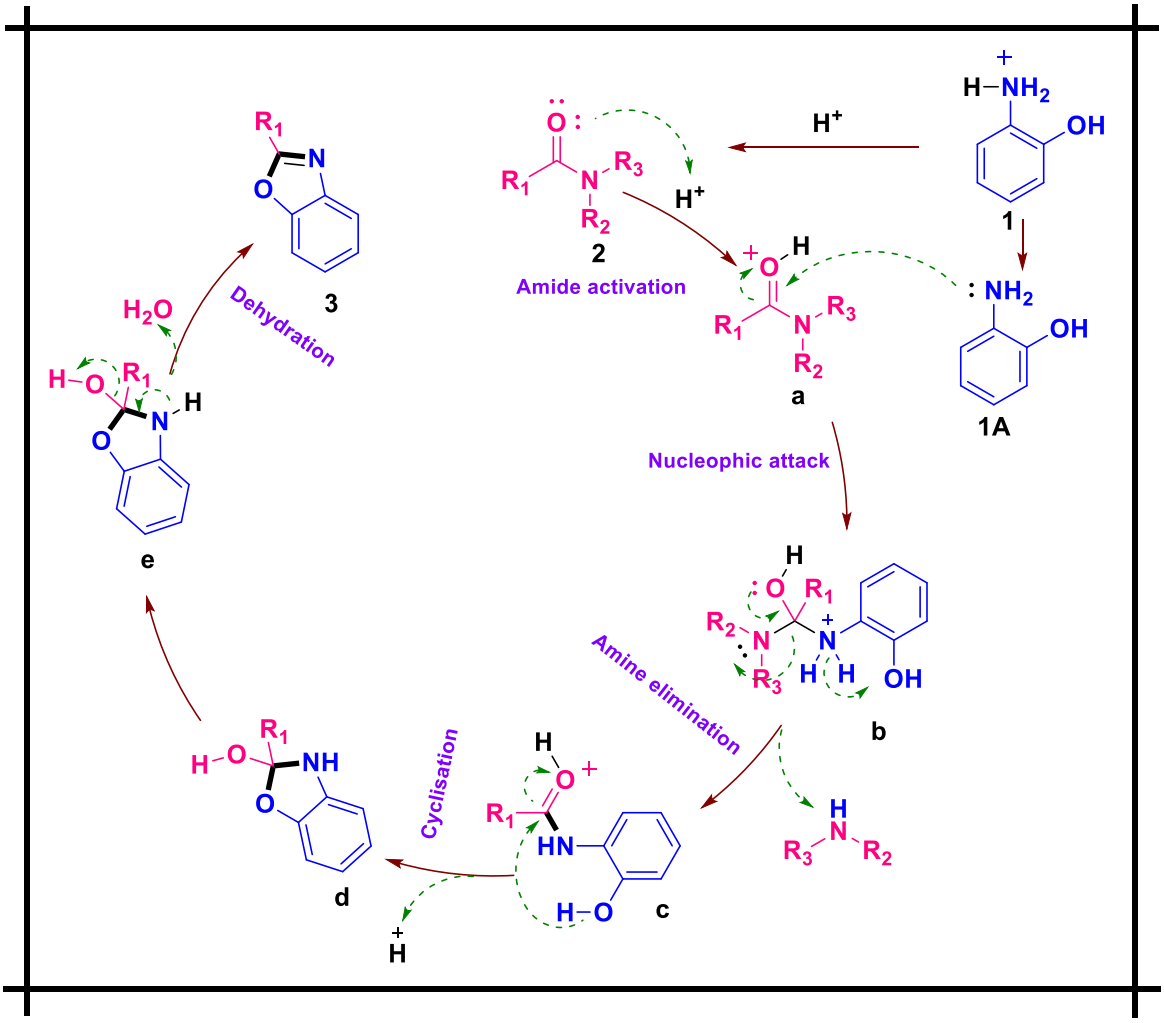

Conclusion

In summary, we have developed a very effective, base- and metal-free approach for synthesising a variety of benzoxazoles and benzothiazoles by employing unactivated amides as carbon sources. This methodology is versatile and applicable to a wide range of substrates to produce corresponding desired products. Furthermore, the protocol is simple and easy to handle, producing amines as by-products. Finally, this methodology is efficient and a more practical process as compared to previously reported methods.

Experimental Section

General Information

All reactions were conducted under standard operating conditions without the use of any stringent conditions. All chemicals were obtained from Aldrich Chemical Co., Alfa Aesar, used as received without additional purification. Lab reagent (LR) grade solvents were used for extraction and column chromatography purchased from Roma-chem. The reaction progress was monitored on Merck TLC Silica gel 60 F254 plates, and the spots were visualized under ultraviolet (UV) light, followed by iodine or ninhydrin staining solution followed by heating.

^{1}H and ^{13}C NMR spectra were recorded on 400, 100 MHz NMR spectrometer using $CDCl_3$ and DMSO-d_6 as solvents unless otherwise stated. Chemical shifts are expressed in parts per million (ppm) relative to TMS is used as an internal standard. Unless otherwise specified, all reagents were weighed and handled in air.

Experimental Procedure (EP-1)

A mixture of amine hydrochloride salt **1** (0.689 mmol) and amide **2** (2.75 mmol) under atmospheric air at 150 °C, stirred for 15.0 hrs in a sealed tube (20.0 ml). After bringing the mixture to room temperature, 10 mL water was added, and the mixture was extracted with DCM (3 X 5 Vol). The combined organic layers were dried with anhydrous Na_2SO_4. Under vacuum, the solvent was evaporated, and the crude product was purified using column chromatography (silica gel, EtOAc/Hexane) in order to obtain a pure product.

Procedure for Gram scale reaction

Gram scale preparation of 3p

A solution of 2-aminophenol hydrochloride salt **1h** (1 g, 6.89 mmol) and benzamide **2i** (3.34 g, 27.47 mmol) was stirred in a sealed tube (20.0 ml) under air at 150 °C for 15.0 hrs. After bringing the reaction was mixture to room temperature, added 10 mL water and the mixture was extracted with ethyl acetate (3 X 10 mL). The combined organic layers were dried with anhydrous Na_2SO_4. The solvent was evaporated under a vacuum. The crude product was purified using column chromatography (silica gel, EtOAc/Hexane 6:4) to obtain a pure product yield of 98% (1.03 g).

Analytical data of compounds

2,6-dimethylbenzo[d]oxazole[13] **(3a) (CAS No- 53012-61-6)**

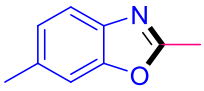

Yellow liquid; **^{1}H** NMR (400 MHz, $CDCl_3$): δ 7.47 (d, J = 8.0 Hz, 1H), 7.21 (s, 1H), 7.06 (d, J = 8.4 Hz, 1H), 2.56 (s, 3H), 2.42 (s, 3H) ppm; **^{13}C** NMR (100 MHz, $CDCl_3$): δ 163.3, 151.2, 139.1, 134.8, 125.3, 118.6, 110.4, 21.6, 14.4.

2,5-Dimethylbenzo[d]oxazole[13] **(3b) (CAS No- 5676-58-4)**

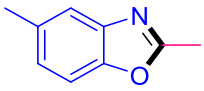

Yellow liquid; **^{1}H** NMR (400 MHz, $CDCl_3$): δ 7.41 (s, 1H), 7.30 (d, J = 8.4 Hz, 1H), 7.06 (d, J = 8.0 Hz, 1H), 2.59 (s, 3H), 2.42 (s, 3H) ppm; **^{13}C** NMR (100 MHz, $CDCl_3$): δ 164.0, 149.2, 141.5, 134.0, 125.7, 119.3, 109.6, 21.4, 14.5 ppm.

5-(Tert-butyl)-2-Methylbenzo[d]oxazole[14] **(3c) (CAS No- 40874-54-2)**

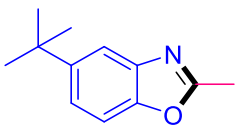

Yellow liquid; **^{1}H** NMR (400 MHz, $CDCl_3$): δ 7.70 (s, 1H), 7.42-7.37 (m, 2H), 2.65 (s, 3H), 1.40 (s, 9H) ppm; **^{13}C** NMR (100 MHz, $CDCl_3$): δ 164.1, 149.0, 147.9, 141.2, 122.3, 116.0, 109.5, 35.0, 31.9, 14.6 ppm.

5-chloro-2-methylbenzo[d]oxazole (3d)[13] **(CAS No- 19219-99-9)**

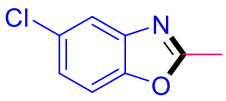

Light yellow solid; **^{1}H** NMR (400 MHz, $CDCl_3$): δ 7.60 (s, 1H), 7.35 (d, J = 8.8 Hz, 1H), 7.24 (d, J = 8.4 Hz, 1H), 2.61 (s, 3H) ppm; **^{13}C** NMR (100 MHz, $CDCl_3$): δ 165.6, 149.5, 142.3, 129.5, 124.9, 119.4, 111.1, 14.6 ppm.

6-chloro-2-methylbenzo[d]oxazole[13] **(3e) (CAS No- 63816-18-2)**

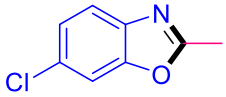

Light yellow solid; **^{1}H** NMR (400 MHz, $CDCl_3$): δ 7.54 (dd, J = 8.4 Hz, 1H), 7.47 (s, 1H), 7.27 (d, J = 8.4 Hz, 1H), 2.63 (s, 3H) ppm; **^{13}C** NMR (100 MHz, $CDCl_3$): δ 168.9, 146.9, 120.6, 119.5, 107.1, 15.0 ppm.

2-Methyl-5-Nitrobenzo[d]oxazole[15] **(3f) (CAS No- 5683-43-2)**

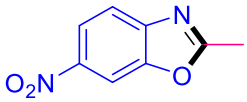

Off white solid; **^{1}H** NMR (400 MHz, $CDCl_3$): δ 8.40 (s, 1H), 8.28 (dd, J = 2.1, 8.8 Hz, 1H), 7.75 (d, J = 8.4 Hz, 1H), 2.73 (s, 3H) ppm; **^{13}C** NMR (100 MHz, $CDCl_3$): δ 168.9, 146.9, 120.6, 119.5, 107.1, 15.0 ppm.

2-methyloxazolo[4,5-b]pyridine[13] **(3g) (CAS No- 86467-39-2)**

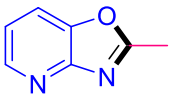

Off White solid; **^{1}H** NMR (400 MHz, $CDCl_3$): δ 7.85 (d, J = 4.0 Hz, 1H), 7.37 (d, J = 8.0 Hz, 1H), 7.12 (dd, J = 8.0, 4.0 Hz, 1H), 2.29 (s, 3H); **^{13}C** NMR (100 MHz, $CDCl_3$): δ 172.1, 145.4, 140.6, 138.2, 128.7, 122.9, 23.5 ppm.

2-methylbenzo[d]oxazole[13] **(3h) (CAS No- 86467-39-2)**

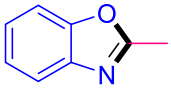

Off White solid; **^{1}H** NMR (400 MHz, $CDCl_3$): δ 7.67-7.65 (m, 1H), 7.47-7.45 (m, 1H), 7.29-7.26 (m, 2H), 2.63 (s, 3H); **^{13}C** NMR (100 MHz, DMSO-d_6): δ 172.1, 145.4, 140.6, 138.2, 128.7, 122.9, 23.5 ppm.

2-propylbenzo[d]oxazole[16] (3i) (CAS No- 2008-05-1)

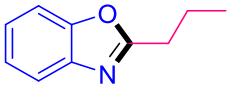

Brown liquid; **^{1}H** NMR (400 MHz, $CDCl_3$): δ 7.64 (dd, J = 7.2, 4.0 Hz, 1H), 7.45 (d, J = 8.0 Hz, 1H), 7.26-7.24 (m, 2H), 2.88 (t, 2H), 1.92-1.87 (m, 2H), 1.03 (t, 3H); **^{13}C** NMR (100 MHz, $CDCl_3$): δ 167.1, 150.6, 141.3, 123.9, 119.4, 110.3, 30.5, 20.3, 13.9 ppm.

2-butylbenzo[d]oxazole[16] (3j) (CAS No- 6797-49-5)

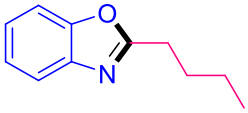

Brown liquid; ^{1}H NMR (400 MHz, DMSO-d_6): δ 7.66-7.63 (m, 1H), 7.59-7.57 (m, 1H), 7.29-7.27 (m, 2H), 2.86 (m, 2H) 1.77-1.69 (m, 2H),1.38-1.29 (m, 2H), 0.86 (t, 3H) ppm. **^{13}C** NMR (100 MHz, DMSO-d_6): δ 166.7, 150.2, 141.0, 124.3, 123.9, 119.1, 110.2, 28.1, 27.4, 21.5, 13.3 ppm.

2-(2,2-dimethylpropyl)-benzo[d]oxazole[17] (3k) (CAS No- 143857-68-5)

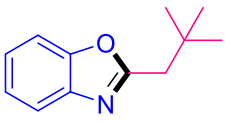

Light yellow solid; **^{1}H** NMR (400 MHz, $CDCl_3$): δ 7.69 (d, J = 3.2 Hz, 1H), 7.51 (m, 1H), 7.29 (m, 2H), 2.82 (s, 2H), 1.11 (s, 9H) ppm; **^{13}C** NMR (100 MHz, $CDCl_3$): δ 166.1, 150.9, 141.4, 124.5, 124.1, 119.7, 110.4, 42.5, 32.2, 29.7 ppm.

2-isopropylbenzo[d]oxazole[16] (3l) (CAS No- 6797-15-5)

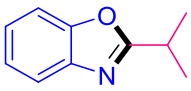

Light brown liquid; **^{1}H** NMR (400 MHz, DMSO-d_6): δ 7.68 (dd, J = 5.4, 3.4 Hz, 1H), 7.47 (dd, J = 5.8, 3.4 Hz, 1H), 7.29 (m, 2H), 3.25 (m, 1H), 1.46 (d, 6H) ppm; **^{13}C** NMR (100 MHz, $CDCl_3$): δ 173.6, 150.9, 141.4, 124.5, 124.1, 119.8, 110.4, 34.3, 28.6 ppm.

2-(tert-butyl)benzo[d]oxazole[16] (3m) (CAS No- 54696-03-6)

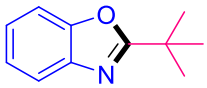

Brown liquid; **^{1}H** NMR (400 MHz, $CDCl_3$): δ 7.65 (dd, J = 5.4, 3.4 Hz, 1H), 7.43 (dd, J = 5.2, 3.6 Hz, 1H), 7.23 (m, 2H), 1.45 (s, 9H) ppm; **^{13}C** NMR (100 MHz, $CDCl_3$): δ 173.6, 150.9, 141.4, 124.5, 124.1, 119.8, 110.4, 34.3, 28.6 ppm.

2-cyclopropylbenzo[d]oxazole[16] (3n) (CAS No- 63359-58-0)

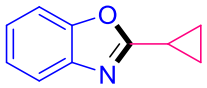

Brown liquid; **^{1}H** NMR (400 MHz, DMSO-d_6): δ 7.58 (d, J = 6.8 Hz, 1H), 7.38 (m, 1H), 7.21 (m, 2H), 2.17 (m, 1H), 1.23 (s, 2H), 1.12 (m, 2H) ppm; **^{13}C** NMR (100 MHz, $CDCl_3$): δ 168.6, 150.4, 141.5, 124.1, 123.9, 118.9, 109.9, 9.3, 9.1 ppm.

2-cyclohexylbenzo[d]oxazole[18] (3o) (CAS No- 104462-82-0)

Brown solid; **^{1}H** NMR (400 MHz, DMSO-d_6): δ 7.67-7.65 (m, 1H), 7.62-7.59 (m, 1H), 7.31-7.28 (m, 2H), 2.92 (tt, 1H), 2.06-2.02 (m, 2H), 1.74-1.69 (m, 2H), 1.63-1.57 (m, 3H), 1.39-1.29 (tq, 2H), 1.23 (tt, 1H); **^{13}C** NMR (100 MHz, DMSO-d_6): δ 169.5, 150.0, 140.9, 124.4, 123.9, 119.2, 110.3, 36.8, 29.8, 25.2, 24.8 ppm.

2-benzylbenzo[d]oxazole[19] (3p) (CAS No- 2008-07-3)

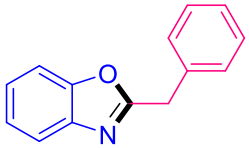

Light yellow solid; **^{1}H** NMR (400 MHz, $CDCl_3$): δ 7.68-7.66 (m, 1H), 7.41-7.39 (m, 1H), 7.35-7.34 (m, 2H), 7.31-7.27 (m, 2H), 7.24-7.22 (m, 3H), 4.22 (s, 2H). ppm; **^{13}C** NMR (100 MHz, $CDCl_3$): δ 165.2, 151.0, 141.3, 134.8, 129.0, 128.8, 127.3, 124.7, 124.2, 119.8, 110.4, 35.2 ppm.

2-phenylbenzo[d]oxazole (3r)[18] (CAS No- 833-50-1)

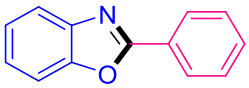

Off white solid; **^{1}H** NMR (400 MHz, $CDCl_3$): δ 8.28 (m, 2H), 7.79 (dd, J = 6.0, 3.2 Hz, 1H), 7.60 (dd, J = 5.6, 3.6 Hz, 1H), 6.54 (m, 3H), 7.37 (dd, J = 5.8, 3.4 Hz, 2H) ppm; **^{13}C** NMR (100 MHz, $CDCl_3$): δ 163.2, 150.8, 141.9, 131.8, 130.6, 129.1, 127.8, 125.4, 124.8, 120.1, 110.8 ppm.

2-(phenoxymethyl)benzo[d]oxazole[20] (3s) (CAS No- 7506-48-1)

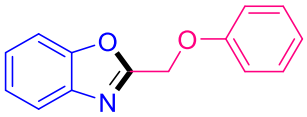

White solid; **^{1}H** NMR (400 MHz, $CDCl_3$): δ 7.65 (m, 1H), 7.43 (m, 1H), 7.22 (m, 4H), 6.95 (d, J = 8.4 Hz, 2H), 6.89 (t, 1H), 5.20 (s, 2H) ppm; **^{13}C** NMR (100 MHz, $CDCl_3$): δ 161.6, 157.9, 151.0, 140.7, 129.7, 125.6, 124.7, 122.0, 120.4, 114.9, 110.0, 62.8 ppm.

2-(trichloromethyl)benzo[d]oxazole[20] (3t) (CAS No- 14468-53-2)

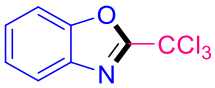

Brown solid; ^{1}H NMR (400 MHz, DMSO-d_6): δ 7.56 (dd, J = 7.96, 1.72 Hz, 1H), 7.10 (dt, 1H), 6.96 (dd, J = 8.12, 1.52 Hz, 1H), 6.85 (dt, 1H) ppm. **^{13}C** NMR (100 MHz, DMSO-d_6): δ 159.3, 149.9, 127.1, 123.8, 123.6, 119.1, 115.6, 92.7 ppm.

2-(thiophen-2-yl)benzo[d]oxazole[18] (3u) (CAS No- 23999-63-5)

Brown solid; ^{1}H NMR (400 MHz, DMSO-d_6): δ 7.96-7.94 (m, 2H), 7.76-7.72 (m, 2H), 7.43-7.36 (3, 1H), 7.31-7.29 (m, 1H) ppm. **^{13}C** NMR (100 MHz, DMSO-d_6): δ 158.3, 149.9, 141.4, 131.9, 130.5, 128.8, 128.5, 125.4, 124.9, 119.5, 110.7 ppm.

2-methylbenzo[d]thiazole[19] (5a) (CAS No- 120-75-2)

Brown liquid; ^{1}H NMR (400 MHz, DMSO-d_6): δ 7.99 (dd, J = 8.24, 1.04 Hz, 2H), 7.92 (d, J = 9.04 Hz, 1H), 7.45 (dt, 1H), 7.37 (dt, 1H), 2.77 (s, 3H) ppm. **^{13}C** NMR (100 MHz, DMSO-d_6): δ 166.8, 152.9, 135.2, 125.9, 124.6, 121.9, 121.8, 19.7 ppm.

5-chloro-2-methylbenzo[d]thiazole[19] (5b) (CAS No- 1006-99-1)

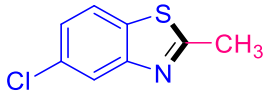

Brown solid; ^{1}H NMR (400 MHz, DMSO-d_6): δ 8.06 (d, J = 8.56 Hz, 1H), 7.97 (d, J = 2.08 Hz, 1H), 7.43 (dd, J = 8.56, 2.08 Hz, 1H), 2.80 (s, 3H) ppm. **^{13}C** NMR (100 MHz, DMSO-d_6): δ 169.6, 153.8, 133.9, 130.7, 124.8, 123.4, 121.4, 19.8 ppm.

References

[1] a) I. J. Turchi, *Industrial and Engineering Chemistry Product Research and Development* **1981**, 20, 1, 32-76; b) I. V. Smolyar, A. K. Yudin, V. G. Nenajdenko, *Chem. Rev.* **2019**, 119, 17, 10032-10240; c) J. Zhang, P. Y. Coqueron, M. A. Ciufolini, *Heterocycles* **2010**, 82, 2, 949-980; d) K. Passador, S. Thorimbert, C. Botuha, *Synthesis (Germany)* **2019**, 51, 02, 384-398.

[2] a) H. Z. Zhang, Z. L. Zhao, C. H. Zhou, *European Journal of Medicinal Chemistry* **2018**, 144, 444-492; b) S. Kakkar, B. Narasimhan, *BMC Chemistry* **2019**, 13, 16; c) N. Y. Guerrero-Pepinosa, M. C. Cardona-Trujillo, S. C. Garzón-Castaño, L. A. Veloza, J. C. Sepúlveda-Arias, *Biomedicine and Pharmacotherapy* **2021**, 138, 111495; d) R. Kaur, K. Palta, M. Kumar, M. Bhargava, L. Dahiya, *Expert Opinion on Therapeutic Patents* **2018**, 28, 11, 783-812.

[3] a) J. T. Mhlongo, E. Brasil, B. G. de la Torre, F. Albericio, *Marine Drugs* **2020**, 18,4 203; b) C.

Lamberth, *J Heterocycl Chem* **2017**, 54, 2974.

[4] a) Z. Jin, *Nat. Prod. Rep.* **2011**, 28, 1143-1191; b) S. Tilvi, K. S. Singh, *Current Organic Chemistry* **2016**, 20, 8, 898-929; c) Z. Jin, *Nat. Prod. Rep.* **2013**, 30, 869-915; d) Z. Jin, *Nat. Prod. Rep.* **2009**, 26, 382-445; e) Z. Jin, Z. Li, R. Huang, *Nat. Prod. Rep.* **2002**, 19, 545-476; f) Z. Jin, *Nat. Prod. Rep.* **2006**, 23, 464-496.

[5] a) X. K. Wong, K. Y. Yeong, *ChemMedChem* **2021**, 16, 21, 3237-3262; b) R. V. Kumar, *Asian Journal of Chemistry* **2004**; c) C. S. Demmer, L. Bunch, *European Journal of Medicinal Chemistry* **2015**, 97, 778-785.

[6] a) S. Bresciani, N. C. O. Tomkinson, *Heterocycles* **2014**, 89, 11, 2479-2543; b) S. Ueda, H. Nagasawa, *Angewandte Chemie* **2008**, 120, 34, 6511-6513; c) A. R. Hajipour, Z. Khorsandi, *New J. Chem.* **2016**, 40, 10474-10481; d) F. Wu, J. Zhang, Q. Wei, P. Liu, J. Xie, H. Jiang, B. Dai, *Org. Biomol. Chem.* **2014**, 12, 9696-9701; e) M. Zhang, *Advanced Synthesis and Catalysis* **2009**, 351, 14-15, 2243-2270; f) K. Oshimoto, H. Tsuji, M. Kawatsura, *Org. Biomol. Chem.* **2019**, 17, 4225-4229; g) L. A. Nguyen, T. T. T. Nguyen, Q. A. Ngo, T. B. Nguyen, *Org. Biomol. Chem.* **2021**, 19, 6015-6020; h) G. Chakraborty, R. Mondal, A. K. Guin, N. D. Paul, *Org. Biomol. Chem.* **2021**, 19, 7217-7233; i) D. B. Nale, B. M. Bhanage, *Synlett* **2015**, 26, 20, 2835-2842.

[7] a) M. S. Rao, S. Hussain, *Synthetic Communications* **2021**, 51, 17, 2684-2694; b) J. Zhang, L. Hu, Y. Liu, Y. Zhang, X. Chen, Y. Luo, Y. Peng, S. Han, B. Pan, *J. Org. Chem.* **2021**, 86, 21, 14485-14492; c) G. H. Sung, I. H. Lee, B. R. Kim, D. S. Shin, J. J. Kim, S. G. Lee, Y. J. Yoon, *Tetrahedron* **2013**, 69, 17, 3530-3535.

[8] a) S. Rajasekhar, B. Maiti, K. Chanda, *Synlett* **2017**, 28, 05, 521-541; b) X. Liu, Z. B. Dong, *European Journal of Organic Chemistry* **2020**, 4, 408-419; c) S. Dhawan, V. Kumar, P. S. Girase, S. Mokoena, R. Karpoormath, *ChemistrySelect* **2021**, 6, 4, 754-787. d) S. R. Shinde, P. Girase, S. Dhawan, S. N. Inamdar, V. Kumar, C. Pawar, M. B. Palkar, M. Shinde, R. Karpoormath, Synthetic Communications **2021**, 52, 1, 1-36.

[9] V. Kumar, S. Dhawan, P. S. Girase, P. Singh, R. Karpoormath, *European Journal of Organic Chemistry* **2021**, 41, 5627-5639.

[10] a) G. Li, M. Szostak, Synthesis **2020**, 52, 18, 2579-2599. b) G. Li, C. Ji, X. Hong, M. Szostak, J. Am. Chem. Soc. **2019**, 141, 28, 11161-11172. c) M. Rahman, G. Li, M. Szostak, J. Org. Chem. **2019**, 84, 18, 12091-12100. d) S. Dhawan, P. S. Girase, V. Kumar, R. Karpoormath, Synthetic Communications **2021**, 51, 24, 3729-3739. e) P. S. Girase, V. Kumar, S. Dhawan, R. Karpoormath, ChemistrySelect 2022, 7, e202103237.

[11] J. Yin, J. Zhang, C. Cai, G. J. Deng, H. Gong, *Org. Lett.* **2019**, 21, 2, 387-392.

[12] a) L. Wang, X. Ren, J. Yu, Y. Jiang, J. Cheng, *J. Org. Chem.* **2013**, 78, 23, 12076-12081; b) K. L. Li, Z. B. Du, C. C. Guo, Q. Y. Chen, *J. Org. Chem.* **2009**, 74, 9, 3286-3292; c) V. Venkateswarlu, K. A. A. Kumar, S. Balgotra, G. L. Reddy, M. Srinivas, R. A. Vishwakarma, S. D. Sawant, *Chemistry - A European Journal* **2014**, 20, 22, 6641-6645.

(13) Mayo, M. S.; Yu, X.; Zhou, X.; Feng, X.; Yamamoto, Y.; Bao, M. Synthesis of Benzoxazoles from 2-Aminophenols and β-Diketones Using a Combined Catalyst of Brønsted Acid and Copper Iodide. *J. Org. Chem.* **2014**. 79, 13, 6310-6314.

(14) Li, K. L.; Du, Z. B.; Guo, C. C.; Chen, Q. Y. Regioselective Syntheses of 2- and 4-Formylpyrido[2,1-b]Benzoxazoles. *J. Org. Chem.* **2009**. 74, 9, 3286-3296.

(15) Zhang, P.; Cedilote, M.; Cleary, T. P.; Pierce, M. E. Mono-Nitration of Aromatic Compounds via Their Nitric Acid Salts. *Tetrahedron Lett.* **2007**. 48, 49, 8659-8664.

(16) Niu, Z. J.; Li, L. H.; Liu, X. Y.; Liang, Y. M. Transition-Metal-Free Alkylation/Arylation of Benzoxazole via Tf2O-Activated-Amide. *Adv. Synth. Catal.* **2019**. 361, 22, 5217-5222.

(17) Dong, K.; Humeidi, A.; Griffith, W.; Arman, H.; Xu, X.; Doyle, M. P. Ag I -Catalyzed Reaction of Enol Diazoacetates and Imino Ethers: Synthesis of Highly Functionalized Pyrroles . *Angew. Chemie* **2021**. 60, 24, 13394-13400.

(18) Putta, R. R.; Chun, S.; Choi, S. H.; Lee, S. B.; Oh, D. C.; Hong, S. Iron(0)-Catalyzed Transfer Hydrogenative Condensation of Nitroarenes with Alcohols: A Straightforward Approach to

Benzoxazoles, Benzothiazoles, and Benzimidazoles. *J. Org. Chem.* **2020**. 85, 23, 15396-15405.

(19) Zhang, J.; Hu, L.; Liu, Y.; Zhang, Y.; Chen, X.; Luo, Y.; Peng, Y.; Han, S.; Pan, B. Elemental Sulfur-Promoted Benzoxazole/Benzothiazole Formation Using a C═C Double Bond as a One-Carbon Donator. *J. Org. Chem.* **2021**. 86, 21, 14485-14492.

(20) Luo, B.; Li, D.; Zhang, A. L.; Gao, J. M. Synthesis, Antifungal Activities and Molecular Docking Studies of Benzoxazole and Benzothiazole Derivatives. *Molecules* **2018**. 23, 10, 2457.

Chapter 5

Cu-Catalysed Transamidation of Unactivated Aliphatic Amides

- **Published:** Organic and Biomolecular Chemistry. DOI:10.1039/D2OB01152B

Graphical Abstract

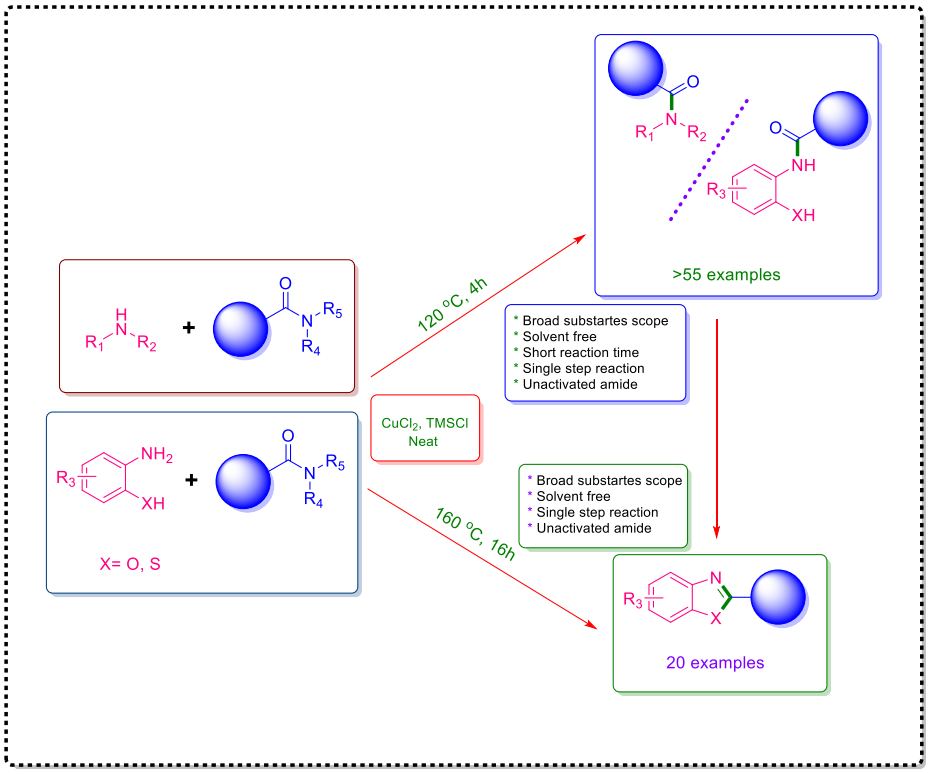

Abstract

Direct transamidation is gaining prominence as a ground-breaking technique that generates a wide variety of amides without the requirement for acid-amine coupling or other intermediate steps. However, transamidation of unactivated aliphatic amides, on the other hand, has been a long-standing issue in comparison to transamidation of activated amides. Herein, we report a transamidation approach of an unactivated aliphatic amide using a copper catalyst and chlorotrimethylsilane as an additive. In addition, we used transamidation as a tool for selective N-C(O) cleavage and O-C(O) formation to synthesise 2-substituted benzoxazoles and benzothiazoles. The reactions were carried out without using any solvents and offered a wide range of substitutions scope.

Keyword

Transamidation, Unactivated, Alipahtic, amide, Annulation, Benzoxazole, Benzothiazole.

Introduction

Amide-bond carried compounds earn an excellent reputation as a fundamental moiety in natural products, chemistry[1,2], biology[3,4], agrochemicals[5], proteins[6,7], lubricants[8], and plastics[9]. In particular, the aliphatic amide bond is a core building block of pharmaceuticals such as Zolpidem[10], levomilnacipran[11], Phenacetin[12], Afatinib[13], and Paracetamol[14] (**Fig 5-1a**). Thus, the amide C-N bond synthesis[1,2,15,16] piques the curiosity of chemists in organic chemistry. The most common method of synthesising amides is through the reaction of acid chloride or acid with amines[17], metal-catalysed hydration of nitriles[18], oxidative amidation[19] of various groups such as aldehyde, benzyl alcohols, methyl ketone or methyl arenes and oxidation of primary benzyl amines, rearrangement of aldoximes[20] and decarboxylative ammoxidation of phenylacetic acid which is also achievable on both a laboratory and commercial scale. Indeed, several naming reactions have been reported for amide bonds formation[21–23]. Nevertheless, these processes exhibit limitations, including chemo- and regioselectivity, narrow substrate scope, and the employment of activating reagents. As a result, these limitations motivate synthetic chemists academics to advance their research into the amide bond N-C(O).

Transamidation is a direct conversion of one amide to another and has risen to prominence in recent decades[17,24,25]. Indeed, transamidation has advantages in pharmaceutical and other industries, such as reduced multistep coupling reactions, activating reagents, and selectivity that is more cost-effective on a wide scale. However, transamidation is a more challenging technique to make amides more diverse because of their conjugated structure making them less reactive than other carbonyl compounds[24,26-29] (**Fig 5-1b**). Consequently, the C-N amide bond is activated in two promising ways: 1) To weaken an amide bond via the nitrogen atom of amide have been activated using boc-anhydride, tosyl, or mesyl functionalisation[28]; however, this step has disadvantages because it is a two-step reaction and only primary and secondary amides have predominantly been explored because an activating group can replace the one proton of amide; 2) catalysed activation of the C-N bond by a transition metal[24,25,17,30].

Numerous research groups have developed and employed transamidation that involves preactivating the N-C(O) amide bond by using an N-protecting group such as N-Boc, N-Ts, pyrazoles, or succinimide[31-33]. Whether or not there is a transition metal, these strategies have worked[25,30]. In particular, the Szostak research group demonstrated that transamidation of activated amide could be carried out with or without the assistance of metal catalysts[31,34-37] (**Fig 5-1c**). In addition, Lee and colleagues described a metal-free transamidation reaction using benzoylpyrrolidinone amide[38] (**Fig 5-1c**). On the other hand, Dander et al. came up with a nickel-mediated system that aliphatic amides diversification could be worked *via* transamidation[39] (**Fig 5-1c**). However, the generation of side products of these approaches as the leaving group adds another disadvantage in terms of atom economy along with other drawbacks.

In recent years, various metal-mediated methodologies have also effectively transformed amides *via* amide bond activation[30]. These approaches performed admirably, but they are limited to individually primary[25], secondary[37,40,41], and tertiary amides[38,42,43], not to all amides. The current work is based on the copper-mediated transamidation of primary, secondary, and tertiary aliphatic amides as well as their application in benzoxazoles/benzothiazoles synthesis *via* intramolecular annulation. Furthermore, the absence of an activating group on the nitrogen atom of amide could widen the scope of reaction as tertiary amide, making this methodology critical.

Result and Discussion

Reaction Condition Optimisation

We chose N,N-dimethylcyclohexanecarboxamide **1I** and aniline **2A** as model substrates and carried out reactions between them under various reaction circumstances to optimise the standard conditions and their results are summarised in **Table 5-1-1**, **Table 5-1-2**, and **Table 5-1-3**. A copper-catalysed model reaction between **1I** and **2A** in toluene was carried out at 120 °C for 10 hours with TMSCl as a Lewis acid that

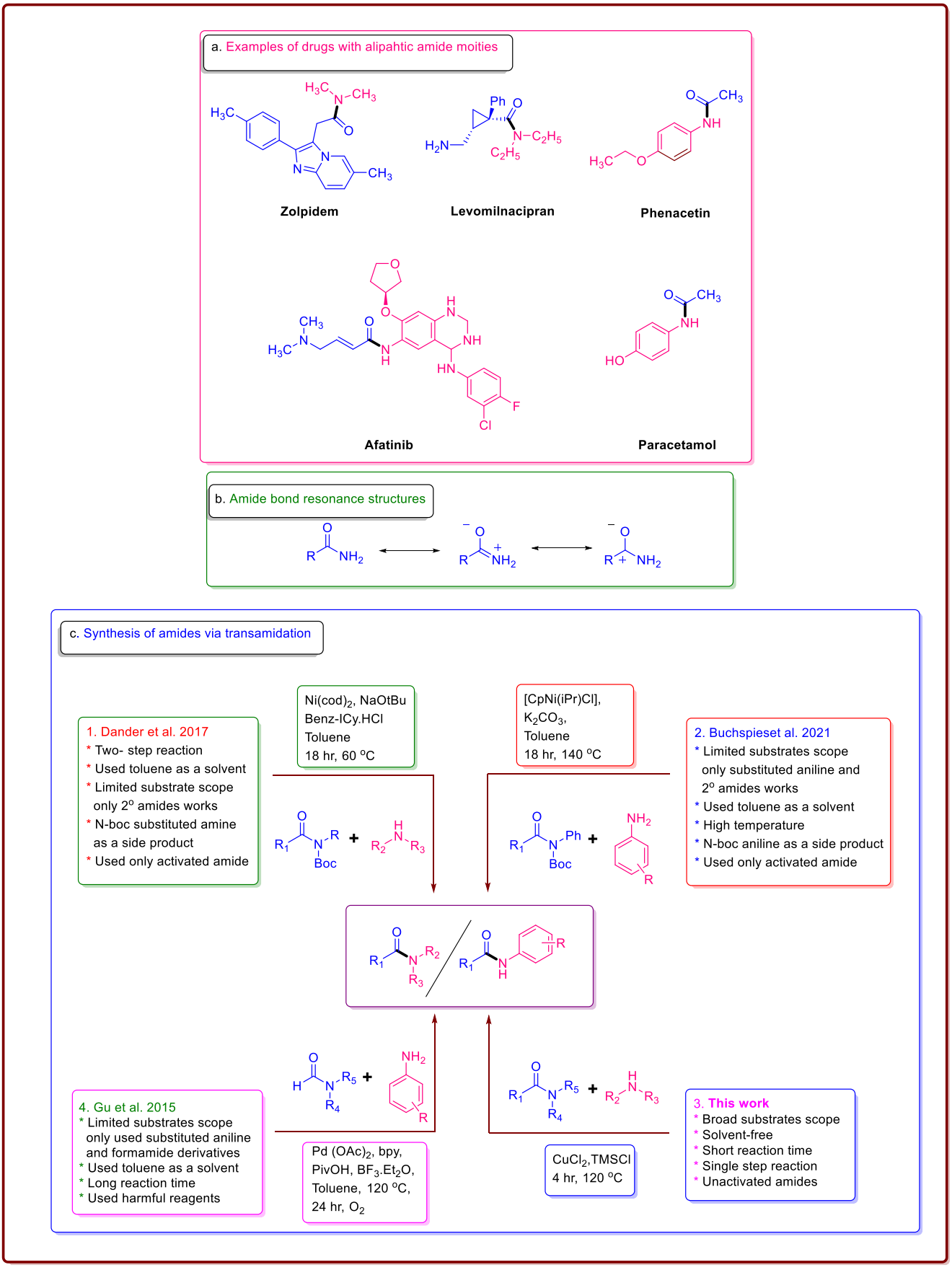

*Figure 5- 1. **Examples of drugs with aliphatic amide moieties***

activated the amide. $CuCl_2$ was used as a catalyst in the transamidation of **1I**, yielding 72 % of the amide product (entry 1 and **Table 5-1-1**). The replacement of $CuCl_2$ with other Cu and metal catalysts (Pd and Ni) did not show any significant improvement (entries 2-9 and **Table 5-1-1**).

Additionally, the other copper catalysts generated acceptable but not optimal results. Next, we looked at Lewis acids that had previously been utilised in transamidation, but none of them expressed satisfaction with the method (entries 1-4 and **Table 5-1-2**). Following that, we evaluated alternate solvents for toluene, including xylene, NMP, and DMSO (entries 2-7 and **Table** 5**-1-3**). Neither one of those solvents performed well in the transformation of **1I**, although the reaction without the solvent produced a higher yield than the toluene reaction (entry 5 and **Table 5-1-3**). Based on the results of the preceding experiments, we chose $CuCl_2$ as a catalyst and TMSCl as a Lewis acid additive, and this reaction proceeded smoothly without the use of a solvent.

Furthermore, we investigated other reaction conditions, including the equivalent (equiv), temperature, and duration, all of which are critical components. First, we started flatulating the proportion of amine, finding that less quantity (1.0 equiv) of **2A** resulted in less transformation and that more quantity (2.0 equiv) had no discernible effect on the results (entries 1-3 and **Table 5-1-4**). Concentrating on the quantity of catalyst, decreasing the mol% from 20 to 0 in various portions such as 15, 10, and 0 led to a decline in yield, however raising the $CuCl_2$ loading to 40 mol% resulted in no significant increase in output (entries 4-8 and **Table 5-1-4**). Reaction temperature studies further revealed that the reaction accelerated slowly at the lower temperature range, whereas the higher temperature did not rise in the impurity profiles and transformation of **1I** (entries 9-13 and **Table 5-1-4**). Turning the focus to the quantity of TMSCl, these trials demonstrated that a less equiv resulted in a lower conversion rate and a higher proportion resulted in similar results (entries 14-17 and **Table 5-1-4**). Finally, we examined the effect of time on reaction outcome. We determined that the reaction was complete after four hours but that more stirring time had no destructive impact on production. From all of these reaction parameters optimisation studies, we found that **2A** (1.5 equiv), $CuCl_2$ (20 mol %), and TMSCl (1.5 equiv) in solvent-free conditions produced the best outcome for this transamidation reaction.

Table 5- 1. Reaction conditions optimisation for transamidation of aliphatic N,N-dimethylcyclohexanecarboxamide with aniline.

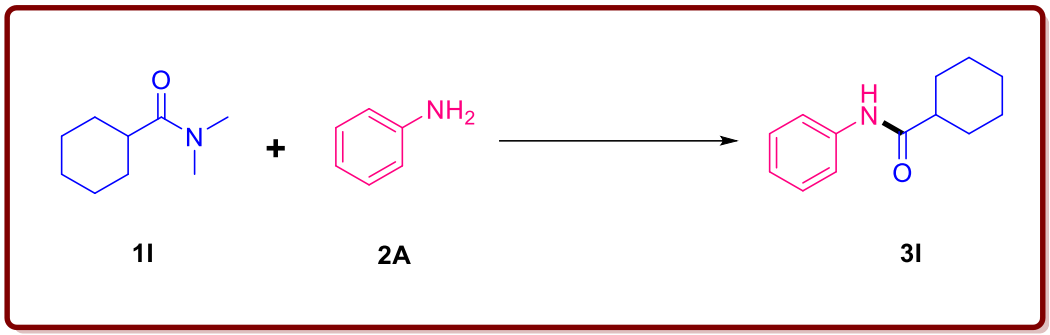

*Table 5-1- 1:- Catalyst Study**

Entry	Catalyst (20 mol%)	Yield[#]
1	**$CuCl_2$**	**72**
2	$CuBr_2$	61
3	CuCl	5
4	CuBr	4
5	CuI	3
6	$Cu(OTf)_2$	41
7	$Cu(OAc)_2$	52
8	$PdCl_2$	traces
9	$NiCl_2$	20

*Reaction conditions: 1I (1.1 mmol), 2A (1.61 mmol) and TMSCl (1.61 mmol) were reacted in Toluene (1.0 mL) at 120 °C for 10 h. [#]Isolation by using column chromatography.

*Table 5-1- 2:- Lewis acid study**

Entry	Lewis acid (Equiv)	Yield (%)[#]
1	**TMSCl**	**72**
2	$FeCl_3$	13
3	$AlCl_3$	9
4	TiCl4	traces

*Reaction conditions: 1I (1.1 mmol), 2A (1.61 mmol) and $CuCl_2$ (0.22 mmol) were reacted in Toluene (1.0 mL) at 120 °C for 10 h. [#]Isolation by using column chromatography.

*Table 5-1- 3:- Solvent-Study**

Entry	Solvent	Yield (%)[#]

1	Toluene	72
2	Xylene	69
3	NMP	79
4	DMSO	traces
5[$]	**Neat**	**87**
6	Chlorobenzene	45
7	n-Butanol	0

*Reaction conditions: 1I (1.1 mmol), 2A (1.61 mmol) and $CuCl_2$ (0.22 mmol) were reacted in Toluene (1.0 mL) at 120 °C for 10 h. [#]Isolation by using column chromatography. [$]Without solvent under same condition.

*Table 5-1- 4:- Equiv, time and temperature study**

Entry	Aniline 2A (equiv)	$CuCl_2$ (mol%)	Temperature (°C)	TMSCl (equiv)	Time (hr)	Yield (%)[#]
1	1.0	20.0	120	1.5	10	56
2	1.5	20.0	120	1.5	10	87
3	2.0	20.0	120	1.5	10	88
4	1.5	0.0	120	1.5	10	10
5	1.5	10.0	120	1.5	10	70
6	1.5	15.0	120	1.5	10	81
7	1.5	30.0	120	1.5	10	86
8	1.5	40.0	120	1.5	10	87
9	1.5	20.0	80	1.5	10	0
10	1.5	20.0	100	1.5	10	35
11	1.5	20.0	110	1.5	10	72
12	1.5	20.0	130	1.5	10	85
13	1.5	20.0	140	1.5	10	88
14	1.5	20.0	120	0	10	0
15	1.5	20.0	120	0.5	10	10
16	1.5	20.0	120	1.0	10	55
17	1.5	20.0	120	2.0	10	89
18	1.5	20.0	120	1.5	2	60
19	**1.5**	**20.0**	**120**	**1.5**	**4**	**87**

20	1.5	20.0	120	1.5	6	85
21	1.5	20.0	120	1.5	8	89

*Reaction conditions: 1A (1.0 eq). #Isolation by using column chromatography.

Scope of Transamidation

Amide Scope

Using optimised reaction parameters, we reacted aniline **2A** and 2-aminophenol **5A** to investigate the scope of this transformation with a variety of aliphatic amides **1** (**Scheme 5-1**). All transamidation amide products **3** conversions proceeded efficiently with good yields following purification. N,N-dimethylformamide **1A** yielded the desired amide **3A** in 94% isolated yield. The corresponding compounds **3B** and **3C** were synthesised in 92% and 90% yields, respectively, from N,N-dimethylacetamide **1B** and N,N-dimethylpentanamide **1C** to react with 2-aminopehnol **5A**. It was found that long-chain amide such as N,N-dimethylpentanamide **1C** performed admirably in the transamidation procedure. However, the transamidation result of N,N,3,3-tetramethylbutanamide **1D** was more reasonable due to less blockage. Despite this, we noticed a steric hindrance effect on yield when N,N-dimethylisobutyramide **1E** and N,N-dimethylpivalamide **1F** were reacted with **2A**. The discrepancy in the results of **3E** and **3F** from their respective reactions indicated that the bulky group affects the transamidation process yield. The steric hindrance of the CCl_3 group on carbonyl may be the explanation for the **1G** transformation's poor performance compared to the other amides. This fact is supported by the subsequent amide **1G** transformation, which produced a meager result compared to the other reactions. In Contrast, cyclic amides such as N,N-dimethylcyclopropanecarboxamide **1H** and N,N-dimethylcyclohexanecarboxamide **1I** achieved acceptable yields (86% and 79%, respectively) of the corresponding products (**3H** and **3I**). While the reaction performed with those aliphatic amides which has aromatic system such as N,N-dimethyl-2-phenylacetamide **1J** and N,N-dimethyl-2-phenoxyacetamide **1K** performed under these conditions and reacted with aniline **2A** formed transamideted products **3J** and **3K**, respectively at 87% and 89% conversion rate, respectively.

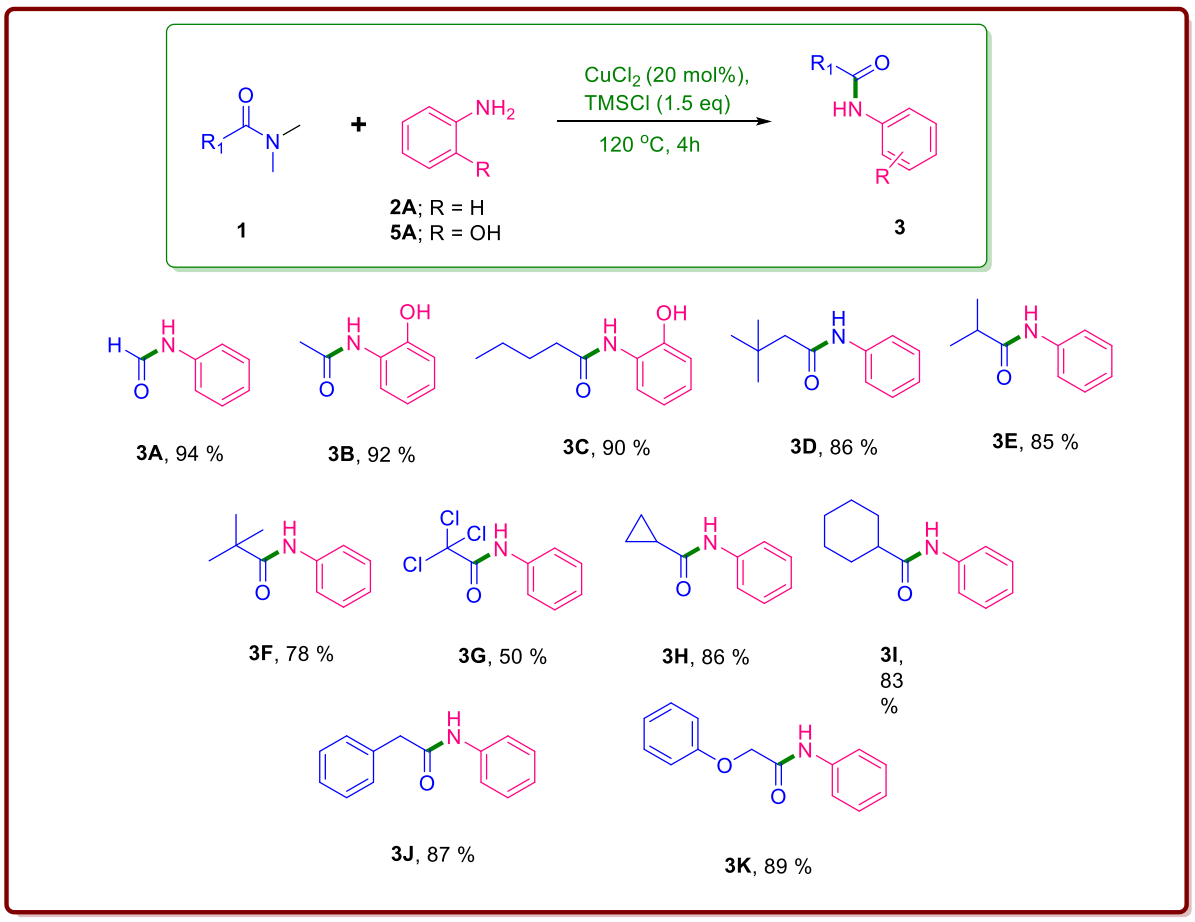

*Scheme 5- 1: Transamidation of aliphatic amides: reaction scope. Amide **1** (1.0 mmol), Amine **2/5** (1.5 mmol), $CuCl_2$ (20.0 mol%), TMSCl (1.5 mmol), 120 °C, 4 h. Isolated yields.*

Amine Scope

Subsequently, we investigated the influence of the various aromatic and aliphatic substituents environment on the nitrogen atom of the amine **2** (**Scheme 5-2**). First, we screened a series of diversely substituted anilines **2** which transform amide **1** to amide **3**. As shown, this N-formylation is compatible with halides decorated anilines, such as chloride and fluoride, at various positions. However, the anilines (**2b** and **2d**) with halogens substituted at *meta* position produced more desired products than their *ortho* and *para* counterparts (**2a**, **2c** and **2e**), probably attributed to their inductive effect of halogens. As expected, the introduction of electronic-donating substituents including methoxy, hydroxy, and alkyl groups on aniline in this transformation led to remarkable *N*-formamide conversion results. Anisidine (**2f** and **2g**) and aminophenol (**2h**, **2i** and **2j**) yielded amides (**3f**-**3j**) in the 89-93% range. In addition, *p*-thioanisidine **2k** provided the desired product **3k** in 88% yield. Notably, this

reaction was tolerant of a wide variety of functional groups such as acid, ester, and ketone. Aminoacetophenones derivatives gave 72% and 80% yields of **3m** and **3n**, respectively. 4-amino benzoic acid and ethyl 4-aminobenzoate provided **3o** and **3p** in 48% and 60% transformation outcomes. Di-substituted anilines (**2q**–**2u**) also produced moderate to good yields of the desired products. It was observed that electron-donating substituted aniline **2v** produced a better yield than electron-withdrawing substituted anilines (**2w**-**2z**) during the *N*-acylation reaction with *N*,*N*-dimethylacetamide. However, when secondary amines (**2aa**-**2ae**) such as *N*-methylaniline, diphenylamine, and aliphatic heterocyclic amine reacted with *N*,*N*-dimethylformamide under optimised circumstances, the predicted corresponding compounds were obtained. Finally, we glanced at heterocyclic anilines as substrates and found that they produced valuable yields, as evidenced by the synthesis of **3af** and **3ag**. This technique affords a substantial amide transamidation by using weak nucleophilic amines with aliphatic amides.

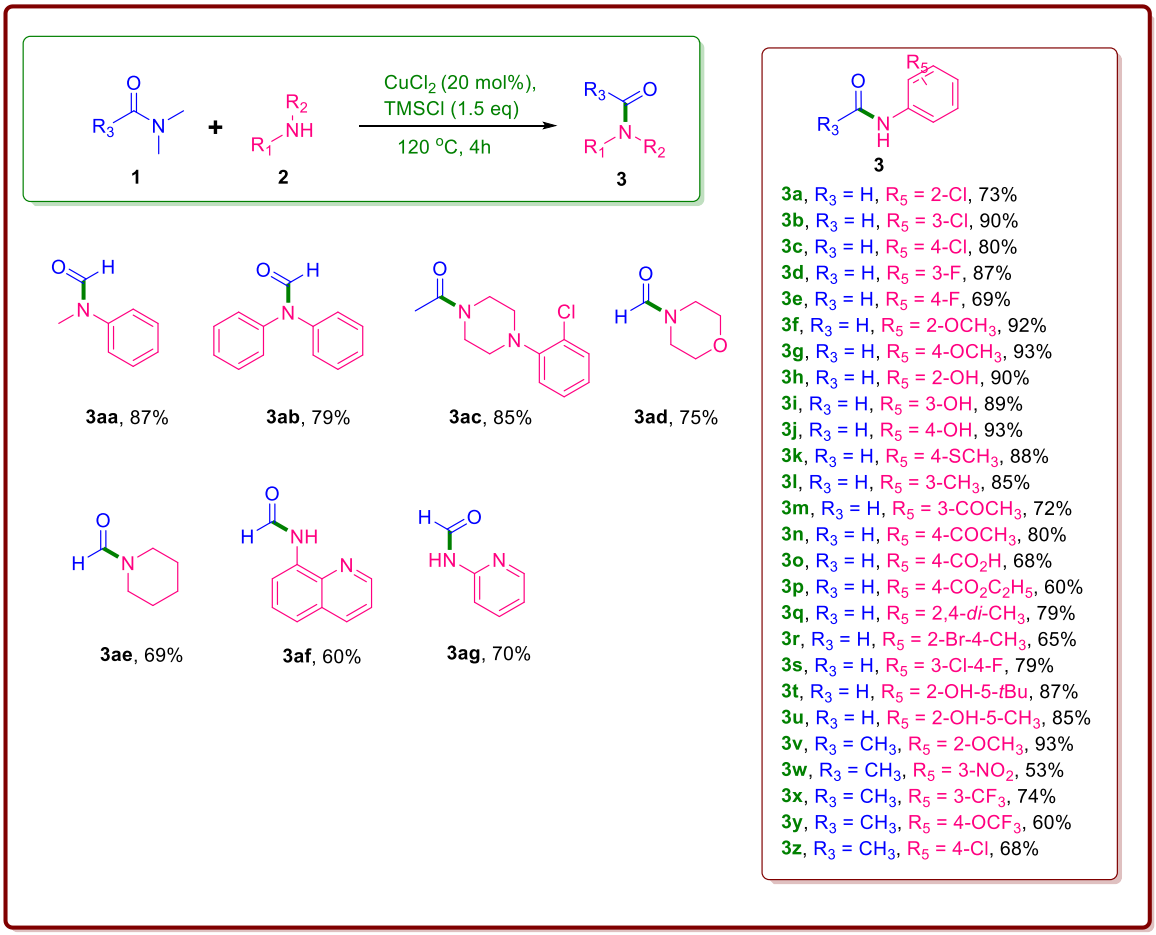

*Scheme 5- 2: Amidation of amines: reaction scope. Amide **1** (1.0 mmol), Amine **2** (1.5 mmol), $CuCl_2$ (20.0 mol%), TMSCl (1.5 mmol), 120 °C, 4 h. Isolated yields.*

Steric Hindrance investigation of Amide

Furthermore, we investigated the steric hindrance of primary, secondary, and tertiary amides in the transamidation reaction to expand their significant potential, as shown in **scheme 5-3**. The development of amide transformation methodologies has piqued researchers' interest since amides are used in a wide range of pharmacological agents and natural ingredients (Chem. Rev. 2016, 116, 12029−12122). As shown, this methodology has a wide range of compatibility. Amides having a lower or higher steric hindrance engage in the reaction. Notably, transamidation of bulky tertiary amides yielded less than secondary and primary amides. However, we were glad to observe that these parameters are compatible with a wide variety of amide substrates.

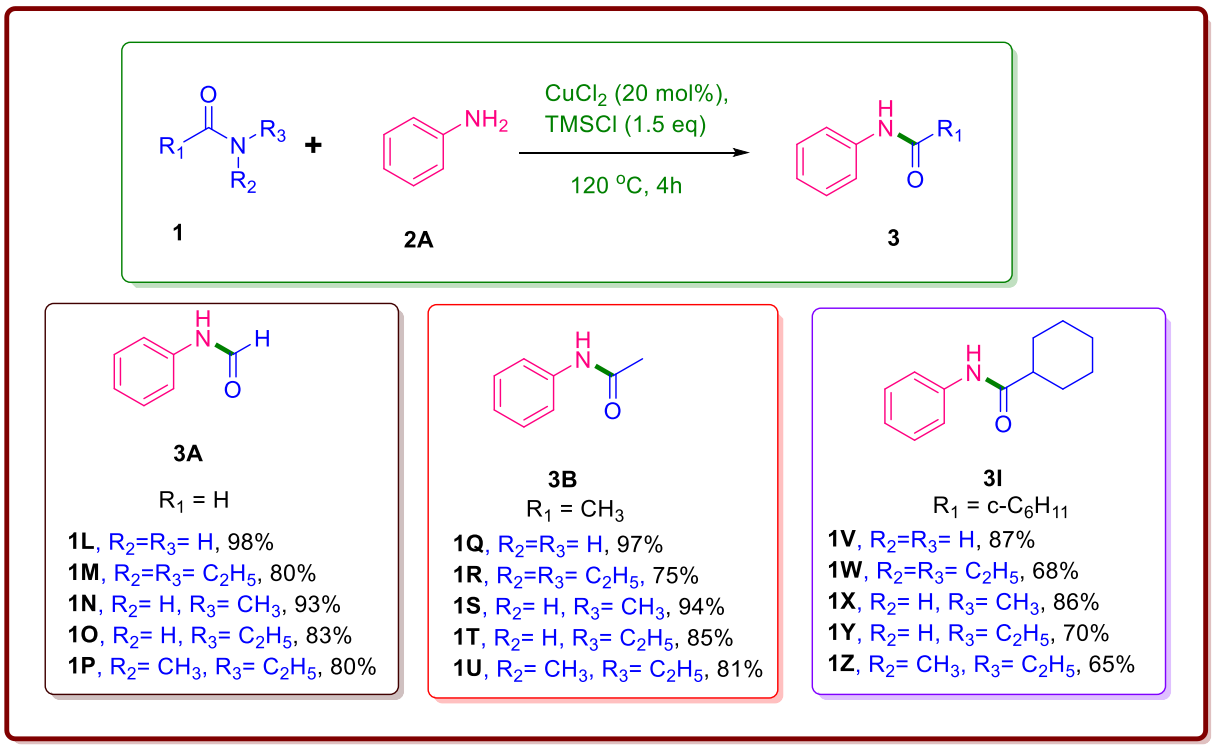

*Scheme 5- 3: Transamidation of different N-substituted amides: reaction scope. Amide **1** (1.0 mmol), Amine **2A** (1.5 mmol), $CuCl_2$ (20.0 mol%), TMSCl (1.5 mmol), 120 °C, 4 h. Isolated yields.*

In organic chemistry, transamidation is still a relatively unknown process. As a result, we wanted to see if this transamidation might be used to synthesise benzoxazole. We performed a reaction between aminophenol **5a** and N,N-dimethylpentamide **1C** stirred overnight at 140 °C. We concluded that the intramolecular annulation of **3F** was occurring after elucidating the structure of the upper spot using NMR spectroscopy, as shown in **scheme 5-4**. Our method directly eliminated the dimethylamine in this transformation of amide **1C** and yielded **6c** in 17 %. Following that, we concentrated on improving the yield of the benzoxazole product to make it a step-economical and cost-effective route to 2-substituted benzoxazole.

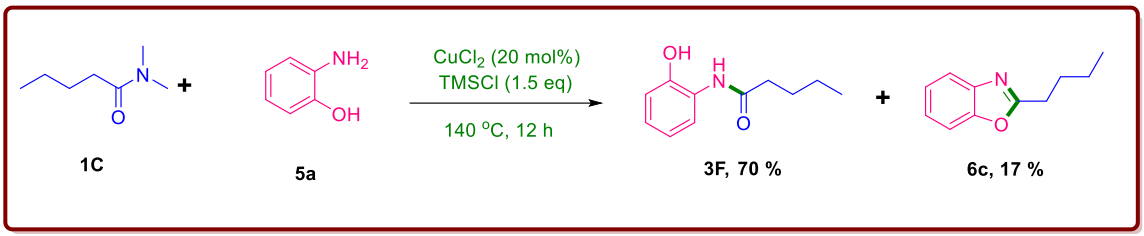

*Scheme 5- 4: Transamidation reaction of N,N-dimethylpentanamide **1C** with 2-aminophenol **5a**. Amide **1** (1.0 mmol), Amine **2** (1.5 mmol), $CuCl_2$ (20.0 mol%), TMSCl (1.5 mmol), 140 °C, 12 h. Isolated yields.*

Optimisation of Benzoxazole

Similarly, for standardising reaction conditions, we chose 2-aminophenol **5a** and N-methylpentanamide **4c** as model substrates. We observed that just three parameters have an impact on the yield of benzoxazole during the optimisation studies; the results are summarised in **Table 5-2**. First, we observed that the temperature significantly affects the reaction transformation. As a result of the experiments, we concluded that a higher temperature was required for benzoxazole annulation. However, the best output of benzoxazole had been at 160 °C (entry 6 and **Table 5-2**). On the other hand, we found that time plays a crucial role in the synthesis of desired compound **6c**. We conducted some studies with both short and long time intervals and found that short time intervals reactions produced lower yields than long-time duration reactions (entries 7-10 and **Table 5-2**). Finally, when the TMSCl quantity was increased by 0.5 equiv compared to the transamidation condition, the yield of **6c** improved (entry 14 and **Table 5-2**). Furthermore, adding more TMSCl did not enhance the production of the desired product.

*Table 5 - 2 :- Equiv, time and temperature study**

Entry	Aniline 5a (equiv)	$CuCl_2$ (mol%)	Temperature (°C)	TMSCl (equiv)	Time (hr)	Yield (%)#
1	1.5	20.0	100	1.5	12	0
2	1.5	20.0	110	1.5	12	0
3	1.5	20.0	130	1.5	12	11
4	1.5	20.0	140	1.5	12	17
5	1.5	20.0	150	1.5	12	45
6	1.5	20.0	**160**	1.5	12	51
7	1.5	20.0	160	1.5	14	61
8	1.5	20.0	160	1.5	**16**	65
9	1.5	20.0	160	1.5	18	65
10	1.5	20.0	160	1.5	20	64
11	1.5	20.0	160	0	16	0
12	1.5	20.0	160	0.5	16	8

13	1.5	20.0	160	1.0	16	40
14	1.5	20.0	160	**2.0**	16	76

*Reaction conditions: 4c (1.0 eq). #Isolation by using column chromatography.

Scope of Amide and 2-Aminophenol scope in the synthesis of Benzoxazole and Benzothiazole

After extensive optimisation, we investigated a variety of substituted 2-aminophenol **5** and aliphatic secondary amides **4** toward the synthesis of their corresponding 2-substituted benzoxazole **6** (**Scheme 5-5a**). When 2-aminophenol **5a** was reacted with unbranched alkyl chain amides such as N-methylacetamide (**4a**), N-methylbutyramide (**4b**), and N-methylpentanamide (**4c**) resulted in excellent yields of the corresponding benzoxazoles. Additionally, β-branched-chain amides and substituted amides including N,3,3-tetramethylbutanamide (**4d**), N-methyl-2-phenylacetamide (**4e**), and N-methyl-2-phenoxyacetamide (**4f**), were produced in a good yield range (70-75%) of 2-neopentyl, 2-benzyl, and 2-(phenoxymethyl)benzoxazole (**6d**, **6e**, and **6f**, respectively) under optimised conditions. Under this annulation condition, some amides with α-branched chains were evaluated, regarded as sterically hindered examples. However, these amides like N-methylisobutyramide (**4g**) and N-methylpivalamide (**4h**) resulted in a good transformation into cyclic products **6g** and **6h**, respectively. Even 2,2,2-trichloro-N-methylacetamide (**4i**) was capable of being reacted, as demonstrated by the formation of **6i**, although with a lower yield. Furthermore, N-methylcyclopropanecarboxamide (**4j**) and N-methylcyclohexanecarboxamide (**4k**) perform as suitable partners in this cyclisation approach.

Moving beyond the area of amides, we sought to investigate a variety of substituted 2-aminophenols that reacts with N-methylacetamide (**4a**) in the annulation process (**Scheme 5-5b**). We explored several electron-withdrawing and electron-donating groups decorated on 2-aminophenol. This cyclised technique was effective with chloro ornamented 2-aminophenols (**5b** and **5c**). However, this study found a similar position effect pattern on yield as transamidation. Furthermore, 5-nitro-2-aminophenol yielded a moderate amount of the desired product (**6n**). After that, we looked at electron-rich groups like 4-methyl, 5-methyl, and 4-tert-butyl 2-aminophenol (**5d**, **5e** and **5f**, respectively). Under these conditions, the relevant annulation compounds were synthesised in good yields. This methodology produced respective benzoxazole (**6r**) with a moderate performance using 3-aminopyridin-2-ol (**5g**).

Finally, we checked the compatibility of a bulky amine such as 1-aminonaphthalen-2-ol (**5h)** and found a moderate result of desired product **6s**.

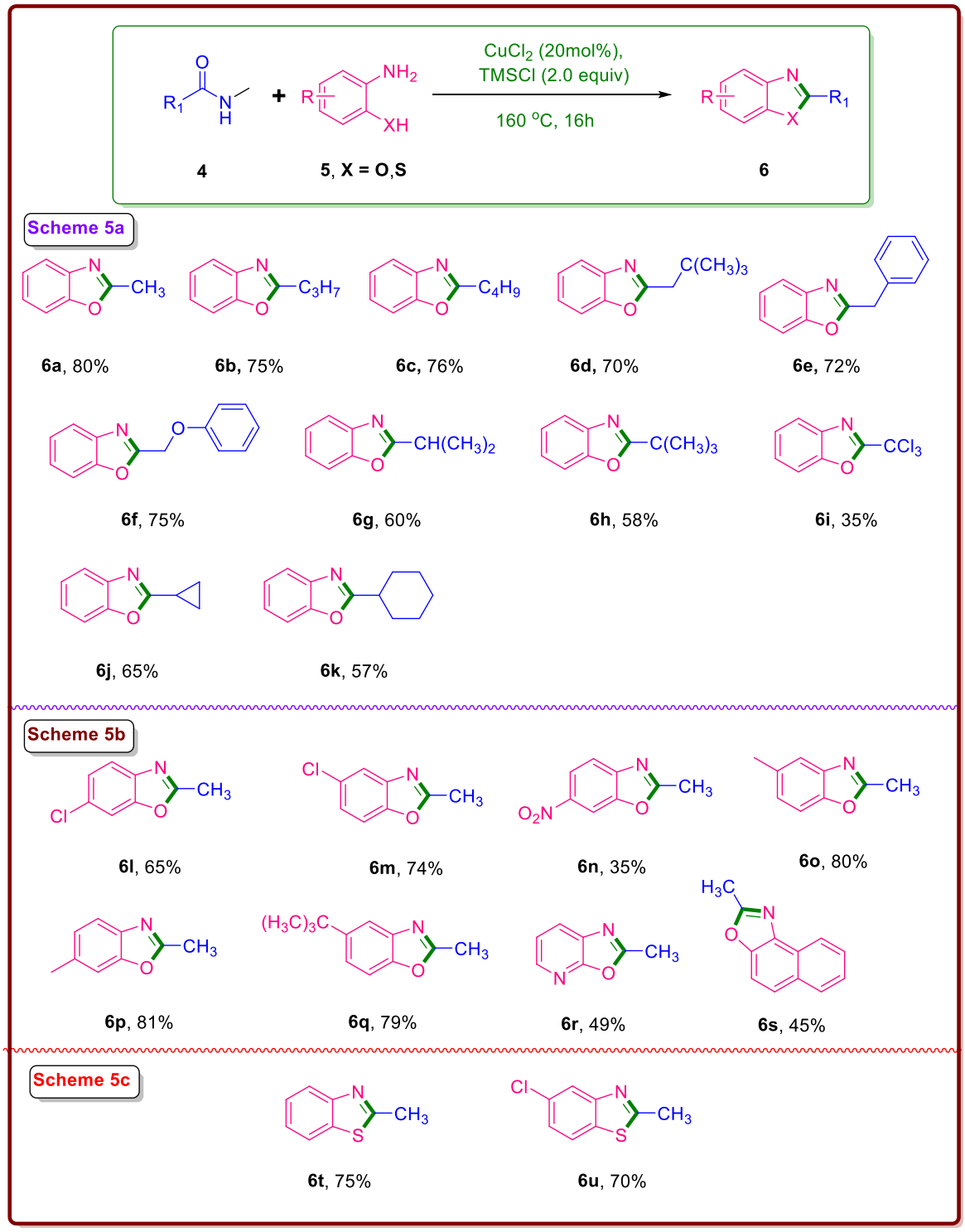

Scheme 5- 5: Annulation of Benzoxazole and thiazole: reaction scope. Amine 4 (1.0 mmol), 5 (1.5 mmol), $CuCl_2$ (20.0 mol%), TMSCl (2.0 mmol), 160 °C, 16 h. Isolated yields.

We were excited to observe that this approach is also consistent with benzothiazole production (**6t** and **6u**) from the reaction of N-methylacetamide (**4a**) with substituted 2-aminothiophenols (**Scheme 5-5c**). The versatility of the annulation promises well for its future usage in organic chemistry.

Competitive Experiments

Additionally, the competitive transamidation performed between aliphatic amide (**1I**), and aromatic amide (**1L** and **1M**) , indicated that aliphatic amide underwent transformation more readily than the aromatic amide (**Scheme 5-6**).

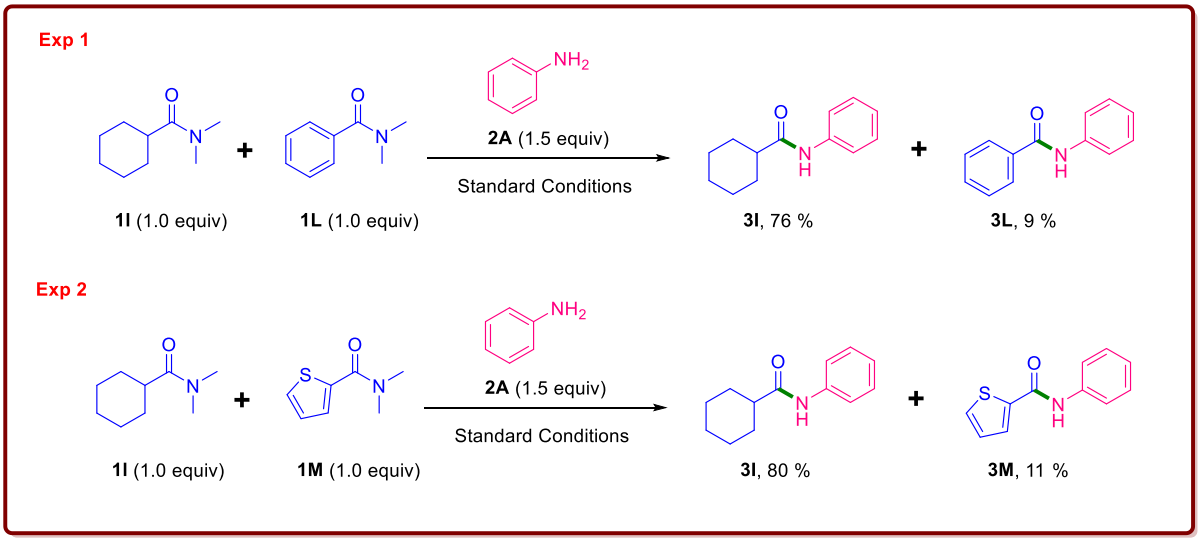

Scheme 5- 6: Competitive Experiments between aliphatic and aromatic amides: Isolated yields.

Mechanistic Investigation

To better understand the mechanistic approach of transamidation, we executed some experiments, as indicated in **Scheme 5-7**. Initially, we sought to dispel the doubt that a radical species drives the transamidation. Therefore, we carried out a reaction in the presence of TEMPO, which serves as a radical trap for that species (**Scheme 5-7a**). As a result, the reaction gave an identical result to those obtained under conventional conditions. Hence, we can deduce that a radical species did not trigger the reaction.

Following that, we assumed that the TMSCl first reacts with the amine and subsequently combines it to the amide for transformation. A reaction using amide and N,N-bis(trimethylsilyl)amine demonstrated this concept (**Scheme 5-7b**), where the transamidation of **1J** did not occur under standardised conditions. Also, we presented a comparison of two reactions to evaluate which oxygen is involved in benzoxazole annulation, as shown in **Scheme 5-7c**. Only a transamidation product resulted when **1J** reacted with **2A** under annulation conditions. On the other hand, a reaction between **1J** and **5a** produced a cyclised compound. We can assume from these studies that the oxygen in 2-aminophenol belongs to the cyclised product. Finally, to explain the temperature influence on the intramolecular annulation, we ran two experiments, one at 120 °C and the other at 160 °C, both stirred under the same conditions (**Scheme 5-7d**). The first experiment came to a halt at the transamidation compound, whereas the second experiment yielded the cyclised product.

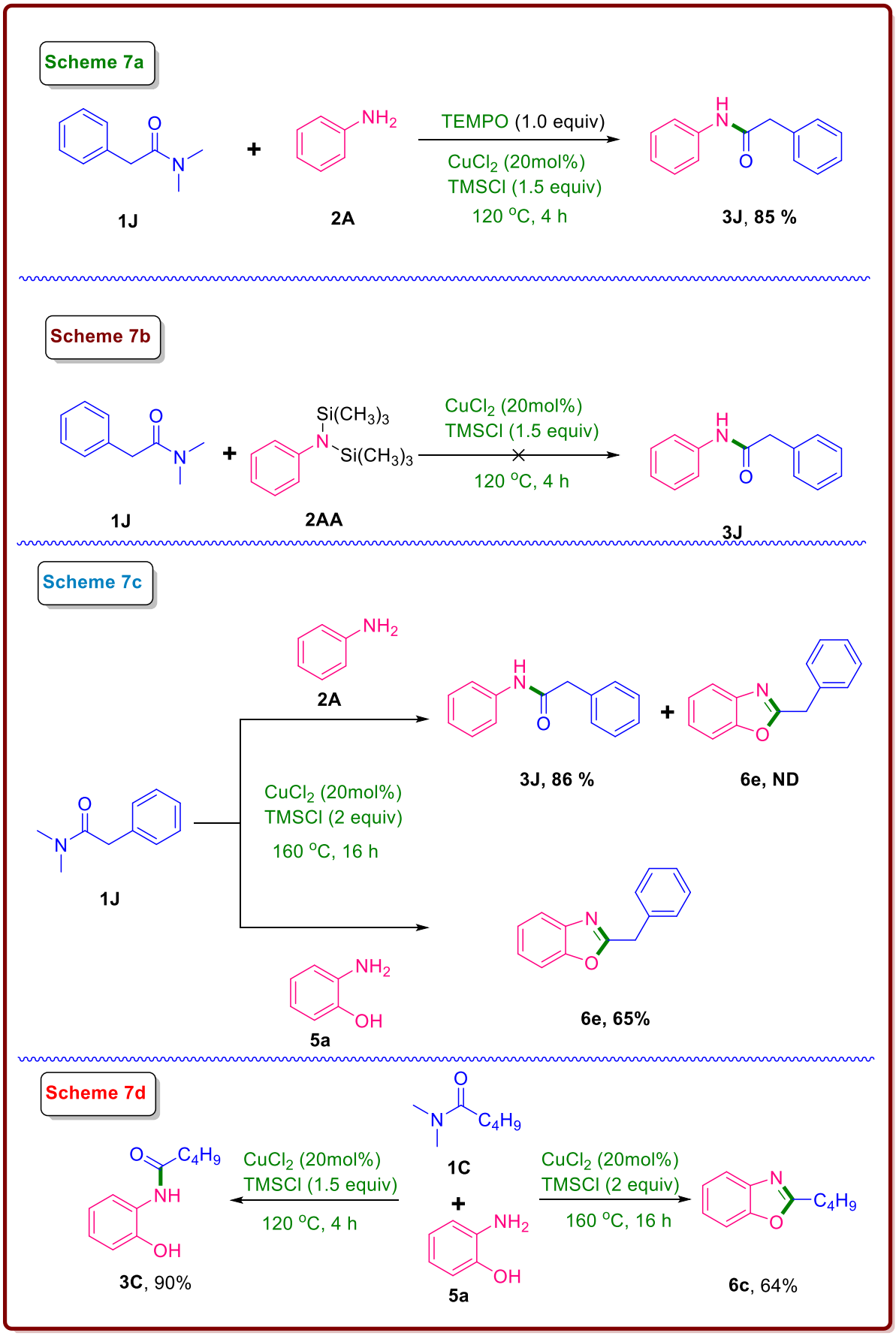

Scheme 5- 7: Mechanistic Investigation experiments. Isolated yields.

Based on mechanistic experiments and previous research, we can provide plausible transamidation (cycle 1) and annulation (cycle 2) mechanism paths, as shown in **Scheme 5-8**. Cu(II) activates the amide bond to generate amidate complex **T1**, which can be synthesised from free Cu(II). When the complex **T1** is treated with TMSCl and an amine, the Cu-N bond of **T1** is cleaved, resulting in the unstable species **T2**, wherein TMSCl could serve as a Lewis acid to accelerate the reaction. Usually, basic ligand amines exchange with the amide, resulting in protonated free ligands; it has been proposed in other similar mechanisms. **T2** annulates occur due to intramolecular interactions between the amine nitrogen atom and the carbonyl carbon atom, leading to intermediate **T3**, which is in equilibrium with its isomer **T4**. **T3** can regenerate **T2** in the same way that **T4** can produce **T5** (an isomer of **T2**). As a result, TMSCl presumably aids in the removal of amine to generate **T7**, which occurs in tandem with the production of the Cu complex species **T6**. Eventually, **T6** splits to give the transamidated product **3** and the Cu catalyst for the next cycle 1. We assume that amine **1** is a 2-aminophenol in the example of benzoxazole formation. As a result, the final intermediate **T6** in cycle 1 should resemble **T6'** in cycle 2. The phenol's oxygen atom reacts with the amidate Cu(II) complex **A1** look like when the **T1** species was transformed to the **T2** intermediate. Subsequently, the intramolecular interaction causes **A1** to transform into **A2**. Ultimately, **A2** eliminates the Cu(II) complex, resulting in the annulated product **6**.

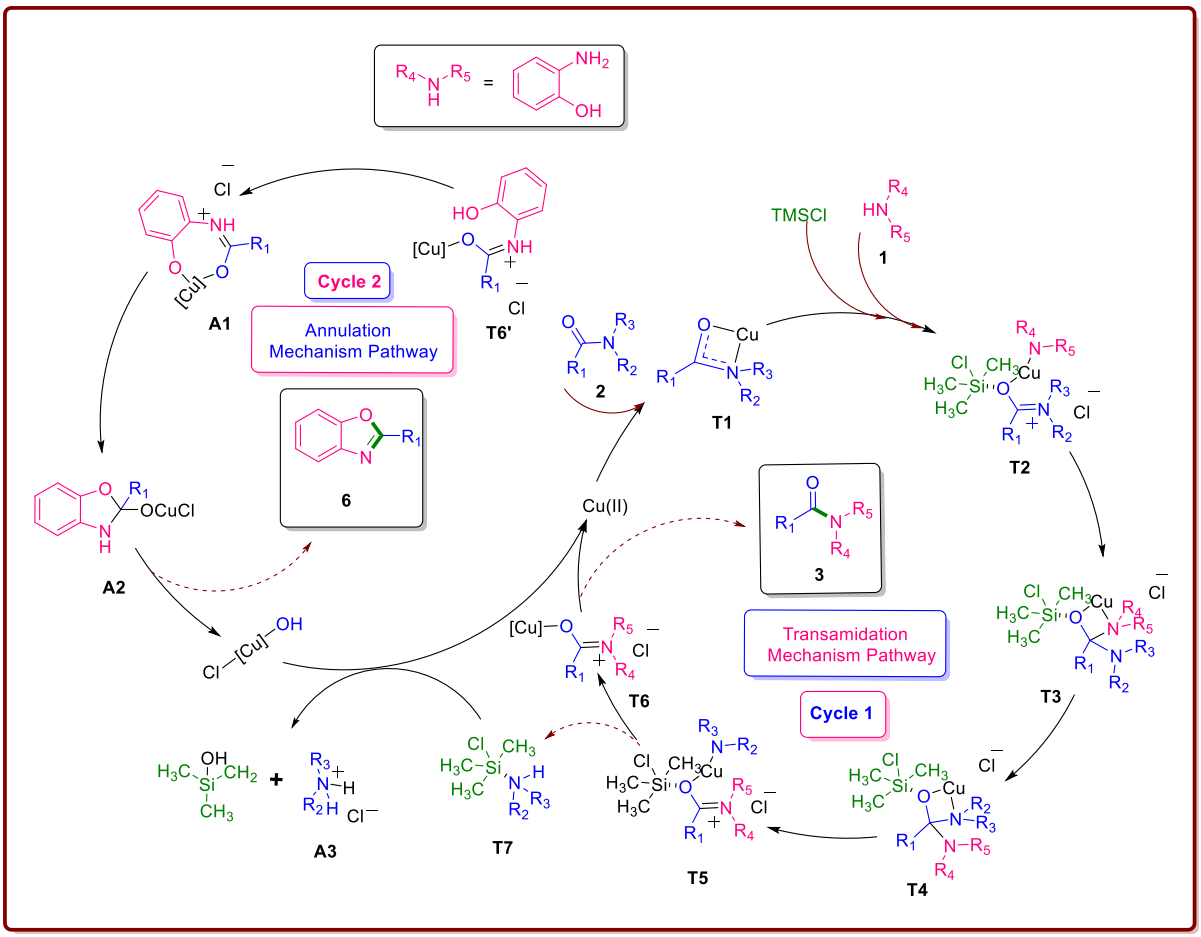

Scheme 5- 8: Plausible Mechanism of Cu-mediated Transamidation and Annulation.

Conclusion

In summary, we have reported an efficient Cu(II)-catalysed transamidation of unactivated aliphatic amides. This protocol provided benzoxazole and benzothiazole in good to excellent yields under solvent-free conditions. Furthermore, all reagents are affordable and straightforward to use, requiring no extra precautions. Hence, this approach could be used to synthesise a variety of substituted benzimidazoles/benzothiazole and transamidation products with a wide range of substrate scopes.

Experimental Section

General Information

General Analytical Information. ^{1}H and ^{13}C NMR spectra were recorded on Bruker AV 400 MHz instrument at 400 MHz (^{1}H NMR), 100 MHz (^{13}C NMR). All ^{1}H NMR spectra were measured in parts per million (ppm) downfield, or were measured relative to the residual proton signals of d^{1}-chloroform

($CDCl_3$, 7.26 ppm) and dimethyl sulfoxide-d_6 (DMSO-d_6, 2.50 ppm). All ^{13}C NMR spectra were reported in ppm relative to residual carbon signals of $CDCl_3$ (77.16 ppm) and DMSO-d_6 (39.52 ppm). Coupling constants (*J*) are reported in hertz (Hz). Multiplicity was indicated as follows: s (singlet), d (doublet), t (triplet), q (quartet), p (pentet), and m (multiplet). Thin-layer chromatography (TLC) was performed on precoated Merck Silica gel 60 F254 plates and compounds were visualized with a UV light at 254 nm. Flash chromatography for purification of compounds were carried out using silica gel (100–200 mesh).

General Reagents Information. Unless otherwise noted, commercially available materials were obtained from Aldrich Chemical Co., Alfa Aesar and used without prior purification. Chlorotrimethylsilane (TMSCl, 98% purity) was purchased from Aldrich Chemical Co. and was stored in refrigerator for storage. $CuCl_2$ (99% purity) was purchased from Aldrich Chemical Co. Lab reagent (LR) grade solvents were used for extraction and column chromatography purchased from Loba-chem.

General Manipulation Considerations. Unless otherwise specified, all reagents were weighed and handled in air, and all reactions performed in a 20 mL sealed vial with an air atmosphere. The eluents used for column chromatography were presented as ratios of solvent volumes. $CuCl_2$ (99% purity) was used for scope study unless otherwise noted. Yields reported in the publication are isolated yields unless otherwise noted. All new starting materials and products were characterized by ^1H and ^{13}C NMR spectroscopies.

Optimization of Reaction Conditions of transamidation

General procedure for optimizations of reaction conditions. An oven-dried 20 mL Teflon screw-capped vial equipped with a stir bar was sequentially charged with amide **1I**, aniline **2A** and catalyst. TMSCl were transferred into the tube via a syringe. The resulting mixture was stirred in a preheated heat block. After full fill the reaction condition of experiment, the reaction mixture was cooled down to room temperature. The reaction mixture was diluted with ethyl acetate and then washed with dilute aqueous HCl solution and saturated brine, dried with anhydrous Na_2SO_4, and finally concentrated in vacuo with the aid of rotary evaporator. The residue was purified by flash chromatography on silica gel using hexane and ethyl acetate as eluent to give the transamidated product **3I**.

Cu-catalyzed transamidation of Aliphatic unactivated amides

Experimental Procedure (EP-1): An oven-dried 20 mL Teflon screw-capped vial equipped with a stir bar was sequentially charged with aliphatic amide (0.5 mmol, 1 equiv.), amine (0.75 mmol, 1.5 equiv.) and $CuCl_2$ (0.075 mmol, 0.15 equiv.). TMSCl (0.75 mmol, 1.5 equiv.) was transferred into the tube via a syringe. The resulting mixture was stirred under an argon atmosphere in a preheated heat block at 120 °C for 4 h. At this point, the reaction mixture was cooled down to room temperature. The reaction mixture was diluted with ethyl acetate and then washed with dilute aqueous HCl solution (~0.1 M, 2 x 30 mL; **note**: water was used for washing instead of HCl (aq) for pyridine/quinoline-containing amide products) and saturated brine (~30 mL), dried with anhydrous Na_2SO_4, and finally concentrated in vacuo with the aid of rotary evaporator. The residue was purified by flash chromatography on silica gel using hexane and ethyl acetate as eluent to give the transamidated product.

Analytical Data

N-phenylformamide[44] **(Scheme 1**, entry **3A)** (CAS No. **103-70-8**)

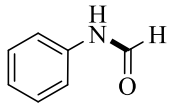

Using the experimental procedure EP-1, the product was obtained as light brown solid in 94% yield; **^{1}H NMR** (400 MHz, $CDCl_3$, ppm): δ = 9.20 (br, 1H), 8.68 (d, J = 11.3 Hz, 1H), 8.57 (br, 1H), 8.31 (s, 1H), 7.56 (d, J = 8.0 Hz, 2H), 7.34-7.27 (m, 4H), 7.16 (t, J = 7.5 Hz, 1H), 7.12-7.08 (m, 3H). **^{13}C NMR** (100 MHz, $CDCl_3$, ppm): δ = 163.23, 159.89, 137.09, 136.85, 129.69, 129.01, 125.25, 124.74, 120.23, 118.78.

N-(2-hydroxyphenyl)acetamide[45] **(Scheme 1**, entry **3B)** (CAS No. **614-80-2**)

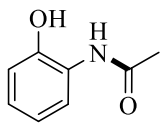

Using the experimental procedure EP-1, the product was obtained as light brown solid in 92% yield; **^{1}H NMR** (400 MHz, DMSO-d_6, ppm): δ = 9.73 (s, 1H), 9.30 (br, 1H), 7.67 (d, J = 8.1 Hz, 1H), 6.98 – 6.89

(m, 1H), 6.85 (d, *J* = 9.5 Hz, 1H), 6.75 (t, *J* = 7.6 Hz, 1H), 2.09 (s, 3H). **^{13}C NMR** (100 MHz, DMSO-d_6, ppm): δ = F3169.03, 147.90, 126.43, 124.66, 122.38, 118.98, 115.96, 23.60.

N-(2-hydroxyphenyl)pentanamide[46] **(Scheme 1**, entry **3C)** (CAS No. **105293-97-8**)

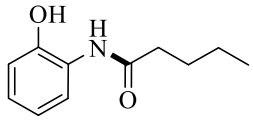

Using the experimental procedure EP-1, the product was obtained as light brown solid in 90% yield; **^{1}H NMR** (400 MHz, DMSO-d_6, ppm): δ = 9.72 (br, 1H), 9.25 (s, 1H), 7.67 (d, *J* = 9.3 Hz, 1H), 6.94 (t, *J* = 7.6 Hz, 1H), 6.86 (d, *J* = 6.6 Hz, 1H), 6.76 (td, *J* = 7.5, 1.6 Hz, 1H), 2.40 (t, *J* = 7.4 Hz, 2H), 1.58 (p, *J* = 7.4 Hz, 2H), 1.33 (h, *J* = 7.4 Hz, 2H), 0.90 (t, *J* = 7.3 Hz, 3H). **^{13}C NMR** (100 MHz, DMSO-d_6, ppm): δ = 172.05, 147.92, 126.47, 124.64, 122.30, 118.99, 116.11, 35.68, 27.44, 21.80, 13.71.

3,3-dimethyl-N-phenylbutanamide[46] **(Scheme 1**, entry **3D)** (CAS No. **72807-56-8**)

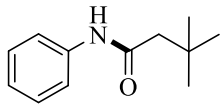

Using the experimental procedure EP-1, the product was obtained as light brown solid in 86% yield; **^{1}H NMR** (400 MHz, DMSO-d_6, ppm): δ = 9.77 (s, 1H), 7.59 (d, *J* = 7.6 Hz, 2H), 7.01 (t, *J* = 7.3 Hz, 2H), 2.18 (s, 2H), 1.02 (s, 9H). **^{13}C NMR** (100 MHz, DMSO-d_6, ppm): δ = 169.96, 139.28, 128.59, 122.95, 119.18, 49.60, 30.83, 29.62.

N-phenylisobutyramide[47] **(Scheme 1**, entry **3E)** (CAS No. **4406-41-1**)

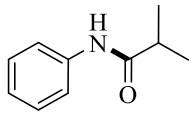

Using the experimental procedure EP-1, the product was obtained as light brown solid in 85% yield; **^{1}H NMR** (400 MHz, $CDCl_3$, ppm): δ = 7.53 (d, *J* = 8.3 Hz, 2H), 7.43 (br, 1H), 7.30 (t, *J* = 7.6 Hz, 2H), 7.09 (t, *J* = 7.4 Hz, 1H), 2.52 (hept, *J* = 7.0 Hz, 1H), 1.25 (s, 3H), 1.23 (s, 3H). **^{13}C NMR** (100 MHz, $CDCl_3$, ppm): δ = 175.72, 138.24, 129.00, 124.23, 120.11, 36.65, 19.69.

N-phenylpivalamide[44] **(Scheme 1**, entry **3F)** (CAS No. **6625-74-7**)

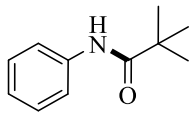

Using the experimental procedure EP-1, the product was obtained as light brown solid in 78% yield; **^{1}H NMR** (400 MHz, $CDCl_3$, ppm): δ = 7.53 (d, J = 8.7 Hz, 2H), 7.31 (t, J = 7.5 Hz, 3H), 7.10 (t, J = 8.0 Hz, 1H), 1.32 (s, 9H). **^{13}C NMR** (100 MHz, $CDCl_3$, ppm): δ = 176.72, 138.15, 129.01, 124.28, 120.16, 39.68, 27.71.

2,2,2-trichloro-N-phenylacetamide[48] **(Scheme 1**, entry **3G)** (CAS No. **2563-97-5**)

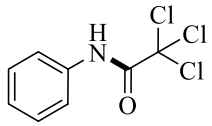

Using the experimental procedure EP-1, the product was obtained as light brown solid in 50% yield; **^{1}H NMR** (400 MHz, $CDCl_3$, ppm): δ = 8.34 (br, 1H), 7.58 (d, J = 8.7 Hz, 2H), 7.41 (t, J = 7.4 Hz, 2H), 7.24 (t, J = 7.4 Hz, 1H). **^{13}C NMR** (100 MHz, $CDCl_3$, ppm): δ = 159.37, 136.06, 129.45, 126.18, 120.52, 92.96.

N-phenylcyclopropanecarboxamide[46] **(Scheme 1**, entry **3H)** (CAS No. **2759-52-6**)

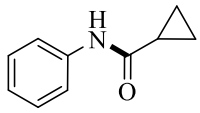

Using the experimental procedure EP-1, the product was obtained as light brown solid in 86% yield; **^{1}H NMR** (400 MHz, $CDCl_3$, ppm): δ = 7.67 (s, 1H), 7.50 (d, J = 8.2 Hz, 2H), 7.34 – 7.27 (m, 2H), 7.08 (t, J = 7.5 Hz, 1H), 1.55-1.49 (m, 1H), 1.13 – 0.97 (m, 2H), 0.83-0.79 (m, 2H).

N-phenylcyclohexanecarboxamide[44] **(Scheme 1**, entry **3I)** (CAS No. **2719-26-8**)

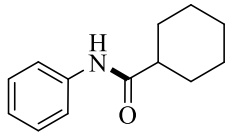

Using the experimental procedure EP-1, the product was obtained as light brown solid in 83% yield; **^{1}H NMR** (400 MHz, DMSO-d_6, ppm): δ = 9.79 (s, 1H), 7.59 (d, J = 8.2 Hz, 2H), 7.26 (t, J = 7.9 Hz, 2H), 2.31 (t, J = 11.6 Hz, 1H), 1.83 – 1.70 (m, 4H), 1.65 (d, J = 9.8 Hz, 1H), 1.51 – 1.33 (m, 2H), 1.33 – 1.13 (m, 3H). **^{13}C NMR** (100 MHz, DMSO-d_6, ppm): δ = 174.29, 139.52, 128.60, 122.83, 119.02, 44.87, 29.15, 25.42, 25.26.

N,2-diphenylacetamide[46] **(Scheme 1**, entry **3J)** (CAS No. **621-06-7**)

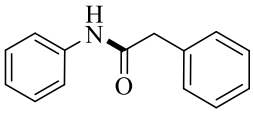

Using the experimental procedure EP-1, the product was obtained as light brown solid in 87% yield; **^{1}H NMR** (400 MHz, DMSO-d_6, ppm): δ = 10.19 (s, 1H), 7.61 (d, J = 8.7 Hz, 2H), 7.40 – 7.19 (m, 7H), 7.03 (t, J = 7.4 Hz, 1H), 3.64 (s, 2H). **^{13}C NMR** (100 MHz, DMSO-d_6, ppm): δ = 169.11, 139.25, 136.04, 129.12, 128.72, 128.31, 126.53, 123.21, 119.10, 43.35.

2-phenoxy-N-phenylacetamide[48] **(Scheme 1**, entry **3K)** (CAS No. **18705-01-6**)

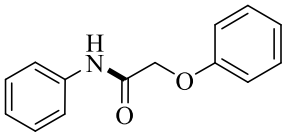

Using the experimental procedure EP-1, the product was obtained as light brown solid in 89% yield; **^{1}H NMR** (400 MHz, DMSO-d_6, ppm): δ = 10.11 (s, 1H), 7.65 (d, J = 8.0 Hz, 2H), 7.32 (t, J = 7.9 Hz, 4H), 7.08 (t, J = 7.4 Hz, 1H), 7.02-6.95 (m, 3H), 4.70 (s, 2H). **^{13}C NMR** (100 MHz, DMSO-d_6, ppm): δ = 166.59, 157.83, 138.41, 129.53, 128.74, 123.70, 121.19, 119.71, 114.66, 67.10.

Scheme 2

N-(2-Hydroxy-4-methylphenyl)formamide[49] **(Scheme 2**, entry **3a)** (CAS No. **2843-27-8**)

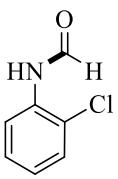

Using the experimental procedure EP-1, the product was obtained as brown solid in 73% yield; 66:34 mixture of rotamers: **^{1}H NMR** (400 MHz, $CDCl_3$, ppm): δ = 8.66 (d, J = 11.1 Hz, 0.47H), 8.45 (s, 1H), 8.35 (d, J = 8.3 Hz, 1H), 7.74 (br, 1.3H), 7.38 (d, J = 8.1 Hz, 0.45H), 7.33 (d, J = 8.1 Hz, 1H), 7.27 – 7.18 (m, 1H), 7.09 (dt, J = 8.3, 4.4 Hz, 0.48H), 7.02 (t, J = 7.8 Hz, 1H). **^{13}C NMR** (100 MHz, $CDCl_3$, ppm): δ = 161.73, 159.03, 133.81, 130.44, 129.24, 128.13, 127.93, 126.10, 125.27, 122.14, 118.87.

N-(3-chlorophenyl) formamide[50] (**Scheme 2**, entry **3b**) (CAS No. **139-71-9**)

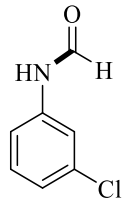

Using the experimental procedure EP-1, the product was obtained as off white solid in 90%; 55:45 mixture of rotamers: **^{1}H NMR** (400 MHz, $CDCl_3$, ppm): δ = 8.69 – 8.61 (m, 2H), 8.56 (s, 0H), 8.33 (s, 1H), 7.70 (s, 0H), 7.62 (s, 1H), 7.35 (d, J = 8.1 Hz, 1H), 7.28 – 7.15 (m, 4H), 7.12 (d, J = 8.1 Hz, 1H), 7.06 (d, J = 7.0 Hz, 2H), 6.95 (d, J = 7.9 Hz, 1H). **^{13}C NMR** (100 MHz, $CDCl_3$, ppm): δ = 162.60, 159.26, 138.08, 135.60, 134.88, 130.95, 130.25, 125.50, 125.05, 120.25, 118.92, 118.08, 116.84.

N-(4-chlorophenyl) formamide[49] (**Scheme 2**, entry **3c**) (CAS No. **2617-79-0**)

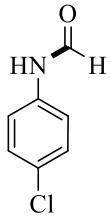

Using the experimental procedure EP-1, the product was obtained as off-white solid in 80% yield; 56:44 mixture of rotamers: **^{1}H NMR** (400 MHz, $CDCl_3$, ppm): δ = 8.71 (br, 0.64H), 8.59 (d, J = 11.2 Hz, 0.77H), 8.31 (s, 1H), 7.75 (br, 0.82H), 7.44 (d, J = 8.9 Hz, 2H), 7.26 (d, J = 8.8 Hz, 1.58H), 7.22 (d, J = 8.8 Hz, 2H), 6.99 (d, J = 8.8 Hz, 1.56H). **^{13}C NMR** (100 MHz, $CDCl_3$, ppm): δ = 162.83, 159.34, 135.54, 135.42, 130.91, 129.99, 129.95, 129.24, 121.40, 120.20.

N-(3-fluorophenyl)formamide[51] (**Scheme 2**, entry **3d**) (CAS No. **1428-10-0**)

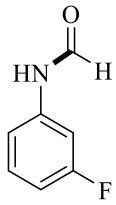

Using the experimental procedure EP-1, the product was obtained as yellow solid in 87% yield; 52:48 mixture of rotamers: **^{1}H NMR** (400 MHz, $CDCl_3$, ppm): δ = 8.88 (br, 0.88H), 8.64 (d, J = 11.2 Hz, 0.95H), 8.30 (s, 1.17H), 8.03 (br, 1.06H), 7.41 (d, J = 10.6 Hz, 1.15H), 7.28 – 7.10 (m, 3.35H), 6.78 (m, 3.96H). **^{13}C NMR** (100 MHz, $CDCl_3$, ppm): δ = 164.68, 164.20, 162.83, 162.22, 161.77, 159.59, 138.59, 138.52, 138.41, 131.29, 131.20, 130.39, 130.29, 115.41, 115.38, 114.18, 114.15, 112.24, 112.03, 111.78, 111.57, 107.89, 107.63, 106.16, 105.91.

N-(4-fluorophenyl) formamide[49] (**Scheme 2**, entry **3e**) (CAS No. **459-25-6**)

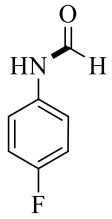

Using the experimental procedure EP-1, the product was obtained as off-white solid in 69% yield; 63:37 mixture of rotamers: **^{1}H NMR** (400 MHz, $CDCl_3$, ppm): δ = 8.63 (br, 0.55H), 8.57 (d, J = 11.1 Hz, 0.82H), 8.34 (s, 1H), 7.76 (br, 0.86H), 7.50 (dd, J = 9.0, 4.9 Hz, 2H), 7.07 (m, 2.87H), 7.01 (t, J = 8.6 Hz, 2.14H). **^{13}C NMR** (100 MHz, $CDCl_3$, ppm): δ = 163.20, 161.80, 160.95, 159.37, 159.30, 158.52, 133.00, 132.86, 122.04, 121.95, 121.34, 121.26, 116.79, 116.56, 116.00, 115.77.

N-(2-methoxyphenyl)formamide[49] (**Scheme 2,** entry **3f**) (CAS No. **23896-88-0**)

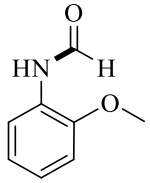

Using the experimental procedure EP-1, the product was obtained as brown solid in 92% yield; 69:31 mixture of rotamers: **^{1}H NMR** (400 MHz, $CDCl_3$, ppm): δ = 8.89 (s, 0.25H), 8.47 (s, 1H), 8.35 (d, J =

7.9 Hz, 1H), 7.92 (s, 0.82H), 7.79 (s, 0.41H), 7.18 (d, *J* = 8.2 Hz, 0.43H), 7.12 (t, *J* = 7.9 Hz, 0.46H), 7.06 (t, *J* = 7.1 Hz, 1H), 6.99 – 6.85 (m, 3H), 3.87 (s, 3H), 3.85 (s, 1.29H). **^{13}C NMR** (100 MHz, $CDCl_3$, ppm): δ = 161.60, 158.91, 148.89, 147.91, 126.81, 126.29, 125.34, 124.36, 121.14, 120.55, 116.85, 111.39, 110.16, 55.80.

N-(4-methoxyphenyl) formamide[49] (**Scheme 2**, entry **3g**) (CAS No. **5470-34-8**)

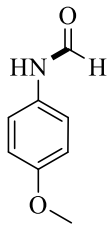

Using the experimental procedure EP-1, the product was obtained as reddish brown solid in 93% yield; 51:49 mixture of rotamers: **^{1}H NMR** (400 MHz, $CDCl_3$, ppm): δ = 8.55 (br, 0.63H), 8.50 (d, *J* = 11.4 Hz, 1H), 8.28 (s, 1H), 7.88 (br, 0.83H), 7.43 (d, *J* = 9.0 Hz, 2H), 7.03 (d, *J* = 8.8 Hz, 1.91H), 6.85 (dd, *J* = 14.4, 8.9 Hz, 4H), 3.78 (s, 2.86H), 3.76 (s, 3H). ^{13}C NMR (101 MHz, $CDCl_3$) δ 163.43, 159.34, 157.68, 156.77, 130.14, 129.74, 121.96, 121.61, 114.97, 114.29, 55.63, 55.55.

N-(2-Hydroxy-4-methylphenyl)formamide[52] **(Scheme 2**, entry **3h)** (CAS No. **2843-27-8**)

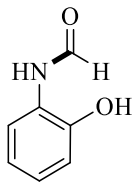

Using the experimental procedure EP-1, the product was obtained as brown solid in 90% yield; 85:15 mixture of rotamers: **^{1}H NMR** (400 MHz, DMSO-d_6, ppm): δ = 9.93 (s, 1H), 9.56 (s, 1H), 9.24 (d, *J* = 11.1 Hz, 0.15H), 8.52 (d, *J* = 11.2 Hz, 0.17H), 8.28 (s, 1H), 8.02 (d, *J* = 7.9 Hz, 1H), 7.12 (d, *J* = 7.7 Hz, 0.17H), 6.98 (t, *J* = 7.6 Hz, 0.19H), 6.94 – 6.82 (m, 2H), 6.75 (t, *J* = 7.6 Hz, 1.2H). **^{13}C NMR** (100 MHz, DMSO-d_6, ppm): δ = 163.48, 160.04, 148.97, 146.74, 126.01, 125.49, 124.20, 121.77, 120.84, 119.45, 119.01, 116.11, 115.11.

N-(3-hydroxyphenyl)formamide[50] (**Scheme 2**, entry **3i**) (CAS No. **24891-35-8**)

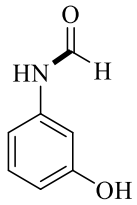

Using the experimental procedure EP-1, the product was obtained as brown oil in 89% yield; 73:27 mixture of rotamers: **^{1}H NMR** (400 MHz, DMSO-d_6, ppm): δ = 10.03 (s, 1H), 10.00 (s, 0.25H), 9.51 (s, 0.37H), 9.41 (s, 1H), 8.72 (d, *J* = 11.0 Hz, 0.36H), 8.22 (s, 1H), 7.18 (s, 1H), 7.08 (t, *J* = 8.1 Hz, 1.44H), 6.93 (d, *J* = 10.0 Hz, 1H), 6.63 (d, *J* = 7.9 Hz, 0.38H), 6.57 (s, 0.38H), 6.48 (t, *J* = 7.0 Hz, 0.39H). **^{13}C NMR** (100 MHz, DMSO-d_6, ppm): δ = 162.38, 159.46, 158.27, 157.70, 139.47, 139.25, 130.20, 129.57, 110.85, 110.80, 109.92, 108.02, 106.40, 104.77.

N-(4-hydroxyphenyl)formamide[52] (**Scheme 2**, entry **3j**) (CAS No. **41656-75-1**)

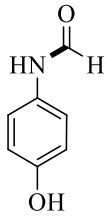

Using the experimental procedure EP-1, the product was obtained as brown solid in 93% yield; 77:23 mixture of rotamers: **^{1}H NMR** (400 MHz, DMSO-d_6, ppm): δ = 9.88 (s, 1H), 9.83 (d, *J* = 11.2 Hz, 0.34H), 9.22 (s, 1.28H), 8.50 (d, *J* = 11.1 Hz, 0.28H), 8.16 (d, *J* = 2.2 Hz, 1H), 7.37 (d, *J* = 8.8 Hz, 2H), 6.98 (d, *J* = 8.8 Hz, 0.61H), 6.76 – 6.66 (m, 2.63H). **^{13}C NMR** (100 MHz, DMSO-d_6, ppm): δ = 162.56, 158.84, 154.23, 153.55, 129.99, 129.66, 120.82, 120.22, 115.87, 115.19.

N-(4-(methylthio)phenyl)formamide[52] (**Scheme 2**, entry **3k**) (CAS No. **170288-29-6**)

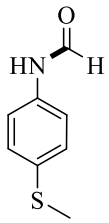

Using the experimental procedure EP-1, the product was obtained as cream solid in 88% yield; 54:46 mixture of rotamers: **^{1}H NMR** (400 MHz, $CDCl_3$, ppm): δ = 8.57 (d, J = 11.4 Hz, 0.92H), 8.51 (br, 0.7H), 8.29 (s, 1H), 7.61 (br, 0.83H), 7.42 (d, J = 8.7 Hz, 2H), 7.23 – 7.13 (m, 4H), 6.98 (d, J = 8.6 Hz, 1.80H), 2.41 (s, 2.56H), 2.40 (s, 3H). **^{13}C NMR** (100 MHz, $CDCl_3$, ppm): δ = 162.82, 159.24, 135.43, 134.51, 134.47, 134.22, 128.52, 127.95, 120.76, 119.76, 16.60, 16.58.

N-m-tolylformamide[49] (**Scheme 2**, entry **3l**) (CAS No. **3085-53-8**)

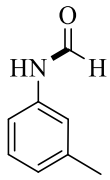

Using the experimental procedure EP-1, the product was obtained as brown oil in 85% yield; 55:45 mixture of rotamers: **^{1}H NMR** (400 MHz, $CDCl_3$, ppm): δ = 8.96 (br, 0.86H), 8.68 (d, J = 11.3 Hz, 1H), 8.33 (d, J = 1.9 Hz, 0.8H), 8.09 (br, 0.66H), 7.40 (s, 0.82H), 7.33 (d, J = 8.1 Hz, 0.79H), 7.20 (dt, J = 12.0, 7.8 Hz, 1.88H), 6.99 (d, J = 7.7 Hz, 1H), 6.96 – 6.88 (m, 2.87H), 2.34 (s, 3.15H), 2.31 (s, 2.52H). **^{13}C NMR** (100 MHz, $CDCl_3$, ppm): δ = 163.16, 159.57, 139.87, 139.06, 137.01, 136.82, 129.57, 128.91, 126.10, 125.61, 120.80, 119.55, 117.24, 115.81, 21.48, 21.42.

N-(3-acetylphenyl)formamide[52] (**Scheme 2**, entry **3m**) (CAS No. **72801-78-6**)

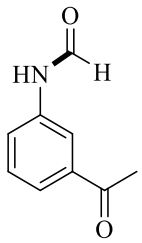

Using the experimental procedure EP-1, the product was obtained as white solid in 72% yield; 64:36 mixture of rotamers: **^{1}H NMR** (400 MHz, $CDCl_3$, ppm): δ = 8.99 (br, 0.52H), 8.86 (d, J = 11.1 Hz, 0.6H), 8.43 (s, 1H), 8.39 (br, 0.71H), 7.96-7.90 (m, 3.17H), 7.67 (d, J = 8.7 Hz, 2H), 7.18 (d, J = 8.7 Hz, 1.24H), 2.57 (s, 1.72H), 2.56 (s, 3H). **^{13}C NMR** (100 MHz, $CDCl_3$, ppm): δ = 197.39, 197.01, 162.26, 159.61, 141.55, 141.36, 133.74, 133.28, 130.51, 129.86, 119.39, 117.34, 26.56.

N-(4-acetylphenyl)formamide[48] (**Scheme 2,** entry **3n**) (CAS No. **41656-75-1**)

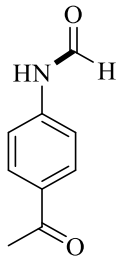

Using the experimental procedure EP-1, the product was obtained as white solid in 80% yield; 66:34 mixture of rotamers: **^{1}H NMR** (400 MHz, $CDCl_3$, ppm): δ = 8.93 (d, J = 11.4 Hz, 0.46H), 8.76 (d, J = 11.2 Hz, 0.54H), 8.48 (br, 0.75H), 8.42 (s, 1H), 8.07 (s, 1H), 7.92 (d, J = 8.1 Hz, 1H), 7.73 (d, J = 7.5 Hz, 1.14H), 7.67 (d, J = 9.3 Hz, 1H), 7.52 – 7.37 (m, 1.57H), 7.32 (d, J = 5.6 Hz, 0.55H), 2.60 (s, 1.56H), 2.57 (s, 3H). **^{13}C NMR** (100 MHz, $CDCl_3$, ppm): δ = 198.34, 197.66, 162.74, 159.83, 138.53, 137.81, 137.78, 137.61, 130.19, 129.53, 125.29, 124.85, 124.69, 123.20, 119.42, 117.84, 26.81.

4-formamidobenzoic acid[48] (**Scheme 2**, entry **3o**) (CAS No. **28533-43-9**)

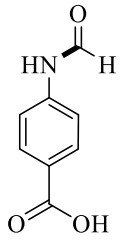

Using the experimental procedure EP-1, the product was obtained as brown oil in 68% yield; 55:45 mixture of rotamers: **^{1}H NMR** (400 MHz, $CDCl_3$, ppm): δ = 8.85 (br, 0.49H), 8.69 (d, J = 11.4 Hz, 0.58H), 8.35 (s, 0.49H), 8.00 (br, 0.45H), 7.55 (d, J = 8.2 Hz, 1H), 7.33 (dt, J = 13.4, 8.1 Hz, 2.15H), 7.18 (t, J = 7.5 Hz, 0.57H), 7.12 (m, 1.6H). **^{13}C NMR** (100 MHz, $CDCl_3$, ppm): δ = 163.09, 159.55, 137.06, 136.87, 129.82, 129.15, 125.37, 124.87, 120.19, 118.91.

Ethyl 4-formamidobenzoate[48] (**Scheme 2**, entry **3p**) (CAS No. **5422-63-9**)

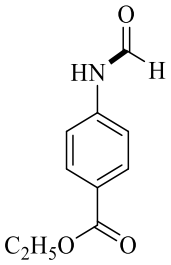

Using the experimental procedure EP-1, the product was obtained as white solid in 60% yield; 75:25 mixture of rotamers: **^{1}H NMR** (400 MHz, DMSO-d_6, ppm): δ = 10.53 (s, 1H), 10.46 (d, J = 10.8 Hz, 0.27H), 8.96 (d, J = 10.6 Hz, 0.26H), 8.35 (d, J = 1.7 Hz, 1H), 7.91 (m,2.65H), 7.71 (d, J = 8.4 Hz, 2H), 7.31 (d, J = 8.1 Hz, 0.77H), 4.28 (q, J = 7.1 Hz, 2.64H), 1.30 (t, J = 7.1 Hz, 4H). **^{13}C NMR** (100 MHz, DMSO-d_6, ppm): δ = 165.24, 162.54, 160.11, 142.90, 142.43, 130.73, 130.33, 124.66, 118.62, 116.43, 60.45, 14.18.

N-(2,4-dimethylphenyl)formamide[53] (**Scheme 2**, entry **3q**) (CAS No. **60397-77-5**)

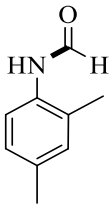

Using the experimental procedure EP-1, the product was obtained as off-white solid in 79% yield; 65:35 mixture of rotamers: **^{1}H NMR** (400 MHz, $CDCl_3$, ppm): δ = 8.45 (d, J = 11.2 Hz, 0.91H), 8.39 (s, 0.53H), 8.18 (br, 0.77H), 7.66 (d, J = 8.7 Hz, 0.51H), 7.35 (br, 0.38H), 7.04 (s, 1H), 7.00 (s, 3H), 2.31 (s, 3H), 2.28 (s, 1.62H), 2.26 (s, 3H), 2.22 (s, 1.65H). **^{13}C NMR** (100 MHz, $CDCl_3$, ppm): δ = 163.82, 159.50, 136.07, 135.45, 132.53, 131.96, 131.31, 130.22, 129.26, 127.63, 127.36, 123.51, 121.46, 20.94, 20.87, 17.79, 17.75.

N-(2-bromo-4-methylphenyl)formamide[52] (**Scheme 2**, entry **3r**) (CAS No. **353284-16-9**)

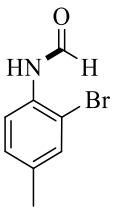

Using the experimental procedure EP-1, the product was obtained as off-white solid in 65% yield; 67:33 mixture of rotamers: **^{1}H NMR** (400 MHz, $CDCl_3$, ppm): δ = 8.62 (d, J = 11.1 Hz, 0.49H), 8.46 (s, 1H), 8.22 (d, J = 8.3 Hz, 1H), 7.62 (br, 1H), 7.42 (s, 0.50H), 7.37 (s, 1H), 7.12 (s, 1H), 7.10 (s, 0.58H), 2.32 (s, 1.48H), 2.30 (s, 3H). **^{13}C NMR** (100 MHz, $CDCl_3$, ppm): δ = 161.90, 158.88, 136.91, 135.93, 133.88, 132.72, 132.35, 129.42, 129.17, 122.24, 119.46, 114.78, 113.04, 20.67, 20.61.

N-(3-chloro-4-fluorophenyl)formamide[52] (**Scheme 2**, entry **3s**) (CAS No. **770-22-9**)

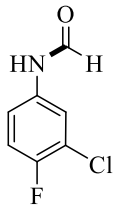

Using the experimental procedure EP-1, the product was obtained as off-white solid in 79% yield; 64:36 mixture of rotamers: **^{1}H NMR** (400 MHz, $CDCl_3$, ppm): δ = 8.66 (br, 0.42H), 8.58 (d, J = 11.1 Hz, 0.56H), 8.35 (s, 1H), 7.78 (br, 0.73H), 7.72 (dd, J = 6.5, 2.5 Hz, 1H), 7.36 (m, 1H), 7.18 (dd, J = 6.2, 2.6 Hz, 0.49H), 7.14 (t, J = 8.6 Hz, 0.57H), 7.08 (t, J = 8.7 Hz, 1H), 7.03 – 6.94 (m, 0.56H). **^{13}C NMR** (100 MHz, $CDCl_3$, ppm): δ = 162.89, 159.30, 157.27, 156.42, 154.80, 153.97, 133.55, 122.47, 121.61, 119.88, 119.81, 119.13, 119.06, 117.81, 117.58, 117.00, 116.78.

N-(5-(tert-butyl)-2-hydroxyphenyl)formamide[48] (**Scheme 2**, entry **3t**) (CAS No. **2305056-85-1**)

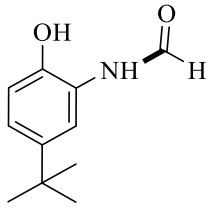

Using the experimental procedure EP-1, the product was obtained as brown solid in 87% yield; 77:23 mixture of rotamers: **^{1}H NMR** (400 MHz, DMSO-d_6, ppm): δ = 9.67 (s, 1H), 9.53 (s, 1H), 9.18 (d, J = 11.2 Hz, 0.14H), 8.52 (d, J = 11.2 Hz, 0.17H), 8.27 (s, 1H), 8.08 (s, 1H), 7.09 (s, 0.18H), 6.99 (dd, J = 8.5, 2.4 Hz, 0.2H), 6.93 (dd, J = 8.4, 2.4 Hz, 1H), 6.82 (s, 0.21H), 6.78 (d, J = 8.4 Hz, 1H), 1.23 (s,

11.58H). **^{13}C NMR** (100 MHz, DMSO-d_6, ppm): δ = 163.64, 159.98, 146.67, 144.42, 141.89, 141.26, 125.41, 124.54, 122.04, 120.81, 119.06, 117.92, 115.62, 114.64, 33.79, 31.37, 31.29.

N-(2-hydroxy-5-methylphenyl)formamide[48] (**Scheme 2**, entry **3u**) (CAS No. **74642-14-1**)

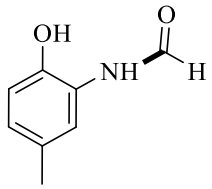

Using the experimental procedure EP-1, the product was obtained as brown solid in 85% yield; 81:19 mixture of rotamers: **^{1}H NMR** (400 MHz, DMSO-d_6, ppm): δ = 9.65 (s, 1H), 9.50 (s, 1H), 9.18 (d, J = 11.6 Hz, 0.15H), 8.51 (d, J = 11.1 Hz, 0.17H), 8.26 (s, 1H), 7.86 (s, 1H), 6.93 (s, 0.18H), 6.76 (d, J = 6.7 Hz, 0.63H), 6.73 (m, 1.8H), 2.18 (s, 3.72H). **^{13}C NMR** (100 MHz, DMSO-d_6, ppm): δ = 163.40, 159.93, 146.52, 144.40, 128.16, 127.53, 124.98, 124.44, 122.12, 121.26, 115.96, 114.89, 20.49, 20.09.

N-(2-methoxyphenyl)acetamide[54] **(Scheme 2**, entry **3v) (**CAS No. **93-26-5)**

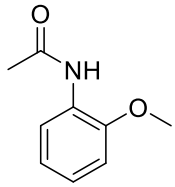

Using the experimental procedure EP-1, the product was obtained as white solid in 93% yield; **^{1}H NMR** (400 MHz, $CDCl_3$, ppm): δ = 8.34 (d, J = 9.7 Hz, 1H), 7.79 (br, 1H), 7.08 – 6.99 (m, 1H), 6.94 (t, J = 7.1 Hz, 1H), 6.86 (d, J = 8.2 Hz, 1H), 3.87 (s, 3H), 2.19 (s, 3H). **^{13}C NMR** (100 MHz, $CDCl_3$, ppm): δ = 168.31, 147.79, 127.78, 123.73, 121.17, 119.92, 109.98, 55.74, 24.97.

N-(3-nitrophenyl)acetamide[55] **(Scheme 2**, entry **3w) (**CAS No. **121-89-1)**

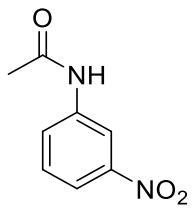

Using the experimental procedure EP-1, the product was obtained as yellow solid in 53% yield; **^{1}H NMR** (400 MHz, DMSO-d_6, ppm): δ = 10.44 (br, 1H), 8.60 (t, J = 2.2 Hz, 1H), 7.87 (dd, J = 8.2, 2.2 Hz, 2H), 7.57 (t, J = 8.2 Hz, 1H), 2.09 (s, 3H). **^{13}C NMR** (100 MHz, DMSO-d_6, ppm): δ = 169.10, 147.95, 140.40, 130.08, 124.87, 117.50, 113.04, 112.94, 24.03.

N-(3-(trifluoromethyl)phenyl)acetamide[48] **(Scheme 2**, entry **3x) (**CAS No. **349-76-8)**

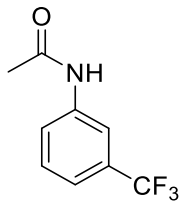

Using the experimental procedure EP-1, the product was obtained as white solid in 74% yield; **^{1}H NMR** (400 MHz, DMSO-d_6, ppm): δ = 10.26 (s, 1H), 8.07 (t, J = 2.0 Hz, 1H), 7.75 (d, J = 8.2 Hz, 1H), 7.52 (t, J = 8.0 Hz, 1H), 7.36 (d, J = 7.7 Hz, 1H), 2.07 (s, 3H). **^{13}C NMR** (100 MHz, DMSO-d_6, ppm): δ = 168.93, 140.04, 129.91, 122.46, 119.36,119.32, 119.29, 119.25, 115.0, 114.96, 24.02, 20.57.

N-(4-(trifluoromethoxy)phenyl)acetamide[48] **(Scheme 2**, entry **3y) (**CAS No. **85013-98-5)**

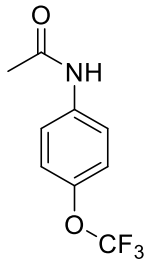

Using the experimental procedure EP-1, the product was obtained as Colourless Solid in 60% yield; **^{1}H NMR** (400 MHz, $CDCl_3$, ppm): δ = 7.95 (s, 1H), 7.53 (d, J = 9.0 Hz, 2H), 7.14 (d, J = 8.8 Hz, 2H), 2.16 (s, 3H). **^{13}C NMR** (100 MHz, $CDCl_3$, ppm): δ = 169.00, 136.71, 121.77, 121.32, 42.44, 24.46.

N-(4-chlorophenyl)acetamide[48] **(Scheme 2**, entry **3z) (**CAS No. **99-91-2)**

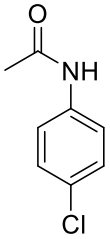

Using the experimental procedure EP-1, the product was obtained as light yellow solid in 68%; **^{1}H NMR** (400 MHz, DMSO-d_6, ppm): δ = 10.05 (br, 1H), 7.60 (d, J = 8.8 Hz, 2H), 7.33 (d, J = 8.9 Hz, 2H), 2.04 (s, 3H). **^{13}C NMR** (100 MHz, DMSO-d_6, ppm): δ = 168.43, 138.26, 128.53, 126.50, 120.48, 23.96.

N-methyl-N-phenylformamide[49] (**Scheme 2**, entry **3aa**) (CAS No. **93-61-8**)

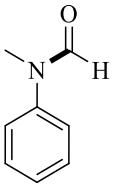

Using the experimental procedure EP-1, the product was obtained as yellow oil in 87% yield; **^{1}H NMR** (400 MHz, $CDCl_3$, ppm): δ = 8.34 (s, 1H), 7.28 (t, J = 8.0 Hz, 2H), 7.14 (t, J = 8.0 Hz, 1H), 7.04 (d, J = 8.6 Hz, 2H), 3.18 (s, 3H). **^{13}C NMR** (100 MHz, $CDCl_3$, ppm): δ = 162.41, 142.21, 129.66, 126.46, 122.41, 32.08.

N,N-diphenylformamide[48] (**Scheme 2**, entry **3ab**) (CAS No. **607-00-1**)

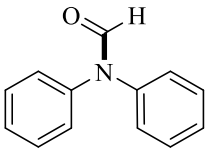

Using the experimental procedure EP-1, the product was obtained as yellow solid in 79% yield. **^{1}H NMR** (400 MHz, $CDCl_3$, ppm): δ = 8.60 (s, 1H), 7.33-7.30 (m, 4H), 7.28 – 7.15 (m, 4H), 7.10 (d, J = 7.9 Hz, 2H). **^{13}C NMR** (100 MHz, $CDCl_3$, ppm): δ = 161.85, 141.91, 139.76, 129.81, 129.29, 127.16, 126.97, 126.23, 125.21.

1-(4-(2-chlorophenyl)piperazin-1-yl)ethan-1-one[48] **(Scheme 2**, entry **3ac) (**CAS No. **150557-82-7)**

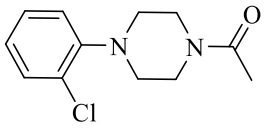

Using the experimental procedure EP-1, the product was obtained as light yellow solid in 85%; **^{1}H NMR** (400 MHz, DMSO-d_6, ppm): δ = 7.42 (d, J = 7.8 Hz, 1H), 7.30 (t, J = 7.7 Hz, 1H), 7.14 (d, J = 8.1 Hz, 1H), 7.06 (t, J = 7.6 Hz, 1H), 3.58 (q, J = 4.9 Hz, 4H), 2.96 (t, J = 4.9 Hz, 2H), 2.90 (t, J = 5.0 Hz, 2H), 2.04 (s, 3H). **^{13}C NMR** (100 MHz, DMSO-d_6, ppm): δ = 168.33, 148.65, 130.31, 128.09, 127.73, 124.23, 121.09, 51.16, 50.74, 45.91, 45.48, 41.03, 21.19.

morpholine-4-carbaldehyde[49] **(Scheme 2**, entry **3ad) (**CAS No. **4394-85-8)**

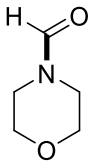

Using the experimental procedure EP-1, the product was obtained as yellow oil in 75%; **^{1}H NMR** (400 MHz, $CDCl_3$, ppm): δ = 7.86 (s, 1H), 3.51-3.48 (m, 2H), 3.48 – 3.41 (m, 2H), 3.40 – 3.32 (m, 2H), 3.26 – 3.18 (m, 2H). **^{13}C NMR** (100 MHz, DMSO-d_6, ppm): δ = 160.56, 66.85, 66.01, 45.42, 40.20.

piperidine-1-carbaldehyde[49] **(Scheme 2**, entry **3ae) (**CAS No. **2591-86-8)**

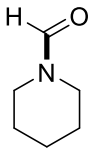

Using the experimental procedure EP-1, the product was obtained as yellow oil in 69%; **^{1}H NMR** (400 MHz, $CDCl_3$, ppm): δ = 7.79 (s, 1H), 3.30 – 3.21 (m, 2H), 3.17 – 3.03 (m, 2H), 1.50 – 1.45 (m, 2H), 1.42 – 1.34 (m, 2H), 1.35 – 1.24 (m, 2H). **^{13}C NMR** (100 MHz, $CDCl_3$, ppm): δ = 160.33, 46.34, 40.11, 26.14, 24.66, 24.23.

N-(quinolin-8-yl)formamide[48] (**Scheme 2**, entry **3af**) (CAS No. **62937-22-8**)

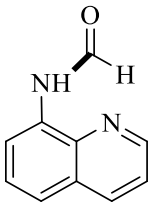

Using the experimental procedure EP-1, the product was obtained as brown solid in 60% yield; 88:12 mixture of rotamers; **^{1}H NMR** (400 MHz, $CDCl_3$, ppm): δ = 9.62 (br, 1H), 9.20 (br, 0.09H), 8.87 (d, *J* = 11.7 Hz, 0.11H), 8.56 (dd, *J* = 4.3, 1.6 Hz, 1.13H), 8.50 (p, *J* = 4.6 Hz, 1H), 8.45 (s, 1H), 7.93 (d, *J* = 8.3 Hz, 1H), 7.89 (d, *J* = 8.1 Hz, 0.15H), 7.29 (s, 1.15H), 7.28 (s, 1H), 7.26 (s, 0.18H), 7.22 (dd, *J* = 8.3, 4.3 Hz, 1.31H), 7.01 (s, 0.1H). **^{13}C NMR** (100 MHz, $CDCl_3$, ppm): δ = 159.39, 148.30, 138.05, 136.88, 133.52, 128.12, 127.51, 122.37, 121.81, 117.99.

N-(pyridin-2-yl)formamide[52] (**Scheme 2**, entry **3ag**) (CAS No. **34813-97-3**)

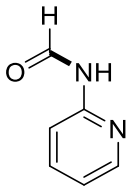

Using the experimental procedure EP-1, the product was obtained as brown solid in 70%; **^{1}H NMR** (400 MHz, DMSO-d_6, ppm): δ = 10.58 (s, 1H), 9.28 (d, *J* = 10.3 Hz, 0.57H), 8.33 (s, 0.82H), 8.25 (s, 0.64H), 7.82 – 7.69 (m, 1.11H), 7.08 (d, *J* = 5.6 Hz, 1.11H), 6.92 (d, *J* = 8.3 Hz, 0.61H). **^{13}C NMR** (100 MHz, DMSO-d_6, ppm): δ = 162.14, 160.32, 151.65, 151.03, 148.08, 138.71, 138.33, 119.78, 119.24, 113.79, 111.14.

Optimization of Reaction Conditions of annulation

General procedure for optimizations of reaction conditions. An oven-dried 20 mL Teflon screw-capped vial equipped with a stir bar was sequentially charged with amide **4c**, aniline **5a** and catalyst. TMSCl were transferred into the tube via a syringe. The resulting mixture was stirred in a preheated heat block. After full fill the reaction condition of experiment, the reaction mixture was cooled down to room temperature. The reaction mixture was diluted with ethyl acetate and then washed with dilute aqueous HCl solution and saturated brine, dried with

anhydrous Na_2SO_4, and finally concentrated in vacuo with the aid of rotary evaporator. The residue was purified by flash chromatography on silica gel using hexane and ethyl acetate as eluent to give the transamidated product **6c**.

Cu-catalyzed annulation of aliphatic unactivated amides with substituted 2-aminophenols

Experimental Procedure (EP-2): An oven-dried 20 mL Teflon screw-capped vial equipped with a stir bar was sequentially charged with aliphatic amide (0.5 mmol, 1 equiv.), amine (0.75 mmol, 1.5 equiv.) and $CuCl_2$ (0.075 mmol, 0.15 equiv.). TMSCl (0.75 mmol, 1.5 equiv.) was transferred into the tube via a syringe. The resulting mixture was stirred under an argon atmosphere in a preheated heat block at 160 °C for 16 h. At this point, the reaction mixture was cooled down to room temperature. The reaction mixture was diluted with ethyl acetate and then washed with dilute aqueous HCl solution (~0.1 M, 2 x 30 mL; **note**: water was used for washing instead of HCl (aq) for pyridine/quinoline-containing amide products) and saturated brine (~30 mL), dried with anhydrous Na_2SO_4, and finally concentrated in vacuo with the aid of rotary evaporator. The residue was purified by flash chromatography on silica gel using hexane and ethyl acetate as eluent to give the annulated benzoxazole product.

Analytical Data

2-methylbenzo[d]oxazole[56] (**Scheme 5a**, entry **6a**) (CAS No. **95-21-6**)

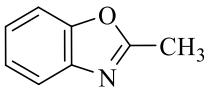

Using the experimental procedure EP-2, the product was obtained as light brown liquid in 80%; **^{1}H NMR** (400 MHz, $CDCl_3$, ppm): δ = 7.66 (dd, J = 6.2, 2.9 Hz, 1H), 7.47 (dd, J = 6.4, 2.9 Hz, 1H), 7.29 (dd, J = 5.3, 3.9 Hz, 2H), 2.65 (s, 3H). **^{13}C NMR** (100 MHz, DMSO-d_6, ppm): δ = 172.1, 145.4, 140.6, 138.2, 128.7, 122.9, 23.5.

2-propylbenzo[d]oxazole[57] (**Scheme 5a**, entry **6b**) (CAS No. **2008-05-1**)

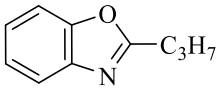

Using the experimental procedure EP-2, the product was obtained as light brown liquid in 76%; **^{1}H NMR** (400 MHz, $CDCl_3$, ppm): δ = 7.64 (dd, J = 7.2, 4.0 Hz, 1H), 7.45 (d, J = 8.0 Hz, 1H), 7.26-7.24 (m, 2H), 2.88 (t, 2H), 1.92-1.87 (m, 2H), 1.03 (t, 3H). **^{13}C NMR** (100 MHz, $CDCl_3$, ppm): δ = 167.1, 150.6, 141.3, 123.9, 119.4, 110.3, 30.5, 20.3, 13.9.

2-butylbenzo[d]oxazole[57] (**Scheme 5a**, entry **6c**) (CAS No. **6797-49-5**)

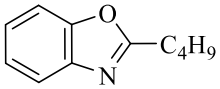

Using the experimental procedure EP-2, the product was obtained as light brown liquid in 75%; **^{1}H NMR** (400 MHz, DMSO-d_6, ppm): δ = 7.68 – 7.61 (m, 1H), 7.61 – 7.52 (m, 1H), 7.33 – 7.23 (m, 2H), 2.86 (t, J = 7.5 Hz, 2H), 1.73 (p, J = 7.5 Hz, 2H), 1.33 (dq, J = 14.8, 7.3 Hz, 2H), 0.85 (t, J = 7.4 Hz, 3H). **^{13}C NMR** (100 MHz, DMSO-d_6, ppm): δ = 166.69, 150.20, 141.02, 124.31, 123.91, 119.07, 110.18, 28.12, 27.35, 21.54, 13.29.

2-neopentylbenzo[d]oxazole[58] (**Scheme 5a**, entry **6d**) (CAS No. **143857-68-5**)

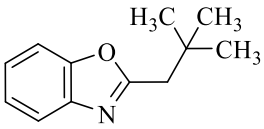

Using the experimental procedure EP-2, the product was obtained as light-yellow solid in 70%; **^{1}H NMR** (400 MHz, $CDCl_3$, ppm): δ = 7.70 (d, J = 3.2 Hz, 1H), 7.55 – 7.43 (m, 1H), 7.32 – 7.24 (m, 2H), 2.82 (s, 2H), 1.08 (s, 9H). **^{13}C NMR** (100 MHz, $CDCl_3$, ppm): δ = 166.05, 150.88, 141.38, 124.52, 124.15, 119.70, 110.40, 42.54, 32.20, 29.73.

2-benzylbenzo[d]oxazole[59] (**Scheme 5a**, entry **6e**) (CAS No. **2008-07-3**)

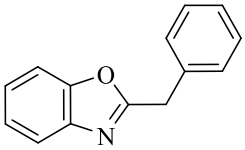

Using the experimental procedure EP-2, the product was obtained as light-yellow solid in 72%; **^{1}H NMR** (400 MHz, $CDCl_3$, ppm): δ = 7.67 (dd, J = 5.9, 2.4 Hz, 1H), 7.49 – 7.38 (m, 1H), 7.34 (d, J = 7.1 Hz, 2H), 7.29 (t, J = 7.8 Hz, 2H), 7.24-7.19 (m, 3H), 4.22 (s, 2H). **^{13}C NMR** (100 MHz, $CDCl_3$, ppm): δ = 165.18, 151.00, 141.29, 134.76, 128.97, 128.78, 127.27, 124.66, 124.16, 119.77, 110.40, 35.18.

2-(phenoxymethyl)benzo[d]oxazole[60] (**Scheme 5a**, entry **6f**) (CAS No. **7506-48-1**)

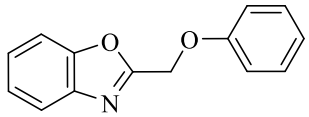

Using the experimental procedure EP-2, the product was obtained as white solid in 75%; **^{1}H NMR** (400 MHz, $CDCl_3$, ppm): δ = 7.65 (dd, J = 5.3, 3.9 Hz, 1H), 7.43 (dd, J = 4.8, 3.2 Hz, 1H), 7.26 – 7.22 (m, 2H), 7.19 (t, J = 7.6 Hz, 2H), 6.97 (s, 1H), 6.94 (s, 1H), 6.92 – 6.85 (m, 1H), 5.20 (s, 2H). **^{13}C NMR** (100 MHz, $CDCl_3$, ppm): δ = 161.56, 157.93, 150.97, 140.74, 129.69, 125.64, 124.69, 121.97, 120.43, 114.87, 110.95, 62.80.

2-isopropylbenzo[d]oxazole[57] (**Scheme 5a**, entry **6g**) (CAS No. **6797-15-5**)

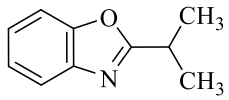

Using the experimental procedure EP-2, the product was obtained as light brown liquid in 60%; **^{1}H NMR** (400 MHz, $CDCl_3$, ppm): δ = 7.70-7.66 (m, 1H), 7.47 (dd, J = 5.6, 3.7 Hz, 1H), 7.35 – 7.23 (m, 2H), 3.25 (hept, J = 7.0 Hz, 1H), 1.46 (d, J = 8.2 Hz, 6H). **^{13}C NMR** (100 MHz, $CDCl_3$, ppm): δ = 171.45, 150.84, 141.27, 124.57, 124.17, 119.72, 110.43, 29.01, 20.41.

2-(tert-butyl)benzo[d]oxazole[57] (**Scheme 5a**, entry **6h**) (CAS No. **54696-03-6**)

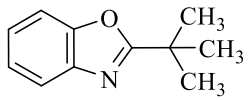

Using the experimental procedure EP-2, the product was obtained as brown liquid in 58%; **^{1}H NMR** (400 MHz, $CDCl_3$, ppm): δ = 7.52-7.48 (m, 1H), 7.30-7.27 (m, 1H), 7.13 – 7.03 (m, 2H), 1.30 (s, 9H).

^{13}C NMR (100 MHz, $CDCl_3$, ppm): δ = 173.61, 150.94, 141.36, 124.51, 124.08, 119.82, 110.42, 34.28, 28.59.

2-(trichloromethyl)benzo[d]oxazole[60] (**Scheme 5a**, entry **6i**) (CAS No. **14468-53-2**)

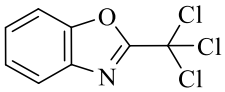

Using the experimental procedure EP-2, the product was obtained as brown solid in 35%; **^{1}H NMR** (400 MHz, $CDCl_3$, ppm): δ = 7.56 (dd, J = 7.9, 1.7 Hz, 1H), 7.19 – 7.08 (m, 1H), 7.03 – 6.87 (m, 1H), 6.89 – 6.76 (m, 1H). **^{13}C NMR** (100 MHz, $CDCl_3$, ppm): δ = 159.31, 149.86, 127.07, 123.84, 123.65, 119.10, 115.61, 92.74.

2-cyclopropylbenzo[d]oxazole[57] (**Scheme 5a**, entry **6j**) (CAS No. **63359-58-0**)

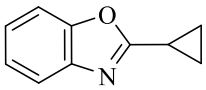

Using the experimental procedure EP-2, the product was obtained as brown liquid in 65%; **^{1}H NMR** (400 MHz, $CDCl_3$, ppm): δ = 7.58 (d, J = 6.7 Hz, 1H), 7.39 (d, J = 7.6 Hz, 1H), 7.23-7.19 (m, 2H), 2.21-2.14 (m, 1H), 1.26-1.21 (m, 2H), 1.23 – 1.07 (m, 2H). **^{13}C NMR** (100 MHz, $CDCl_3$, ppm): δ = 168.64, 150.45, 141.54, 124.11, 123.99, 118.98, 110.02, 9.30, 9.17.

2-cyclohexylbenzo[d]oxazole[61] (**Scheme 5a**, entry **6k**) (CAS No. **104462-82-0**)

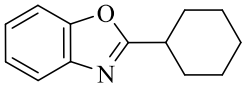

Using the experimental procedure EP-2, the product was obtained as brown solid in 57%; **^{1}H NMR** (400 MHz, $CDCl_3$, ppm): δ = 7.70 – 7.63 (m, 1H), 7.63 – 7.55 (m, 1H), 7.35 – 7.24 (m, 2H), 2.92 (tt, J = 11.0, 3.7 Hz, 1H), 2.04 (dd, J = 12.9, 3.1 Hz, 2H), 1.71 (dt, J = 13.1, 3.8 Hz, 2H), 1.65 – 1.50 (m, 3H), 1.35 (qt, J = 12.2, 3.2 Hz, 2H), 1.28 – 1.13 (m, 1H). **^{13}C NMR** (100 MHz, $CDCl_3$, ppm): δ = 169.50, 149.99, 140.85, 124.40, 123.96, 119.23, 110.32, 36.78, 29.85, 25.24, 24.82.

6-chloro-2-methylbenzo[d]oxazole[54] (**Scheme 5a**, entry **6l**) (CAS No. **63816-18-2**)

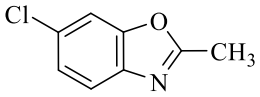

Using the experimental procedure EP-2, the product was obtained as brown solid in 57%; **^{1}H NMR** (400 MHz, $CDCl_3$, ppm): δ = 7.54 (dd, J = 8.4 Hz, 1H), 7.47 (s, 1H), 7.27 (d, J = 8.4 Hz, 1H), 2.63 (s, 3H). **^{13}C NMR** (100 MHz, $CDCl_3$, ppm): δ = 168.9, 146.9, 120.6, 119.5, 107.1, 15.0.

5-chloro-2-methylbenzo[d]oxazole[56] (**Scheme 5b**, entry **6m**) (CAS No. **19219-99-9**)

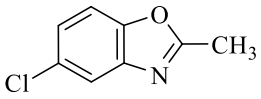

Using the experimental procedure EP-2, the product was obtained as light-yellow solid in 74%; **^{1}H NMR** (400 MHz, $CDCl_3$, ppm): δ = 7.60 (s, 1H), 7.36 (d, *J* = 8.6 Hz, 1H), 7.24 (d, *J* = 8.6 Hz, 1H), 2.61 (s, 3H). **^{13}C NMR** (100 MHz, $CDCl_3$, ppm): δ = 165.57, 149.53, 142.31, 129.48, 124.95, 119.39, 111.07, 14.56.

2-methyl-6-nitrobenzo[d]oxazole[62] (**Scheme 5b**, entry **6n**) (CAS No. **5683-43-2**)

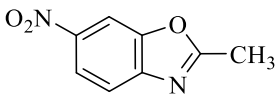

Using the experimental procedure EP-2, the product was obtained as off-white solid in 35%; **^{1}H NMR** (400 MHz, $CDCl_3$, ppm): δ = 8.40 (s, 1H), 8.28 (d, *J* = 8.8 Hz, 1H), 7.75 (d, *J* = 8.8 Hz, 1H), 2.73 (s, 3H). **^{13}C NMR** (100 MHz, $CDCl_3$, ppm): δ = 168.97, 150.28, 146.98, 120.57, 119.53, 107.06, 15.02.

2,5-dimethylbenzo[d]oxazole[56] (**Scheme 5b**, entry **6o**) (CAS No. **5676-58-4**)

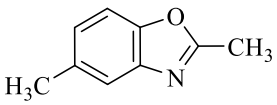

Using the experimental procedure EP-2, the product was obtained as yellow liquid in 80%; **^{1}H NMR** (400 MHz, $CDCl_3$, ppm): δ = 7.41 (s, 1H), 7.31 (d, *J* = 8.2 Hz, 1H), 7.06 (d, *J* = 10.1 Hz, 1H), 2.59 (s,

3H), 2.42 (s, 3H). **^{13}C NMR** (100 MHz, $CDCl_3$, ppm): δ = 163.99, 149.21, 141.51, 133.97, 125.56, 119.33, 109.60, 21.43, 14.51.

2,6-dimethylbenzo[d]oxazole[56] (**Scheme 5b**, entry **6p**) (CAS No. **53012-61-6**)

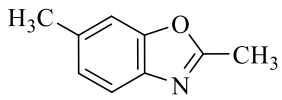

Using the experimental procedure EP-2, the product was obtained as yellow liquid in 81%; **^{1}H NMR** (400 MHz, $CDCl_3$, ppm): δ = 7.48 (d, J = 8.2 Hz, 1H), 7.22 (s, 1H), 7.06 (d, J = 8.3 Hz, 1H), 2.56 (s, 3H), 2.42 (s, 3H). **^{13}C NMR** (100 MHz, $CDCl_3$, ppm): δ = 163.28, 151.20, 139.05, 134.76, 125.26, 118.62, 110.40, 21.58, 14.37.

5-(tert-butyl)-2-methylbenzo[d]oxazole[63] (**Scheme 5b**, entry **6q**) (CAS No. **40874-54-2**)

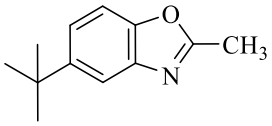

Using the experimental procedure EP-2, the product was obtained as yellow liquid in 79%; **^{1}H NMR** (400 MHz, $CDCl_3$, ppm): δ = 7.70 (s, 1H), 7.44 – 7.34 (m, 2H), 2.65 (s, 3H), 1.40 (s, 9H). **^{13}C NMR** (100 MHz, $CDCl_3$, ppm): δ = 164.12, 149.04, 147.85, 141.23, 122.26, 116.00, 109.45, 34.97, 31.89, 14.59.

2-methyloxazolo[4,5-b]pyridine[56] (**Scheme 5b**, entry **6r**) (CAS No. **86467-39-2**)

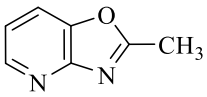

Using the experimental procedure EP-2, the product was obtained as off-white solid in 49%; **^{1}H NMR** (400 MHz, $CDCl_3$, ppm): δ = 7.84 (d, J = 6.2 Hz, 1H), 7.37 (d, J = 8.2 Hz, 1H), 7.12 (dd, J = 8.1, 4.6 Hz, 1H), 2.29 (s, 3H). **^{13}C NMR** (100 MHz, $CDCl_3$, ppm): δ = 172.13, 145.36, 140.59, 138.15, 128.68, 122.86, 23.46.

2-methylnaphtho[1,2-d]oxazole[64] (**Scheme 5b**, entry **6s**) (CAS No. **85-15-4**)

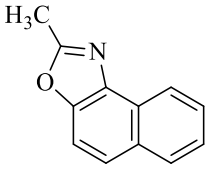

Using the experimental procedure EP-2, the product was obtained as brown liquid in 55%; **^{1}H NMR** (400 MHz, $CDCl_3$, ppm): δ = 8.46 (d, J = 8.2 Hz, 1H), 7.93 (d, J = 8.2 Hz, 1H), 7.72 (d, J = 8.8 Hz, 1H), 7.67 – 7.58 (m, 2H), 7.51 (t, J = 7.6 Hz, 1H), 2.72 (s, 3H). **^{13}C NMR** (100 MHz, $CDCl_3$, ppm): δ = 162.94, 148.18, 136.63, 131.10, 128.58, 126.98, 126.31, 125.35, 125.19, 122.00, 110.70, 14.68.

2-methylbenzo[d]thiazole[59] (**Scheme 5b**, entry **6t**) (CAS No. **120-75-2**)

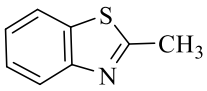

Using the experimental procedure EP-2, the product was obtained as brown liquid in 75%; **^{1}H NMR** (400 MHz, DMSO-d_6, ppm): δ = 8.00-7.97 (m, 1H), 7.93 – 7.90 (m, 1H), 7.47-7.43 (m, 1H), 7.39-7.34 (m, 1H), 2.77 (s, 3H). **^{13}C NMR** (100 MHz, DMSO-d_6, ppm): δ = 166.8, 153.0, 135.2, 125.9, 124.6, 121.9, 121.8, 19.6.

5-chloro-2-methylbenzo[d]thiazole[59] (**Scheme 5b**, entry **6u**) (CAS No. **1006-99-1**)

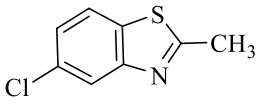

Using the experimental procedure EP-2, the product was obtained as brown liquid in 70%; **^{1}H NMR** (400 MHz, DMSO-d_6, ppm): δ = 8.06 (d, J = 8.6 Hz, 1H), 7.97 (d, J = 2.0 Hz, 1H), 7.43 (dd, J = 8.6, 2.1 Hz, 1H), 2.80 (s, 3H). **^{13}C NMR** (100 MHz, DMSO-d_6, ppm): δ = 169.63, 153.84, 133.96, 130.73, 124.78, 123.38, 121.40, 19.80.

References

(1) Allen, C. L.; Williams, J. M. J. Metal-Catalysed Approaches to Amide Bond Formation. *Chem. Soc. Rev.* **2011**. https://doi.org/10.1039/c0cs00196a.

(2) Valeur, E.; Bradley, M. Amide Bond Formation: Beyond the Myth of Coupling Reagents.

Chem. Soc. Rev. **2009**. https://doi.org/10.1039/b701677h.

(3) Maruyama, C.; Hamano, Y. TRNA-Dependent Amide Bond–Forming Enzymes in Peptide Natural Product Biosynthesis. *Current Opinion in Chemical Biology*. 2020. https://doi.org/10.1016/j.cbpa.2020.08.002.

(4) Sánchez, A.; Vázquez, A. Bioactive Peptides: A Review. *Food Quality and Safety*. 2017. https://doi.org/10.1093/fqsafe/fyx006.

(5) Kay-Shoemake, J. L.; Watwood, M. E.; Sojka, R. E.; Lentz, R. D. Soil Amidase Activity in Polyacrylamide-Treated Soils and Potential Activity toward Common Amide-Containing Pesticides. *Biol. Fertil. Soils* **2000**. https://doi.org/10.1007/s003740050643.

(6) Cotesta, S.; Stahl, M. The Environment of Amide Groups in Protein-Ligand Complexes: H-Bonds and Beyond. *J. Mol. Model.* **2006**. https://doi.org/10.1007/s00894-005-0067-x.

(7) Mahesh, S.; Tang, K. C.; Raj, M. Amide Bond Activation of Biological Molecules. *Molecules* **2018**. https://doi.org/10.3390/molecules23102615.

(8) Lee, P. C.; Ha, J. U.; Kim, B. R.; Jeoung, S. K.; Jung, W.; Shin, D.; Han, J. H.; Bang, Y. K. Melt Flow Improvement of Polyamide 6/Glass Fiber Composite Using Amide-Type Lubricant. *Polym.* **2018**. https://doi.org/10.7317/pk.2018.42.4.568.

(9) Biundo, A.; Subagia, R.; Maurer, M.; Ribitsch, D.; Syrén, P. O.; Guebitz, G. M. Switched Reaction Specificity in Polyesterases towards Amide Bond Hydrolysis by Enzyme Engineering. *RSC Adv.* **2019**. https://doi.org/10.1039/c9ra07519d.

(10) Badillo, S. P. J.; Jamora, R. D. G. Zolpidem for the Treatment of Dystonia. *Frontiers in Neurology*. 2019. https://doi.org/10.3389/fneur.2019.00779.

(11) Saraceni, M. M.; Venci, J. V.; Gandhi, M. A. Levomilnacipran (Fetzima): A New Serotonin-Norepinephrine Reuptake Inhibitor for the Treatment of Major Depressive Disorder. *Journal of Pharmacy Practice*. 2014. https://doi.org/10.1177/0897190013516504.

(12) Clissold, S. P. Paracetamol and Phenacetin. *Drugs* **1986**. https://doi.org/10.2165/00003495-198600324-00005.

(13) Harvey, R. D.; Adams, V. R.; Beardslee, T.; Medina, P. Afatinib for the Treatment of EGFR Mutation-Positive NSCLC: A Review of Clinical Findings. *Journal of Oncology Pharmacy Practice*. 2020. https://doi.org/10.1177/1078155220931926.

(14) Przybyła, G. W.; Szychowski, K. A.; Gmiński, J. Paracetamol – An Old Drug with New Mechanisms of Action. *Clinical and Experimental Pharmacology and Physiology*. 2021. https://doi.org/10.1111/1440-1681.13392.

(15) De Figueiredo, R. M.; Suppo, J. S.; Campagne, J. M. Nonclassical Routes for Amide Bond Formation. *Chemical Reviews*. 2016. https://doi.org/10.1021/acs.chemrev.6b00237.

(16) Pattabiraman, V. R.; Bode, J. W. Rethinking Amide Bond Synthesis. *Nature*. 2011. https://doi.org/10.1038/nature10702.

(17) Lanigan, R. M.; Sheppard, T. D. Recent Developments in Amide Synthesis: Direct Amidation of Carboxylic Acids and Transamidation Reactions. *European Journal of Organic Chemistry*. 2013. https://doi.org/10.1002/ejoc.201300573.

(18) Naka, H.; Naraoka, A. Recent Advances in Transfer Hydration of Nitriles with Amides or Aldoximes. *Tetrahedron Letters*. 2020. https://doi.org/10.1016/j.tetlet.2019.151557.

(19) Gaspa, S.; Porcheddu, A.; De Luca, L. Recent Developments in Oxidative Esterification and Amidation of Aldehydes. *Tetrahedron Letters*. 2016. https://doi.org/10.1016/j.tetlet.2016.06.115.

(20) Debnath, P. Recent Advances in the Synthesis of Amides via Oxime Rearrangements and Its Applications. *Curr. Org. Synth.* **2018**. https://doi.org/10.2174/1570179415666180416151039.

(21) Rocha, R. O.; Rodrigues, M. O.; Neto, B. A. D. Review on the Ugi Multicomponent Reaction Mechanism and the Use of Fluorescent Derivatives as Functional Chromophores. *ACS Omega* **2020**. https://doi.org/10.1021/acsomega.9b03684.

(22) Wolff, H. The Schmidt Reaction. *Org. React.* **2012**. https://doi.org/10.1002/0471264180.or003.08.

(23) Jiang, D.; He, T.; Ma, L.; Wang, Z. Recent Developments in Ritter Reaction. *RSC Advances*. 2014. https://doi.org/10.1039/c4ra10784e.

(24) Acosta-Guzmán, P.; Mateus-Gómez, A.; Gamba-Sánchez, D. Direct Transamidation Reactions: Mechanism and Recent Advances. *Molecules*. 2018. https://doi.org/10.3390/molecules23092382.

(25) Kolympadi Marković, M.; Marković, D.; Laclef, S. Amide Synthesis by Transamidation of Primary Carboxamides. *Synth.* **2020**. https://doi.org/10.1055/s-0040-1707133.

(26) Li, G.; Ma, S.; Szostak, M. Amide Bond Activation: The Power of Resonance. *Trends in Chemistry*. 2020. https://doi.org/10.1016/j.trechm.2020.08.001.

(27) PAULING, L.; COREY, R. B.; BRANSON, H. R. The Structure of Proteins; Two Hydrogen-Bonded Helical Configurations of the Polypeptide Chain. *Proc. Natl. Acad. Sci. U. S. A.* **1951**. https://doi.org/10.1073/pnas.37.4.205.

(28) Meng, G.; Shi, S.; Szostak, M. Cross-Coupling of Amides by N-C Bond Activation. *Synlett* **2016**. https://doi.org/10.1055/s-0036-1588080.

(29) Kovács, E.; Rózsa, B.; Csomos, A.; Csizmadia, I. G.; Mucsi, Z. Amide Activation in Ground and Excited States. *Molecules* **2018**. https://doi.org/10.3390/molecules23112859.

(30) Chaudhari, M. B.; Gnanaprakasam, B. Recent Advances in the Metal-Catalyzed Activation of Amide Bonds. *Chemistry - An Asian Journal*. 2019. https://doi.org/10.1002/asia.201801317.

(31) Li, G.; Szostak, M. Non-Classical Amide Bond Formation: Transamidation and Amidation of Activated Amides and Esters by Selective N-C/O-C Cleavage. *Synthesis (Germany)*. 2020. https://doi.org/10.1055/s-0040-1707101.

(32) Bourne-Branchu, Y.; Gosmini, C.; Danoun, G. N-Boc-Amides in Cross-Coupling Reactions.

Chemistry - A European Journal. 2019. https://doi.org/10.1002/chem.201802635.

(33) Chen, J.; Xia, Y.; Lee, S. Transamidation for the Synthesis of Primary Amides at Room Temperature. *Org. Lett.* **2020**. https://doi.org/10.1021/acs.orglett.0c00958.

(34) Buchspies, J.; Rahman, M. M.; Szostak, M. Transamidation of Amides and Amidation of Esters by Selective N-C(O)/O-C(O) Cleavage Mediated by Air- and Moisture-Stable Half-Sandwich Nickel(II)-NHC Complexes. *Molecules* **2021**. https://doi.org/10.3390/molecules26010188.

(35) Li, G.; Szostak, M. Transition-Metal-Free Activation of Amides by N−C Bond Cleavage. *Chemical Record*. 2020. https://doi.org/10.1002/tcr.201900072.

(36) Liu, C.; Lalancette, R.; Szostak, R.; Szostak, M. Sterically Hindered Ketones via Palladium-Catalyzed Suzuki-Miyaura Cross-Coupling of Amides by N-C(O) Activation. *Org. Lett.* **2019**. https://doi.org/10.1021/acs.orglett.9b02961.

(37) Rahman, M. M.; Li, G.; Szostak, M. Metal-Free Transamidation of Secondary Amides by N-C Cleavage. *J. Org. Chem.* **2019**. https://doi.org/10.1021/acs.joc.9b02013.

(38) Idris, M. A.; Lee, S. Transamidation: Via C-N Bond Cleavage of Amides and Tertiary Amines. *Org. Chem. Front.* **2020**. https://doi.org/10.1039/d0qo00713g.

(39) Dander, J. E.; Baker, E. L.; Garg, N. K. Nickel-Catalyzed Transamidation of Aliphatic Amide Derivatives. *Chem. Sci.* **2017**. https://doi.org/10.1039/c7sc01980g.

(40) Liu, Y.; Shi, S.; Achtenhagen, M.; Liu, R.; Szostak, M. Metal-Free Transamidation of Secondary Amides via Selective N-C Cleavage under Mild Conditions. *Org. Lett.* **2017**. https://doi.org/10.1021/acs.orglett.7b00429.

(41) Tang, L.; Li, X. M.; Matuska, J. H.; He, Y. H.; Guan, Z. Intramolecular Transamidation of Secondary Amides via Visible-Light-Induced Tandem Reaction. *Org. Lett.* **2018**. https://doi.org/10.1021/acs.orglett.8b02303.

(42) Stephenson, N. A.; Zhu, J.; Gellman, S. H.; Stahl, S. S. Catalytic Transamidation Reactions Compatible with Tertiary Amide Metathesis under Ambient Conditions. *J. Am. Chem. Soc.* **2009**. https://doi.org/10.1021/ja8094262.

(43) Cheung, C. W.; Ma, J. A.; Hu, X. Manganese-Mediated Reductive Transamidation of Tertiary Amides with Nitroarenes. *J. Am. Chem. Soc.* **2018**. https://doi.org/10.1021/jacs.8b03739.

(44) Qu, E.; Li, S.; Bai, J.; Zheng, Y.; Li, W. Nickel-Catalyzed Reductive Cross-Coupling of N-Acyl and N-Sulfonyl Benzotriazoles with Diverse Nitro Compounds: Rapid Access to Amides and Sulfonamides. *Org. Lett.* **2022**, *24* (1), 58–63. https://doi.org/10.1021/acs.orglett.1c03535.

(45) Jain, I.; Sharma, R.; Malik, P. Manganese-Mediated Acetylation of Alcohols, Phenols, Thiols, and Amines Utilizing Acetic Anhydride. *Synth. Commun.* **2019**. https://doi.org/10.1080/00397911.2019.1650282.

(46) Yi, X.; Yi, X.; Lei, S.; Liu, W.; Che, F.; Yu, C.; Liu, X.; Wang, Z.; Zhou, X.; Zhang, Y. Copper-Catalyzed Radical N-Demethylation of Amides Using N-Fluorobenzenesulfonimide as an Oxidant. *Org. Lett.* **2020**. https://doi.org/10.1021/acs.orglett.0c00863.

(47) Ning, Y.; Wang, S.; Li, M.; Han, J.; Zhu, C.; Xie, J. Site-Specific Umpolung Amidation of Carboxylic Acids via Triplet Synergistic Catalysis. *Nat. Commun.* **2021**. https://doi.org/10.1038/s41467-021-24908-w.

(48) Kumar, V.; Dhawan, S.; Girase, P. S.; Singh, P.; Karpoormath, R. An Environmentally Benign, Catalyst-Free N−C Bond Cleavage/Formation of Primary, Secondary, and Tertiary Unactivated Amides. *European J. Org. Chem.* **2021**. https://doi.org/10.1002/ejoc.202101114.

(49) Leong, B. X.; Teo, Y. C.; Condamines, C.; Yang, M. C.; Su, M. Der; So, C. W. A NHC-Silyliumylidene Cation for Catalytic N-formylation of Amines Using Carbon Dioxide. *ACS Catal.* **2020**. https://doi.org/10.1021/acscatal.0c03795.

(50) Jiang, J.; Li, L.; Zhang, L.; Chen, Q.; Sun, H.; Liao, S.; Li, C.; Zhang, L. Organophosphoric Acid Promoted Transamidation: Using N,N-Dimethylformamide and N,N-Dimethylacetamide

as the Acyl Sources. *ChemistrySelect* **2021**, *6* (45), 12834–12837. https://doi.org/https://doi.org/10.1002/slct.202103932.

(51) Kandula, V.; Gudipati, R.; Chatterjee, A.; Yennam, S.; Behera, M. An Efficient Method for the Preparation of N -Formamides Using Propylphosphonic Anhydride (T3P®). *SynOpen* **2018**. https://doi.org/10.1055/s-0036-1591584.

(52) Dhawan, S.; Girase, P. S.; Kumar, V.; Karpoormath, R. HCl-Mediated Transamidation of Unactivated Formamides Using Aromatic Amines in Aqueous Media. *Synth. Commun.* **2021**. https://doi.org/10.1080/00397911.2021.1989597.

(53) Jiang, X.; Huang, Z.; Makha, M.; Du, C. X.; Zhao, D.; Wang, F.; Li, Y. Tetracoordinate Borates as Catalysts for Reductive Formylation of Amines with Carbon Dioxide. *Green Chem.* **2020**. https://doi.org/10.1039/d0gc01741h.

(54) Sutar, S. M.; Kalkhambkar, R. G. Ultrasonic Assisted Facile Synthesis of N-Arylamides Using Nitriles and 1-Aryltriazenes Precursors Promoted by Brønsted Acidic Ionic Liquid under Metal-Free Conditions. *ChemistrySelect* **2021**. https://doi.org/10.1002/slct.202101855.

(55) Zhou, X. Y.; Chen, X.; Yang, D. Iodine and Brønsted Acid Catalyzed C–C Bond Cleavage of 1,3-Diketones for the Acylation of Amines. *Synth. Commun.* **2020**. https://doi.org/10.1080/00397911.2019.1691736.

(56) Mayo, M. S.; Yu, X.; Zhou, X.; Feng, X.; Yamamoto, Y.; Bao, M. Synthesis of Benzoxazoles from 2-Aminophenols and β-Diketones Using a Combined Catalyst of Brønsted Acid and Copper Iodide. *J. Org. Chem.* **2014**. https://doi.org/10.1021/jo500604x.

(57) Niu, Z. J.; Li, L. H.; Liu, X. Y.; Liang, Y. M. Transition-Metal-Free Alkylation/Arylation of Benzoxazole via Tf2O-Activated-Amide. *Adv. Synth. Catal.* **2019**. https://doi.org/10.1002/adsc.201901078.

(58) Dong, K.; Humeidi, A.; Griffith, W.; Arman, H.; Xu, X.; Doyle, M. P. Ag I -Catalyzed Reaction of Enol Diazoacetates and Imino Ethers: Synthesis of Highly Functionalized Pyrroles

. *Angew. Chemie* **2021**. https://doi.org/10.1002/ange.202101641.

(59) Zhang, J.; Hu, L.; Liu, Y.; Zhang, Y.; Chen, X.; Luo, Y.; Peng, Y.; Han, S.; Pan, B. Elemental Sulfur-Promoted Benzoxazole/Benzothiazole Formation Using a C═C Double Bond as a One-Carbon Donator. *J. Org. Chem.* **2021**. https://doi.org/10.1021/acs.joc.1c01357.

(60) Luo, B.; Li, D.; Zhang, A. L.; Gao, J. M. Synthesis, Antifungal Activities and Molecular Docking Studies of Benzoxazole and Benzothiazole Derivatives. *Molecules* **2018**. https://doi.org/10.3390/molecules23102457.

(61) Putta, R. R.; Chun, S.; Choi, S. H.; Lee, S. B.; Oh, D. C.; Hong, S. Iron(0)-Catalyzed Transfer Hydrogenative Condensation of Nitroarenes with Alcohols: A Straightforward Approach to Benzoxazoles, Benzothiazoles, and Benzimidazoles. *J. Org. Chem.* **2020**. https://doi.org/10.1021/acs.joc.0c02191.

(62) Zhang, P.; Cedilote, M.; Cleary, T. P.; Pierce, M. E. Mono-Nitration of Aromatic Compounds via Their Nitric Acid Salts. *Tetrahedron Lett.* **2007**. https://doi.org/10.1016/j.tetlet.2007.10.027.

(63) Li, K. L.; Du, Z. B.; Guo, C. C.; Chen, Q. Y. Regioselective Syntheses of 2- and 4-Formylpyrido[2,1-b]Benzoxazoles. *J. Org. Chem.* **2009**. https://doi.org/10.1021/jo900267c.

(64) Katritzky, A. R.; Wang, Z.; Hall, C. D.; Akhmedov, N. G.; Shestopalov, A. A.; Steel, P. J. Cyclization of α-Oxo-Oximes to 2-Substituted Benzoxazoles. *J. Org. Chem.* **2003**. https://doi.org/10.1021/jo026771y.

Chapter 6

Summary and Conclusion

Synthetic chemists are usually faced with a difficult problem when it comes to amide synthesis. Thus, the acid amine coupling reagents, acid chloride preparation, metal-catalysed hydration of nitriles, oxidative amidation of various groups such as aldehyde, benzyl alcohols, methyl ketone or methyl arenes and oxidation of primary benzyl amines, rearrangement of aldoximes and decarboxylative ammoxidation of phenylacetic acid methods came to limelight. Additionally, Transamidation has recently shown promising results in obtaining amide compounds from other amides. However, transamidation is classified into two types based on the amides. The first is activated amides, which have had their nitrogen atoms activated utilising boc-anhydride, mesyl, and tosyl functionalization to weaken the C-N bond. The benefit of this activation is the mild reaction condition for this conversion; nevertheless, the two-step process is a downside. On the other hand, unactivated amides without an activation group demand moderate to harsh conditions for transformation. The methodologies of unactivated amides based on metal and non-metal catalysed processes are briefly described in **Chapter 2**. We have also looked into the mechanistic processes of reactions. Thus, we decided to investigate innovative, eco-friendly, and wide-scope transamidation methodologies and their applications.

In **Chapter 3**, we developed a simple, efficient, single-step, metal-free, and environmentally friendly amide synthesis with excellent yields. In the absence of any catalyst or additive, amides are converted to other amides using amine hydrochloride salts. The reaction's mechanistic pathway is as follows: initially, the carbonyl group of the amide is activated by salt, then amine attacks the amide intermediate as a nucleophile, resulting in the desired amide via amine elimination as a by-product. Furthermore, this versatile new transamidation opens up a wide range of possibilities for the synthesis of another amide to amide, which can be exploited by academics, agrochemical companies, and pharmaceutical companies in the development of new building blocks for the synthesis of new active pharmaceutical ingredients (APIs), drugs, and pesticides. This research finding was published in European Journal of

Organic Chemistry in year **2021**, volume **2021**, issue **41** and page number **5627-5639** (**10.1002/ejoc.202101114**).

In addition to looking for alternative transamidation pathways, we established a new framework for producing 2-substituted 1,3-benzoxazole and 1,3-benzothiazole derivatives in **Chapter 4**. This method is a continuation of the work described in **Chapter 3**, in which only substituted 2-aminophenol hydrochloride salts as an amine salt reacts with various amides to synthesize 2-substituted 1,3-benzoxazole and 1,3-benzothiazole compounds. The same mechanism as in **Chapter 3** employs to obtain the desired products in this reaction. First, an amide is converted to another amide by salt activation, followed by the nucleophilic attack and amine elimination, ending in a transamide amide as an intermediate. The intermolecular attack of the oxygen atom of phenol on the carbonyl group of the amide, followed by dihydroxylation, produces final annulated products. We conducted some experiments at various temperatures in order to generate these cyclized products. Surprisingly, 150 °C temperature produced the desired compounds in moderate to excellent yields under neat conditions. Additionally, this annulation is also one application of transamidation. This article is currently being proofread in the Tetrahedron journal with manuscript id (**10.1016/j.tet.2022.132794**).

We established a Cu mediated transamidation of unactivated aliphatic amides in **Chapter 5**. Under neat conditions, the reaction between amine and amides was carried out in the presence of $CuCl_2$ and TMSCl as a catalyst-Lewis acid combination. The effect of several catalysts on the reaction was investigated, and it was observed that $CuCl_2$ is the best catalyst for the reaction. We can only access the transformation of aliphatic amides with this method. Furthermore, an increased mol ratio of TMSCl and high temperature with the same conditions were used to produce 2-substituted 1,3-benzoxazole and 1,3-benzothiazole by annulation substituted 2-aminophenol and 2-aminothiophenol with aliphatic amides. This transamidation and annulation are carried out via initially the formation of a Cu-amide complex followed by TMSCl and the amine reacts with this complex, resulting in a transamide product by the elimination of the amine salt and trimethyl silanol as by-products. Furthermore, in the presence of additional TMSCl equiv and at high temperatures, annulated compounds result from 2-aminophenol and 2-aminothiophenol. This study is currently being under revision in the Organic & Biomolecular Chemistry journal with manuscript id (OB-ART-04-2022-000704).

Future work

Throughout the course, a thorough study on the modification of two transamidation reactions and their applications was carried out. Thus, annulation protocols of polysubstituted benzoxazole and benzothiazole derivatives by the application of non-metal and metal catalysts transamidation in two different methodologies were also reported. A total of three different strategies were reported for the present investigation, namely, Catalyst-Free N-C bond cleavage/formation of Primary, Secondary and Tertiary Unactivated Amides (published in EJOC journal)[1], Metal-free direct annulation of 2-aminophenols and 2-aminothiophenols with unactivated amides through transamidation (published in Tetrahedron journal)[2], and Cu-Catalysed Transamidation of Unactivated Aliphatic Amides (under review in OBC journal). Environmentally benign methods were applied for transamidation and cyclization reactions, and in future, this catalyst can also be applied for other important organic transformations. The synthetically synthesised derivatives can also be used as reaction intermediates to prepare marketed drugs, agrochemicals and other fields. As stated previously, the current strategy employed amine hydrochloride salts and a copper catalyst, and the amines can be further modified with specific functionality to develop more active species. In future, it could be interesting to consider the other metal catalysts to perform these reactions with extended scope and yield. In addition, the synthesis of polysubstituted benzoxazole and benzothiazole will be try with other reagents such as TMSCl[3]. Furthermore, these methods can be used for other heterocyclic moieties[4–6]. Thus, a deeper analysis of mechanisms using DFT studies and new proposals to explore different approaches are required.

References

1 V. Kumar, S. Dhawan, P. S. Girase, P. Singh and R. Karpoormath, European J. Org. Chem., , DOI:10.1002/ejoc.202101114.

2 V. Kumar, S. Dhawan, R. Bala, P. S. Girase, P. Singh and R. Karpoormath, Tetrahedron, 2022, 115, 132794.

3 S. Yu, K. Ho Song and S. Lee, Asian J. Org. Chem., , DOI:10.1002/ajoc.201900216.

4 X. Zhang, S. Liao, A. Liu, X. Liu, Q. Kuang, Y. Wang, P. Xu, X. Huang, H. Wu and J. Yuan, Tetrahedron Lett., 2022.

5 X. Wang, Y. Wang, X. Liu, T. He, L. Li, H. Wu, S. Zhou, D. Li, S. Liao, P. Xu, X. Huang and J. Yuan, Tetrahedron, , DOI:10.1016/j.tet.2021.132496.

6 X. Wang, S. Shang, Q. Tian, Y. Wang, H. Wu, Z. Li, S. Zhou, H. Liu, Z. Dai, W. Luo, D. Li, X. Xiao, S. Wang and J. Yuan, Tetrahedron, , DOI:10.1016/j.tet.2020.131480.

APPENDIX-I

SUPPLEMENTARY INFORMATION

CHAPTER 3

An Environmentally Benign, Catalyst-Free N-C bond cleavage/formation of Primary, Secondary and Tertiary Unactivated Amides

Article published in European Journal of Organic Chemistry Journal with DOI: 10.1002/ejoc.202101114

1H and 13C NMR Spectra

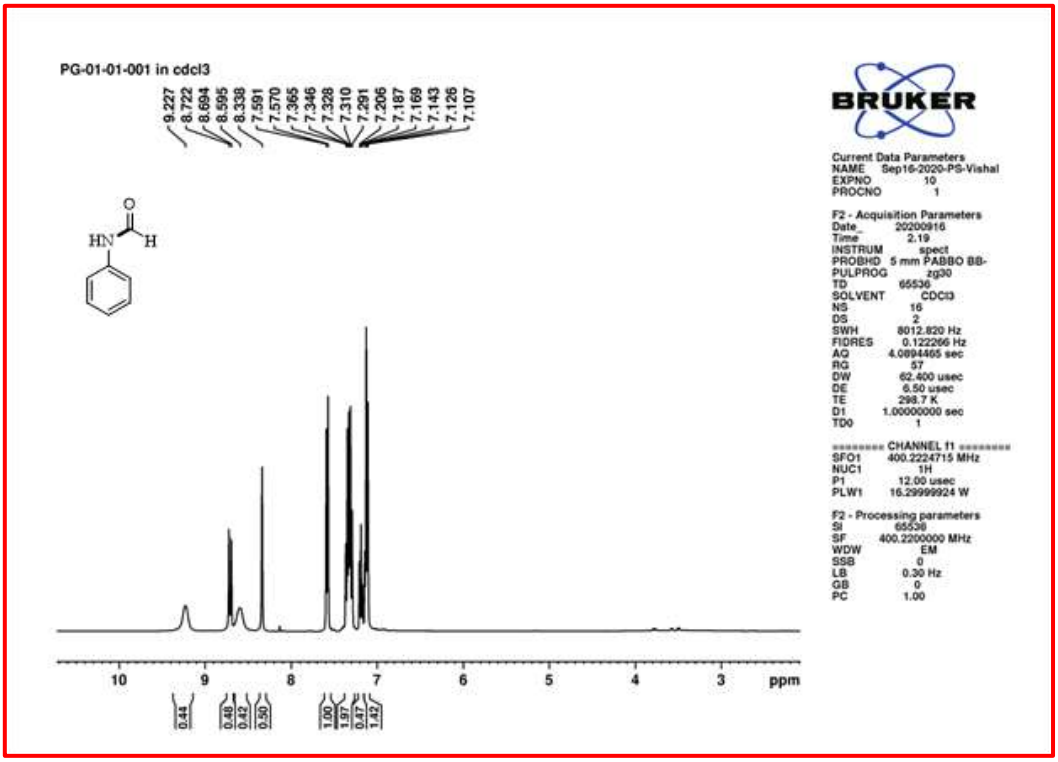

^{1}H NMR spectra of **3A**.

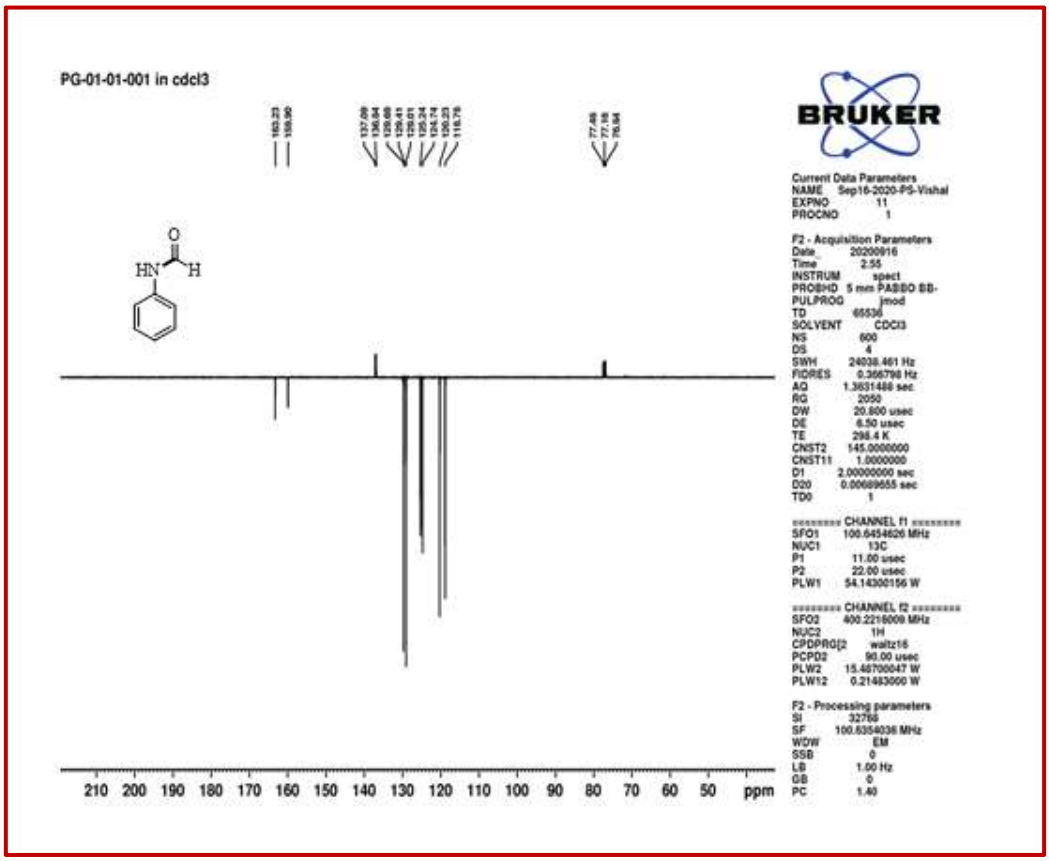

^{13}C NMR spectra of **3A.**

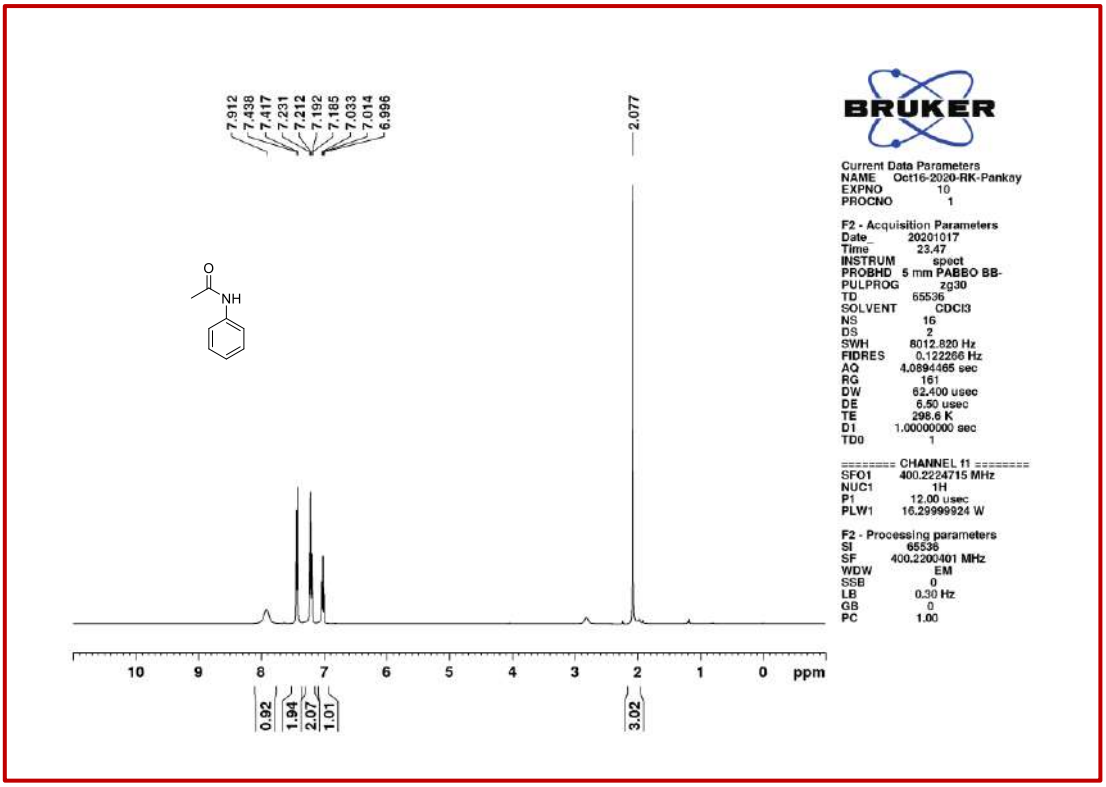

^{1}H NMR spectra of **3B.**

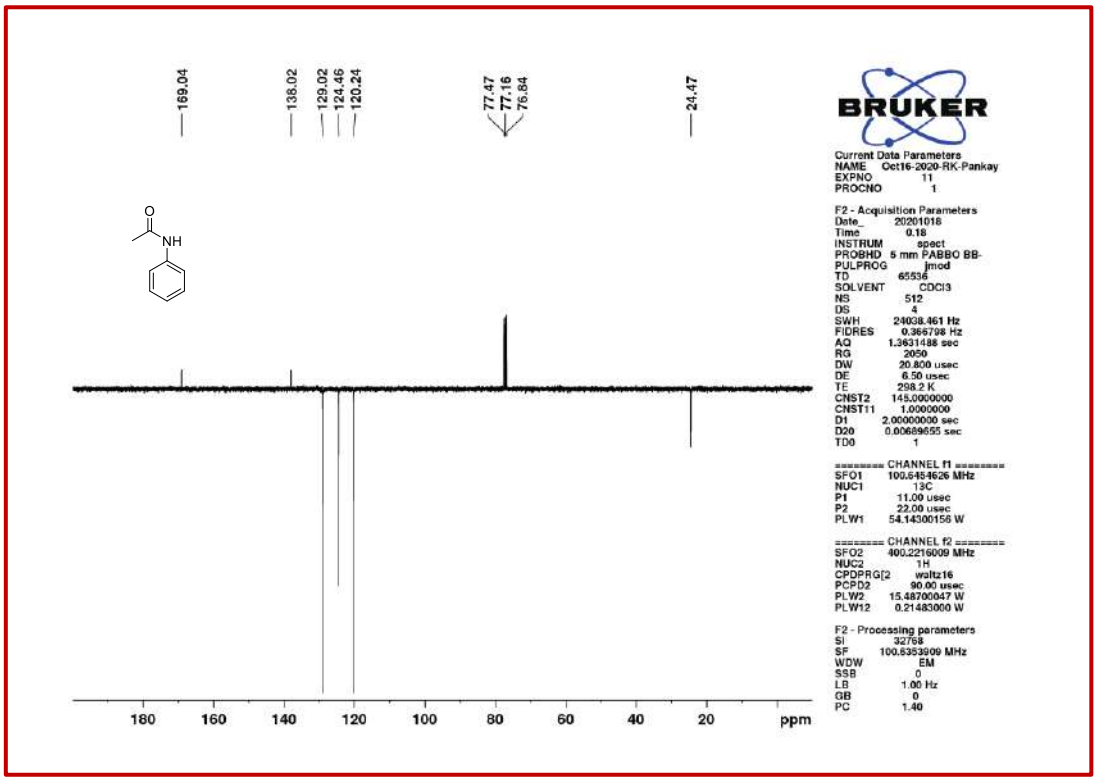

^{13}C NMR spectra of **3B.**

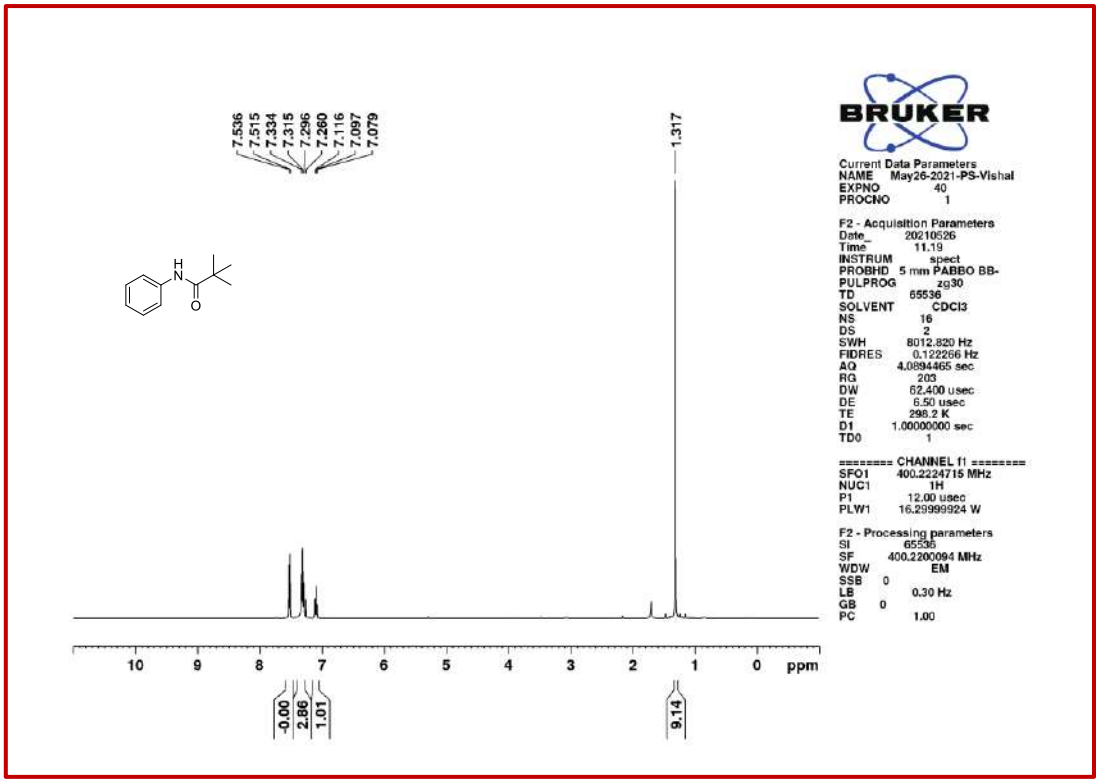

^{1}H NMR spectra of **3C.**

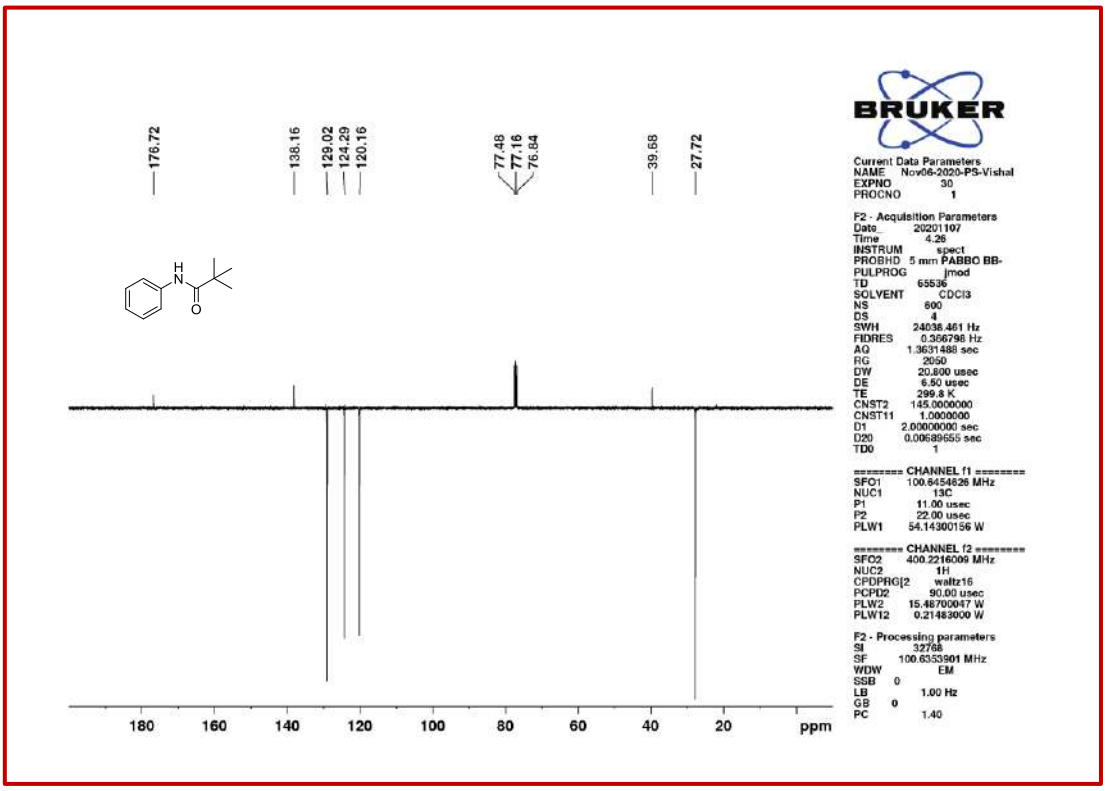

^{13}C NMR spectra of **3C.**

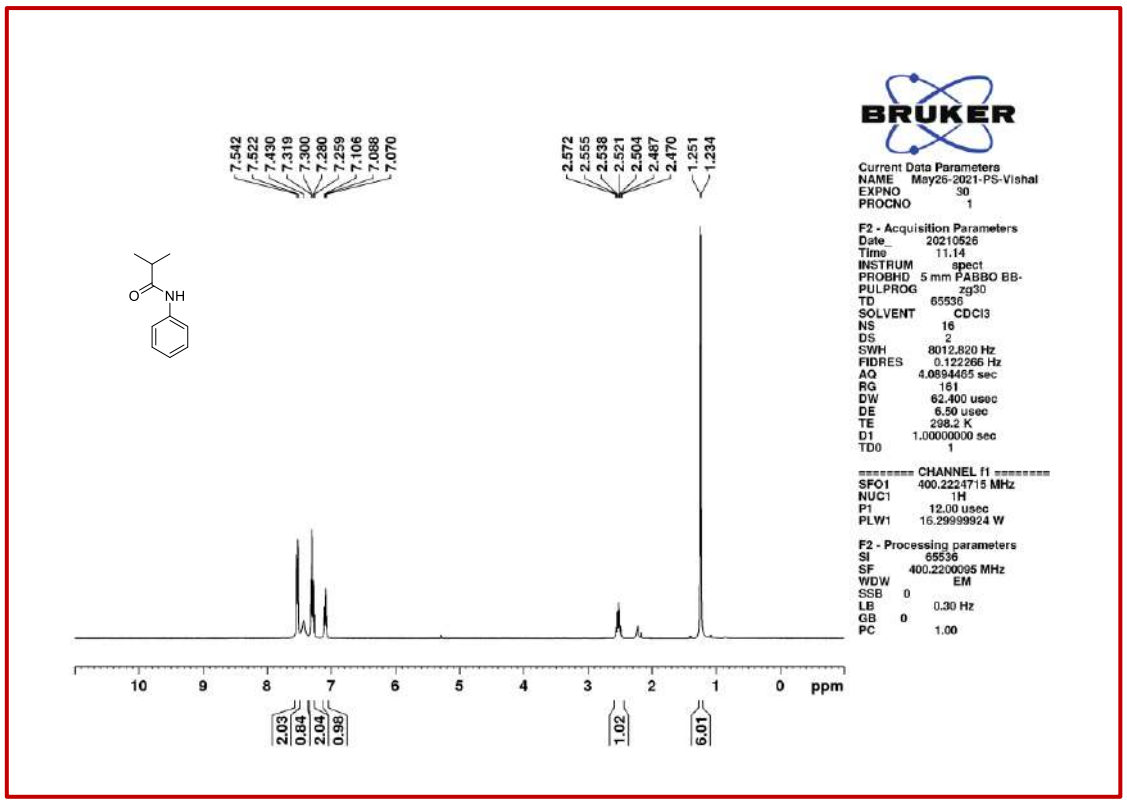

^{1}H NMR spectra of **3D.**

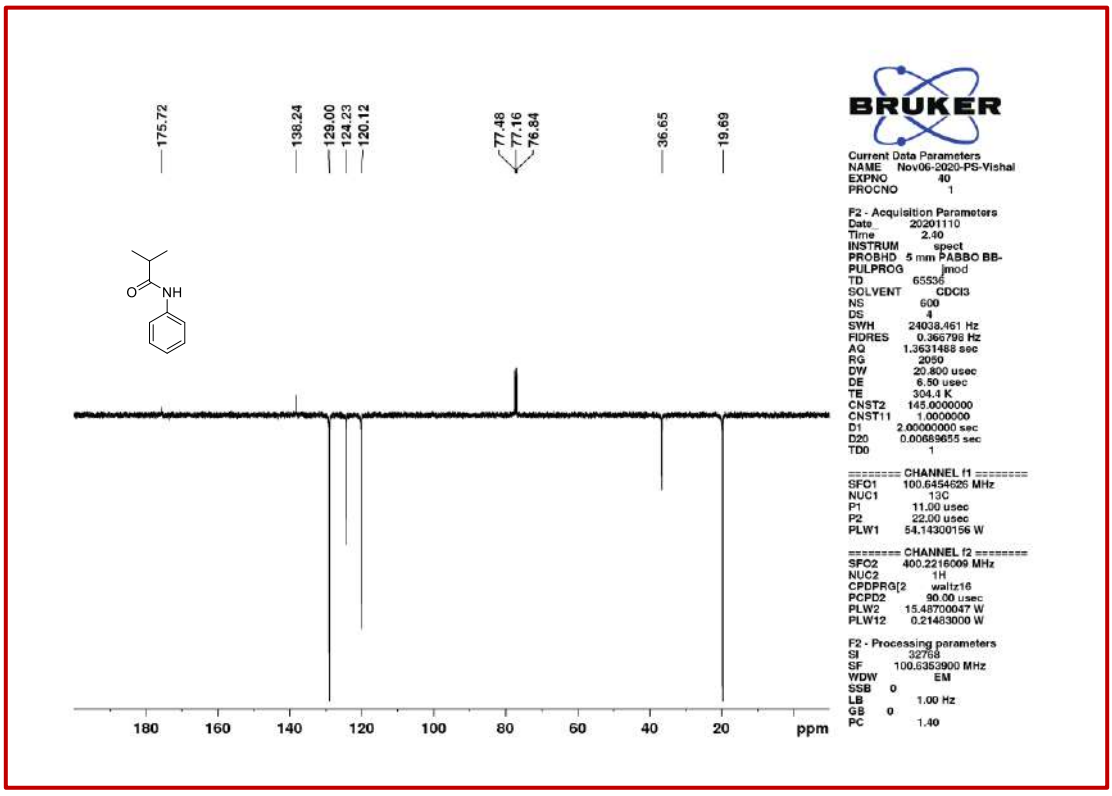

^{13}C NMR spectra of **3D.**

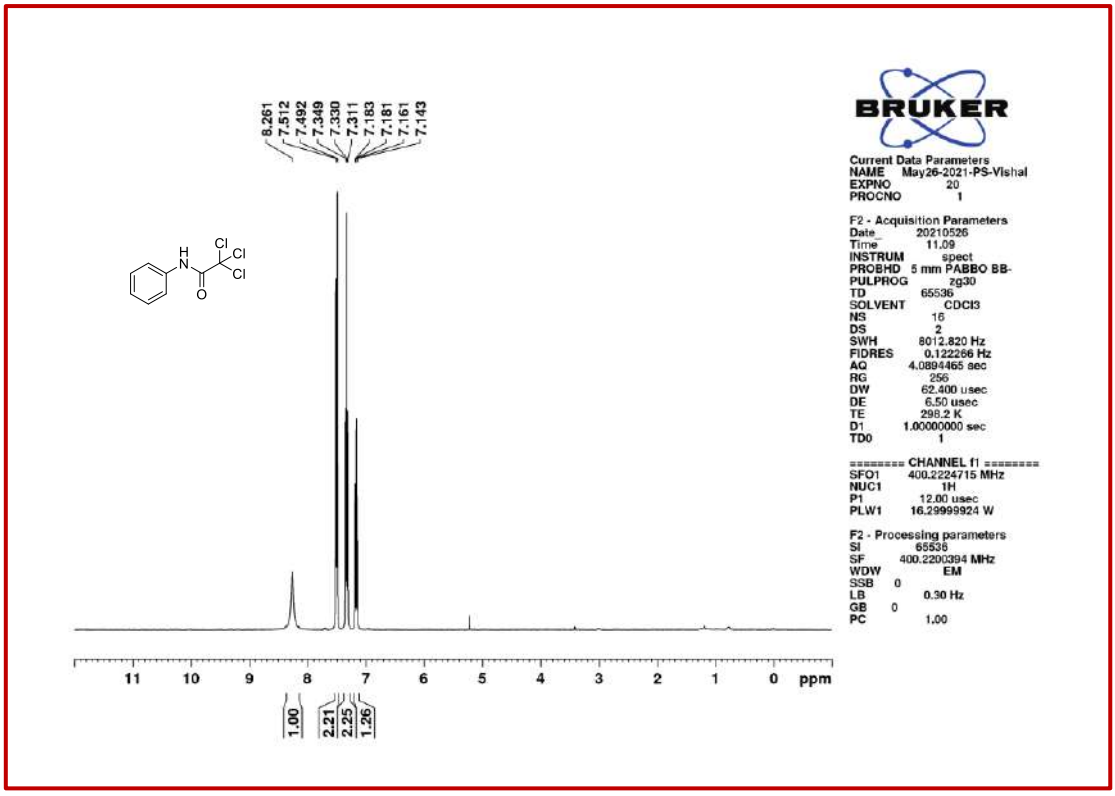

^{1}H NMR spectra of **3E.**

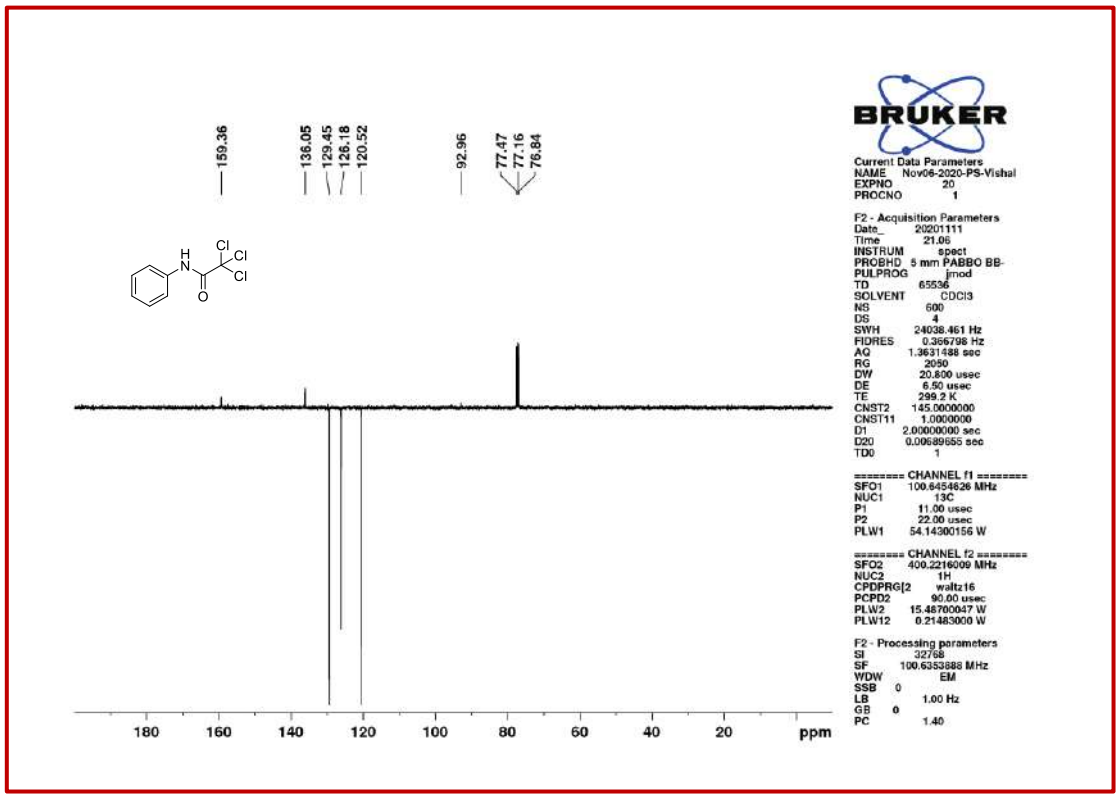

^{13}C NMR spectra of **3E.**

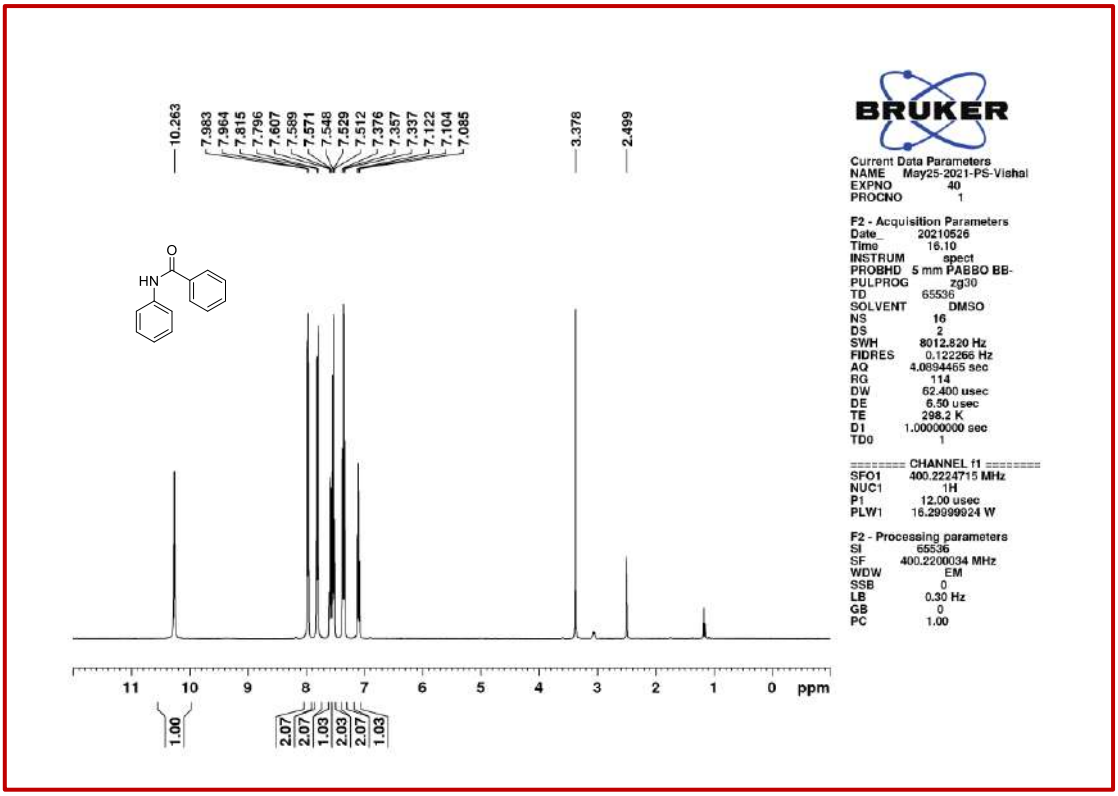

^{1}H NMR spectra of **3F.**

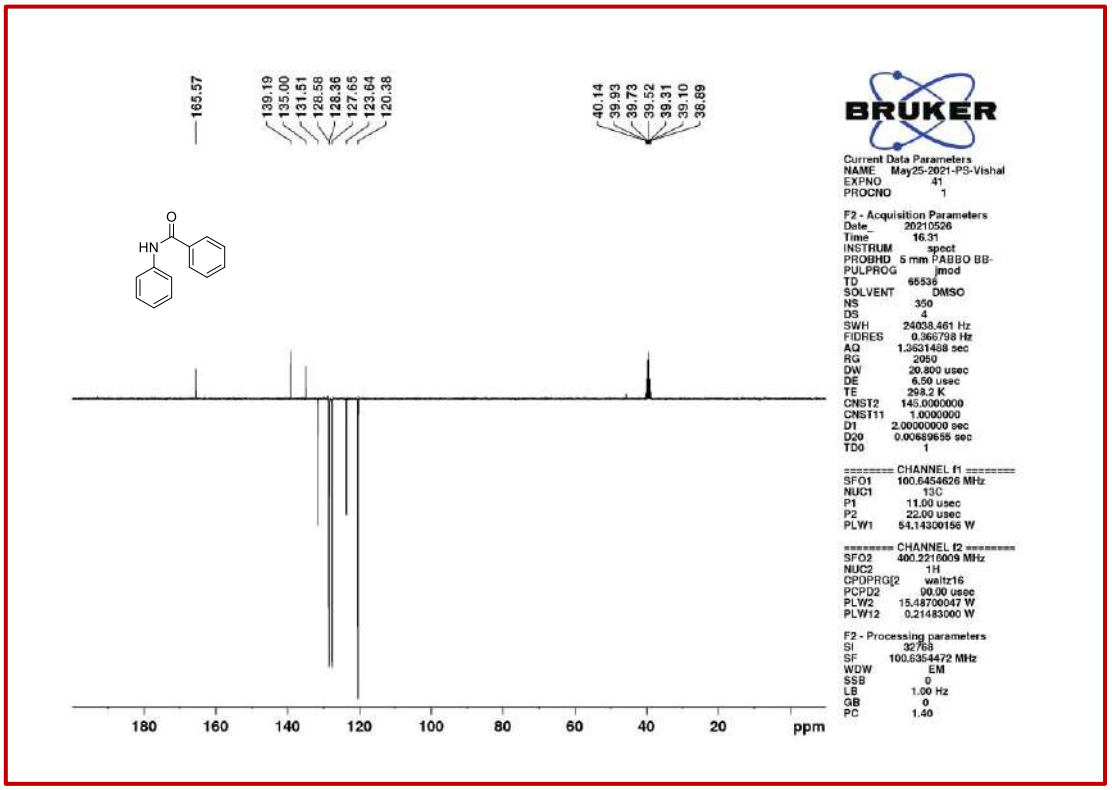

^{13}C NMR spectra of **3F.**

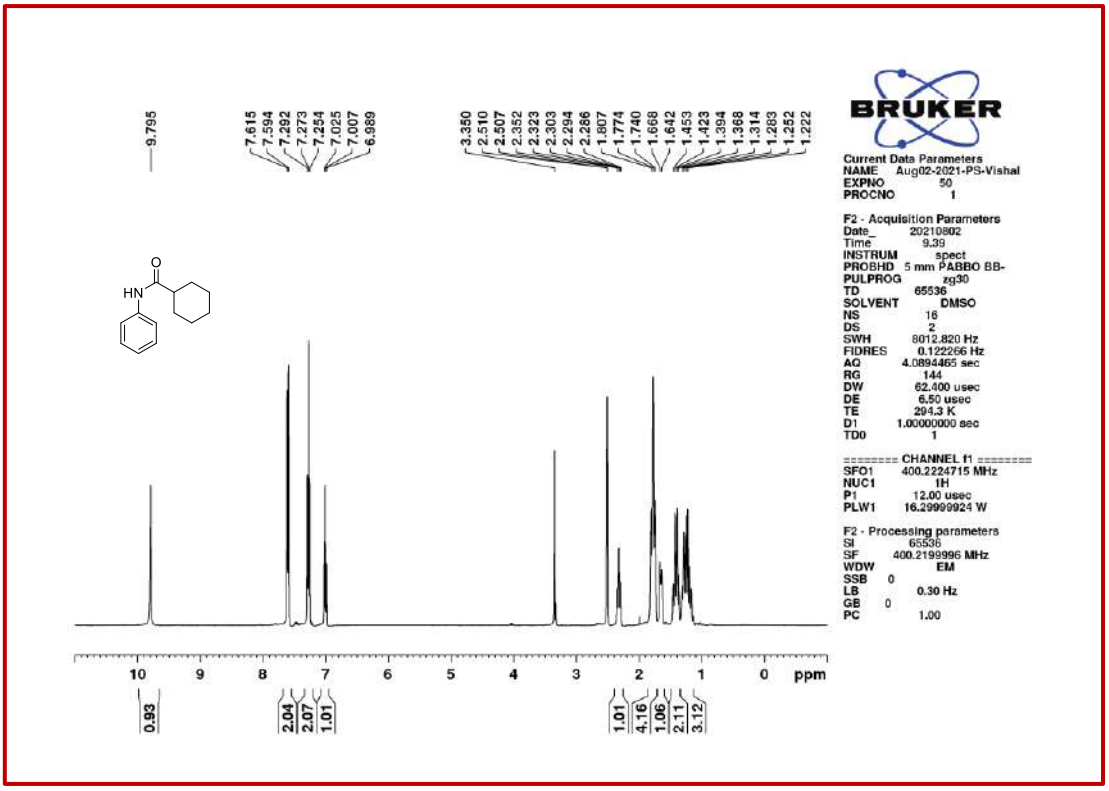

^{1}H NMR spectra of **3G.**

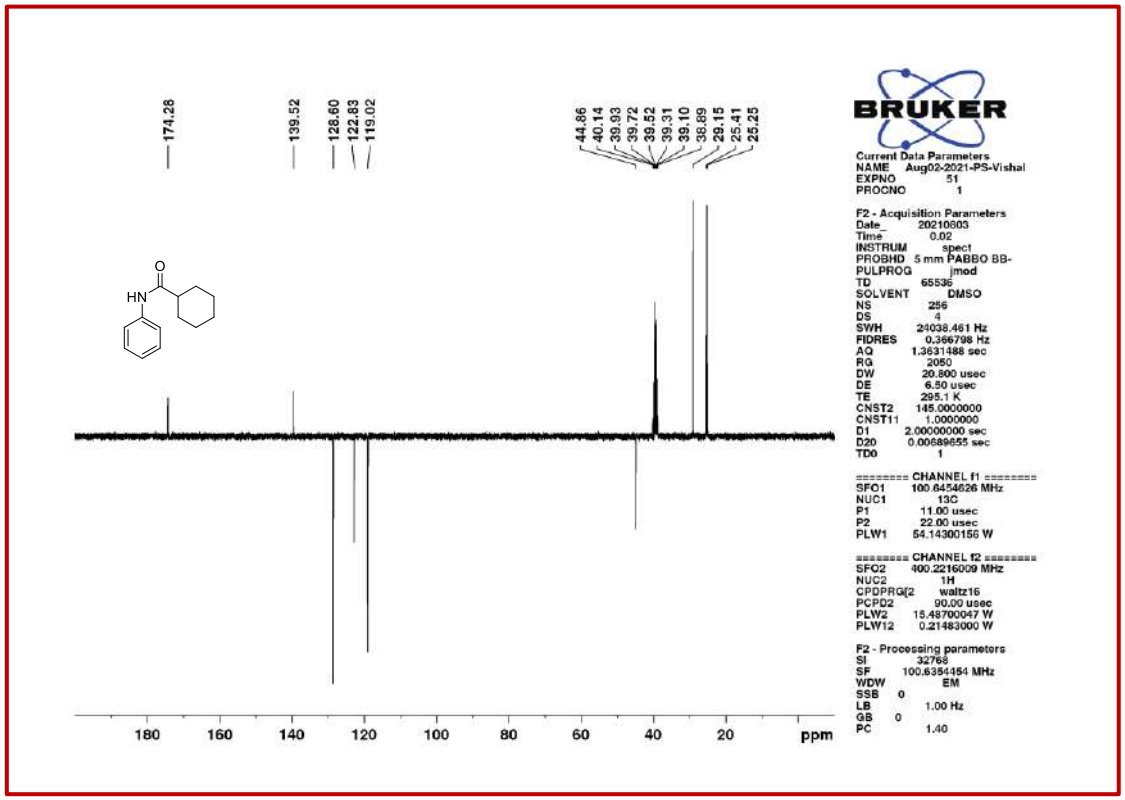

^{13}C NMR spectra of **3G.**

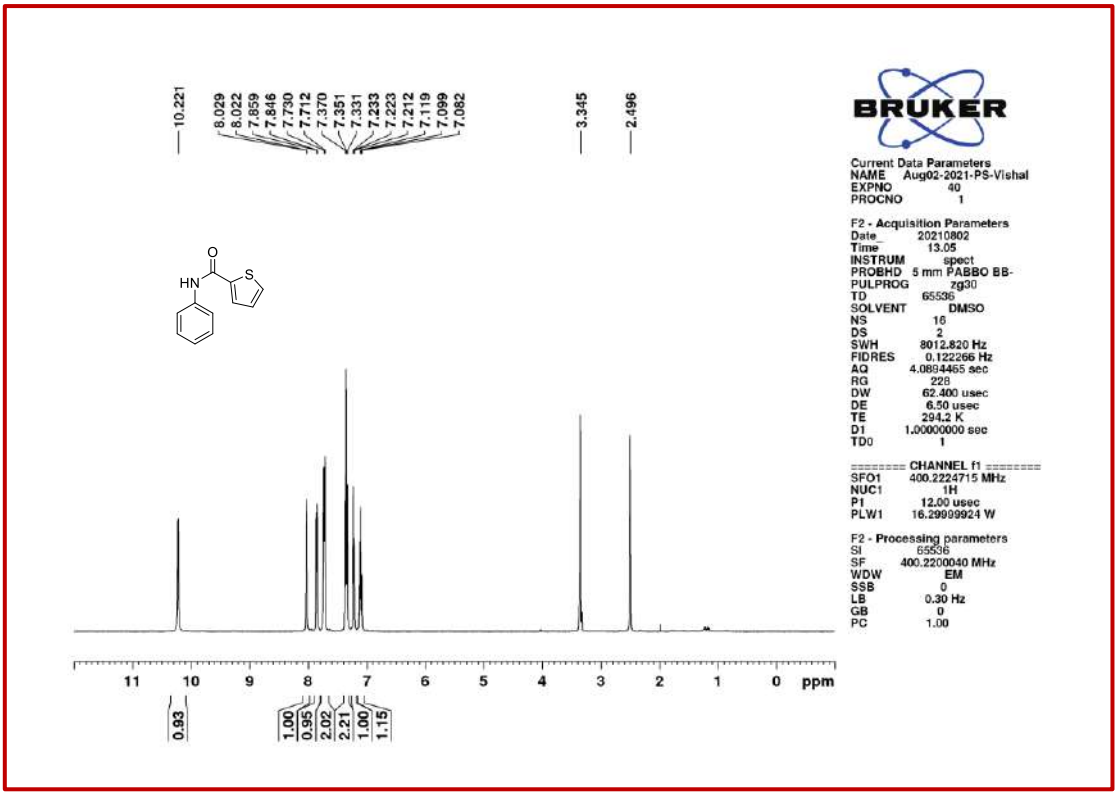

^{1}H NMR spectra of **3H.**

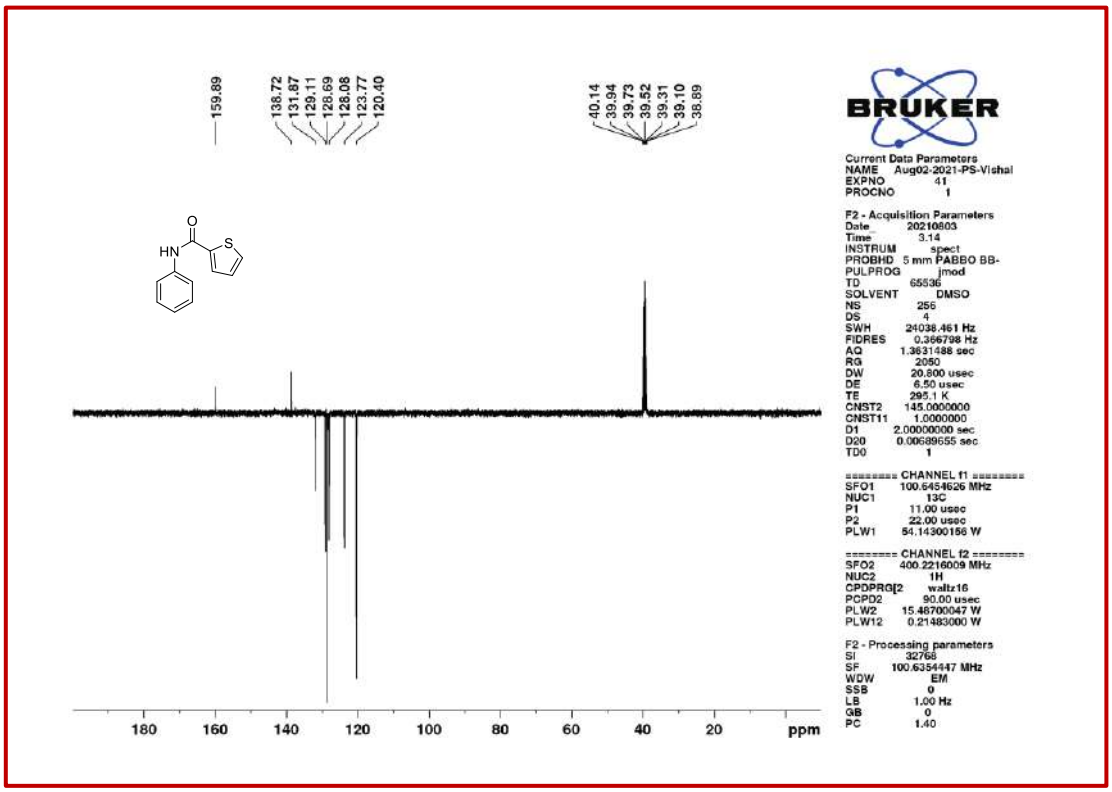

^{13}C NMR spectra of **3H.**

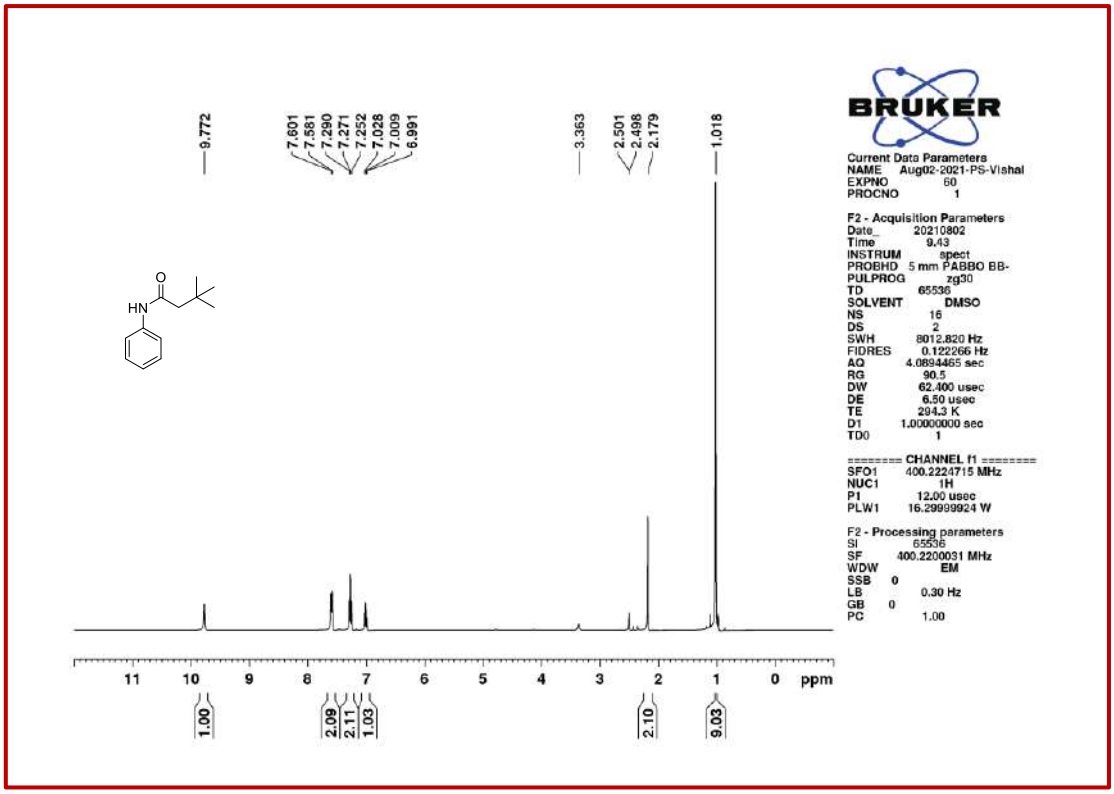

^{1}H NMR spectra of **3I.**

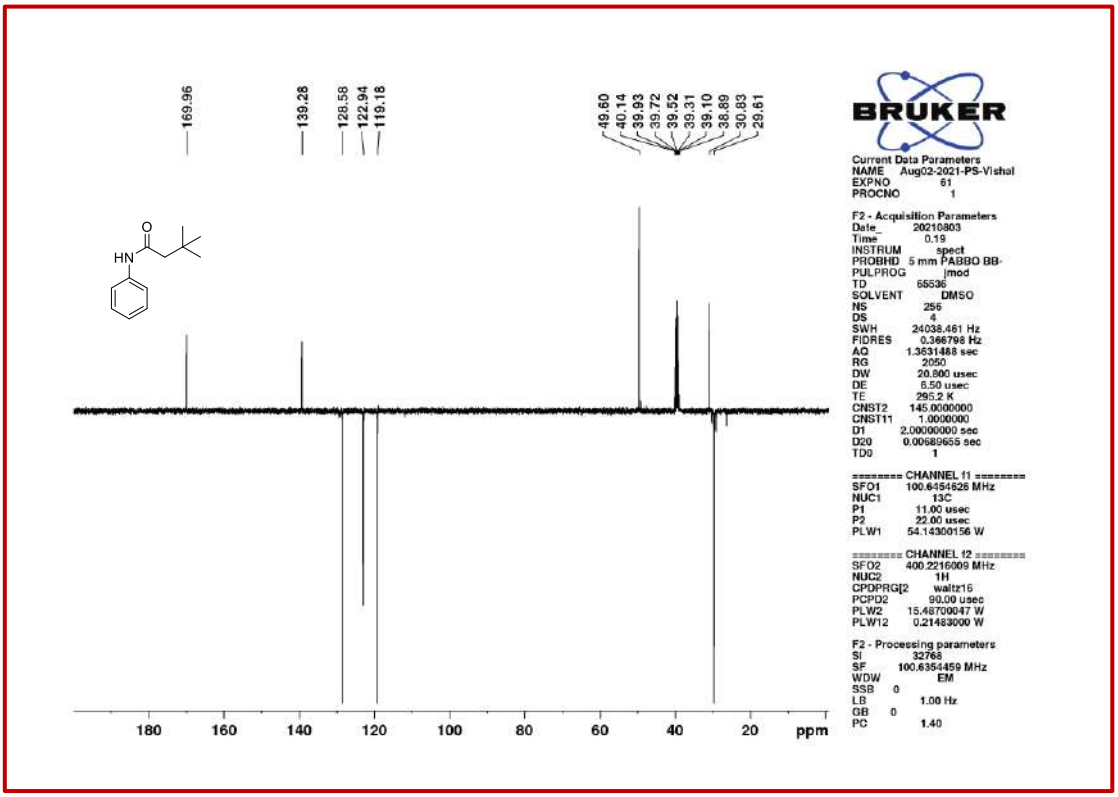

^{13}C NMR spectra of **3I.**

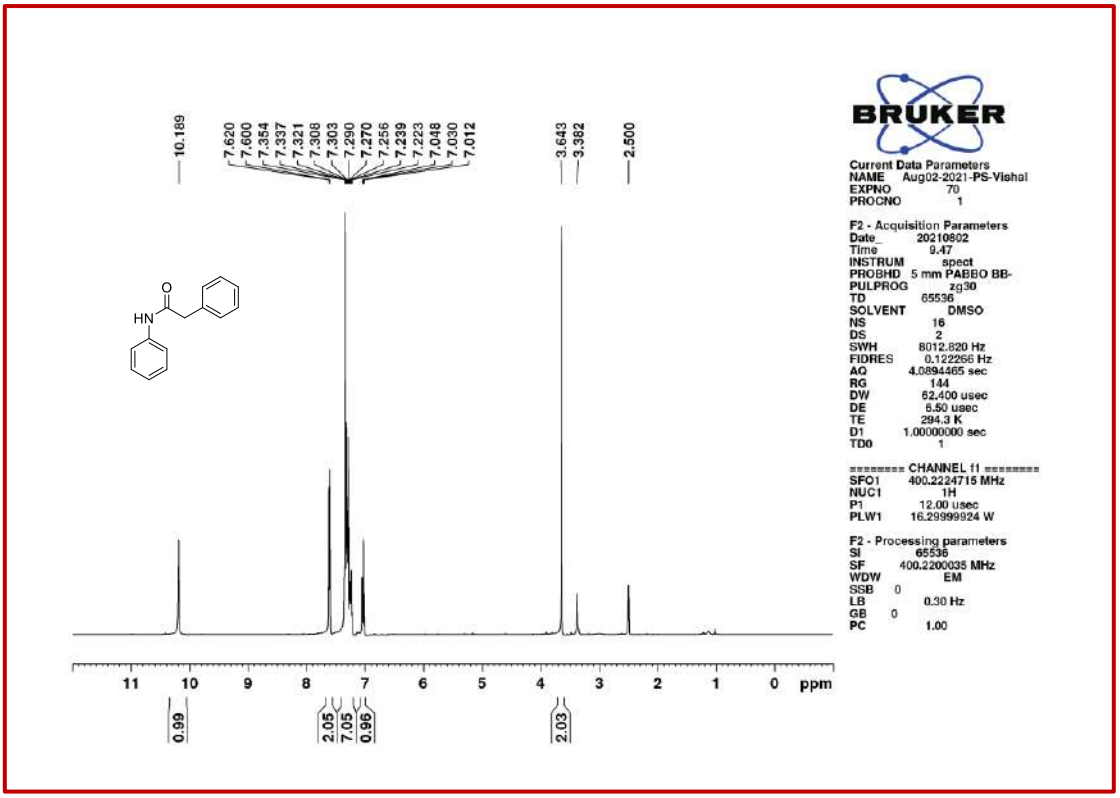

^{1}H NMR spectra of **3J.**

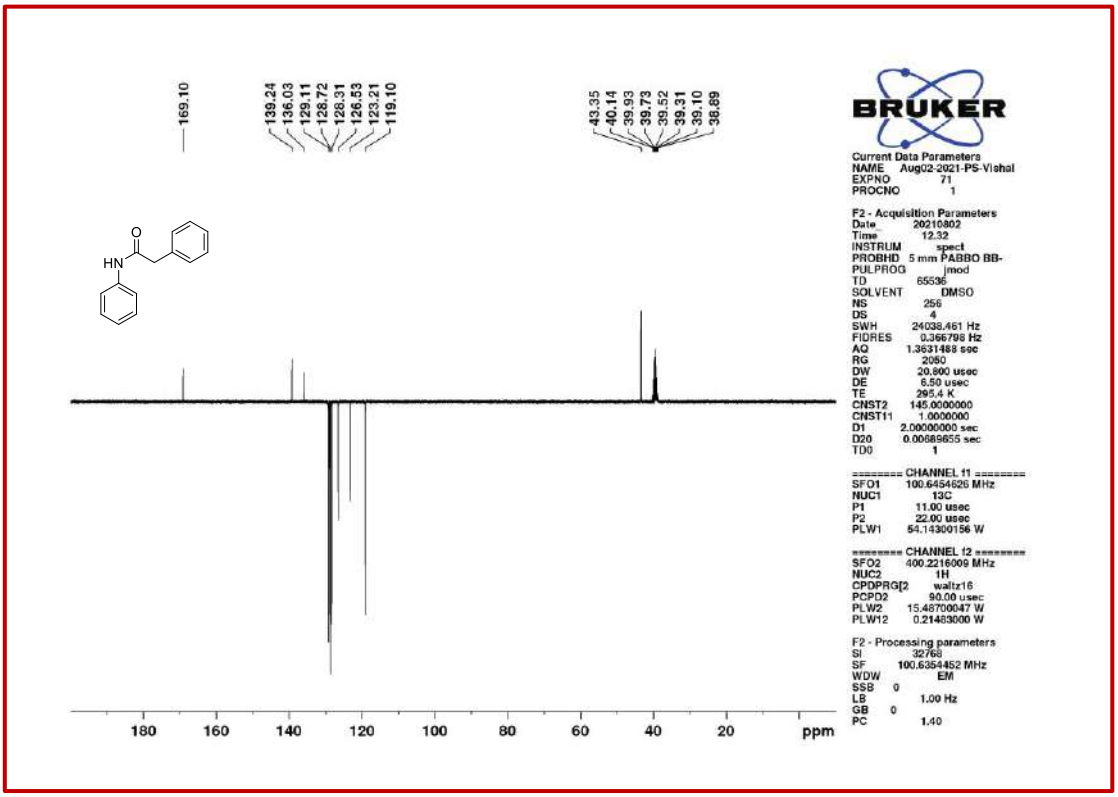

^{13}C NMR spectra of **3J.**

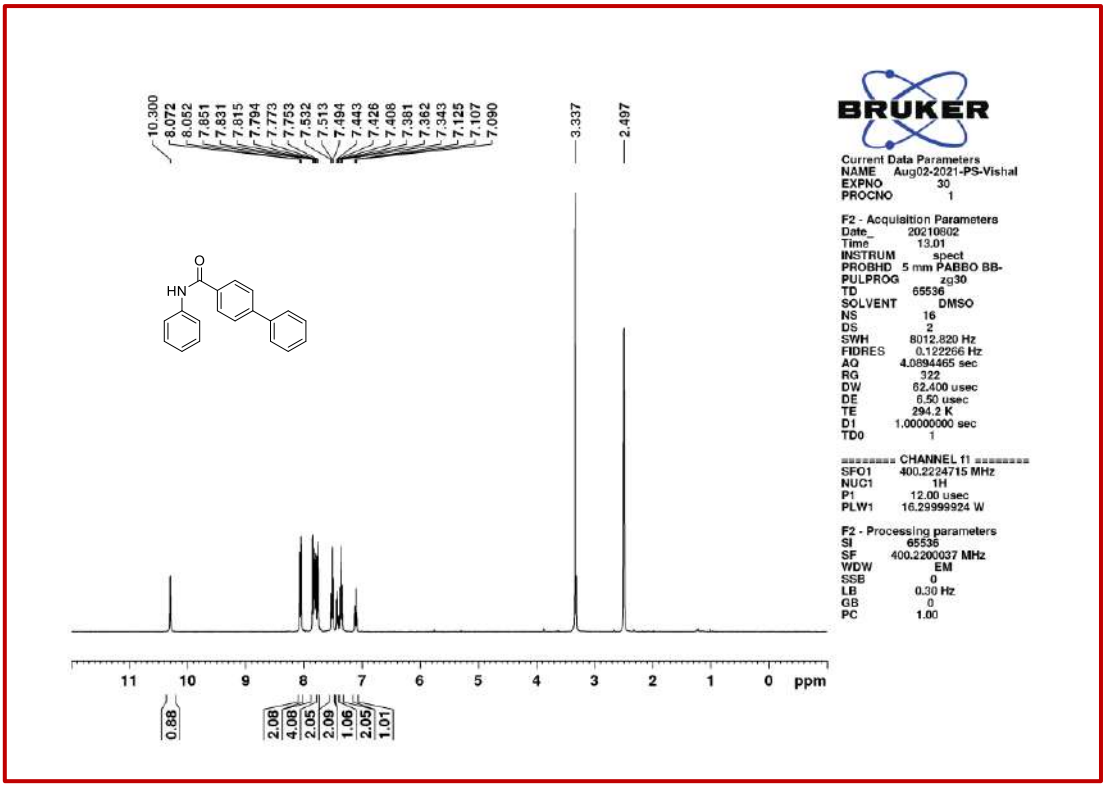

^{1}H NMR spectra of **3K.**

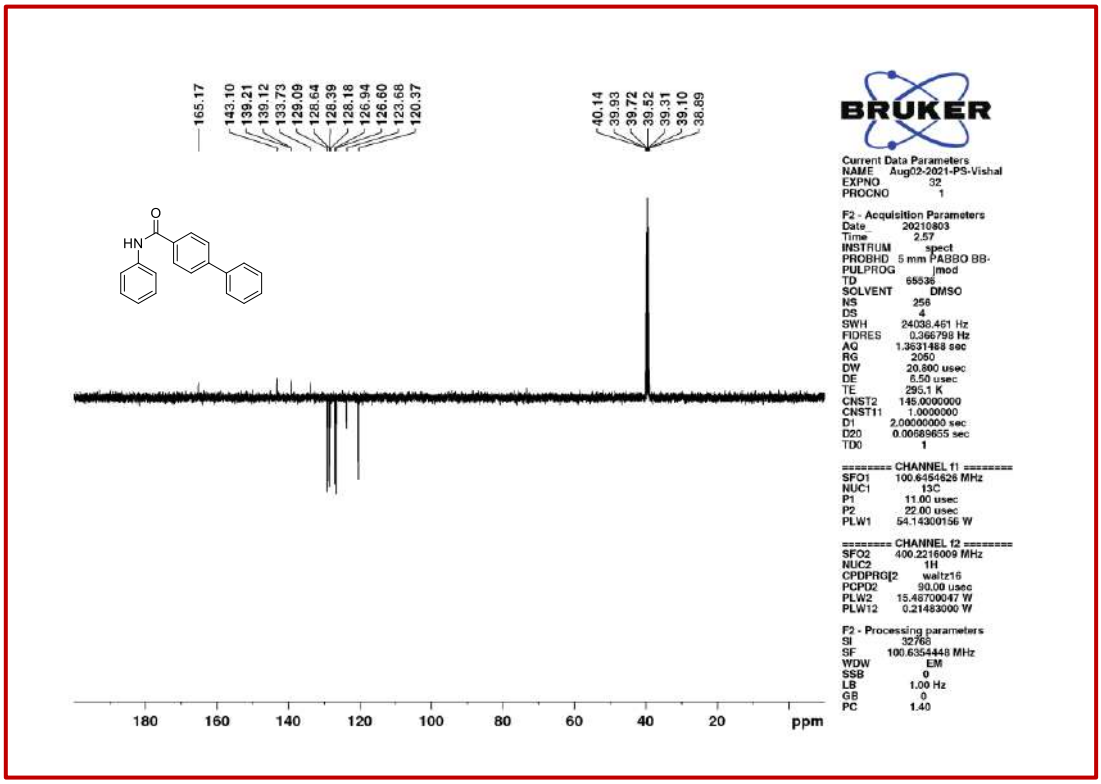

^{13}C NMR spectra of **3K.**

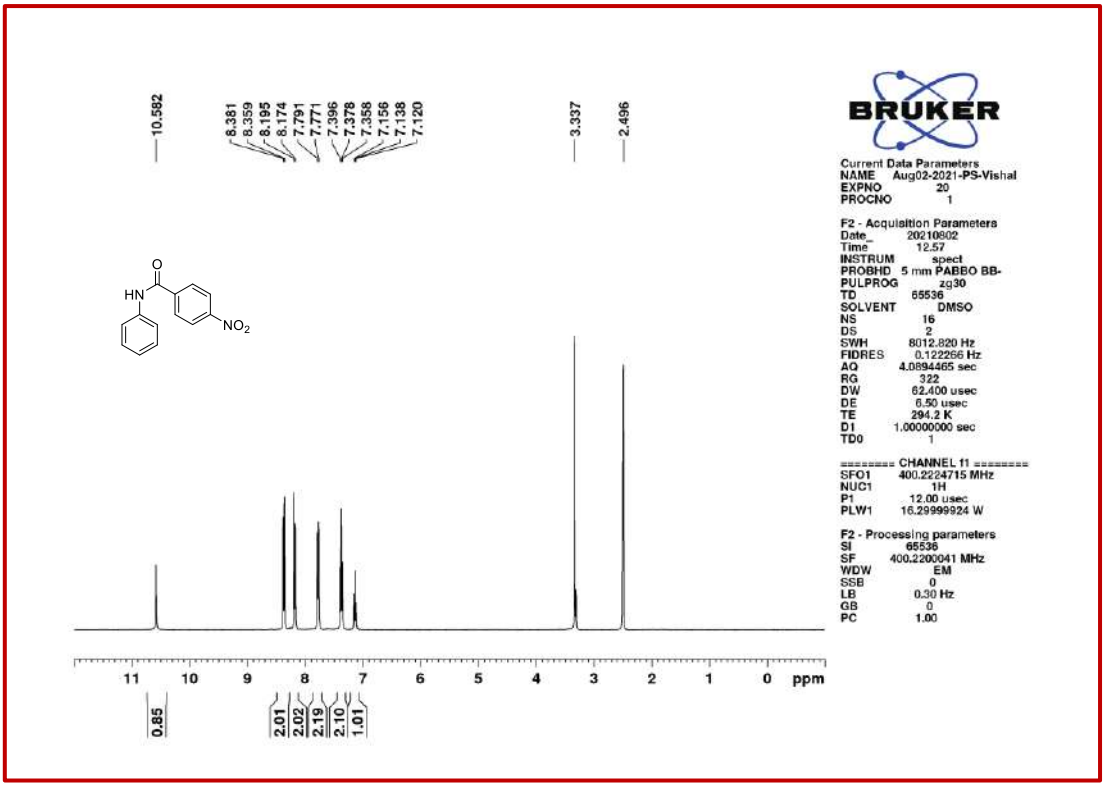

^{1}H NMR spectra of **3L.**

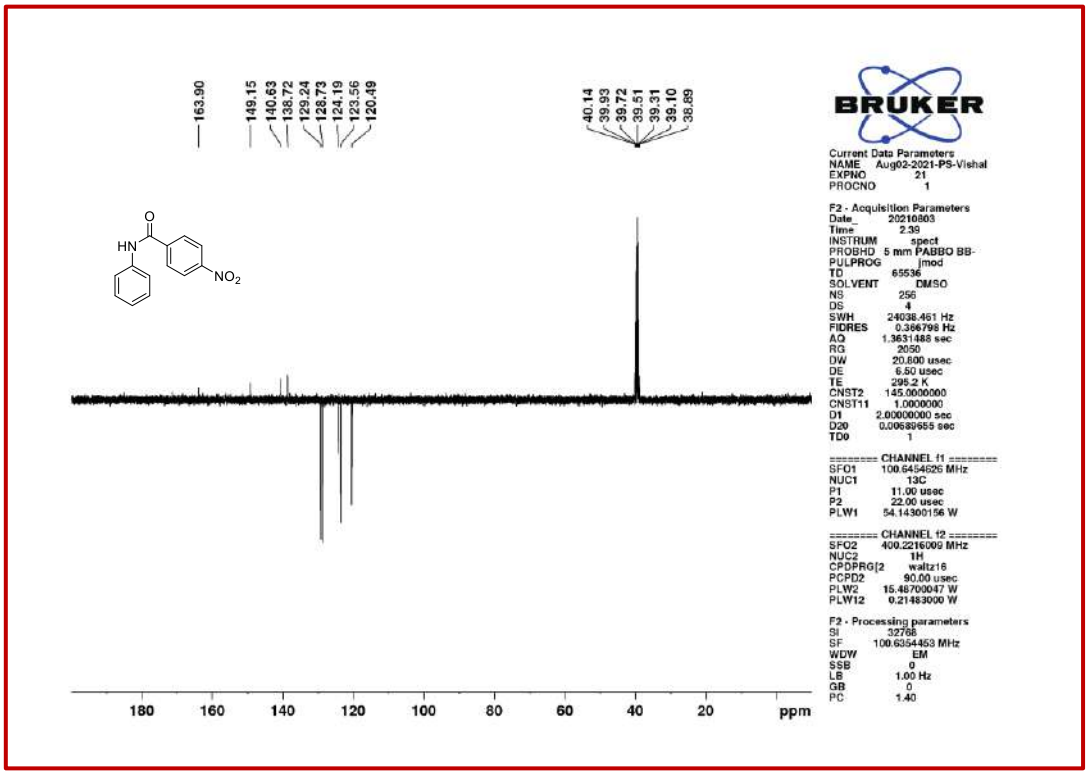

^{13}C NMR spectra of **3L.**

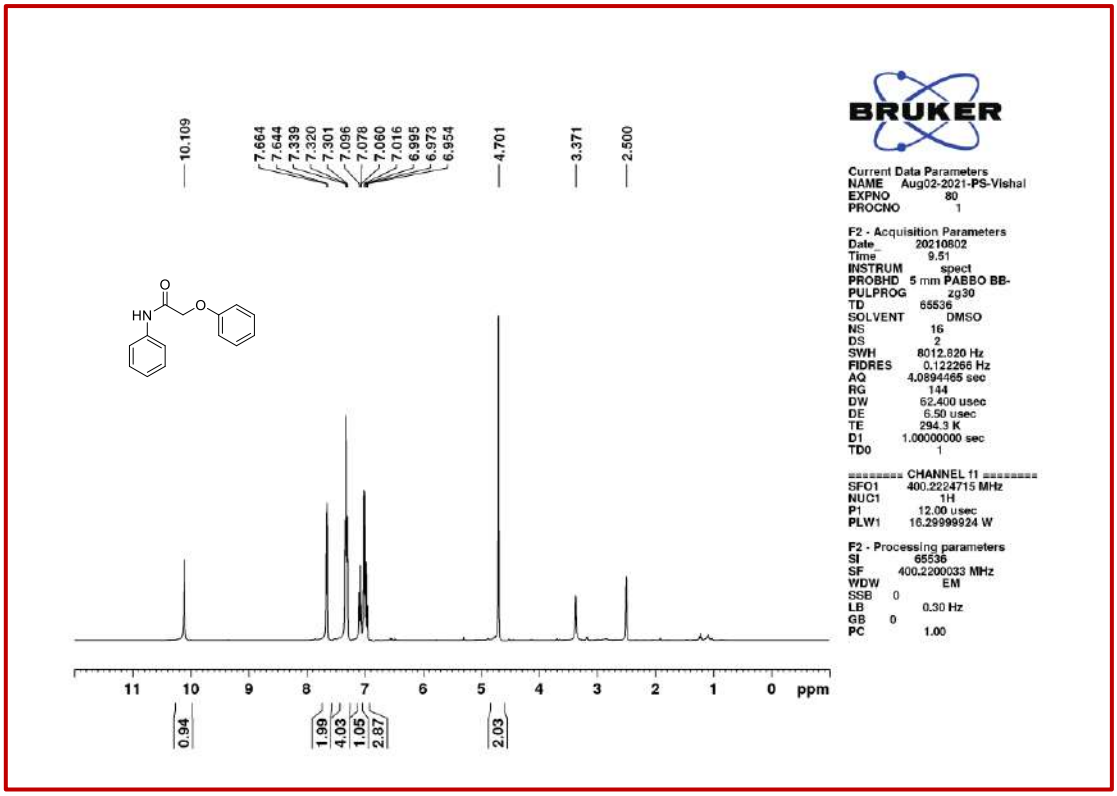

^{1}H NMR spectra of **3M.**

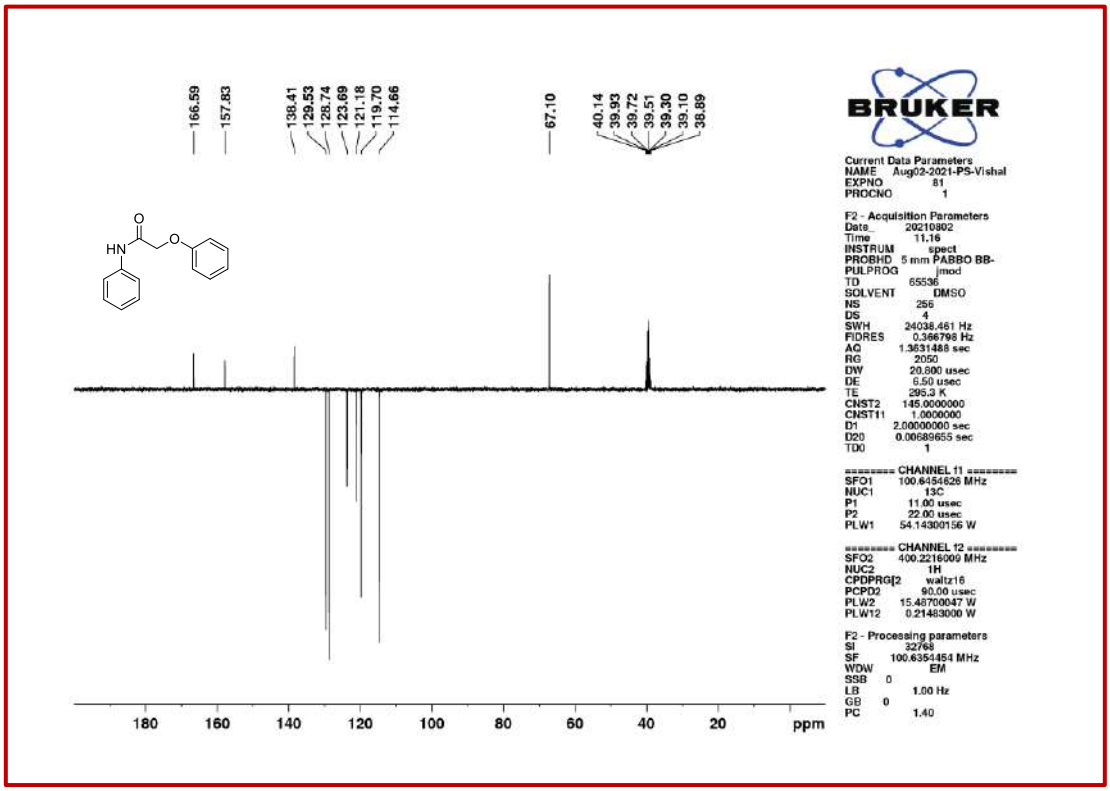

^{13}C NMR spectra of **3M.**

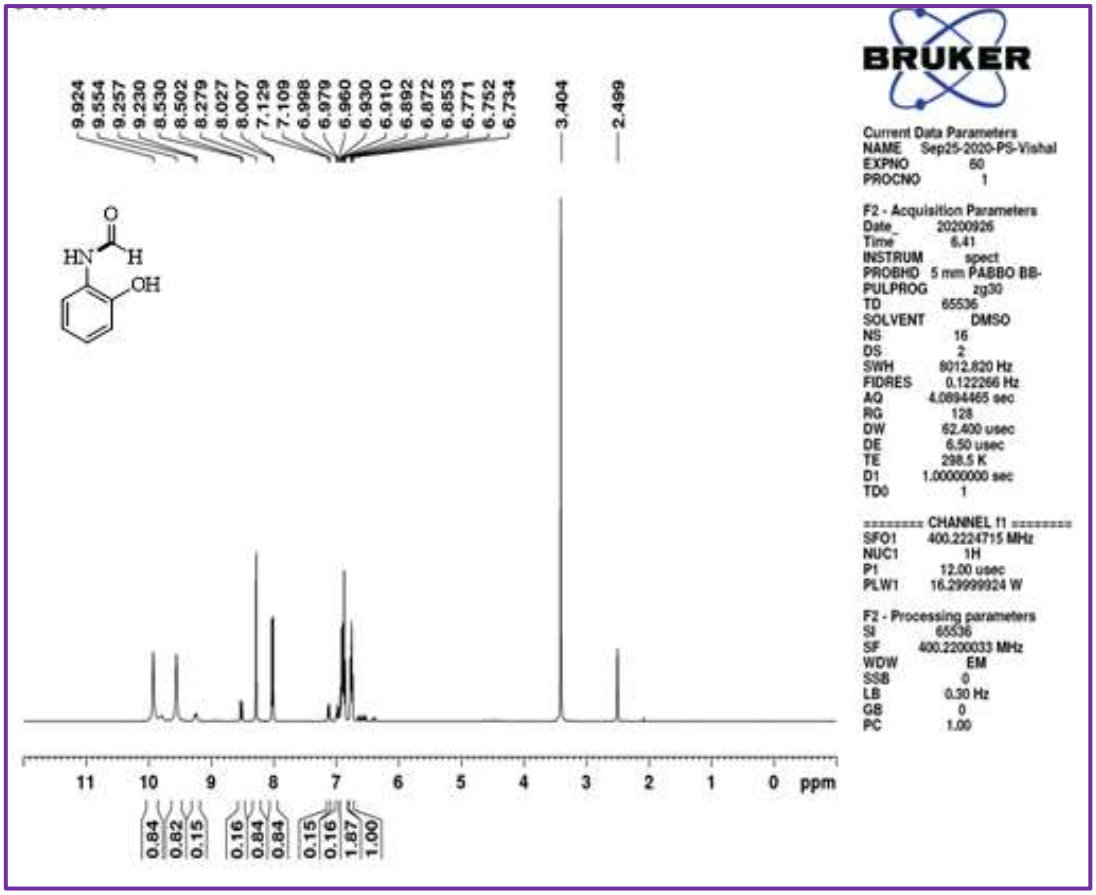

^{1}H NMR spectra of **3a**.

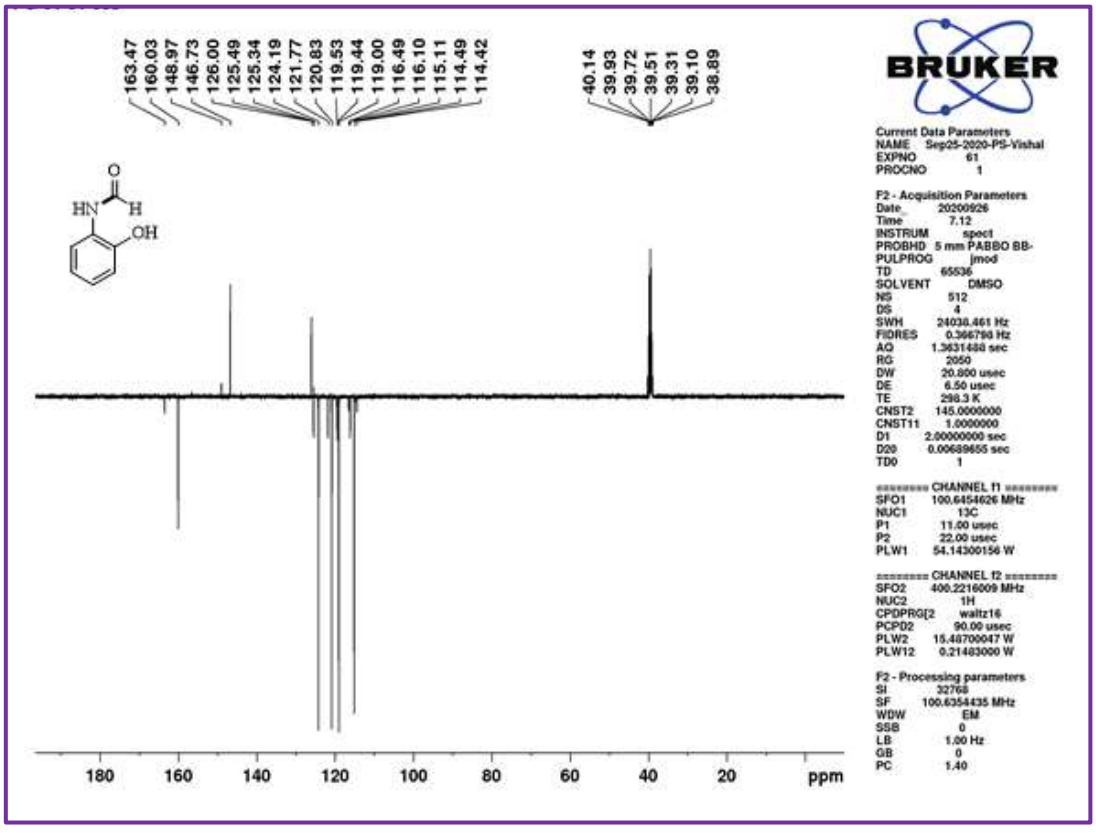

^{13}C NMR spectra of **3a.**

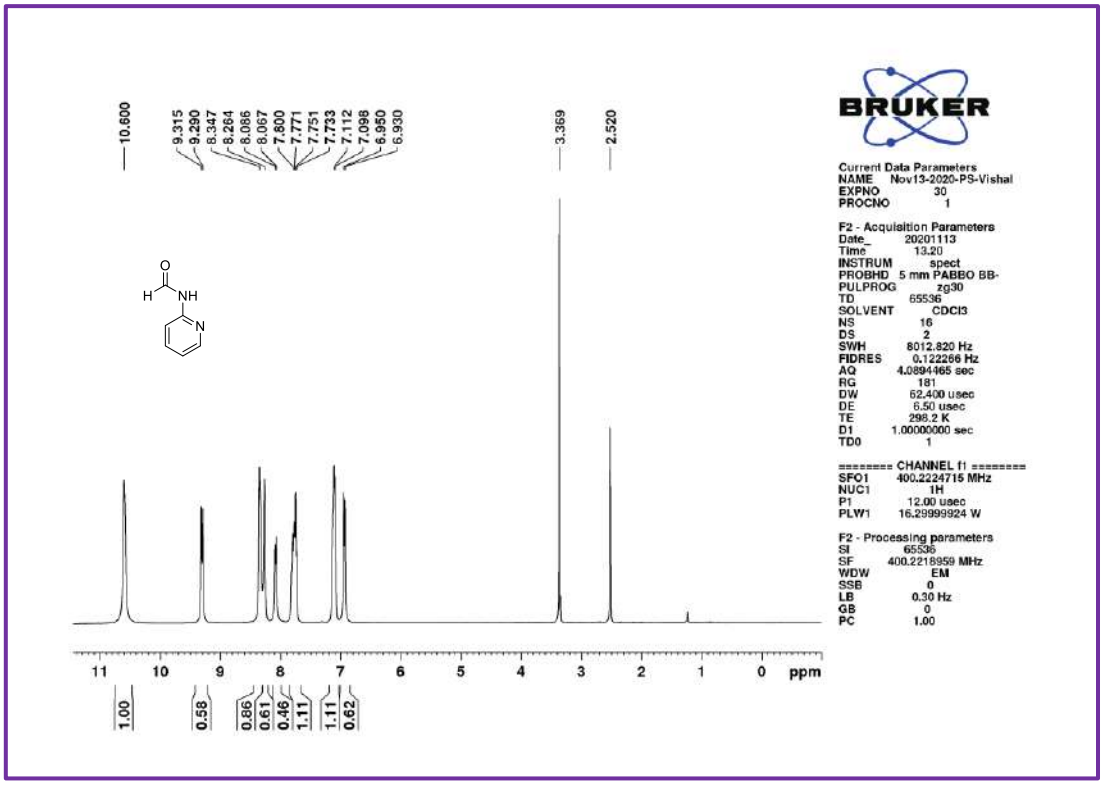

^{1}H NMR spectra of **3b.**

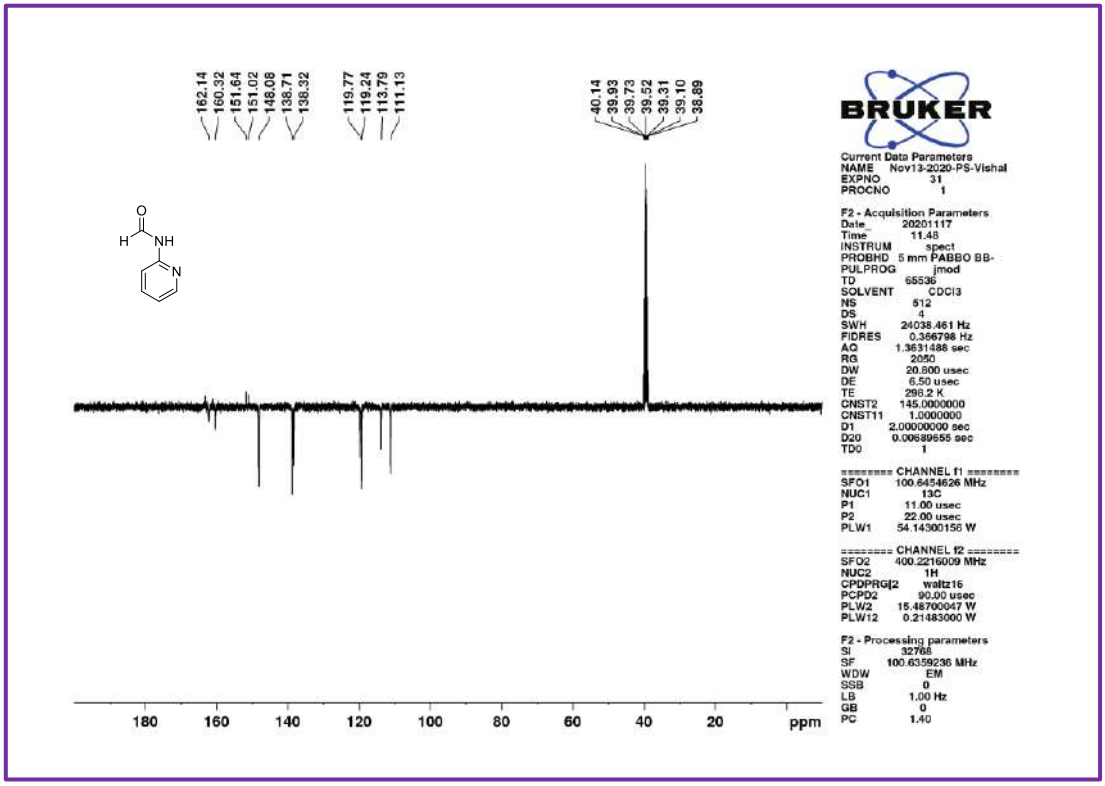

^{13}C NMR spectra of **3b.**

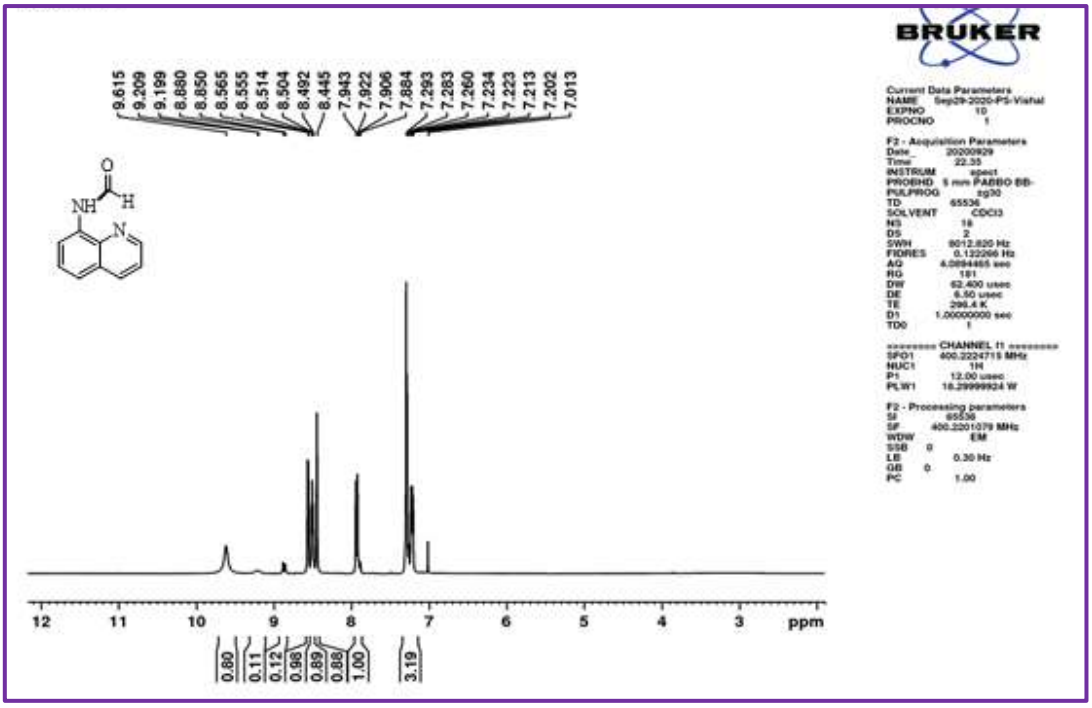

^{1}H NMR spectra of **3c.**

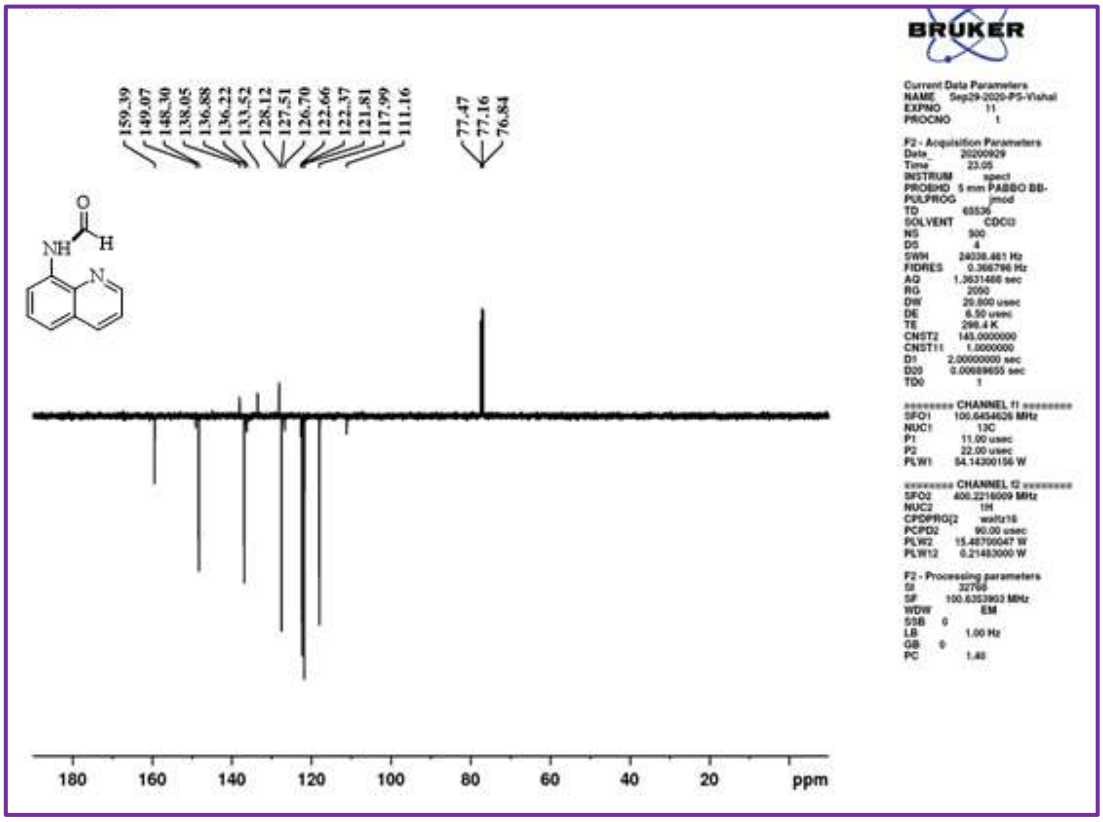

^{13}C NMR spectra of **3c.**

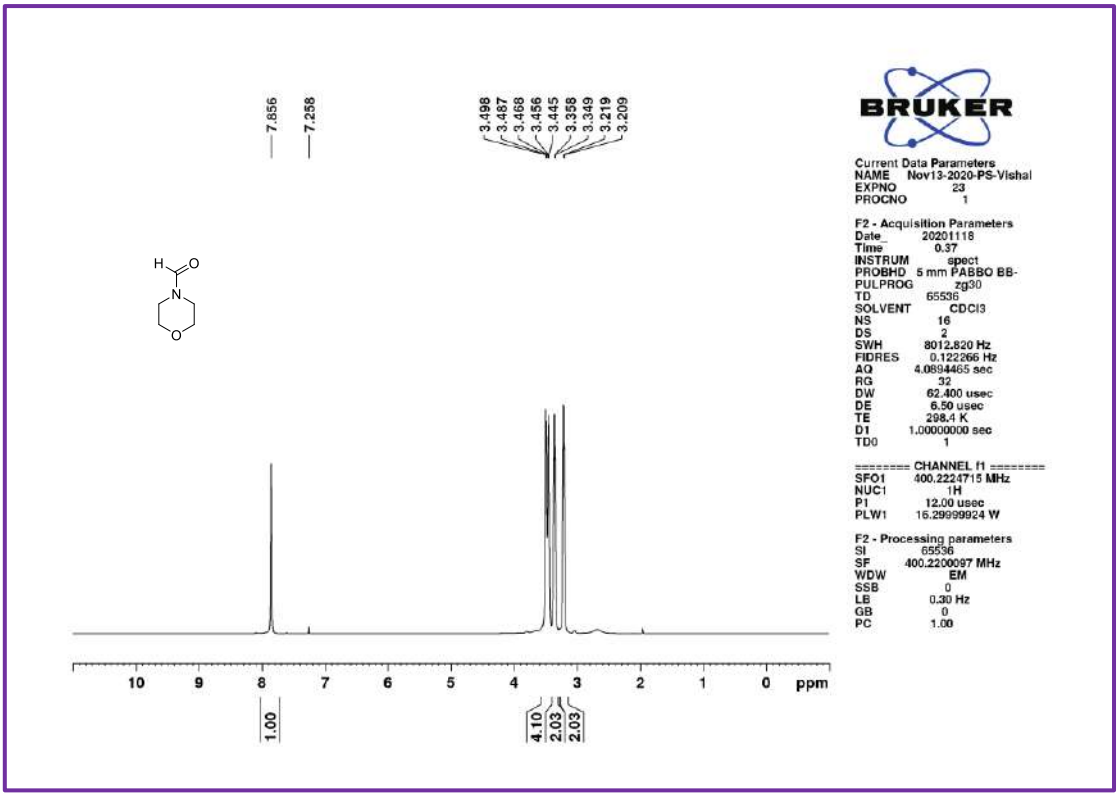

^{1}H NMR spectra of **3d.**

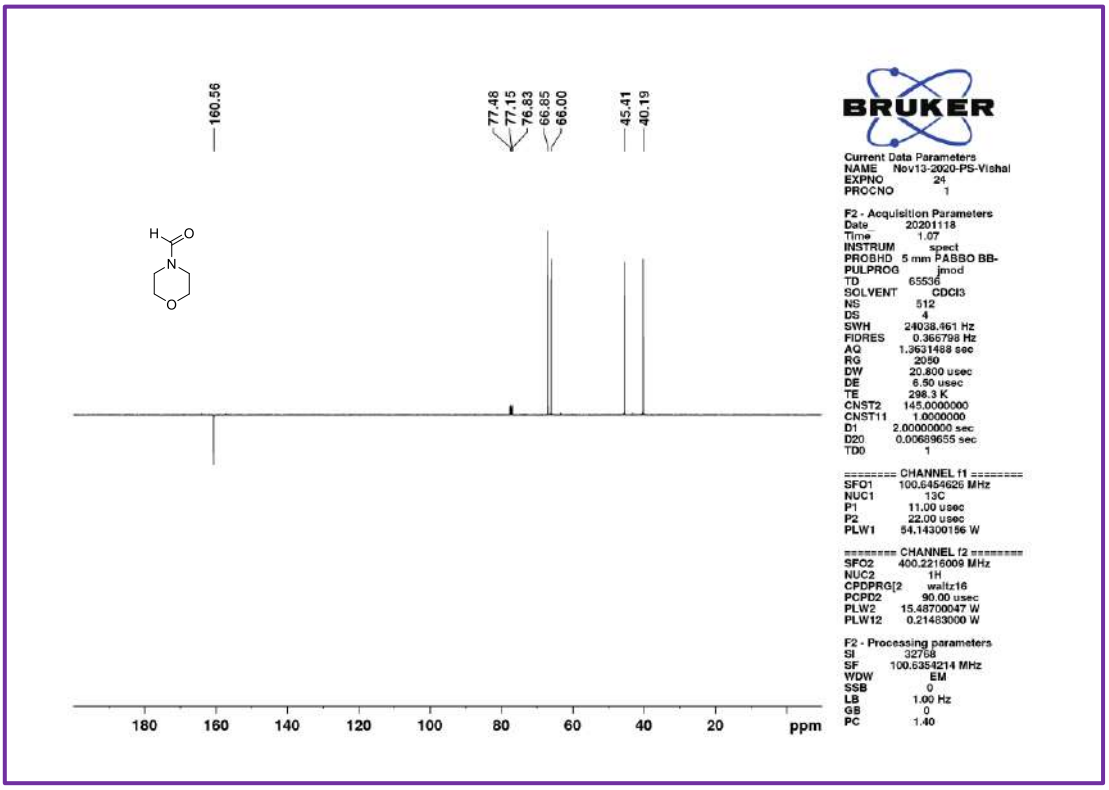

^{13}C NMR spectra of **3d.**

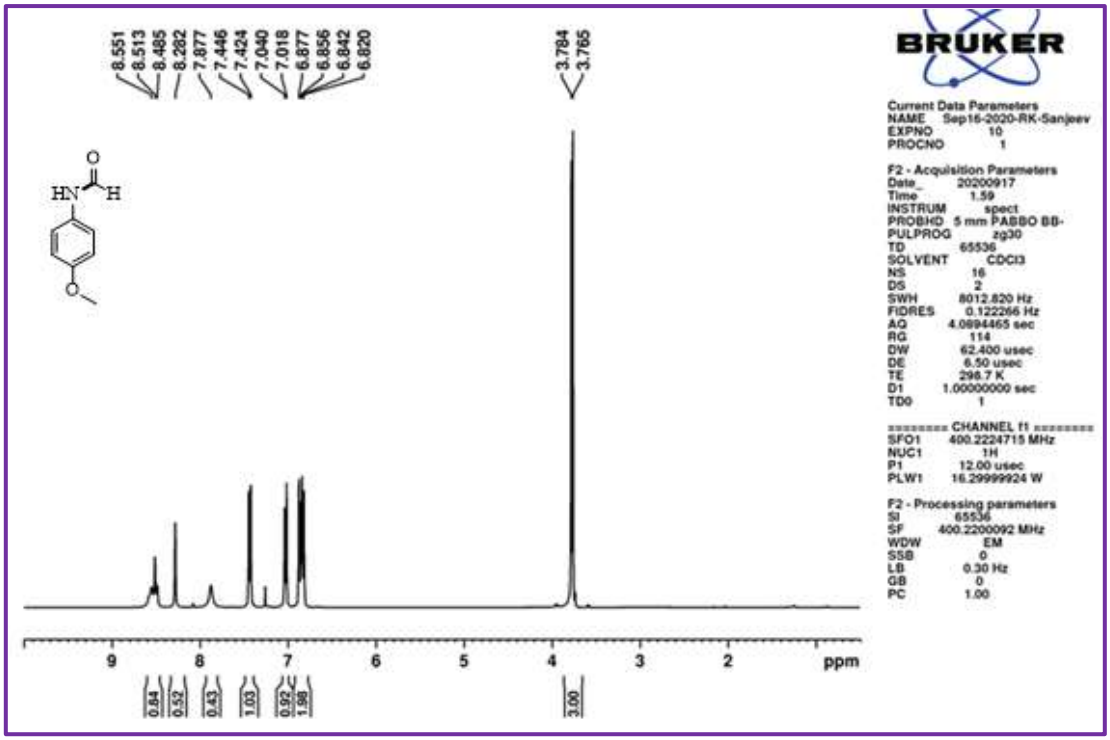

^{1}H NMR spectra of **3e.**

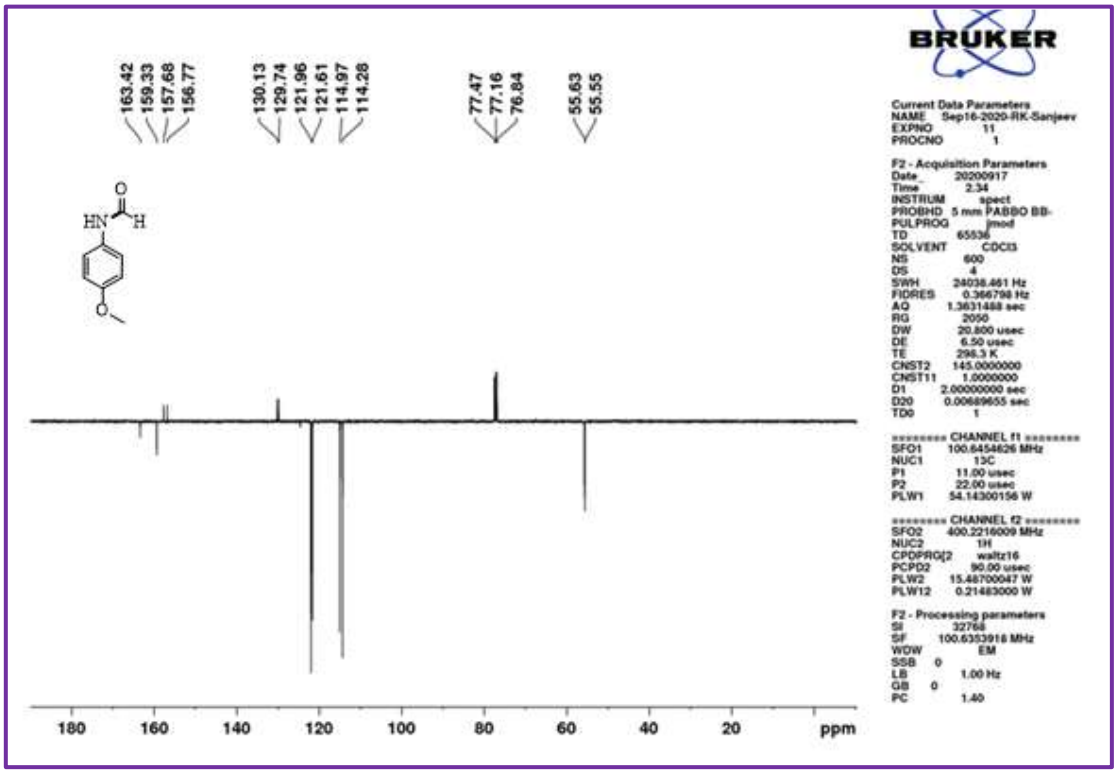

^{13}C NMR spectra of **3e.**

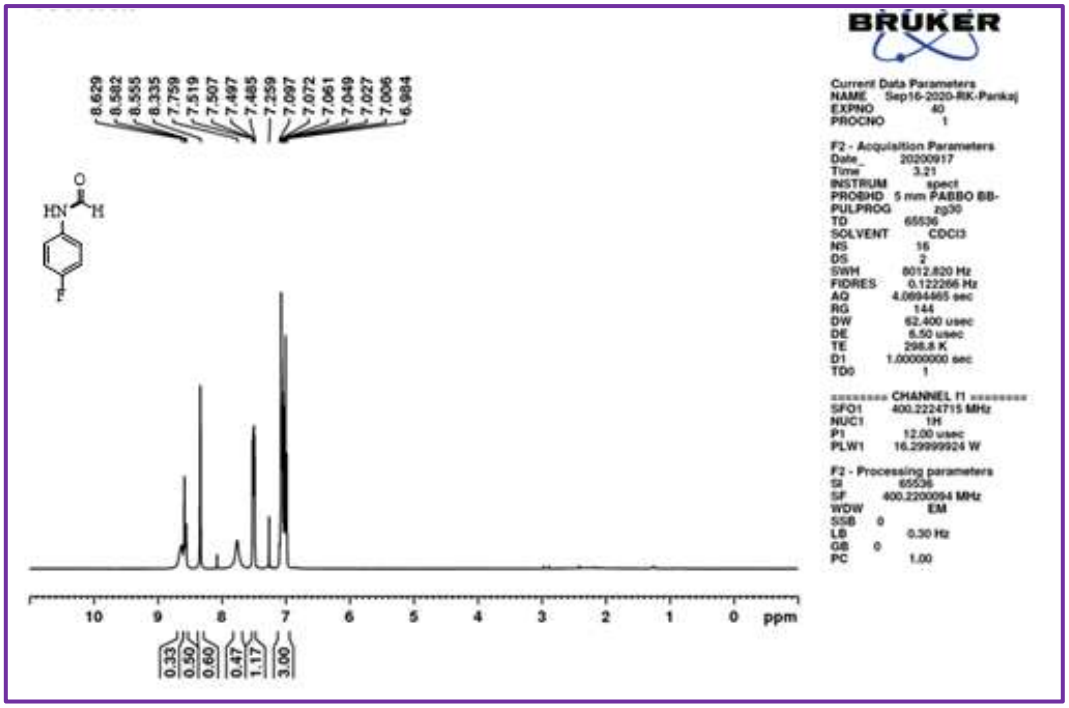

^{1}H NMR spectra of **3f.**

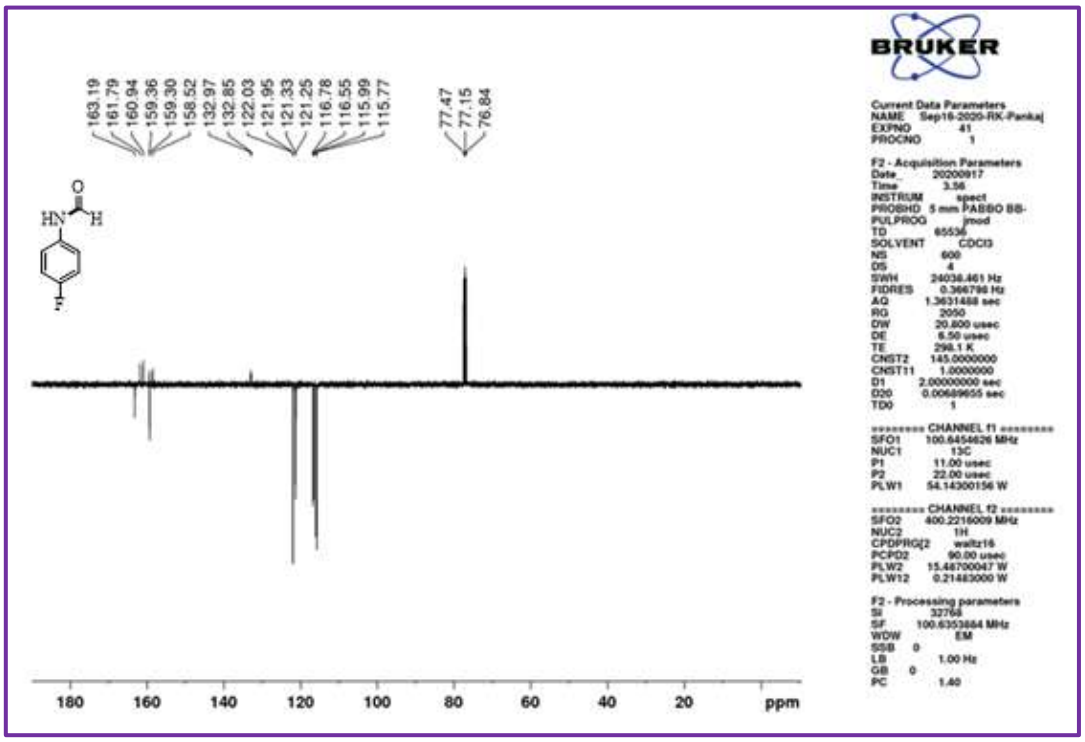

^{13}C NMR spectra of **3f.**

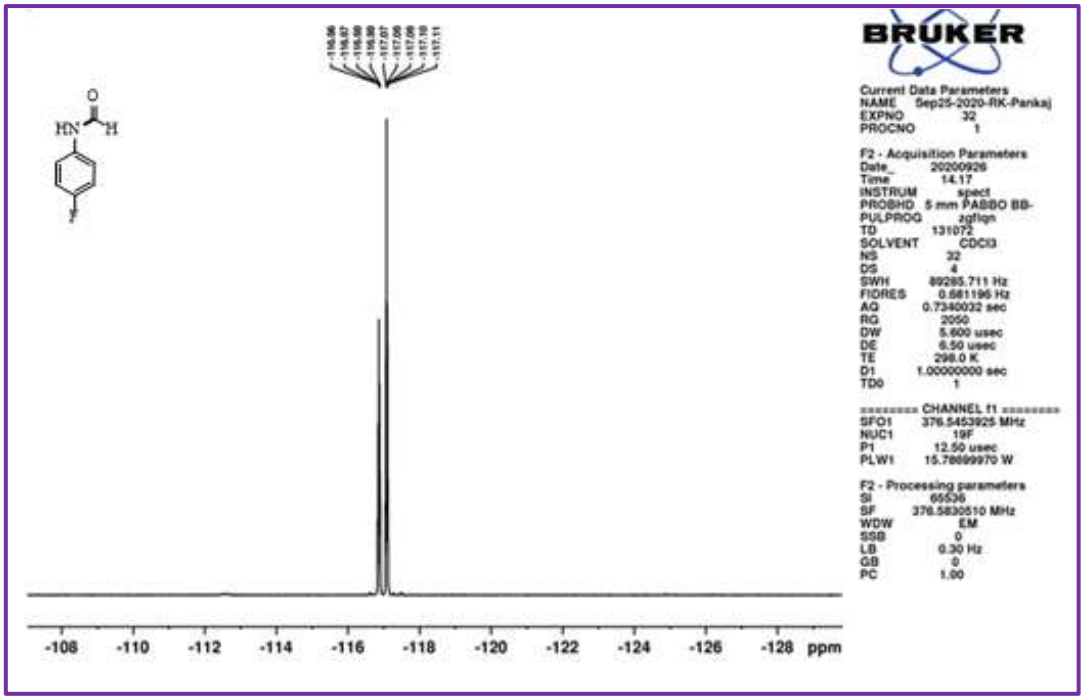

^{19}F NMR spectra of **3f.**

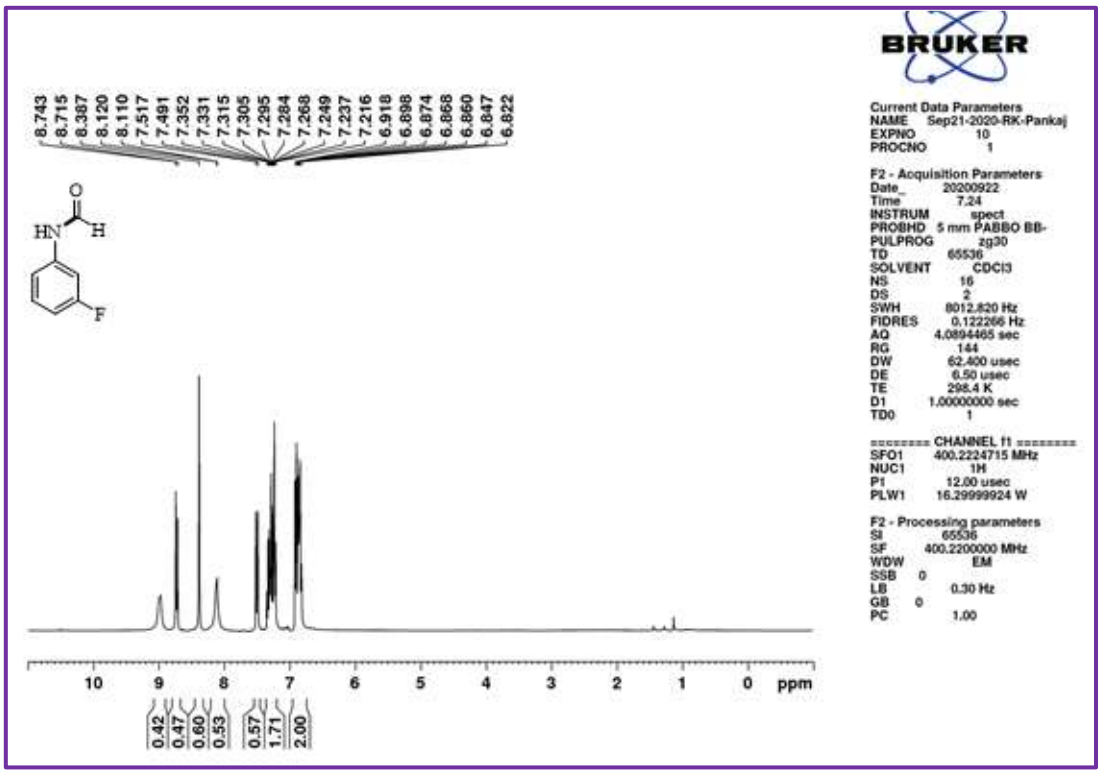

^{1}H NMR spectra of **3g.**

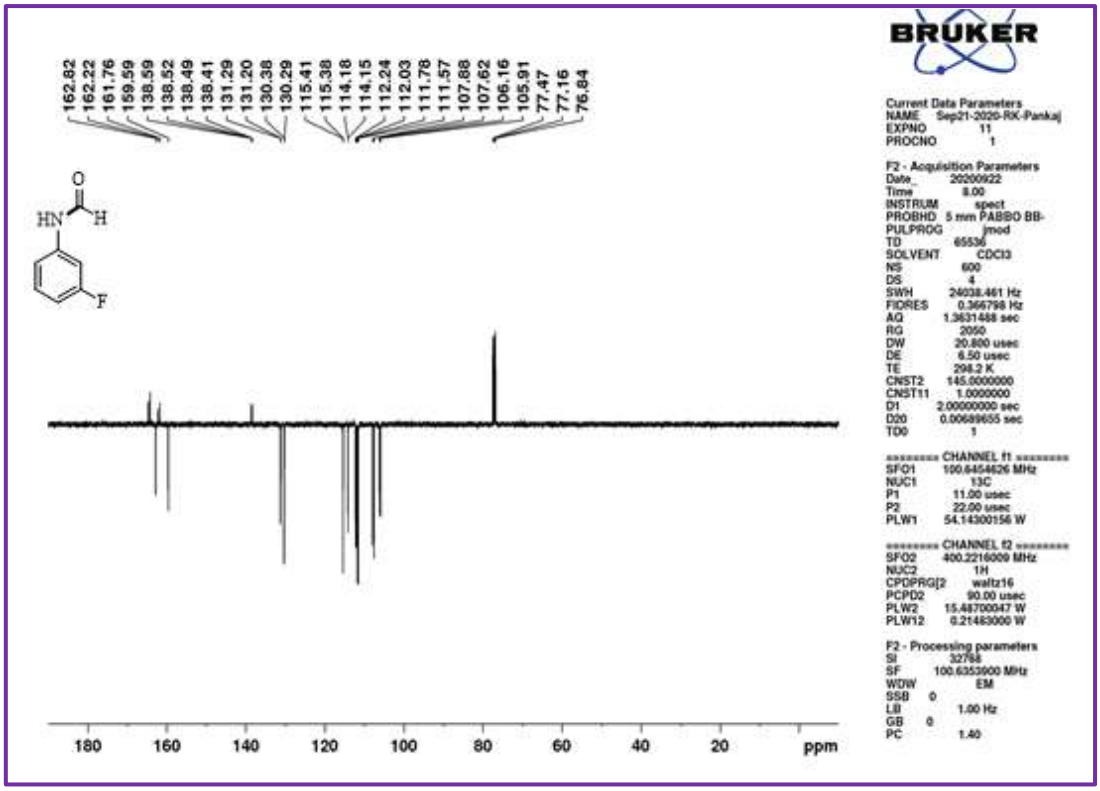

^{13}C NMR spectra of **3g.**

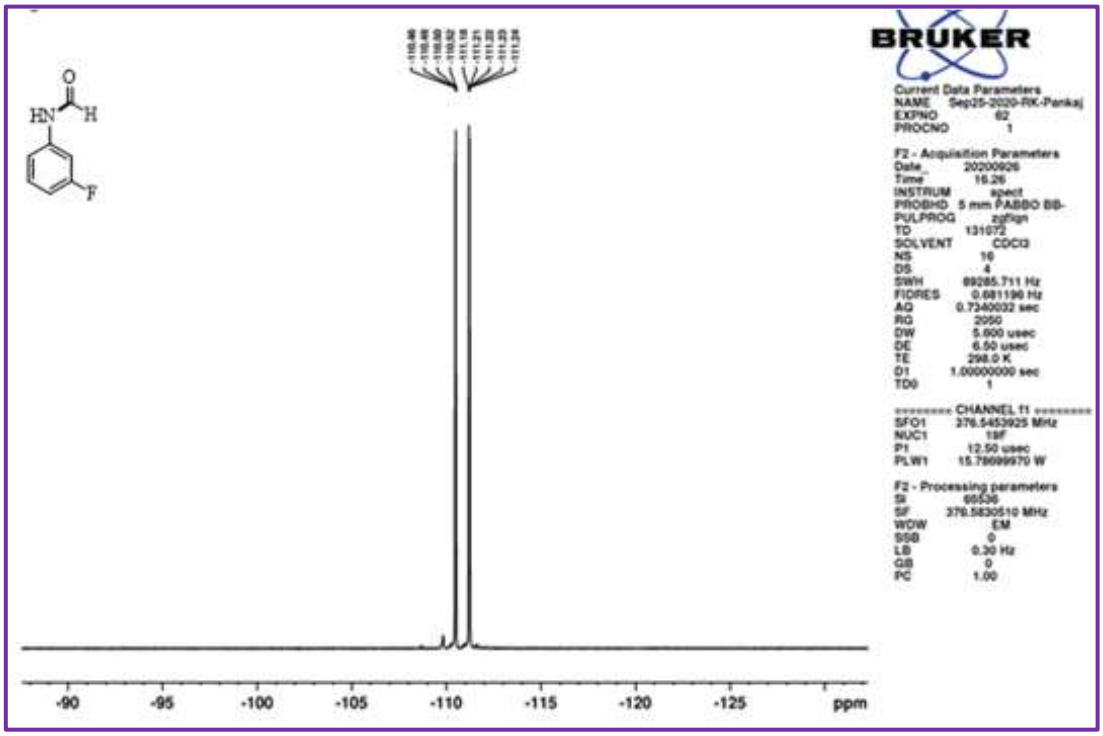

^{19}F NMR spectra of **3g.**

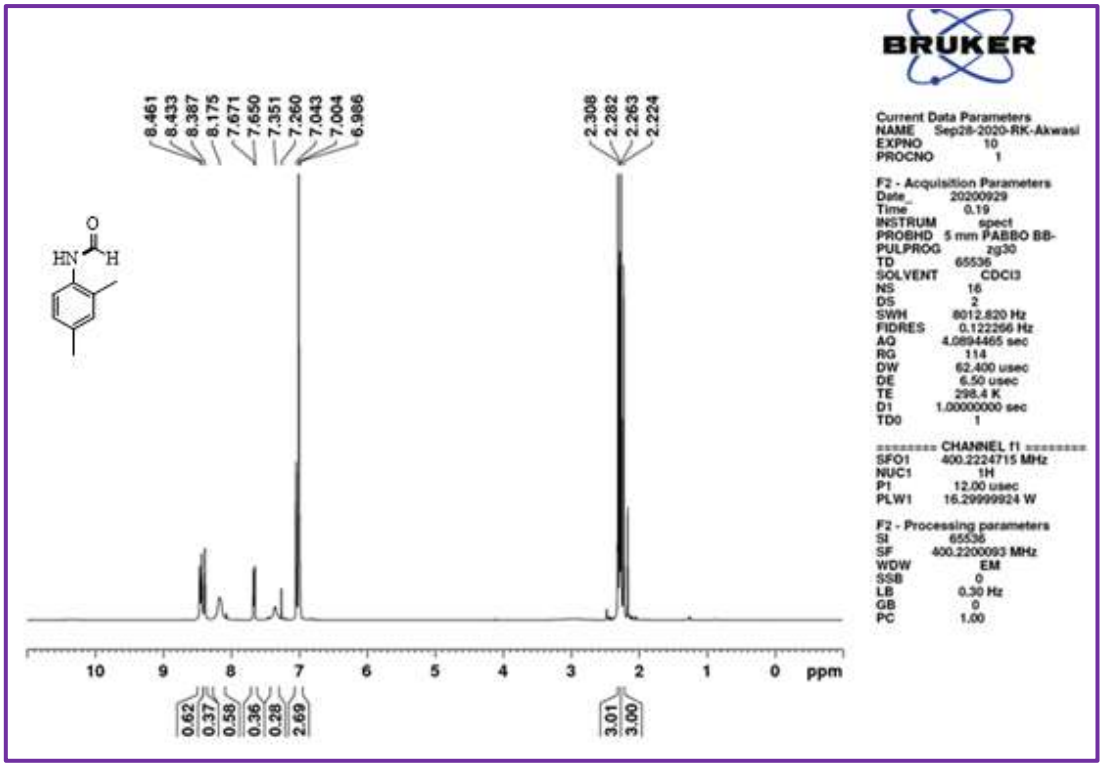

^{1}H NMR spectra of **3h.**

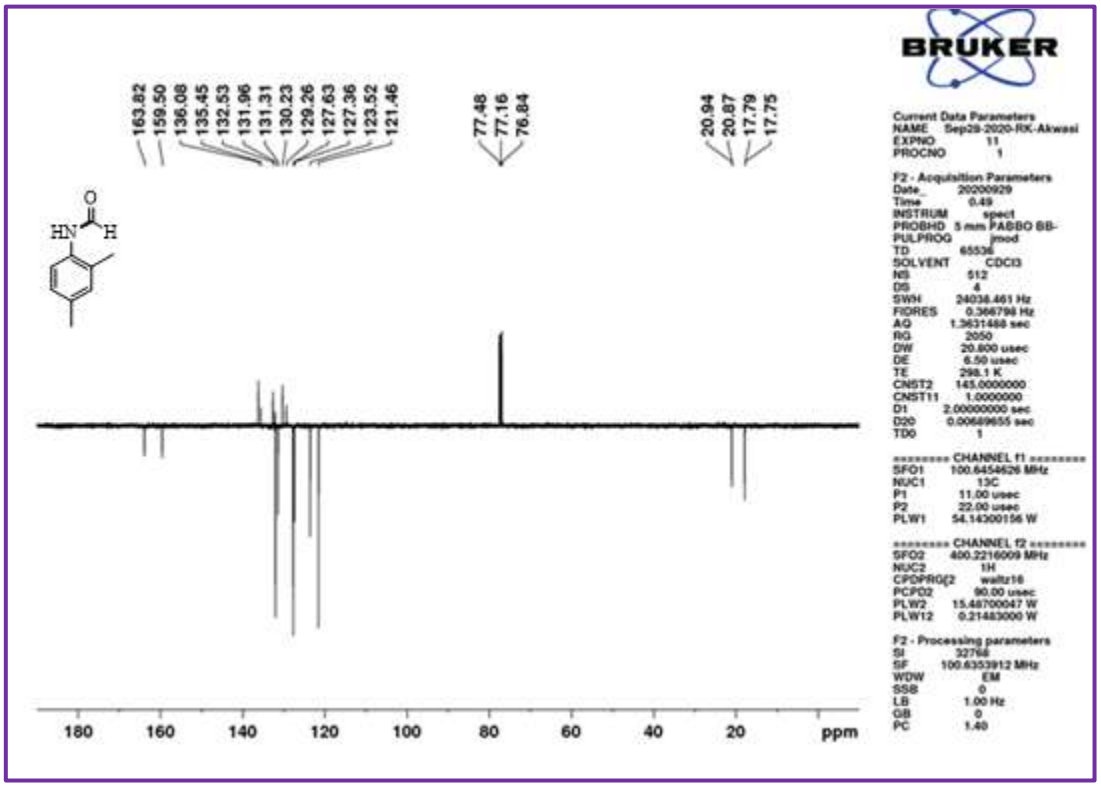

^{13}C NMR spectra of **3h.**

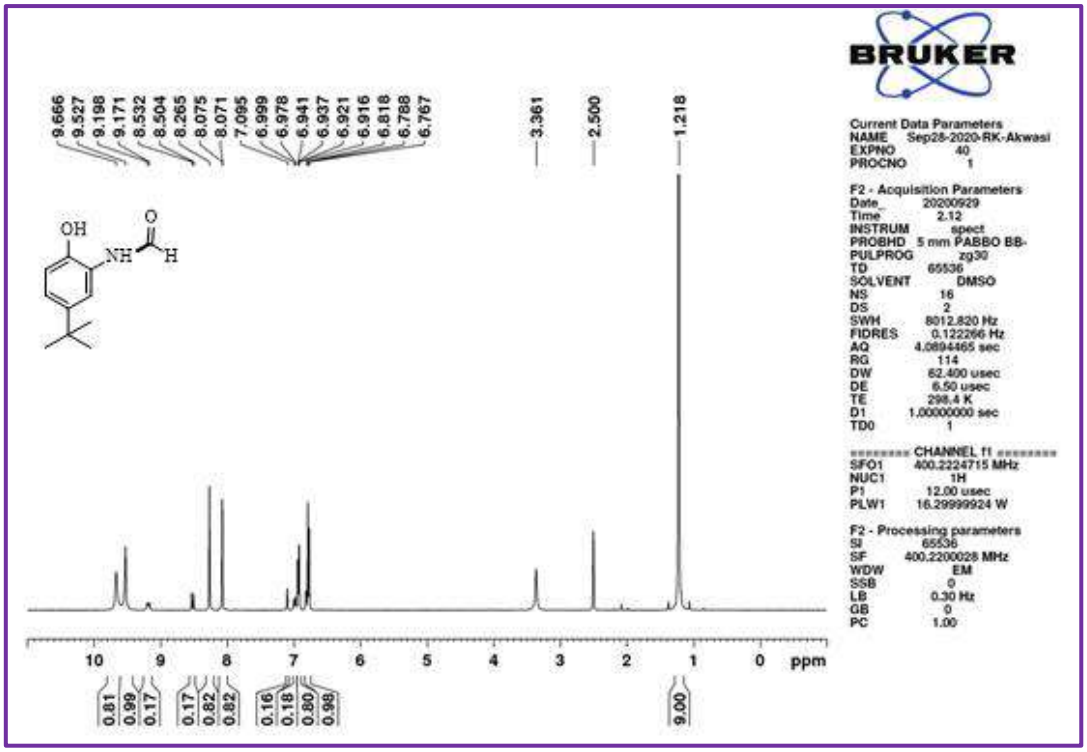

^{1}H NMR spectra of **3i.**

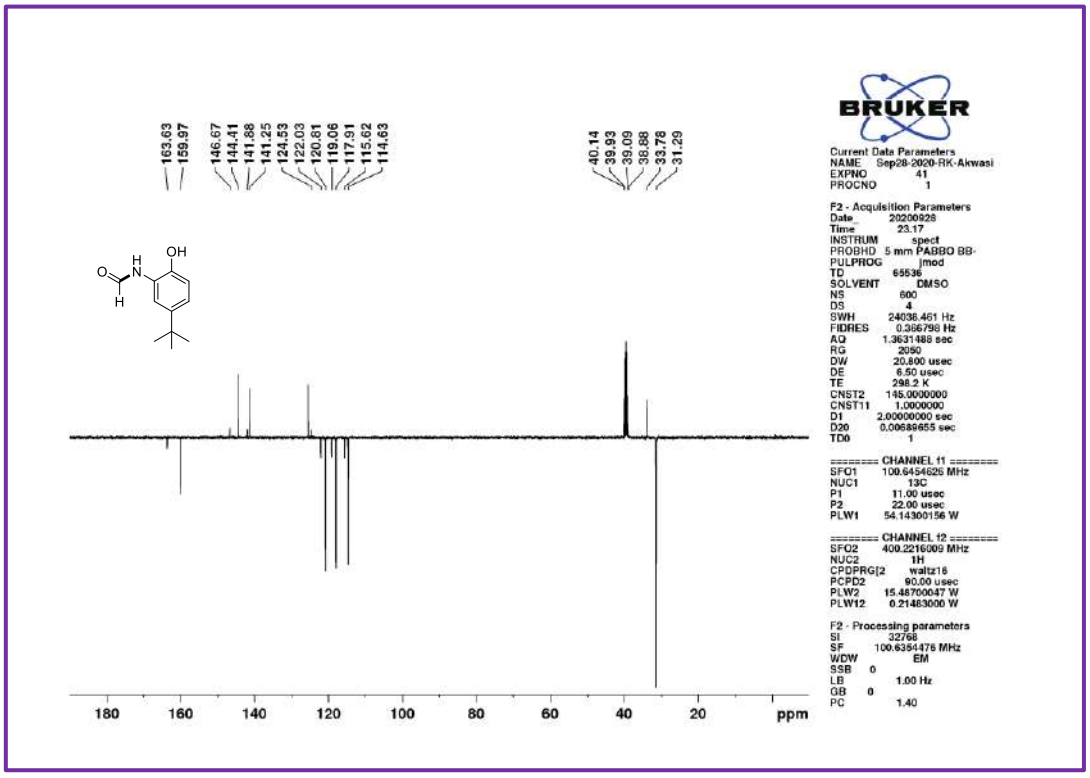

^{13}C NMR spectra of **3i.**

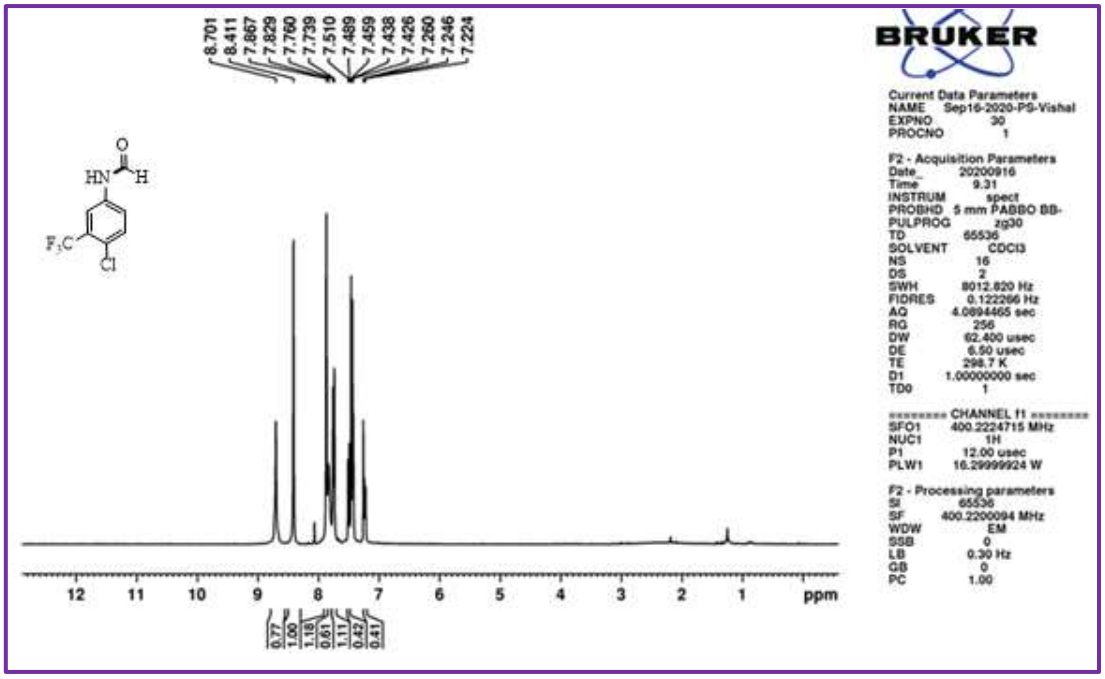

^{1}H NMR spectra of **3j.**

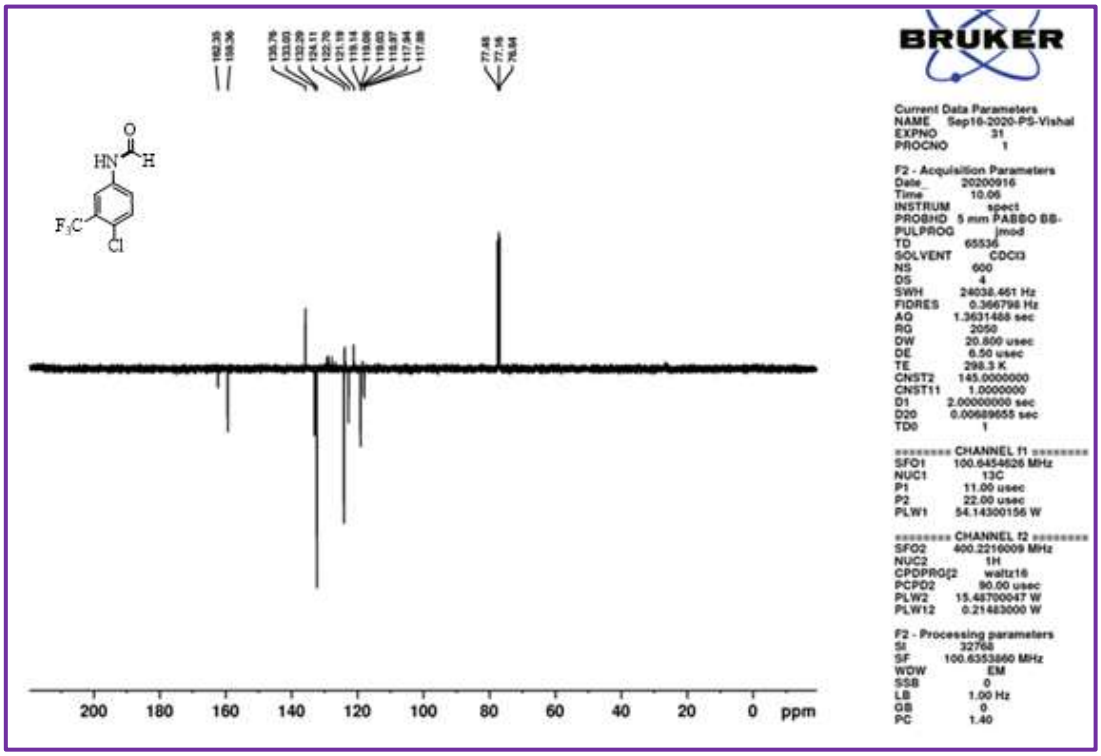

^{13}C NMR spectra of **3j.**

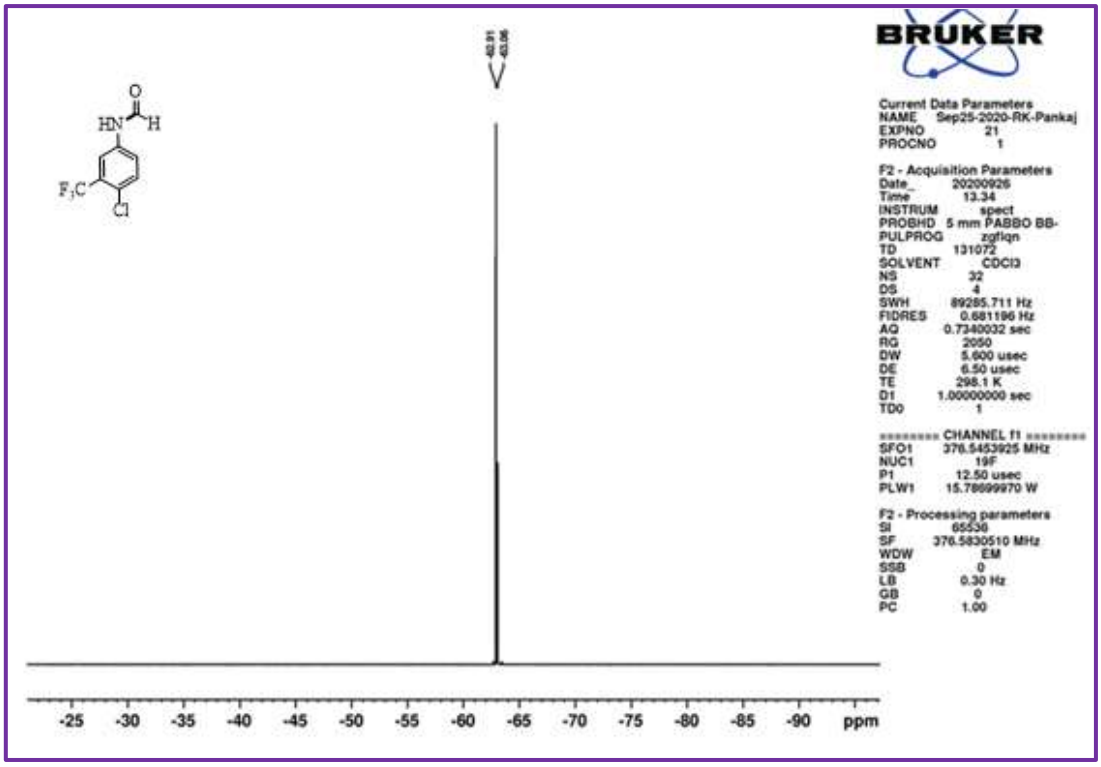

^{19}F NMR spectra of **3j.**

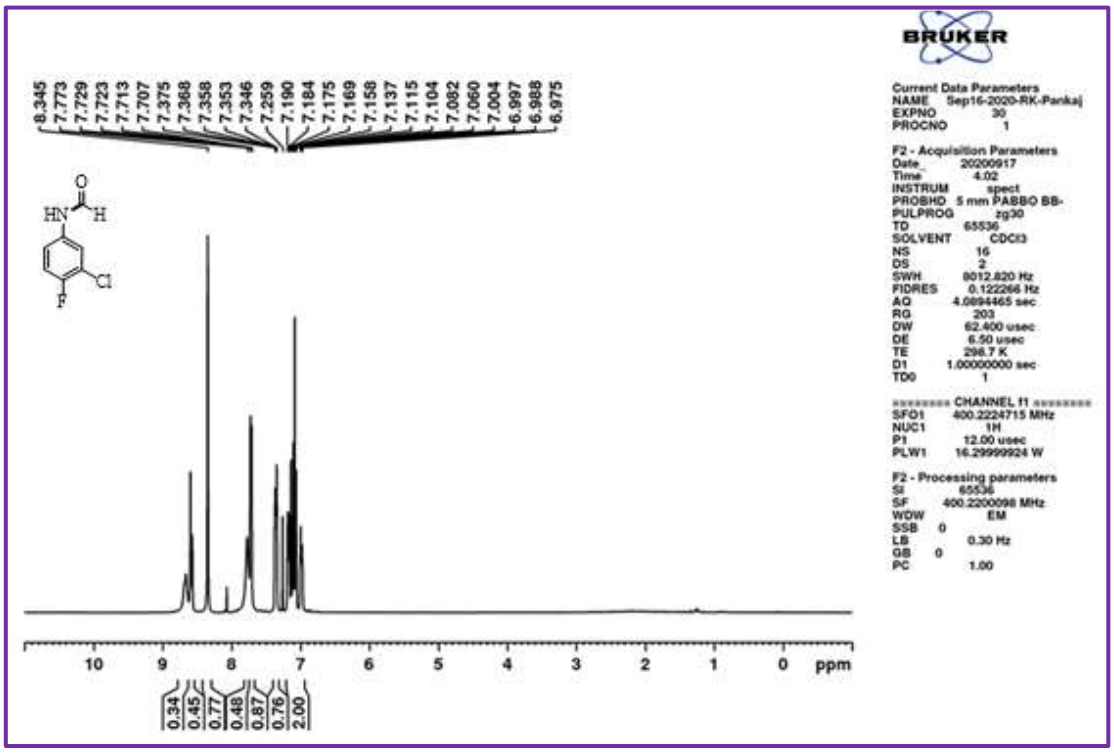

^{1}H NMR spectra of **3k.**

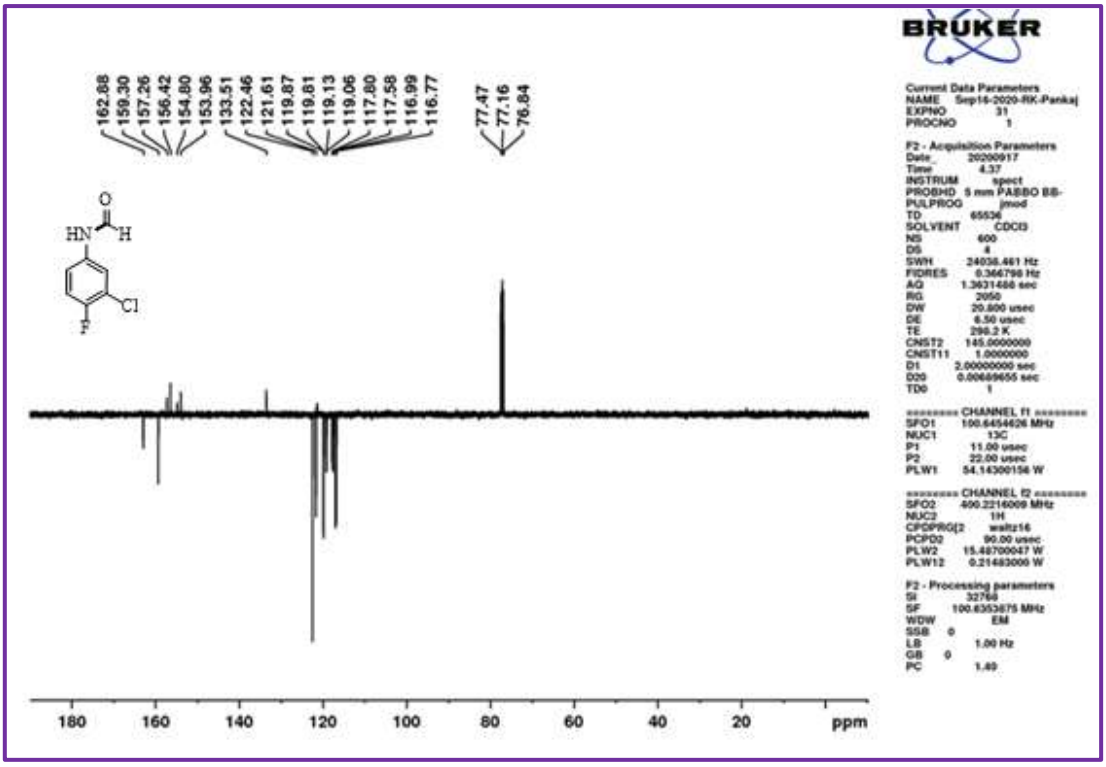

^{13}C NMR spectra of **3k.**

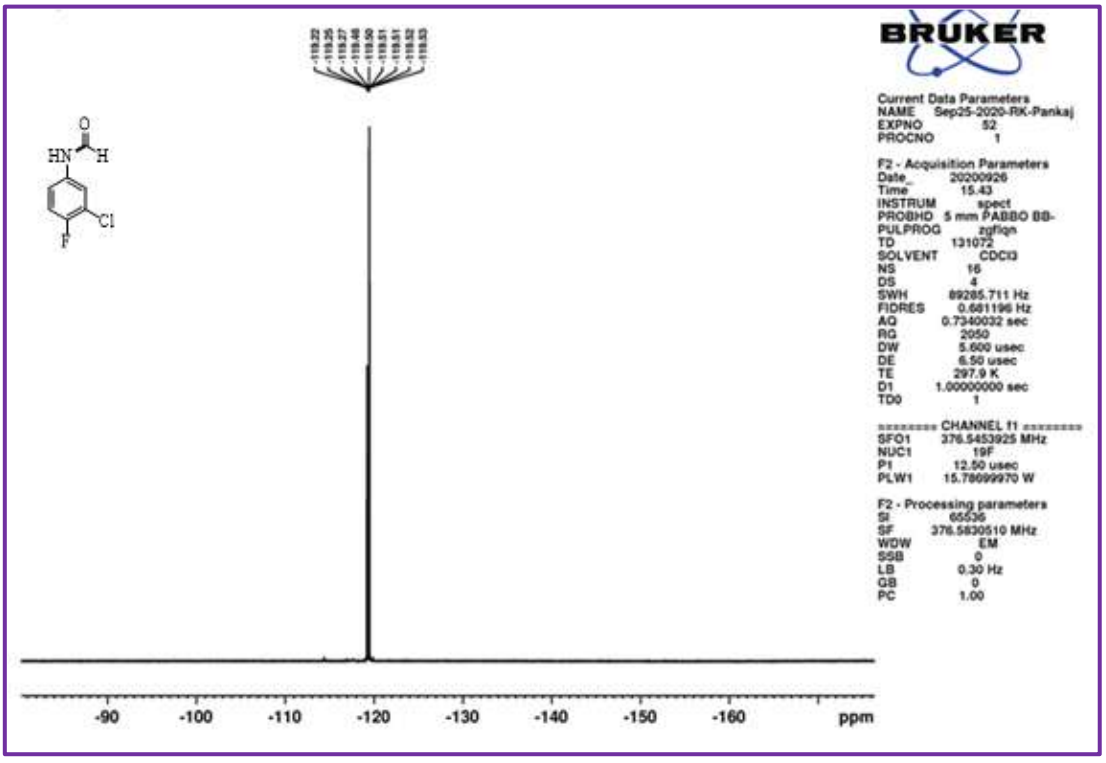

^{19}F NMR spectra of **3k.**

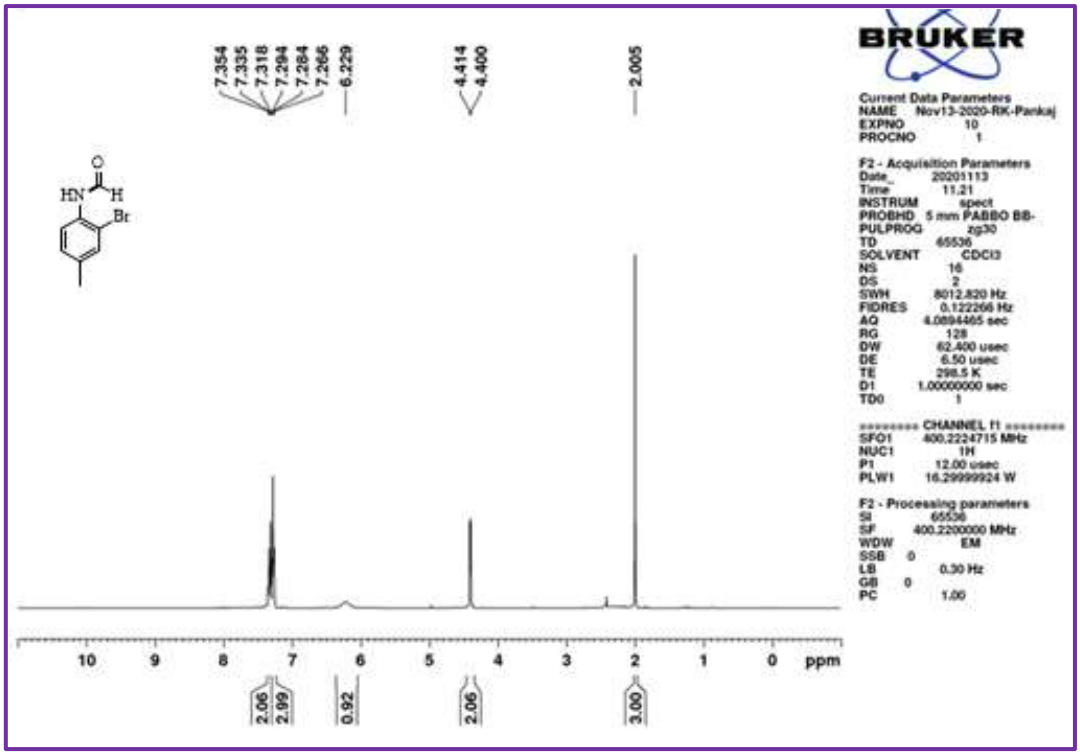

^{1}H NMR spectra of **3l.**

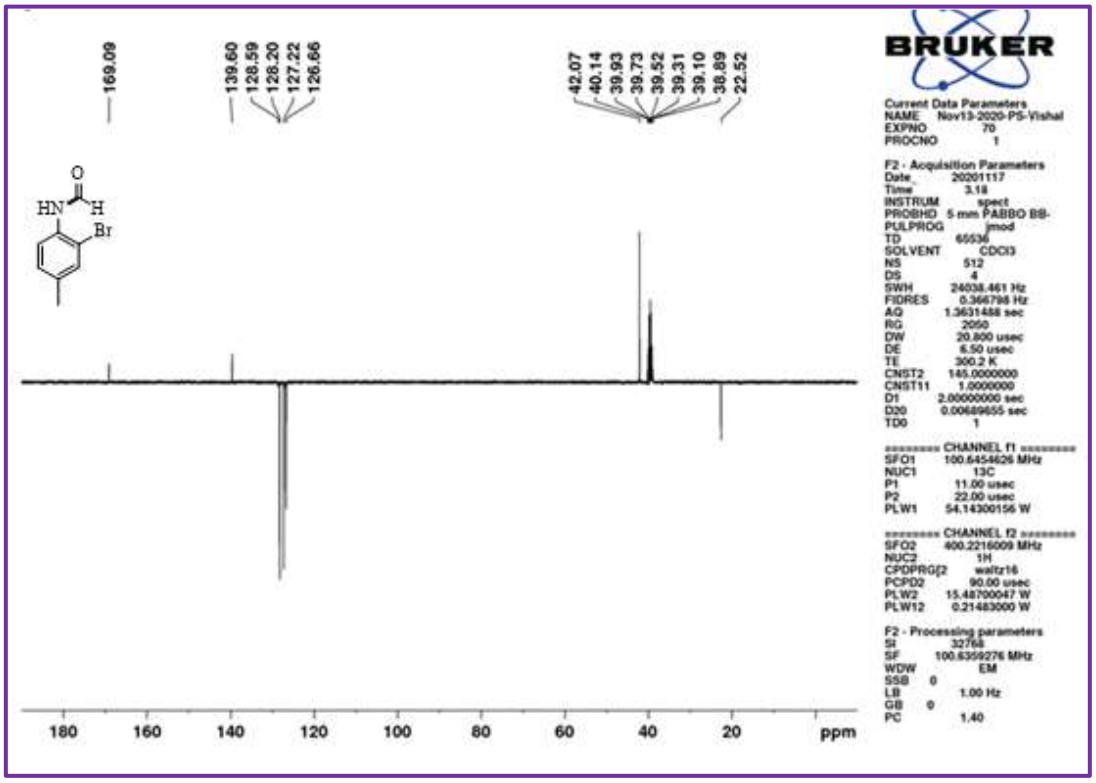

^{13}C NMR spectra of **3l.**

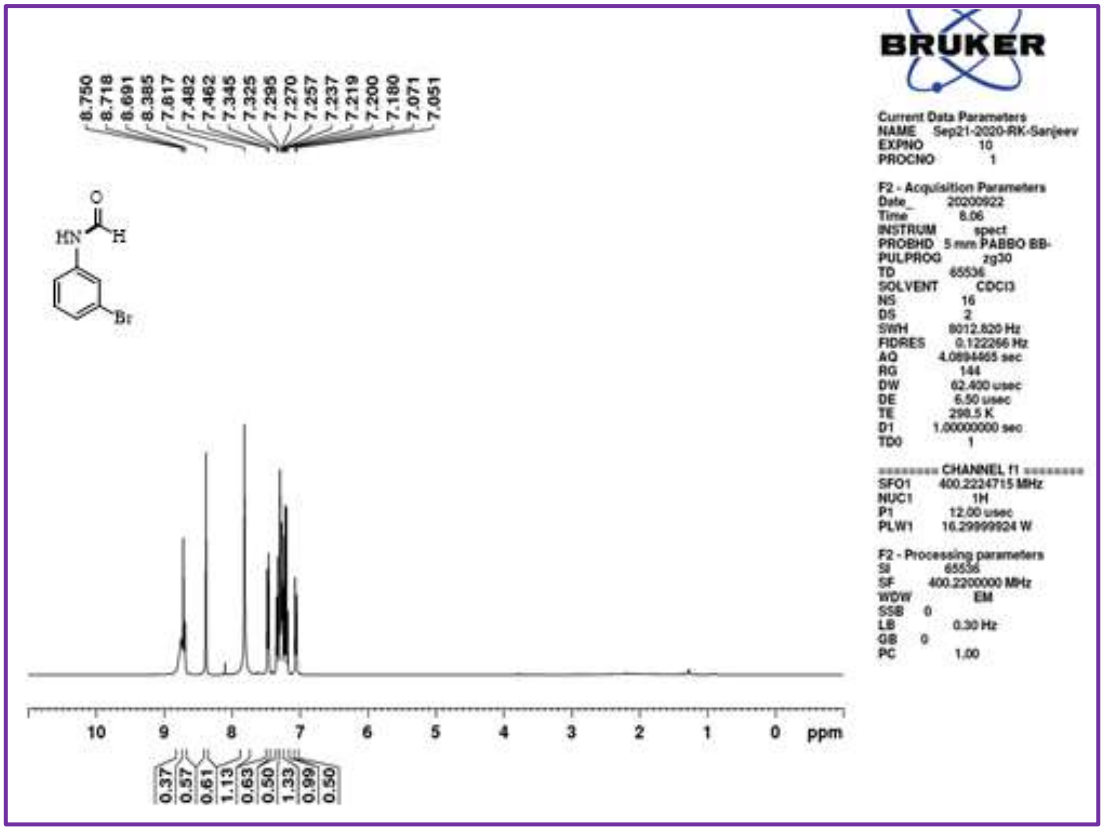

^{1}H NMR spectra of **3m.**

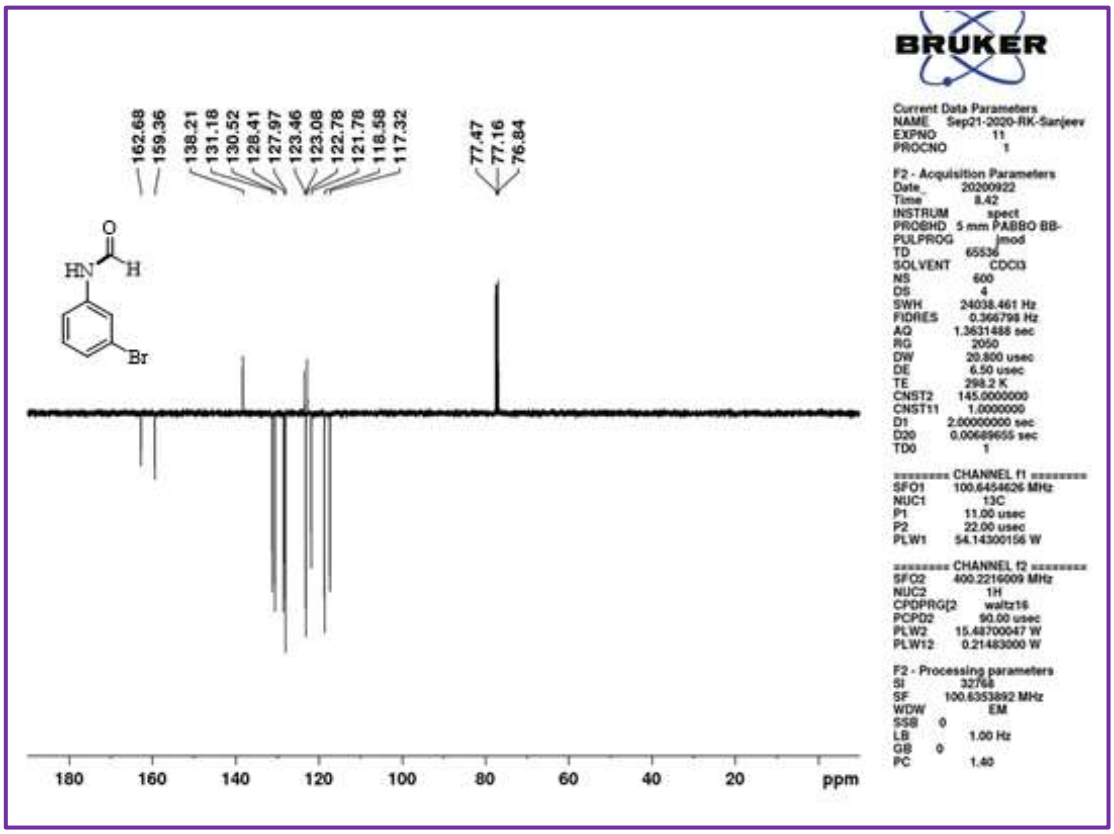

^{13}C NMR spectra of **3m.**

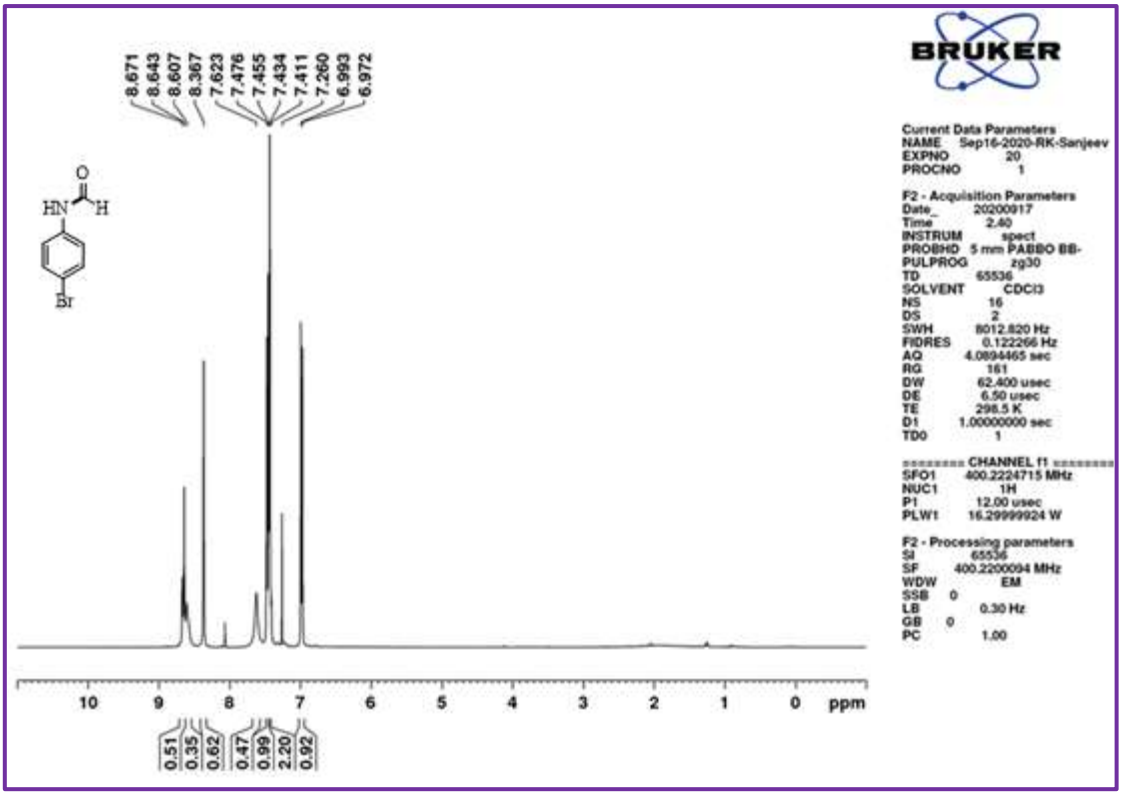

^{1}H NMR spectra of **3n.**

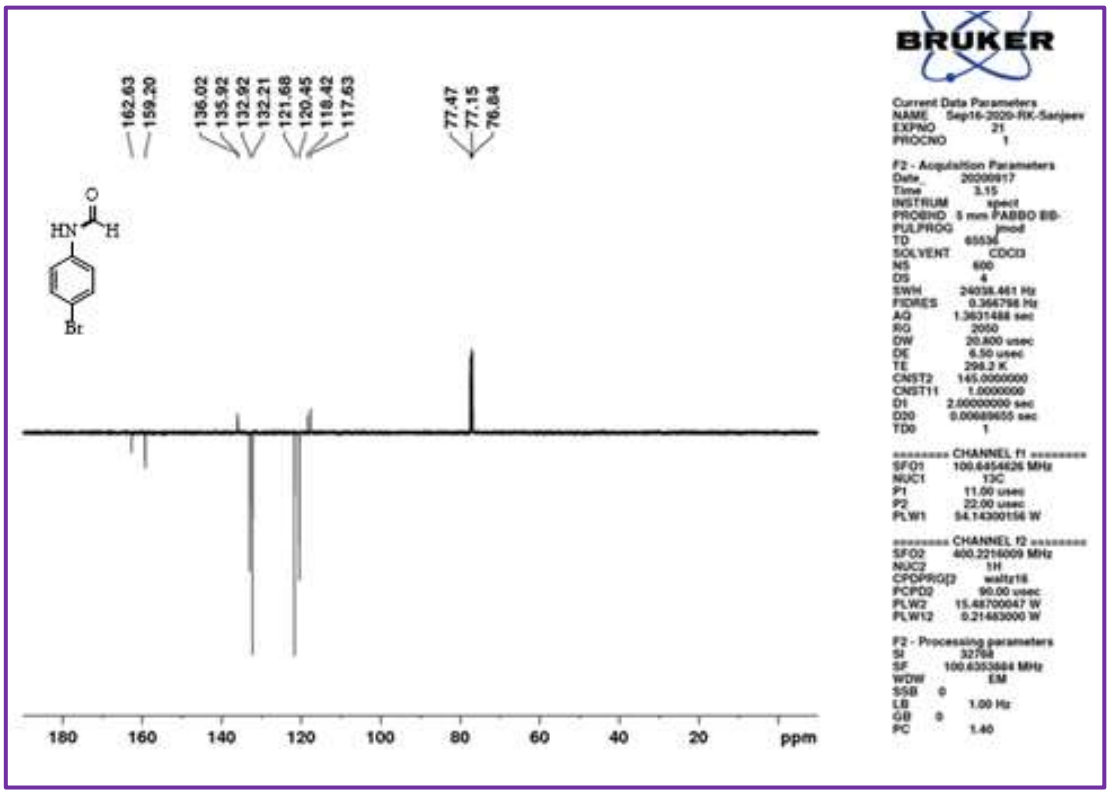

^{13}C NMR spectra of **3n.**

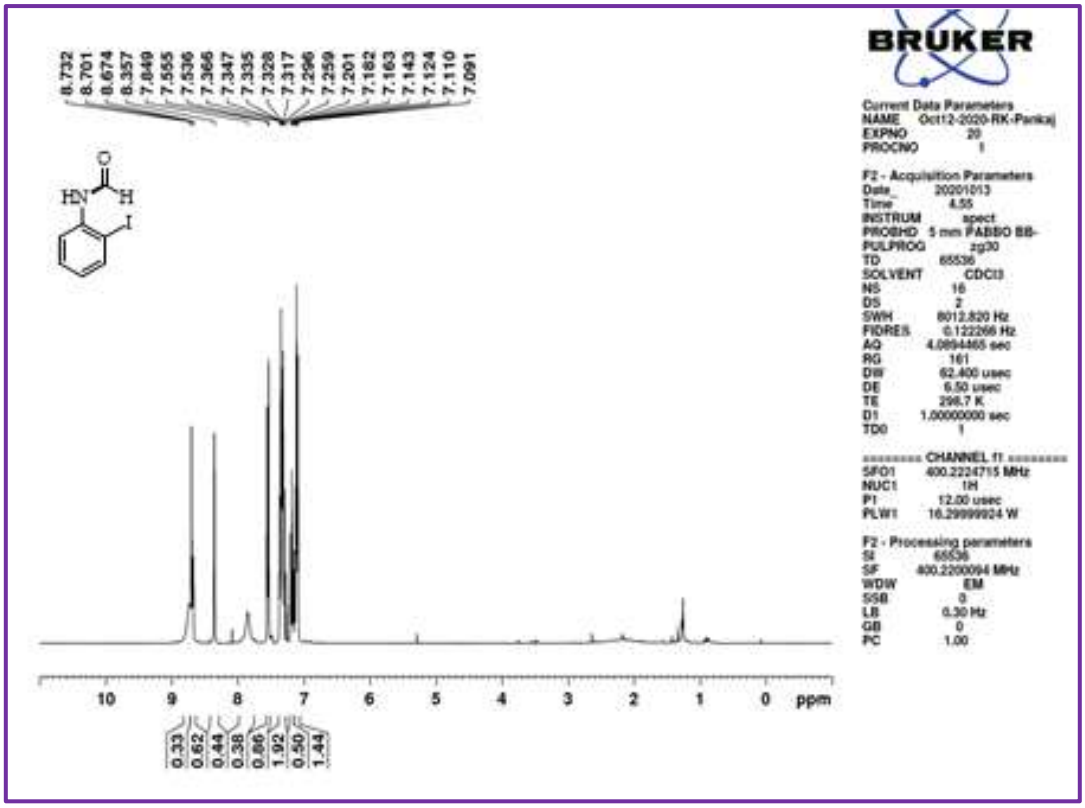

^{1}H NMR spectra of **3o.**

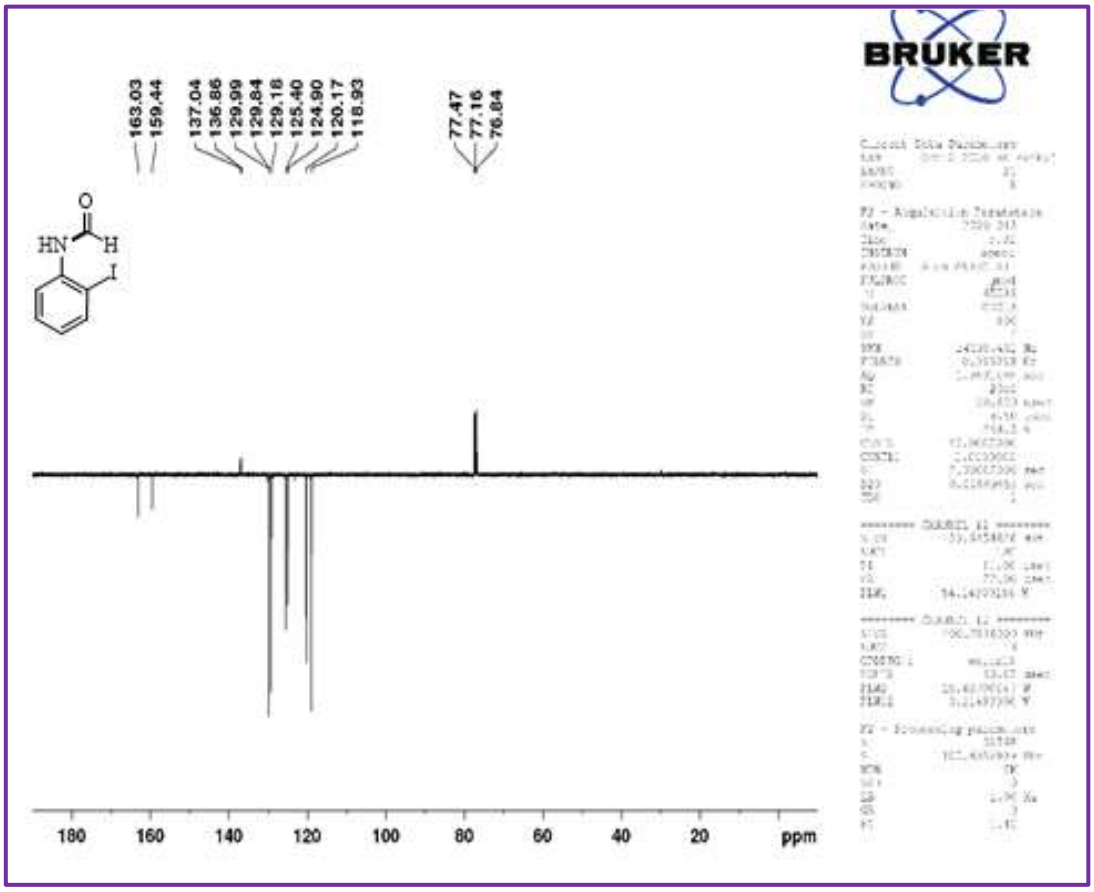

^{13}C NMR spectra of **3o.**

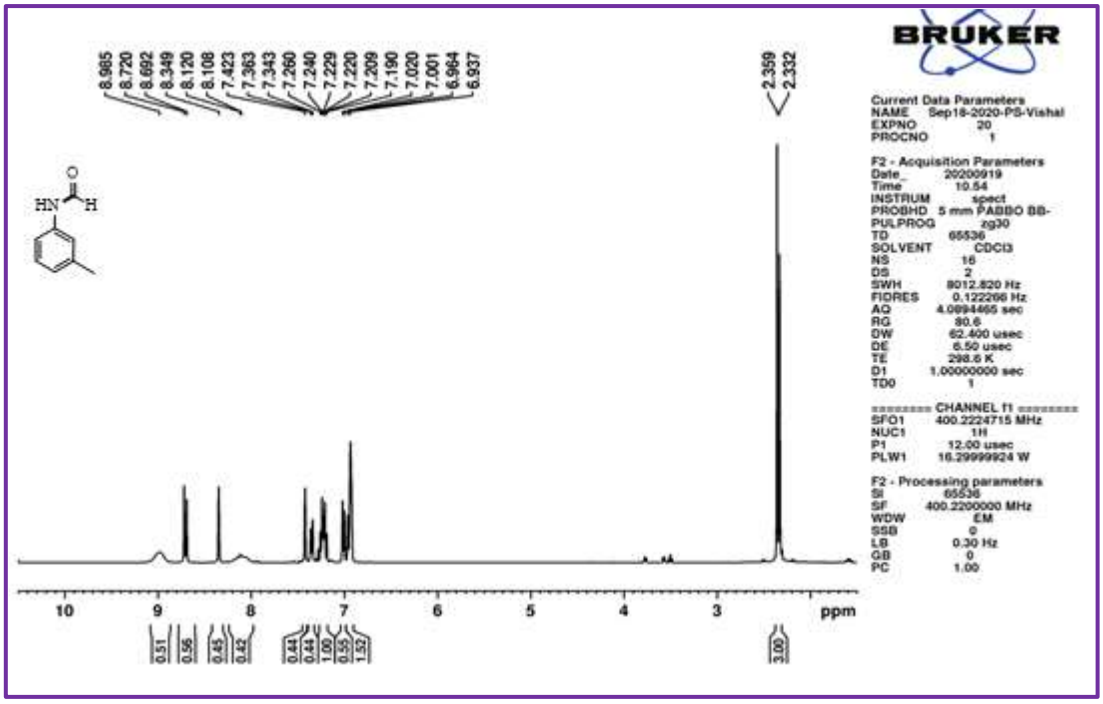

^{1}H NMR spectra of **3p.**

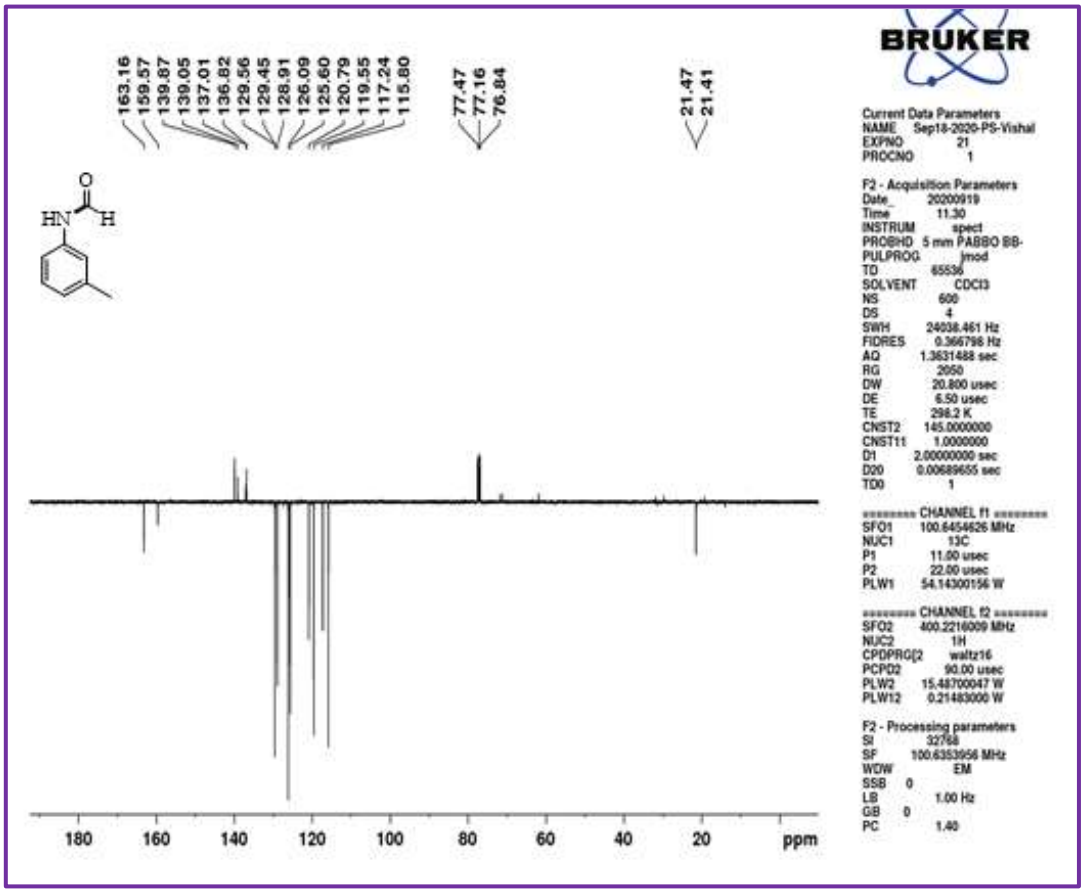

^{13}C NMR spectra of **3p.**

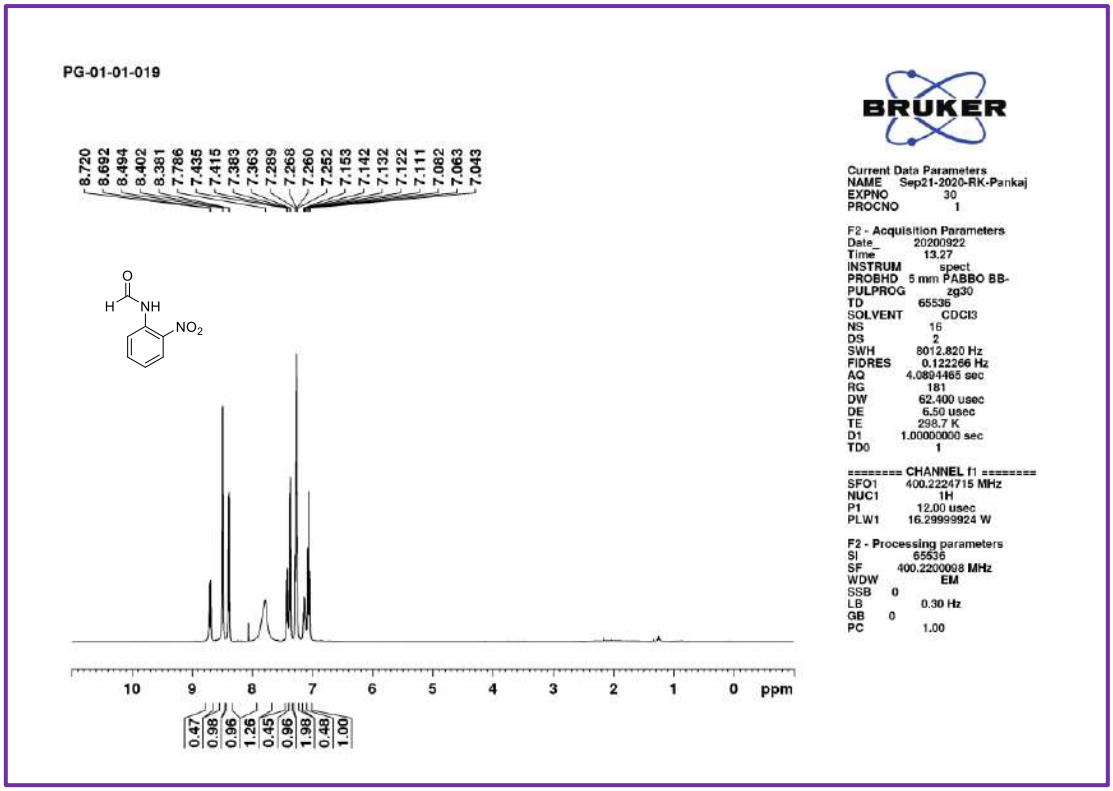

^{1}H NMR spectra of **3q.**

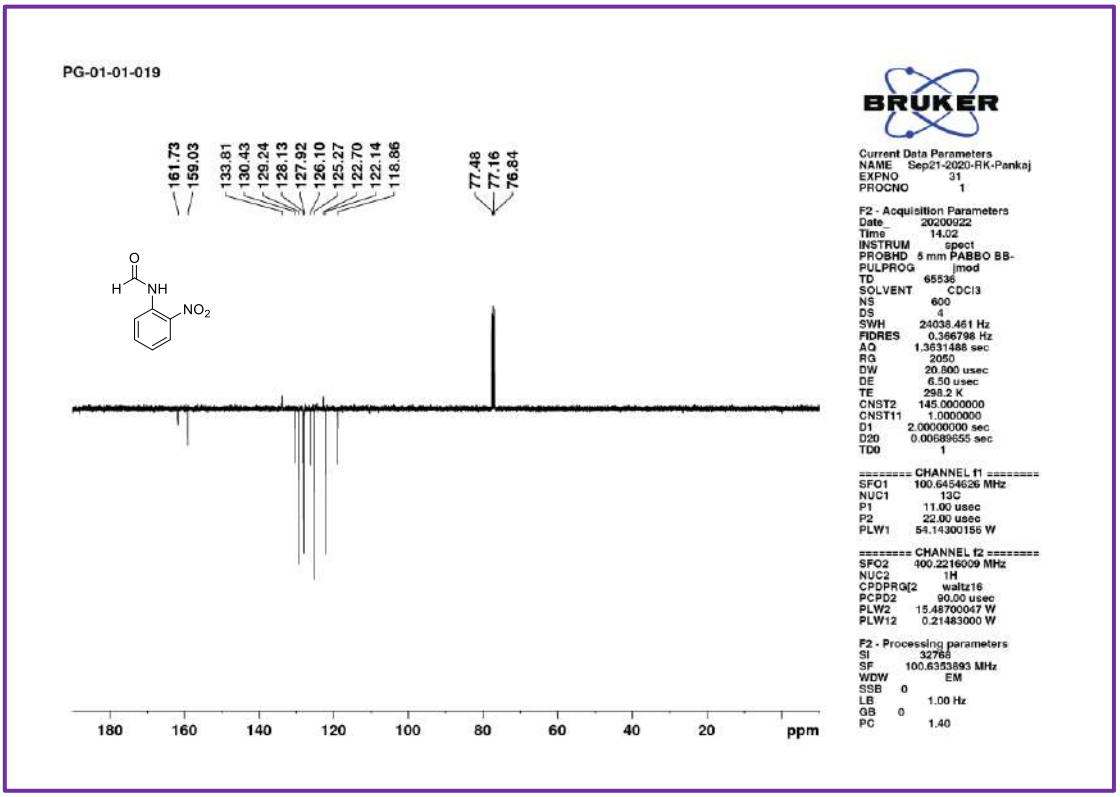

^{13}C NMR spectra of **3q.**

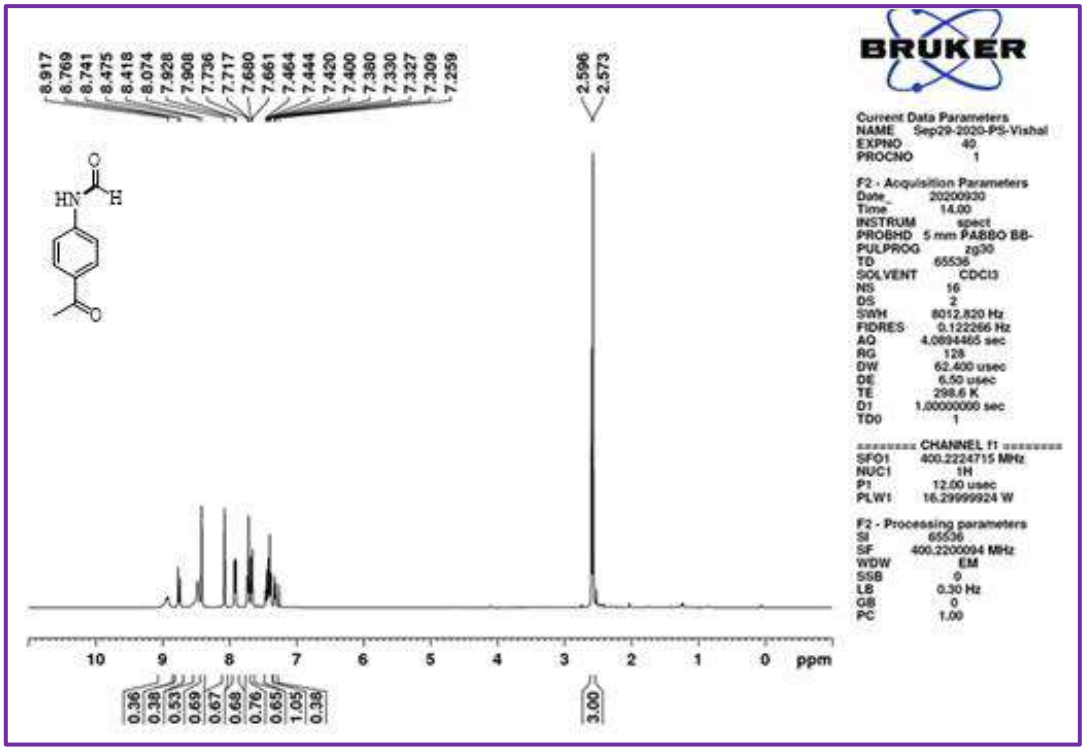

^{1}H NMR spectra of **3r.**

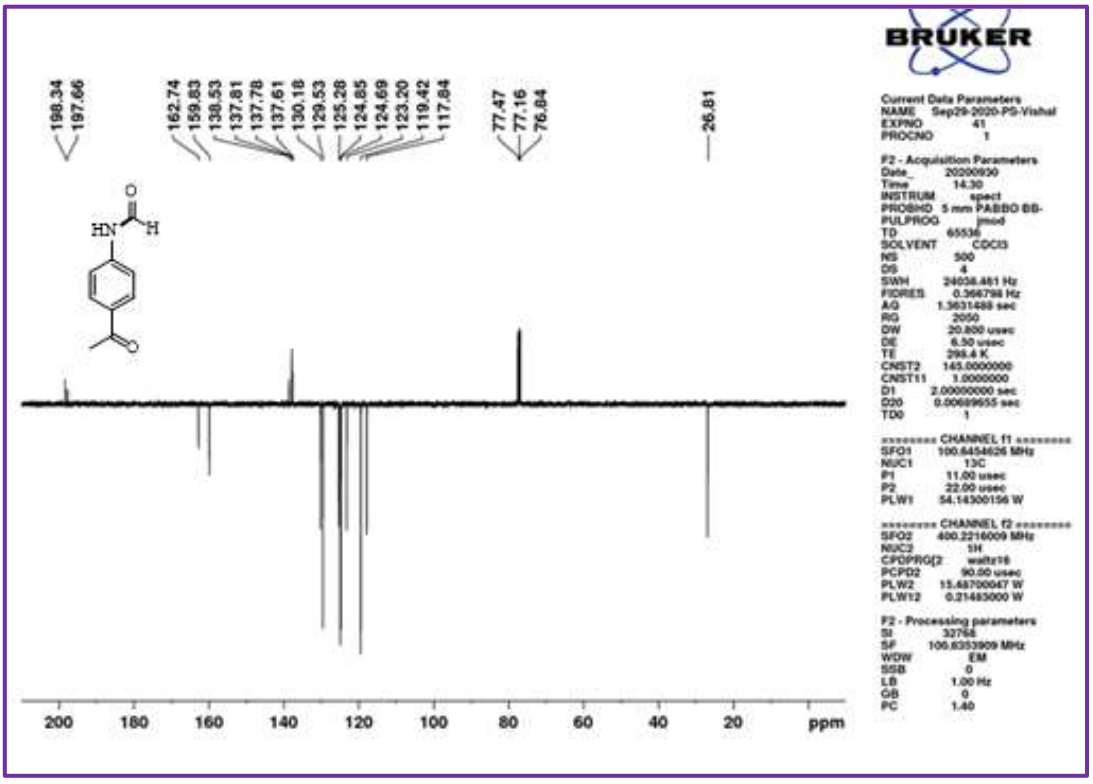

^{13}C NMR spectra of **3r.**

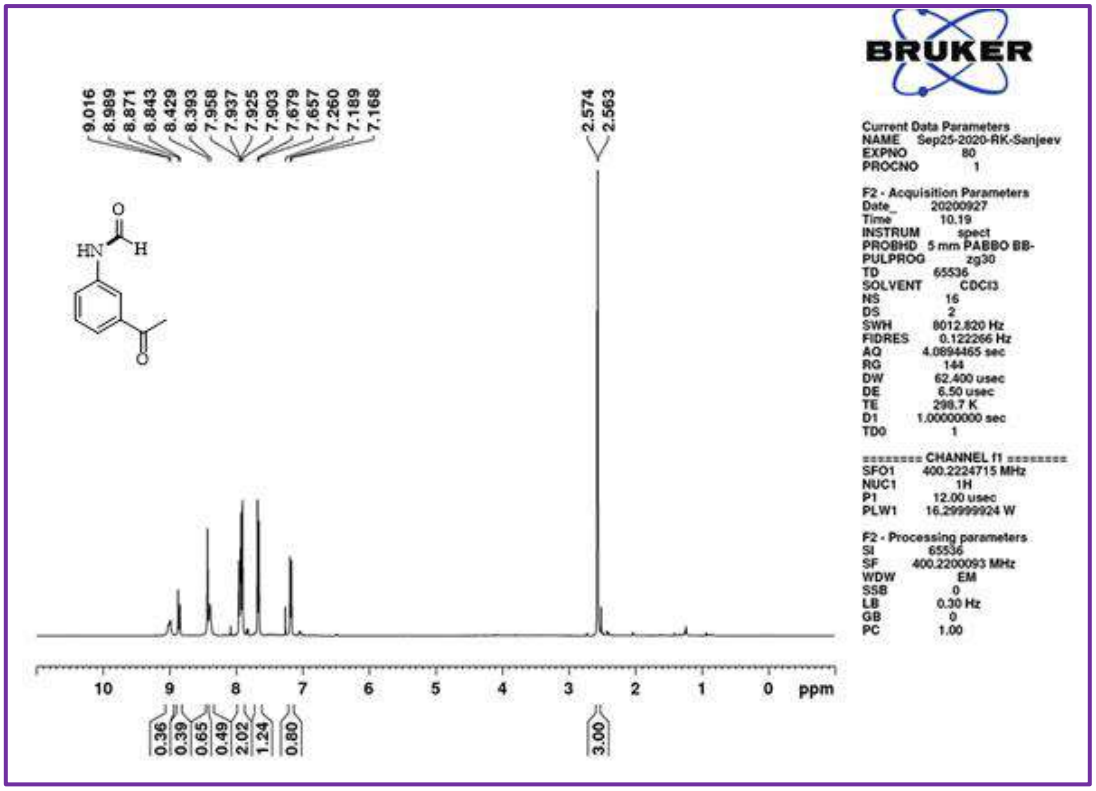

^{1}H NMR spectra of **3s.**

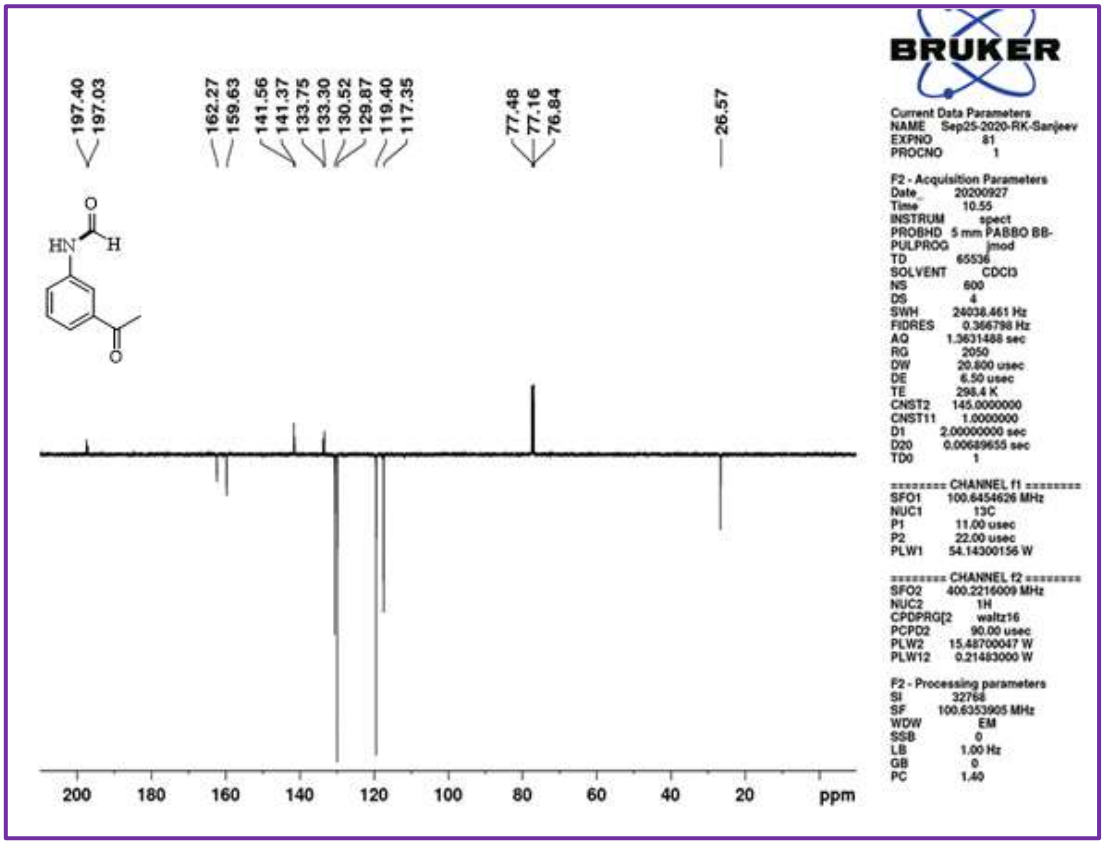

^{13}C NMR spectra of **3s.**

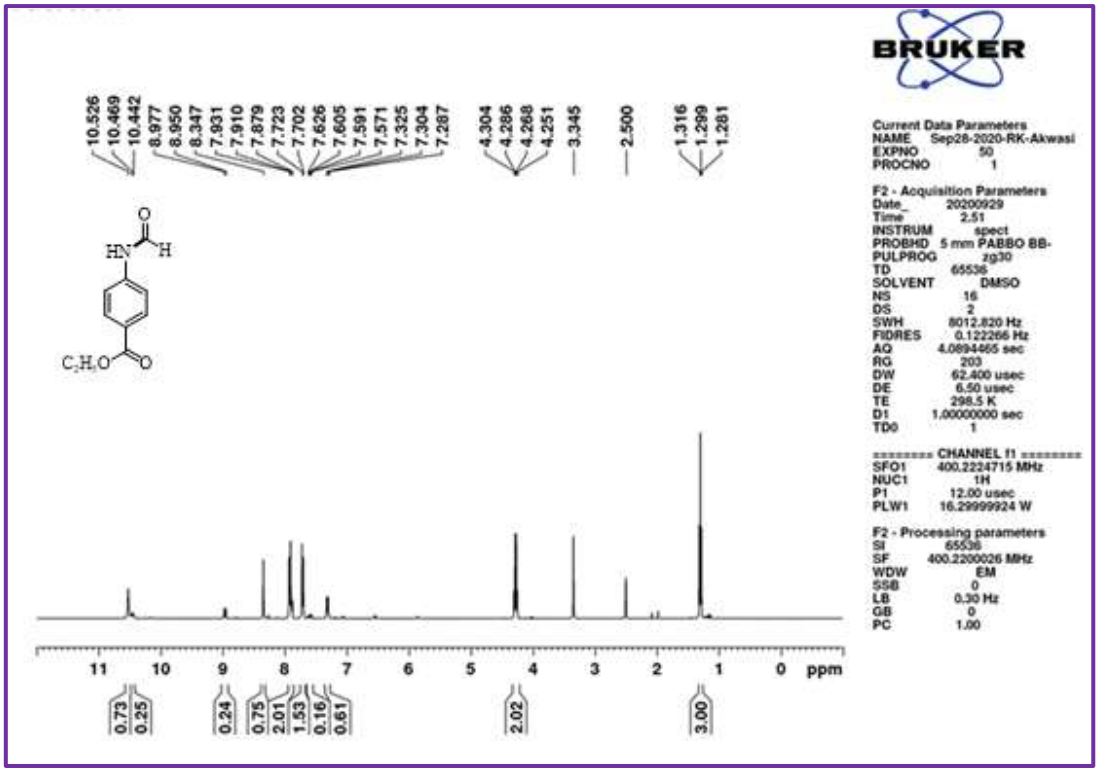

^{1}H NMR spectra of **3t.**

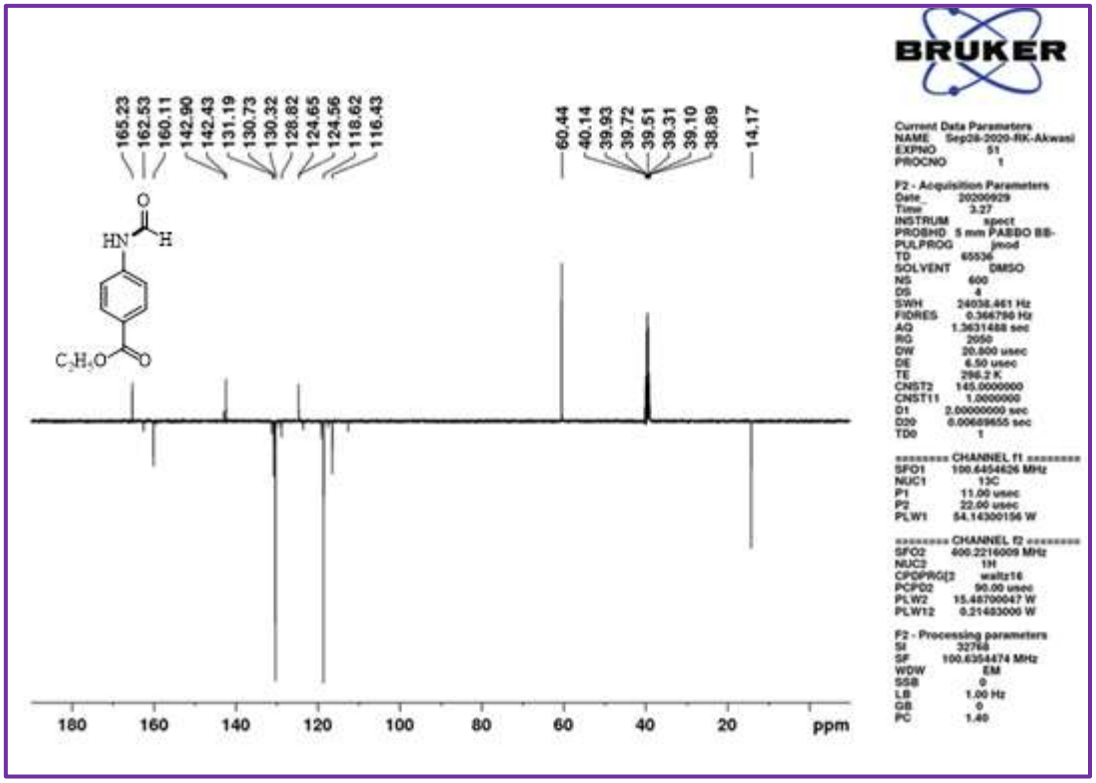

^{13}C NMR spectra of **3t.**

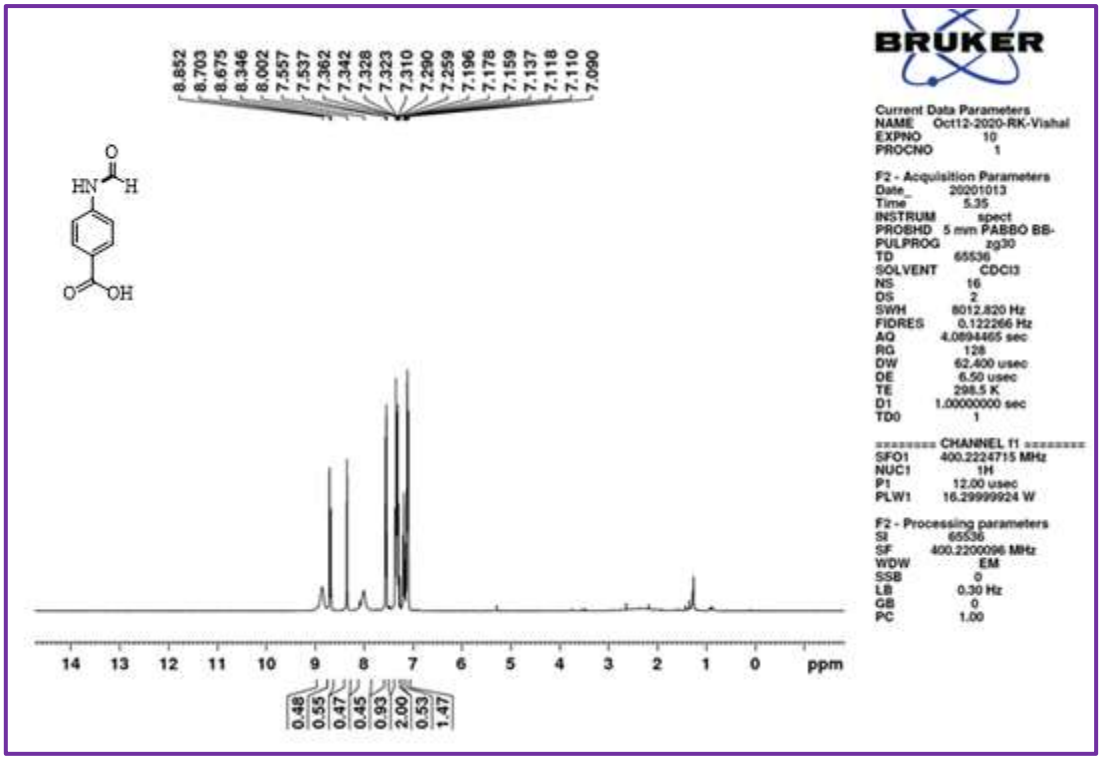

^{1}H NMR spectra of **3u.**

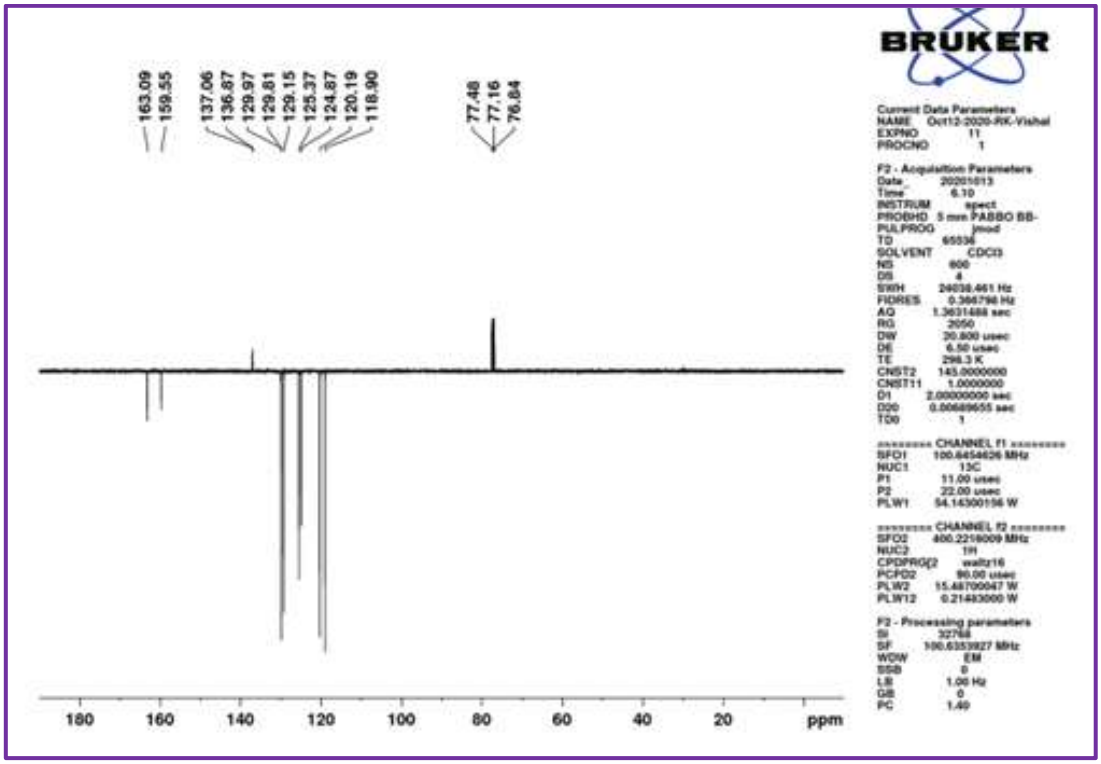

^{13}C NMR spectra of **3u.**

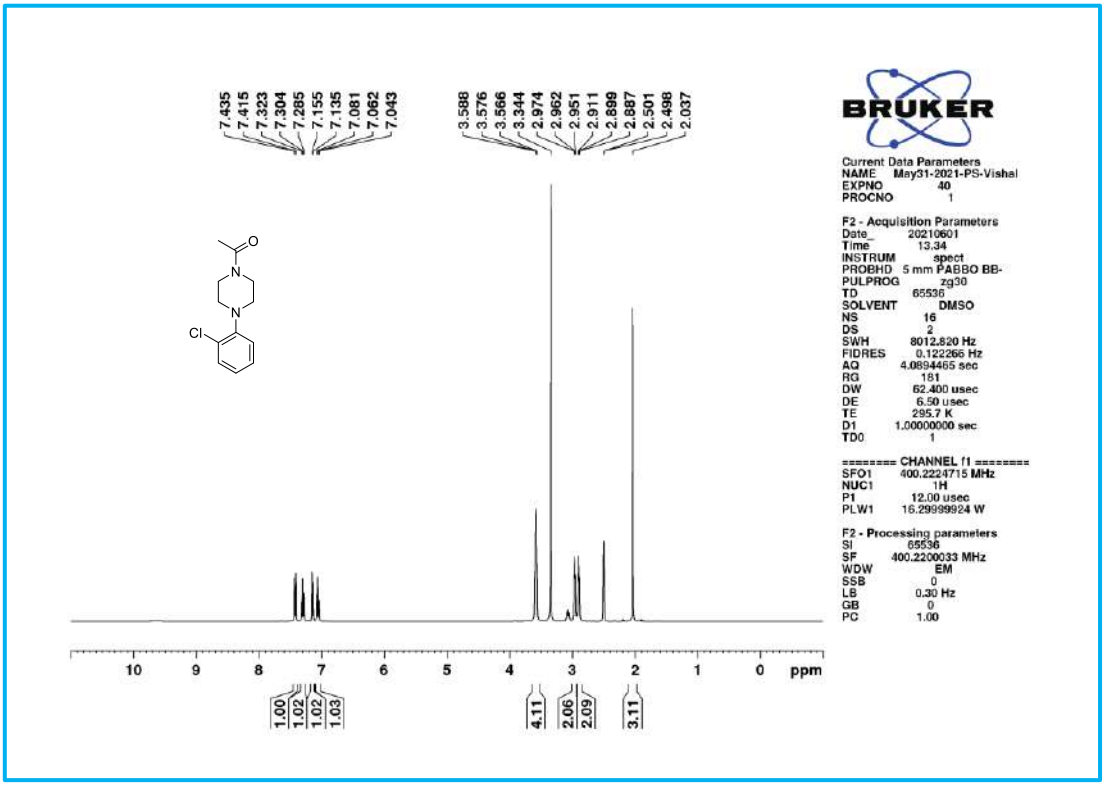

^{1}H NMR spectra of **4a.**

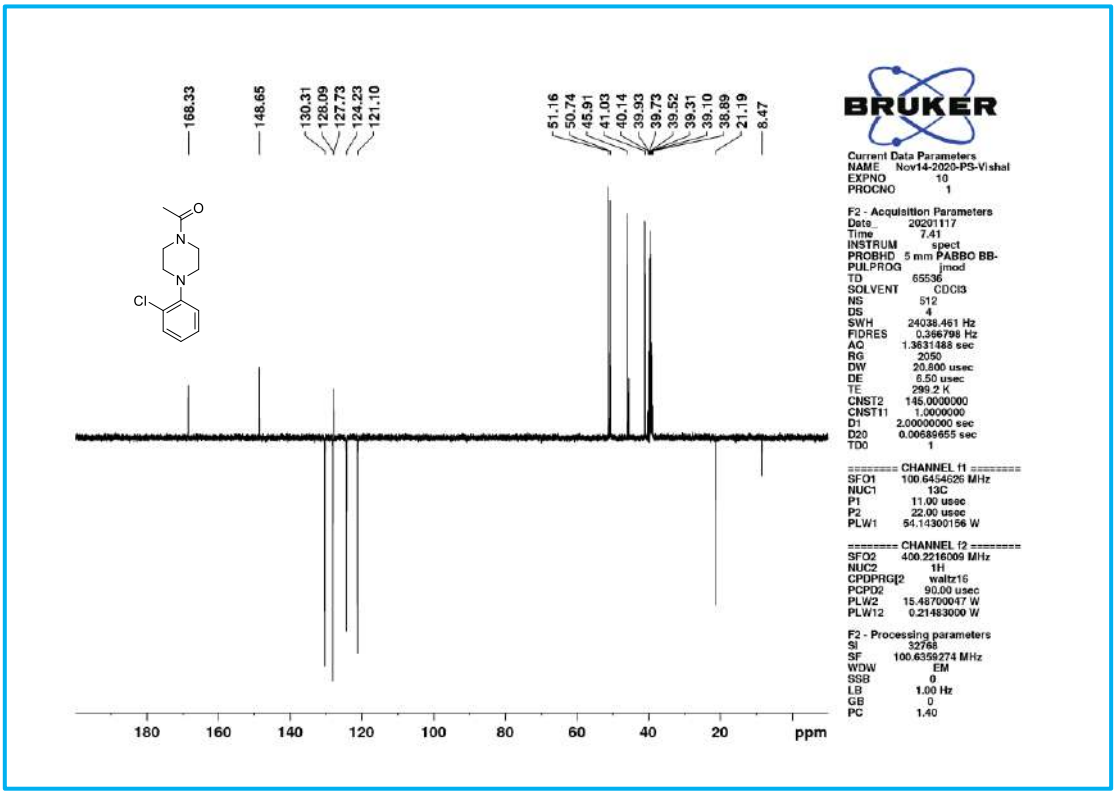

^{13}C NMR spectra of **4a.**

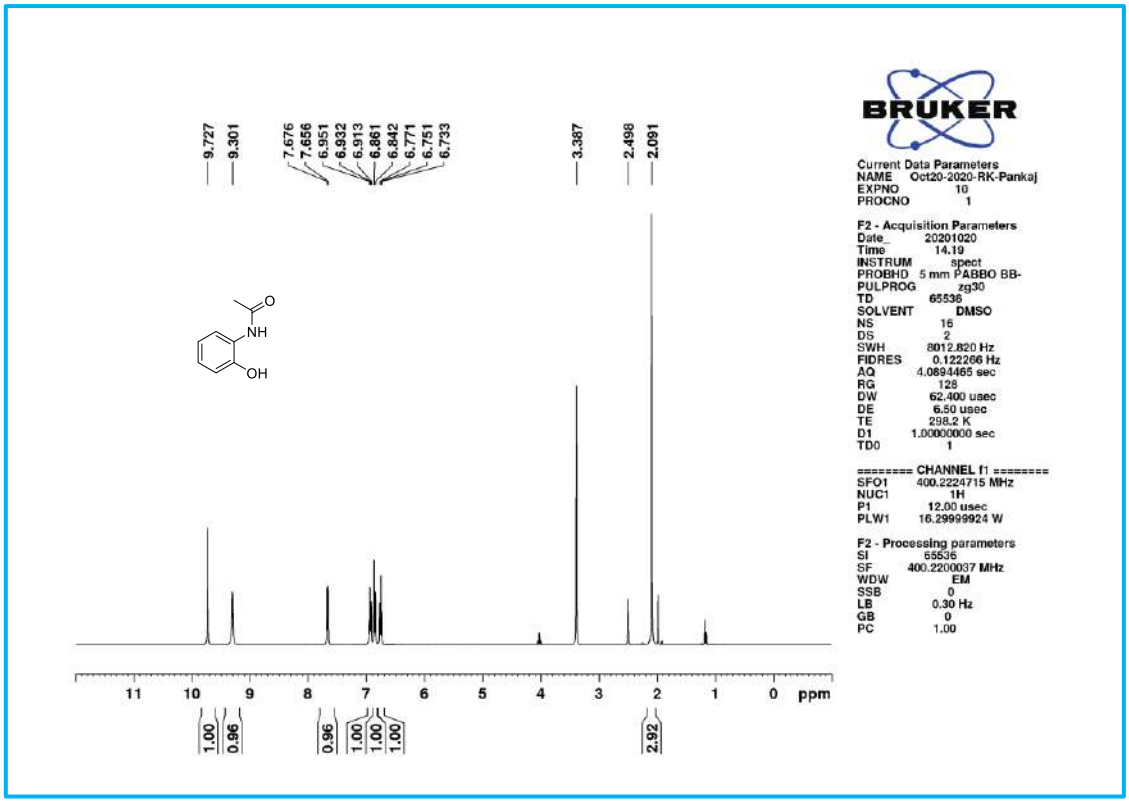

^{1}H NMR spectra of **4b.**

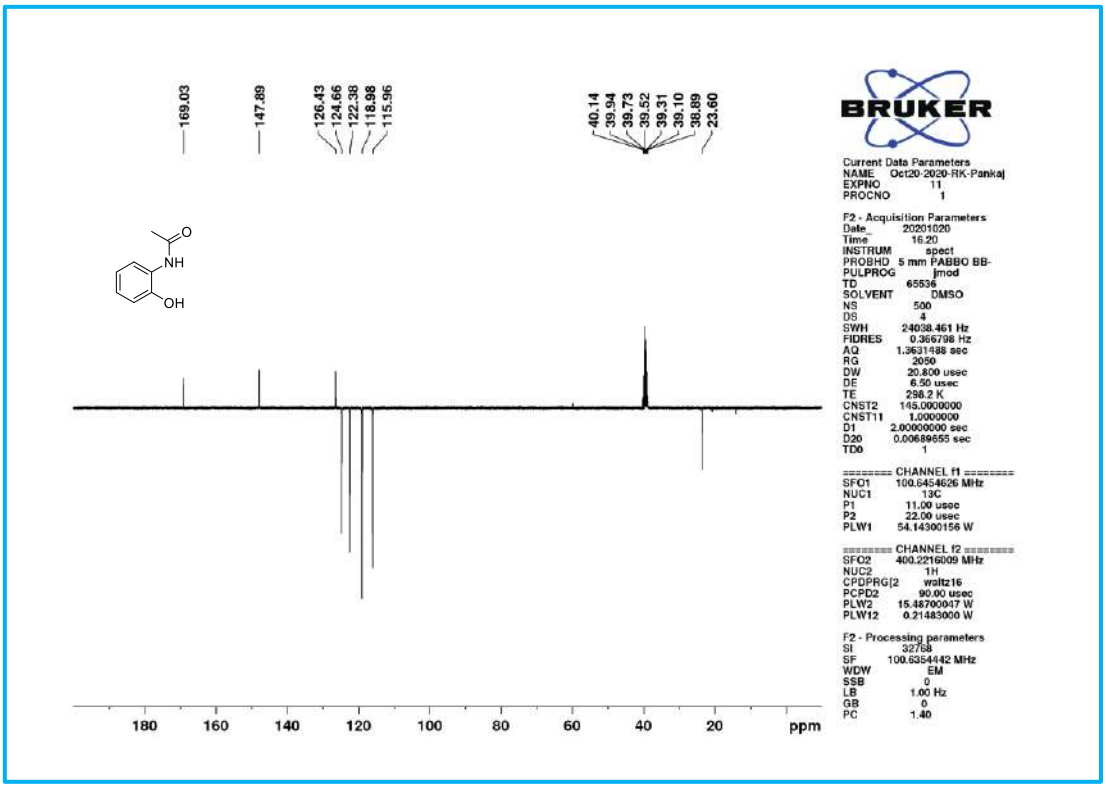

^{13}C NMR spectra of **4b.**

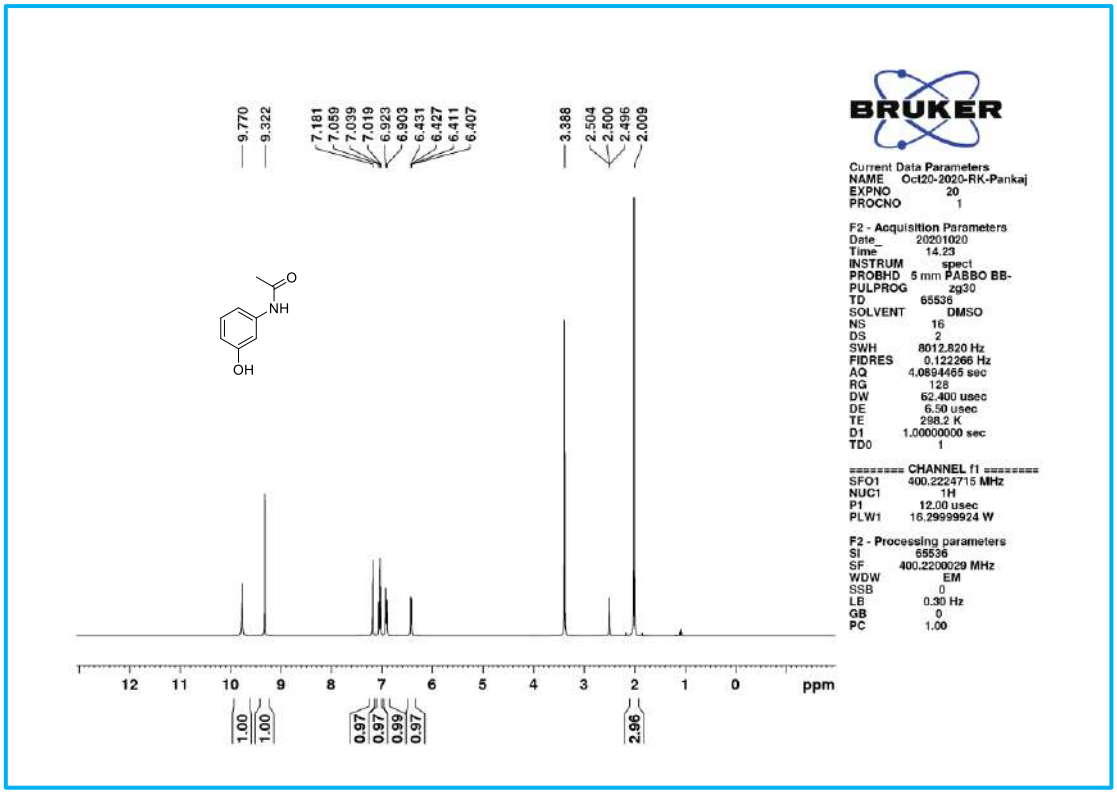

^{1}H NMR spectra of **4c.**

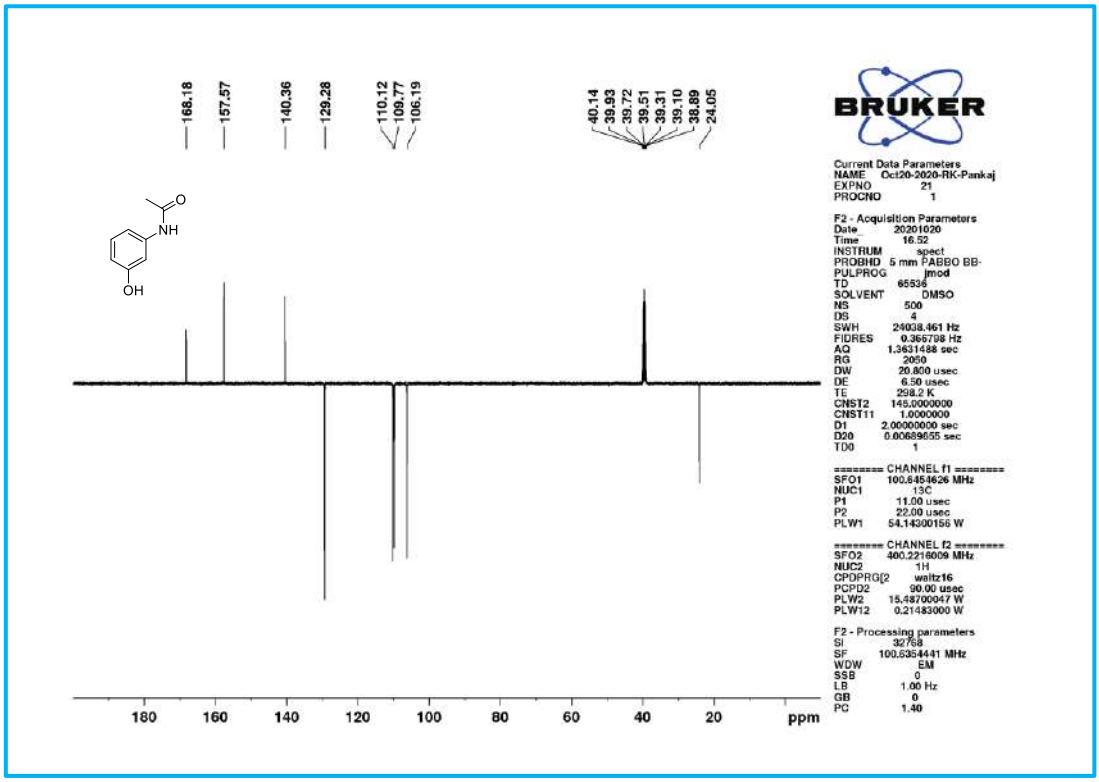

^{13}C NMR spectra of **4c.**

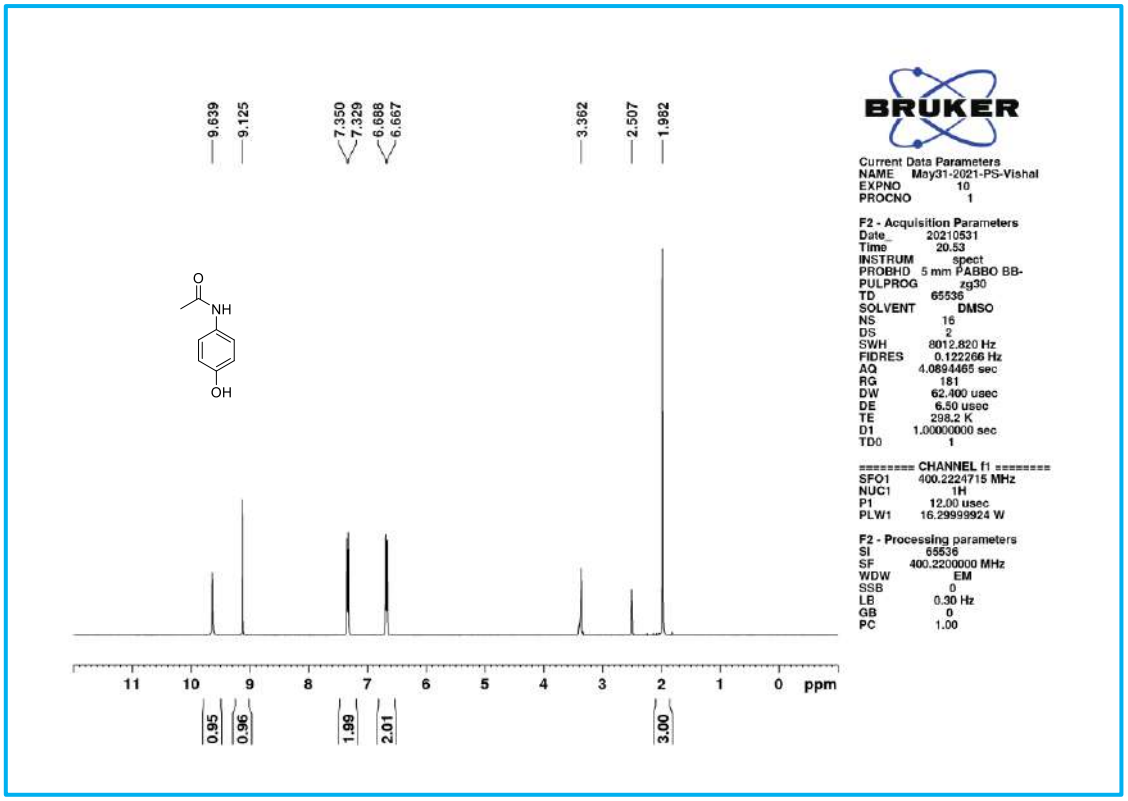

^{1}H NMR spectra of **4d.**

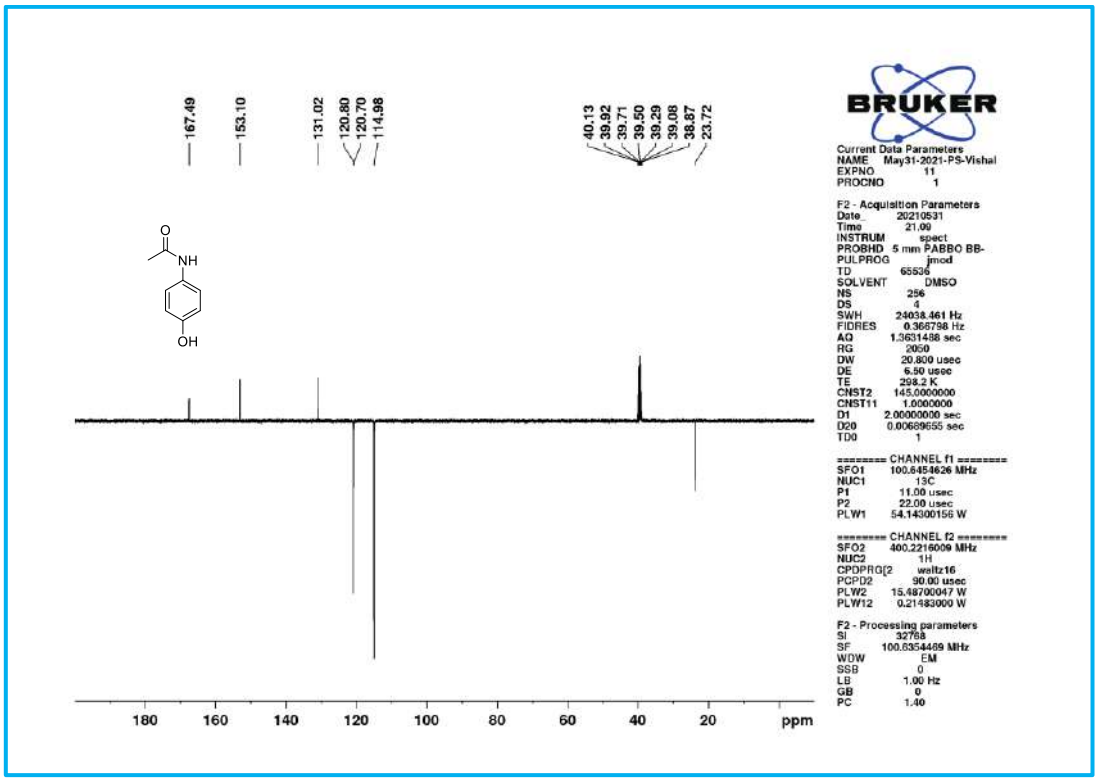

^{13}C NMR spectra of **4d.**

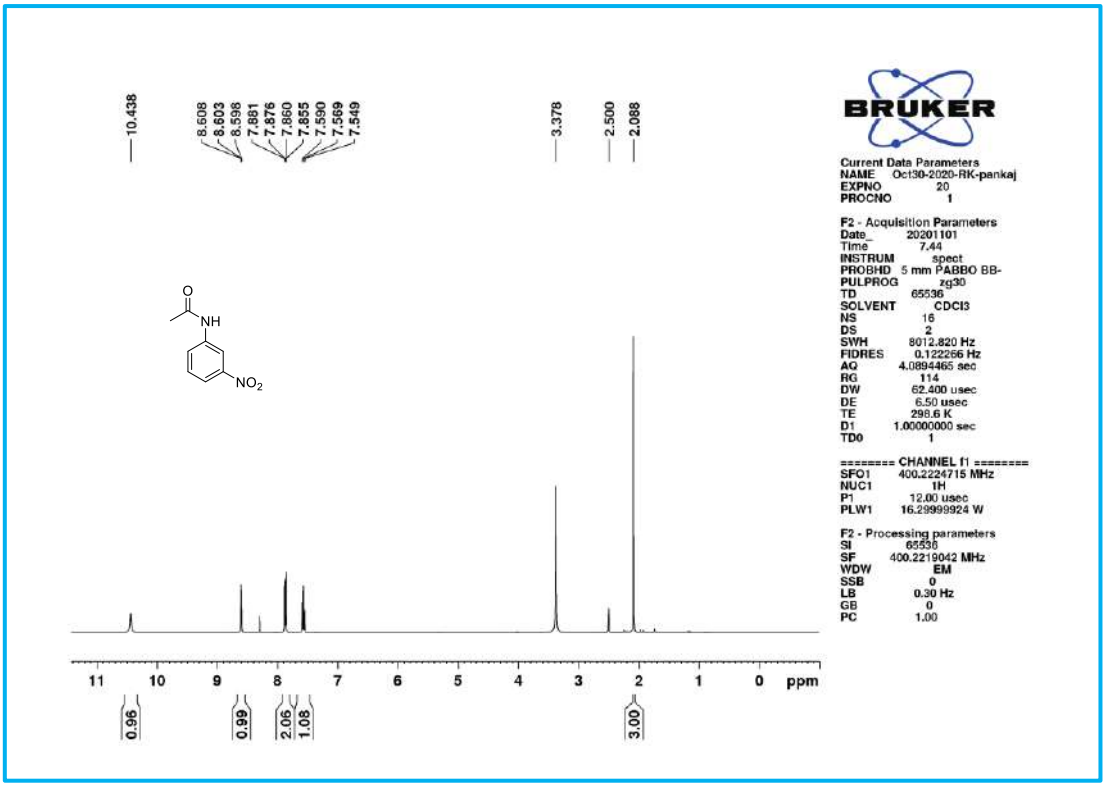

^{1}H NMR spectra of **4e.**

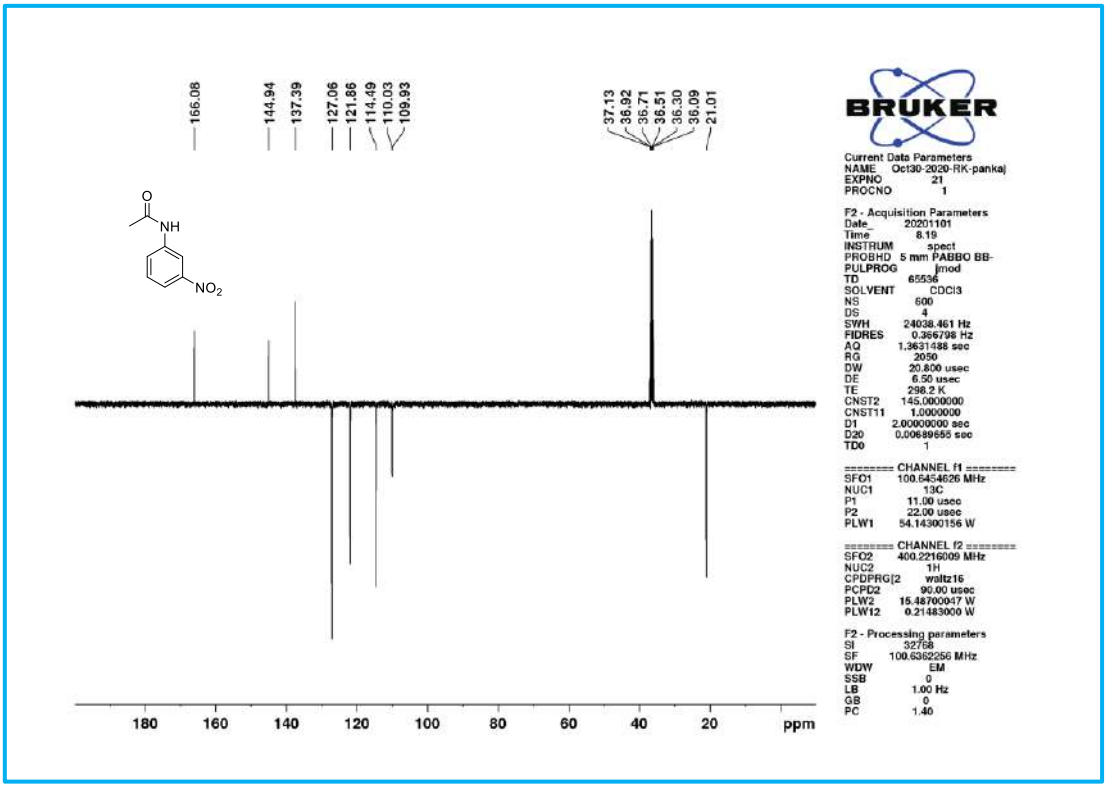

^{13}C NMR spectra of **4e.**

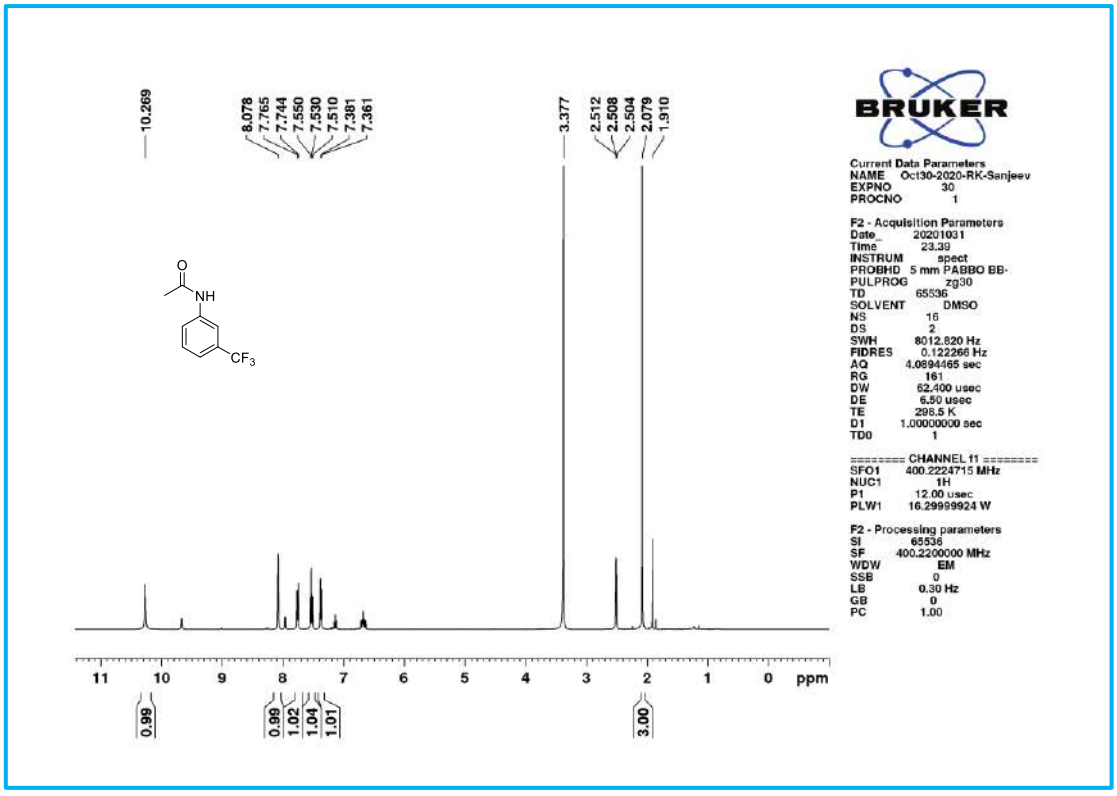

^{1}H NMR spectra of **4f.**

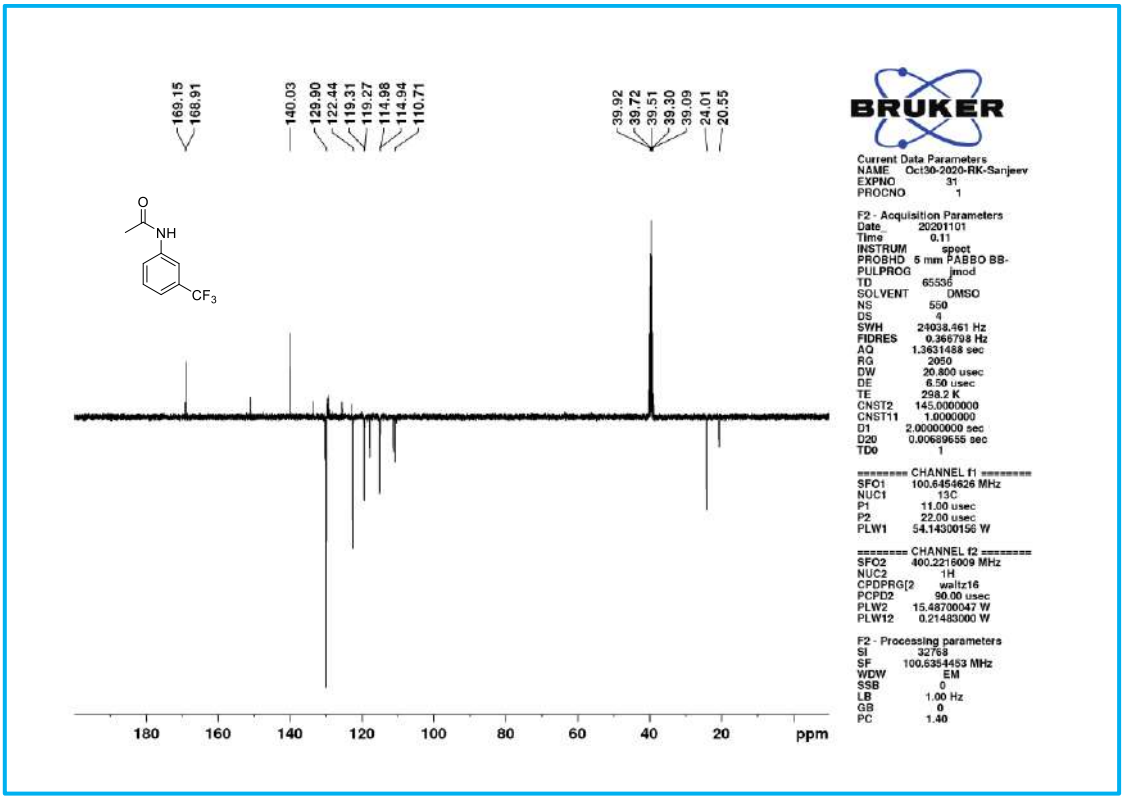

^{13}C NMR spectra of **4f.**

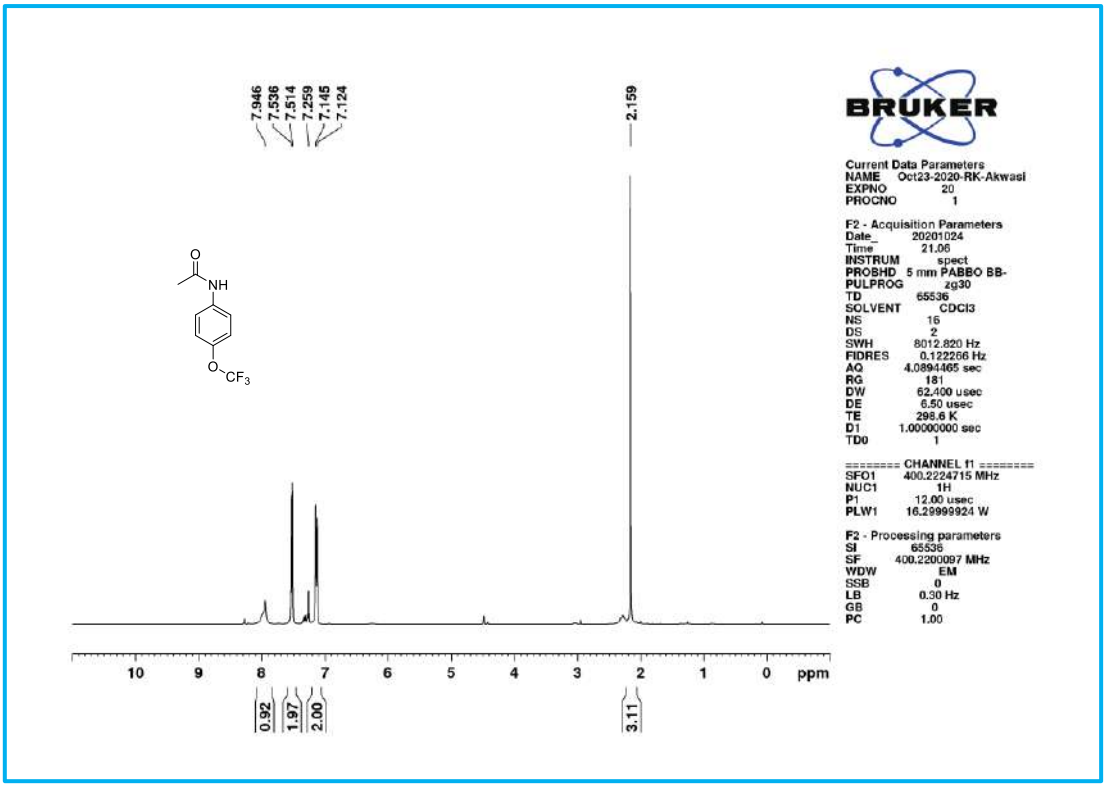

^{1}H NMR spectra of **4g.**

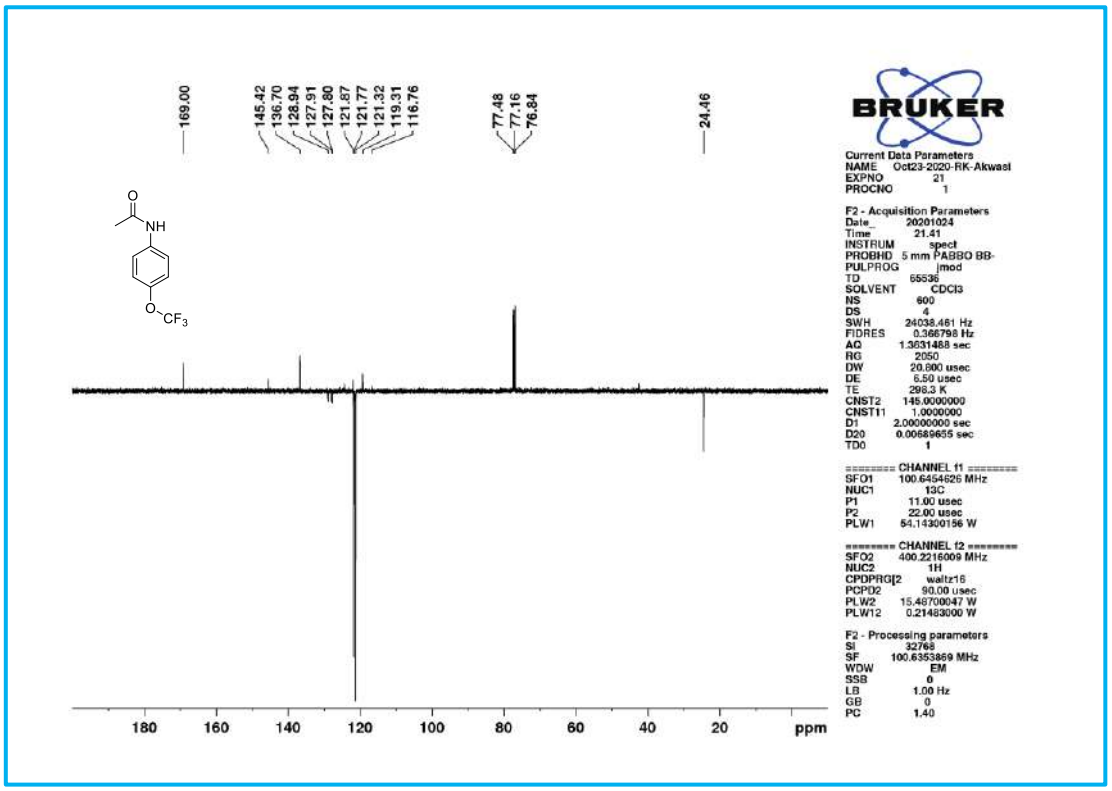

^{13}C NMR spectra of **4g.**

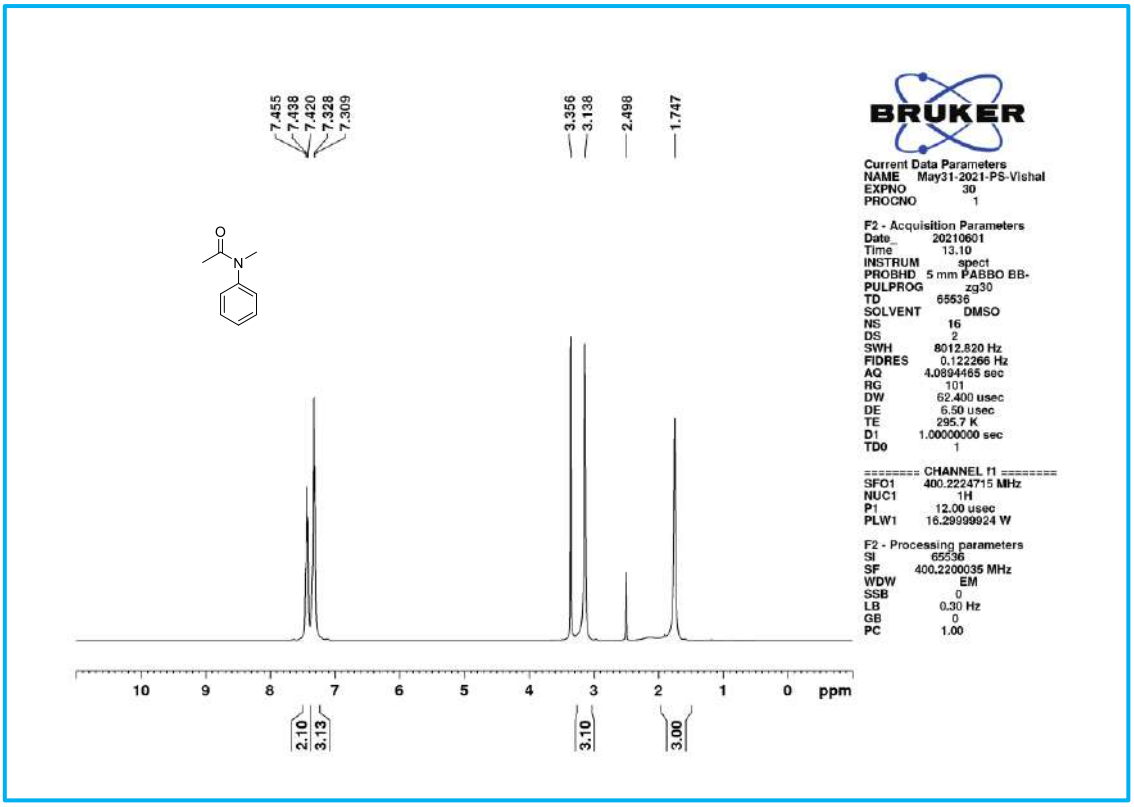

^{1}H NMR spectra of **4h.**

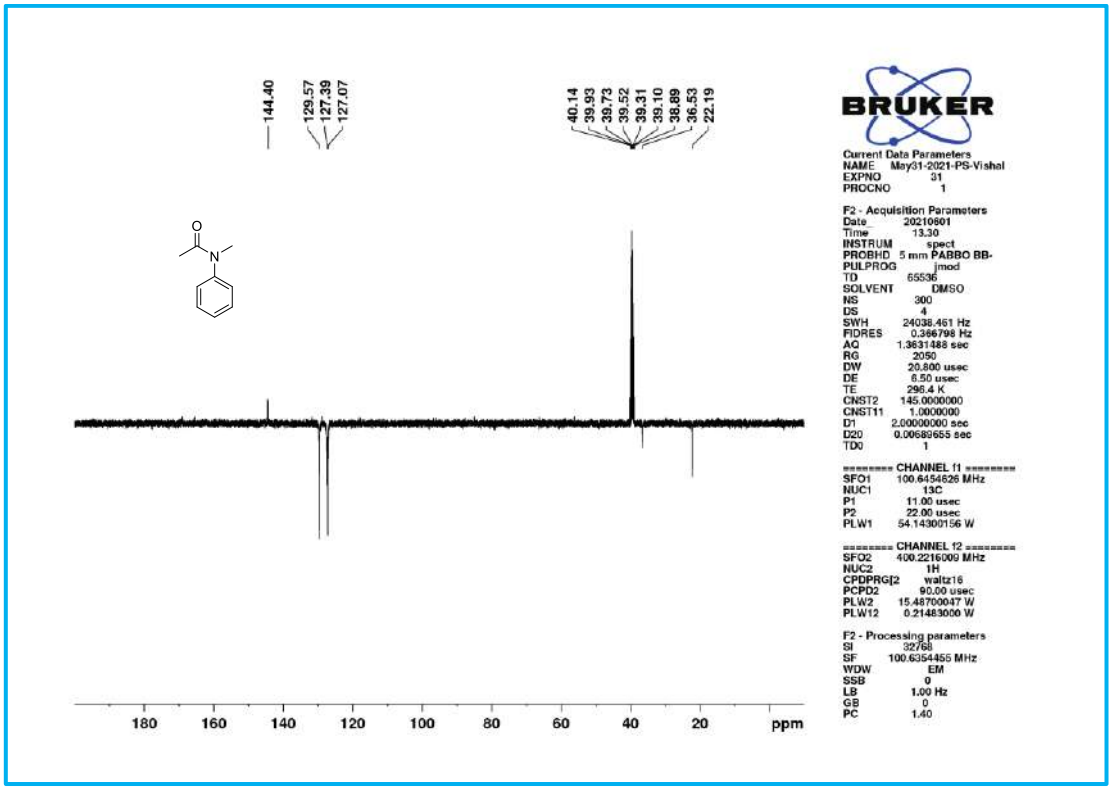

^{13}C NMR spectra of **4h.**

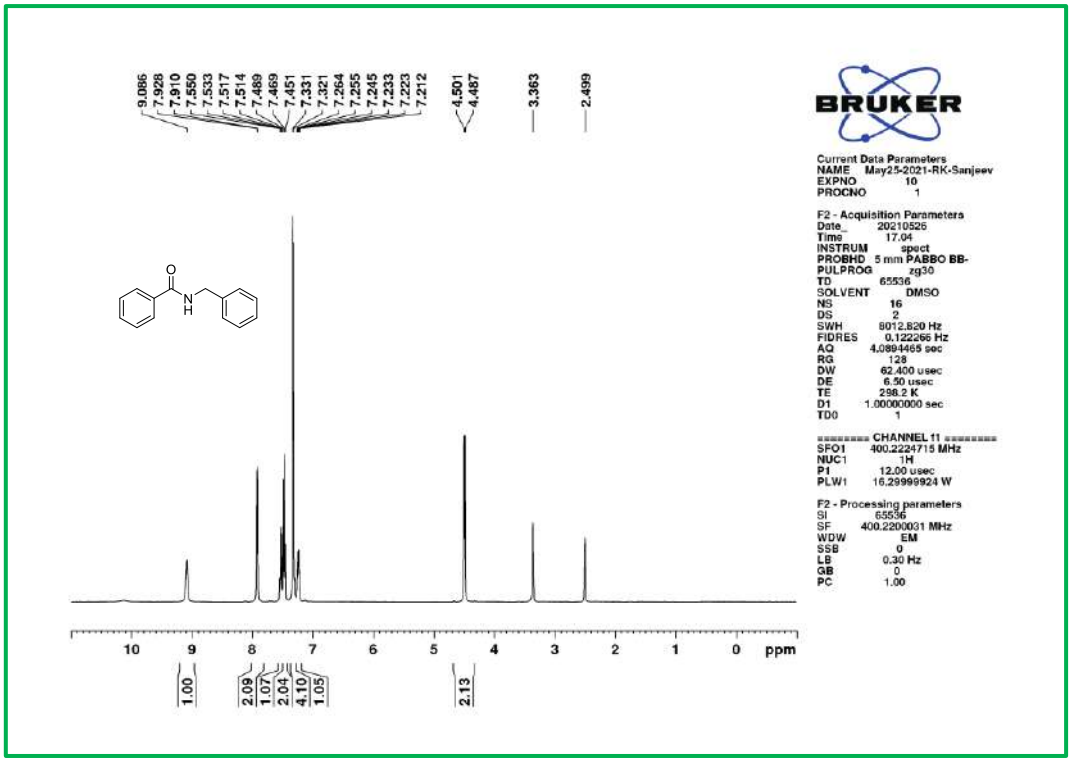

^{1}H NMR spectra of **5a.**

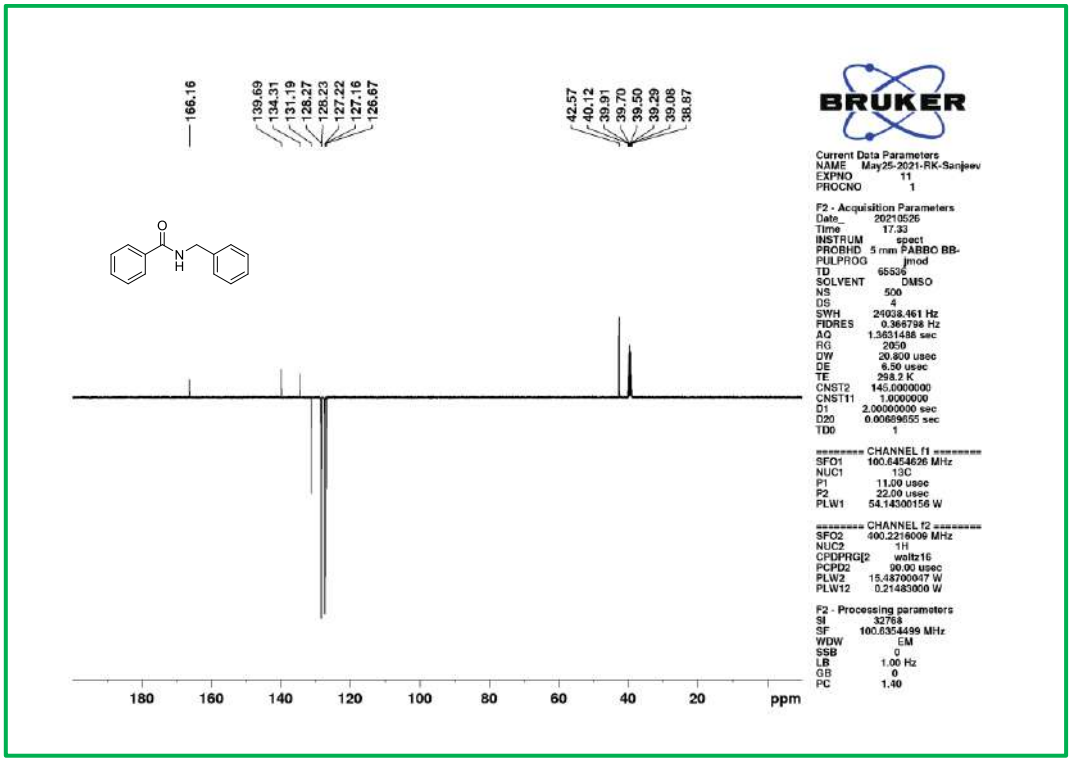

^{13}C NMR spectra of **5a.**

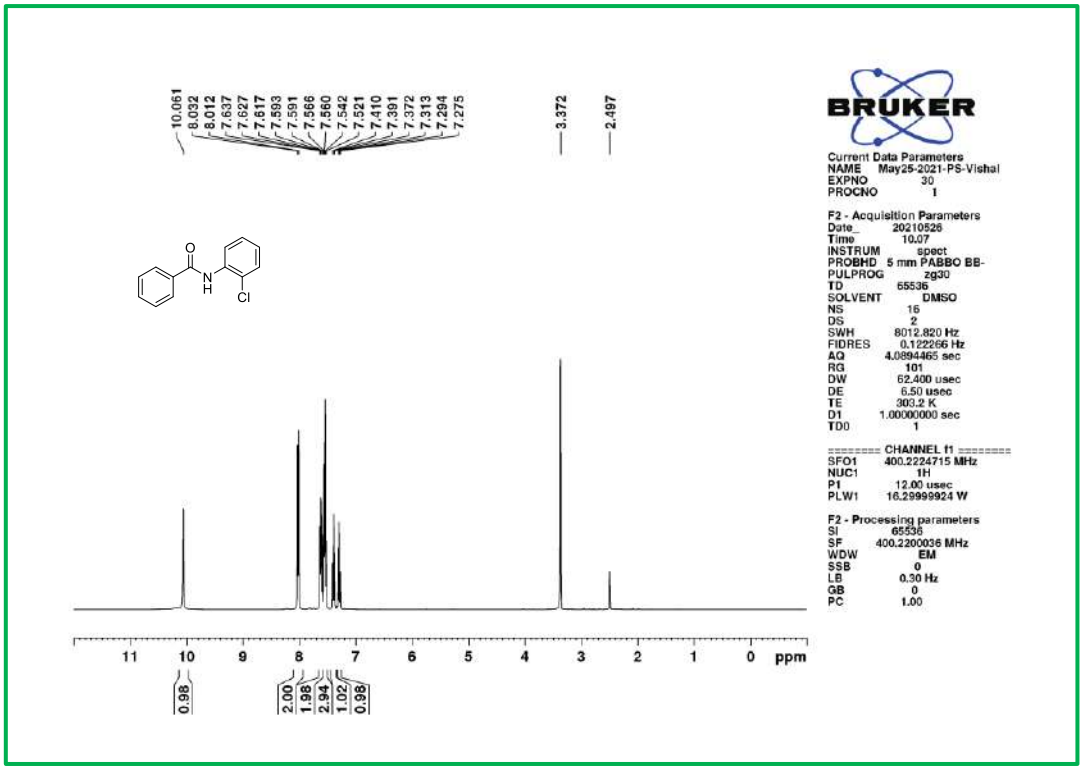

^{1}H NMR spectra of **5b.**

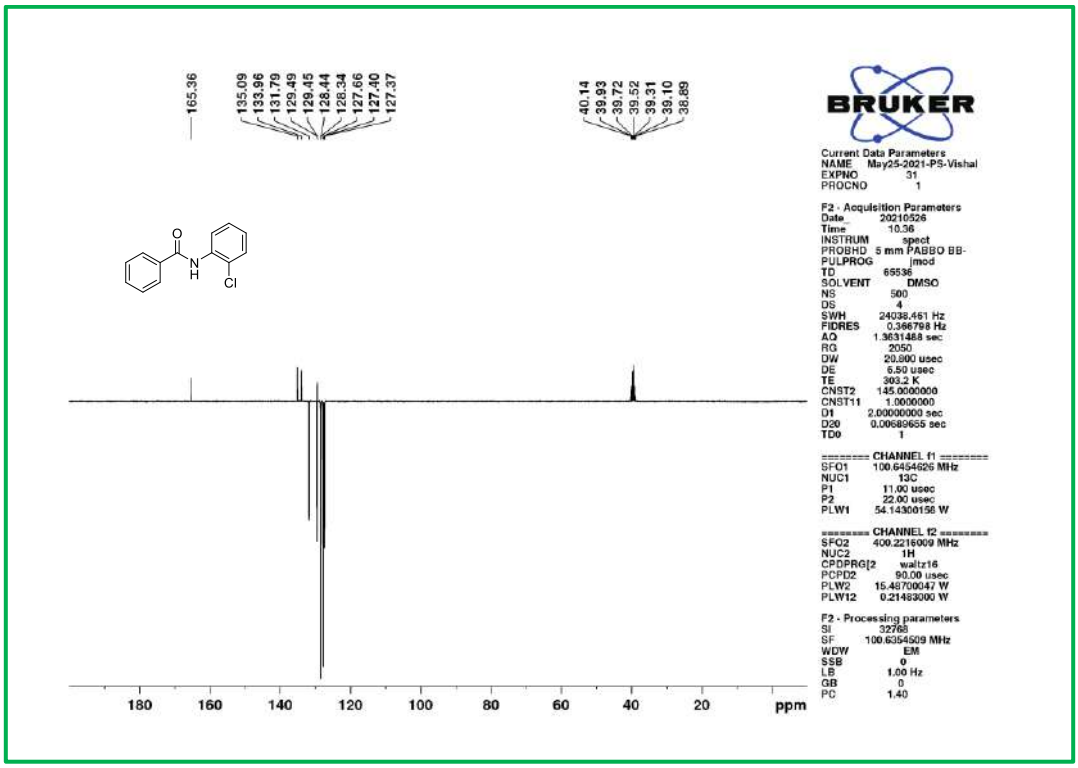

^{13}C NMR spectra of **5b.**

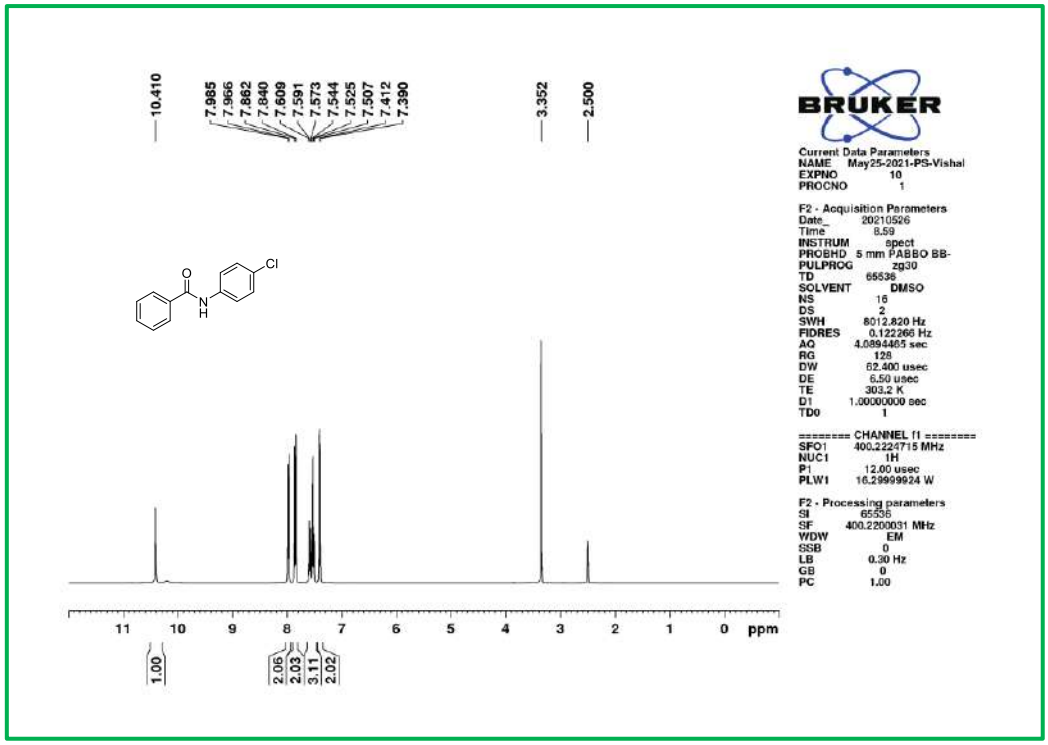

^{1}H NMR spectra of **5c.**

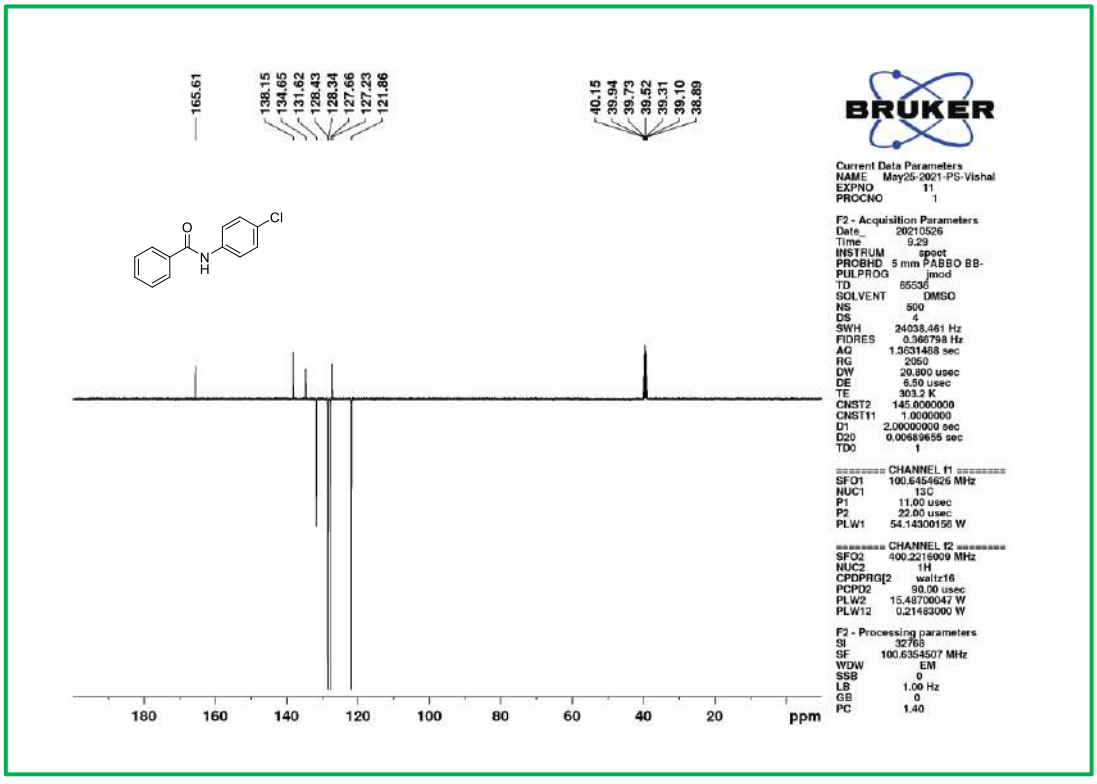

^{13}C NMR spectra of **5c.**

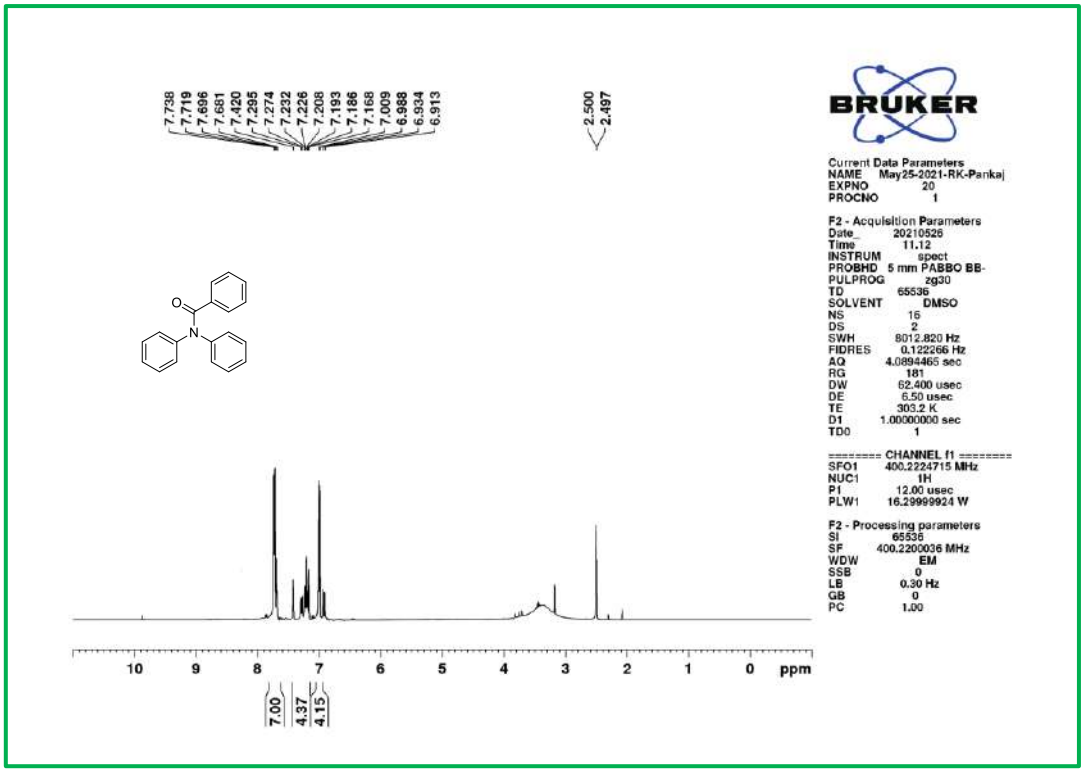

^{1}H NMR spectra of **5d.**

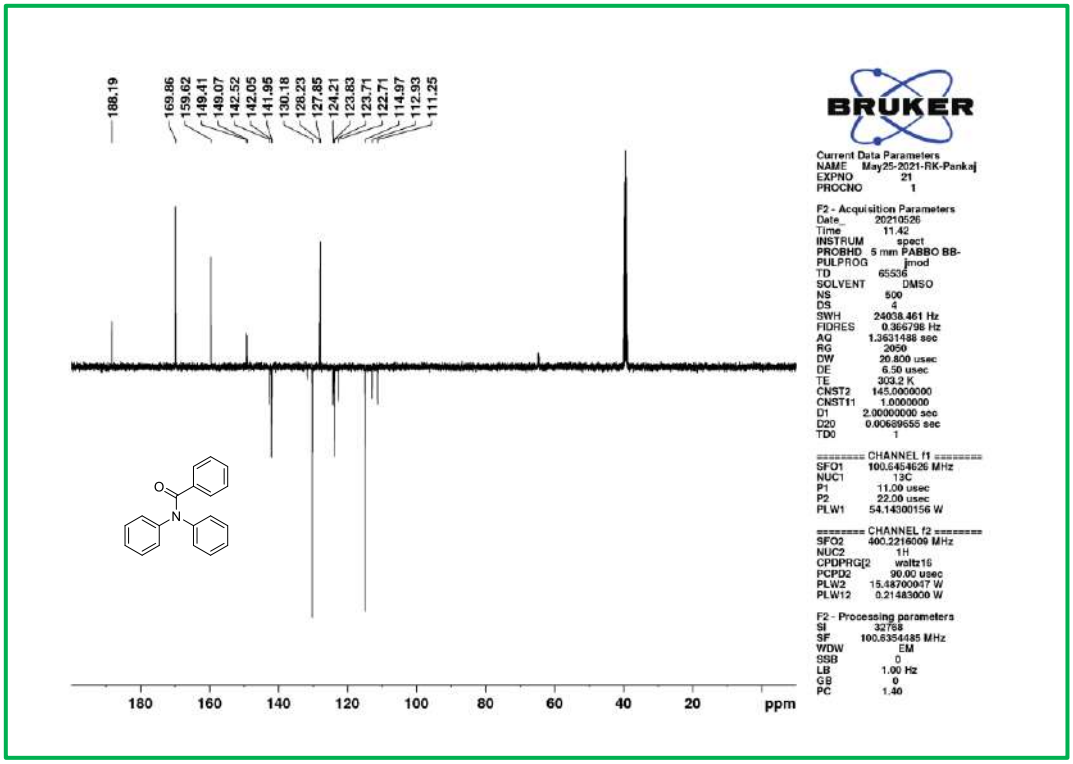

^{13}C NMR spectra of **5d.**

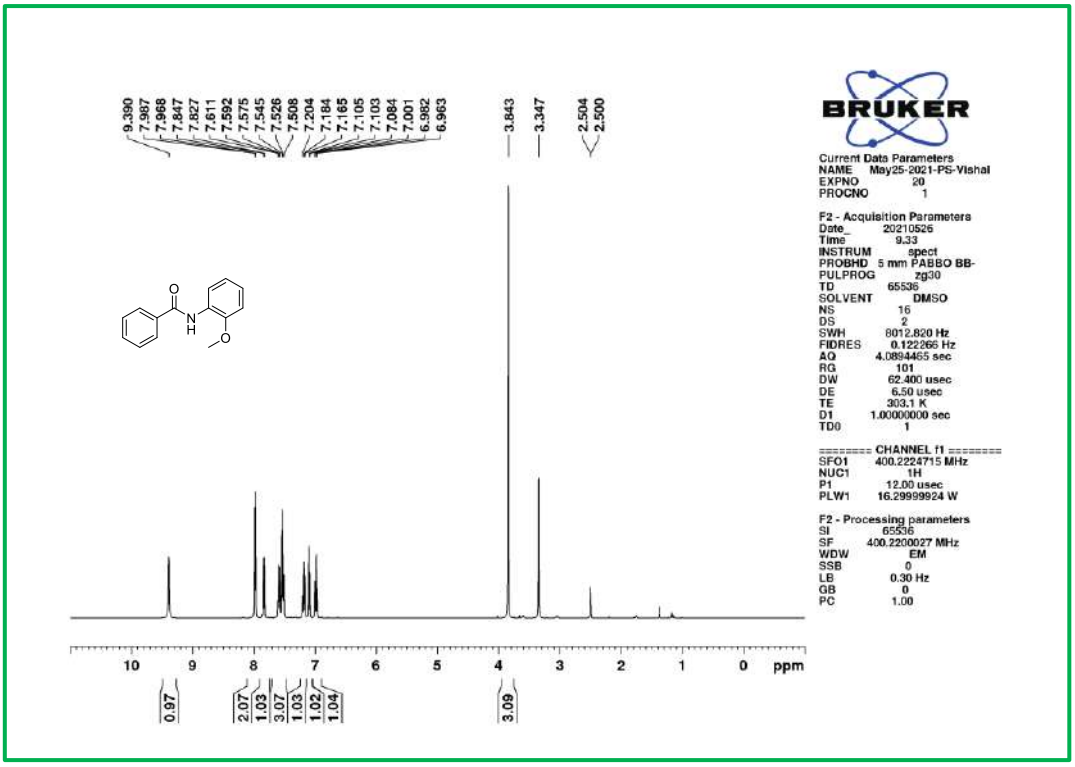

^{1}H NMR spectra of **5e.**

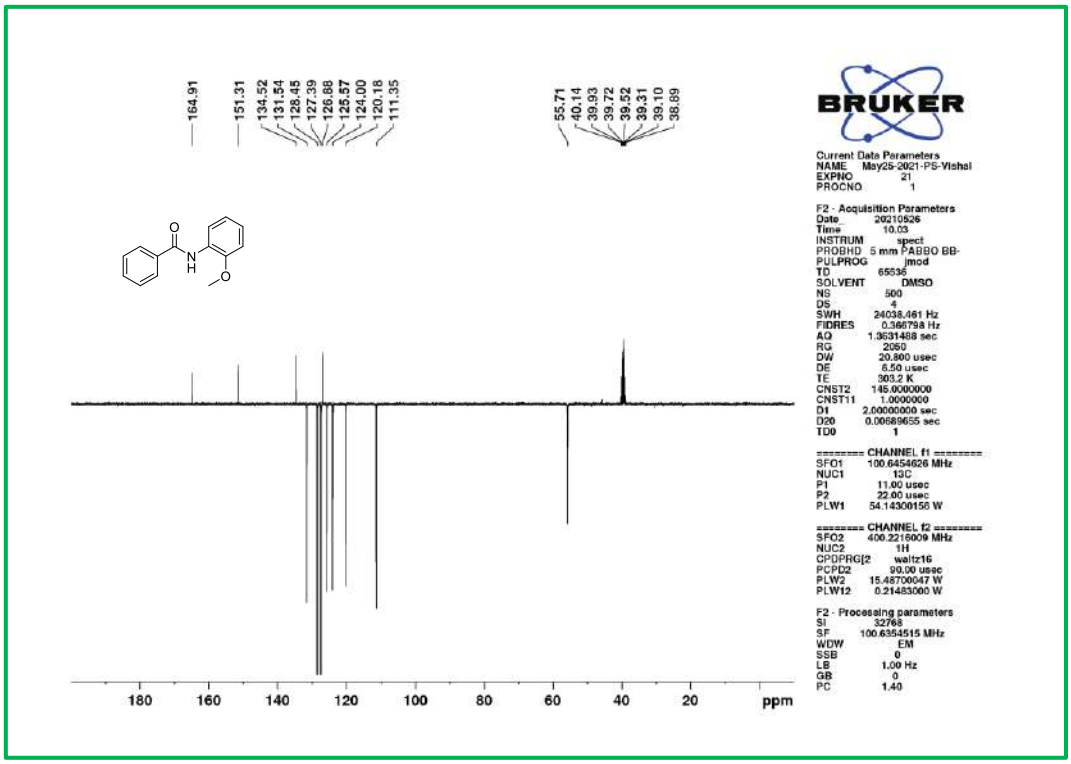

^{13}C NMR spectra of **5e.**

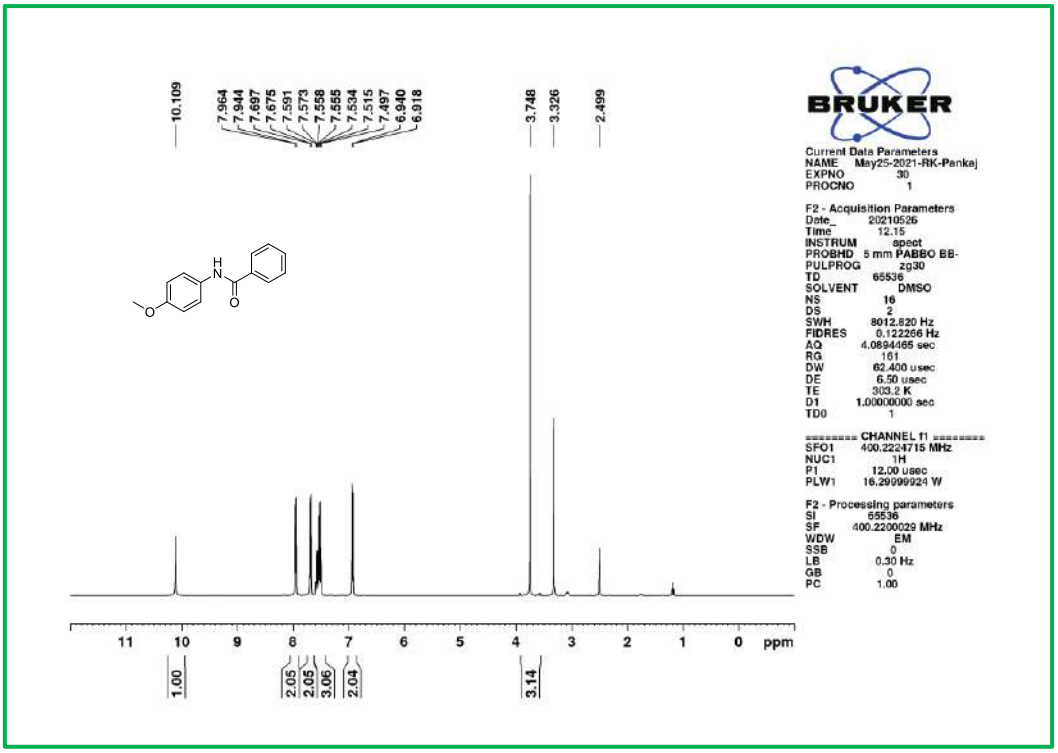

^{1}H NMR spectra of **5f.**

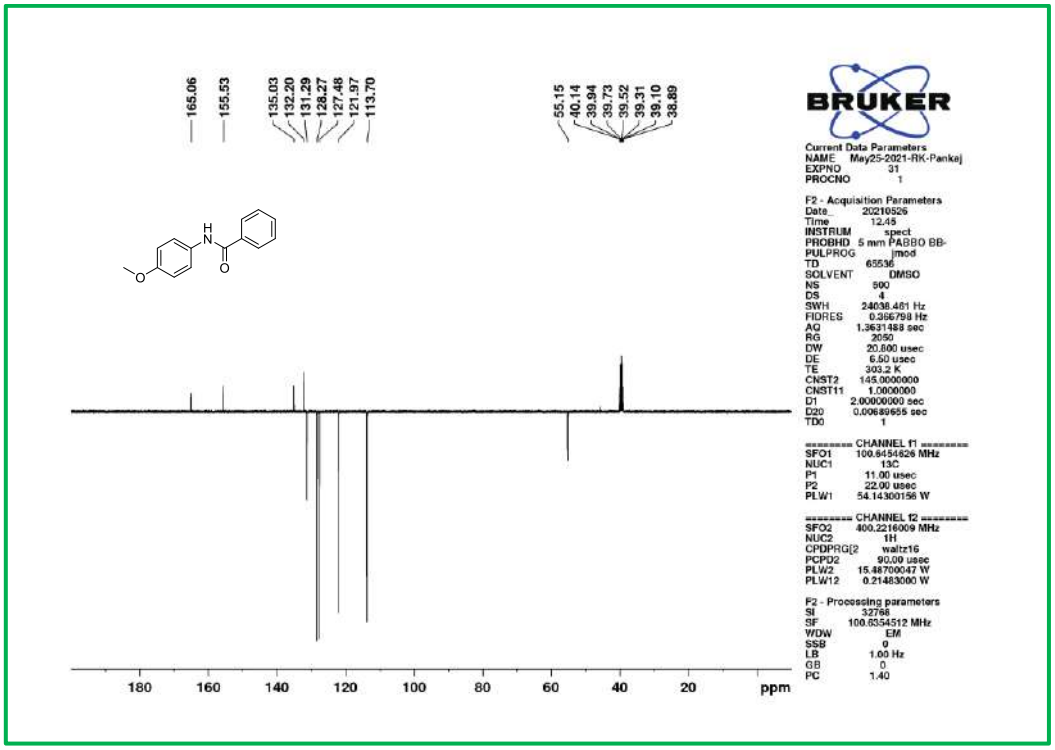

^{13}C NMR spectra of **5f.**

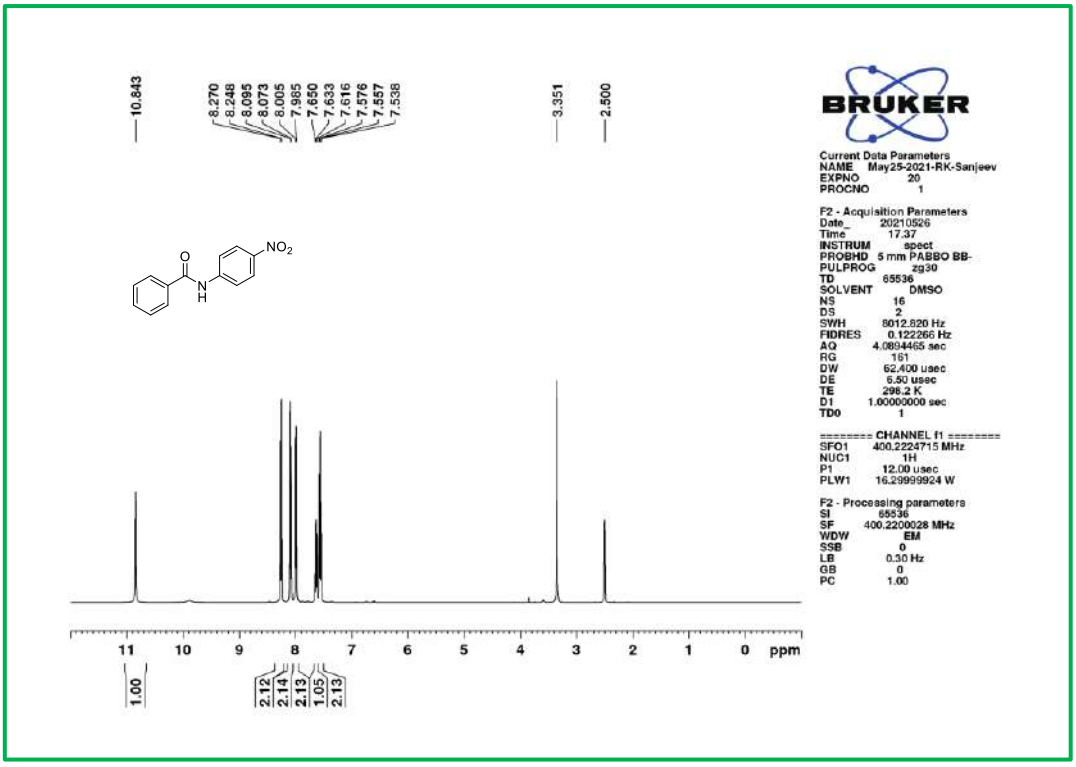

^{1}H NMR spectra of **5g.**

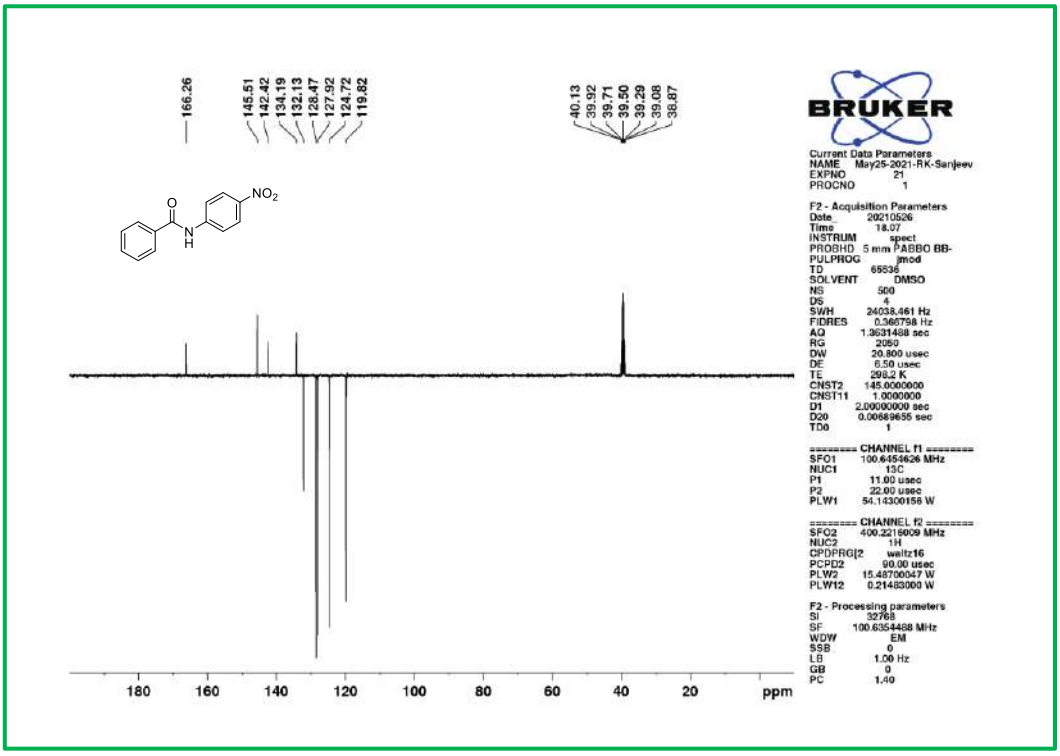

^{13}C NMR spectra of **5g.**

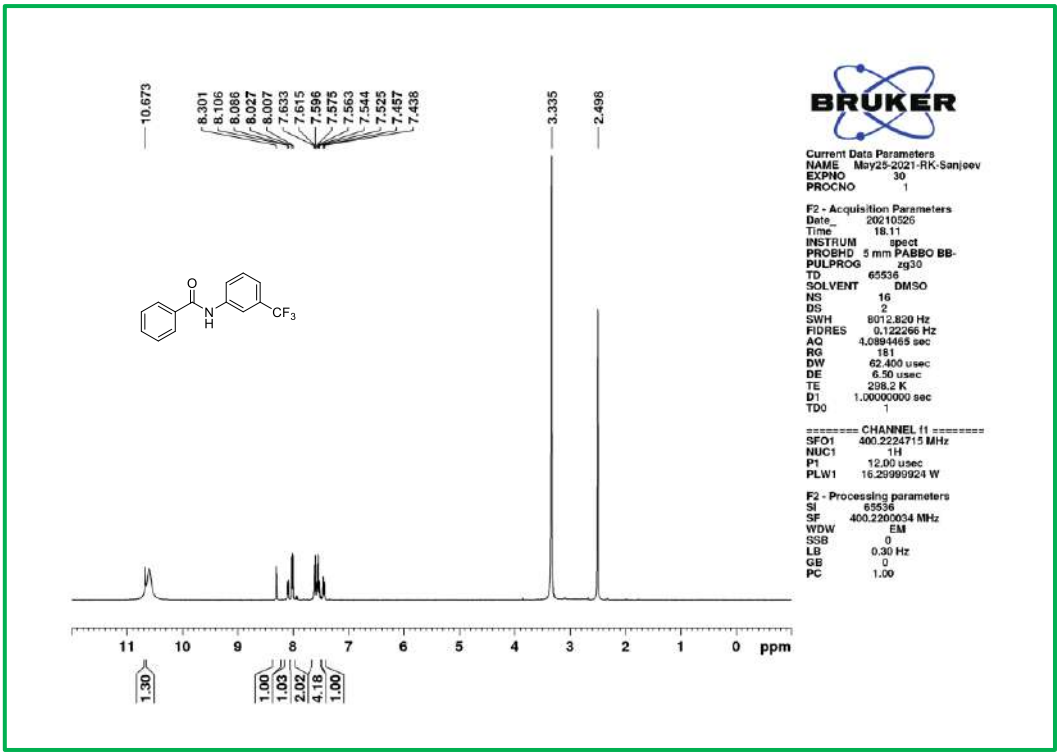

^{1}H NMR spectra of **5h.**

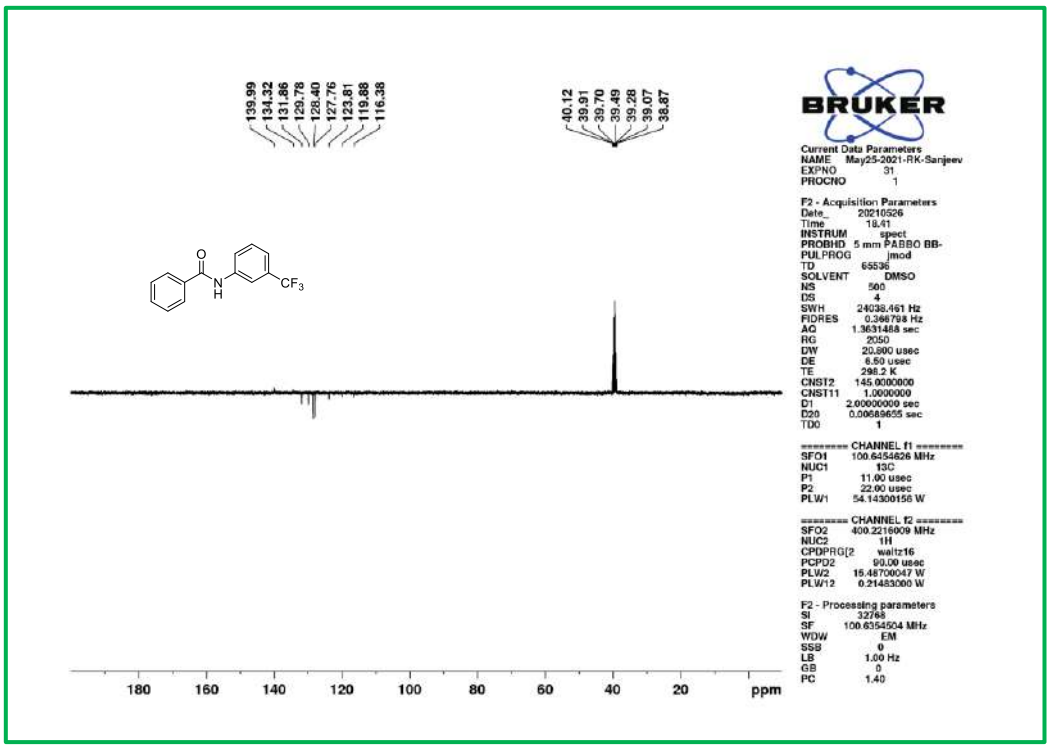

^{13}C NMR spectra of **5h.**

APPENDIX-II

SUPPLEMENTARY INFORMATION

CHAPTER 4

Metal-free direct annulation of 2-aminophenols and 2-aminothiophenols with unactivated amides through transamidation: Access to polysubstituted benzoxazole and benzothiazole derivatives

Published in Tetrahedron Journal

^{1}H and ^{13}C NMR Spectra

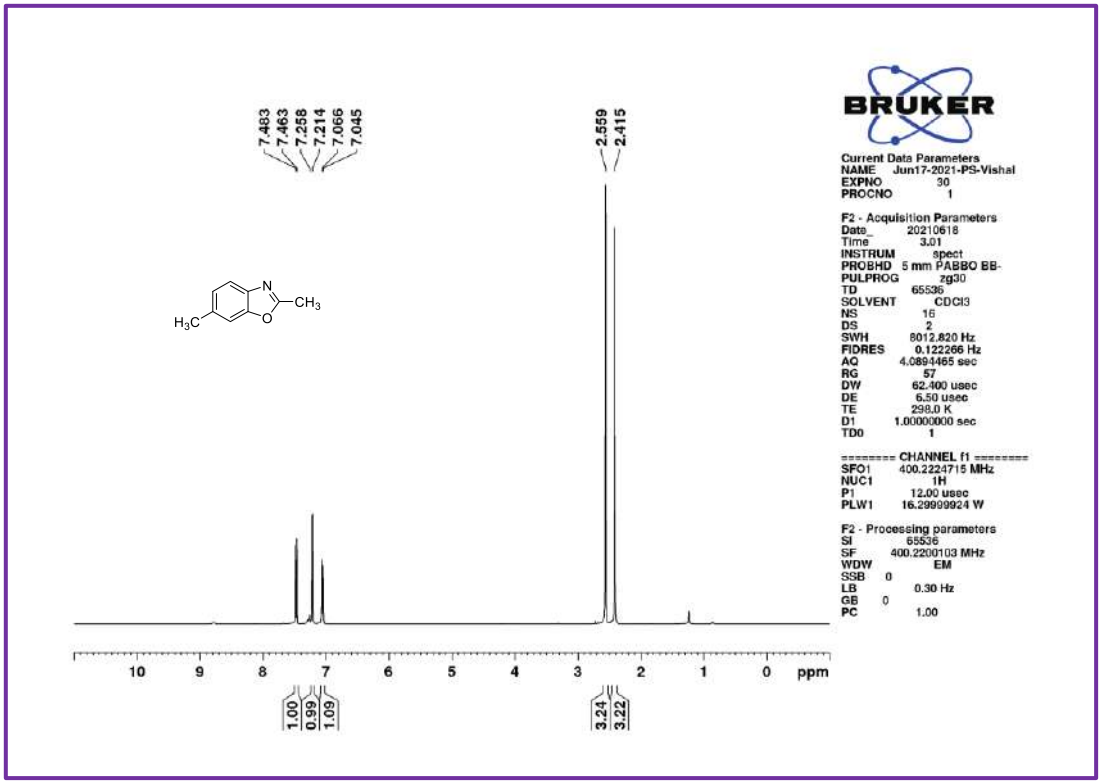

^{1}H NMR spectra of **3a**.

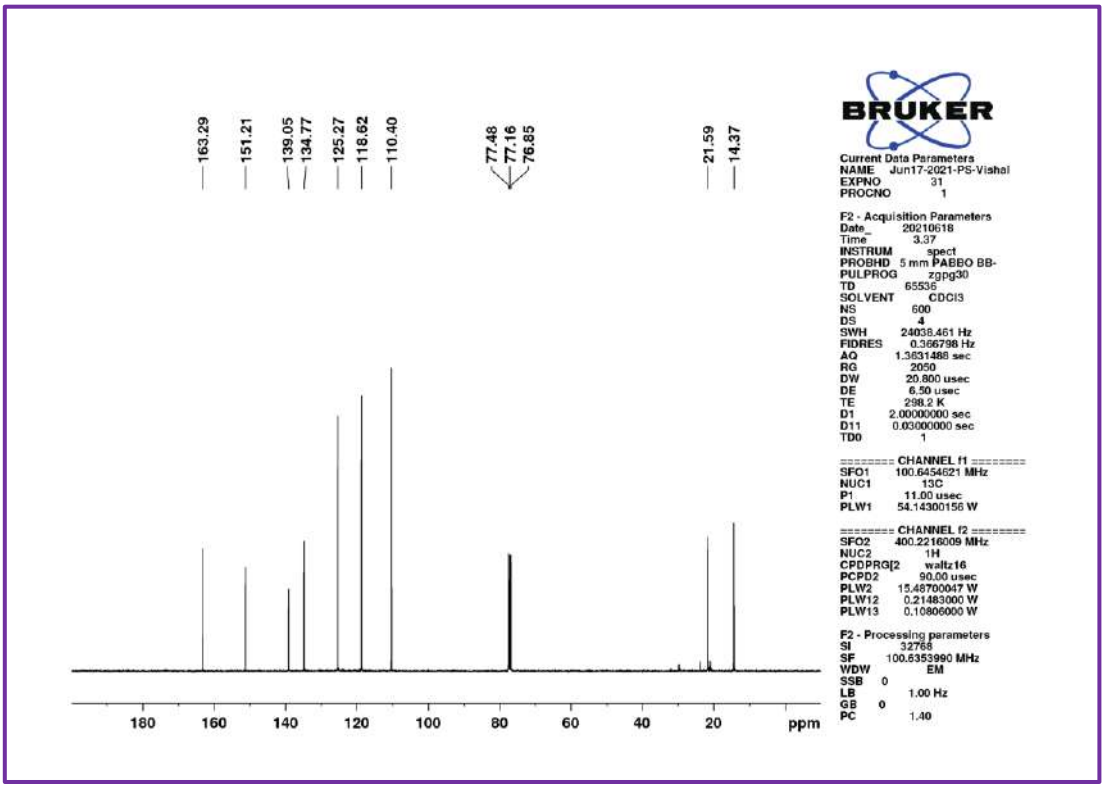

^{13}C NMR spectra of **3a.**

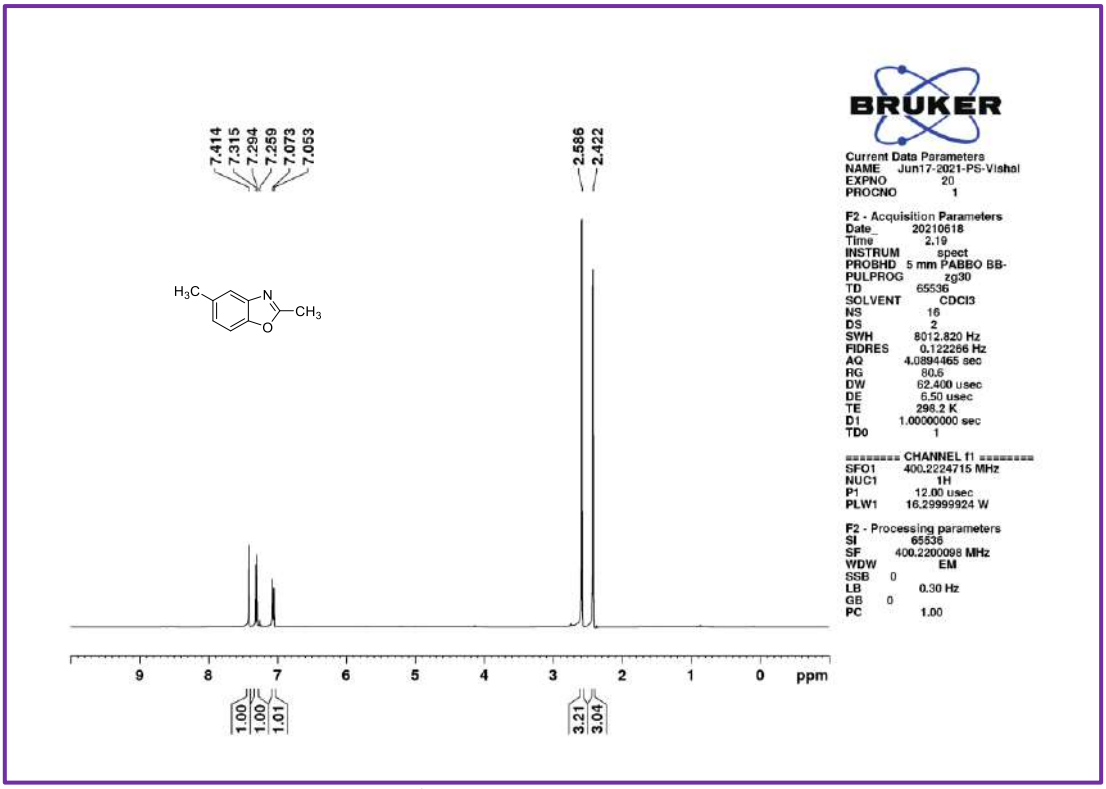

^{1}H NMR spectra of **3b**.

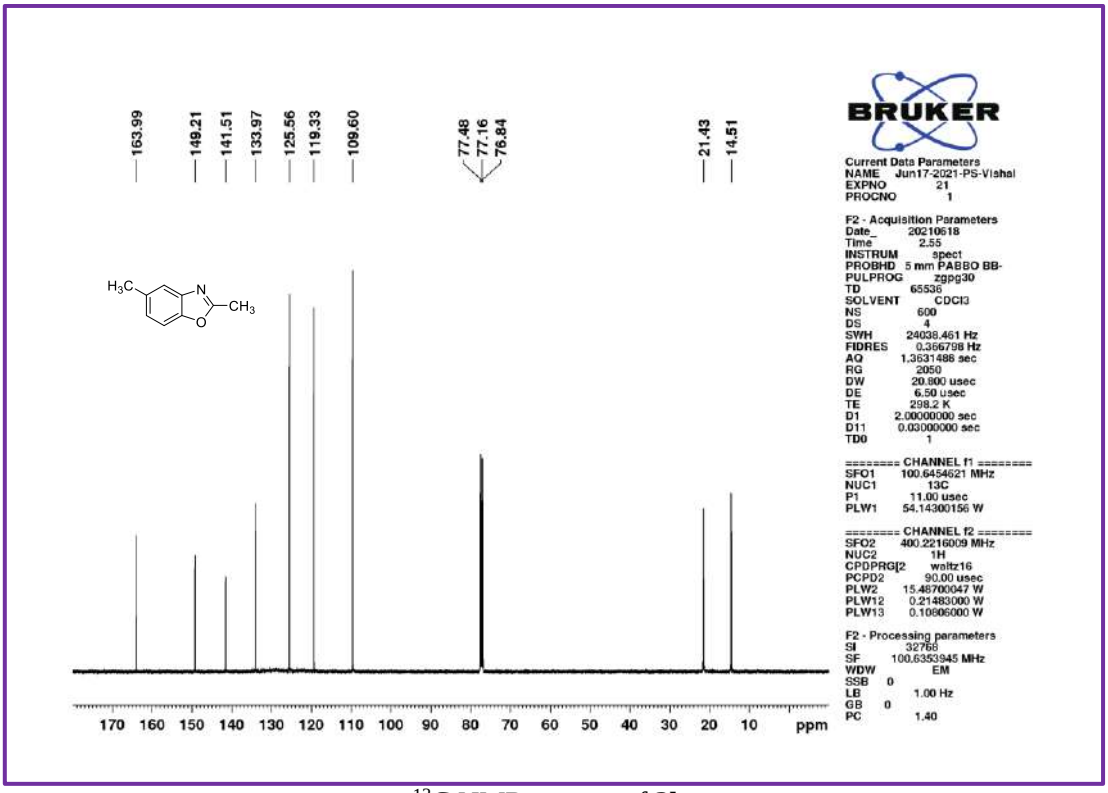

^{13}C NMR spectra of **3b.**

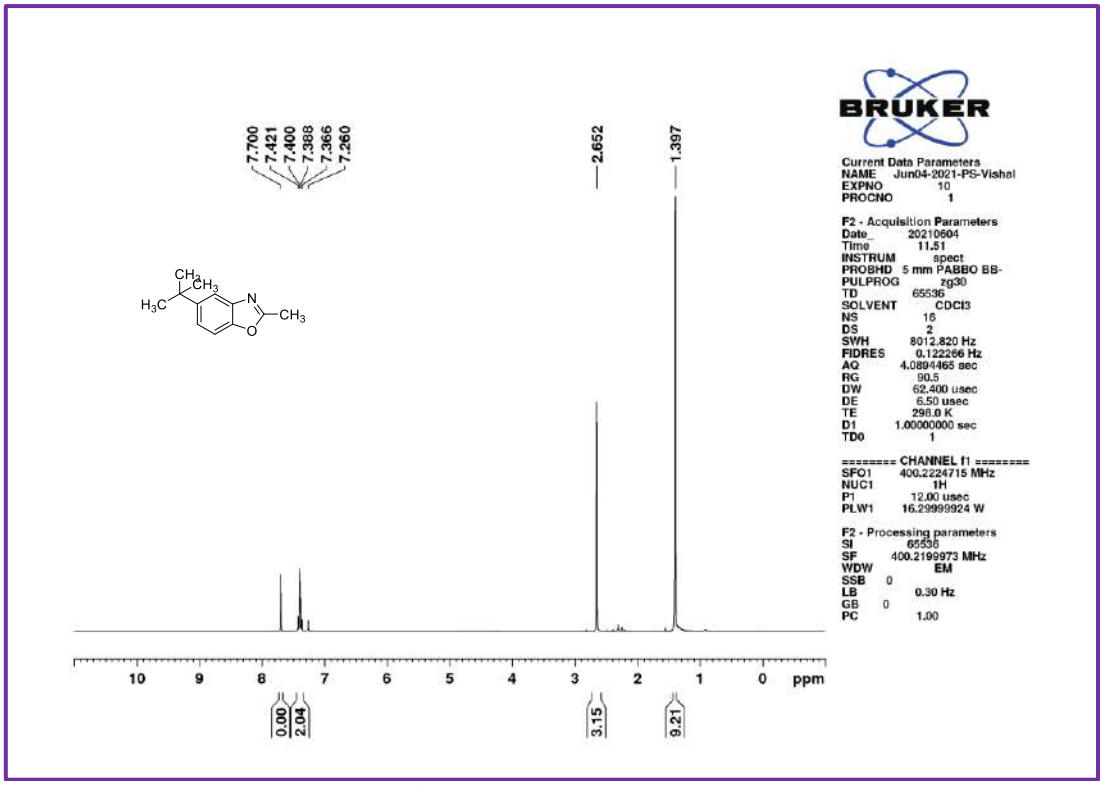

^{1}H NMR spectra of **3c**.

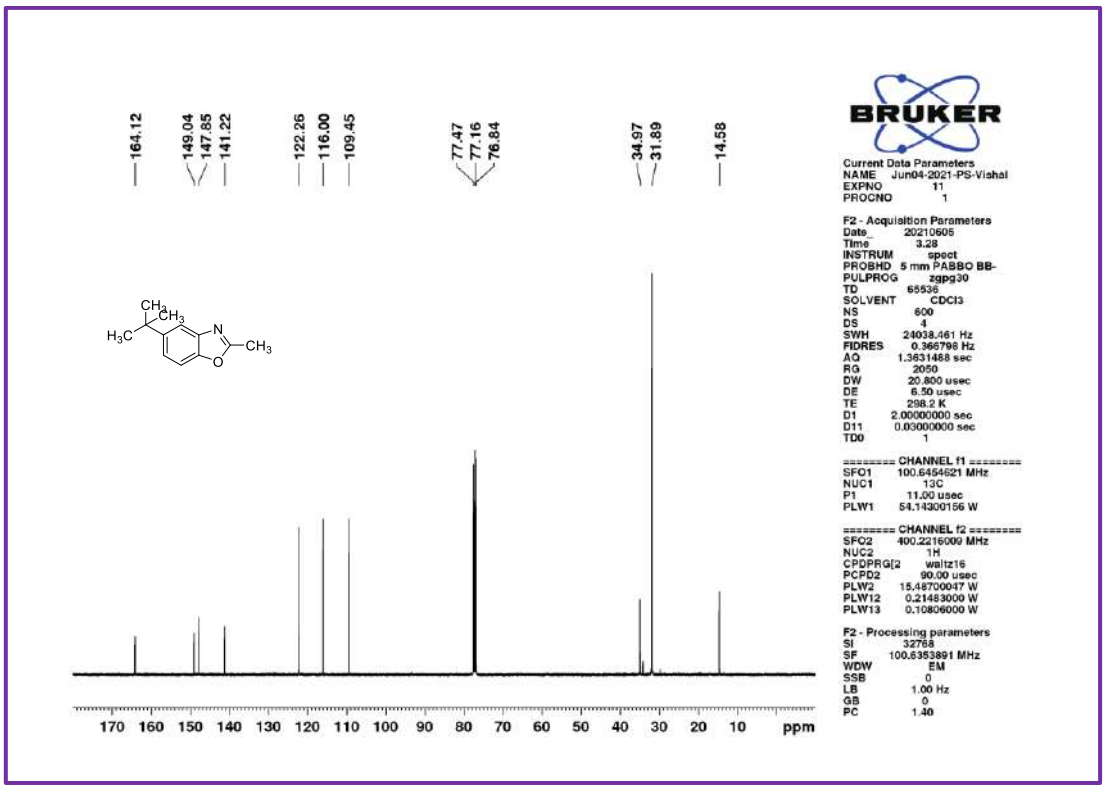

^{13}C NMR spectra of **3c.**

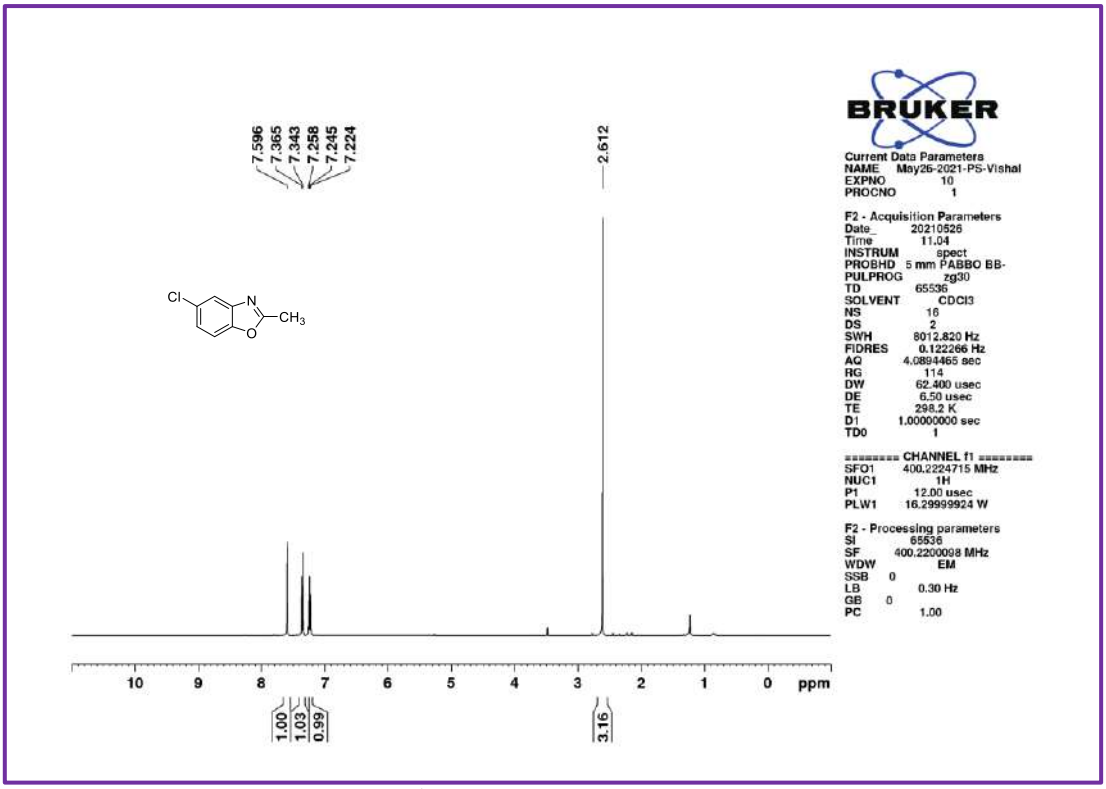

^{1}H NMR spectra of **3d**.

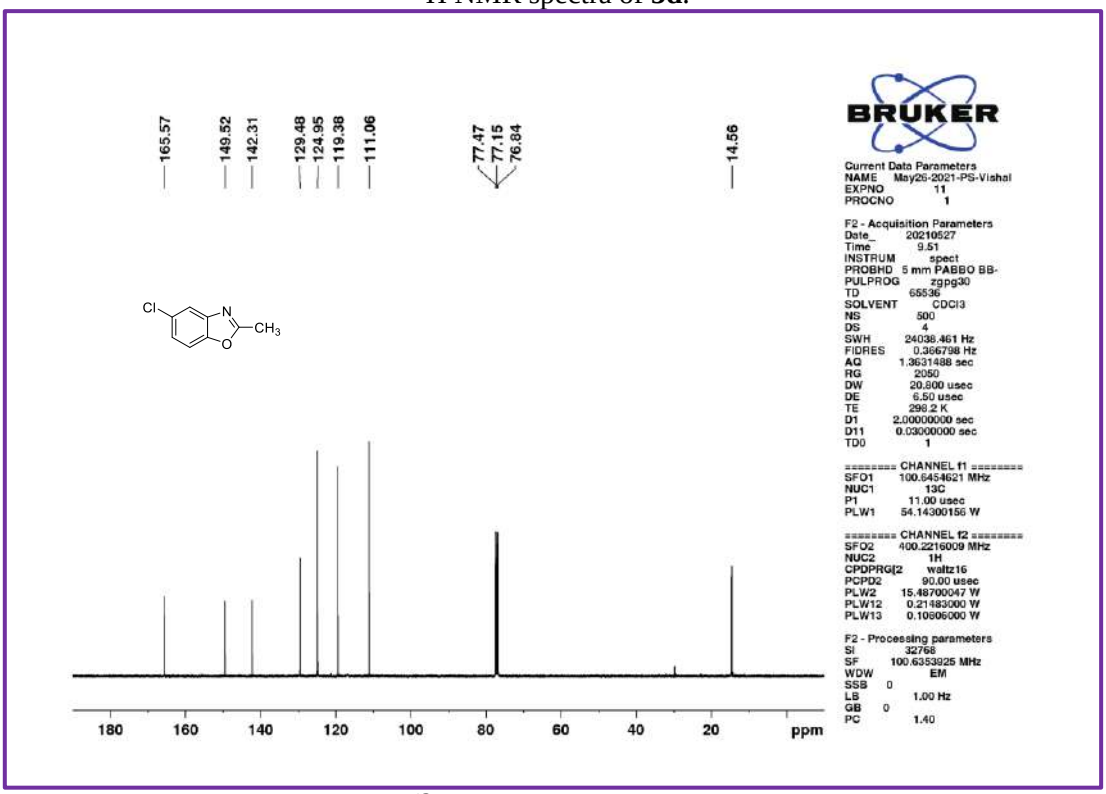

^{13}C NMR spectra of **3d.**

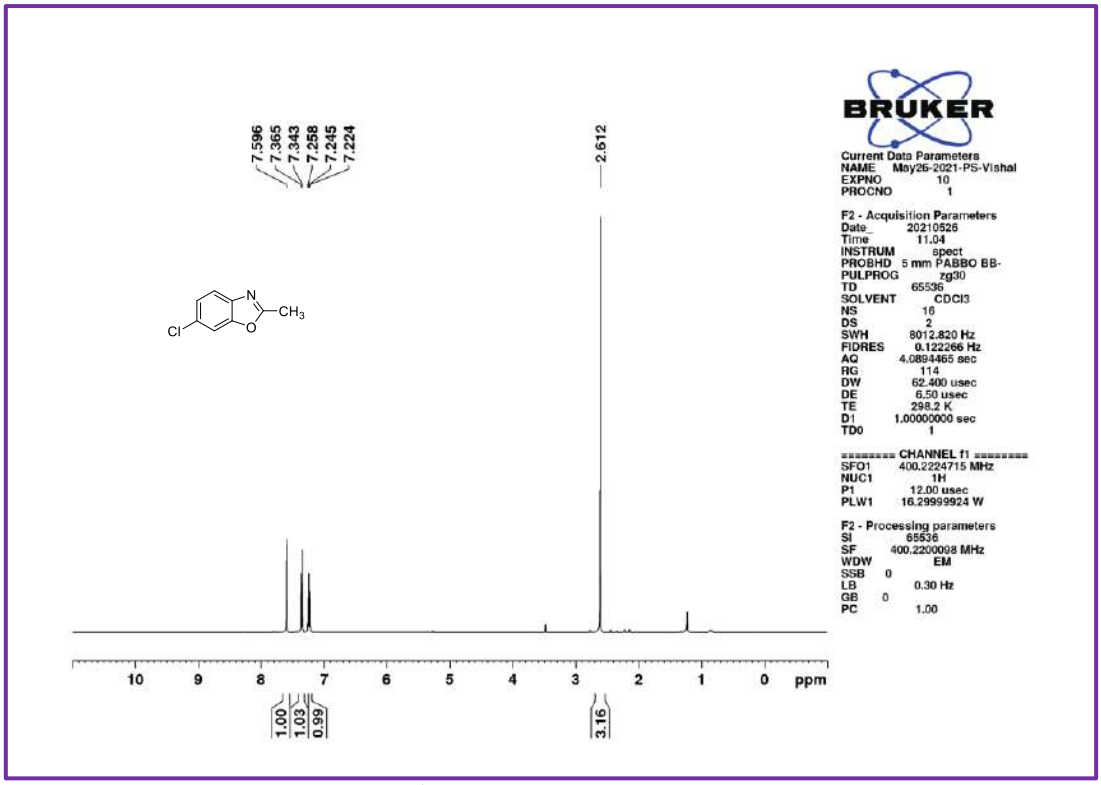

^{1}H NMR spectra of **3e.**

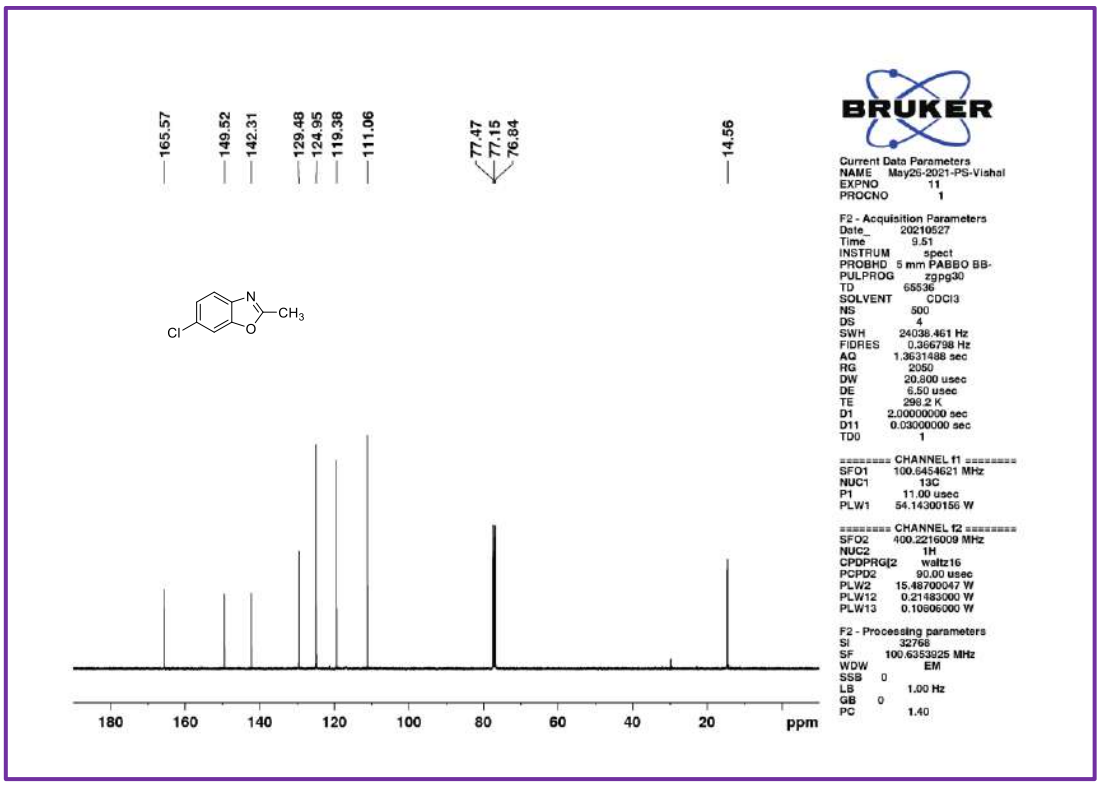

^{13}C NMR spectra of **3e.**

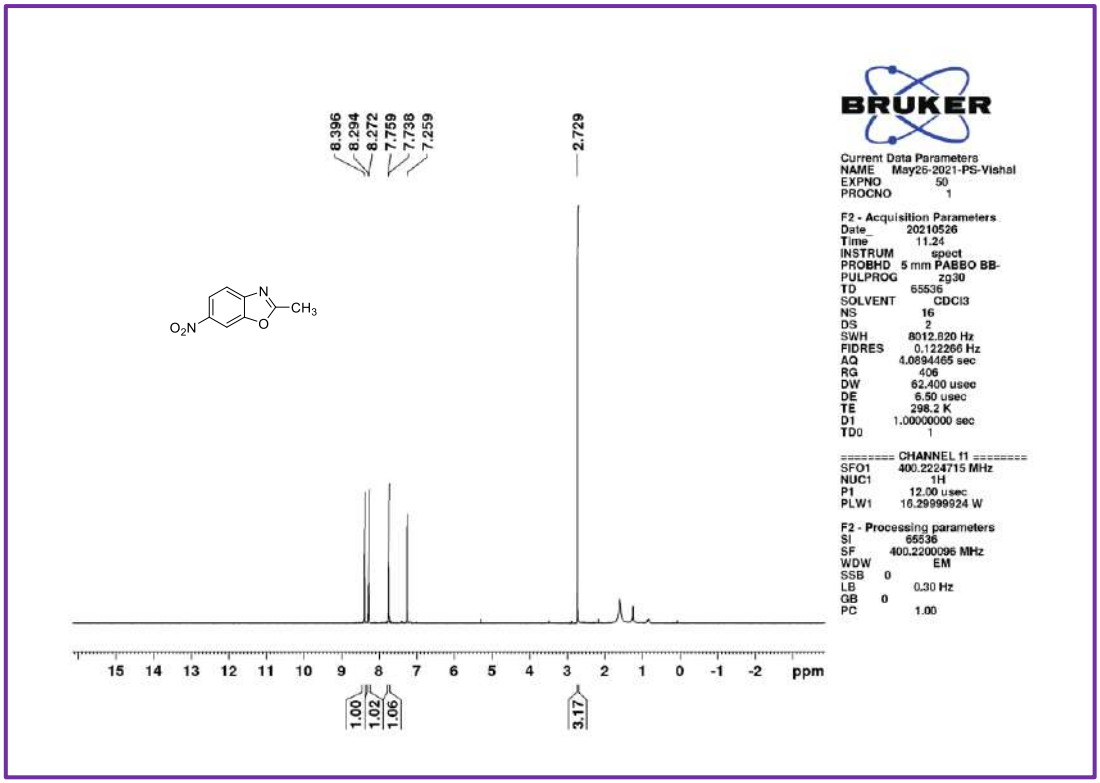

^{1}H NMR spectra of **3f**.

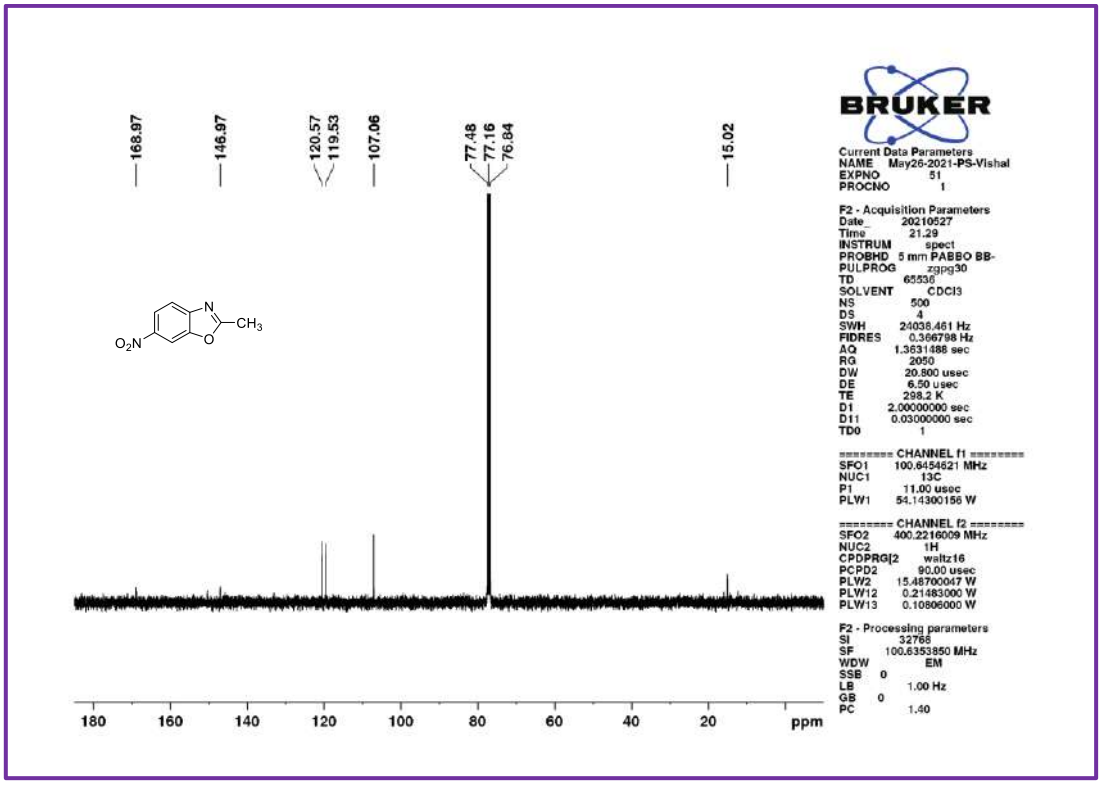

^{13}C NMR spectra of **3f.**

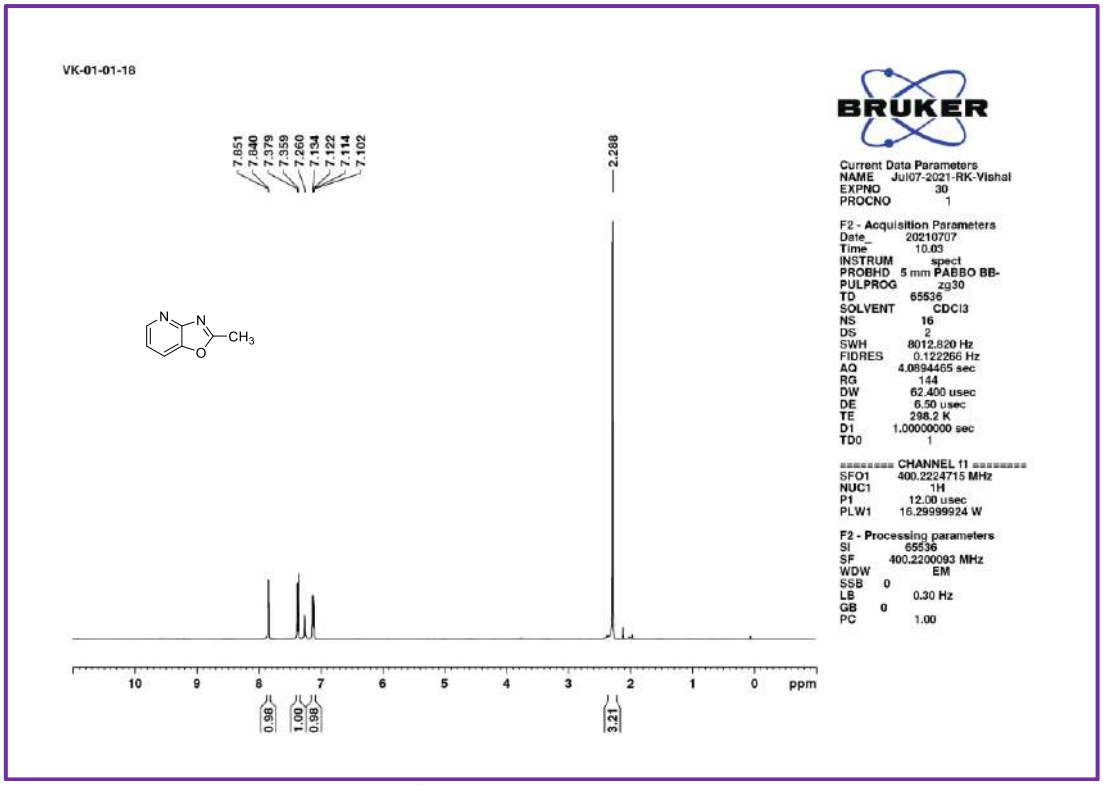

^{1}H NMR spectra of **3g**.

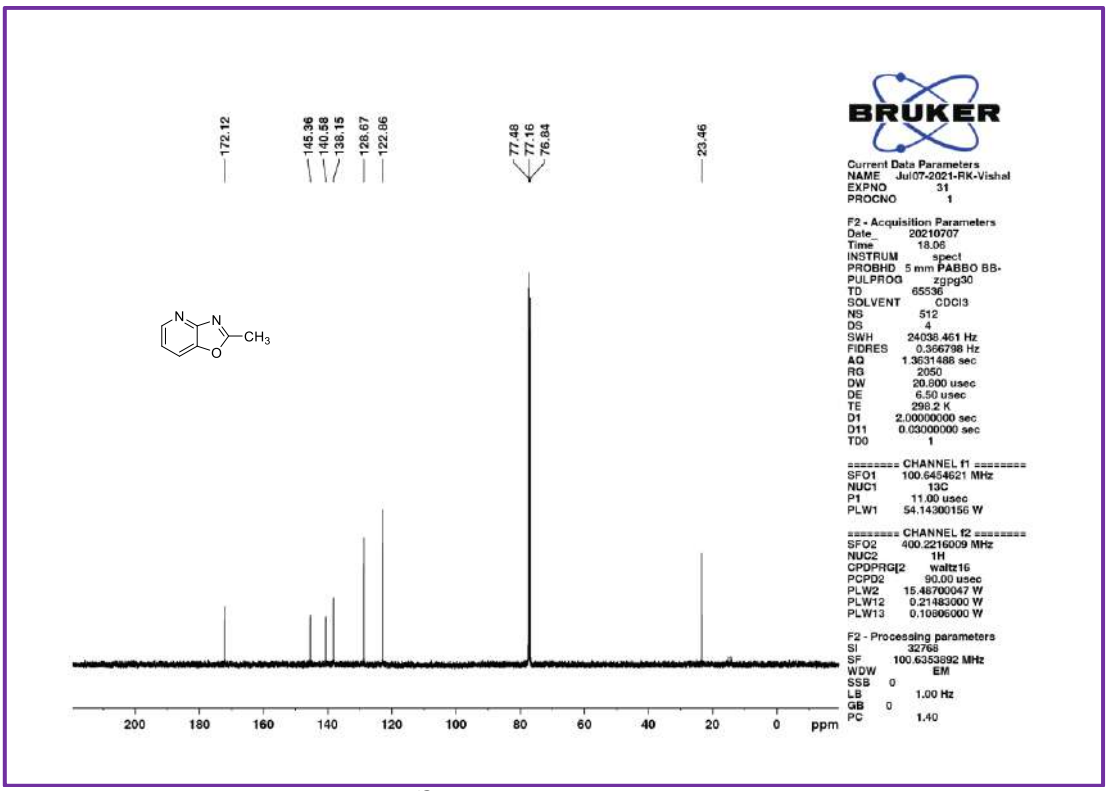

^{13}C NMR spectra of **3g.**

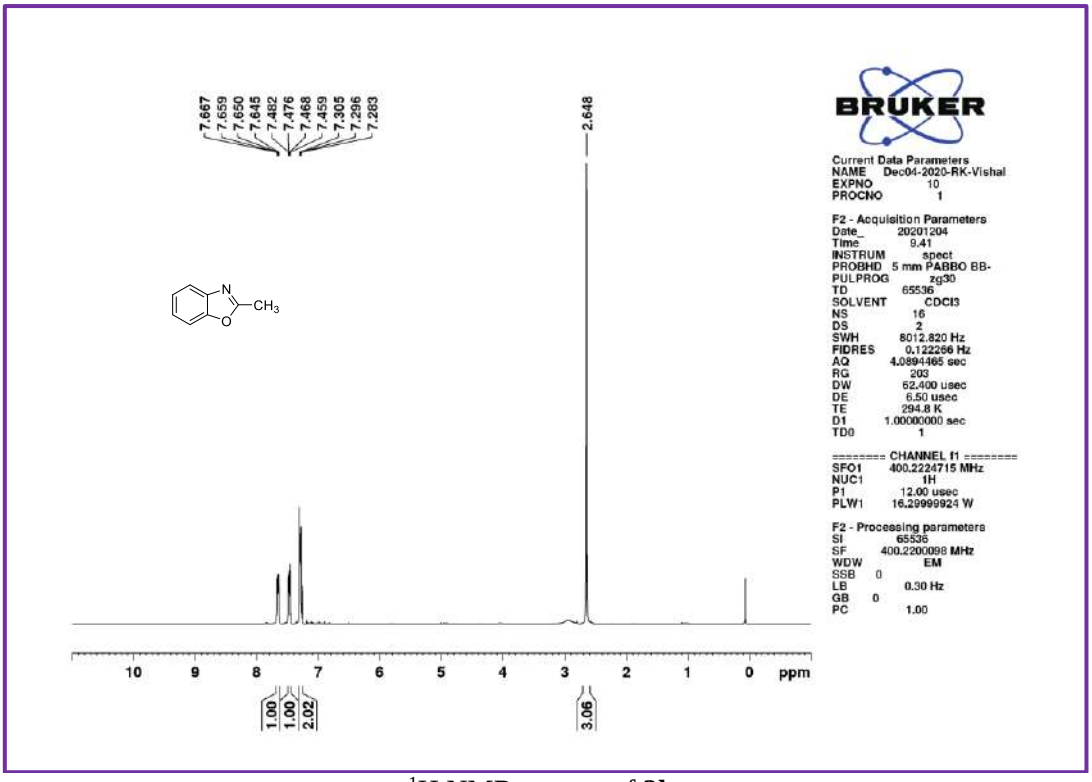

^{1}H NMR spectra of **3h**.

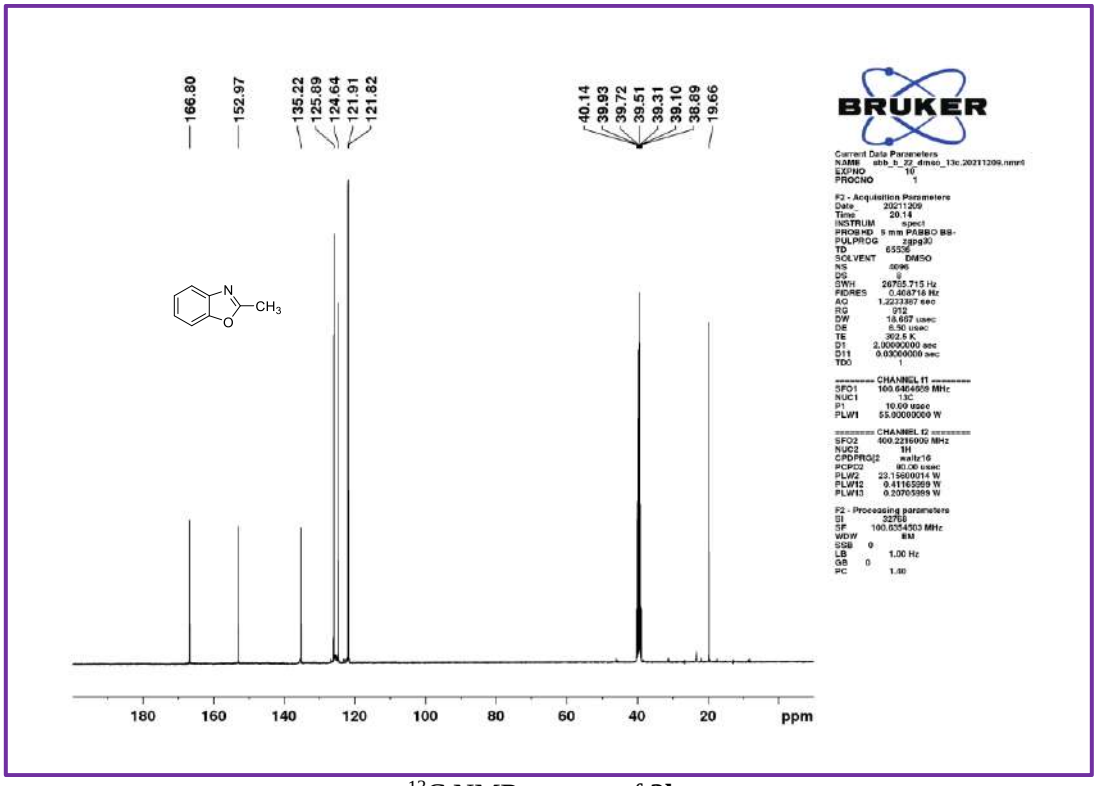

^{13}C NMR spectra of **3h.**

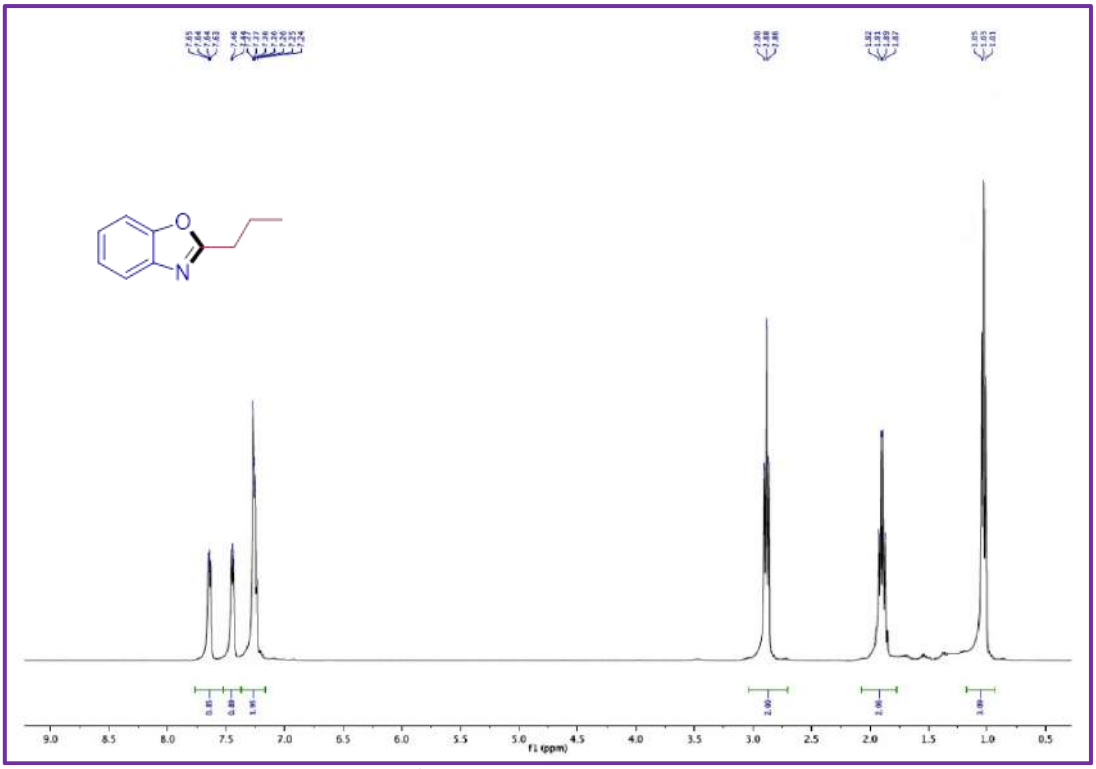

^{1}H NMR spectra of **3i**.

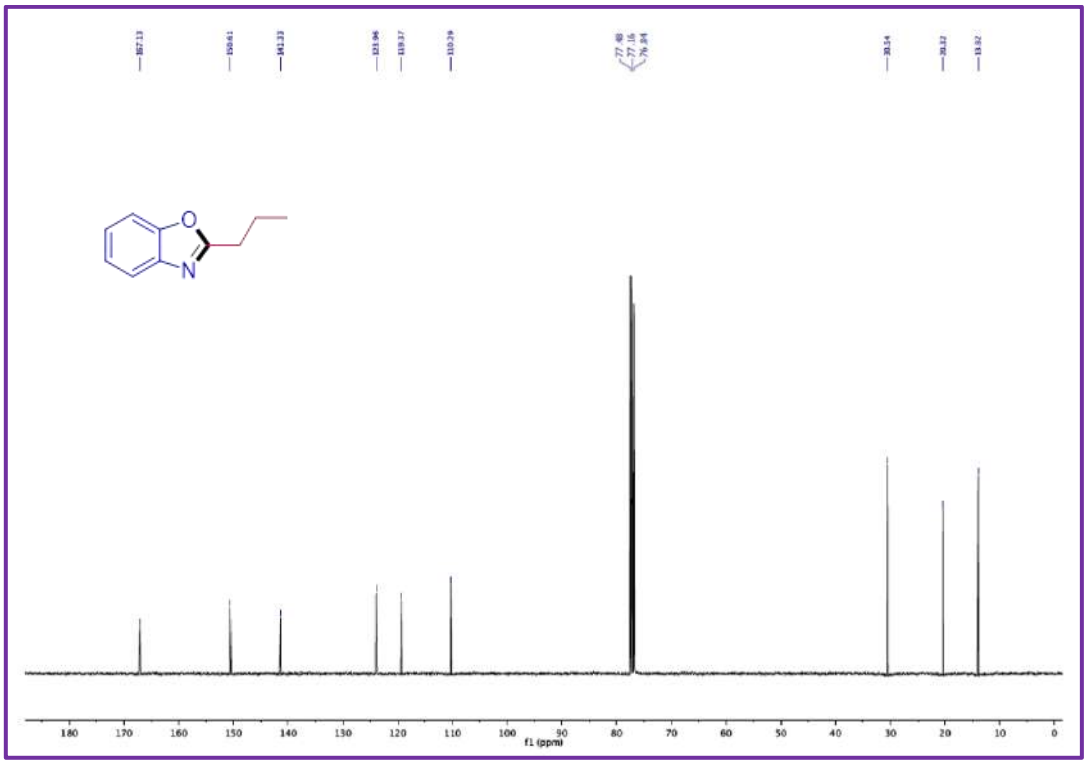

^{13}C NMR spectra of **3i.**

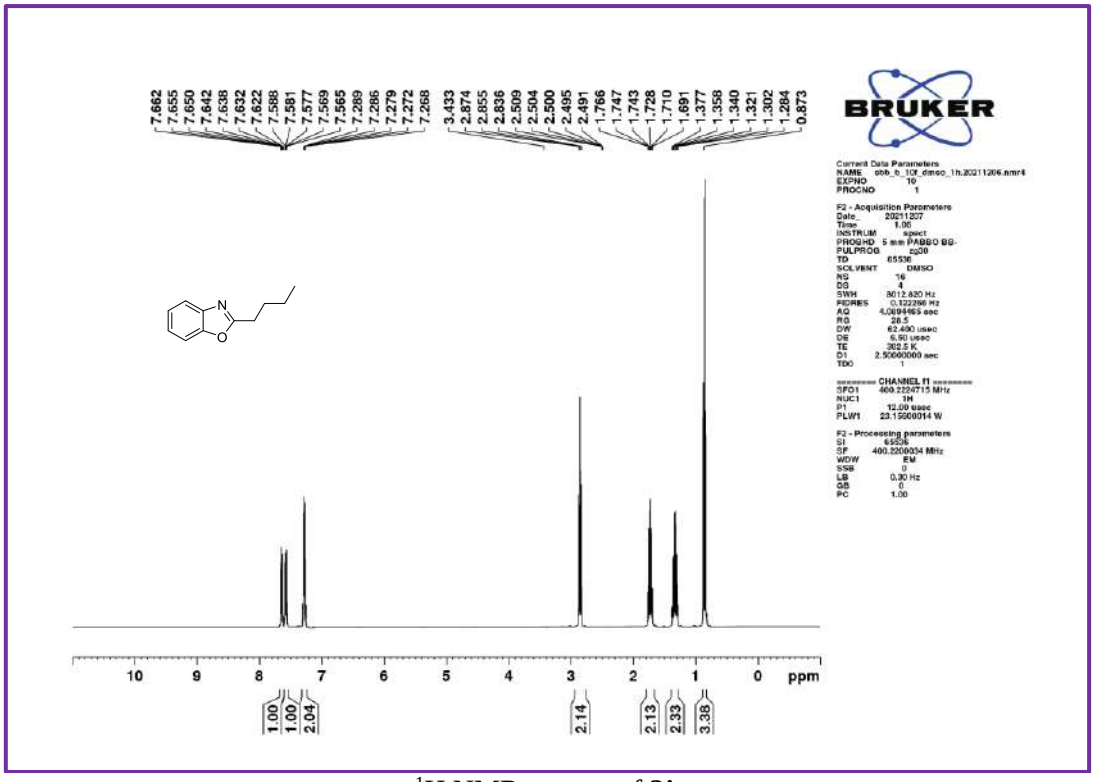

^{1}H NMR spectra of **3j**.

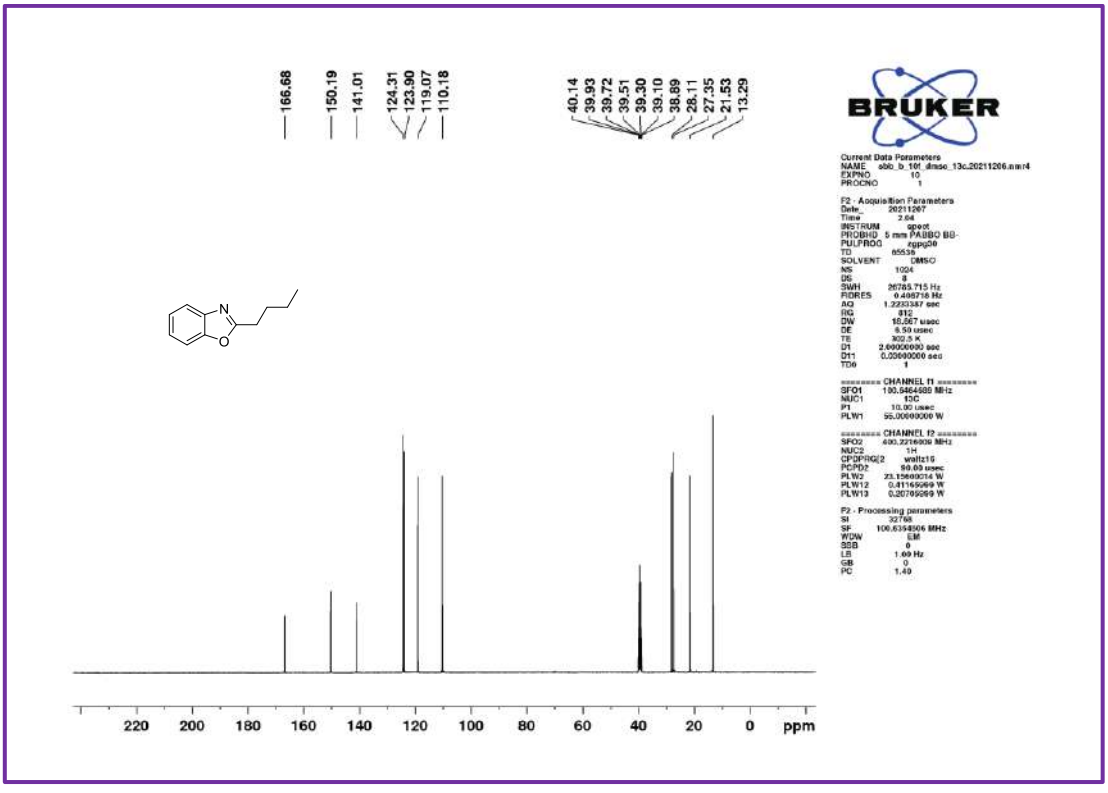

^{13}C NMR spectra of **3j.**

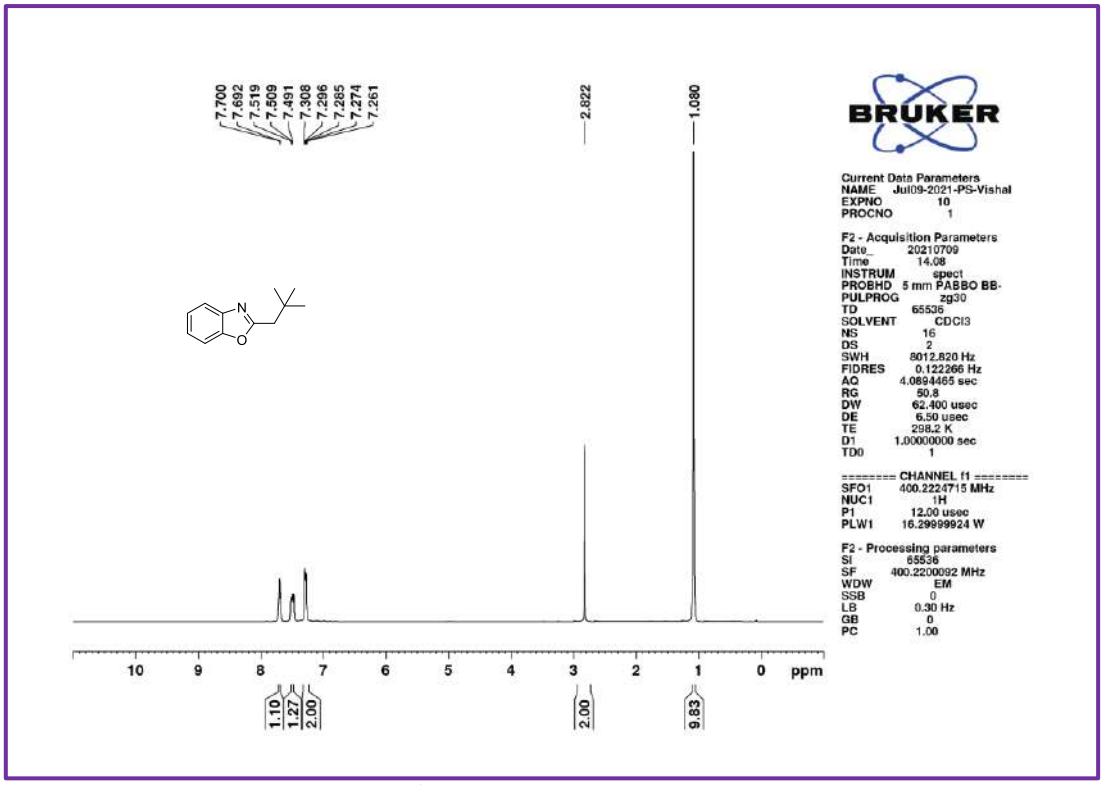

^{1}H NMR spectra of **3k**.

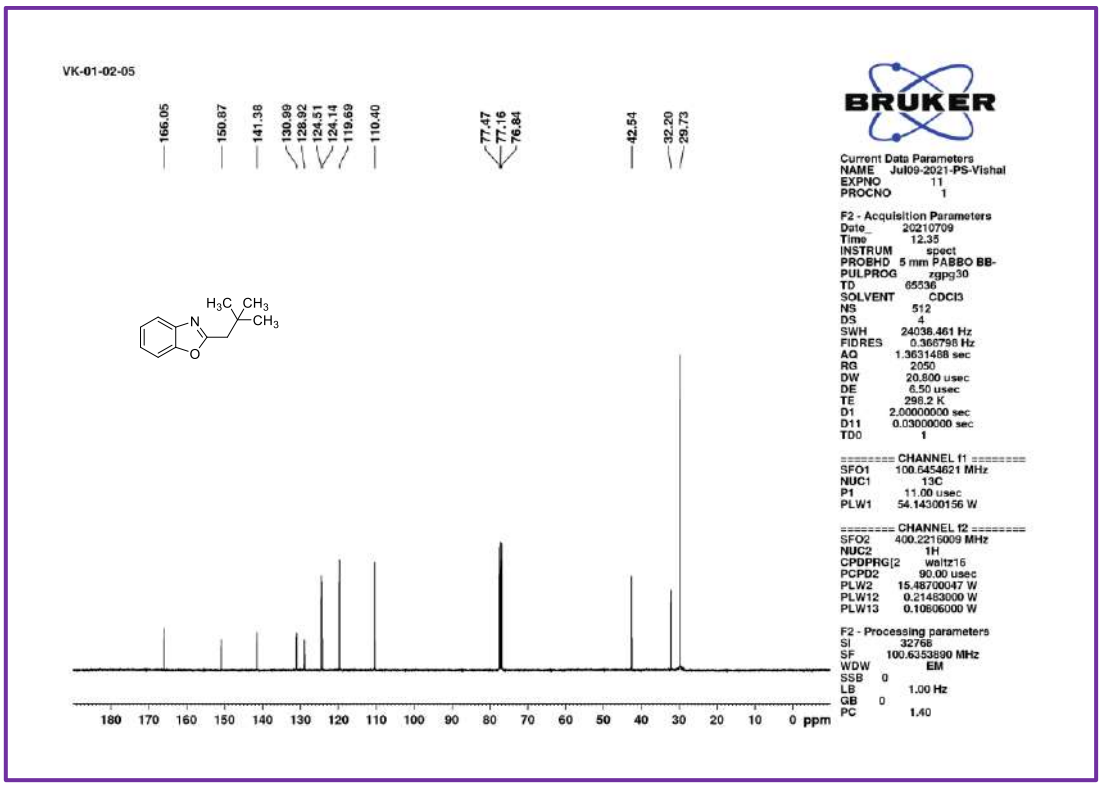

^{13}C NMR spectra of **3k.**

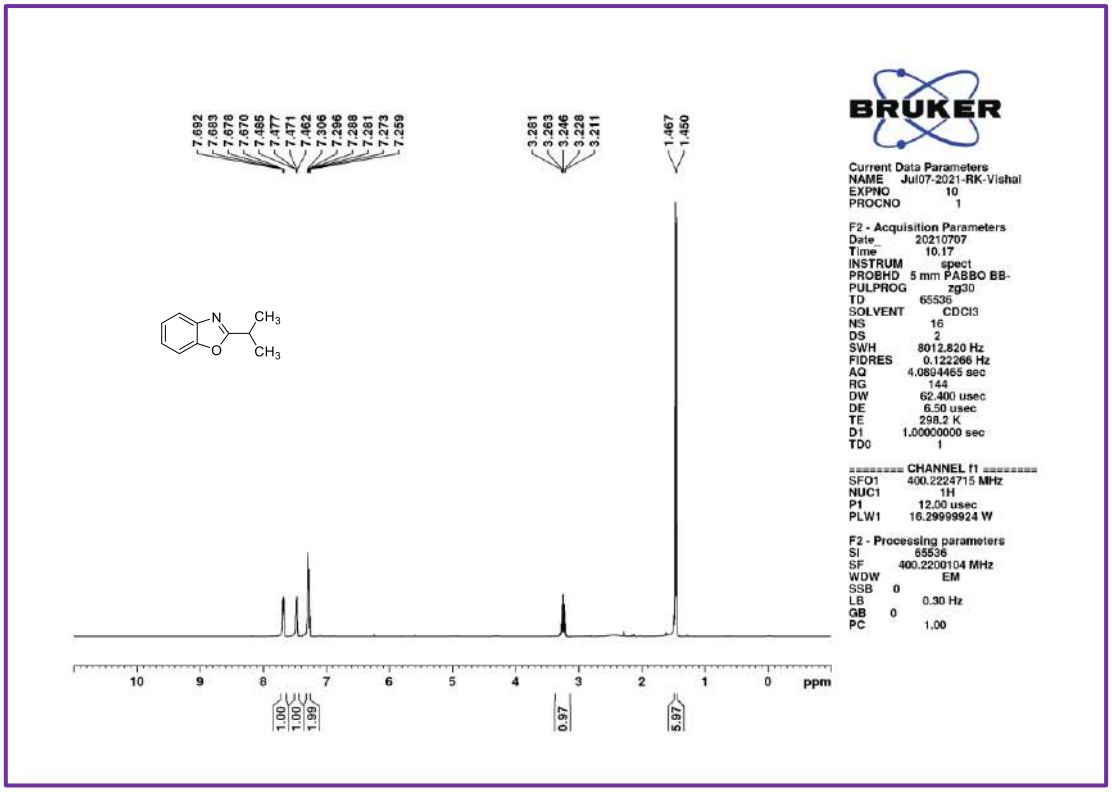

^{1}H NMR spectra of **3l**.

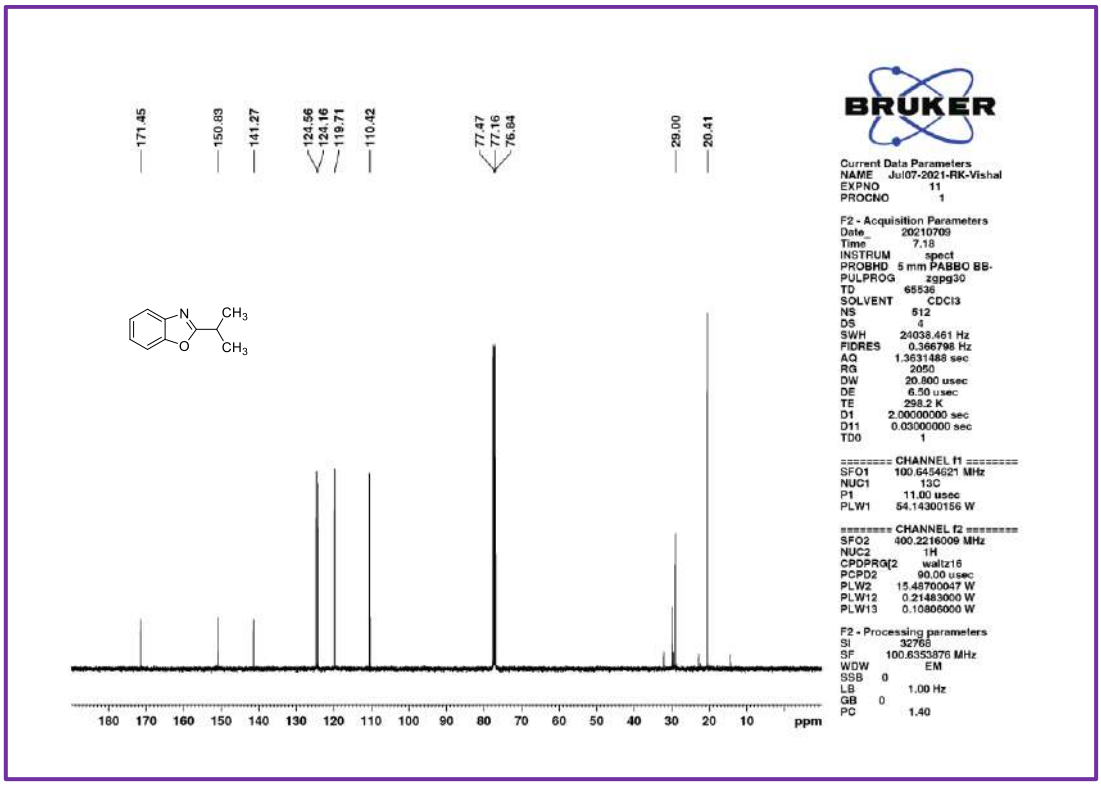

^{13}C NMR spectra of **3l.**

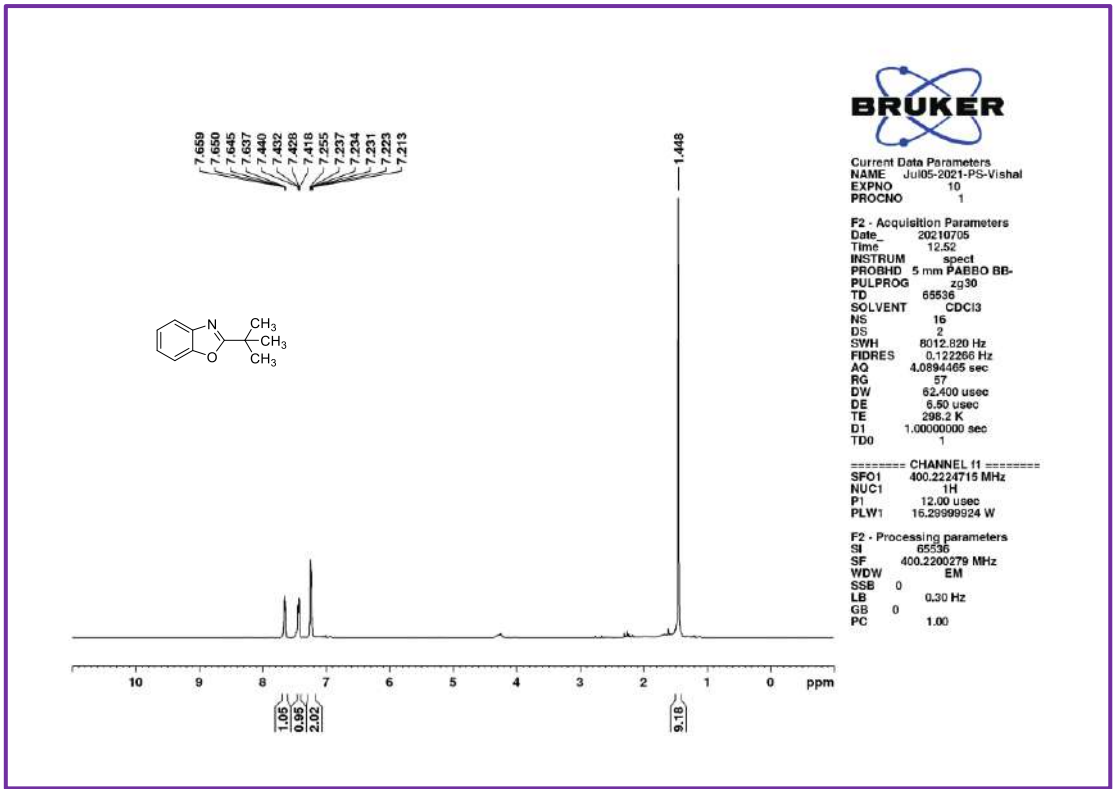

^{1}H NMR spectra of **3m**.

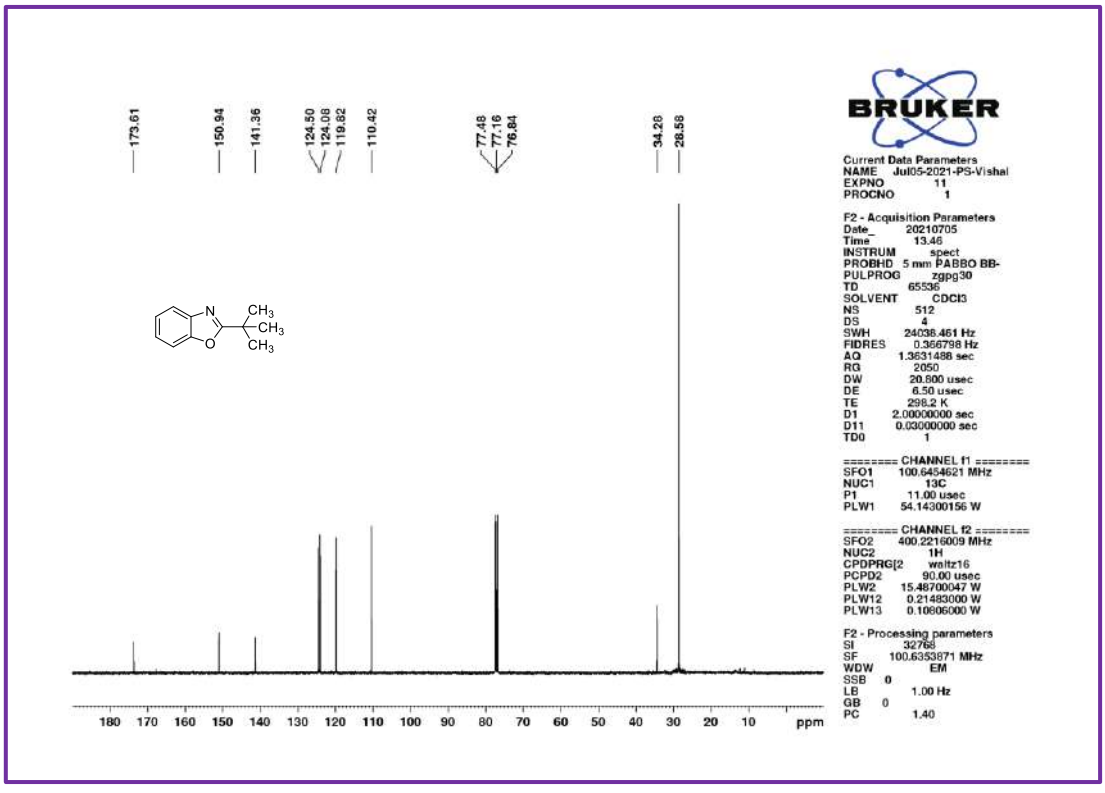

^{13}C NMR spectra of **3m.**

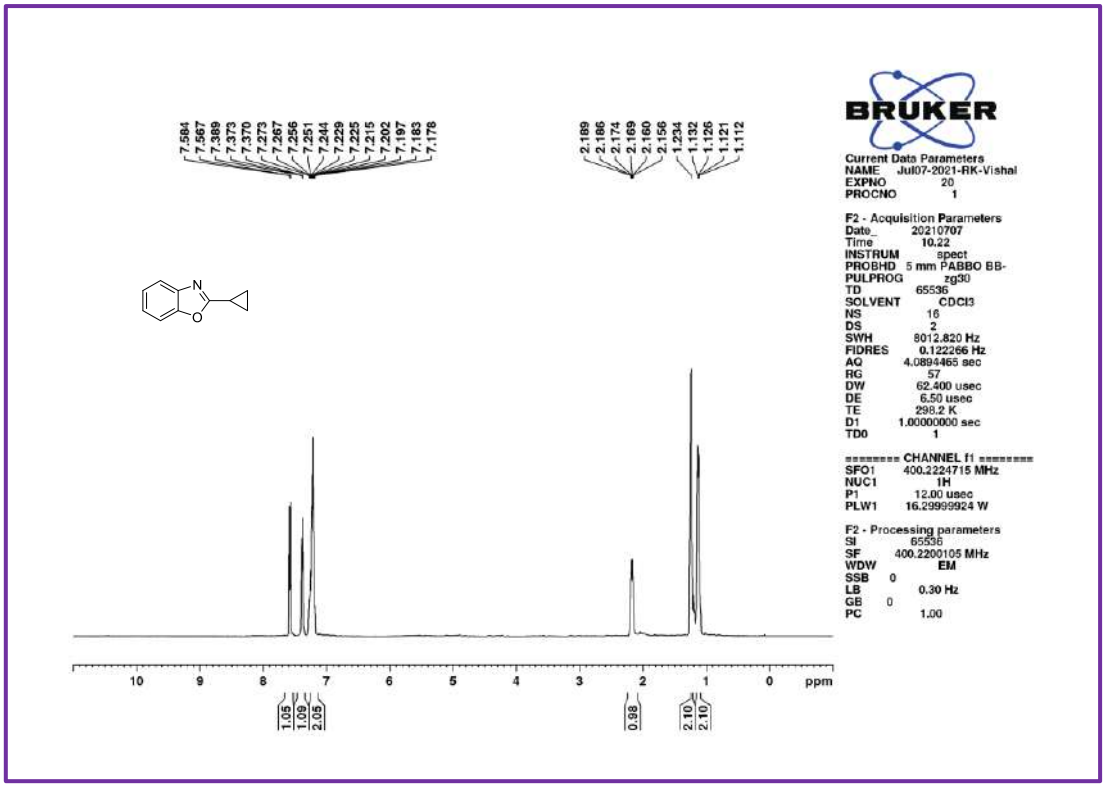

^{1}H NMR spectra of **3n**.

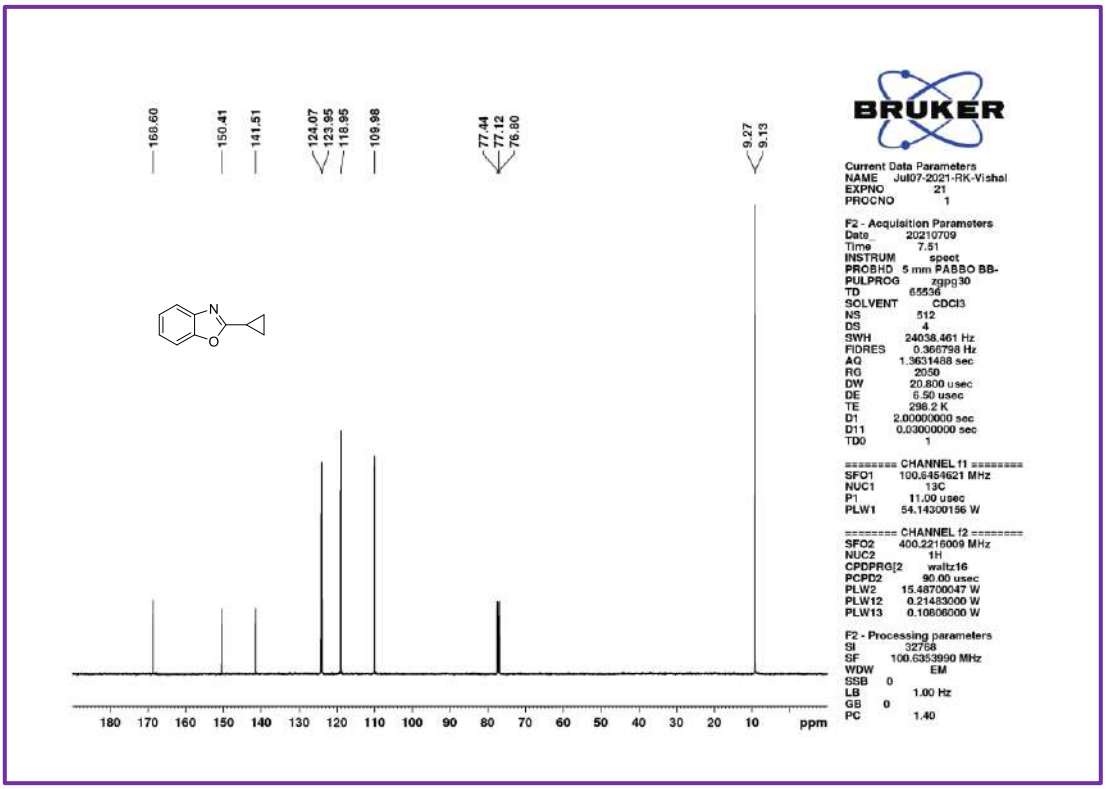

^{13}C spectra of **3n.**

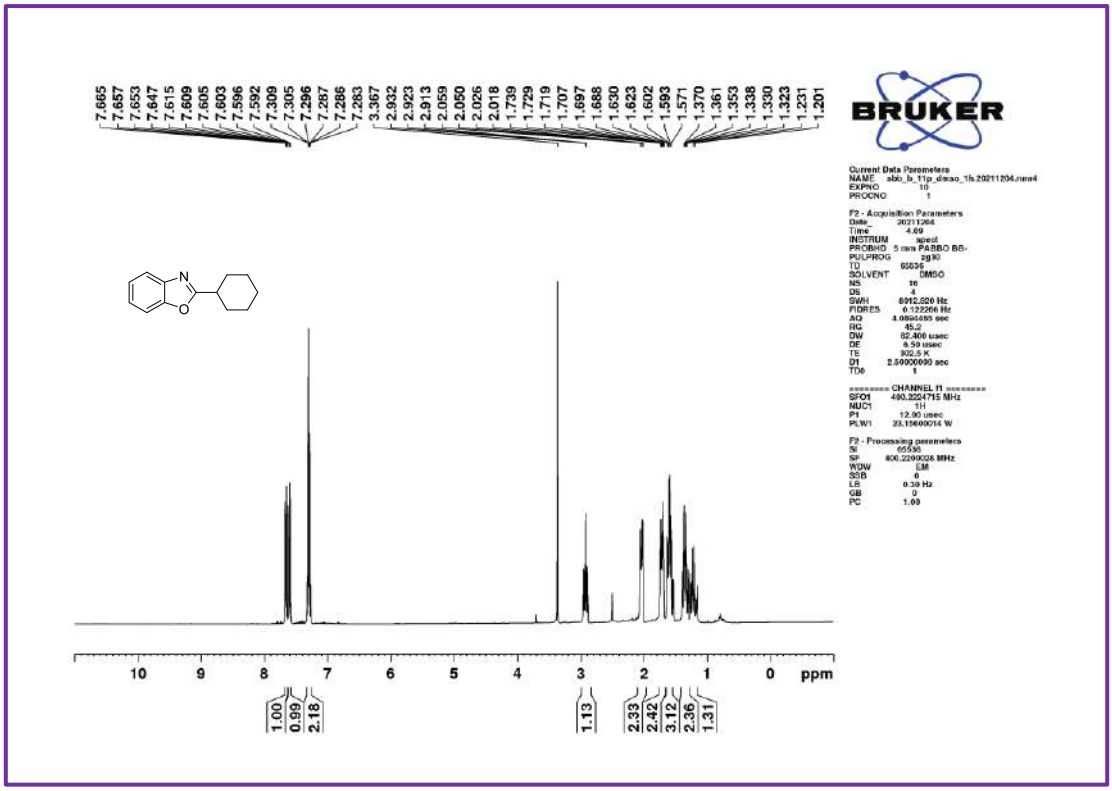

^{1}H NMR spectra of **3o**.

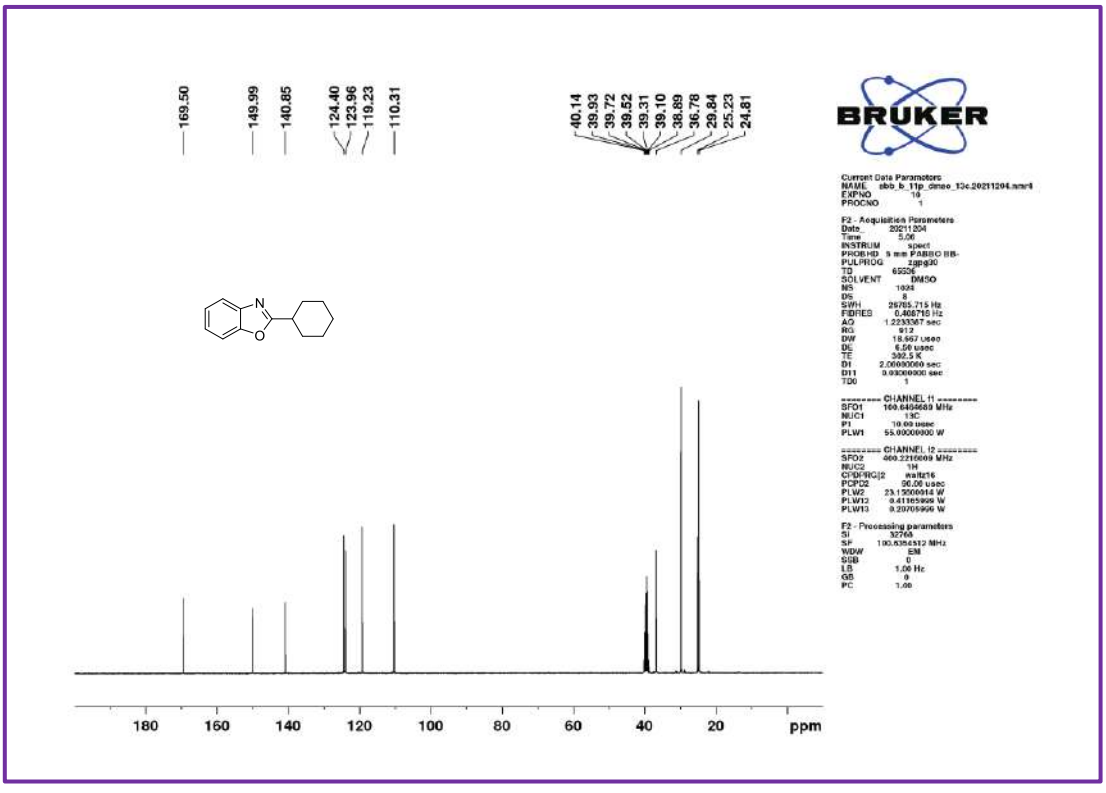

^{13}C NMR spectra of **3o.**

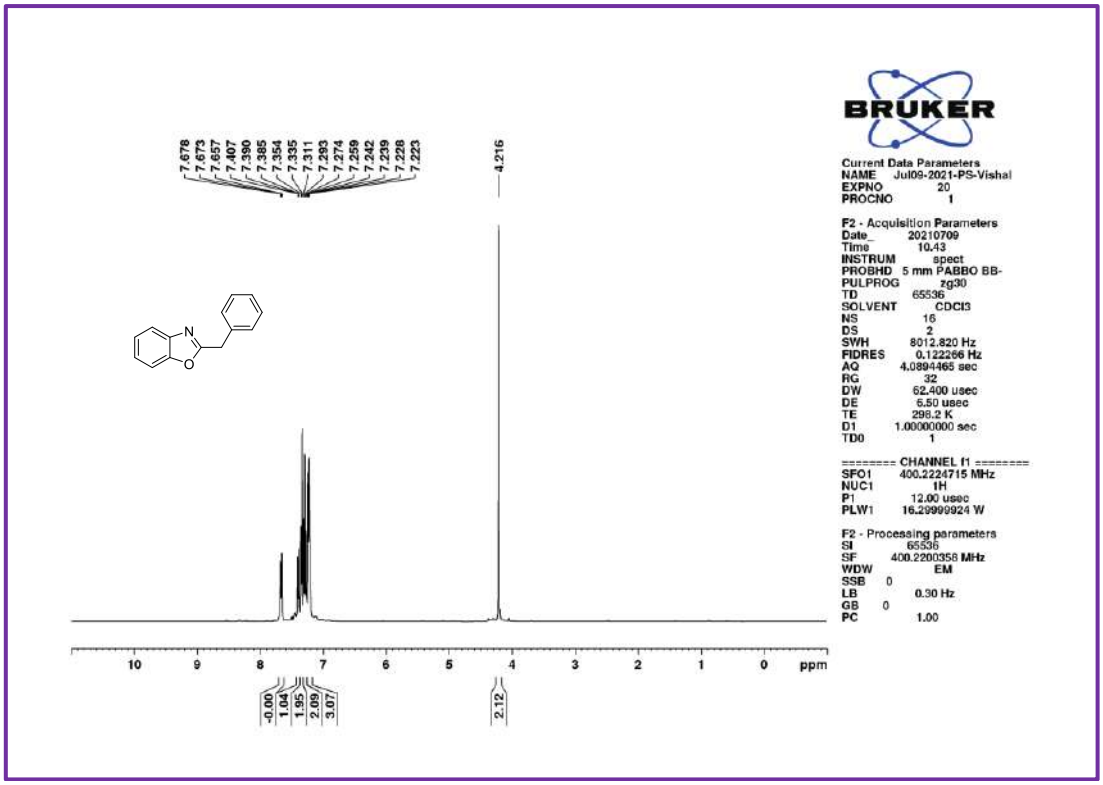

^{1}H NMR spectra of **3p**.

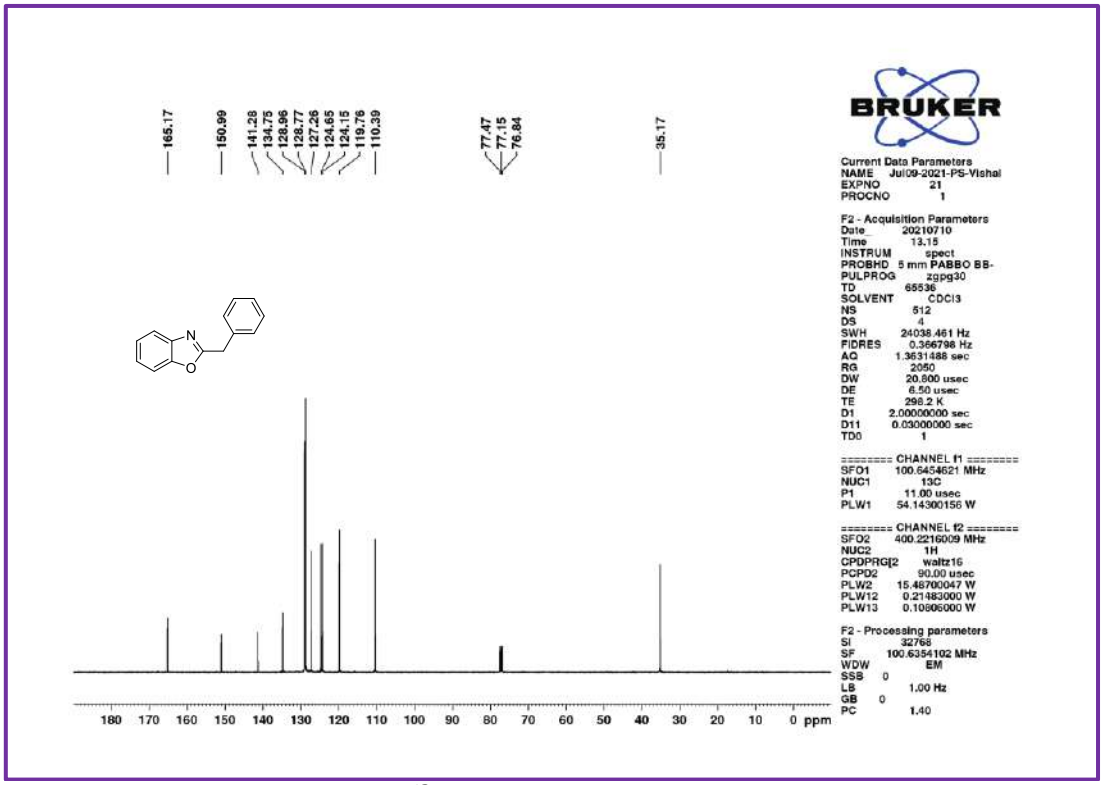

^{13}C NMR spectra of **3p.**

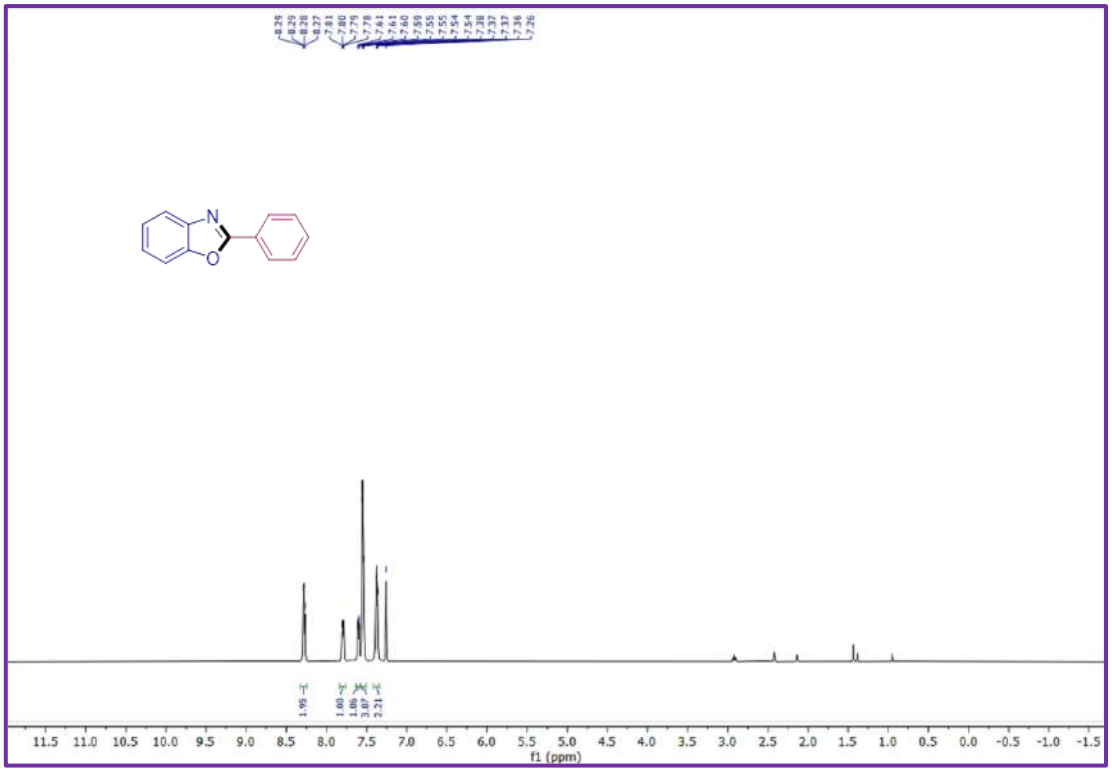

^{1}H NMR spectra of **3r**.

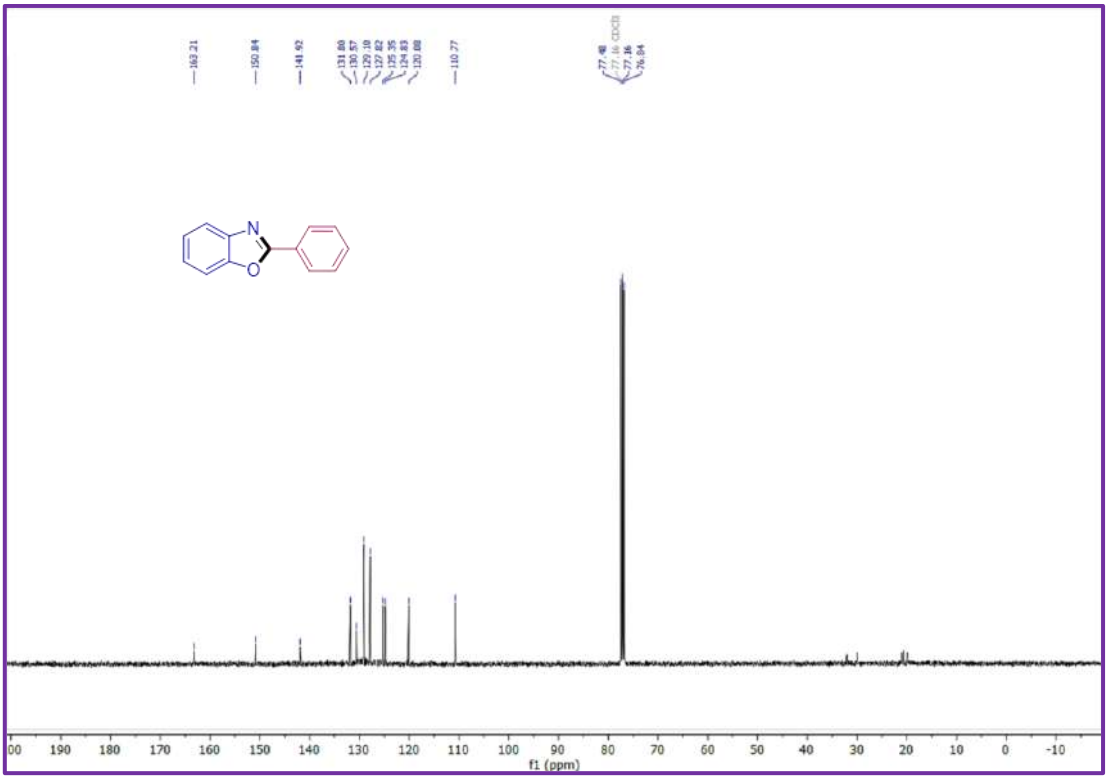

^{13}C NMR spectra of **3r.**

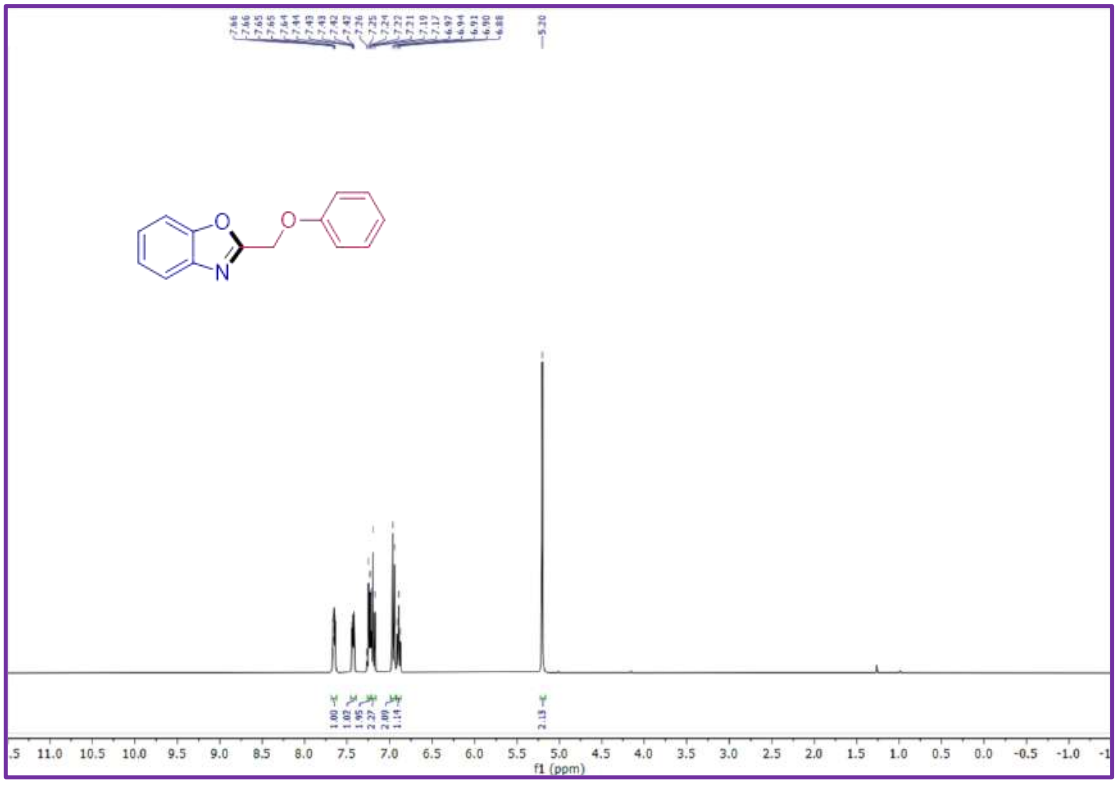

^{1}H NMR spectra of **3s**.

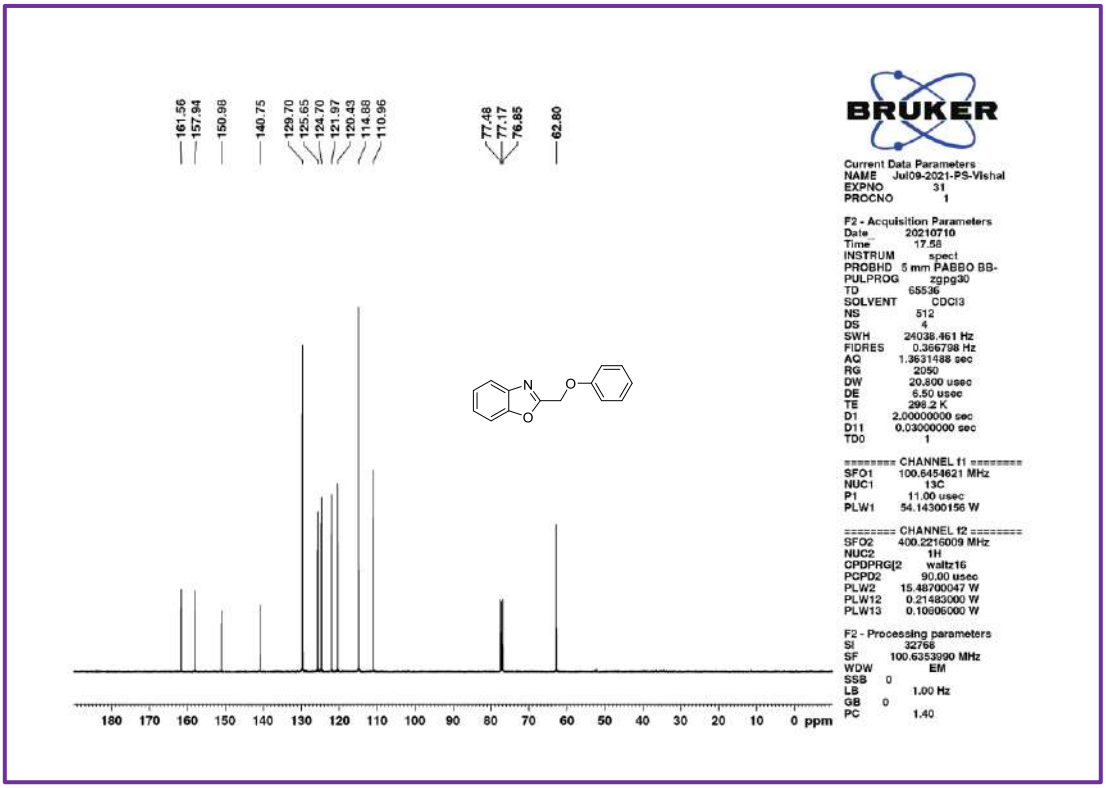

^{13}C NMR spectra of **3s.**

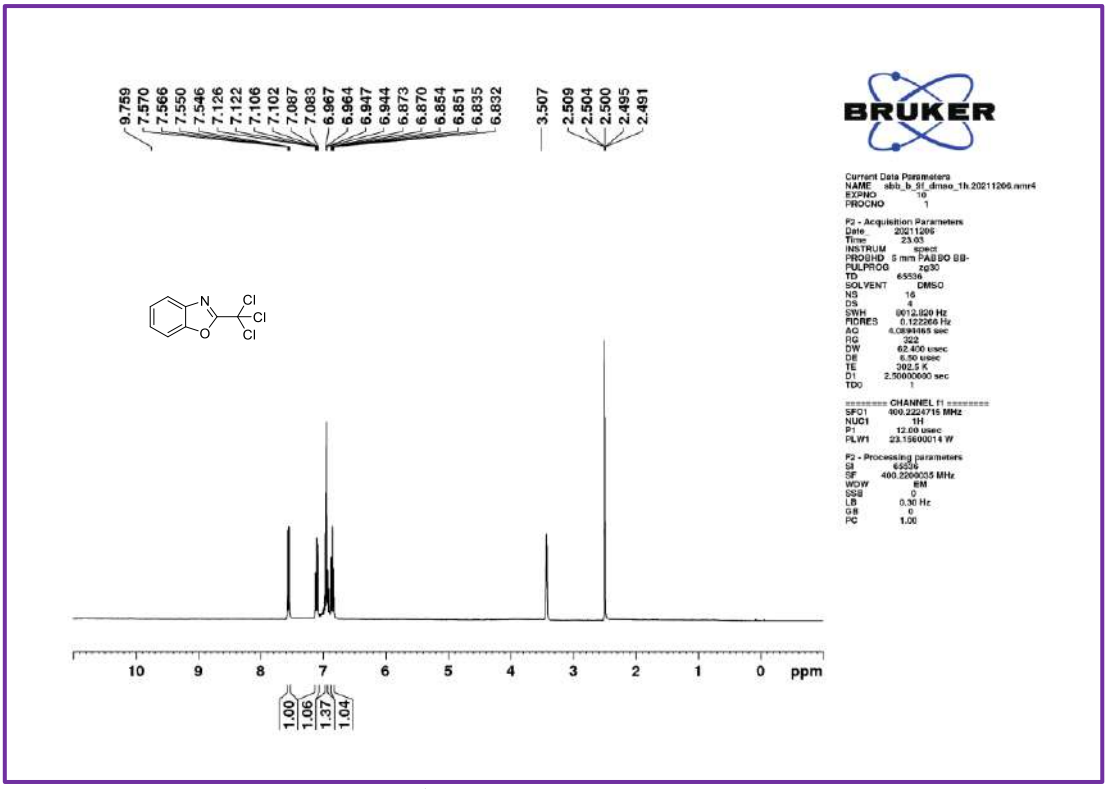

^{1}H NMR spectra of **3t.**

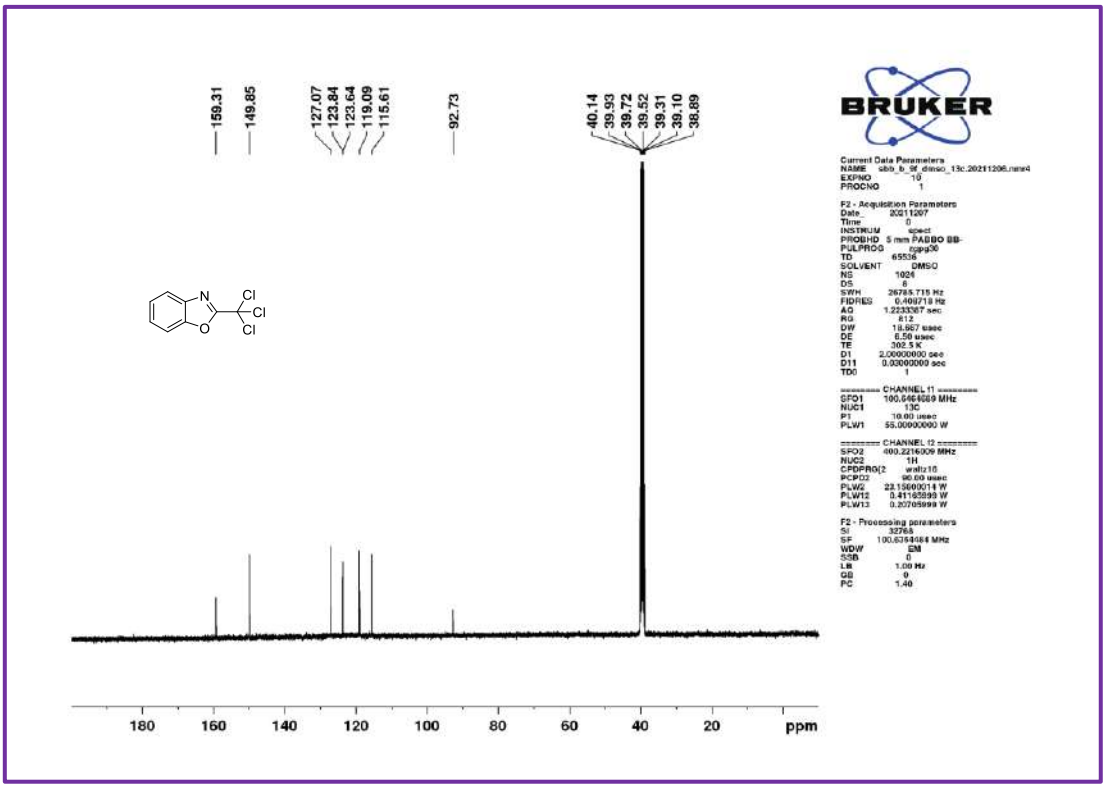

^{13}C NMR spectra of **3t.**

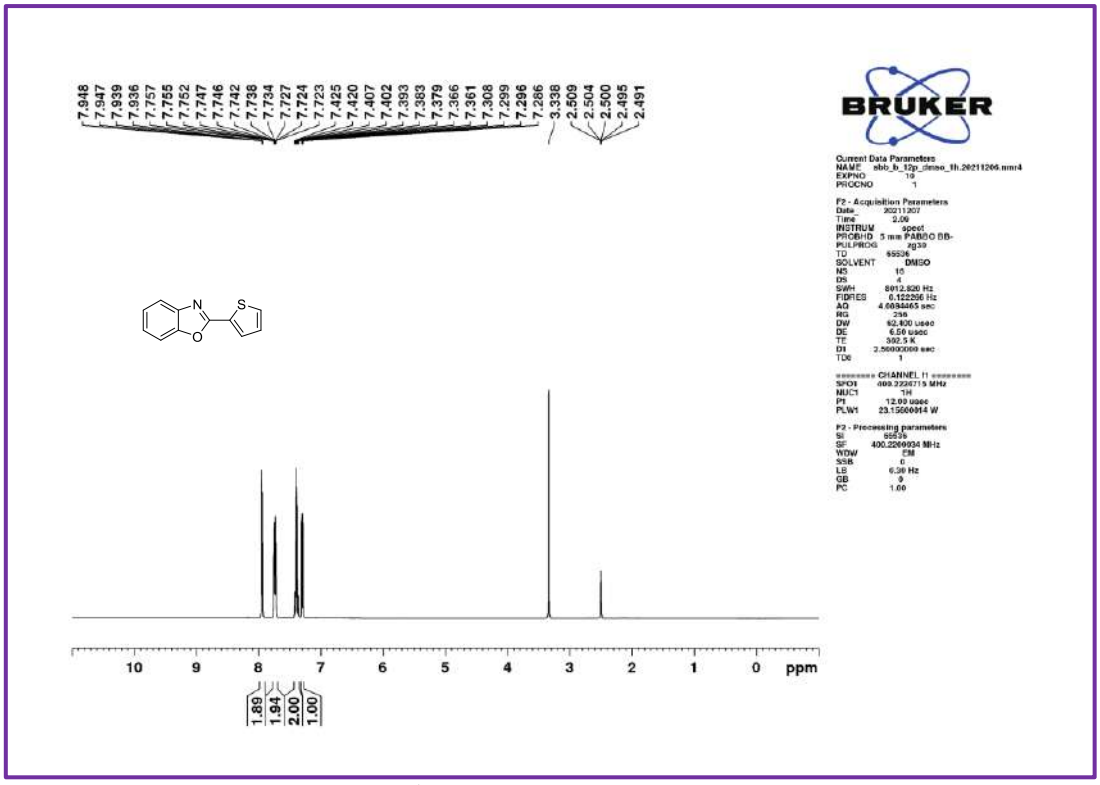

^{1}H NMR spectra of **3u.**

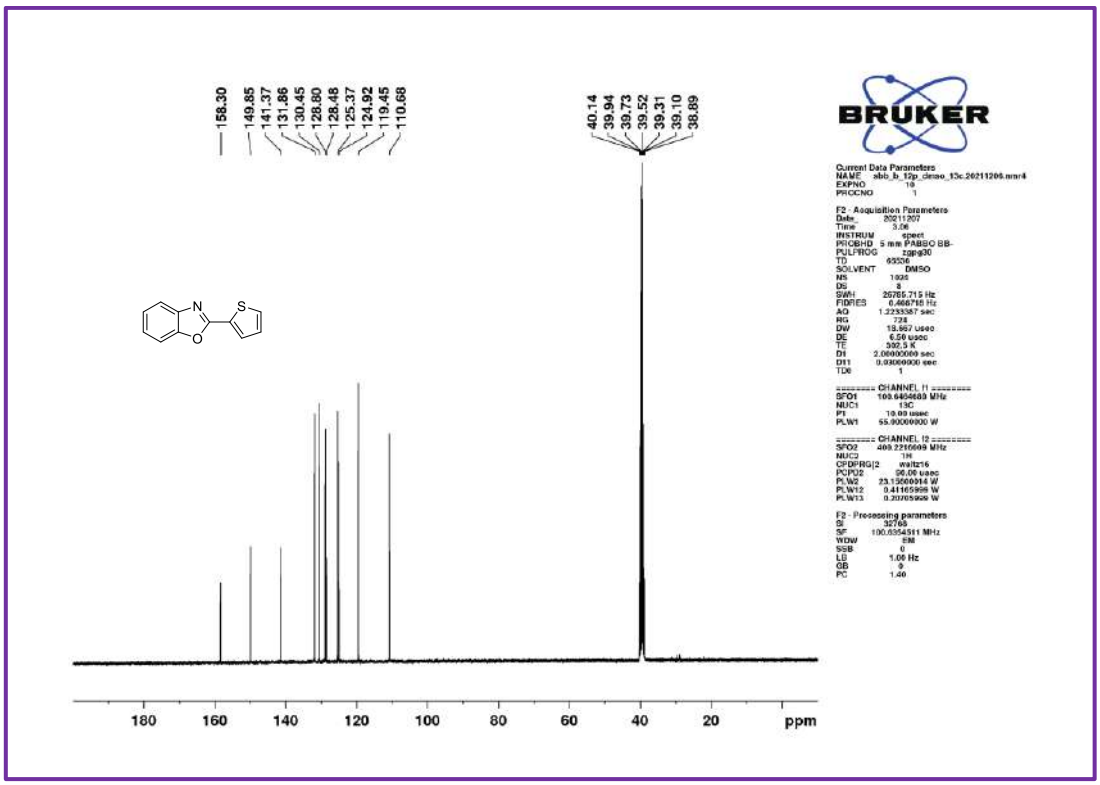

^{13}C NMR spectra of **3u.**

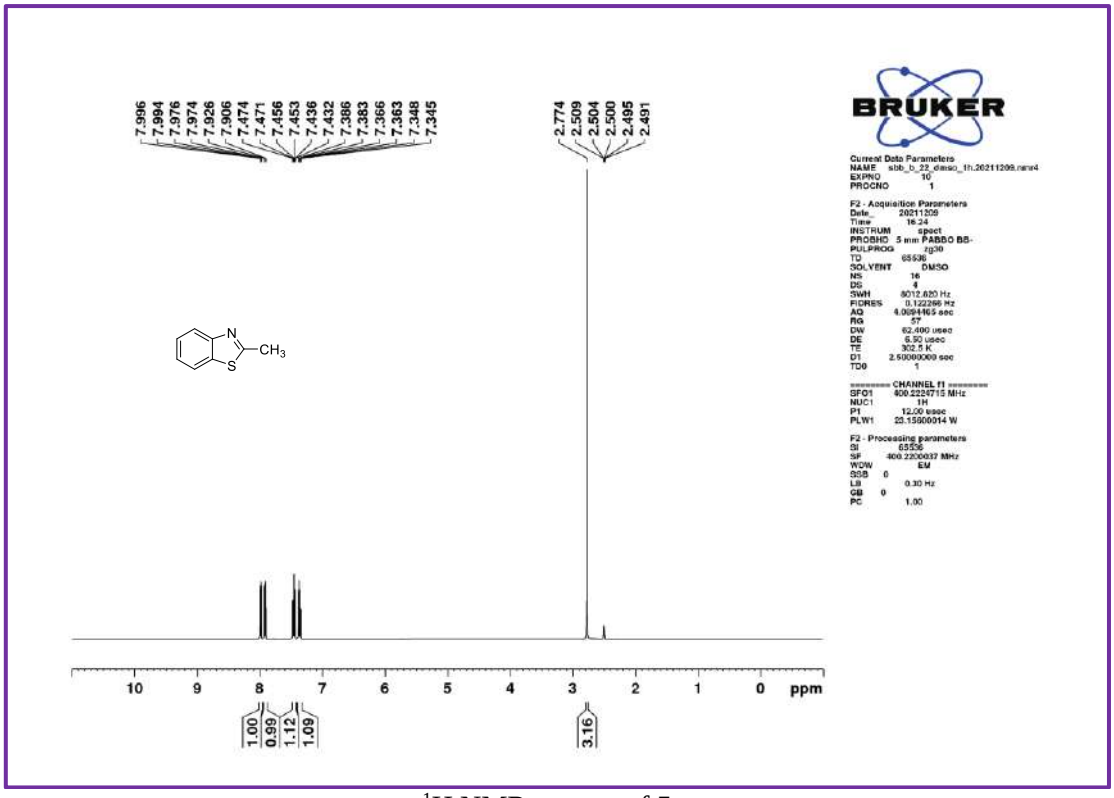

^{1}H NMR spectra of **5a.**

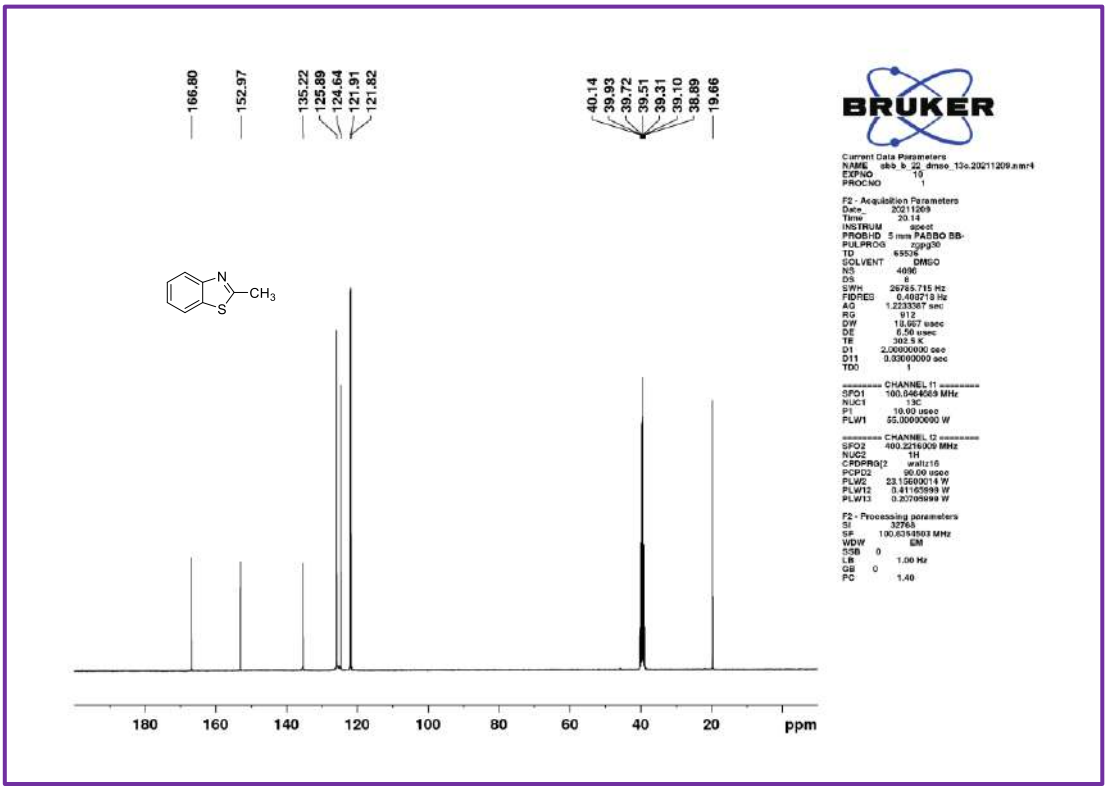

^{13}C NMR spectra of **5a.**

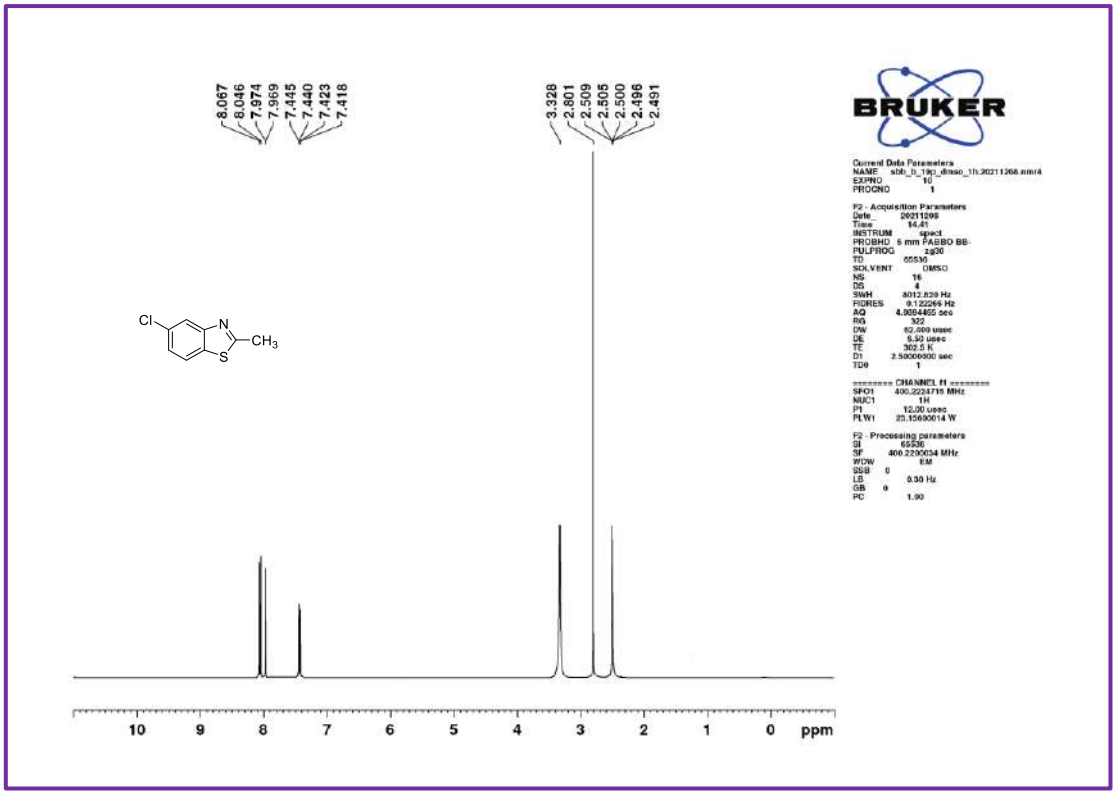

^{1}H NMR spectra of **5b.**

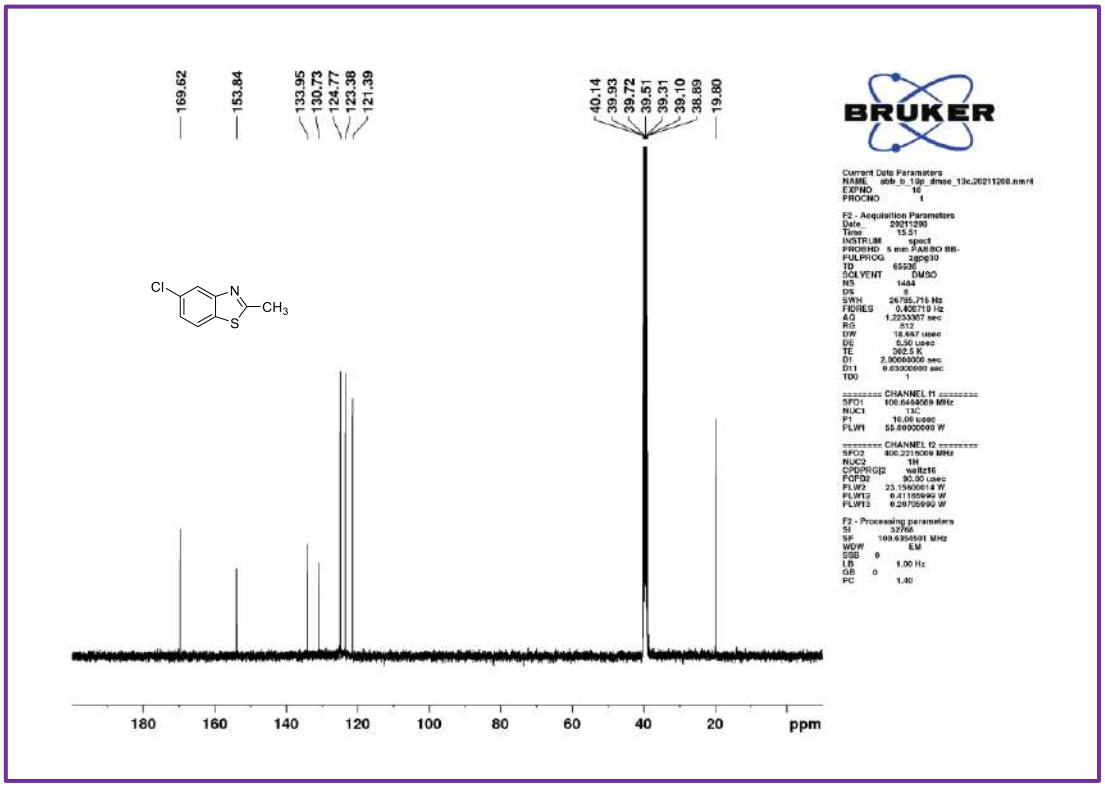

^{13}C NMR spectra of **5b.**

APPENDIX-III

SUPPLEMENTARY INFORMATION

CHAPTER 5

Cu-Catalysed Transamidation of Unactivated Aliphatic Amides

Under review in Organic and Bimolecular Chemistry.

^{1}H and ^{13}C NMR Spectra

^{1}H NMR spectra of **3A** is similar to 3A, Scheme 2 and Chapter 3**.**

^{13}C NMR spectra of **3A** is similar to 3A, Scheme 2 and Chapter 3**.**

^{1}H NMR spectra of **3B** is similar to 4b, Scheme 3 and Chapter 3**.**

^{13}C NMR spectra of **3B** is similar to 4b, Scheme 3 and Chapter 3**.**

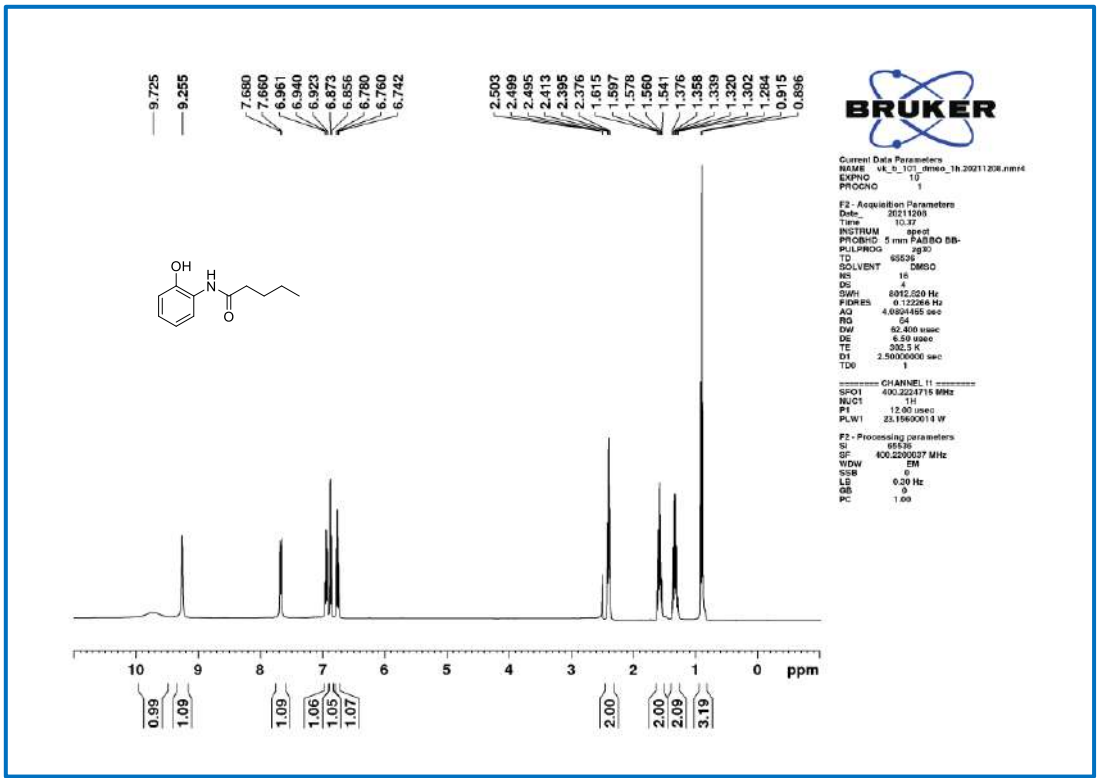

^{1}H NMR spectra of **3C.**

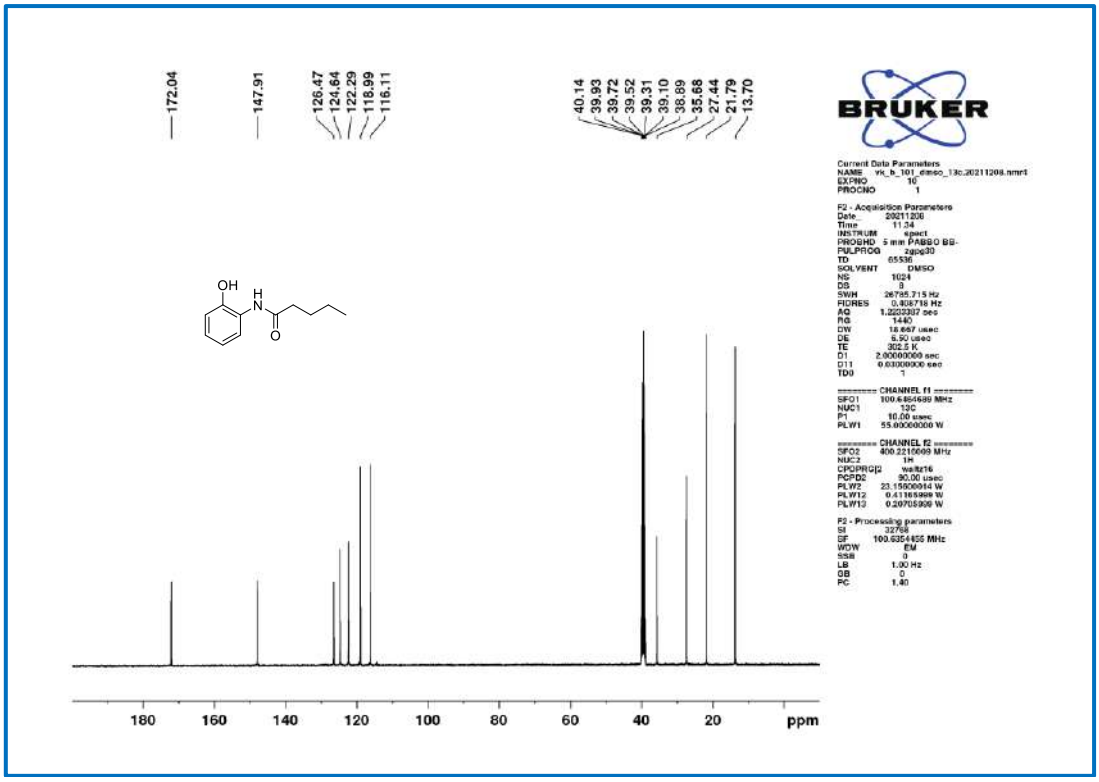

^{13}C NMR spectra of **3C.**

^{1}H NMR spectra of **3D** is similar to 3I, Scheme 2 and Chapter 3**.**

^{13}C NMR spectra of **3D** is similar to 3I, Scheme 2 and Chapter 3**.**

^{1}H NMR spectra of **3E** is similar to 3D, Scheme 2 and Chapter 3**.**

^{13}C NMR spectra of **3E** is similar to 3D, Scheme 2 and Chapter 3**.**

^{1}H NMR spectra of **3F** is similar to 3C, Scheme 2 and Chapter 3**.**

^{13}C NMR spectra of **3F** is similar to 3C, Scheme 2 and Chapter 3**.**

^{1}H NMR spectra of **3G** is similar to 3E, Scheme 2 and Chapter 3**.**

^{13}C NMR spectra of **3G** is similar to 3E, Scheme 2 and Chapter 3**.**

^{1}H NMR spectra of **3H** is similar to 3F, Scheme 2 and Chapter 3**.**

^{13}C NMR spectra of **3H** is similar to 3F, Scheme 2 and Chapter 3**.**

^{1}H NMR spectra of **3I** is similar to 3G, Scheme 2 and Chapter 3**.**

^{13}C NMR spectra of **3I** is similar to 3G, Scheme 2 and Chapter 3**.**

^{1}H NMR spectra of **3J** is similar to 3J, Scheme 2 and Chapter 3**.**

^{13}C NMR spectra of **3J** is similar to 3J, Scheme 2 and Chapter 3**.**

^{1}H NMR spectra of **3K** is similar to 3M, Scheme 2 and Chapter 3**.**

^{13}C NMR spectra of **3K** is similar to 3M, Scheme 2 and Chapter 3**.**

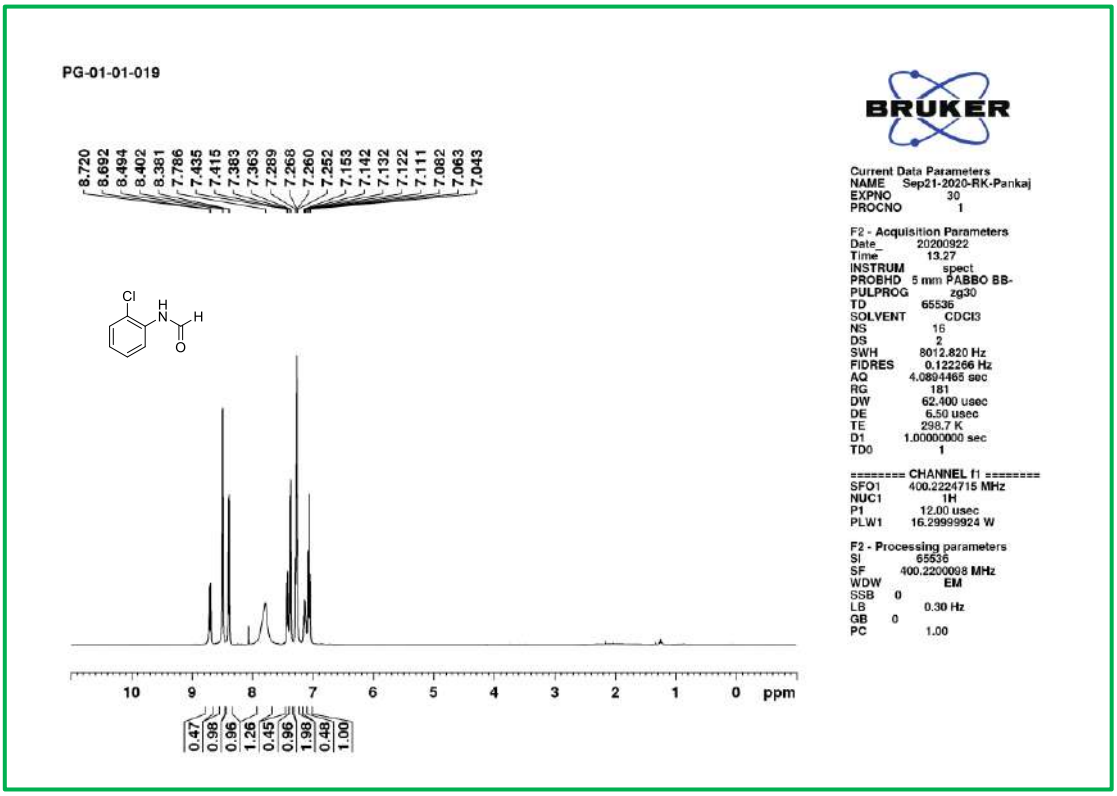

^{1}H NMR spectra of **3a.**

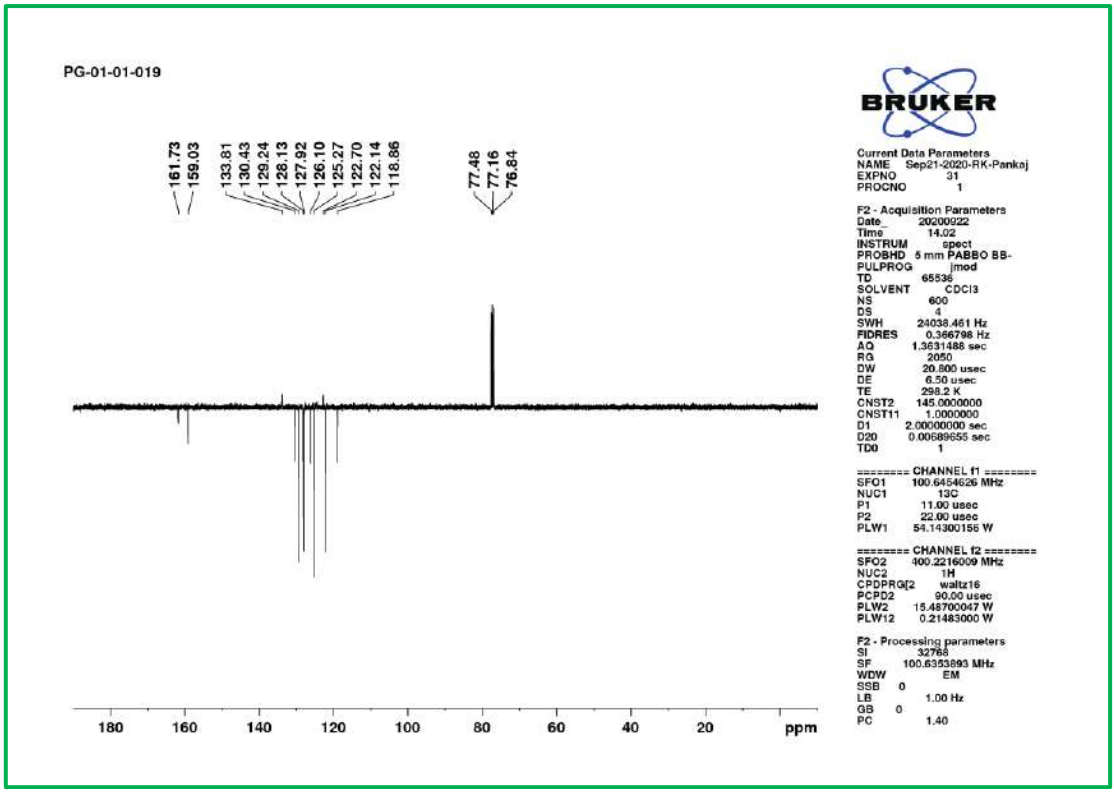

^{13}C NMR spectra of **3a.**

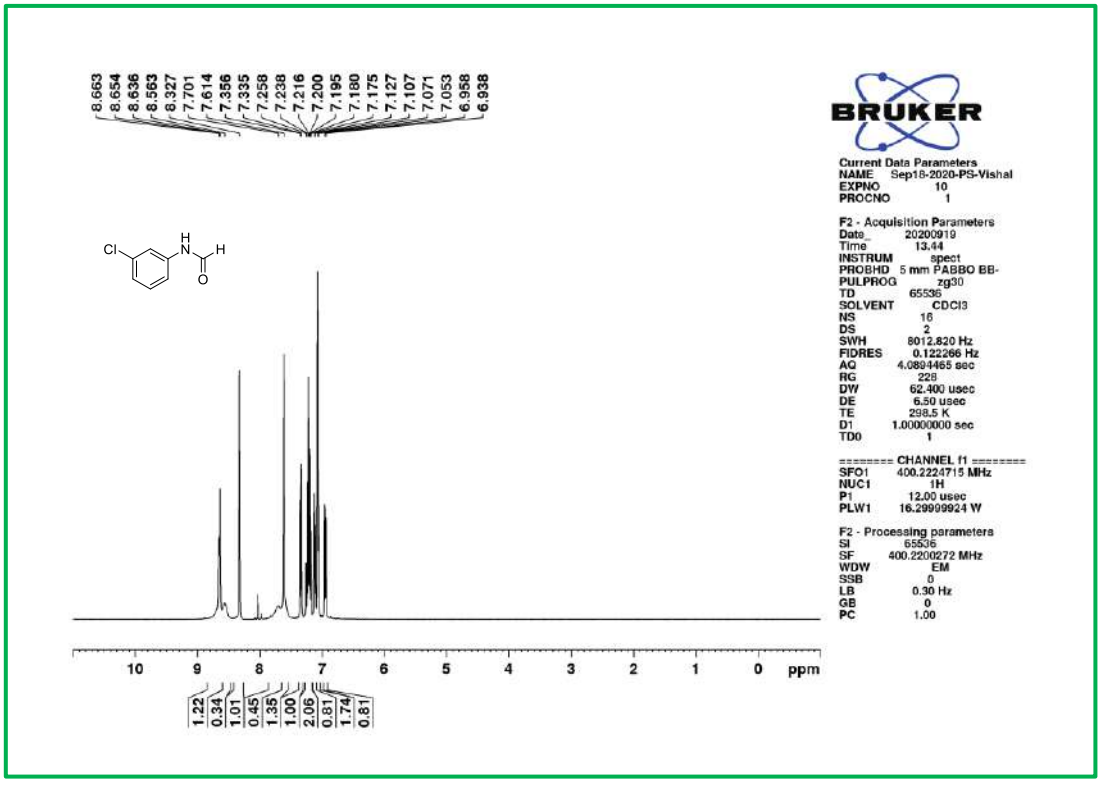

^{1}H NMR spectra of **3b.**

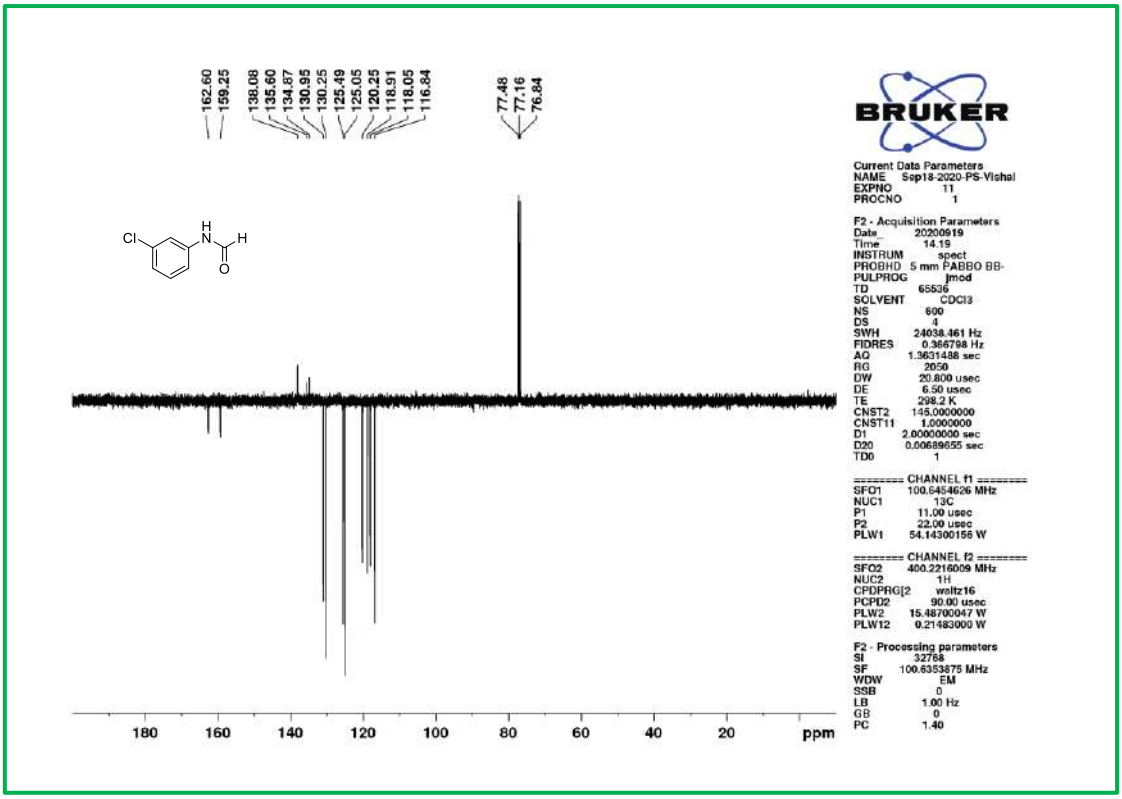

^{13}C NMR spectra of **3b.**

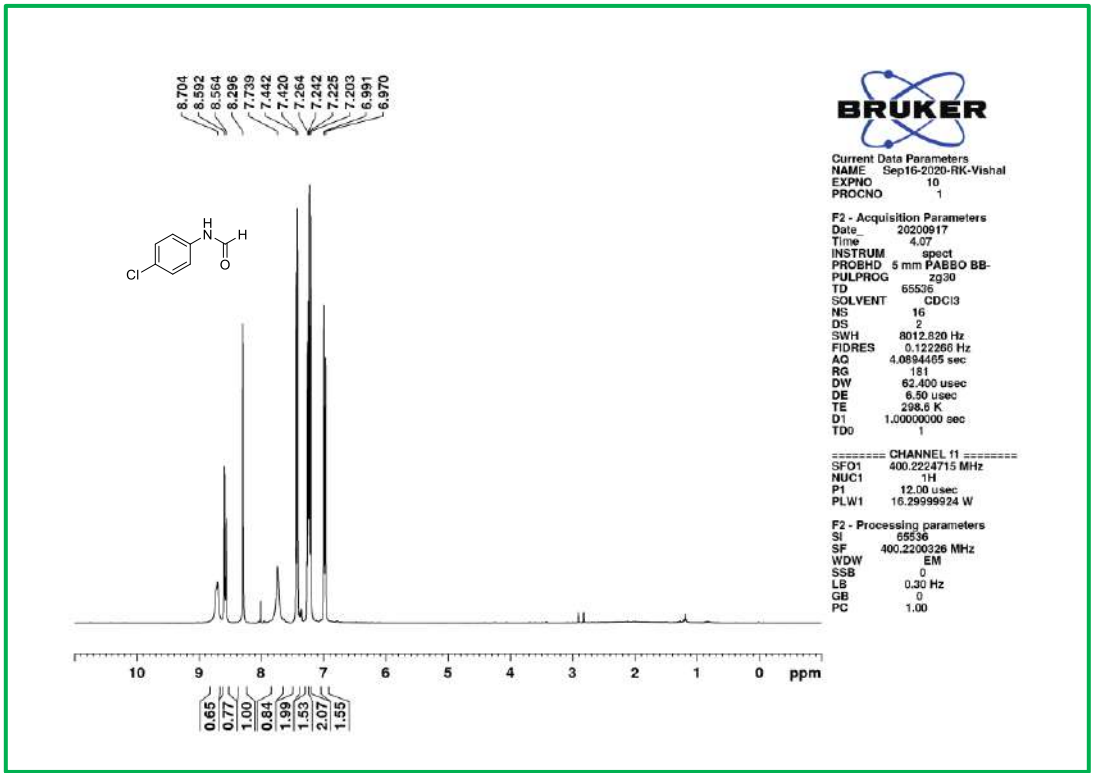

^{1}H NMR spectra of **3c.**

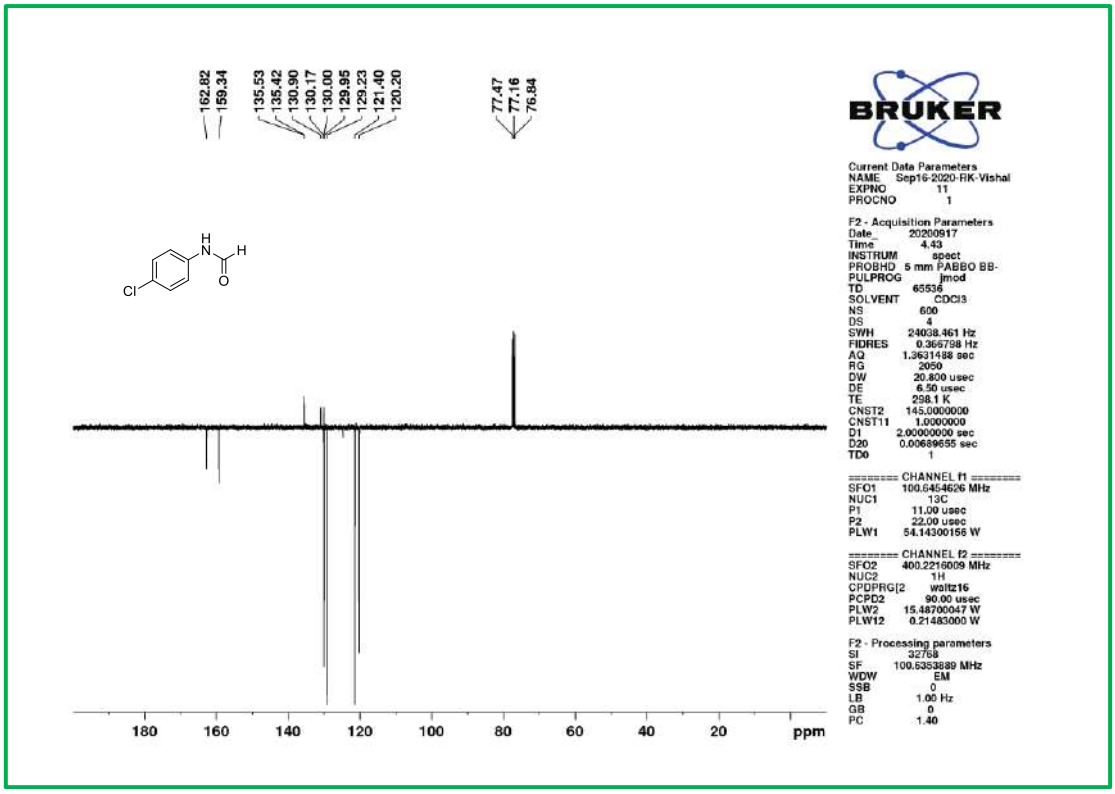

^{13}C NMR spectra of **3c.**

^{1}H NMR spectra of **3d** is similar to 3g, Scheme 3 and Chapter 3**.**

^{13}C NMR spectra of **3d** is similar to 3g, Scheme 3 and Chapter 3**.**

^{1}H NMR spectra of **3e** is similar to 3f, Scheme 3 and Chapter 3**.**

^{13}C NMR spectra of **3e** is similar to 3f, Scheme 3 and Chapter 3**.**

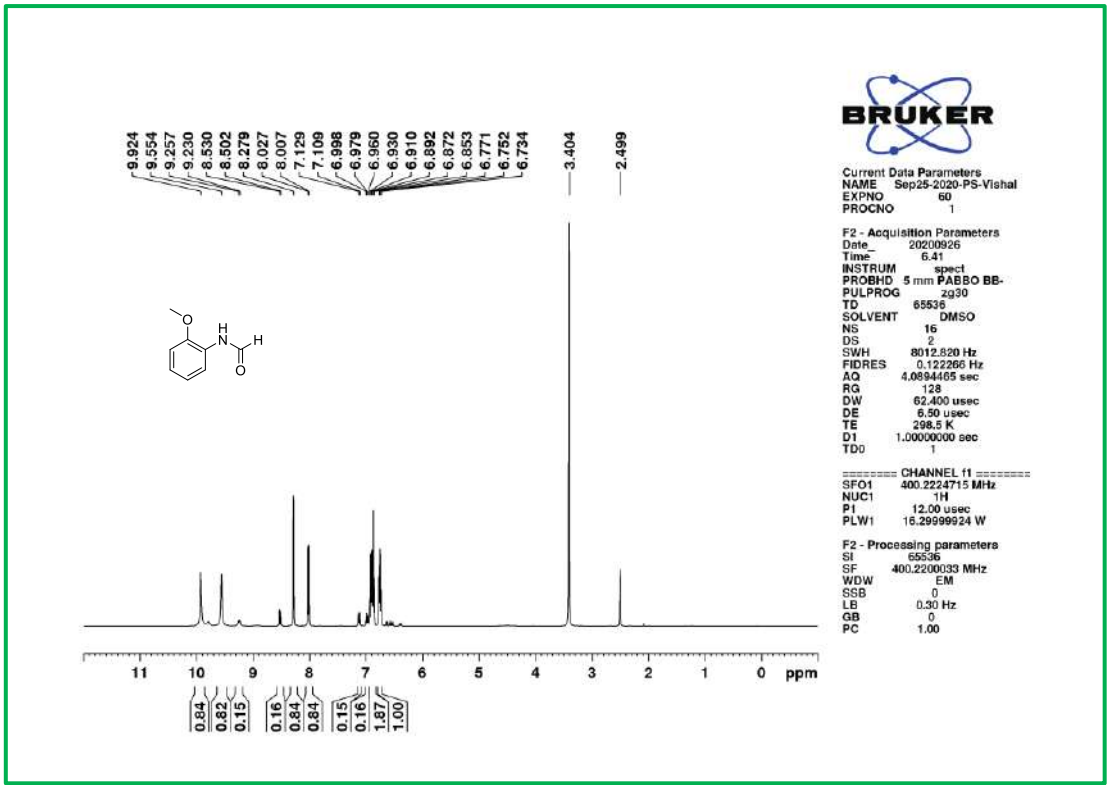

^{1}H NMR spectra of **3f.**

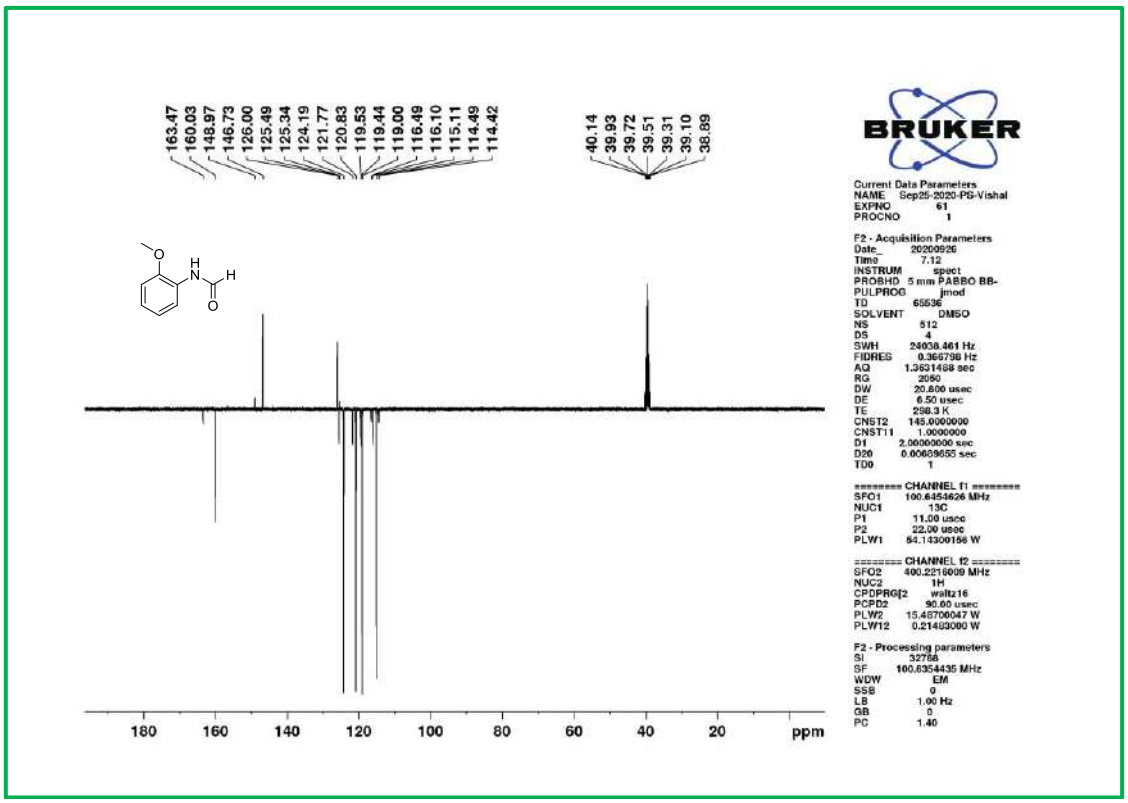

^{13}C NMR spectra of **3f.**

^{1}H NMR spectra of **3g** is similar to 3e, Scheme 3 and Chapter 3**.**

^{13}C NMR spectra of **3g** is similar to 3e, Scheme 3 and Chapter 3**.**

^{1}H NMR spectra of **3h** is similar to 3a, Scheme 3 and Chapter 3**.**

^{13}C NMR spectra of **3h** is similar to 3a, Scheme 3 and Chapter 3**.**

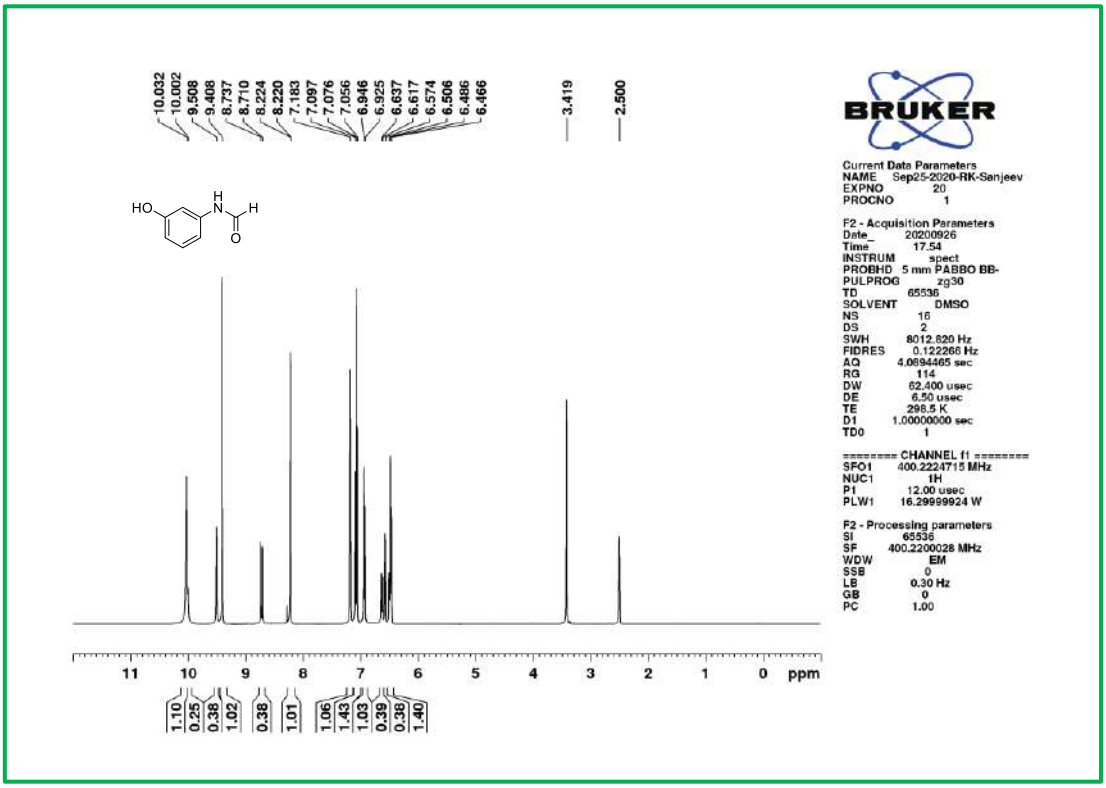

^{1}H NMR spectra of **3i.**

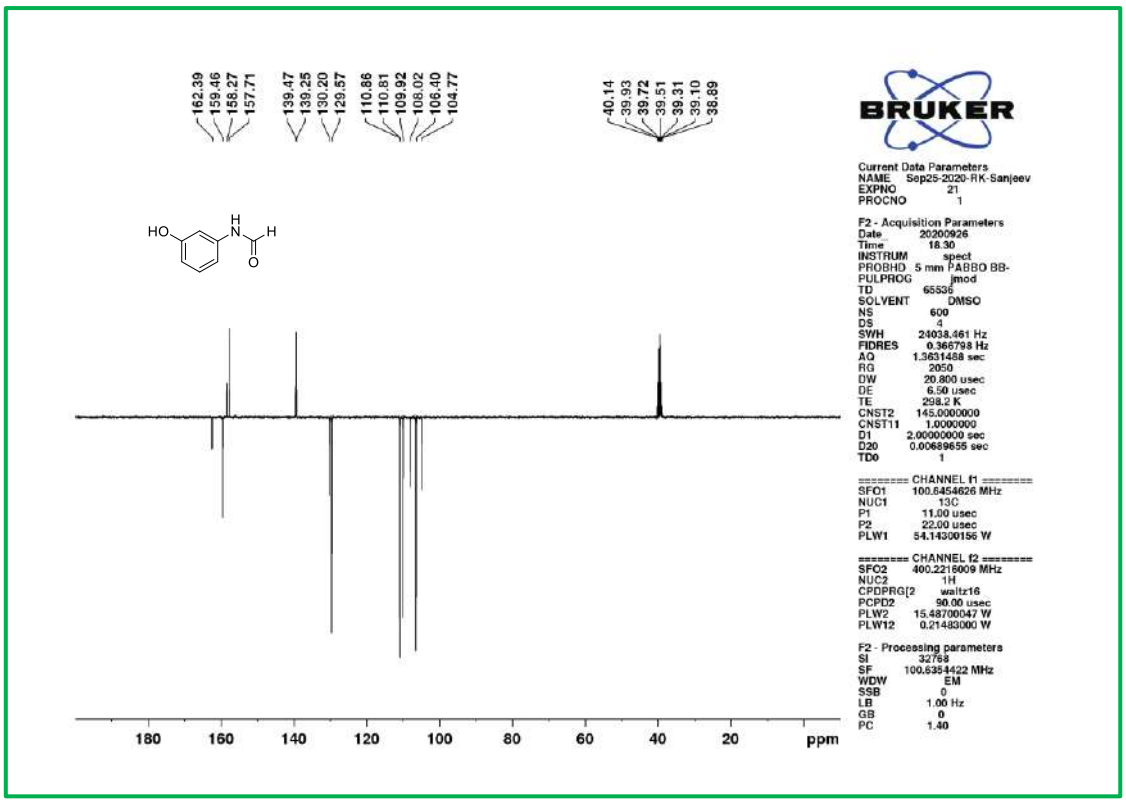

^{13}C NMR spectra of **3i.**

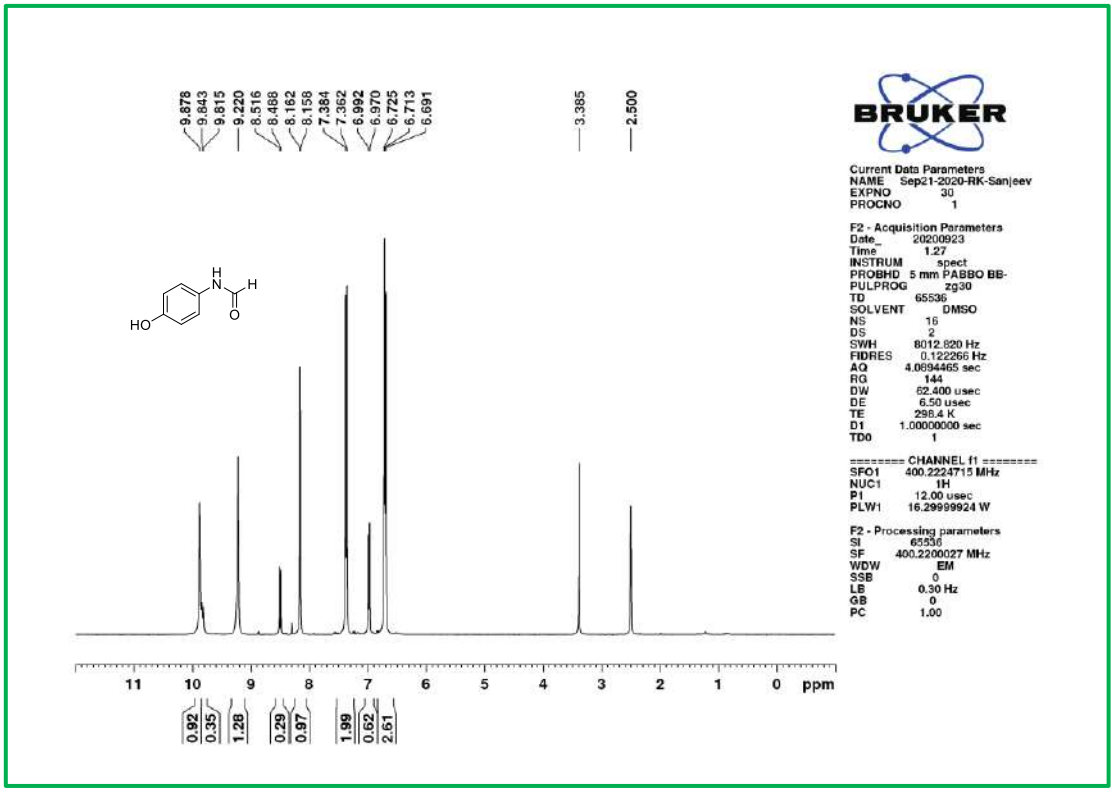

^{1}H NMR spectra of **3j.**

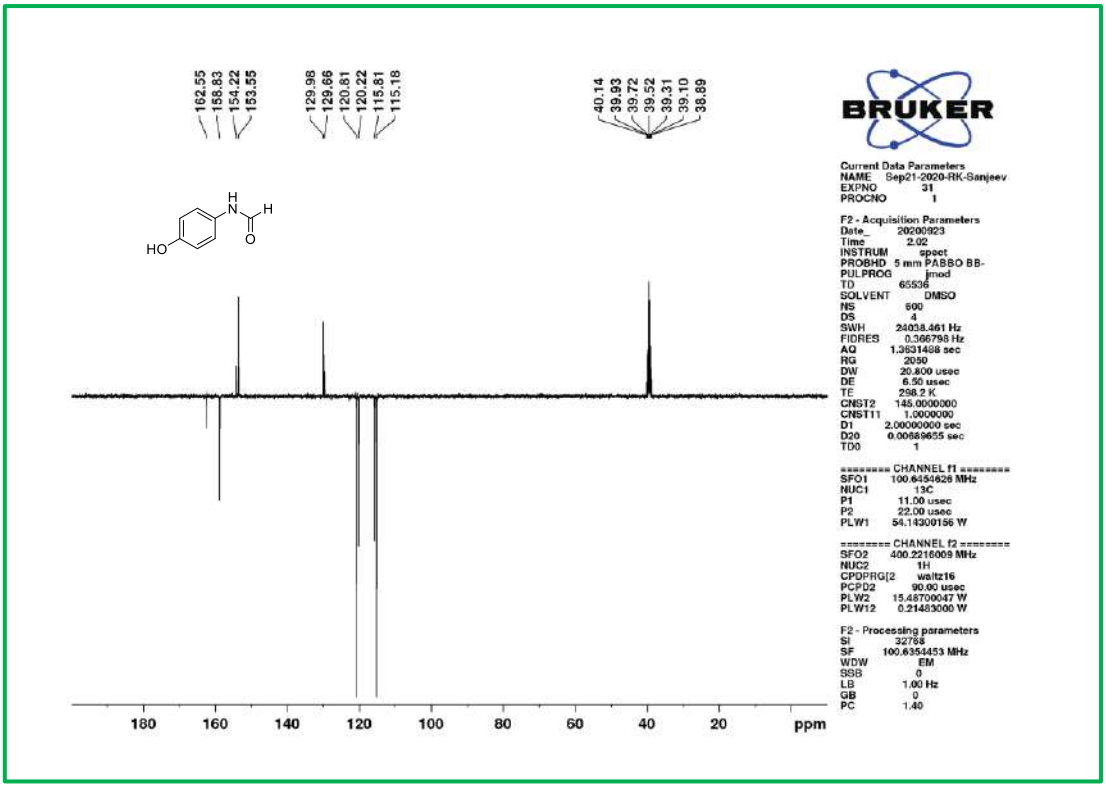

^{13}C NMR spectra of **3j.**

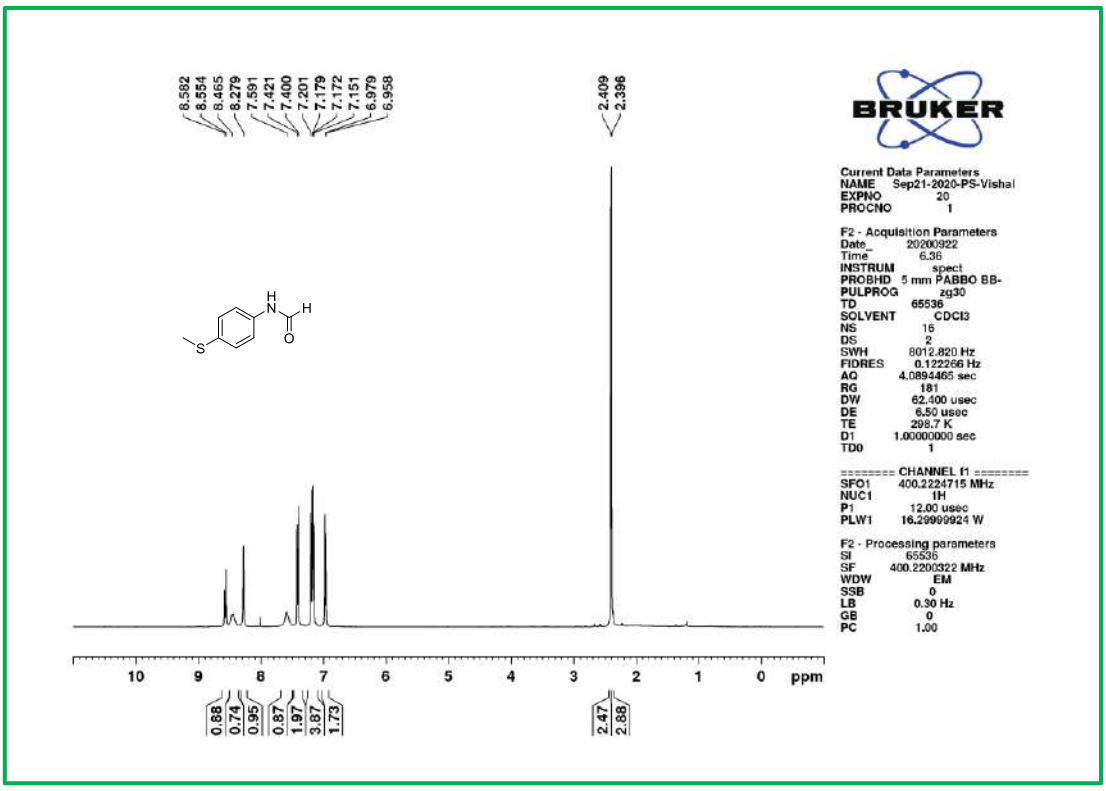

^{1}H NMR spectra of **3k.**

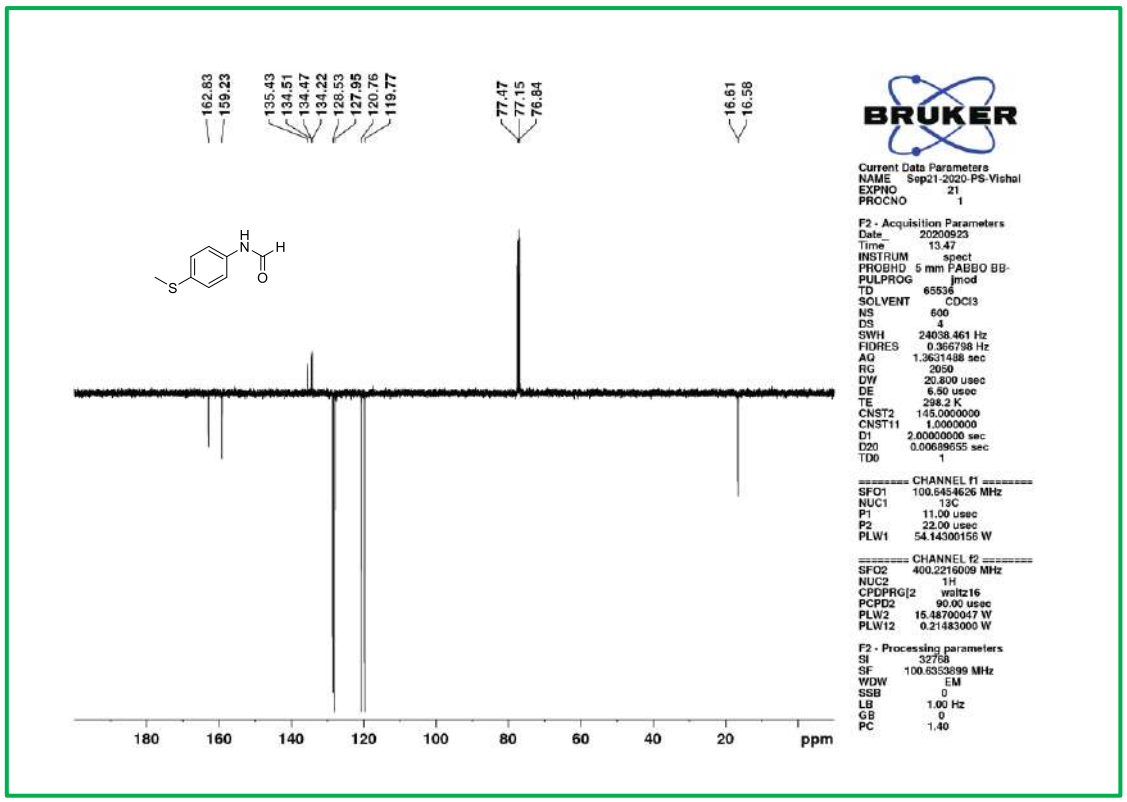

^{13}C NMR spectra of **3k.**

^{1}H NMR spectra of **3l** is similar to 3p, Scheme 3 and Chapter 3**.**

^{13}C NMR spectra of **3l** is similar to 3p, Scheme 3 and Chapter 3**.**

^{1}H NMR spectra of **3m** is similar to 3s, Scheme 3 and Chapter 3**.**

^{13}C NMR spectra of **3m** is similar to 3s, Scheme 3 and Chapter 3**.**

^{1}H NMR spectra of **3n** is similar to 3r, Scheme 3 and Chapter 3**.**

^{13}C NMR spectra of **3n** is similar to 3r, Scheme 3 and Chapter 3**.**

^{1}H NMR spectra of **3o** is similar to 3u, Scheme 3 and Chapter 3**.**

^{13}C NMR spectra of **3o** is similar to 3u, Scheme 3 and Chapter 3**.**

^{1}H NMR spectra of **3p** is similar to 3t, Scheme 3 and Chapter 3**.**

^{13}C NMR spectra of **3p** is similar to 3t, Scheme 3 and Chapter 3**.**

^{1}H NMR spectra of **3q** is similar to 3h, Scheme 3 and Chapter 3**.**

^{13}C NMR spectra of **3q** is similar to 3h, Scheme 3 and Chapter 3**.**

^{1}H NMR spectra of **3r** is similar to 3l, Scheme 3 and Chapter 3**.**

^{13}C NMR spectra of **3r** is similar to 3l, Scheme 3 and Chapter 3**.**

^{1}H NMR spectra of **3s** is similar to 3k, Scheme 3 and Chapter 3**.**

^{13}C NMR spectra of **3s** is similar to 3k, Scheme 3 and Chapter 3**.**

^{1}H NMR spectra of **3t** is similar to 3i, Scheme 3 and Chapter 3**.**

^{13}C NMR spectra of **3t** is similar to 3i, Scheme 3 and Chapter 3**.**

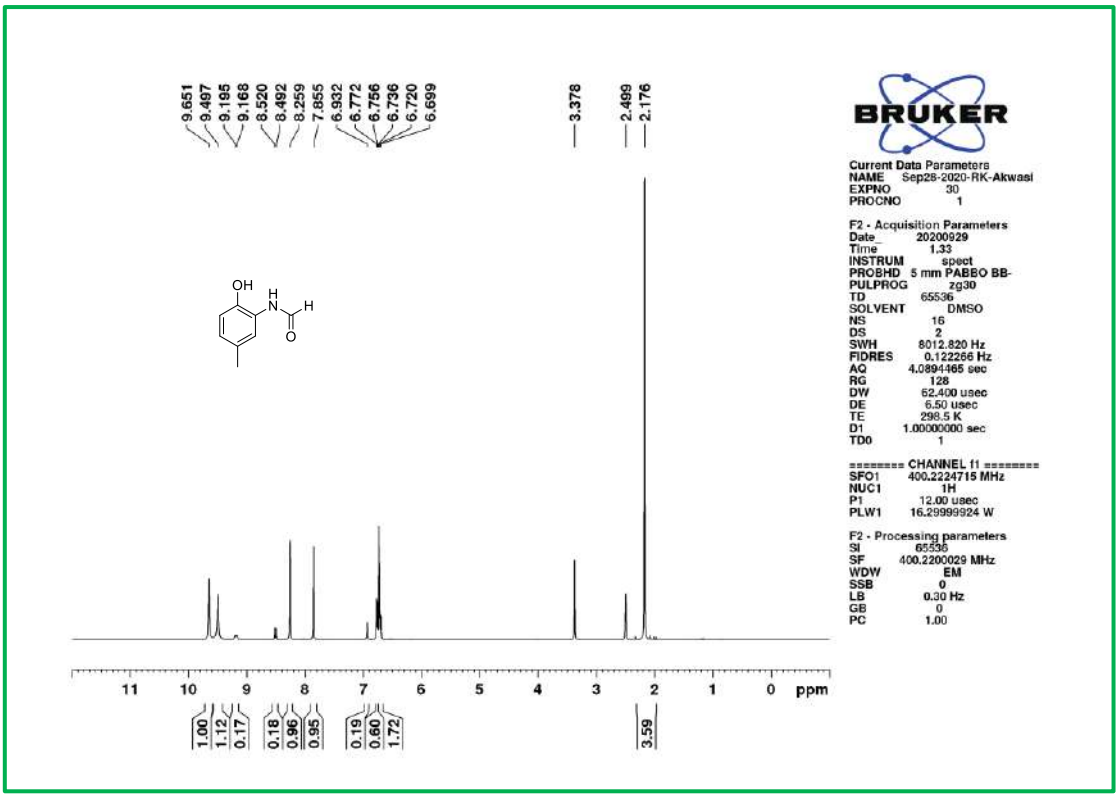

^{1}H NMR spectra of **3u.**

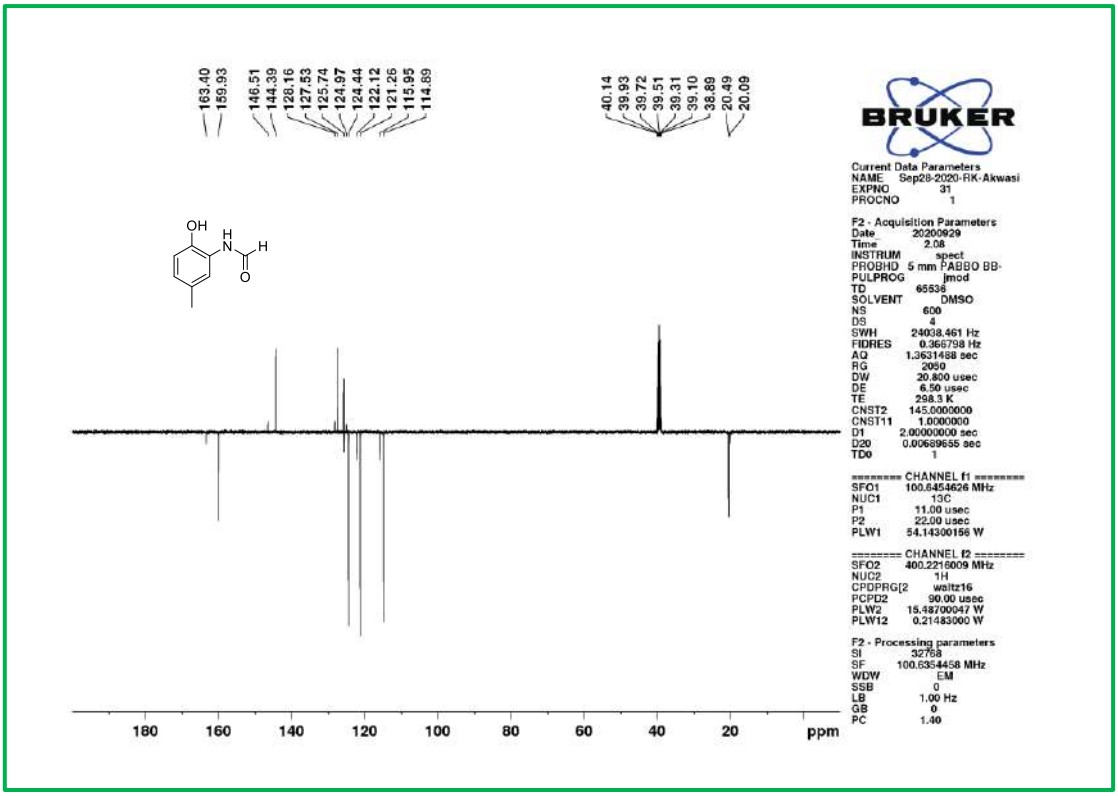

^{13}C NMR spectra of **3u.**

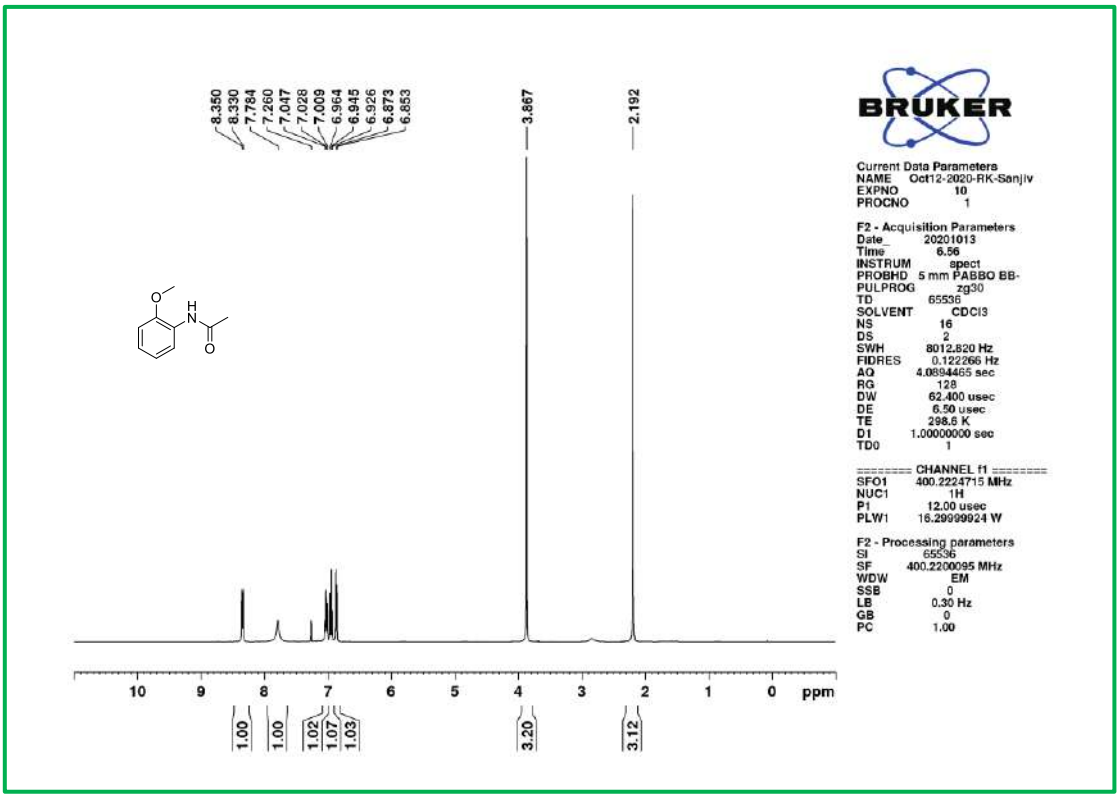

^{1}H NMR spectra of **3v.**

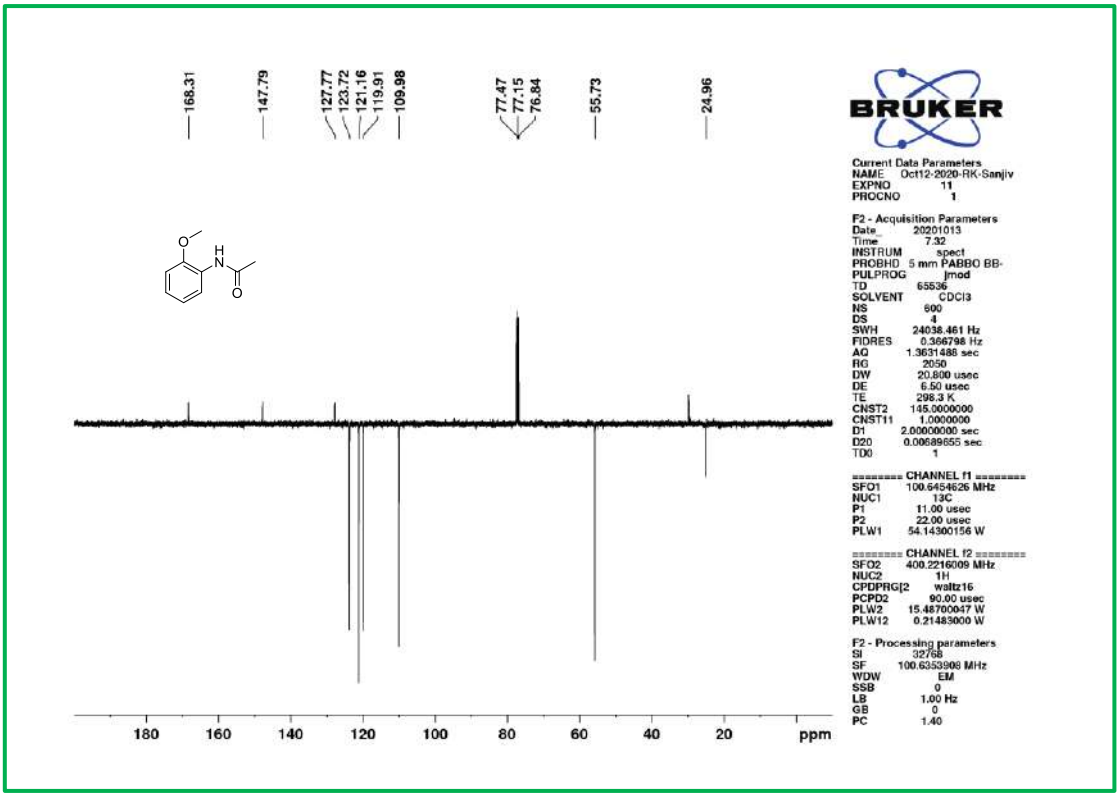

^{13}C NMR spectra of **3v.**

^{1}H NMR spectra of **3w** is similar to 4e, Scheme 3 and Chapter 3**.**

^{13}C NMR spectra of **3w** is similar to 4e, Scheme 3 and Chapter 3**.**

^{1}H NMR spectra of **3x** is similar to 4f, Scheme 3 and Chapter 3**.**

^{13}C NMR spectra of **3x** is similar to 4f, Scheme 3 and Chapter 3**.**

^{1}H NMR spectra of **3y** is similar to 4g, Scheme 3 and Chapter 3**.**

^{13}C NMR spectra of **3y** is similar to 4g, Scheme 3 and Chapter 3**.**

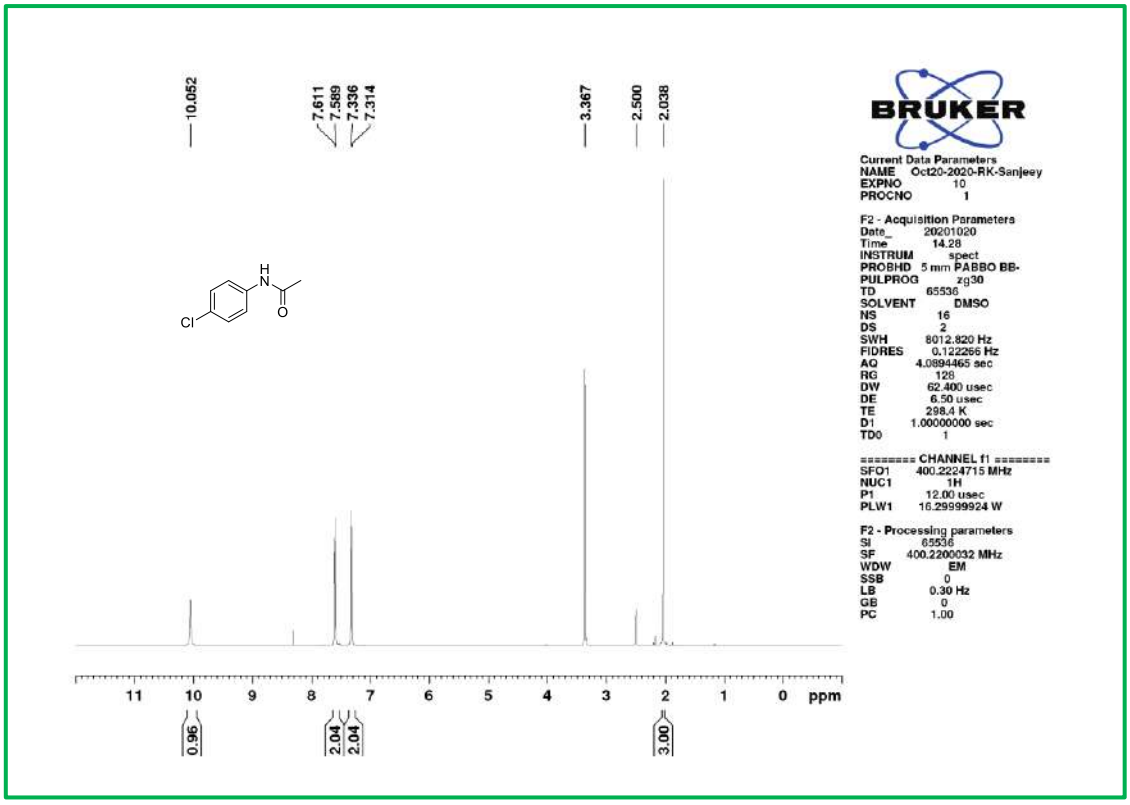

^{1}H NMR spectra of **3z.**

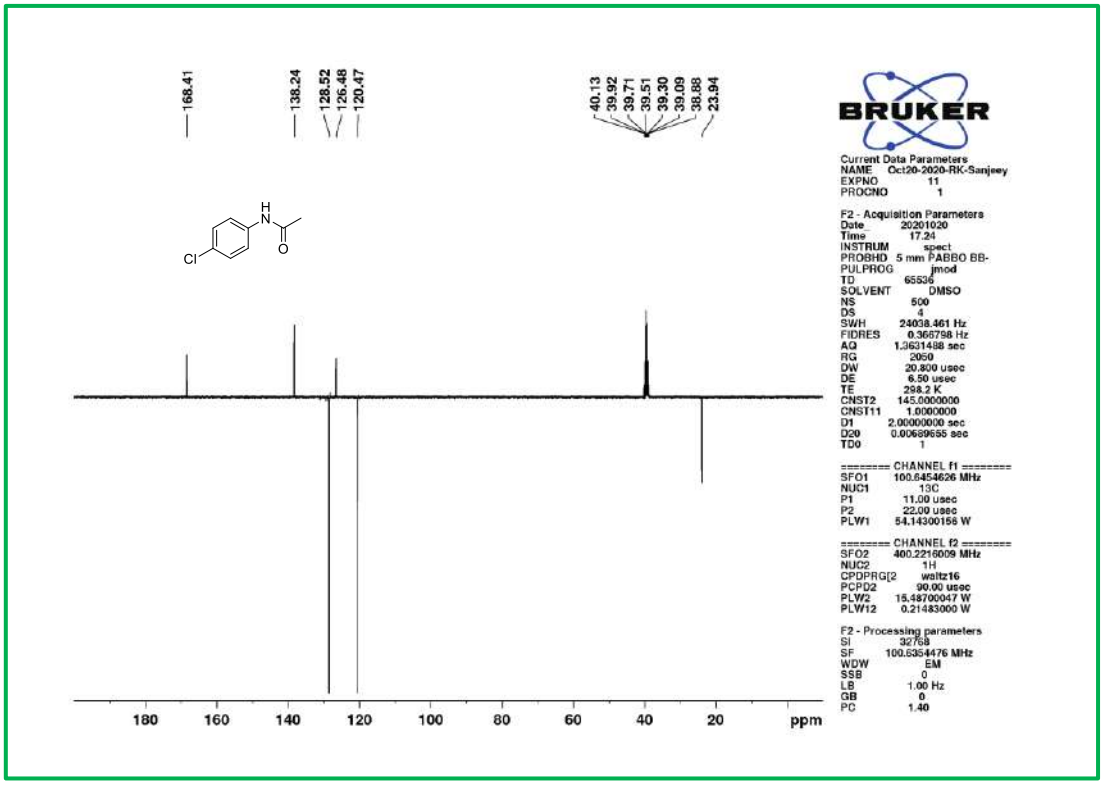

^{13}C NMR spectra of **3z.**

^{1}H NMR spectra of **3aa** is similar to 4h, Scheme 3 and Chapter 3**.**

^{13}C NMR spectra of **3aa** is similar to 4h, Scheme 3 and Chapter 3**.**

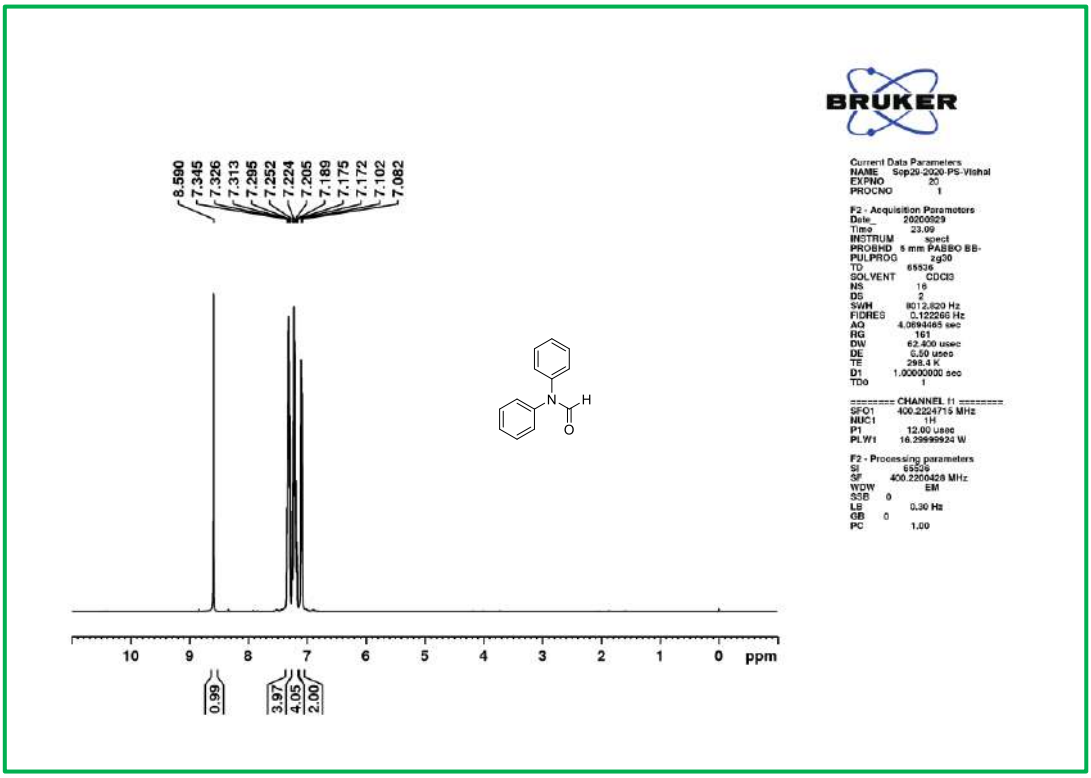

^{1}H NMR spectra of **3ab.**

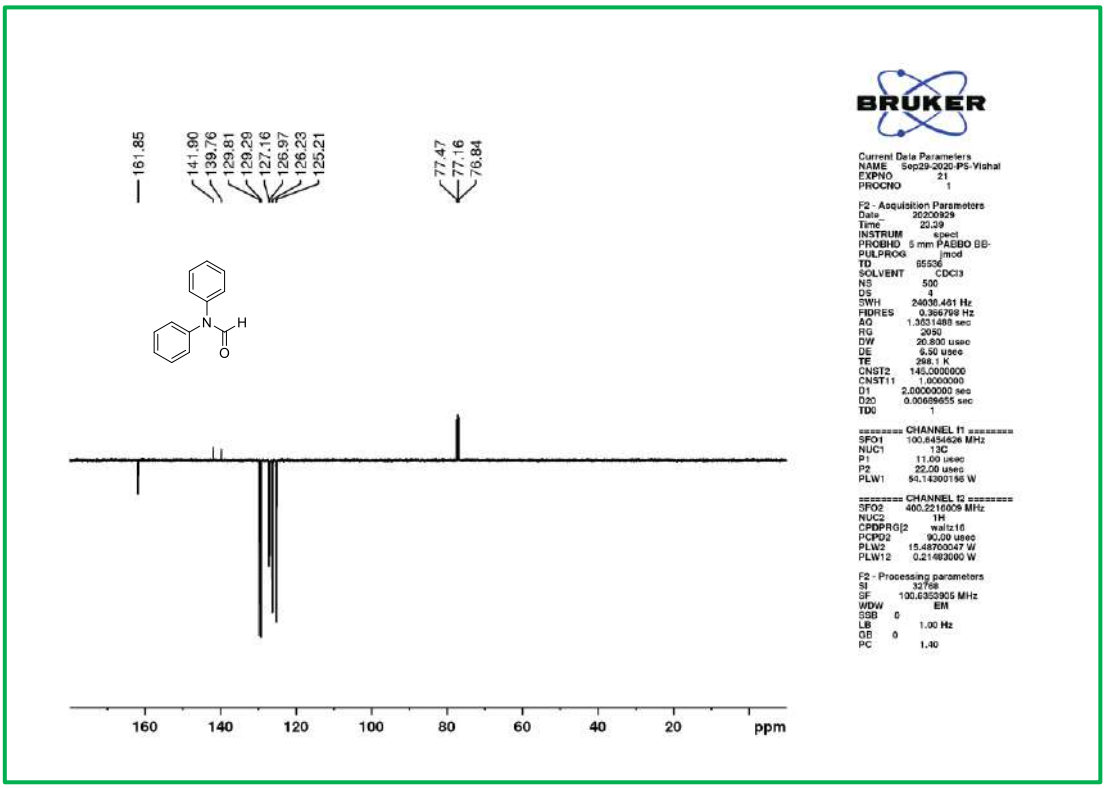

^{13}C NMR spectra of **3ab.**

^{1}H NMR spectra of **3ac** is similar to 4a, Scheme 3 and Chapter 3**.**

^{13}C NMR spectra of **3ac** is similar to 4a, Scheme 3 and Chapter 3**.**

^{1}H NMR spectra of **3ad** is similar to 3d, Scheme 3 and Chapter 3**.**

^{13}C NMR spectra of **3ad** is similar to 3d, Scheme 3 and Chapter 3**.**

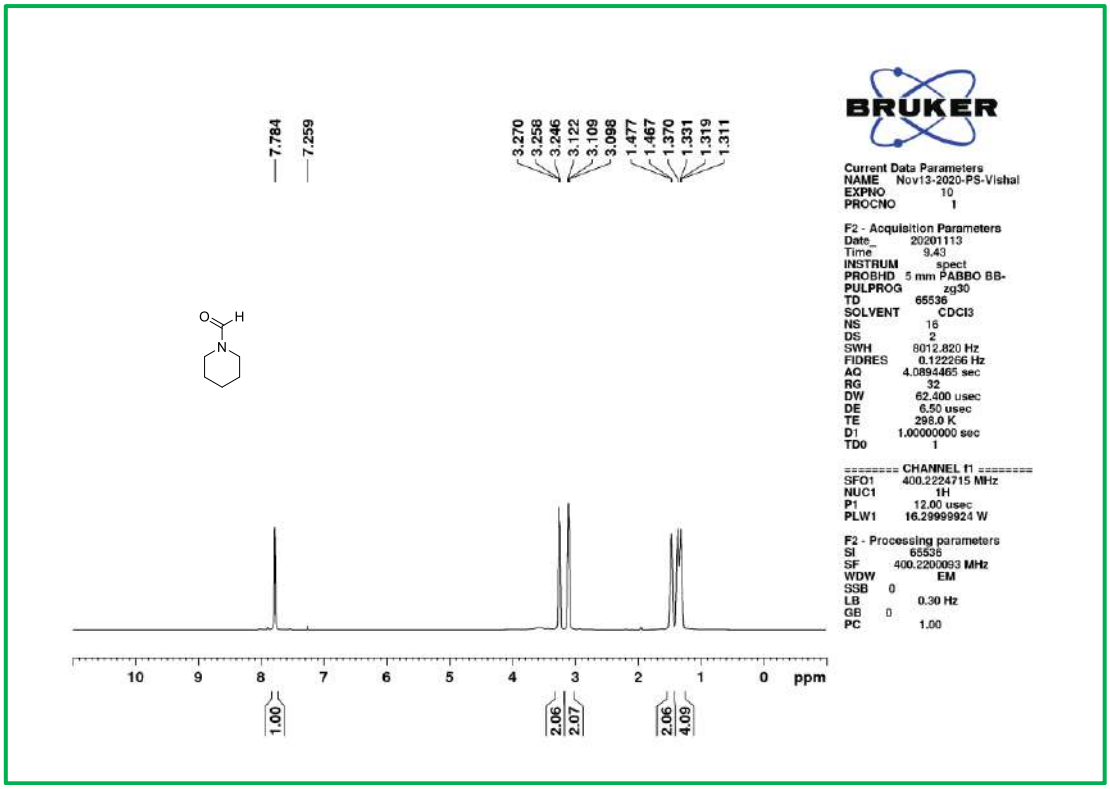

^{1}H NMR spectra of **3ae.**

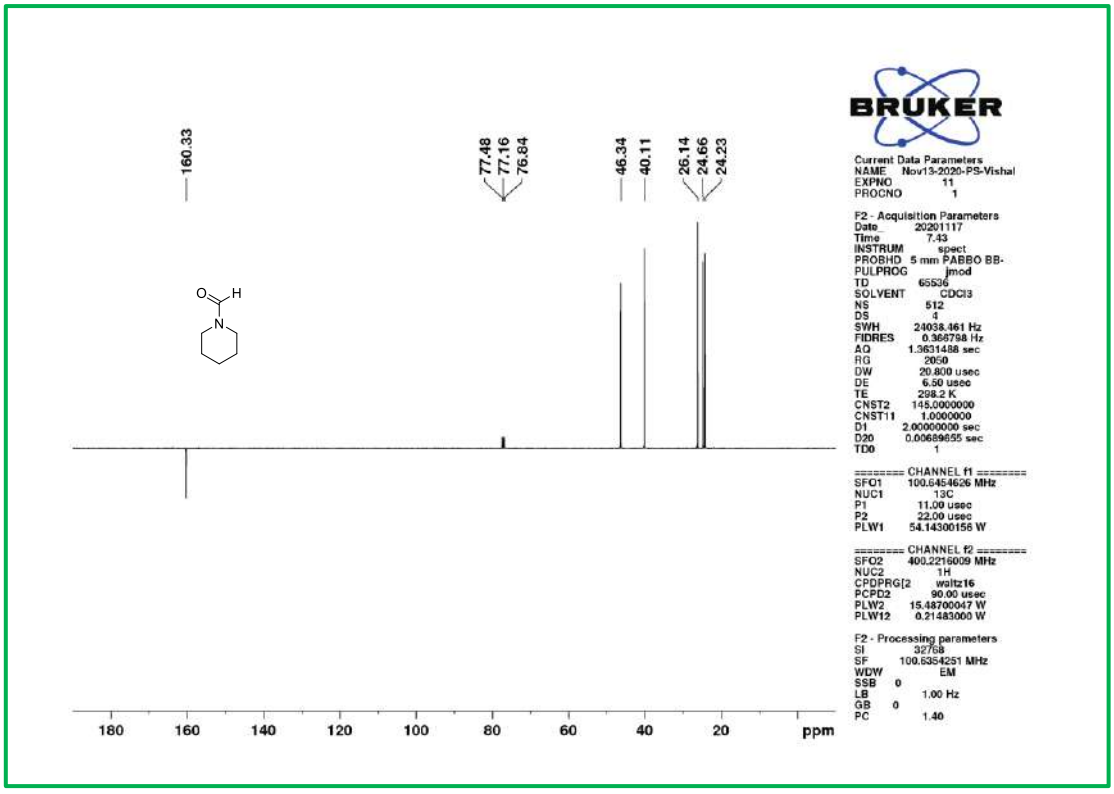

^{13}C NMR spectra of **3ae.**

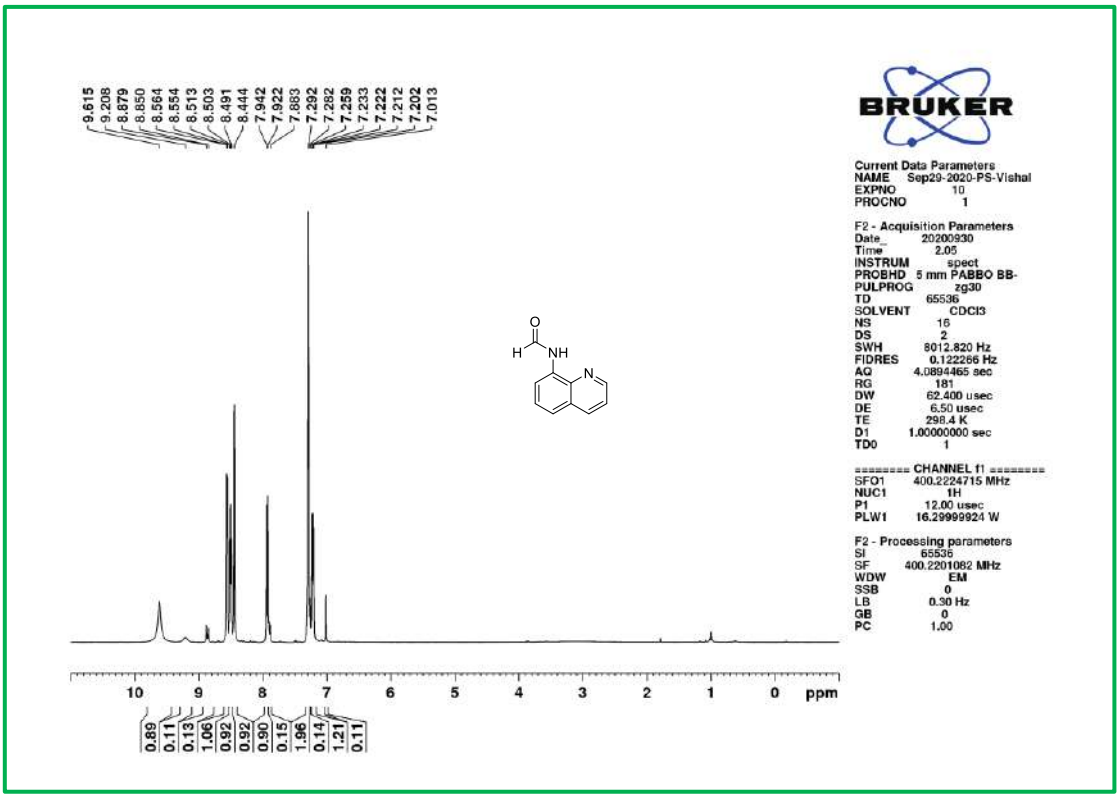

^{1}H NMR spectra of **3af.**

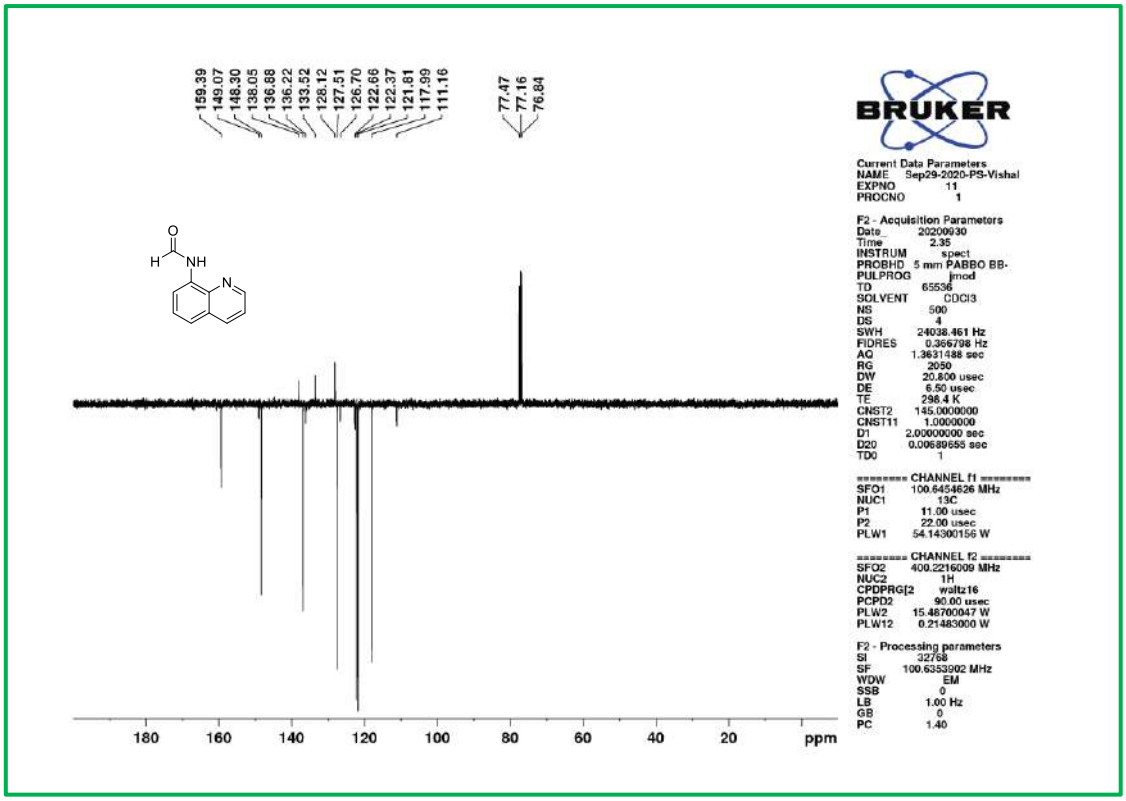

^{13}C NMR spectra of **3af.**

^{1}H NMR spectra of **3ag** is similar to 3b, Scheme 3 and Chapter 3**.**

^{13}C NMR spectra of **3ag** is similar to 3b, Scheme 3 and Chapter 3**.**

^{1}H NMR spectra of **6a** is similar to 3h, Table 2 and Chapter 4**.**

^{13}C NMR spectra of **6a** is similar to 3h, Table 2 and Chapter 4**.**

^{1}H NMR spectra of **6b** is similar to 3i, Table 2 and Chapter 4**.**

^{13}C NMR spectra of **6b** is similar to 3i, Table 2 and Chapter 4**.**

^{1}H NMR spectra of **6c** is similar to 3j, Table 2 and Chapter 4**.**

^{13}C NMR spectra of **6c** is similar to 3j, Table 2 and Chapter 4**.**

^{1}H NMR spectra of **6d** is similar to 3k, Table 2 and Chapter 4**.**

^{13}C NMR spectra of **6d** is similar to 3k, Table 2 and Chapter 4**.**

^{1}H NMR spectra of **6e** is similar to 3p, Table 2 and Chapter 4**.**

^{13}C NMR spectra of **6e** is similar to 3p, Table 2 and Chapter 4**.**

^{1}H NMR spectra of **6f** is similar to 3r, Table 2 and Chapter 4**.**

^{13}C NMR spectra of **6f** is similar to 3r, Table 2 and Chapter 4**.**

^{1}H NMR spectra of **6g** is similar to 3l, Table 2 and Chapter 4**.**

^{13}C NMR spectra of **6g** is similar to 3l, Table 2 and Chapter 4**.**

^{1}H NMR spectra of **6h** is similar to 3m, Table 2 and Chapter 4**.**

^{13}C NMR spectra of **6h** is similar to 3m, Table 2 and Chapter 4**.**

^{1}H NMR spectra of **6i** is similar to 3s, Table 2 and Chapter 4**.**

^{13}C NMR spectra of **6i** is similar to 3s, Table 2 and Chapter 4**.**

^{1}H NMR spectra of **6j** is similar to 3n, Table 2 and Chapter 4**.**

^{13}C NMR spectra of **6j** is similar to 3n, Table 2 and Chapter 4**.**

^{1}H NMR spectra of **6k** is similar to 3o, Table 2 and Chapter 4**.**

^{13}C NMR spectra of **6k** is similar to 3o, Table 2 and Chapter 4**.**

^{1}H NMR spectra of **6l** is similar to 3e, Table 2 and Chapter 4**.**

^{13}C NMR spectra of **6l** is similar to 3e, Table 2 and Chapter 4**.**

^{1}H NMR spectra of **6m** is similar to 3d, Table 2 and Chapter 4**.**

^{13}C NMR spectra of **6m** is similar to 3d, Table 2 and Chapter 4**.**

^{1}H NMR spectra of **6n** is similar to 3f, Table 2 and Chapter 4**.**

^{13}C NMR spectra of **6n** is similar to 3f, Table 2 and Chapter 4**.**

^{1}H NMR spectra of **6o** is similar to 3b, Table 2 and Chapter 4**.**

^{13}C NMR spectra of **6o** is similar to 3b, Table 2 and Chapter 4**.**

^{1}H NMR spectra of **6p** is similar to 3a, Table 2 and Chapter 4**.**

^{13}C NMR spectra of **6p** is similar to 3a, Table 2 and Chapter 4**.**

^{1}H NMR spectra of **6q** is similar to 3c, Table 2 and Chapter 4**.**

^{13}C NMR spectra of **6q** is similar to 3c, Table 2 and Chapter 4**.**

^{1}H NMR spectra of **6r** is similar to 3g, Table 2 and Chapter 4**.**

^{13}C NMR spectra of **6r** is similar to 3g, Table 2 and Chapter 4**.**

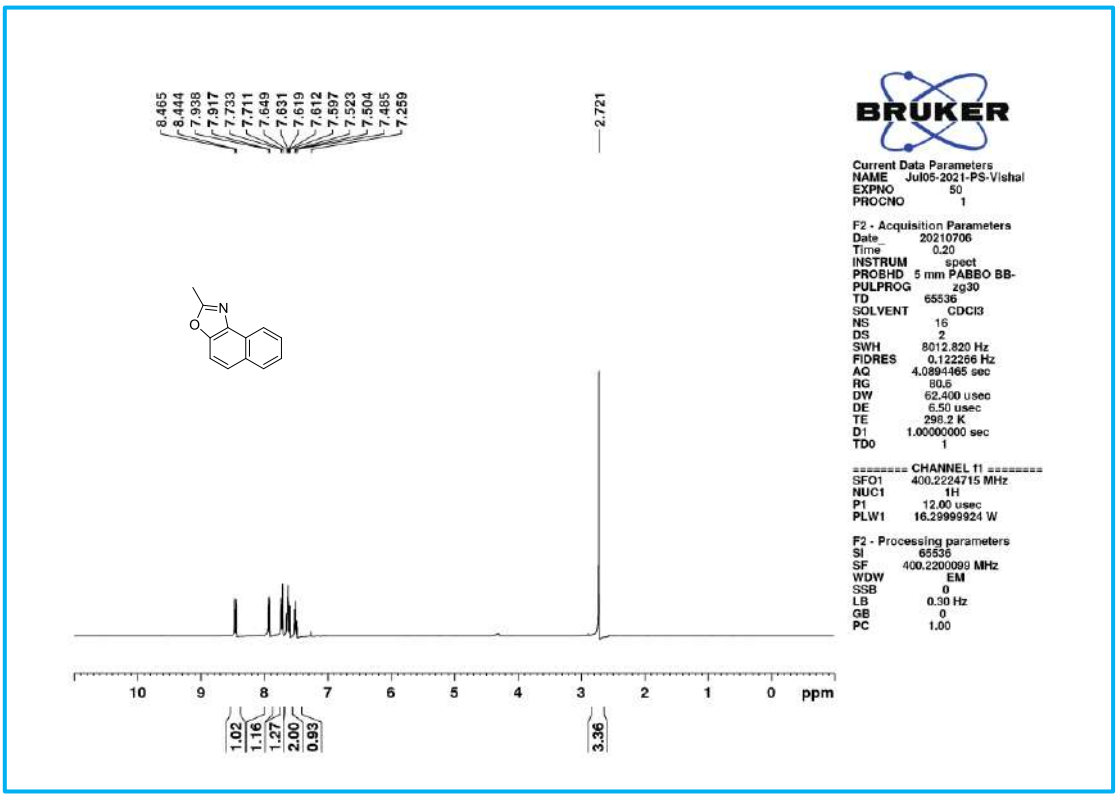

^{1}H NMR spectra of **6s.**

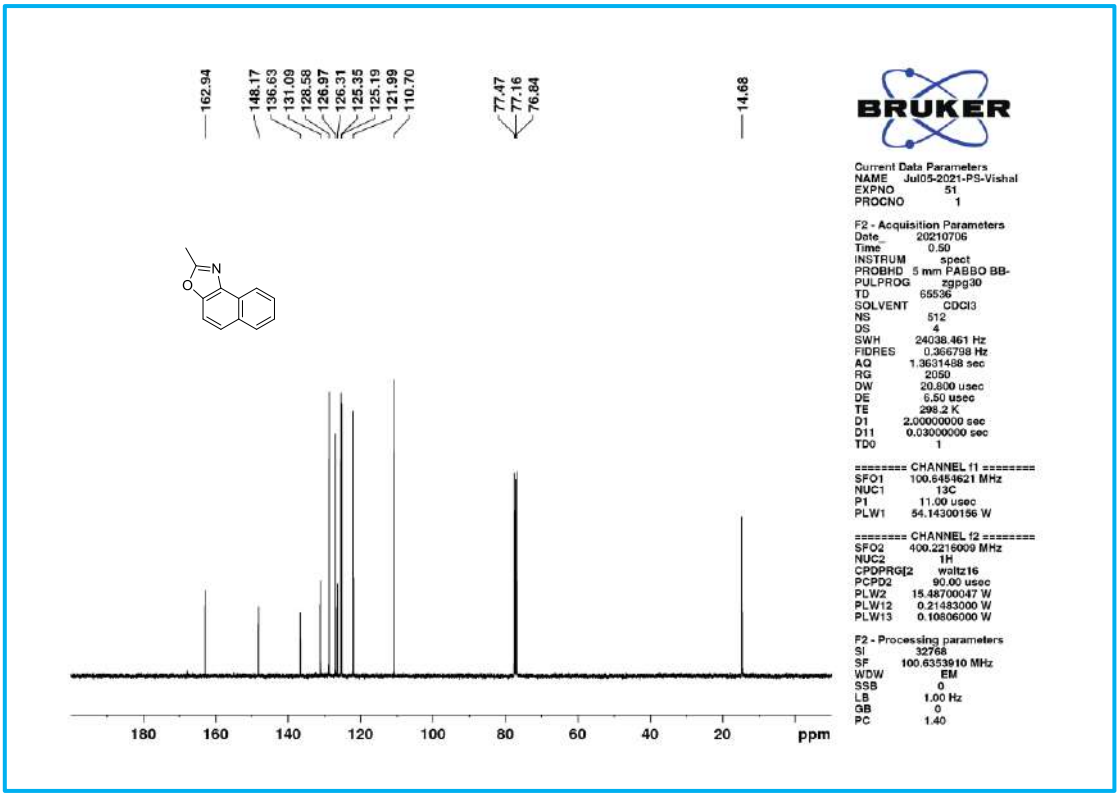

^{13}C NMR spectra of **6s.**

^{1}H NMR spectra of **6t** is similar to 5a, Scheme 3 and Chapter 4**.**

^{13}C NMR spectra of **6t** is similar to 5a, Scheme 3 and Chapter 4**.**

^{1}H NMR spectra of **6u** is similar to 5b, Scheme 3 and Chapter 4**.**

^{13}C NMR spectra of **6u** is similar to 5b, Scheme 3 and Chapter 4**.**

APPENDIX-IV

Published Articles

EurJOC
European Journal of Organic Chemistry

Full Papers
doi.org/10.1002/ejoc.202101114

Chemistry Europe
European Chemical Societies Publishing

Special Collection

An Environmentally Benign, Catalyst-Free N–C Bond Cleavage/Formation of Primary, Secondary, and Tertiary Unactivated Amides

Vishal Kumar,[a] Sanjeev Dhawan,[a] Pankaj Sanjay Girase,[a] Parvesh Singh,[b] and Rajshekhar Karpoormath*[a]

Herein, we report an operationally simple, cheap, and catalyst-free method for the transamidation of a diverse range of unactivated amides furnishing the desired products in excellent yields. This protocol is environmentally friendly and operates under extremely mild conditions without using any promoter or additives. Significantly, this strategy has been implied in the chemoselective synthesis of a pharmaceutical molecule, paracetamol, on a gram-scale with excellent yield. We anticipate that this universally applicable strategy will be of great interest in drug discovery, biochemistry, and organic synthesis.

Introduction

In chemistry and biology, the amide bond is the most fundamental functional group.[1] The amide linkages are widely used in the organic synthesis of pharmaceuticals,[2a] natural products,[2b] pesticides,[2c] polymers[2d] and biologically relevant molecules.[2e] Recent studies signify that the amide bond is prevalent in 25% of pharmaceuticals,[3] whereas amidation reactions depict the most common reaction conducted to synthesise new drugs.[4] In particular, amide bonds are the most prevalent form of bond found in various drugs, such as formoterol, tetrahydrolipstatin, leucovorin, penicillin G, lacosamide, and paracetamol (Figure 1). As a consequence of the prevalence of amide bonds, novel methods for the synthesis of amides significantly impact every branch of organic chemistry.[4]

Transamidation has recently garnered significant interest from a variety of research groups.[5] However, due to the amide bond's stability, various catalysts or activating agents are used for the transamidation of amines.[6] Several transition-metal based catalytic systems employed in the transamidation reactions *viz*: Pd,[7a] Ni[7b] (Scheme 1B), Fe,[7c] Cu,[7d] Mn,[7e] lanthanides,[8a] Ti,[8b] Zr,[8c] Al,[8d] and sulfated tungstate[8e] are widely used in academia and industry for the preparation of amides.[9] Additionally, metal-catalysed reactions are undesirable due to waste metal and increasing synthetic costs. Despite these challenges, numerous discoveries in metal-free approaches have been reported, including the use of benzotriazole, boric acid derivatives,[10a] chitosan,[10b] *N,N*-di-alkyl formamide,[10c] hypervalent iodine,[11a] L-proline,[11b] hydroxylamine hydrochloride[11c] (Scheme 1A) and imidazole derivatives,[11d] as well as microwave irradiation processes. The Szostak group recently reported a LiHMDS promoted chemoselective transamidation of amides at room temperature through N–C (acyl) cleavage[12] (Scheme 1A). While these metal-free protocols have several benefits, some pitfalls remain, including the need for stoichiometric catalysts, low selectivity, and challenges with catalysts separation. Despite these breakthroughs, a realistic solution to the transamidation is only restricted to active 1° amides, while the challenging aliphatic 2° and 3° amides remained less exploited.[13] Recent advances, as reported, are incompatible with highly valuable less-nucleophilic amines and low reactive, secondary and tertiary amides under metal- or catalyst-free conditions.

In thinking through the consequences noted earlier, in this paper, we describe the successful realisation of a high-yielding transition metal-free strategy for transamidation reactions using amine hydrochloride salts and unactivated amide derivatives as carbonyl sources (Scheme 1C) *via* highly selective N–C bond cleavage. The protocol is extremely versatile across a wide variety of structurally diverse substrates (>60 examples) and operationally easy and cost-effective due to the absence of an acid, bases, catalyst, ligands, or other additives with prolonged reaction time. We believe that this straightforward N–C cleavage/formation will be of great interest, offers a robust approach to the classic problem of 2° and 3° unactivated aliphatic/aromatic amide transamidation, and it is expected that this work will influence future efforts to synthesise pharmaceuticals, natural products, and polymers.

[a] V. Kumar, Dr. S. Dhawan, P. S. Girase, Dr. R. Karpoormath
Department of Pharmaceutical Chemistry,
Discipline of Pharmaceutical Sciences, College of Health Sciences,
University of KwaZulu-Natal (Westville),
Durban-4000, South Africa
E-mail: karpoormath@ukzn.ac.za
[b] Prof. Dr. P. Singh
School of Chemistry and Physics,
University of KwaZulu-Natal,
P/Bag X54001, Westville, Durban-4000, South Africa

Supporting information for this article is available on the WWW under https://doi.org/10.1002/ejoc.202101114

This article belongs to the Joint Special Collection "Biological and Medicinal Chemistry in Africa".

EurJOC
European Journal of Organic Chemistry
Full Papers
doi.org/10.1002/ejoc.202101114
Chemistry Europe
European Chemical Societies Publishing

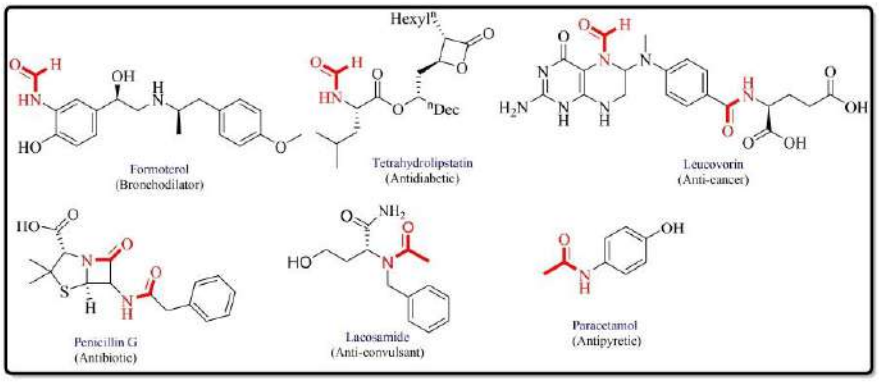

Figure 1. Marketed bioactive compounds with amide framework.

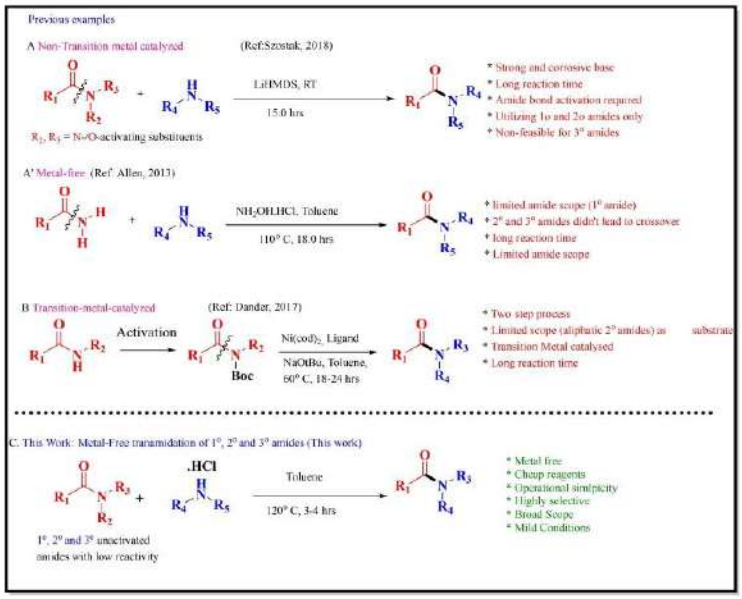

Scheme 1. LiHMDS, $NH_2OH.HCl$ and nickel-catalyzed transamidation reactions of amides with amines: previously reported protocols (**A**–**B**) and (**C**) This work, depicting transamidation using 1°, 2° and 3° unactivated amides.

Results and Discussion

We selected readily available formamide (**2o**) as a formyl source and *p*-anisidine (**1e**) as the reaction partners to initiate our studies. The outcomes are illustrated in Table 1. As previously shown in classical nucleophilic substitution reactions, solvent selection, temperature, acids, and time significantly impact yield. So initially, various commercially available acids such as trifluoroacetic acid, hydrochloric acid, sulphuric acid, acetic acid, and nitric acid (Table 1, entries 1–5) were investigated but revealed a decrease in yield when compared to HCl. Subsequently, we investigated transamidation in various organic solvents (Table 1, entries 6–10); however, toluene emerged as the most optimal solvent and provided the desired product **3e** in 97% yield (Table 1, entry 6). Moreover, an increase in the reaction time to 4 h does not affect the outcome of correspond-

EurJOC
European Journal of Organic Chemistry
Full Papers
doi.org/10.1002/ejoc.202101114
Chemistry Europe
European Chemical Societies Publishing

Table 1. Reaction conditions optimisation for *N*-Formylation of *p*-anisidine with formamide.

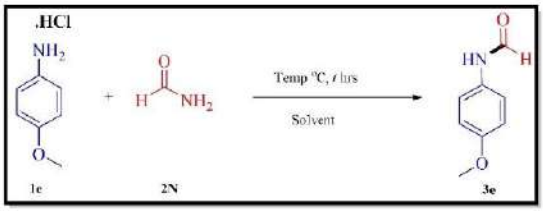

Acid Study

S.No.	Acid	Solvent [5.0 Vol]	Temp [°C]	Time [h]	[%] Yield[c]
1[a]	CF_3COOH	Toluene	120	4	**20**
2[a]	**HCl**	**Toluene**	**120**	**4**	**97**
3[a]	H_2SO_4	Toluene	120	4	**5**
4[a]	CH_3COOH	Toluene	120	4	**30**
5[a]	HNO_3	Toluene	120	4	**10**

Solvent Study

S.NO.	Solvent [5.0 Vol]	Temp [°C]	Time [h]	Yield[c]
6[a]	**Toluene**	**120**	**4**	**97**
7[a]	DMSO	120	4	20
8[a]	Xylene	120	4	88
9[a]	NMP	120	4	52
10[a]	Water	120	4	81

Formamide Equivalents Study

S.NO.	Eq (2o)	Temp [°C]	Time [h]	Yield[c]
15[b]	1	120	3	56
16[b]	2	120	3	86
17[b]	**3**	**120**	**3**	**98**
18[b]	4	120	3	97
19[b]	5	120	3	98

Time Study

S.NO.	Solvent [5.0 Vol]	Temp [°C]	Time [h]	Yield[c]
11[a]	Toluene	120	1	72
12[a]	Toluene	120	2	83
13[a]	**Toluene**	**120**	**3**	**98**
14[a]	Toluene	120	4	97

Temperature Study

S.NO.	Solvent [5.0 Vol]	Temp [°C]	Time [h]	Yield[c]
20[a]	Toluene	80	3	5
21[a]	Toluene	100	3	30
22[a]	**Toluene**	**120**	**3**	**98**

[a] Conditions: *p*-anisidine **1e** (1.0 mmol), formamide **2N** (3.0 mmol). [b] Conditions: *p*-anisidine 1e (1.0 mmol), Solvent: Toluene (5.0 Vol), all the reactions were conducted under air. [c] Isolated yields.

ing products (Table 1, entry 14). To increase the yield of **3e**, we analysed other parameters such as formamide equivalents and temperature. Further, it was observed that when 1.0 to 5.0 eq. of **2o** was used as the formylating agent in toluene, the amide **3e** was obtained in moderate to an excellent yield of 56–98% (Table 1, entries 15–19). The utilisation of **2o** to 4.0 and 5.0 eq. had no discernible impact on the yield of **3e** (Table 1, entries 18 and 19). Notably, the reduction of reaction temperature to 80 and 100 °C afforded the poor result of the desired product (5–30%), emphasising the importance of temperature in facilitating the net transamidation reaction (Table 1, entries 20 and 21). Thus, the optimum result was obtained when 3.0 eq of **2o** was used as the formyl source, using toluene as a solvent and extending the reaction time to 3.0 h at 120 °C (Table 1, entries 13, 17 and 22).

With the optimised reaction conditions, we examined the scope of carbonyl sources (**2A–Y**) for the transamidation of aniline **1**[5]**a** (Scheme 2). From **2A–M** are tertiary amides (*N*,*N*-dimethyl), while **2N–Y** are amides with various nitrogen substitutions. Fortunately, the aliphatic amides like the *N*-formylation (**2A**), and *N*-acylation (**2B**) reactions proceeded smoothly when 3,3-dimethylbutanamide (**2I**) was used as carbonyl sources, provided a good yield of 78%, respectively. However, Due to the hindrance of branched/cyclic alkyl groups, the resultant *tert*-butylate (**2C**), isobutyramide (**2D**) and cyclohexanecarboxamide (**3G**) products were obtained in the moderate yields. Tri-chloroacetamide (**2E**), 2-phenylacetamide (**2J**) and 2-phenoxyacetamide (**2M**) were also employed effectively as an acyl source yielding the desired products (**3E**, **3J** and **3M**) in moderate to good yields of 64–78%. Further,

EurJOC
European Journal of Organic Chemistry
Full Papers
doi.org/10.1002/ejoc.202101114
Chemistry Europe
European Chemical Societies Publishing

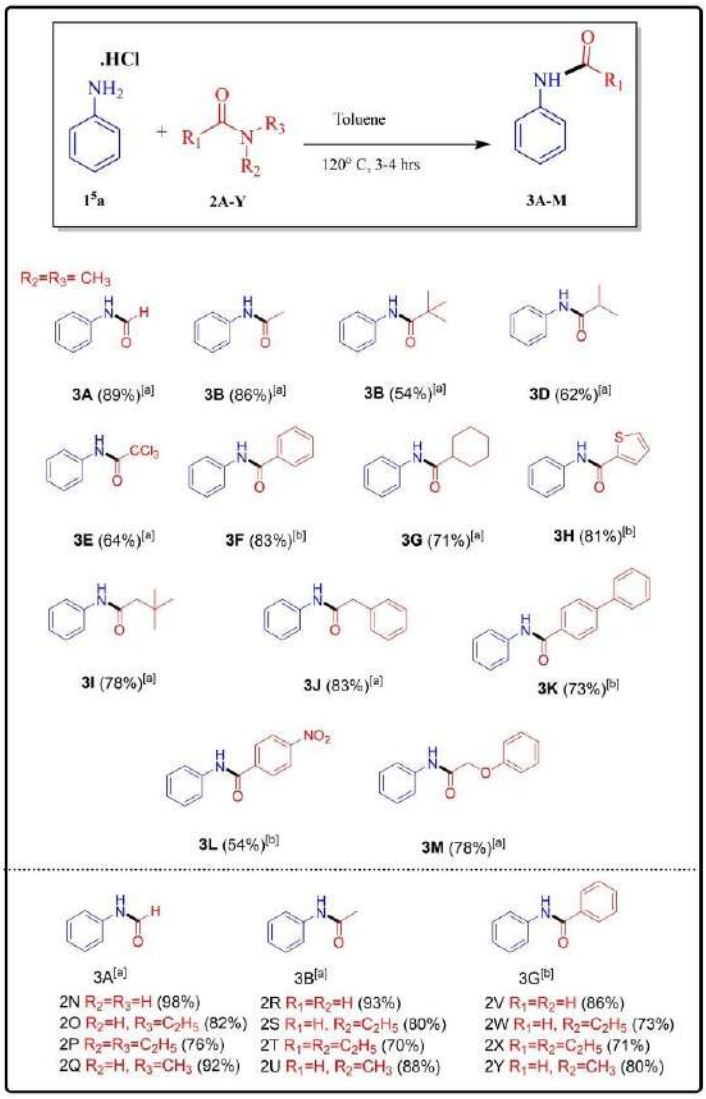

Scheme 2. The substrate scope of 1°, 2° and 3° unactivated amides. [a] All the reactions were conducted on a 1.0 mmol scale, 3.0 mmol of amide, under air for 3 h, using toluene (5.0 Vol). [b] Time = 4.0 h.

multiple benzamide derivatives were used as benzoyl sources. The results indicate that the nitro substituted benzamide provided less yield comparable to other benzamides. We got moderate results when N,N-diethyl amides (**2P**, **2T**, and **2X**) were utilised for their respective compounds due to steric hindrance.

The universality of the transamidation was explored using a wide variety of amines (Scheme 3). We performed the *N*-formylation, *N*-acetylation and *N*-benzoylation of multiple amines, including 1°, 2°, electron-donating and withdrawing substitutions aromatic, heterocyclic, and aliphatic amines (Scheme 3). The current protocol is compatible with a wide range of anilines substituted with functional groups such as

EurJOC
European Journal of Organic Chemistry
Full Papers
doi.org/10.1002/ejoc.202101114
Chemistry Europe
European Chemical Societies Publishing

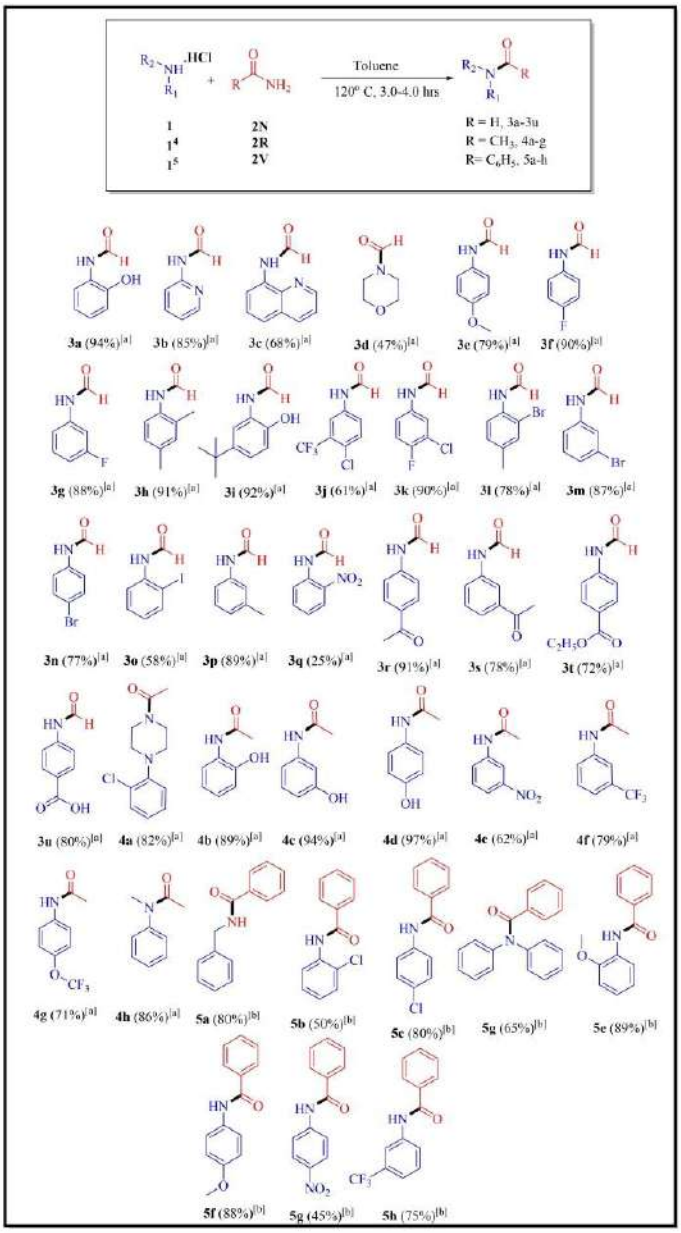

Scheme 3. The substrate scope of diversified amines with formamide. Isolated yields were reported. [a] t = 3 h and [b] t = 4 h.

alkyl (**3h**, **3p** and **3r**), alkoxyl (**3e**, **5e** and **5f**), hydroxyl (**3a**, **3r**, and **4b–d**), nitro (**3q** and **4e**), halo (**3f–g**, **3i–3o**, **4d**, and **5b–c**), keto (**3s–t**), and ester (**3u**), heteroaromatic (**3b** and **3d**), quinoline (**3c**), secondary amines (**3w**, **4a**, **4h**, **5c** and **5g**), and

EurJOC
European Journal of Organic Chemistry
Full Papers
doi.org/10.1002/ejoc.202101114
Chemistry Europe
European Chemical Societies Publishing

aliphatic amines (**3d**, **3w**, **4a**, **5c** and **5h**), respectively. We also analysed various aromatic amines with different substituents and obtained the resulting *N*-formylated products in good to excellent yields (Scheme 2). Pleasingly, the heterocyclic aromatic anilines rapidly converted to the corresponding products (**3b–d**) in the range of 68–85% yield, whereas **3c** had a lower yield, possibly due to steric hindrance, as we observed when synthesising the **5g** product. Interestingly, substrates containing a hydroxyl group have afforded excellent yields (89–97%) without any difficulty (**3a**, **3r** and **4b–d**). Furthermore, methoxy substituted anilines also performed well in the synthesis of *N*-formylation (**3e**) and *N*-benzoylation (**5e–f**) products at all substituent positions. When aniline contained strong electron-withdrawing nitro groups, only low to moderate yields (25 and 62%) of the corresponding products were obtained (**3q** and **4e**). In this study, we found that *meta*-nitro aniline, 4-(trifluoromethoxy)-aniline and 3-trifluoromethyl aniline converted into their corresponding products (**4f–g**) with good yields (71–79%). Additionally, the halogenated anilines tested afforded the corresponding *N*-formylated/benzoylated products (**3f–g**, **3m–o** and **5b–c**) in moderate to excellent yields (50–90%). *ortho* halogen-substituted anilines were also shown to be less reactive than *meta* and *para*-substituted anilines in these experiments. On the other hand, di-substituted anilines produced a good product yield, whether both were electron-donating groups (EWG) or electron-donating groups (EDG). To our delight, amines with acid-sensitive functionalities, such as an ester, were well tolerated, yielding formamide (**3u**) in 72% yields. Similarly, when aniline substituted acetophenone, and carboxylic acid analogues (**3s–t** and **3zn**) were used as substrates, the reaction proceeded well and yielded the expected products in moderate to excellent yields (78–91%). Finally, the transamidation reaction of aliphatic 1° and 2° amines were investigated, and the corresponding products (**3d**, and **5a**) were obtained in good yields.

Further, only *N*-formylation reaction occurred in the presence of water (Scheme 4A); the other reactions, such as *N*-acylation and *N*-benzoylation, did not produce the desired products. Likewise, similar results were obtained in the presence of in concentrated HCl (Scheme 4B). Subsequently, the same reaction was attempted under NET conditions utilising various amides, namely formamide, acetamide, and benzamide derivatives. Under standard reaction conditions, the corresponding

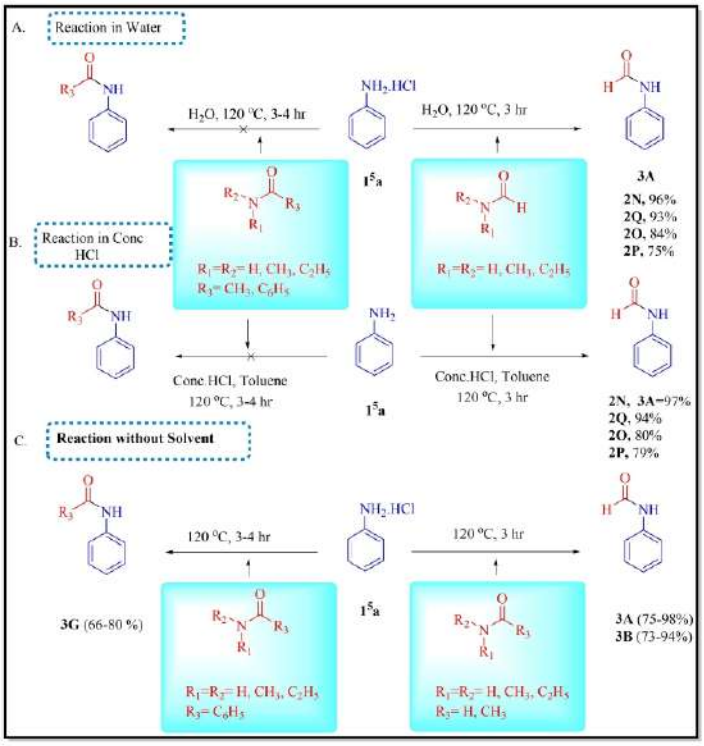

Scheme 4. The road map for transamidation under different reactions conditions.

EurJOC
European Journal of Organic Chemistry
Full Papers
doi.org/10.1002/ejoc.202101114
Chemistry Europe
European Chemical Societies Publishing

products were obtained in moderate to excellent yields (Scheme 4C).

Mechanistic study

To depict the current protocol's reaction mechanism, four control experiments were carried out, and the results are illustrated in Scheme 5. First, transamidation of acetamide (**2R**) showed that the free amine **1[4]d** exerted an indicative impact, producing the target product (**4d**) in traces. Second, the yield of acylated product (**1[4]d**) remained the same when HCl gas purged through reaction mass containing free amine (**1[4]d**) in toluene (Scheme 5A). Lastly, the yield of *N*-acetylated product (**4d**) remained the same using TEMPO as a radical trap. It was found that TEMPO did not suppress the yield of the transamidation product as a radical scavenger (Scheme 5B). The results indicated that no radical intermediates were formed during the transamidation process.

Based on the experimental results, the plausible reaction mechanism is presented in Scheme 6. Initially, the carbonyl group of **2** is activated with HCl followed by a nucleophilic attack of amine (**1**) on **A** (**A** and **B** are in resonance) and resulted in the formation of intermediate **C**. Then, **C** could transform into **D** through tautomerisation. In the next step, intermediate **E** is formed through the elimination of amine (**D1**). Finally, the deprotonation step results in the formation of the final product **3**.

Ultimately, the viability of the pharmaceutical of this metal-free protocol for the synthesis of the marketed drug acetaminophen (Antipyretic drug) was demonstrated on a grams-scale (Scheme 7). In contrast to conventional methods, the current protocol is beneficial for API (Active pharmaceutical ingredients) products and intermediates as it does not include the utilisation of metal residues. Subsequently, we examined the chemoselectivity between amino and hydroxyl groups present in the same substrate. Pleasantly, we got selective *N*-formylated and *N*-acetylated products, demonstrating the selectivity of the current transamidation process.

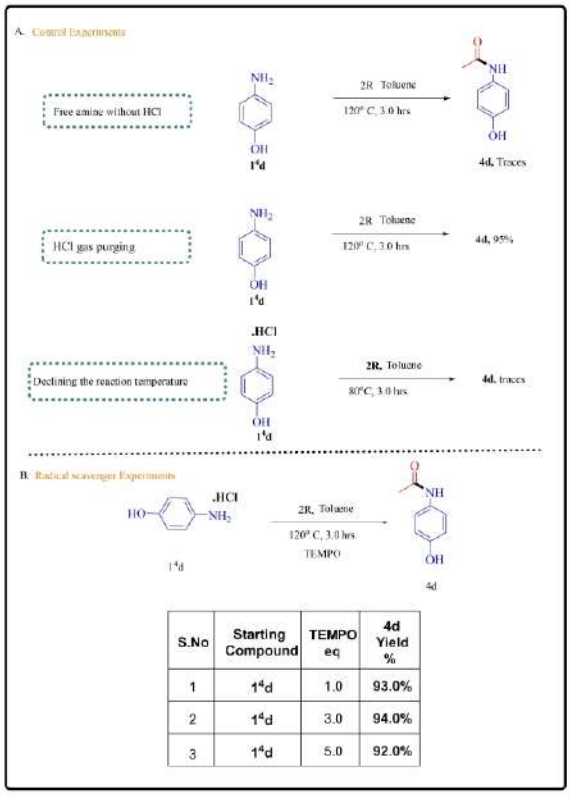

S.No	Starting Compound	TEMPO eq	4d Yield %
1	1[4]d	1.0	93.0%
2	1[4]d	3.0	94.0%
3	1[4]d	5.0	92.0%

Scheme 5. Some control experiments and the reaction in radical scavenger conditions.

EurJOC
European Journal of Organic Chemistry
Full Papers
doi.org/10.1002/ejoc.202101114
Chemistry Europe
European Chemical Societies Publishing

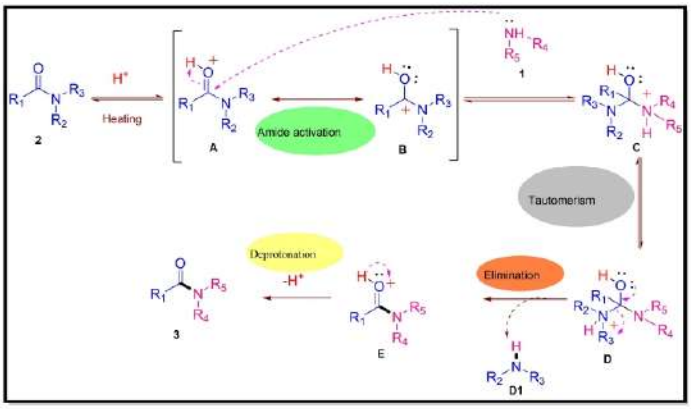

Scheme 6. The plausible reaction mechanism.

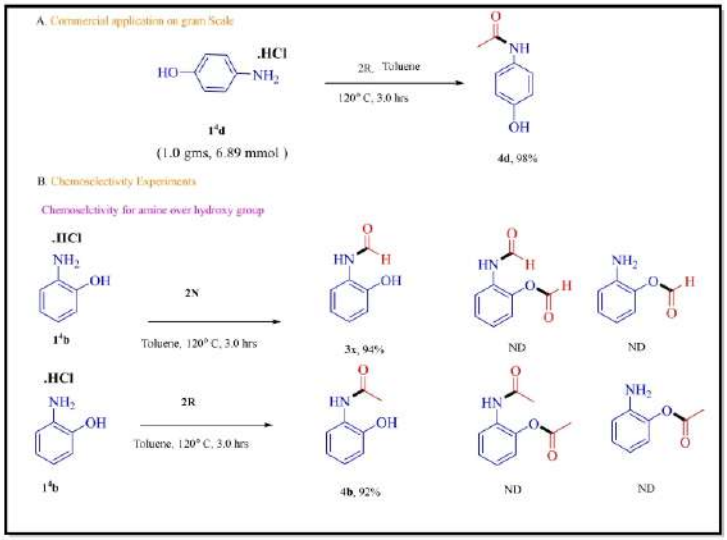

Scheme 7. Commercial application of protocol on Gram-Scale and chemo-selectivity experiments.[14a-c] *ND = Not developed.

Conclusion

A highly efficient, catalyst-free, and convenient protocol for the synthesis of amides through transamidation of diverse amines has been reported using amine hydrochloride salt as a reactant as well as the catalyst. This amidation reaction is well tolerated for a wide variety of amines with diverse functionalities, namely acids, ester, and ketones. The environmental compatibility, mild reaction conditions, adaptability, and accessible and easily accessible starting materials are all strengths of this strategy. It is noteworthy that amides have the potential to be highly efficient transamidation agents.

Experimental Section

General information: All reactions were conducted under standard operating conditions without the use of any stringent conditions. All chemicals were obtained from Aldrich Chemical Co., Alfa Aesar, used as received without additional purification. Lab reagent (LR) grade solvents were used for extraction and column chromatog-

EurJOC
European Journal of Organic Chemistry
Full Papers
doi.org/10.1002/ejoc.202101114
Chemistry Europe
European Chemical Societies Publishing

raphy purchased from Roma-chem. The reaction progress was monitored on Merck TLC Silica gel 60 F254 plates, and the spots were visualized under ultraviolet (UV) light, followed by iodine or ninhydrin staining solution followed by heating. ^1H, ^{13}C and ^{19}F NMR spectra were recorded on 400, 100, 377 MHz NMR spectrometer using $CDCl_3$ and DMSO-d_6 as solvents unless otherwise stated. Chemical shifts are expressed in parts per million (ppm) relative to TMS is used as an internal standard. Unless otherwise specified, all reagents were weighed and handled in air.

Experimental procedure for N-formylation of amines (EP-1): A mixture of amine salt 1 (1.0 eq), amide 2 (3.0 eq), and Toluene (5.0 Vol) was stirred in a vial under atmospheric air at 120 °C for 3 h. After bringing the mixture to room temperature, 10 mL water was added and the mixture was extracted with ethyl acetate (3×20 mL). The EtOAc layer was washed with 3×5 mL of 1 M sodium bicarbonate solution. The combined organic layers were dried with anhydrous Na_2SO_4. Under vacuum, the solvent was evaporated, and the crude product was purified using column chromatography (silica gel, EtOAc/Hexane) in order to obtain a pure product.

Experimental procedure for N-benzoylation of amines (EP-2): A mixture of amine salt 1 (1.0 eq), amide 2 (3.0 eq), and Toluene (5.0 Vol) was stirred in vial under atmospheric air at 120 °C for 4 h. After bringing the mixture to room temperature, 10 mL water was added and the mixture was extracted with ethyl acetate (3×20 mL). The EtOAc layer was washed with 3×5 mL of 1 M sodium bicarbonate solution. The combined organic layers were dried with anhydrous Na_2SO_4. Under vacuum, the solvent was evaporated, and the crude product was purified using column chromatography (silica gel, EtOAc/Hexane) in order to obtain a pure product.

Experimental procedure for gram scale preparation of paracetamol (PCM): A solution of 4-aminophenol (1 g, 6.89 mmol) and acetamide (1.22 g, 20.66 mmol) was stirred in a round bottom flask (25 mL) under atmosphere of air at 120 °C for 3 h. After bringing the mixture to room temperature, 20 mL water was added and the mixture was extracted with ethyl acetate (3×20 mL). The EtOAc layer was washed with 3×5 mL of 1 M sodium bicarbonate solution. The combined organic layers were dried with anhydrous Na_2SO_4. Under vacuum, the solvent was evaporated, and the crude product was purified using column chromatography (silica gel, EtOAc/Hexane 6:4) in order to obtain a pure product in a yield of 98% (1.03 g).

***N*-Phenylformamide**[15a] **(3A):** Using the experimental procedure **EP-1**, the product was obtained as yellow solid in 94% yield; A mixture of rotamers is observed; ^1H NMR (400 MHz, $CDCl_3$) δ 9.22 (Minor rotamer, s, 0.44H), 8.71 (Major rotamer, d, J=11.3 Hz, 0.48H), 8.60 (Minor rotamer, s, 0.42H), 8.34 (Major rotamer, s, 0.50H), 7.58 (d, J=8.2 Hz, 1.0H), δ 7.36–7.29 (m, 2.0H), 7.19 (t, J=7.4 Hz, 0.47H), 7.13 (t, J=7.1 Hz, 1.42H); ^{13}C NMR (100 MHz, $CDCl_3$) δ major rotamer 163.23, 136.84, 129.41, 125.24, 118.78, minor rotamer 159.90, 137.09, 129.69, 124.74, 120.23.

***N*-Phenylacetamide**[15b] **(3B):** Using the experimental procedure **EP-1**, the product was obtained as colourless oil in 93%; ^1H NMR (400 MHz, $CDCl_3$) δ 7.91 (s, 1H), 7.43 (d, J=8.0 Hz, 2H), 7.21 (t, J=7.7 Hz, 2H), 7.02 (t, J=7.4 Hz, 1H), 2.08 (s, 3H). ^{13}C NMR (100 MHz, $CDCl_3$) δ 169.05, 138.03, 129.03, 124.47, 120.25, 24.47.

***N*-Phenylpivalamide**[15c] **(3C):** Using the experimental procedure **EP-1**, the product was obtained as white solid in 54%; ^1H NMR (400 MHz, $CDCl_3$) δ 7.52 (d, J=8.3 Hz, 2H), 7.31 (t, J=7.7 Hz, 3H), 7.10 (t, J=7.4 Hz, 1H), 1.32 (s, 9H). ^{13}C NMR (100 MHz, $CDCl_3$) δ 176.73, 138.16, 129.02, 124.29, 120.17, 39.68, 27.72.

***N*-Phenylisobutyramide**[15d] **(3D):** Using the experimental procedure **EP-1**, the product was obtained as white solid in 62%; ^1H NMR (400 MHz, $CDCl_3$) δ 7.53 (d, J=8.0 Hz, 2H), 7.43 (s, 1H), 7.30 (t, J=7.7 Hz, 2H), 7.09 (t, J=7.3 Hz, 1H), 2.57–2.47 (m, 1H), 1.24 (d, J=6.8 Hz, 6H). ^{13}C NMR (100 MHz, $CDCl_3$) δ 176.72, 138.24, 128.99, 124.23, 120.11, 77.47, 77.15, 76.84, 36.64, 19.69.

2,2,2-Trichloro-*N*-phenylacetamide[15e] **(3E):** Using the experimental procedure **EP-1**, the product was obtained as white solid in 64%; ^1H NMR (400 MHz, $CDCl_3$) δ 8.26 (s, 1H), 7.50 (d, J=8.3 Hz, 2H), 7.33 (t, J=7.7 Hz, 2H), 7.16 (t, J=7.6 Hz, 1H). ^{13}C NMR (100 MHz, $CDCl_3$) δ 136.05, 129.45, 126.18, 120.52.

***N*-Phenylbenzamide**[15e] **(3F):** Using the experimental procedure **EP-2**, the product was obtained as white solid in 83%; ^1H NMR (400 MHz, DMSO-d_6) δ 10.26 (s, 1H), 7.97 (d, J=7.2 Hz, 2H), 7.81 (d, J=8 Hz, 2H), 7.59 (t, J=8.3 Hz, 1H), 7.53 (t, J=8.3 Hz, 2H), 7.36 (t, J=7.7 Hz, 2H), 7.10 (t, J=7.6 Hz, 1H). ^{13}C NMR (100 MHz, DMSO-d_6) δ 165.57, 139.19, 135.01, 131.52, 128.85, 128.59, 128.36, 127.65, 123.64, 120.38.

N-Phenylcyclohexanecarboxamide[16e] **(3G):** Using the experimental procedure **EP-1**, the product was obtained as light white solid in 71% yield; ^1H NMR (400 MHz, DMSO-d_6) δ 9.78 (s, 1H), 7.60 (d, J=8.4 Hz, 2H), 7.27 (t, 2H), 7.01 (t, 1H), 2.32 (m, 1.0H), 1.77 (t, 4.0H), 1.65 (d, J=10.4 Hz, 1H), 1.41 (m, 2H), 1.27 (m, 3H); ^{13}C NMR (100 MHz, DMSO-d_6) δ 174.27, 139.51, 128.58, 122.81, 119.00, 44.85, 29.13, 25.40, 25.24.

N-Phenylthiophene-2-carboxamide[16b] **(3H):** Using the experimental procedure **EP-2**, the product was obtained as light white solid in 81% yield; ^1H NMR (400 MHz, DMSO-d_6) δ 10.22 (s, 1H), 8.03 (d, J=2.8 Hz, 1H), 7.85 (d, J=5.2 Hz, 1H), 7.72 (d, J=7.6 Hz, 2H), 7.35 (t, 2H), 7.22 (t, 1H), 7.10 (t, 1H); ^{13}C NMR (100 MHz, DMSO-d_6) δ 159.88, 138.71, 131.86, 129.10, 128.68, 128.07, 123.75, 120.39.

3,3-Dimethyl-N-phenylbutanamide[16c] **(3I):** Using the experimental procedure **EP-1**, the product was obtained as light brown solid in 78% yield; ^1H NMR (400 MHz, DMSO-d_6) δ 9.77 (s, 1H), 7.59 (d, J=8 Hz, 2H), 7.27 (t, 2H), 7.01 (t, 1H), 2.18 (s, 2H), 1.02 (s, 9H); ^{13}C NMR (100 MHz, DMSO-d_6) δ 169.96, 139.28, 128.58, 122.94, 119.18, 49.60, 30.83, 29.62.

N,2-Diphenylacetamide[16d] **(3J):** Using the experimental procedure **EP-1**, the product was obtained as light brown solid in 83% yield; ^1H NMR (400 MHz, DMSO-d_6) δ 10.19 (s, 1H), 7.61 (d, J=8 Hz, 2H), 7.29 (m, 7H), 7.03 (t, 1H), 3.64 (s, 2H); ^{13}C NMR (100 MHz, DMSO-d_6) δ 169.10, 139.24, 136.03, 129.11, 128.71, 128.30, 126.52, 123.20, 119.10, 43.35.

N-Phenyl-[1,1'-biphenyl]-4-carboxamide[16e] **(3K):** Using the experimental procedure **EP-2**, the product was obtained as light white solid in 73% yield; ^1H NMR (400 MHz, DMSO-d_6) δ 10.30 (s, 1H), 8.06 (d, J=8 Hz, 2H), 7.82 (dd, J=14.4, 8 Hz, 4H), 7.76 (d, J=8 Hz, 2H), 7.51 (t, 2H), 7.43 (t, 1H), 7.36 (t, 2H), 7.11 (t, 1H); ^{13}C NMR (100 MHz, DMSO-d_6) δ 165.17, 143.10, 139.21, 139.12, 133.73, 129.09, 128.64, 128.39, 128.18, 126.94, 126.60, 123.68, 120.37.

4-Nitro-N-phenylbenzamide[16d] **(3L):** Using the experimental procedure **EP-2**, the product was obtained as light white solid in 54% yield; ^1H NMR (400 MHz, DMSO-d_6) δ 10.58 (s, 1H), 8.37 (d, J=8.4 Hz, 2H), 8.19 (d, J=8.4 Hz, 2H), 7.78 (d, J=8.4 Hz, 2H), 7.38 (t, 2H), 7.14 (t, 1H); ^{13}C NMR (100 MHz, DMSO-d_6) δ 163.90, 149.15, 140.64, 138.72, 129.24, 128.74, 124.19, 123.57, 120.49.

2-Phenoxy-N-phenylacetamide[17a] **(3M):** Using the experimental procedure **EP-1**, the product was obtained as light white solid in 78% yield; ^1H NMR (400 MHz, DMSO-d_6) δ 10.11 (s, 1H), 7.65 (d, J=8.0 Hz, 2H), 7.32 (t, 4H), 7.01 (t, 1H), 6.98 (m, 3H); ^{13}C NMR (100 MHz, DMSO-d_6) δ 166.59, 157.83, 138.41, 129.53, 128.74, 123.70, 121.19, 119.71, 114.66, 67.10.

EurJOC
European Journal of Organic Chemistry
Full Papers
doi.org/10.1002/ejoc.202101114
Chemistry Europe
European Chemical Societies Publishing

N-(2-Hydroxy-4-methylphenyl)formamide[17b] (**3a**): Using the experimental procedure **EP-1**, the product was obtained as brown solid in 94% yield; ^{1}H NMR (400 MHz, DMSO) δ 9.92 (s, 1H), 9.55 (s, 1H), 8.28 (s, 1H), 8.02 (d, J=7.9 Hz, 1H), 6.94–6.82 (m, 2H), 6.75 (t, J=7.4 Hz, 1H); ^{13}C NMR (100 MHz, DMSO): δ 163.47, 160.03, 148.97, 146.73, 126.00, 125.48, 125.34, 124.19, 121.76, 120.83, 119.53, 119.00, 116.10, 115.10.

N-(Pyridin-2-yl)formamide[17c] (**3b**): Using the experimental procedure **EP-1**, the product was obtained as brown solid in 85%; ^{1}H NMR (400 MHz, $CDCl_3$) δ 10.58 (s, 1H), 9.28 (d, J=10.0 Hz, 0.57H), 8.33 (s, 1H), 8.24 (s, 0.60H), 8.06 (d, J=7.9 Hz, 0.45H), 7.78–7.771 (m, 1H), 7.08 (d, J=5.6 Hz, 1H), 6.92 (d, J=7.9 Hz, 0.59H). ^{13}C NMR (100 MHz, $CDCl_3$) δ 162.13, 160.31, 151.65, 148.06, 138.70, 138.31, 119.76, 119.22, 113.78, 111.12.

N-(Quinolin-8-yl)formamide[17d] (**3c**): Using the experimental procedure **EP-1**, the product was obtained as brown solid in 68% yield. A mixture of rotamers is observed; ^{1}H NMR (400 MHz, $CDCl_3$) δ 9.61 (br, s, 0.80H), 9.20 (br, s, 0.11H), 8.84 (t, J=18.7 Hz, 0.12H), 8.56 (d, J=4.1 Hz, 0.98H), 8.49 (dd, J=11.5, 7.0 Hz, 0.89H), 8.44 (s, 0.88H), 7.93 (d, J=8.3 Hz, 1.0H), 7.29–7.01 (m, 3.19H); ^{13}C NMR (100 MHz, $CDCl_3$) δ Major rotamer: 159.98, 144.41, 141.25, 125.41, 120.81, 117.92, 114.64, minor rotamer: 163.63, 146.67, 141.89, 124.54, 122.03, 119.06, 115.62.

Piperidine-1-carbaldehyde[17d] (**3d**): Using the experimental procedure **EP-1**, the product was obtained as yellow oil in 52%; ^{1}H NMR (400 MHz, $CDCl_3$) δ 7.78 (s, 1H), 3.26 (t, J=4.8 Hz, 2H), 3.10 (t, J=4.8 Hz, 2H), 1.47 (d, J=4.2 Hz, 2H), 1.37–1.31 (m, 4H).^{13}C NMR (100 MHz, $CDCl_3$) δ 160.34, 46.34, 40.11, 26.31, 26.14, 24.66, 24.23.

N-(4-Methoxyphenyl) formamide[18a] (**3e**): Using the experimental procedure **EP-1**, the product was obtained as reddish brown solid in 98% yield. A mixture of rotamers is observed; ^{1}H NMR (400 MHz, $CDCl_3$) δ 8.52 (t, J=13.2 Hz, 0.84H), 8.28 (Major rotamer, s, 0.52H), 7.88 (Minor rotamer, s, 0.43H), 7.43 (d, J=8.8 Hz, 1.03H), 7.03 (d, J=8.7 Hz, 0.92H), 6.85 (dd, J=14.3, 8.8 Hz, 1.98H), 3.77 (d, J=7.5 Hz, 3H). ^{13}C NMR (100 MHz, $CDCl_3$) δ Major rotamer: 159.33, 157.68, 129.74, 121.74, 114.97, 55.55, minor rotamer: 163.42, 156.77, 130.13, 121.61, 114.28, 55.63.

***N*-(4-Fluorophenyl) formamide**[18b] (**3f**): Using the experimental procedure **EP-1**, the product was obtained as off-white solid in 90% yield. A mixture of rotamers is observed; ^{1}H NMR (400 MHz, $CDCl_3$) δ 8.63 (Minor rotamer, s, 0.33H), 8.57 (Major rotamer, d, J=11.0 Hz, 0.50H), 8.33 (Major rotamer, s, 0.60H), 7.76 (Minor rotamer, s, 0.47H), 7.50 (dd, J=8.7, 4.8 Hz, 1.17H), 7.11–6.96 (m, 3H); ^{13}C NMR (100 MHz, $CDCl_3$) δ Major rotamer: 159.36, 160.94, 158.52, 122.03, 115.99, minor rotamer: 163.19, 161.79, 159.30, 121.95, 115.77; ^{19}F NMR (377 MHz, $CDCl_3$) δ −116.84, −116.85, −116.86, −116.87, −116.89, −116.89, −116.91, −117.06, −117.07, −117.08, −117.09, −117.10, −117.11, −117.12.

***N*-(3-Fluorophenyl)formamide**[18c] (**3g**): Using the experimental procedure **EP-1**, the product was obtained as yellow solid in 88% yield. A mixture of rotamers is observed; ^{1}H NMR (400 MHz, $CDCl_3$) δ 8.98 (Minor rotamer, s, 042H), 8.73 (Minor rotamer, d, J=11.2 Hz, 0.47H), 8.39 (Major rotamer, s, 0.60H), 8.11 (Major rotamer, d, J=4.0 Hz, 0.53H), 7.50 (d, J=10.7 Hz, 0.57H), 7.39–6.81 (m, 1.71H), 6.95–6.82 (m, 2H); ^{13}C NMR (100 MHz, $CDCl_3$) δ Major rotamer: 159.59, 130.3 (d, J=9.3 Hz), 115.39 (d, J=2.9 Hz), 107.88, 107.88, 107.62, Minor rotamer: 162.82, 131.2 (d, J=9.3 Hz), 114.16 (d, J=2.9 Hz), 106.15, 105.9; ^{19}F NMR (377 MHz, $CDCl_3$) δ −110.46, −110.48, −110.50, −110.52, −111.18, −111.21, −111.22, −111.23, −111.24.

***N*-(2,4-Dimethylphenyl)formamide**[18d] (**3h**): Using the experimental procedure **EP-1**, the product was obtained as off-white solid in 91% yield. A mixture of rotamers is observed; ^{1}H NMR (400 MHz, $CDCl_3$) δ 8.45 (d, J=11.2 Hz, 0.62H), 8.39 (s, 0.37H), 8.17 (br, s, 0.58H), 7.66 (d, J=8.6 Hz, 0.36H), 7.35 (br, s, 0.28H), 7.00 (t, J=7.2 Hz, 2.69H), 2.29 (d, J=10.3 Hz, 3H), 2.24 (d, J=15.6 Hz, 3H). ^{13}C NMR (100 MHz, $CDCl_3$) δ Major rotamer: 159.50, 136.08, 132.53, 130.23, 127.63, 121.46, minor rotamer: 163.82, 135.45, 131.96, 129.26, 127.26, 127.36, 123.52.

***N*-(5-(tert-butyl)-2-hydroxyphenyl)formamide**[18e] (**3i**): Using the experimental procedure **EP-1**, the product was obtained as brown solid in 92% yield. A mixture of rotamers is observed; ^{1}H NMR (400 MHz, DMSO) δ 9.67 (s, 0.81H), 9.53 (s, 0.99H), 9.18 (Minor rotamer, d, J=11.0 Hz, 0.17H), 8.52 (Minor rotamer, d, J=11.2 Hz, 0.17H), 8.27 (Major rotamer, s, 0.82H), 8.07 (Major rotamer, d, J=1.4 Hz, 0.82H), 7.10 (s, 0.16H), 6.99 (d, J=8.4 Hz, 0.18H), 6.93 (dd, J=8.4, 1.8 Hz, 0.80H), 6.79 (t, J=10.1 Hz, 0.98H), 1.22 (s, 9H). ^{13}C NMR (100 MHz, DMSO) δ Major: 159.98, 144.41, 141.25, 125.41, 120.81, 117.92, 115.62, minor rotamer: 163.63, 146.67, 141.89, 124.54, 122.03, 122.03, 119.06, 114.64.

***N*-(4-Chloro-3-(trifluoromethyl)phenyl)formamide** (**3j**): Using the experimental procedure **EP-1**, the product was obtained as yellow solid in 61% yield. A mixture of rotamers is observed; ^{1}H NMR (400 MHz, $CDCl_3$) δ 8.70 (s, 0.77H), 8.41 (s, 1H), 7.85 (d, J=15.4 Hz, 1.18H), 7.75 (d, J=8.6 Hz, 0.61H), 7.50 (d, J=8.5 Hz, 1.11H), 7.47–7.40 (m, 0.42H), 7.24 (d, J=8.5 Hz, 0.41H); ^{13}C NMR (100 MHz, $CDCl_3$) δ Major rotamer: 159.36, 132.29, 121.19, 11.94, minor rotamer: 162.35, 133.03, 119.08, 117.89; ^{19}F NMR (377 MHz, $CDCl_3$) δ −62.91 (minor, s), −63.05 (minor, s).

***N*-(3-Chloro-4-fluorophenyl)formamide**[19a] (**3k**): Using the experimental procedure **EP-1**, the product was obtained as off-white solid in 65% yield. A mixture of rotamers is observed; ^{1}H NMR (400 MHz, $CDCl_3$) δ 8.64 (d, J=19.6 Hz, 0.34H), 8.58 (d, J=11.0 Hz, 0.45H), 8.35 (s, 0.77H), 7.72 (dd, J=6.4, 2.1 Hz, 0.48H), 7.39–7.32 (m, 0.87H), 7.20–7.04 (m, 0.76H), 7.02–6.95 (m, 2H). ^{13}C NMR (100 MHz, $CDCl_3$) δ Major rotamer: 159.30, 156.42, 153.96, 122.46, 116.77, minor rotamer: 162.88, 157.26, 154.80, 121.61, 116.99; ^{19}F NMR (377 MHz, $CDCl_3$) δ −119.23, −119.25, −119.27, −119.48, −119.50, −119.51, −119.51, −119.52, −119.53.

***N*-(2-Bromo-4-methylphenyl)formamide**[19b] (**3l**): Using the experimental procedure **EP-1**, the product was obtained as off-white solid in 78% yield. A mixture of rotamers is observed; ^{1}H NMR (400 MHz, $CDCl_3$) δ 8.62 (d, J=11.2 Hz, 0.35H), 8.45 (s, 0.66H), 8.22 (d, J=8.3 Hz, 0.66H), 7.62 (br, s, 0.82H), 7.42 (s, 0.48H), 7.36 (s, 0.49H), 7.12 (t, J=8.8 Hz, 1.32H), 2.30 (d, J=7.8 Hz, 3H). ^{13}C NMR (100 MHz, CDCl3) δ Major rotamer: 158.88, 133.88, 132.72, 129.42, 122.24, 114.78, minor rotamers: 161.90, 135.93, 132.88, 129.17, 119.17, 119.46, 113.04.

***N*-(3-Chlorophenyl)formamide**[17b] (**3m**): Using the experimental procedure **EP-1**, the product was obtained as yellow solid in 87% yield. A mixture of rotamers is observed; ^{1}H NMR (400 MHz, $CDCl_3$) δ 8.72 (t, J=11.9 Hz, 0.83H), 8.38 (s, 0.55H), 7.82 (s, 1.0H), 7.47 (d, J=8.0 Hz, 0.56H), 7.36–7.17 (m, 2.4H), 7.06 (d, J=8.0 Hz, 0.44H), ^{13}C NMR (100 MHz, $CDCl_3$) δ Major rotamer: 159.36, 130.52, 127.97, 123.08, 122.78, 118.58, minor rotamers: 162.68, 131.18, 128.41, 123.46, 121.78, 117.32.

***N*-(4-Bromophenyl)formamide**[19c] (**3n**): Using the experimental procedure **EP-1**, the product was obtained as yellow solid in 77% yield. A mixture of rotamers is observed; ^{1}H NMR (400 MHz, $CDCl_3$) δ 8.66 (Major rotamer, d, J=11.1 Hz, 0.51H), 8.61 (Minor rotamer, s, 0.35H), 8.37 (Major rotamer, s, 0.62H), 7.62 (minor rotamer, s, 0.47H), 7.48 (s, 0.99H), 7.44 (d, J=8.2 Hz, 2.20H), 6.98 (d, J=8.6 Hz, 0.92H); ^{13}C NMR (100 MHz, $CDCl_3$) δ Major rotamer: 159.20, 132.21, 121.21, 117.63, minor rotamer: 162.63, 132.92, 120.45, 118.42.

EurJOC
European Journal of Organic Chemistry
Full Papers
doi.org/10.1002/ejoc.202101114
Chemistry Europe
European Chemical Societies Publishing

***N*-(2-Iodophenyl)formamide**[17b] (**3o**): Using the experimental procedure **EP-1**, the product was obtained as brown solid in 58% yield; A mixture of rotamers is observed; ^{1}H NMR (400 MHz, $CDCl_3$) δ 8.73 (Minor rotamer, s, 0.33H), 8.69 (Major rotamer, d, *J*=11.0 Hz, 0.62H), 8.36 (Major rotamer, s, 0.44H), 7.85 (Minor rotamer, s, 0.38H), 7.55 (d, *J*=7.9 Hz, 0.86H), 7.37–7.30 (m, 1.92H), 7.21–7.07 (m, 1.44H). ^{13}C NMR (100 MHz, $CDCl_3$) δ major rotamer: 163.03, 137.04, 129.99, 125.40, 118.93, minor rotamer: 159.44, 136.84, 129.84, 124.90, 120.17.

***N*-*m*-Tolylformamide**[19d] (**3p**): Using the experimental procedure **EP-1**, the product was obtained as brown oil in 89% yield; A mixture of rotamers is observed; ^{1}H NMR (400 MHz, $CDCl_3$) δ 8.98 (Major rotamer, br s, 0.51H), 8.71 (Major rotamer, d, *J*=11.4 Hz, 0.56H), 8.35 (Minor rotamer, s, 0.45H), 8.11 (Minor rotamer, br d, *J*=5.0 Hz, 0.42H), 7.39 (s, 0.44H), 7.33 (d, *J*=8.1 Hz, 0.44H), 7.20 (dt, *J*=12.0, 7.9 Hz, 1.0H), 6.99 (d, *J*=7.6 Hz, 0.55H), 6.93 (d, *J*=10.8 Hz, 1.52H), 2.32 (d, *J*=10.8 Hz, 3H). ^{13}C NMR (100 MHz, $CDCl_3$) δ Major rotamer: 163.16, 139.87, 136.81, 129.56, 125.60, 119.54, 115.80, 21.41, minor rotamer: 159.57, 139.05, 137.01, 128.91, 126.09, 120.79, 117.24, 21.47.

***N*-(2-Nitrophenyl)formamide**[19e] (**3q**): Using the experimental procedure **EP-1**, the product was obtained as yellow oil in 25% yield; A mixture of rotamers is observed; ^{1}H NMR (400 MHz, $CDCl_3$) δ 8.73 (Minor rotamer, d, *J*=11.1 Hz, 0.32H), 8.52 (Major rotamer, s, 0.69H), 8.41 (d, *J*=8.2 Hz, 0.67H), 7.81 (s, 0.89), 7.43 (d, *J*=8.0 Hz, 0.33H), 7.37 (d, *J*=8.0 Hz, 0.67H), 7.27 (dd, *J*=8.9, 5.8 Hz, 1.38H), 7.15–7.11 (m, 0.31H), 7.06 (t, *J*=7.7 Hz, 0.70H). ^{13}C NMR (100 MHz, CDCl3) δ Major rotamer: 159.03, 129.23, 127.92, 125.26, 122.70, 161.73, 130.43, 128.13, 126.09, 122.14.

***N*-(4-Acetylphenyl)formamide**[20a] (**3r**): Using the experimental procedure **EP-1**, the product was obtained as white solid in 91% yield. A mixture of rotamers is observed; ^{1}H NMR (400 MHz, $CDCl_3$) δ 8.93 (Minor rotamer, d, *J*=10.8 Hz, 0.36H), 8.75 (Minor rotamer, d, *J*=11.2 Hz, 0.38H), 8.47 (Major rotamer, s, 0.53H), 8.42 (Major rotamer, s, 0.69H), 8.07 (s, 0.67H), 7.92 (d, *J*=8.1 Hz, 0.68H), 7.73 (d, *J*=7.5 Hz, 0.76H), 7.67 (d, *J*=7.7 Hz, 0.65H), 7.46–7.38 (m, 1.05H), 7.32 (d, *J*=8.3 Hz, 0.38H), 2.58 (d, *J*=9.2 Hz, 3H), ^{13}C NMR (100 MHz, $CDCl_3$) δ Major rotamer: 198.34, 159.83, 137.83, 129.53, 124.85, 119.42, minor rotamer: 197.66, 162.74, 138.53, 130.18, 123.20, 117.84.

***N*-(3-Acetylphenyl)formamide**[20b] (**3s**): Using the experimental procedure **EP-1**, the product was obtained as white solid in 78% yield. A mixture of rotamers is observed; ^{1}H NMR (400 MHz, $CDCl_3$) δ 9.00 (d, *J*=10.5 Hz, 0.36H), 8.86 (Minor rotamer, d, *J*=11.1 Hz, 0.39H), 8.42 (Major rotamer, s, 0.65H), 8.38 (br, s, 0.73H), 7.93 (dd, *J*=13.4, 8.5 Hz, 0.2.02H), 7.67 (d, *J*=8.5 Hz, 1.24H), 7.18 (d, *J*=8.4 Hz, 0.80H), 2.57 (d, *J*=4.4 Hz, 3H); ^{13}C NMR (100 MHz, $CDCl_3$) δ Major rotamer: 159.27, 133.30, 129.87, 119.40, minor rotamer: 162.27, 133.75, 130.52, 117.35.

Ethyl 4-formamidobenzoate[20c] (**3t**): Using the experimental procedure **EP-1**, the product was obtained as white solid in 72% yield. A mixture of rotamers is observed; ^{1}H NMR (400 MHz, DMSO-d_6) δ 10.53 (Major rotamer, s, 0.73H), 10.46 (Minor rotamer, d, *J*=10.7 Hz, 0.25H), 8.96 (Minor rotamer, d, *J*=10.7 Hz, 0.24H), 8.35 (Major rotamer, s, 0.75H), 7.91 (t, *J*=10.5 Hz, 2.01H), 7.71 (d, *J*=8.5 Hz, 1.53H), 7.31 (t, *J*=7.6 Hz, 0.61H), 4.28 (q, *J*=7.1 Hz, 2H), 1.30 (t, *J*=7.1 Hz, 3H); ^{13}C NMR (100 MHz, DMSO-d_6) δ Major rotamer: 160.11, 142.43, 130.32, 118.62, minor rotamer: 162.53, 142.90, 121.19, 116.43.

4-Formamidobenzoic acid[20d] (**3u**): Using the experimental procedure **EP-1**, the product was obtained as brown oil in 80% yield. A mixture of rotamers is observed; ^{1}H NMR (400 MHz, $CDCl_3$) δ 8.85 (s, 0.48H), 8.69 (d, *J*=11.3 Hz, 0.55H), 8.35 (s, 0.47H), 8.00 (s, 0.45H), 7.55 (d, *J*=8.1 Hz, 0.93H), 7.39–7.27 (m, 2H), 7.18 (t, *J*=7.4 Hz, 0.53H), 7.11 (dd, *J*=10.9, 8.0 Hz, 1.47H); ^{13}C NMR (100 MHz, $CDCl_3$) δ Major rotamer: 163.09, 136.87, 129.97, 125.37, 118.90, minor rotamer: 159.55, 137.06, 129.15, 124.87, 120.19.

1-(4-(2-Chlorophenyl)piperazin-1-yl)ethan-1-one (**4a**): Using the experimental procedure **EP-1**, the product was obtained as light yellow solid in 82%; ^{1}H NMR (400 MHz, DMSO-d_6) δ 7.43 (d, *J*=7.9 Hz, 1H), 7.31 (t, *J*=7.7 Hz, 1H), 7.15 (d, *J*=8.0 Hz, 1H), 7.07 (t, *J*=7.6 Hz, 1H), 3.58 (t, *J*=4.4 Hz, 4H), 2.97 (t, *J*=4.4 Hz, 2H), 2.90 (t, *J*=4.4 Hz, 2H), 2.05 (s, 3H). ^{13}C NMR (100 MHz, DMSO-d_6) δ 168.32, 148.64, 130.30, 128.08, 127.72, 124.22, 121.09, 51.15, 50.73, 45.90, 45.47, 41.02, 21.18, 8.45.

***N*-(2-Hydroxyphenyl)acetamide**[21a] (**4b**): Using the experimental procedure **EP-1**, the product was obtained as white solid in 89%; ^{1}H NMR (400 MHz, DMSO-d_6) δ 9.73 (s, 1H), 9.30 (s, 1H), 7.67 (d, *J*=7.9 Hz, 1H), 6.93 (t, *J*=7.5 Hz, 1H), 6.85 (d, *J*=7.7 Hz, 1H), 6.75 (t, *J*=7.6 Hz, 1H), 2.09 (s, 3H). ^{13}C NMR (100 MHz, DMSO-d_6) δ 169.02, 147.89, 126.42, 124.65, 122.37, 118.98, 115.95, 23.59.

***N*-(3-Hydroxyphenyl)acetamide**[21b] (**4c**): Using the experimental procedure **EP-1**, the product was obtained as colourless semisolid in 94%; ^{1}H NMR (400 MHz, DMSO-d_6) δ 9.78 (s, 1H), 9.33 (s, 1H), 7.19 (s, 1H), 7.05 (t, *J*=8.0 Hz, 1H), 6.92 (d, *J*=8.1 Hz, 1H), 6.43 (dd, *J*=8.0, 1.7 Hz, 1H), 2.02 (s, 3H). ^{13}C NMR (100 MHz, DMSO-d_6) δ 168.18, 157.56, 140.36, 129.27, 110.12, 109.77, 106.19, 24.05.

***N*-(4-Hydroxyphenyl)acetamide**[21c] (**4d**) Using the experimental procedure **EP-1**, the product was obtained as light yellow solid in 97%; ^{1}H NMR (400 MHz, DMSO-d_6) δ 9.64 (s, 1H), 9.13 (s, 1H), 7.34 (d, *J*=8.5 Hz, 2H), 6.68 (d, *J*=8.5 Hz, 2H), 1.98 (s, 3H). ^{13}C NMR (100 MHz, DMSO-d_6) δ 167.50, 153.11, 131.02, 120.81, 114.98, 23.72.

***N*-(3-Nitrophenyl)acetamide**[18d] (**4e**): Using the experimental procedure **EP-1**, the product was obtained as yellow solid in 62%; ^{1}H NMR (400 MHz, DMSO-d_6) δ 10.44 (s, 1H), 8.60 (t, *J*=2.0 Hz, 1H), 7.87 (dd, *J*=8.2, 2.1 Hz, 2H), 7.57 (t, *J*=8.2 Hz, 1H), 2.09 (s, 3H). ^{13}C NMR (100 MHz, DMSO-d_6) δ 166.08, 144.94, 137.39, 127.07, 121.86, 114.49, 110.03, 109.93, 21.01.

***N*-(3-(Trifluoromethyl)phenyl)acetamide**[21d] (**4f**): Using the experimental procedure **EP-1**, the product was obtained as white solid in 79%; ^{1}H NMR (400 MHz, DMSO-d_6) δ 10.27 (s, 1H), 8.08 (s, 1H), 7.75 (d, *J*=8.2 Hz, 1H), 7.53 (t, *J*=8.0 Hz, 1H), 7.36 (t, *J*=11.5 Hz, 1H), 2.08 (s, 3H). ^{13}C NMR (100 MHz, DMSO-d_6) δ 168.91, 151.00, 140.03, 130.32, 129.90, 122.44, 119.31, 119.27, 117.78, 114.98, 114.94, 111.27, 110.71, 24.00, 20.55.

***N*-(4-(Trifluoromethoxy)phenyl)acetamide**[21e] (**4g**): Using the experimental procedure **EP-1**, the product was obtained as Colourless Solid in 71%; ^{1}H NMR (400 MHz, $CDCl_3$) δ 7.95 (s, 1H), 7.53 (d, *J*=8.8 Hz, 2H), 7.14 (d, *J*=8.5 Hz, 2H), 2.16 (s, 3H). ^{13}C NMR (100 MHz, $CDCl_3$) δ 169.00, 145.43, 136.71, 128.95, 127.92, 127.80, 121.87, 121.77, 121.32, 119.32, 24.46.

***N*-Methyl-N-phenylacetamide**[17c] (**4h**): Using the experimental procedure **EP-1**, the product was obtained as light brown solid in 86%; ^{1}H NMR (400 MHz, DMSO-d_6) δ 7.44 (t, *J*=7.0 Hz, 2H), 7.32 (d, *J*=7.5 Hz, 3H), 3.14 (s, 3H), 1.75 (s, 3H). ^{13}C NMR (100 MHz, DMSO-d_6) δ 144.39, 129.56, 127.38, 127.06, 36.52, 22.17.

***N*-Benzylbenzamide**[22a] (**5a**): Using the experimental procedure **EP-2**, the product was obtained as white solid in 80%; ^{1}H NMR (400 MHz, DMSO-d_6) δ 9.08 (s, 1H), 7.92 (d, *J*=7.2 Hz, 2H), 7.55–7.50 (m, 1H), 7.47 (t, *J*=7.5 Hz, 2H), 7.33 (d, *J*=4.1 Hz, 4H), 7.26–7.21 (m, 1H). ^{13}C NMR (100 MHz, DMSO-d_6) δ 166.17, 139.70, 134.32, 131.19, 128.28, 128.24, 127.23, 127.17, 126.68.

***N*-(2-Chlorophenyl)benzamide**[22b] (**5b**): Using the experimental procedure **EP-2**, the product was obtained as white solid in 50%; ^{1}H

EurJOC
European Journal of Organic Chemistry
Full Papers
doi.org/10.1002/ejoc.202101114
Chemistry Europe
European Chemical Societies Publishing

NMR (400 MHz, DMSO-d_6) δ 10.06 (s, 1H), 8.02 (d, J=7.8 Hz, 2H), 7.66–7.58 (m, 2H), 7.55 (dd, J=12.4, 5.4 Hz, 3H), 7.39 (t, J=7.6 Hz, 1H), 7.30 (t, J=7.7 Hz, 1H). ^{13}C NMR (100 MHz, DMSO-d_6) δ 165.35, 135.08, 133.95, 131.78, 129.48, 129.44, 128.43, 128.33, 127.65, 127.39, 127.36.

N-(4-Chlorophenyl)benzamide[22c] **(5c)**: Using the experimental procedure **EP-2**, the product was obtained as white solid in 80%; ^{1}H NMR (400 MHz, DMSO-d_6) δ 10.41 (s, 1H), 7.98 (d, J=7.5 Hz, 2H), 7.85 (d, J=8.8 Hz, 2H), 7.61–7.50 (m, 3H), 7.40 (d, J=8.8 Hz, 2H). ^{13}C NMR (100 MHz, DMSO-d_6) δ 165.60, 138.14, 134.64, 131.61, 128.42, 128.33, 127.65, 127.22, 121.85, 121.76.

***N,N*-Diphenylbenzamide**[23a] **(5d)**: Using the experimental procedure **EP-2**, the product was obtained as yellow solid in 65%; ^{1}H NMR (400 MHz, DMSO-d_6) δ 7.73–7.64 (m, 7H), 7.32–7.14 (m, 4H), 7.00 (t, J=8.4 Hz, 4H). ^{13}C NMR (100 MHz, DMSO-d_6) δ 188.20, 169.86, 159.63, 149.42, 149.08, 142.53, 142.05, 141.96, 130.18, 128.24, 127.86, 124.21, 123.83, 123.71, 122.71, 114.98, 112.94, 111.25.

***N*-(2-Methoxyphenyl)benzamide**[23b] **(5e)**: Using the experimental procedure **EP-2**, the product was obtained as white solid in 89%; ^{1}H NMR (400 MHz, DMSO-d_6) δ 9.39 (s, 1H), 7.98 (d, J=7.4 Hz, 2H), 7.84 (d, J=7.9 Hz, 1H), 7.59 (t, J=7.3 Hz, 3H), 7.18 (t, J=7.8 Hz, 1H), 7.09 (d, J=7.5 Hz, 1H), 6.98 (t, J=7.6 Hz, 1H), 3.84 (s, 3H). ^{13}C NMR (100 MHz, DMSO-d_6) δ 164.90, 151.30, 134.51, 131.53, 128.44, 127.38, 126.87, 125.55, 123.99, 120.17, 111.34, 55.69.

***N*-(4-Methoxyphenyl)benzamide**[15c] **(5f)**: Using the experimental procedure **EP-2**, the product was obtained as white solid in 88%; ^{1}H NMR (400 MHz, DMSO-d_6) δ 10.12 (s, 1H), 7.96 (d, J=7.8 Hz, 2H), 7.69 (d, J=8.8 Hz, 2H), 7.61–7.47 (m, 3H), 6.94 (d, J=8.8 Hz, 2H), 3.75 (s, 3H). ^{13}C NMR (100 MHz, DMSO-d_6) δ 165.06, 155.53, 135.02, 132.20, 131.29, 128.27, 127.48, 121.96, 113.69.

***N*-(4-Nitrophenyl)benzamide**[23c] **(5g)**: Using the experimental procedure **EP-1**, the product was obtained as brown solid in 75%; ^{1}H NMR (400 MHz, DMSO-d_6) δ 10.84 (s, 1H), 8.26 (d, J=9.0 Hz, 2H), 8.08 (d, J=9.0 Hz, 2H), 8.00 (d, J=7.9 Hz, 2H), 7.63 (t, J=6.9 Hz, 1H), 7.56 (t, J=7.6 Hz, 2H). ^{13}C NMR (100 MHz, DMSO-d_6) δ 166.27, 145.52, 142.44, 134.20, 132.14, 128.48, 127.93, 124.74, 119.83, 119.75.

***N*-(3-(Trifluoromethyl)phenyl)benzamide**[22c] **(5h)**: Using the experimental procedure **EP-1**, the product was obtained as white solid in 45%; ^{1}H NMR (400 MHz, DMSO-d_6) δ 10.68 (s, 1H), 8.30 (s, 1H), 8.10 (d, J=8.0 Hz, 1H), 8.02 (d, J=7.9 Hz, 1H), 7.65–7.51 (m, 2H), 7.45 (d, J=7.8 Hz, 1H). ^{13}C NMR (101 MHz, DMSO-d_6) δ 140.00, 131.87, 129.79, 128.41, 127.77, 123.82.

Author contributions

Authorship was assigned on the basis of the contributions of each author to the work described in the manuscript (detailed below) following a discussion involving all authors. S.D. and V.K. wrote the manuscript, compiled the supplementary information and all authors contributed to the reading and editing of the manuscript and supporting information. V.K., and P.S.G. conducted the chemical reactions described in the manuscript. P.S. and R.K. supervised the entire study.

Acknowledgments

The authors are thankful to the Discipline of Pharmaceutical Sciences, College of Health Sciences, University of Kwa-Zulu Natal (UKZN), Durban, South Africa, for providing all the necessary facilities. R.K. gratefully acknowledges National Research Foundation-South Africa (NRF-SA) for funding this project (Grant Nos. 103728 and 112079).

Conflict of Interest

The authors declare no conflict of interest.

Keywords: Amine · Amide · Hydrochloride salt · Metal-free chemistry · Transamidation

[1] Y. L. Zheng, S. G. Newman, *ACS Catal.* **2019**, *9*, 5, 4426–4433.
[2] a) M. R. Petchey, G. Gregan, *Adv. Synth. Catal.* **2019**; b) D. Kaiser, A. Bauer, M. Lemmerer, N. Maulide, *Chem. Soc. Rev.* **2018**; c) M. B. Chaudhari, B. Gnanaprakasam, *Chem. Asian J.* **2019**; d) A. C. Fonseca, M. H. Gil, P. N. Simões, *Prog. Polym. Sci.* **2014**; e) M. Todorovic, D. M. Perrin, *Pept. Sci.* **2020**.
[3] T. Narendar Reddy, A. Beatriz, V. Jayathirtha Rao, D. P. de Lima, *Chem. Asian J.* **2019**, *14*, 3, 344–388.
[4] S. Mahesh, K. C. Tang, M. Raj, *Molecules* **2018**, *23*, 10, 2615.
[5] P. Acosta-Guzmán, A. Mateus-Gómez, D. Gamba-Sánchez, *Molecules* **2018**, *23*, 9, 2382.
[6] R. Sanichar, J. C. Vederas, *Org. Lett.* **2017**, *19*, 1950–1953.
[7] a) I. S. Young, A. L. Glass, T. Cravillion, C. Han, H. Zhang, F. Gosselin, *Org. Lett.* **2018**, *20*, 3902–3906; b) J. E. Dander, E. L. Baker, N. K. Garg, *Chem. Sci.* **2017**, *8*, 6433–6438; c) Y. Li, F. Jia, Z. Li, *Chem. A Eur. J.* **2013**, *19*, 1, 82–86; d) G. Pelletier, D. A. Powell, *Org. Lett.* **2006**, *8*, 26, 6031–6034; e) X. Kong, B. Xu, *Org. Lett.* **2018**, *20*, 15, 4495–4498.
[8] a) Z. Li, C. Guo, J. Chen, Y. Yao, Y. Luo, *Appl. Organomet. Chem.* **2020**, *34*, 4, 5517; b) H. Jiang, Z. Hu, C. Gan, B. Sun, S. Kong, F. Bian, *J. Mol. Catal.* **2021**, *504*, 111490; c) D. C. Lenstra, D. T. Nguyen, J. Mecinović, *Tetrahedron* **2015**, *71*, 34, 5547–5553; d) E. Bon, D. C. H. Bigg, G. Bertrand, *J. Org. Chem.* **1994**, *59*, 15, 4035–4036; e) S. P. Pathare, A. K. H. Jain, K. G. Akamanchi, *RSC Adv.* **2013**, *21*, 3, 7697–7703.
[9] J. Briffa, E. Sinagra, R. Blundell, *Heliyon* **2020**, *6*, 9, e04691.
[10] a) T. B. Nguyen, J. Sorres, M. Q. Tran, L. Ermolenko, A. Al-Mourabit, *Org. Lett.* **2012**, *14*, 12, 3202–3205; b) S. Nageswara Rao, D. Chandra Mohan, S. Adimurthy, *Green Chem.* **2014**, *16*, 9, 4122–4126; c) J. Yin, J. Zhang, C. Cai, G. J. Deng, H. Gong, *Org. Lett.* **2019**, *21*, 387–392.
[11] a) R. Vanjari, B. Kumar Allam, K. Nand Singh, *RSC Adv.* **2013**, *3*, 6, 1691–1694; b) S. Adimurthy, *J. Biomol. Res. Ther.* **2016**, 5, 2; c) C. L. Allen, B. N. Atkinson, J. M. J. Williams, *Angew. Chem. Int. Ed.* **2012**, 51, 1383–1386; *Angew. Chem.* **2012**, *124*, 1412–1415; d) A. K. Brel, S. V. Lisina, S. S. Popov, Y. N. Budaeva, *Russ. J. Gen. Chem.* **2016**, *86*, 3, 549–551.
[12] G. Li, M. Szostak, *Nat. Commun.* **2018**, *9*, 1–8.
[13] E. L. Baker, M. M. Yamano, Y. Zhou, S. M. Anthony, N. K. Garg, *Nat. Commun.* **2016**, *7*, 1–5.
[14] a) R. Chutia, B. Chetia, *New J. Chem.* **2018**, *42*, 18, 15200–15206; b) C. Chen, Y. Pan, H. Zhao, X. Xu, J. Xu, Z. Zhang, S. Xi, L. Xu, H. Li, *Org. Chem. Front.* **2018**, *5*, 3, 415–422; c) U. V. Mallavadhani, L. Sahoo, S. Roy, *Indian J. Chem. Sect. B* **2004**, *43B*, 10, 2175–2177.
[15] a) W. D. Li, D. Y. Zhu, G. Li, J. Chen, J. B. Xia, *Adv. Synth. Catal.* **2019**, *361*, 22, 5098–5104; b) P. V. Ramachandran, H. J. Hamann, *Org. Lett.* **2021**, *23*, 8, 2938–2942; c) Z. Fu, X. Wang, S. Tao, Q. Bu, D. Wei, N. Liu, *J. Org. Chem.* **2021**, *86*, 3, 2339–2358; d) J. S. Li, X. Y. Xie, S. Jiang, P. P. Yang, Z. W. Li, C. H. Lu, W. D. Liu, *Org. Chem. Front.* **2021**, *8*, 4, 697–701; e) T. Imanishi, Y. Fujiwara, Y. Sawama, Y. Monguchi, H. Sajiki, *Adv. Synth. Catal.* **2012**, *354*, 5, 771–776.
[16] a) F. F. Feng, X. Y. Liu, C. W. Cheung, J. A. Ma, *ACS Catal.* **2021**, *11*, 12, 7070–7079; b) K. Wang, J. Hou, T. Wei, C. Zhang, R. Bai, Y. Xie, *Tetrahedron Lett.* **2021**, *62*, 152623; c) X. Yi, X. Yi, S. Lei, W. Liu, F. Che, C. Yu, X. Liu, Z. Wang, X. Zhou, Y. Zhang, *Org. Lett.* **2020**, *22*, 12, 4583–

EurJOC
European Journal of Organic Chemistry
Full Papers
doi.org/10.1002/ejoc.202101114
Chemistry Europe
European Chemical Societies Publishing

4587; d) Y. J. Wang, G. Y. Zhang, A. Shoberu, J. P. Zou, *Tetrahedron Lett.* **2021**, *80*, 153316; e) D. Joseph, M. S. Park, S. Lee, *Org. Biomol. Chem.* **2021**, *19*, 28, 6227–6232.
[17] a) R. Sallio, P. A. Payard, P. Pakulski, I. Diachenko, L. Fabre, S. Berteina-Raboin, C. Colas, I. Ciofini, L. Grimaud, I. Gillaizeau, *RSC Adv.* **2021**, *11*, 15885–15889; b) T. Ghosh, S. Jana, J. Dash, *Org. Lett.* **2019**, *21*, 6690–6694; c) C. Li, M. Wang, X. Lu, L. Zhang, J. Jiang, L. Zhang, *ACS Sustainable Chem. Eng.* **2020**, *8*, 11, 4353–4361; d) M. C. Pichardo, G. Tavakoli, J. E. Armstrong, T. Wilczek, B. E. Thomas, M. H. G. Prechtl, *ChemSusChem* **2020**, *13*, 5, 882–887; e) K. Zhang, L. Zong, X. Jia, *Adv. Synth. Catal.* **2021**, *363*, 5, 1335–1340.
[18] a) S. Wu, Z. Huang, X. Jiang, F. Yan, Y. Li, C. X. Du, *ChemSusChem* **2021**, *14*, 7, 1763–1766; b) M. Amirsoleimani, M. A. Khalilzadeh, D. Zareyee, *J. Mol. Struct.* **2021**, *1225*, 129076; c) R. B. Sonawane, N. K. Rasal, D. S. Bhange, S. V. Jagtap, *ChemCatChem* **2018**, *10*, 17, 3907–3913; d) M. R. Mutra, G. K. Dhandabani, J. J. Wang, *Adv. Synth. Catal.* **2018**, *360*, 20, 3960–3968; e) Y. Yang, Y. Li, Z. Zhang, Y. Zhao, W. Feng, *Synth. Commun.* **2019**, *49*, 8, 1040–1046.
[19] a) B. Kaboudin, M. Khodamorady, *Synlett* **2010**, *19*, 2905–2907; b) W. Mazumdar, N. Jana, B. T. Thurman, D. J. Wink, T. G. Driver, *J. Am. Chem. Soc.* **2017**, *139*, 14, 5031–5034; c) R. Zhang, J. C. Zhang, W. Y. Zhang, Y. Q. He, H. Cheng, C. Chen, Y. C. Gu, *Synthesis.* **2020**, *52*, 3286–3294; d) L. S. R. Yadav, R. Venkatesh, M. Raghavendra, T. Ramakrishnappa, N. Dhananjaya, G. Nagaraju, *Curr. Nanomater.* **2020**, *5*, 1, 66–78(13); e) N. Vodnala, R. Gujjarappa, S. Polina, V. Satheesh, D. Kaldhi, A. K. Kabi, C. C. Malakar, *New J. Chem.* **2020**, *44*, 48, 20940–20944.
[20] a) J. Li, D. huai Tu, J. Zhang, J. Li, Y. Xue, Q. Xu, Y. Du, C. Li, J. Lu, *Catal. Commun.* **2020**, *147*, 106138; b) B. Karimi, F. Mansouri, H. Vali, *ChemPlusChem* **2015**, *80*, 12, 1750–1759; c) K. Škoch, I. Císařová, P. Štěpnička, *Chem. A Eur. J.* **2018**, *24*, 52, 13788–13791; d) M. Tajbakhsh, R. Hosseinzadeh, Heshmatollah, Alinezhad, Parizad, Rezaee, M. Tajbakhsh, *Lett. Org. Chem.* **2013**, *10*, 657–663.
[21] a) X. Wang, T. Gensch, A. Lerchen, C. G. Daniliuc, F. Glorius, *J. Am. Chem. Soc.* **2017**, *139*, 18, 6506–6512; b) G. Lu, Y. Ren, B. Dong, B. Zhou, J. Ren, Y. Ke, B. B. Zeng, *Tetrahedron Lett.* **2019**, *60*, 39, 150859; c) R. Ma, X. Chen, Z. Xiao, M. Natarajan, C. Lu, X. Jiang, W. Zhong, X. Liu, *Tetrahedron Lett.* **2021**, *63*, 19, 152707; d) S. M. Mali, R. D. Bhaisare, H. N. Gopi, *J. Org. Chem.* **2013**, *78*, 11, 5550–5555; e) K. N. Lee, Z. Lei, C. A. Morales-Rivera, P. Liu, M. Y. Ngai, *Org. Biomol. Chem.* **2016**, *14*, 24, 5599–5605.
[22] a) Z. Wang, A. Matsumoto, K. Maruoka, *Chem. Sci.* **2020**, *11*, 12323–12328; b) Y. X. Liang, M. Yang, B. W. He, Y. L. Zhao, *Org. Lett.* **2020**, *22*, 19, 7640–7644; c) A. Sen, R. N. Dhital, T. Sato, A. Ohno, Y. M. A. Yamada, *ACS Catal.* **2020**, *10*, 14410–14418.
[23] a) M. Fairley, L. J. Bole, F. F. Mulks, L. Main, A. R. Kennedy, C. T. O'Hara, J. García-Alvarez, E. Hevia, *Chem. Sci.* **2020**, *11*, 6500–6509; b) B. A. Mair, M. H. Fouad, U. S. Ismailani, M. Munch, B. H. Rotstein, *Org. Lett.* **2020**, *22*, 7, 2746–2750; c) D. S. Barak, D. J. Dahatonde, S. U. Dighe, R. Kant, S. Batra, *Org. Lett.* **2020**, *22*, 23, 9381–9385.

Manuscript received: September 11, 2021
Revised manuscript received: October 3, 2021
Accepted manuscript online: October 7, 2021

Send Orders for Reprints to reprints@benthamscience.net

Current Medicinal Chemistry, 2021, *28*, 1-40 1

REVIEW ARTICLE

Recent Advances in Chalcone-based Anticancer Heterocycles: A Structural and Molecular Target Perspective

Vishal Kumar[1], Sanjeev Dhawan[1], Pankaj Sanjay Girase[1], Paul Awolade[2], Suraj Raosaheb Shinde[1], Rajshekhar Karpoormath[1,*] and Parvesh Singh[2,*]

[1]*Department of Pharmaceutical Chemistry, Discipline of Pharmaceutical Sciences, College of Health Sciences, University of KwaZulu-Natal (Westville Campus),Durban-4000, South Africa;* [2]*School of Chemistry and Physics, University of KwaZulu-Natal (Westville campus), Private Bag X01, Scottsville, Durban, South Africa*

ARTICLE HISTORY

Received: October 17, 2020
Revised: February 15, 2021
Accepted: February 23, 2021

DOI:
10.2174/0929867328666210322102856

Abstract: Chalcones are an interesting class of compounds endowed with a plethora of biological activities beneficial to human health. These chemotypes have continued to attract increased research attention over the years; hence, numerous natural and synthetic chalcones have found with interesting anticancer activities through the inhibition of various molecular targets including ABCG2, BCRP, P-glycoprotein, 5α-reductase, Androgen receptor (AR), Histone deacetylases (HDAC), Sirtuin 1, proteasome, Vascular endothelial growth factor (VEGF), Cathepsin-K, tubulin, CDC25B phosphatase, Topoisomerase, EBV, NF-κB, mTOR, BRAF, and Wnt/β-catenin. Moreover, the study of intrinsic mechanisms of action, particularly relating to specific cellular pathways and modes of engagement with molecular targets, may help medicinal chemists to develop more effective, selective, and cost-effective chalcone-based anticancer drugs. This review, therefore, sheds light on the effect of structural variations on the anticancer potency of chalcone hybrids reported in 2018-2019 alongside their mechanism of action, molecular targets, and potential impacts on effective cancer chemotherapy.

Keywords: Chalcone, anticancer hybrids, cancer, molecular target, mechanism of action, structure-activity relationship.

1. INTRODUCTION

Cancer is the second leading cause of mortality worldwide and a major public health concern. The recent Global Cancer Statistics (GLOBOCAN) report about 18.1 million new cancer cases, and 9.6 million mortalities were recorded in 2018 (Fig. **1**), and the disease burden is projected to become more onerous if urgent action is not taken [1]. Despite the tremendous efforts to develop new chemotherapies and regimens for different types of cancer, high mortality and morbidity rates still persist as a significant threat to man's existence, especially, countries with higher number of cases. The disease hallmarks, *i.e.* an unregulated proliferation of malignant cells and the associated heterogeneity of the tumour milieu also continue to complicate the outcome of therapeutic interventions [2].

The increasing knowledge on the pathogenesis of typical and aberrant neoplasms and their dependence on the deregulation of critical proteins and enzymes controlling cell division and apoptosis has made the biological mechanisms involved in the transformation of healthy to cancerous cells the focus of modern biomedical research [3,4]. However, despite the progress in diagnosis to designing the therapeutic intervention, drug resistance, drug-induced toxicities, and poor patient compliance are major hurdles in the development of new and clinically significant chemotherapeutic agents [5].

*Address correspondence to these authors at the Department of Pharmaceutical Chemistry, Discipline of Pharmaceutical Sciences, College of Health Sciences, University of KwaZulu-Natal(Westville Campus), Durban-4000, South Africa; Tel: +27 31 260 7179; Fax: +27 (0)31 260 7792;
E-mail: Karpoormath@ukzn.ac.za (R.K)
School of Chemistry and Physics, University of KwaZulu-Natal (Westville campus), Private Bag X01, Scottsville, Durban, South Africa; Tel: +27-31-2602181; +27745147754; Fax: +27(0)31 260 3091; Email: singhp4@ukzn.ac.za (P.S)

0929-8673/21 $65.00+.00

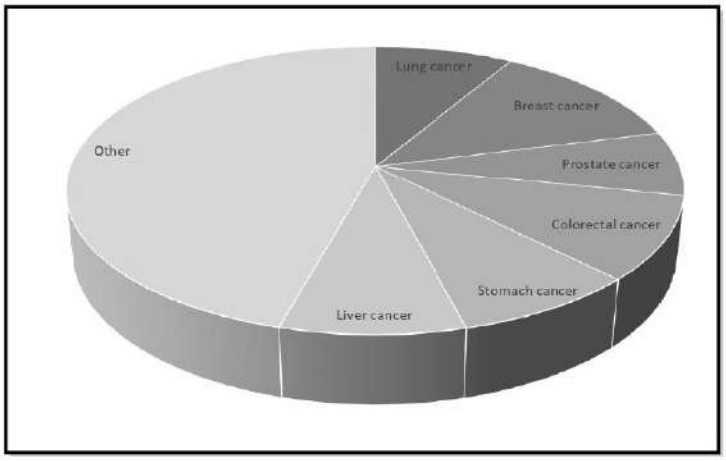

Fig. (1). World's mortality rate of cancer in males and females.

Furthermore, the reduced clinical success of available anticancer agents can be attributed to poor selectivity, off-target toxicity, and the debilitating role of ATP-binding cassette (ABC) transporters [6,7]. These drawbacks of chemotherapy have therefore encouraged the paradigm shift towards alternative therapies for cancer treatment such as apoptosis regulation, anti-angiogenesis therapy, molecular target therapy, immunotherapy, differentiation therapy, targeted radionuclide therapy, nucleic-acid, and signal-transduction-based therapies [8]. Precisely, targeted chemotherapy (Table **1**) exerts its cytotoxic effects through multiple mechanisms, including apoptosis induction, anti-proliferation, immune suppression, and multidrug-resistant(MDR) reversal [9].

The chemical space of natural products has consistently delivered a wide variety of chemotypes with interesting anticancer activities. Among them, chalcones are open-chain flavonoids found in a variety of plant species [10, 11]. Chemically, chalcones are 1,3-diphenyl-2-propene-1-one/benzylidene-acetophenone, they are not only an important structural component of the natural product family but also an essential moiety in synthetic and marketed drugs (Fig. **2**) [12]. Although various synthetic routes have been adopted to access structurally diverse chalcones (Fig. **3**), the Claisen-Schmidt condensation in acid or base, under homogenous conditions remains the most prominent [13]. The traditional strong alkaline media employed includes natural phosphates, KOH, NaOH, $Ba(OH)_2$, and LiHMDS.

The medicinal chemistry and therapeutic relevance of chalcone derivatives are resplendent in literature with many reports highlighting the significance of α,β-unsaturated carbonyl moiety to drug-target interaction and biological activity [14]. Thus, in the current review, a particular focus is given to molecular targets of chalcones for the treatment of cancers and the structurally related chalcones that have been published in the last two years (2018-2019). Their mechanism of action and structure-activity relationship (SAR) were also discussed based on the substitution pattern on rings A and B of the chalcone's structure (Fig. **2**).

2. MOLECULAR TARGETS OF ANTI-CANCER CHALCONES

2.1. P-glycoprotein Inhibitors

Encoded by the ABC subfamily B member 1 (ABCB1) gene, the permeability P-gp also referred to as MDR-1, is a significant cell membrane protein widely expressed to pump exogenous materials out from the cells by ATP-efflux pump, thus playing a vital role in cellular defence mechanism [38]. However, the overexpression of P-gps by cancerous cells thwarts the efficacy of chemotherapeutic agents by reducing the active drugs' concentration. Some chalcone-based compounds exhibiting excellent P-gp inhibition are discussed below [17,39].

A library of chalcone hybrids (**1**, Fig. **4**) was synthesized by Yin and co-workers based on molecular docking simulations [40]. The compounds were evaluated *in vitro* for their anticancer activity against

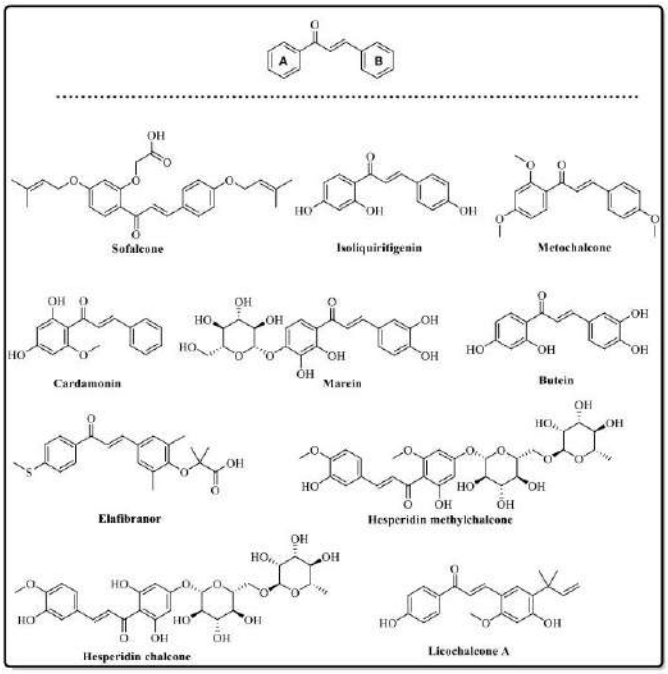

Fig. (2). Chalcone ring pattern and clinically approved chalcone-based drugs.

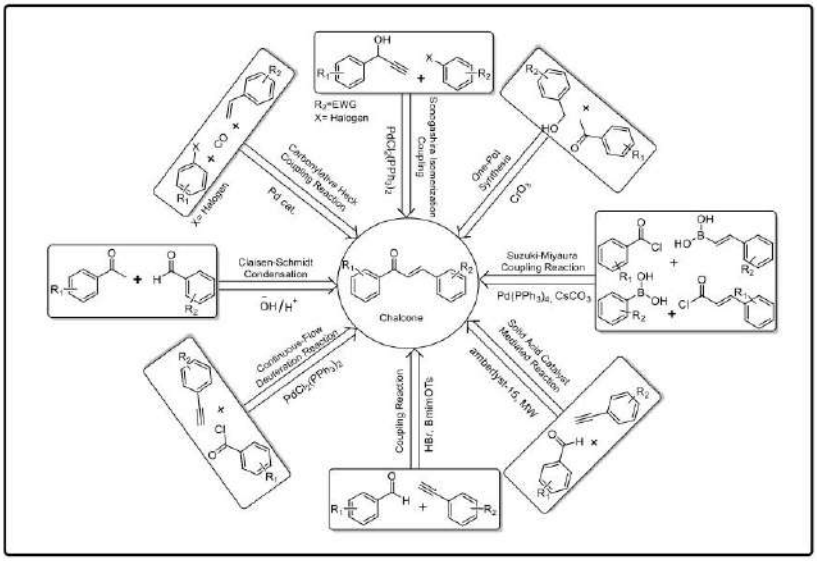

Fig. (3). Different synthetic routes to the chalcone nucleus.

Table 1. Cellular targets of anti-cancer agents.

Channel Involved	Targets	Functions	References
Multi-drug resistance (MDR) Channels			
Multidrug resistance-associated protein (MRP-1) inhibitors	• ABCC1 gene	• Protecting cancer stem cells involved in the MDR	[15]
ATP-binding cassette super-family G member 2 (ABCG2) inhibitors	• ABCG2 gene	• The defense mechanism of the body	[16]
P-glycoprotein inhibitors (P-gp)	• ABCB1 protein of cell membrane	• Pump foreign material out from the cells	[17]
Hormonal Milieu inhibitor			
5α-reductase inhibitor	• 5α-Reductase 1/2/3	• Steroid metabolism	[18]
Androgen receptor (AR)translocation inhibitor (NR3C4)	• AR gene on the X chromosome	• Translocation	[19]
Sex hormone synthesis inhibitor	• Members of the cytochrome • P450 (CYP) system.	• Sexual development and reproduction	
Protein deacetylation inhibitors			
Histone deacetylases inhibitor (HDAC)	• Histone and non-histone proteins	• Removal of acetyl functional groups	[20]
Sirtuin 1 inhibitor	• Nicotinamide adenine dinucleotide (NAD+)dependent-histone deacetylases	• Apoptosis, • Cell proliferation, • Metabolism, • Deoxyribonucleic Acid (DNA) repair • Caloric restriction	[21]
p53 degradation inhibitors			
Oncoprotein interaction inhibitor	• Cancer cell	• Aggressive cancer growth	[22]
Proteasome inhibitor	• Adenosine triphosphate (ATP)-dependent proteolytic activity	• Proteolysis	[23]
Janus kinases (JAKs), signal transducer and activator of transcription proteins (STAT) signaling pathway inhibitor	• DNA	• Activation of cytokine receptor signaling	[24]
Angiogenesis inhibitor			
Vascular endothelial growth factor (VEGF) inhibitor	• Tumour cells	• Formation of new blood vessels	[25]
Vascular endothelial growth factor receptor two inhibitor	• Tumor cells	• Regulates endothelial migration and proliferation	[26]
Matrix-metalloproteinases-2/9 (MMP) inhibitor	• Protease extracellular matrix	• Extracellular matrix (ECM) degradation	[27]
Cellular proliferation inhibitor			
Cathepsin-K inhibitor	• Bone matrix	• Degradation of the organic phase of bone during bone resorption.	[28]
Tubulin inhibitor	• Centrosomes and spindle pole bodies	• Microtubules formation	[29]
M-phase inducer phosphatase 2 (CDC25B) phosphatase inhibitor	• Cell cycle	• G2/M phase transition • Cyclin-dependent kinases activating	[30]

(Table 1) contd....

Channel Involved	Targets	Functions	References
Topoisomerase expression inhibitor	• Topoisomerase I and II	• Replication, • Transcription, • Translation • Recombination of DNA	[31]
Epstein Barr (EBV) induced cancer inhibitor	• Cell nucleus	• Signaling • Transcriptional pathways	[32]
Wnt inhibitors	• Frizzled-related proteins (sFRPs).	• Signaling pathways	[33]
Kinase inhibitors	• Enzyme	• Transfer of phosphate groups	[34]
mTOR inhibitors	• Serine/threonine-specific protein kinase	• Cellular metabolism, • Growth • Proliferation	[35]
BRAF inhibitors	• BRAF gene	• Blocks signaling of the MAPK pathway	[36]
NF-κB (nuclear factor kappa-light-chain-enhancer of activated B cells) inhibitors	• Nuclear factor NF-kappa-B p105 subunit (NF-κB1) • Nuclear factor NF-kappa-B p100 subunit (NF-κB2) • nuclear factor NF-kappa-B p65 subunit (RelA) • Transcription factor RelB (RelB) • c-Rel	• Controls transcription of DNA, • Cytokine production • Cell survival	[37]

parental MDCK II (Madin-Darby canine kidney), H69 (small cell lung cancer), and MCF-7 (breast cancer) cell lines. The most potent compound **1a** (Fig. **4**) exhibited an IC_{50} (half maximal inhibitory concentration) value of 1.02 μM against the HepG2 cell line, compared to the reference drug verapamil and doxorubicin (IC_{50} = 10.10 and 51.19 μM).

Riaz *et al.* conducted a comprehensive study of 40 novel α-substituted chalcones hybrids(**2**, Fig. **4**) and examined their anti-cancer activity *in vitro* against HCC1954 (breast) and HCT116 (colo-rectal) cancer cell lines using the SRB (sulforhodamine B) proliferation assay [41]. SAR analysis showed that α-substituted chalcones with chloro and methoxy groups enhanced the anticancer potency; hence, compounds **2a** and **2b** displayed promising anticancer activities against HCC1954 and HCT116 cell line at GI_{50}(half-maximal growth inhibition) values of 0.63, 0.725, and 0.69, 1.59 μM superior to the reference drug, Paclitaxel. Both compounds, **2a** and **2b,** induced apoptosis by cell growth arrest at the G2/M phase, p53 induction, and PARP (Poly (ADP-ribose) polymerase) cleavage, MDR-1 in the cell line.

An interesting study on aspirin-chalcone analogs (**3**, Fig. **4**) as anti-colorectal cancer agents was conducted by Shan Lu *et al.* [42].The authors reported that compound **3a** displayed superior anti-proliferative activity *in vitro* against HCT-8, DLD-1, and CCD841 cell lines compared to 5-Fluorouracil. Their mechanistic studies further revealed that compound **3a** arrests the cell cycle at the G1 phase and induced apoptosis of CRC (Colorectal cancer) cells as well as the ROS in HCT-8 cells.

Mu *et al.* [43] examined some curcumin derivatives L6H4 on gastric cancer cells (BGC- 823). The *in vivo* evaluation using mouse xeno-transplant gastric tumour model and western blot analysis showed that curcumin L6H4 decreases the expression levels of p53, p21, Bax, and Bcl- 2 and inhibited metastasis and invasiveness. In animal models, curcumin L6H4 analogs suppress the growth of tumor cells and induced the apoptosis of BGC- 823 cells.

In a report by Y. Shang *et al.* [44] two series of coumarin–chalcone hybrids (**4**, Fig. **4**) were prepared from Claisen–Schmidt condensation as cytotoxic agents against A549(human lung adenocarcinoma) cells and inhibitors of ROS accumulation. The preliminary screening showed compound **4a** as the most promising coumarin-chalcone hybrid overall while SAR studies concluded that the chalcone moiety as Michael acceptor plays a crucial role in enhancing cytotoxicity than the position of the hydroxyl (Fig. **4**).

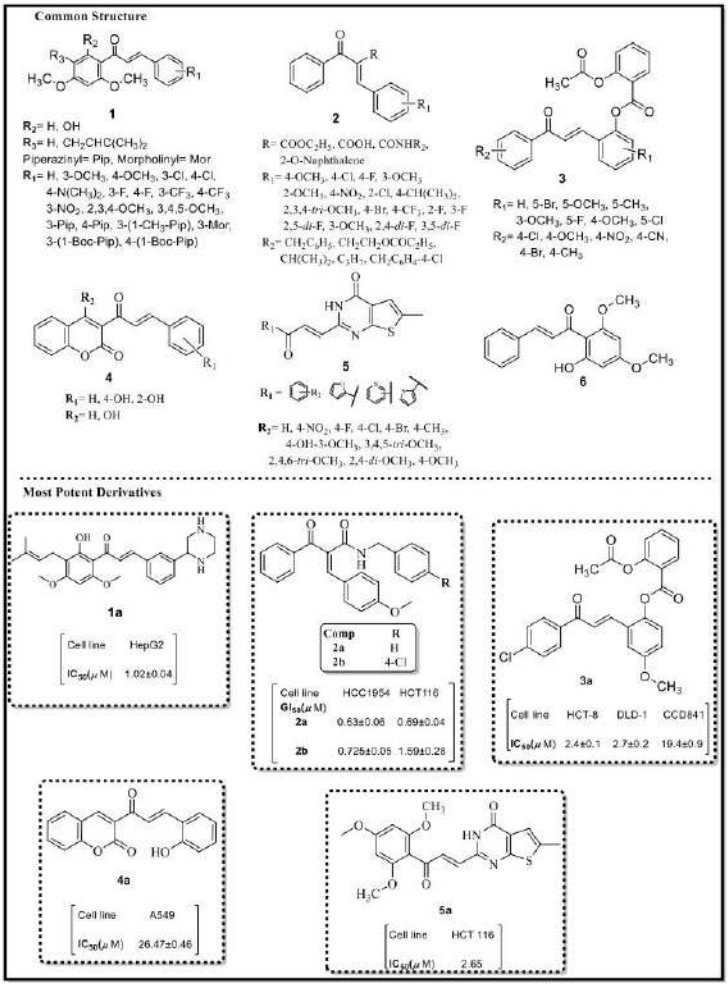

Fig. (4). Substituted chalcones (**1**-**6**) as P-glycoprotein inhibitors.

A series of chalcone analogs (**5**, Fig. **4**) containing thienos [2,3-d] pyrimidin-2-yl nucleus was disclosed by Wang, *et al.* as chemotherapeutic agents against A549 and HCT-116 cell lines [45]. Compound **5a** showed excellent cytotoxicity with an IC_{50} value of 2.65 μM against HCT-116 cells. It was concluded that due to an increase in cleavage of PARP-1 and caspases 3/7/9, compound **5a** induced apoptosis in HCT-116 cells *via* the mitochondrial death pathway.

Hseu *et al.* [46] studied the anticancer efficacy of chalcone flavo-kawain B (FKB) (**6**, Fig. **4**). The study demonstrated that compound **6** induced cell death through apoptosis by hindering PARP-1 and caspase 9/3 signalling pathways and autophagy of A549 cells. Further, the increased ATG7 expression and reduction in the mTOR phosphorylation levels in A549 cells induced autophagy in the cancer cells.

3. HORMONAL MILIEU INHIBITORS

3.1. Androgen Receptor Translocation Inhibitor

The androgen receptor (AR) is a nuclear receptor (NR) that communicates with various genetic

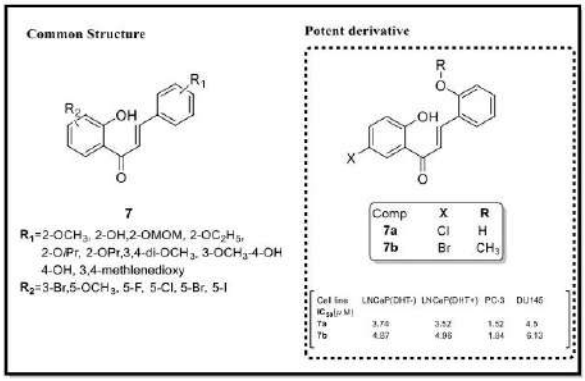

Fig. (5). Chalcone analogs (**7**) as androgen receptor translocation inhibitor.

components that rapidly encode and regulates intracellular cascades. In the absence of an agonist (dihydrotestosterone), ARs are bound to heat shock protein (Hsp-90). As in most NRs, ligand binding initiates direct dissociation of Hsp-90, which subsequently translocates AR into the nucleus to induce gene transcription. Inhibition of this process forestalls the hormonal spread of prostate tumors [47].

Saito *et al.* [48] discovered a novel series of 5'-Chloro-2,2'-dihydroxychalcone as an apoptosis inducer(**7**, Fig. **5**). The compounds were evaluated against taxane-resistant prostate and androgen-independent (AR) cancer along with a multidrug-resistant subline. Compounds **7a** and **7b** exhibited the best potency at an IC_{50} value range of 1-6 μM against PC-3 and DU145 cell lines. Compound **7a** (IC_{50} = 1.52 μM) also interfered with the microtubule network and inhibited sub-G1 aggregation in PC-3 cells. Further, SAR elucidation showed the effect of different substitution patterns on rings A and B on cytotoxicity.

4. p53 DEGRADATION INHIBITORS

p53 is a crucial protein that controls the cell cycle and serves as a tumor suppressor in neoplastic environments.The protein also plays a significant role in regulating DNA repair, gene activation, genomic stability, angiogenesis inhibition, and apoptosis (Fig. **6**). MDM2 and Sirtuin-1 promote the degradation of p53. Thus, inhibiting p53 protein degradation is considered an effective strategy for anticancer therapy [49].

4.1. Oncoprotein Interaction INHIBITORS

Zhao *et al.* synthesized a series of molecular hybrids (**8**, Fig. **7**) as antiproliferative agents against four human cancer cell lines, namely, MGC803, A549, TE-1, and THP-1 [50]. All the examined compounds displayed promising antiproliferative effects in a dose-dependent manner on each cancer cell line. The representative compound **8a** showed the highest activity against MGC803 with an IC_{50} value of 0.84 μM, which is 10-fold more potent than reference drug 5-fluorouracil (5-FU). Mechanistically, the active analogs induced apoptosis in MGC803 *via* up-regulation of Bax and down-regulation of Bcl-2 alone with PARP cleavage. SAR analysis further disclosed that the compounds' antiproliferative activity is mainly influenced by the electron richness or deficiency of the chalcone scaffold.

MDM2 is an E3 ubiquitin ligase and a primary p53 cell antagonist. It functions in unstressed cells by limiting the suppressive role of p53. MDM2 present in mono-ubiquitinates p53 unstressed cells and its mediation destroys the nuclear and cytoplasmic proteasomes. Disruption by multiple routes of the complex p53-MDM2, which leads to the induction and biological response of p53, is a crucial event for p53 activation [51].

Magda *et al.* synthesized a library of 1,2,4-triazolo-tetrahydroisoquinolines (**9**, Fig. **7**) and evaluated their anticancer potentials against MCF-7, A549, HCT116, and Hepg2 cell lines [52]. SAR studies suggested the positive influence of methoxy groups on potency;hence, compounds **9a** and **9b** displayed promising anticancer activities against the estrogen-dependent breast cancer cell line, MCF-7, at IC_{50} values of 50.05 and 27.15 μM, respectively, superior to the positive control 5-FU (IC_{50} = 178 μM). In the MCF-7 cell line, compounds **9a** and **9b** effectively induced cell growth arrest at the G1 phase of the cell cycle.

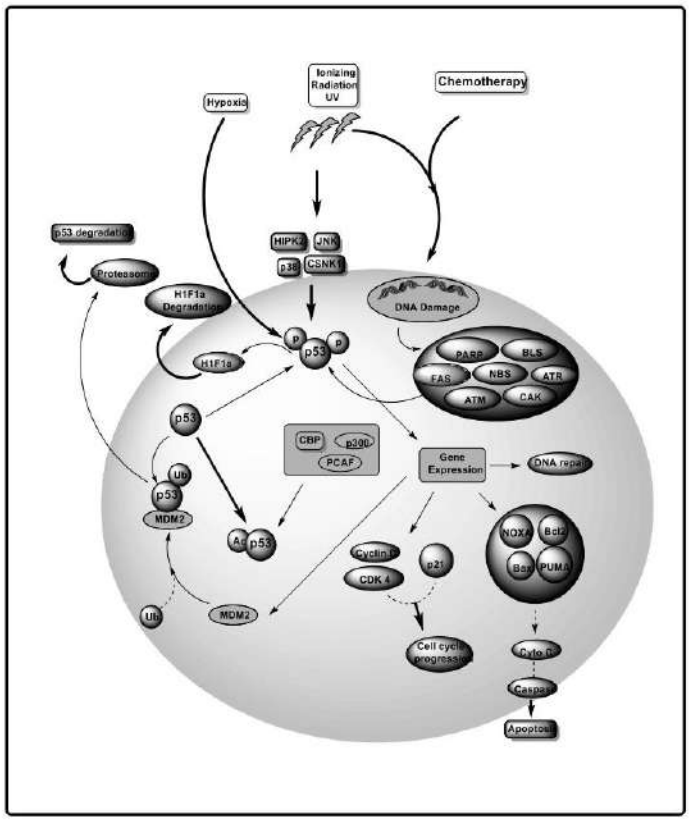

Fig. (6). Cellular pathways involved in p53 degradation inhibition.

Using a base-promoted Claisen–Schmidt condensation reaction, Bandeira *et al.* [53] synthesized a series of chalcone hybrids (**10**, Fig. **7**) containing amino/acetamide groups and evaluated for their anticancer activity. Compound **10a** exhibited significant antiproliferative activity with an IC_{50} value of 3.56 μM against the HCT-116 (colon cancer) cell line.In contrast, the insertion of the electron-donating group (EDG)on ring B inverted the inhibition profile (IC_{50}> 20 μM). Mechanistically, compound **10a** induced cell apoptosis *via* G2/M cell cycle arrest in HCT 116 cells.

Brandao *et al.* [54] reported the synthesis of prenylchalconeshybrids (**11**, Fig. **7**) and evaluated their *in vitro* antitumor activity against HCT116, MCF-7, HepG2, and A375 cancer cell lines. Compound **11a** exhibited the highest cytotoxicity at an IC_{50} range of 1.6-3.6 μM against the tested cancer cell lines HepG2 cells and was superior to standard drug Nutlin. The molecular docking studies suggested the anti-cancer activity is due to their strong hydrogen-bonding interactions with MDM2-p53 proteins.

Among the chalcone-Schiff base derivatives (**12**, Fig. **7**) synthesised by Marwa *et al.* [55] , compound **12** emerged as the most potent cytotoxic agent against HepG2 and MCF-7 cancer cell lines with IC_{50} values of 10.3 and 6.4 μM, respectively, which is comparative to the reference drug doxorubicin (IC_{50} = 8.4 μM and 7.8 μM). The apoptotic effect of compound **12a** was due to the overexpression level of caspase-3. The compound also exerted its anti-proliferative effect *via* phenoxide radical formation. Moreover, SAR analysis demonstrated that electron-withdrawing (EWG) and electron-donating groups (EDG) on chalcone and Schiff bases significantly influenced anticancer activity.

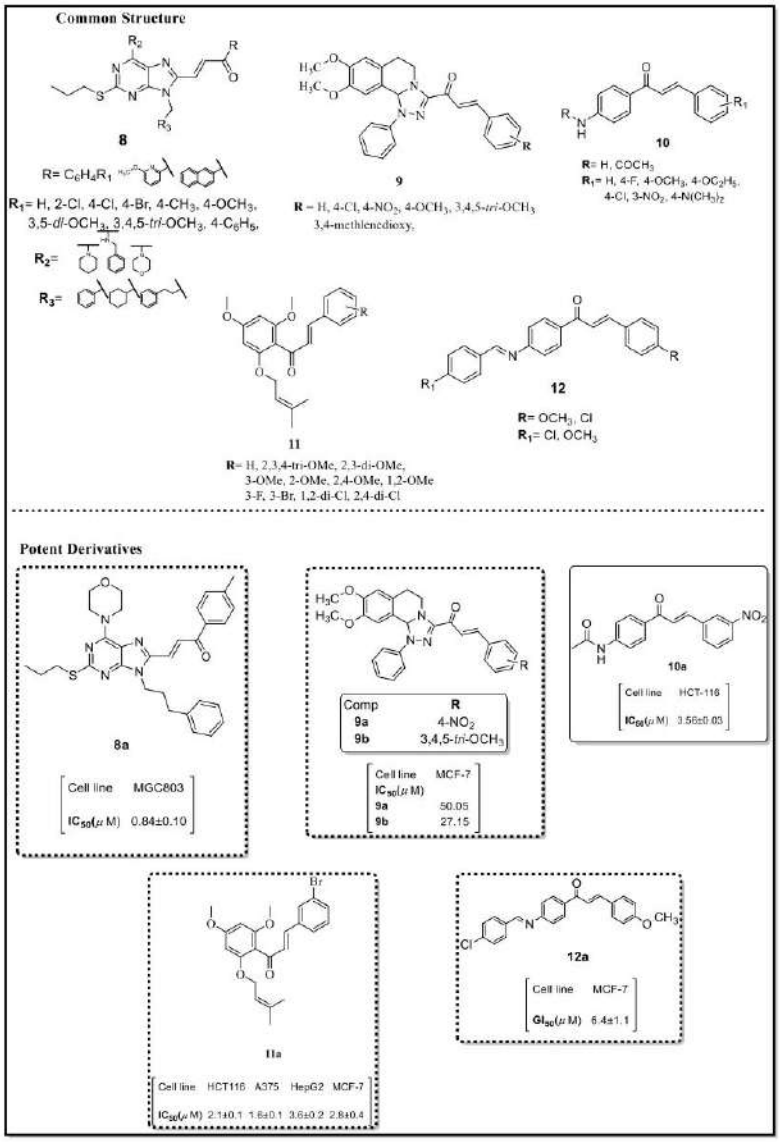

Fig. (7). Chalcone analogs (**8**-**12**) as Oncoprotein interaction Inhibitors.

5. JAK/STAT SIGNALLING PATHWAY INHIBITION

There are many important cellular functions *viz:* apoptosis, proliferation, and immune response mediated by JAK/STAT signalling cascade (Fig. **8**). Sudden stimulation of such a pathway induces severe metastatic transformation and unusual development of several tumours. Increased STAT phosphorylation leads to breast cancer, and STAT3 expression in mitochondria (mitoStat-3) appears to influence cell growth and

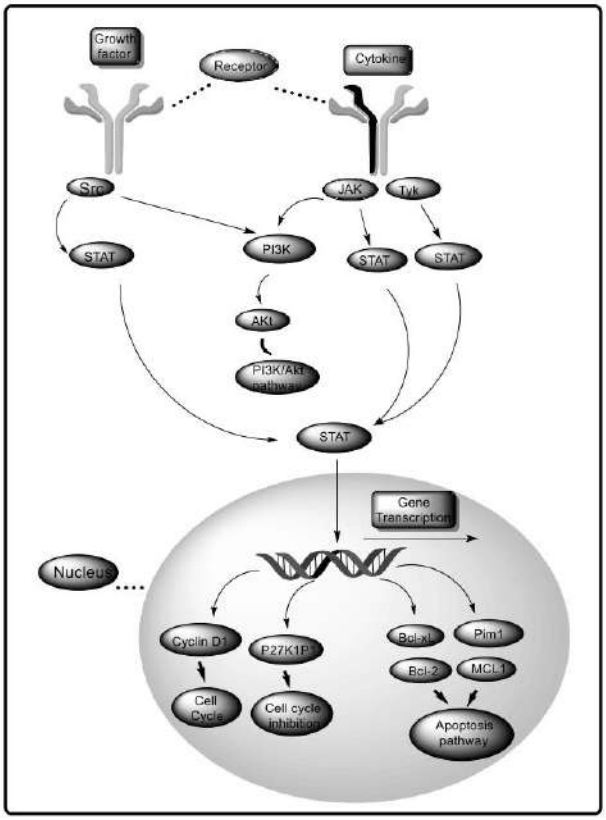

Fig. (8). Cellular pathway involved in JAK/STAT inhibition.

proliferation. Modulating this route by reducing aberrant phosphorylation reduces the growth of various malignancies [56, 57].

Recently, Kanyani *et al.* [58, 59] reported some chalcone derivatives (**13**, Fig. **9**) as anticancer agents due to their *in vitro* cytotoxicity against EGFR (Epidermal growth factor receptor) (A549, and A431), and EGFR mutant (H1975 and H1650) cancer cell lines. Among the examined chalcones, compounds **13a-c** showed over 50% inhibition of the EGFR-TK cell line. Moreover, molecular dynamic simulations demonstrated that the active analogs strongly bind to ATP-binding pocket residue *via* hydrogen bonding interactions which is well-stabilized over the 80 ns (Nanoseconds) simulation period.

In a rationally designed study, Marwa *et al.* [60] tethered chalcone to 1,3,4-oxadiazole and evaluated the cytotoxicity of resulting hybrids(**14**, Fig. **9**) as Src, IL-6, and EGFR inhibitors. Compound **14a** exhibited strong anticancer activity with an IC_{50} value of 3.45, 2.36, and 1.95 µM, against KG-1a, Jurkat, and K-562 cell lines, respectively. Compound **14a** also activated transcription 3 (STAT3) and its phosphorylation by a down-regulating phospho-signal transducer and the rise of p53 level. SAR study showed the impact of phenyl ring substitutions on anticancer activity.

6. ANGIOGENESIS INHIBITORS

Angiogenesis is the biological process in which new blood vessels form from pre-existing vessels. It leads to the development of tumour pro-angiogenic factors, such as TGF-b, fibroblast growth factor (FGF), vascular endothelial growth factor (VEGF), and angiogenin. These factors are observed to facilitate the growth of new blood vessel networks. Angiogenesis inhibition

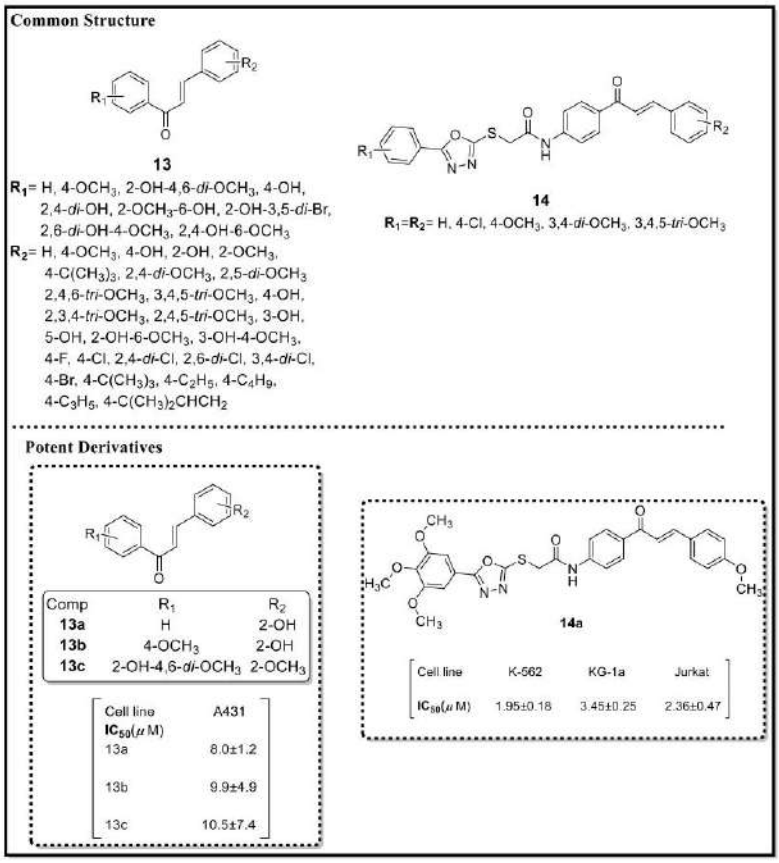

Fig. (9). Chalcone analogue (**13-14**) as JAK/STAT signalling pathway inhibitors.

contributes to the suppression of "angiogenic signalling" which inhibits activation of pro-angiogenic factors and thus slows tumour development [61].

6.1. Vascular Endothelial Growth Factor (VEGF) Inhibitor

Vascular endothelial growth factor (VEGF) is a cell-produced signal protein that activates angiogenesis. VEGF expression is prominent in embryonic stages and is known to play an important role in vascular growth (vasculogenesis).In case of injury and heart block, it is also reported to play a significant role in creating new blood vessels. In certain solid tumors, VEGF over-expression contributes to accelerated tumor development and metastasis, which could be attributed to enhanced nutritional replenishment to the metabolizing cell [25]. Some chalcone-hybrids have been reported with potential VEGF antagonistic activity.

For instance, Wang *et al.* [62] reported the synthesis and anticancer activity of chalcone-modified estradiol analogs (**15**, Fig. **10**) by coupling 2-methoxyestrone and aromatic aldehydes. Compound **15a** displayed promising anti-proliferative activities and established good VEGFR inhibitory activities with IC_{50} values of 77.0 and 78.6 μM against MCF7 (ER+), MDA-MB-231 (ER-) breast cancer cell lines, respectively. The anti-angiogenic effect of **15a** was mediated by inhibition of migration and down-regulating VEGFR expression in human endothelial cells. The presence of EWG substituents on the phenyl ring of benzylidene was crucial for anticancer activity.

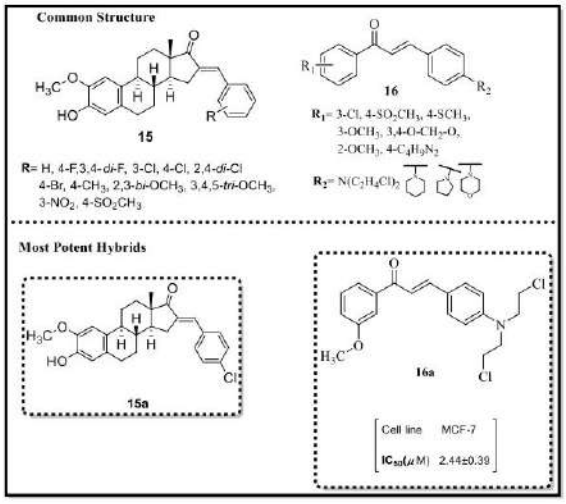

Fig. (10). Chalcone-hybrids (**15**–**16**) as vascular endothelial growth factor (VEGF) inhibitor.

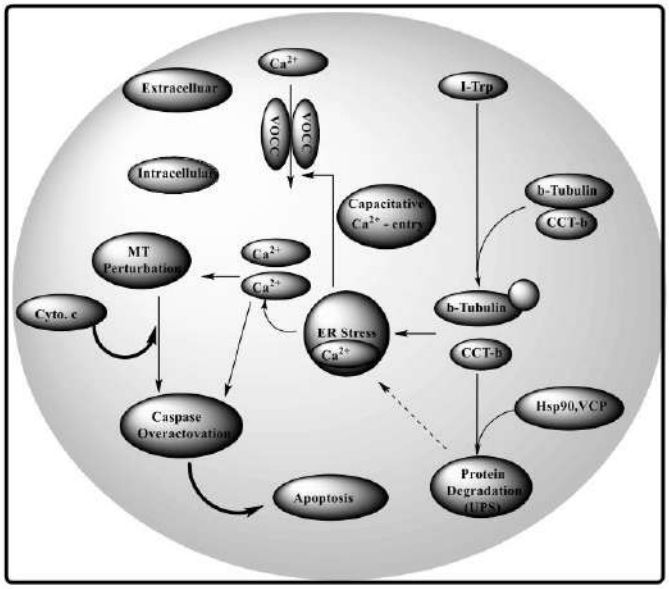

Fig. (11). Cellular pathway involved in Tubulin-polymerization inhibition.

Elkhalifa *et al.* [63] disclosed a set of nitrogen-based chalcone analogs (**16**, Fig. **10**) as triple-negative breast cancer (TNBC) agents. Compound **16a** emerged as lead with good activity against TNBC against all cancer cell lines. Compound **16a** effectively inhibited the cluster formation of MDA-MB-231, MDA-MB-468, and MCF-7 cell lines and cell invasion as well as the migration of MDA-MB-231 and MCF-7 breast cancer cell lines. The compound's mode of action was established as BAXup-regulation, Bcl-2 proteins down-

regulation, stimulated apoptosis, and TNBC cell cycle arrest at the G2/M phase.

7. CELLULAR PROLIFERATION INHIBITOR

7.1. Tubulin-Polymerization Inhibitor

Microtubules are cellular structures that play significant roles in eukaryotic organisms (Fig. **11**)such as intracellular transportation, secretion, motility, mitosis, and cytoskeletal architecture. Tubulin is a di-meric protein molecule comprised of two similar, but non-identical subunits **a** and **b**, which are the main structural element of microtubules, with a molecular weight of 55,000 Da. Chalcones bind and prevent the polymerisation of the micro-tubular protein tubulin, which is an integral step of mitosis, thereby stimulating an untimely disruption of the mitotic spindle panel and interrupt cytoskeletal structure and mitotic arrest [64].

Recently, the anticancer activity of benzo [*d*] imidazo [2,1-*b*] thiazole-chalcone derivatives (**17**, Fig. **12**) was evaluated by Faria *et al.* [65] against breast (MDA MB-231), lung (A-549), colon cancer (HT-29), and prostrate (DU-145) cancer cell lines and compounds **17a** and **17b** were identified as the most potent anti-breast cancer agents with IC_{50} = 1.3 and 1.2 µM, respectively. The active analogs induced apoptosis by cell cycle arrest at the S and G2/M phases. SAR studies showed that substitutions on the chalcone nucleus drastically improved the cytotoxicity activity, while molecular docking studies further highlighted the significance of chalcone core through strong hydrogen bond interaction of the compounds with the protein binding pocket residue.

Guangcheng and co-workers reported the hybridisation of naphthalene and chalcone pharmacophores (**18**, Fig. **12**) and subsequent examination of the hybrids' cytotoxicity on HCT116 and HepG2 cancer cell lines [66]. Compounds **18a** displayed 4-fold superior anticancer activity on HCT116 (IC_{50} = 1.20 µM) and HepG2 (IC_{50} = 1.02 µM) cell line compared to the reference drug millepachine (IC_{50} = 1.51 and 4.66 µM), respectively. The compound inhibited tubulin polymerization in a dose-dependent manner at the G2/M phase of HepG2 cells. SAR analysis further showed that hybrids with EWG(-Cl, -Br) on the *m*-position of phenyl ring improved anticancer activity, while the same groups on *o* and *p*-position resulted in decrease inactivity. *In silico* studies confirmed strong binding interactions of compound **18a** at the colchicine binding site of tubulin.

Natural plants have been recognized since prehistoric times as an inexhaustible source of compounds with excellent bioactivities and high safety. In this regard, Kim *et al.* [67] , isolated a variety of chalcones and lanceolein A–G analogs (**19**, Fig. **12**), from the methanolic extract of *Coreopsis lanceolata* flowers and examined their cytotoxicity on the human colon (HCT15) cancer cell lines using tali assay. The isolated compounds**19a-c** exhibited significant anti-cancer activity with IC_{50} values of 43.7, 35.6, and 47.9 µM, respectively. Mechanistic studies showed that these compounds interfered with cascade-3 and PARP expression in apoptotic cells.

Huang and Wang [68] reported the reactions of Pt(IV) precursor with different chalcone derivatives to give chalcone-Pt(IV) complexes (**20**, Fig. **12**). The complexes were evaluated *in vitro* against three human cancer cell lines (NCI-H460, lung hepatoma; SK-OV-3, HepG-2, ovarian), and two human normal cell lines (BEAS-2B, lung; HL-7702, liver) using MTT (3-(4,5-dimethylthiazol-2-yl)-2,5-diphenyltetrazolium bromide) assay. The most potent compounds **20a-b** displayed 3- and 6-fold enhanced anticancer activity against NCI-H460 and HePG2 cancer cell lines with IC_{50} = 4.65, 3.66, and 2.23, 0.97 µM, compare to reference drug cisplatin (IC_{50} =8.51 and 10.42 µM). Compounds **20a-b** also induced apoptosis in NCI-H460 and HePG2 cells by arresting the cell cycle at the G2/M phase, increasing the production of reactive oxygen species (ROS), and regulating the mitochondria-mediated apoptosis of the Bcl-2 protein family.

A series of chalcone-thiophene analogs(**21**, Fig. **12**), prepared by Pinto *et al.* [69] were evaluated for their anticancer activity against three cancer cell lines *viz*., A375-C5 (melanoma), NCI-H460 (non-small cell lung cancer), and MCF-7 (breast adenocarcinoma), respectively. SAR study revealed the dependence of anticancer activity on the presence of methoxy (-OCH_3) group at 3, 4, 5-positions of the chalcone phenyl ring. Further, the thiophene core enhanced the hybrids' lipophilicity for increased penetration of the cell membrane. The most active compound **21a** exhibited excellent cytotoxicity against MCF-7 with an IC_{50} value of 3.26 µM, fractionally lower than Doxorubicin (IC_{50} = 0.009 µM).

Xu *et al.* [70] reported a library of chalcone-pyridine conjugates (**22**, Fig. **12**) and their *in vitro* cytotoxicity evaluation against a panel of human cancer cell lines (HepG2, KB, HCT-8, MDA-MB-231, H22, and L-O2 cell lines). SAR analysis revealed that the presence of substituted methyl at the α-position of the unsaturated carbonyl group was essential for strong activity anticancer activity. Thus, compound **22a** was

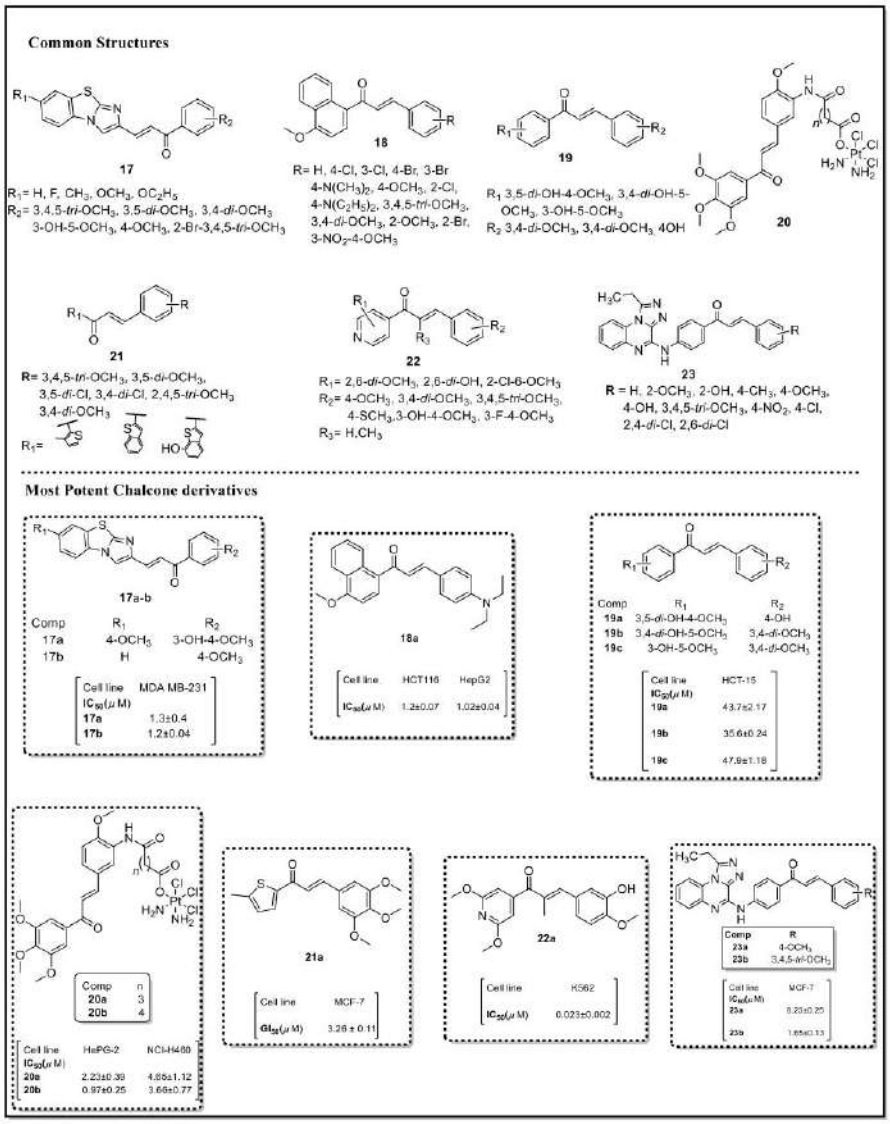

Fig. (12). Chalcone analogs (**17**-**23**) as Tubulin-polymerization inhibitor.

identified as the most promising anti-proliferative agent with IC_{50} values ranging from 0.023 to 0.045 μM.

The anti-breast cancer potential of triazole-quinoxaline-chalcone hybrids (**23**, Fig. **12**) against HCT-116, MCF-7, and HepG-2 were evaluated by Mohamed Alswah and his co-workers [71]. The preliminary results identified compounds **23a** and **23b** as the most promising cytotoxic agents; the compounds induced EGFR kinase and inhibited tubulin polymerization. SAR study concluded that -OH or -OCH_3 groups on aromatic ring B exhibited more potent anti-EGFR and tubulin polymerization compared to other

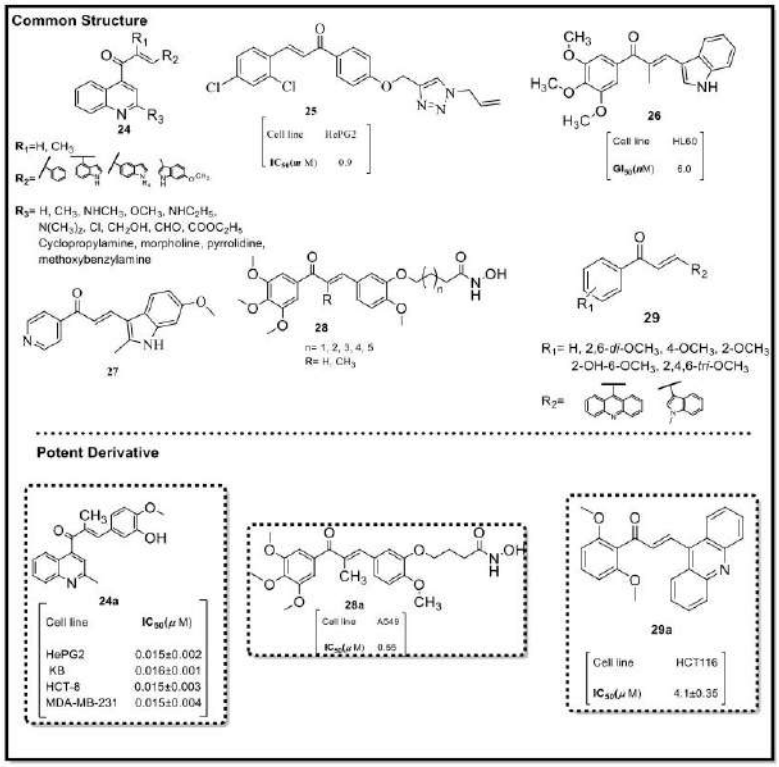

Fig. (13). Chalcone analogs (**24-29**) as Tubulin-polymerization inhibitor.

units. *In silico* studies also suggested that the aromatic stacking interactions played a significant role in the overall anti-breast cancer activity.

Wenlong Li *et al.* [72] disclosed a series of chalcone-quinoline hybrids (**24**, Fig. **13**) as antitumor agents and inhibitors of microtubule polymerization. Compound **24a** showed an excellent cytotoxicity profile against HepG2, KB, HCT-8, MDA-MB-231cancer cell lines with IC_{50} values of 0.015, 0.016, 0.015, and 0.015 μM, respectively, comparable to Combretastatin A-4 (CA-4) used as reference drug. The compound also achieved an effective inhibition of tubulin polymerization at an IC_{50} value of 1.71μM. SAR analysis revealed that the activity in this series depends on the EDG on the quinoline ring.

Wang Yan *et al.* [73] synthesized a series of chalcone-triazole hybrid as anti-tubulin agents for liver cancer treatment. The *in vitro* cytotoxicity study against HepG2, SNU-423, SMMC7221, and SNU-398 liver cancer cell lines established compound **25**(Fig. **13**) as the best cytotoxic agent against HepG2 cells (IC_{50} = 0.90 μM) and a potent inhibitor of tubulin polymerization (IC_{50} = 2.34 μM).

Hui *et al.* [74] synthesized α-methyl-substituted indole-chalcone hybrids and tested their cytotoxicity against a panel of NCI-60 cancer cell lines. Compound **26** (Fig. **13**) emerged as the most potent analog with a GI_{50} value of 6 nM against the HL60 cell line, compared to three standard drugs (vinblastine doxorubicin, and paclitaxel) and excellent cytotoxicity against MDR cancer cells at an IC_{50} value range of 1–53.4 nM. Mechanistic studies showed that compound **26** inhibited the microtubule protein and prevent its polymerization reaction by arresting the cell cycle at the G2/M phase.

Shengnan *et al.* [75] reported 3-(6-Methoxy-2-methyl-1H-indol-3-yl)-1-(4-pyridinyl)-2-propene-1-one (6-MOMIPP) as tubulin inhibitor for brain tumour

chemotherapy. 6-MOMIPP is also capable of crossing the BBB to inhibit the growth of U251 glioblastoma xenografts. The active compound **27** (Fig. **13**) showed their activity in glioblastoma cells due to binding with the colchicine site on β-tubulin and arrest mitotic function.

A series of chalcone derivatives (**28**, Fig. **13**) synthesized by Wang *et al.* [76] have also displayed potent tubulin/HDAC inhibition. The compounds' cytotoxicity was also evaluated in MTT assay against HeLa, SGC-7901, and A549 cancer cell lines. Compound **28a** showed promising anticancer activity against A549 tumour cell lines with the IC_{50} value of0.55μM, with respect to the standard drug SAHA (IC_{50} = 2.61 μM). The mechanistic study established that compound **28a** inhibited tubulin polymerization and arrest the cell cycle at the G2/M phase resulting in apoptosis. Further, molecular docking displayed the inhibitory activity of the compound against HDAC6 and tubulin is due to hydrogen bond and hydrophobic interactions with Phe643 residue.

Takac *et al.* [77] reported seven chalcone derivatives (**29**, Fig. **13**) as tubulin inhibitors. Compound **29a** showed the best potency against human colorectal HCT116 cells line with an IC_{50} value of 4.1 μM. The chalcone analog **29a** arrested the cell cycle in the G2/M phase and induced apoptosis by up and down-regulation of Bax and Bcl-2 protein expression, respectively. The compounds also interfered with Akt and MAPk signalling pathways. The SAR analysis further showed that methoxy and acridine groups are essential for strong anticancer activity.

Delia *et al.* [78] disclosed a series of **1**-(3′,4′,5′-trimethoxyphenyl)-**3**-(2′-alkoxycarbonylindolyl)-**2**-propen-**1**-one derivatives (**30**, Fig. **14**) as tubulin inhibitors. The chalcone-indolehybrids were tested *in vitro* against four human cancer cell lines *viz:* HeLa, HT29, MCF-7, and HL-60, and their cytotoxicity was compared with reference drug CA-4. Compound **30a**-**b** showed the most potent antiproliferative activity and inhibition of tubulin polymerization in MCF-7 cells. Mechanistic studies showed that the compounds induced apoptosis in MCF-7 cells by arresting cell cycle progression at the G2/M phase and overexpression of human U-937/Bcl-2. SAR studies revealed that hybrids with *N*-unsubstituted and methyl substitution at 6 positions are preferred for anticancer activity.

By adopting, Wang *et al.* [66] also adopted the molecular hybridization strategy to synthesize a library of chalcone derivatives (**31**, Fig. **14**) containing indole and naphthalene moiety as tubulin polymerization inhibitors. Compound **31a** showed the most potent cytotoxic activity against HepG2, HCT116, and MCF-7 cells with IC_{50} values of 0.65, 1.13, and 0.82 μM, respectively, in an MTT assay. The compound also inhibited tubulin polymerization at an IC_{50} value of3.9 μM and arrested the cancer cell cycle in the G2/M phase. It was concluded from the SAR studies that *N*-methyl-substituted indole ring enhances anticancer activity while docking studies of compound **31a** showed the H-bond interaction at the colchicine binding site.

In a study presented by Malose *et al.* [79] , compounds **32a-b** emerged from a series of 2-arylbenzo [c] furan-chalcone analogs (**32**, Fig. **14**) as dual tubulin and EGFR-tyrosine kinase inhibitor and the most promising antiproliferative agents against MCF-7 breast cancer cells. The compounds also induced apoptosis through caspase-3 activation. Compound **32b**displayed superior inhibition of tubulin polymerization and EGFR-tyrosine kinase at IC_{50} values of 5.51×10^{-5} μM and 0.09 μM respectively, compared to compound **32a.**

7.2. Topoisomerase Inhibitor

Topoisomerase II enzymes could cut both strands with double-stranded DNA molecules, move via fraction of the duplex, and reattach the slice in a pathway utilizing ATP. Respectively type II topoisomerases catalyse the catenation and de-catenation of two different DNA duplexes. Inhibitors are active stimulators of double-strand breaks in DNA and can induce cell cycle arrest at the G2 phase by disrupting the relationship between topoisomerase II and cell cycle regulators. Topoisomerase II inhibitors may induce a broad variety of chromosome abnormalities, either by sustaining quickly cleaved topoisomerase II-DNA complexes or by interfering with the enzyme's catalytic function, all resulting in DNA double-strand breaks [80].

In a rational based study, Duddukuri *et al.* [81] discovered a series of chalcone-thiophene hybrids (**33**, Fig. **15**)with stronger cytotoxicity to lung (A-549) cancer cell line than prostate (PC-3) and breast (MDA-MB-453, MCF-7) cancer cell lines (IC_{50} = 6.3 and GI_{50} = 1.9 μM). SAR elucidation revealed that the presence of methoxy group on phenyl ring improved cytotoxicity, whereas nitro (NO_2), hydroxyl (-OH), naphthalene, and anthracene groups resulted in inferior activities. The most active compound **33a**showed superior activity (GI_{50} = 1.9 μM) against the A-549 cell line compared to the standard drug, cisplatin (GI_{50} = 4.1 μM). Mechanistic studies established that cell growth inhibition in A549 cells is due to cell cycle arrest at the G0/G1 phase.

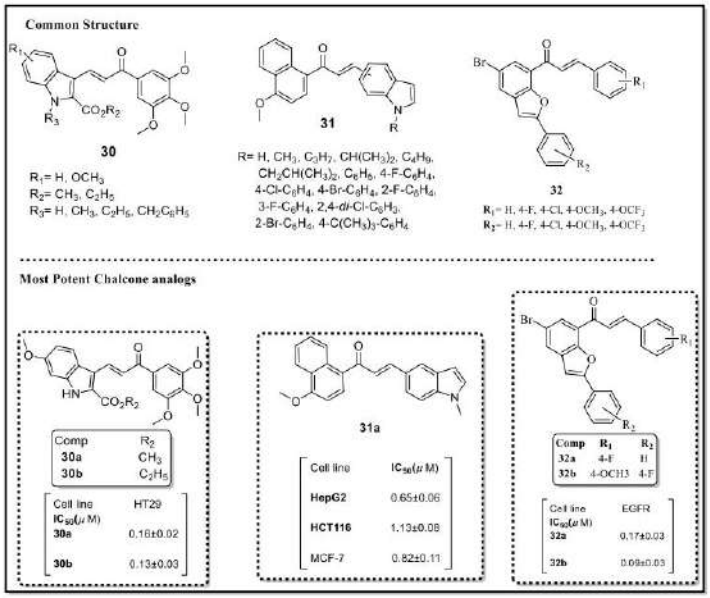

Fig. (14). Chalcone analogs (**30-32**) as Tubulin-polymerization inhibitor.

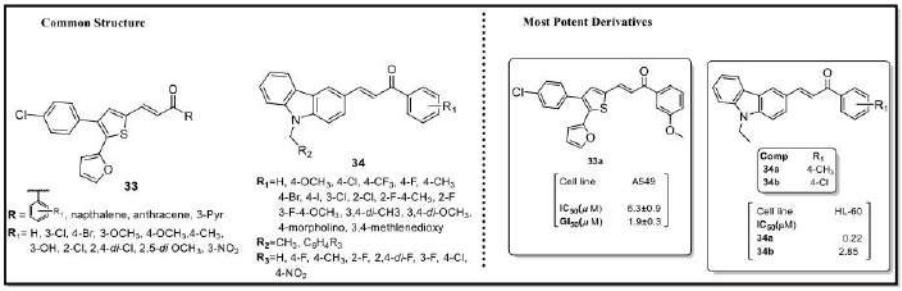

Fig. (15). Chalcone-hybrids (**33-34**) Topoisomerase inhibitor.

By hybridising the chalcone nucleus with carbazole (**34**, Fig. **15**), Jiang *et al.* [82] obtained a series of molecular hybrids as cytotoxic agents against prostate cancer (PC-3), alveolar basal epithelial (A549), acute leukaemia (HL-60), and cervical cancer (HeLa). Hybrid **34a** exhibited the highest inhibitory activity against PC-3, A549, HL-60, and HeLa cell lines with an IC_{50} value of 0.62, 2.16, 0.22, and 0.36 μM and comparatively more potent than control drug etoposide (IC_{50} = 5.73, 32.61, 0.19 and 22.35 μM). Compound **34b** was equally effective against cancer cells, although it had inferior activities (> 2.5 μM) compared to compound **34a**. Mechanistic studies displayed that the chalcone-carbazole hybrids function as a non-intercalative Topo-II catalytic inhibitor.

7.3. Kinase Inhibitors

The ErbB tyrosine kinases play an essential role in normal physiology and neoplasms. The ErbB family of tyrosine kinases (RTKs) is comprised of four members: The Epidermal Growth Factor Receptor (EGFR1), HER-2 (ErbB2), HER-3 (ErbB3), and HER-4 (ErbB4).In several epithelial tumours, epidermal growth factor receptor (EGFR), particularly, ErbB-2, mutates and clinical studies reveal they play a major role in cancer progression. Based on the relevance of

ErbB receptors in cancer therapy, tremendous efforts were made to develop targeted therapies [83, 84].

Cell cycle arrest is a significant stage in cellular pathways associated with cell division and replication. Chalcones have been found to detain different phases of the cell cycle including the G0/G1 phase resulting in apoptosis. In this regard, Lina *et al.* [85] evaluated a series of chalcone-sulfonamide hybrids (**35**, Fig. **16**) and compound **35a** displayed impressive GI_{50} values varying from 0.57 to 12.4 μM against the K562 cancer cell line. SAR study concluded that the presence of 4-chloro substituted chalcones is important for anticancer activity. Additionally, these compounds also showed good activity against *Mycobacterium tuberculosis* H37Rv with MIC values between 14-42 μM, respectively.

Mahmoud *et al.* [86] have reported a series of thienoquinoline-2-carboxamide chalcone derivatives (**36**, Fig. **16**)as EGFR kinase inhibitors (IC_{50} value range of 0.5-3.2 μM). Compounds **36a**-**b** demonstrated the most potent inhibition towards EGFR at IC_{50} value of 0.5 and 0.7 μM, respectively while compound **36b** showed a superior anticancer profile compared to compound **36a**. SAR data illustrated the importance of rigid thieno-quinoline heterocyclic ring to anticancer activity whereas the EGFR inhibitory activity was attributed to the strong interactions of compounds **36a** and **36b** at the enzyme's allosteric site. Preliminary mechanistic studies observed that the most potent compound **36b** affected pre G1 apoptosis and cycle arrest at the G2/M phase.

Inspired by the concept of molecular hybridization, Hesham *et al.* [87] prepared a class of xanthine-chalcone hybrids(**37**, Fig. **16**) as cytotoxic agents against Panc-1 (pancreatic cancer), MCF7 (breast cancer), HT-29 (colon cancer), and A549 (alveolar basal epithelial) cell lines. Compound **37a** displayed impressive activity against Panc-1, MCF7, HT-29 and A549 cancer cell lines with IC_{50} = 1.3, 1.0, 1.2 and 1.5 μM, respectively comparable to reference drug Doxorubicin (IC_{50} = 1.41, 0.90, 1.01 and 1.21 μM). Compound **37b** also displayed significant inhibition (IC_{50} = 0.3 μM) of EGFR in compared to staurosporine (IC_{50} = 0.4 μM). SAR elucidation showed that methyl and EWGs on xanthine and phenyl rings, respectively, favours antiproliferative activity against Panc-1 cells. Mechanistically, compound **37b** induced apoptosis by arresting the cell cycle at the G2/M phase.

Dong *et al.* [88] synthesized various chalcone-dithiocarbamate analogs (**38**, Fig. **16**) and evaluated their cytotoxicity on PC-3, MCF-7, and MGC803 cancer cell lines. The results revealed that compounds **38a** displayed potent anticancer activity against PC3 cells with an IC_{50} value of 1.05 μM while other compounds showed moderate potency with IC_{50} values> 40 μM. Compound **38a** controls the proteins-related expression by arresting the cell cycle at the G2/M phase. Detailed mechanistic studies also showed that compound **38a** induced mitochondrial apoptosis in PC-3 cells by caspase activation, catalase (CAT) inhibition, decreased MMP and ROS production.

The *in vitro* anticancer evaluation of 1,4-dihydroindeno [1,2-c] pyrazole chalcone hybrids(**39**, Fig. **16**) against a panel of cell lines by Khan *et al.* [89] has identified compounds **39a-c** with superior activities (IC_{50} = 3.82, 5.21 and 4.33 μM) against A549 cells compared to standard drug erlotinib (IC_{50} = 10.26 μM). SAR analysis showed that the existence of methoxy substitution on ring-A along with the trimethoxy substitution on ring-D enhances the anticancer activity. Mechanistic studies established that **39a-c** effectively arrested the cell cycle in the G2/M phase in A549 cancer cells.

Zhou *et al.* [90] reported the antitumor activity of chalcone-based natural product butein, (**40**, Fig. **16**) isolated from *Rhusverniciflua*. Butein suppressed the overexpression of Aurora B in HCC cells, which resulted in the inhibition of HCC cell proliferation, colony formation, and delayed tumour growth in nude mice. Further, butein significantly induced apoptosis by decreasing Aurora B and histone H3 phosphorylation as well as arresting the G2/M phase of the HCC cell cycle.Docking analysis also demonstrated the antitumor activity of butein is due to its hydrophobic interactions with Aurora B kinase.

Using ultrasound irradiation, ArtaniaAdnin *et al.* [91] synthesized a set of chloro chalcones analogs (**41**, Fig. **16**) as anti-proliferative agents against MCF7, T47D, HeLa, and WiDr cell lines. Compound **41a** emerged as the most active overall against all tested cancer cells as shown in Fig. **16**. It was depicted that anticancer activity of chalcone was because of hydrogen bonding and π-cation interactions of EGFR receptor with chalcone carbonyl and methoxy group.

7.4. mTOR Inhibitors

Rapamycin (mTOR) signalling pathway integrates both intra and extracellular signals and act as a key regulator for cell survival, metabolism, development, and proliferation. Recent advancements have shown that the mTOR pathway is stimulated during different biological processes and deregulated in cancer. mTOR

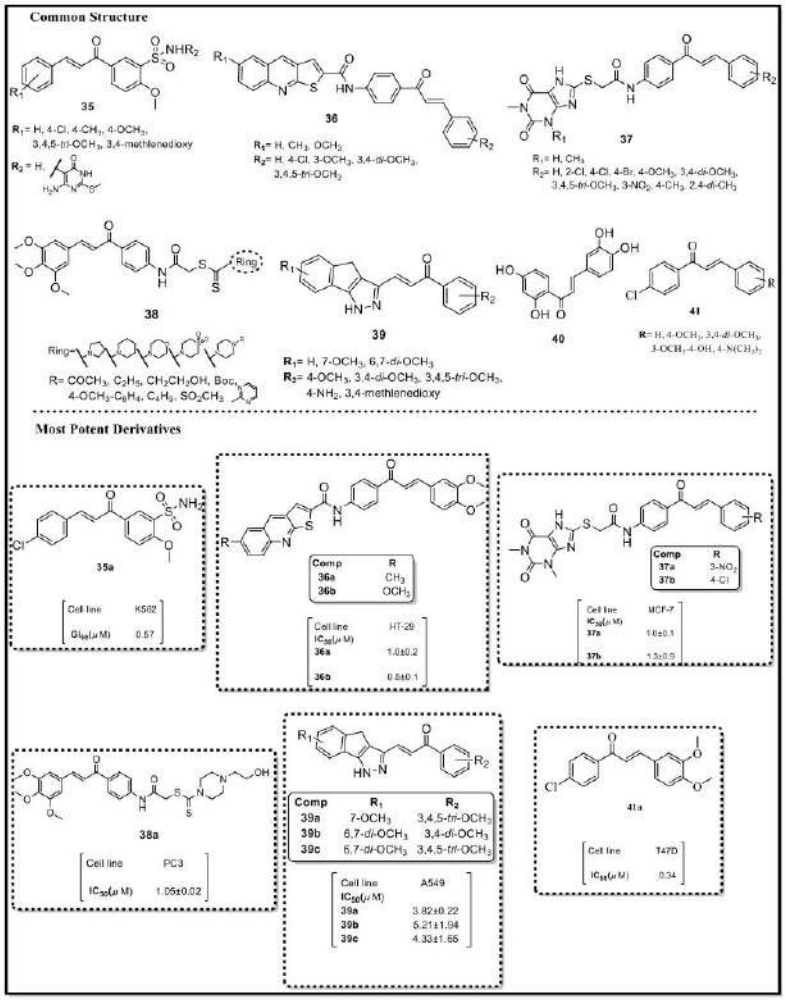

Fig. (16). Chalcone-hybrids (**35-41**) as Kinase inhibitors.

protein is a 289kDa serine-threonine kinase that relates to the kinase family of phosphor-inositide-3-kinase (P-I3K) and is maintained during transformation. mTOR controls cell division by regulating mRNA, autophagy, ribosome, metabolism, and biogenesis [92]. Rapamycin can prevent AKT by interrupting the mTORC2 unit in certain types of cells. Available reports have established that chalcones show potent mTOR inhibition.

Break *et al.* [93] designed and synthesized cardamonin analogs (**42,** Fig. **17**) and screened them for their anticancer activity against A549 and HK1 cell lines. Among all synthesized hybrids, a total of eight analogs showed more effective cytotoxic activities, than natural cardamonin. Compound **42a** displayed the most potent anticancer activity with an IC_{50} value of 13.2 and 0.7 μM against A549 and HK1 cells, respectively. Moreover, the compound decreased the expression levels of p-mTOR and p-4EBP1 in A549 and HK1 cells. Mechanistic studies also showed that compound **42a** caused an accumulation of cells in the G2/M phase and induced caspase-dependent apoptosis in A549 and HK1 cells.

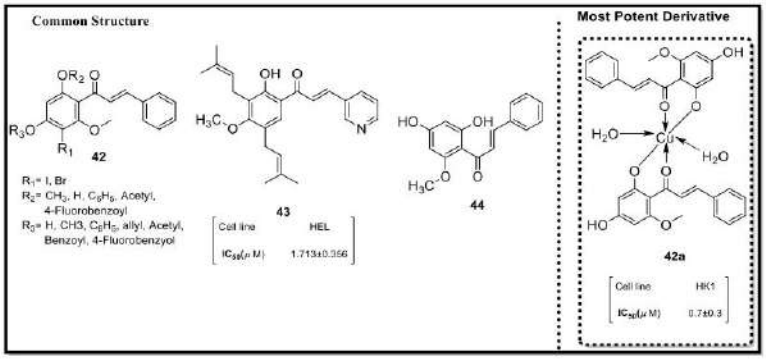

Fig. (17). Chalcone analogs (**42**-**44**) as mTOR inhibitors.

The antiproliferative effects of (*E*)-1-(2-hydroxy-4-methoxy-3,5-diprenyl)phenyl-3-(3-pyridinyl)-propene-1-one (**43**, Fig. **17**) on HEL and K562 leukemia cells in MTT assay and its molecular mechanistic study has been investigated by Zhang *et al.* [94]. Compound **43** displayed selective growth inhibition of HEL cells over K562 cells as well as superior anticancer potential compared to reference drug cisplatin. The compound's apoptotic effect was due to an increase of Bax/Bcl-2 ratio and a decreased expression of Caspase-3/8 and PARP levels in HEL and K562 cells. Moreover, compound **43** induced cell apoptosis in HEL cells by down-regulating Fli-1 protein expression while the down-regulation of phosphorylation levels in AKT/m-TOR and AMPK proteins triggered cell autophagy in HEL and K562 cells.

Natural chalcone cardamonin (**44**, Fig. **17**) was studied by Zhou *et al.* [95]. Itsanticancer potential was investigated on human non-small-cell lung cancer cells (NSCLC). It was concluded from mechanistic studies that cardamonin induced apoptosis of A549 and H460 (NSCLC) cells by activating caspase-3, upregulating Bax, and downregulating Bcl-2 and also, induced G2/M cell cycle arrest by inhibiting the cyclin D1/CDK4 complex. It was further established that cardamonin inhibited the PI3K/Akt/mTOR pathways by reducing the phosphorylation levels PI3K and decreased the expression rates of Ki-67, p-Akt, and p-mTOR.

7.5. NF-kB Inhibitors

The NF-kB pathway controls the viability of healthy and malignant B cells by regulating gene expression (Fig. **18**) [96]. The exogenous apoptotic route is activated by the involvement of tumour necrosis factor (TNF)-family death receptors (TNF receptor-1 and Fas-CD95), and the intrinsic apoptotic mechanism is stimulated by translocating pro-apoptotic members of the Bcl-2. TNF activation and other stimulation (including B-cell receptor, CD-40, and Toll receptor involvement) also trigger the NF-kB pathway and boost the expression of specific genes. Such target of NF-kB genes improves cell viability by modulating TNF signalling, inhibiting FAS-mediated apoptosis, and restricting pro-apoptotic Bcl2 family members' involvement in exposure to several other effects. The NF-kB pathway includes convincing rational therapeutic potential. Chalcone-based hybrids with potent NF-kB inhibition are presented below.

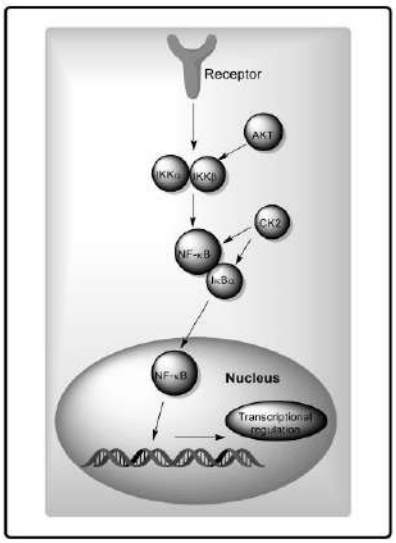

Fig. (18). Cellular pathway involved in NF-kB inhibition.

Novel chalcone-based homoserine lactones derivatives (**45**, Fig. **19**) were synthesized by Bin *et al.* [97] and tested against prostate cancer DU145, PC-3 MGC-803, and MCF-7 cell lines using an MTT assay. Compound **45a** showed potent anticancer activity with IC_{50} = 3.0 and 5.0 μM against DU145 and PC-3 cell lines, respectively, compared to the reference drug OdDHL. The authors also reported the synergistic effect of **45a** and OdDHL with Apo-2L/NFSF10/TRAIL (TNF-related apoptosis-inducing ligand) on growth inhibition and cell apoptosis. Brief SAR studies implied that the compounds' antiproliferative activity is due to the presence of the chalcone scaffold.

Xue *et al.* [98] tested the anti-proliferative potential of 4-oxoquinazolin-2-yl hybrids (**46**, Fig. **19**) bearing a chalcone nucleus against HCT-116 (human colorectal) and MCF-7 (breast cancer) cancer cell lines. SAR study showed the dependence of potency on the position and nature of phenyl ring's substituent. The presence of EDGs (*i.e.* CH_3, OH, and OCH_3) favoured cytotoxicity more than EWGs (*i.e.* Br, F, and OCF_3). Hence, compound **46a** emerged as the most potent analog with an IC_{50}value of 4.08 and 3.56 μM against MCF-7 and HCT-116 cells, respectively, which was comparable to the positive control 5-FU. Mechanistic studies proved that the compounds' cytotoxicity is due to the induction of apoptosis through the mitochondrial pathway.

In a recent study, Silvia *et al.* [99] reported the synthesis and anticancer evaluation of 2'-hydroxy-4'-alkoxy chalcone analogs (**47**, Fig. **19**) against MCF7, HF-6, PC-3, and CaSki cell lines. Their results showed that compounds **47a-e** inhibited cell growth in PC-3 cancer cell lines at an IC_{50} range of 8.08-13.75 μM. Compounds **47a** and **47c** also induced cell cycle arrest at the G2/M phase in PC-3 cancer cells. Their apoptotic results on PC-3 cells showed that these hybrids induced mitochondrial apoptosis by enhancing caspase 3/7 activation while regulating Bcl-2 and Bax transcription. The QSAR (Quantitative-SAR) model reveals that the double bond of α,β-unsaturated carbonyl moiety, along with the planar geometry, are crucial for strong cytotoxicity.

Ahmed *et al.* [100] reported the synthesis and anticancer activity of 1,2,4-triazole-chalcone hybrids (**48**, Fig. **19**) against the NCI-60 cells panel using sulforhodamine B colorimetric assay. Among the tested hybrids, compounds **48a-e** withIC_{50} = 6.06, 4.4, 7.55, 16.04, and 8.04 μM, respectively, exhibited potent cell growth inhibition compared to the standard drug cisplatin (IC_{50}= 15.3 μM). These hybrids also displayed good antitumor activity on nine tumour subpanels with GI_{50} values range of 0.15-23.30 μM. The mechanism of action of these active hybrids was identified as induced apoptosis *via* elevated levels of cytochrome c from mitochondria, pro-apoptotic protein Bax, and activation of the caspase-3/8/9 protein. Further, SAR analysis showed that the presence of *N*-4-allyl triazole significantly improved the compounds' inhibitory activity.

In a rational-based design, Malave*et al.* [101] reported a series of piperidine-chalcones (**49**, Fig. **19**) using the pharmacophore approach. The cytotoxicity was evaluated against LoVo (colorectal), COLO-205, and CCD18Co (normal colorectal) cell lines. Compounds **49a-b** showed good cytotoxicity against all colorectal cell lines while other compounds exhibited cytotoxicity toward normal colorectal (CCD18Co) cell line than LoVo and COLO-205 cancer cells. SAR study showed the dependence of activity on the nature of aromatic ring substituents. Further, these hybrids induced apoptosis *via* multiple mechanisms involving caspases 3/7 activation and NF-κB inhibition. Moreover, compound **49b** potently decreased cell viability in PC-3 and 22RV1 cells by decreasing NF-κB activity in human prostate cancer cell lines.

Recently, Kocyigit *et al.* [102] reported chalcone-imide analogs (**50**, Fig. **19**) as an anticancer agent. All synthesized compounds were evaluated for their anticancer activity against C6 (Glio carcinoma cell in rats) cell, using proliferation BrdU ELISA assay. Most of the evaluated compounds displayed high activity with IC_{50} values in the range of 7.06–67.46μM, compared to standard 5-FU (IC_{50} = 90.36 μM). SAR study showed that the maleimide ring is essential for anticancer activity. The active analogs also exhibited effective inhibition of hCA I, hCA II, and AChE enzymes.

Liu *et al.* [103] isolated Xanthohumol from the flowers of *Humulus lupulus* and established the isolate's *in vitro* effect on the cell viability of HT-29 (colon cancer) cells at an IC_{50} value of 10 μM. The chalcone induced apoptosis by nuclear fragmentation of the HT-29 cells *via* up and down-regulation of Bax and Bcl-2 expression, respectively, in a dose-dependent manner. Further, during a drug resistance the caspase-3/8/9 level increased in HT-29 cells. Mechanistically, xanthohumol caused cell cycle arrest in HT-29 cells at the G2/M phase by down-regulating the expression of cyclin A and B1.

Saavedra *et al.* [104] analysed the cytotoxicity of 6′-Benzyloxy-4-bromo-2′-hydroxychalcone (**51**, Fig. **19**) against human leukemia cells U-937, HL-60, K-562, NALM-6, MOLT-3, Bcl-2 overexpressing U-937/Bcl-2

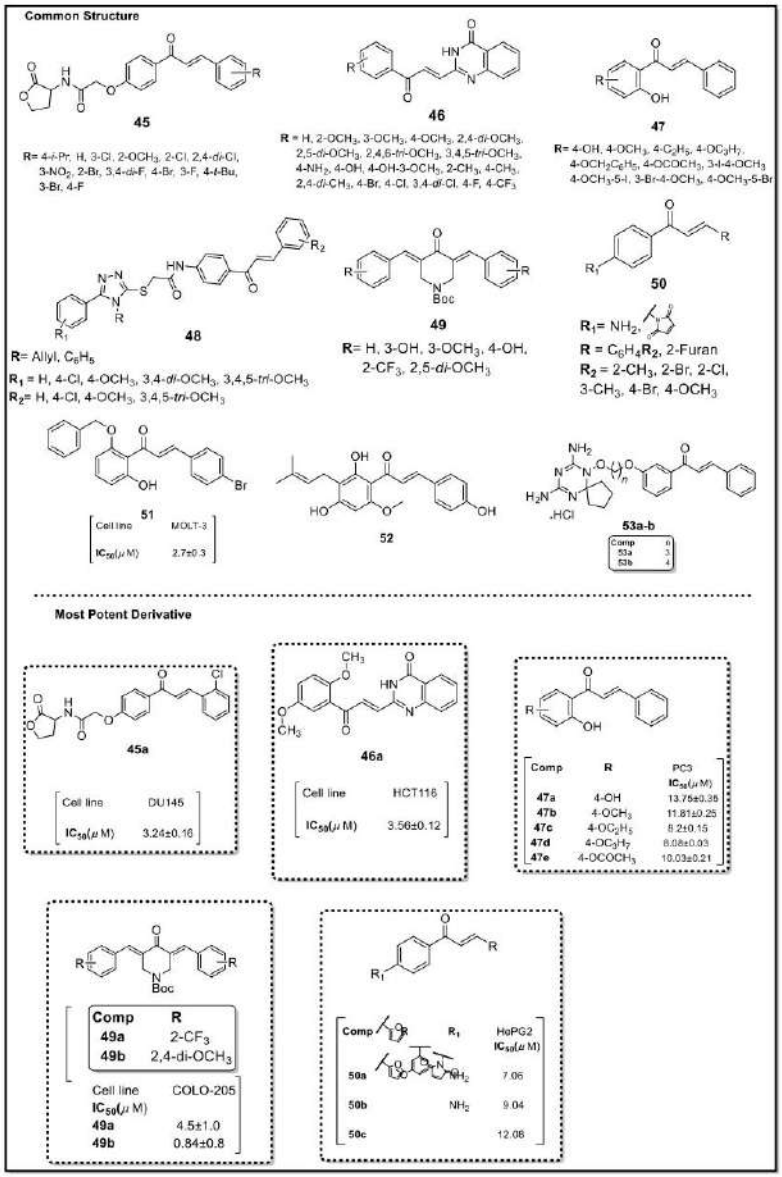

Fig. (19). Chalcone analogs (**45-53**) as NF-kB inhibitors.

and P-glycoprotein overexpressing K-562/ADR. The compound displayed effective cytotoxicity against all human leukemia cell lines but relatively non-toxic to peripheral blood mononuclear cells (PBMC). More importantly, the decreased level of Bcl-2 expression, an increase in Bax protein expression, and cleavage of caspases-3/7/8/9 induced by compound **51** resulted in apoptotic cell death of U-937 cells. It was also con-

cluded that the compound's inhibition of ROS generation in U-937 cells caused cell death.

The therapeutic effect of Xanthohumol (**52**, Fig. **19**) on the neuroblastoma (NB) cell line was examined by Samuel *et al.* [105]. In MTT assay, xanthohumol displayed IC_{50} values of 12 μM and inhibited colony formation of NGP, SH-SY-5Y, and SK-N-AS cells. Xanthohumol also triggered apoptosis in NB cells by cleaving PARP, caspase-3/7, Bax, decreased expression of the Bcl-2 and AKT pathway, respectively. Further, the transcriptional mechanism revealed the up-regulation of micro-RNA DR5 caused TRAIL to affect in NB cells.

From a set of dihydro-triazine-chalcone analogs (**53**, Fig. **19**), Gan *et al.* [106] identified compounds **53a-b** with strong anti-invasive and anti-inflammatory effects on MDA-MB-231 breast carcinoma cells. The most potent analog **53b** controlled the expression of MMP-9 genes in MDA-MB-231 cells *via* the NF-κB signalling pathway in a dose-dependent manner. The ether linkage in the chalcone-tiazine ring tremendously enhanced the bioactivity of these analogs.

8. MISCELLANEOUS CHALCONE-BASED CYTOTOXIC AGENTS

Yali *et al.* [107] conducted the anti-tumour activity evaluation of chalcone benzamide/benzenesulfonamide hybrids (**54**, Fig. **20**) against breast cancer cell lines HCT116, MCF- 7, and 143B using MTT assay. Compound **54a** inhibited cell colony formation in HCT116, MCF-7, and 143B cancer cell lines with an IC_{50} value of 0.597, 0.886, and 0.791 μM, respectively. SAR study revealed that the benzenesulfonamide group is more favoured for high potency than the benzamide group and *meta*-substituted compounds are better cytotoxic agents compared to the corresponding *o*- and *p*-substituted hybrids. Molecular docking studies illustrated the anti-tumour activity of compound **54a** controlled by Cat L and Cat K.

Gupta *et al.* [108] have also adopted the concept of molecular hybridization in the synthesis of a library of indole-chalcone-based chromene hybrids (**55**, Fig. **20**)as cytotoxic agents against MDA-MB-231 (breast cancer), DLD-1 (colon cancer), 4T1 (mouse breast cancer), HepG2 (liver cancer), HeLa (cervical cancer), and HEK-293 (human embryonic kidney) cell lines. Colon cancer cell line (DLD-1) was specifically analysed using a DNA ligation assay. Compound **55a**, containing a free NH_2 unit and *tert*-butyl groups at C-2 and C-8 position of benzopyran ring, respectively, inhibited the proliferation of MDA-MB-231 (IC_{50}= 6.090 μM), DLD-1 (IC_{50}= 4.656 μM), 4T1 (IC_{50}= 5.756 μM), HepG2 (IC_{50}= 6.457 μM), HeLa (IC_{50}= 6.398), and HEK-293 (IC_{50}= 12.4 μM) cancer cell lines.Mechanistic studies showed that compound **55a** did not interact with DNA substrate through ligation but efficiently interacted with hLigI in a competing fashion.

A series of fluorinated bis-chalcone derivatives (**56**, Fig. **20**)was recently prepared by Burmaoglu *et al.* [109] as anticancer agents against ER+ (MCF-7) and Caco-2 cancer cell lines using MTT assay. SAR studies showed that the fluoro substituent at 2,5-position of the chalcone ring enhanced the anticancer activity. Compound **56a** displayed excellent activity (IC_{50}= 1.9 μM) toward MCF-7 cells superior to reference drug cisplatin (IC_{50}= 5.7 μM). Also, both compounds **56a-b** showed the highest inhibitory activity against the Caco-2 cell line (IC_{50} = 7.3 and 6.8 μM, respectively). Compound **56a** also showed good activity against xanthine oxidase (XO) enzyme with the IC_{50} value of 0.76 μM, respectively.

Durgapal *et al.* [110] synthesized a class of structurally diverse3-aminomethyl pyridine chalcone hybrids (**57**, Fig. **20**) and evaluated their cytotoxic activity against MCF7 (Breast cancer) and A549 (Lungs) cancer cell lines *in vitro*. SAR study revealed that the molecular hybrids with substituted chalcone ring showed significantly different cytotoxicity compared to their phenyl analog. Anti-proliferative activity was also dependent on the nature and position of substituents on the chalcone ring. Precisely, the chloro substituted chalcones displayed very good activity against A 549 cell line, while the shifting of halogen position resulted in diminished anti-proliferative activity. Compound **57a** emerged as the most potent compound with IC_{50} values of 0.0067 and 0.245 μM against MCF-7 and A549 cell lines, respectively, compared to the positive control Fluorouracil (IC_{50} = 45.04 μM for MCF-7and 11.13 μM for A549). DNA binding studies of compound **57a** showed the apoptosis of MCF7 cells due to binding with CT-DNA.

Adileh *et al.* [111] have reported a set of 4-amino-5-cinnamoylthiazoles conjugates(**58**, Fig. **20**)as anti-proliferative agents against MCF7, SW480, and HepG2 cancer cell lines. Compound **58a** exhibited the highest growth inhibition (IC_{50}= 10.6 μM) against the HepG2 cancer cell line, however, the effect was less than etoposide (IC_{50} = 6.2 μM). SAR studies illustrated that the presence of substituents on the 5-cinnamoyl moiety and type of cyclic amine attached to the C-2 of thiazole ring enhanced the anti-proliferative activity. Flow

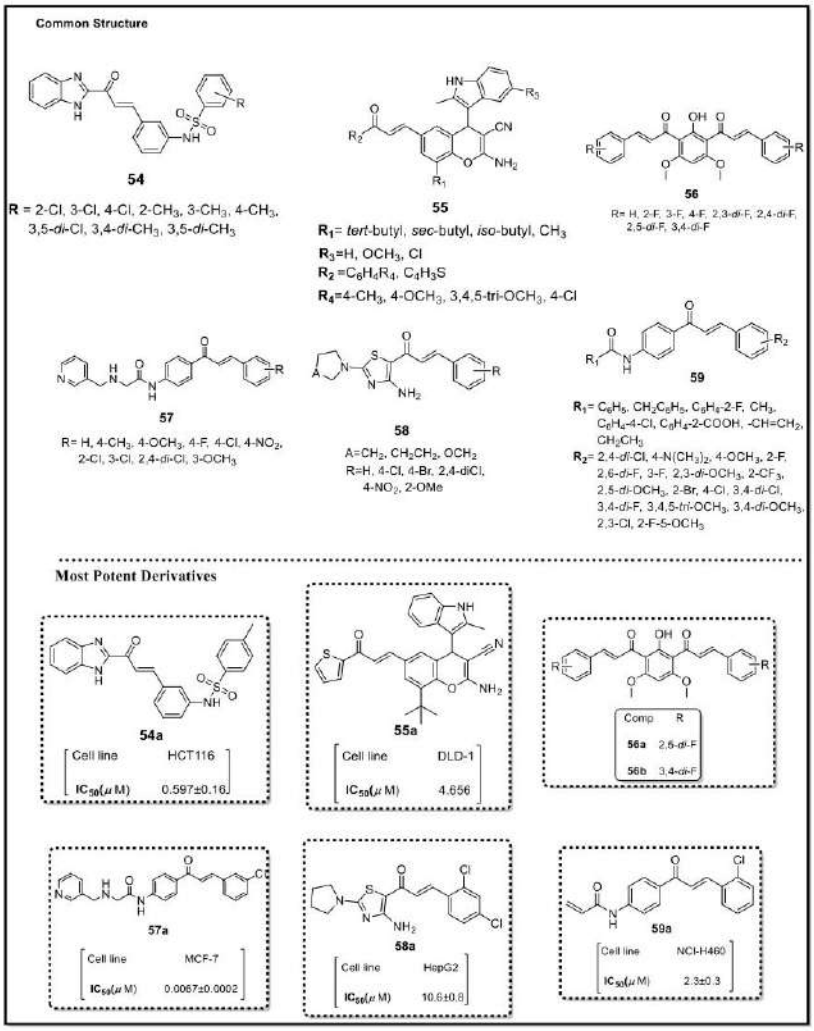

Fig. (20). Chalcone analogs (**54-59**) with anti-cancer activity.

cytometry analysis also showed that the most potent compound **58a** induced apoptosis in HepG2 cells by blocking the cell cycle at the G2 phase.

A series of chalcone compounds (**59**, Fig. **20**) bearing an amide pendant on ring A was designed by Zhu *et al*. [112] and evaluated for their anticancer potential against three human cancer cell lines using MTT assay.Compound **59a** exhibited potent anticancer activities against H1975, NCI-H460, and A549 cell lines with IC_{50} values of 5.7, 2.3, and 3.2 μM, their respectively. The active hybrid exerted its activity by triggering caspase-3 and promoting intracellular ROS levels in NCI-H460 cells. SAR studies showed that the presence of acrylamide unit enhanced the anticancer potential of these analogs.

Charris *et al*. [113] synthesized a set of quinoline-chalcone hybrids (**60**, Fig. **21**) as cytotoxic agents against HL60, E6.1, and Jurkat cancer cell lines using

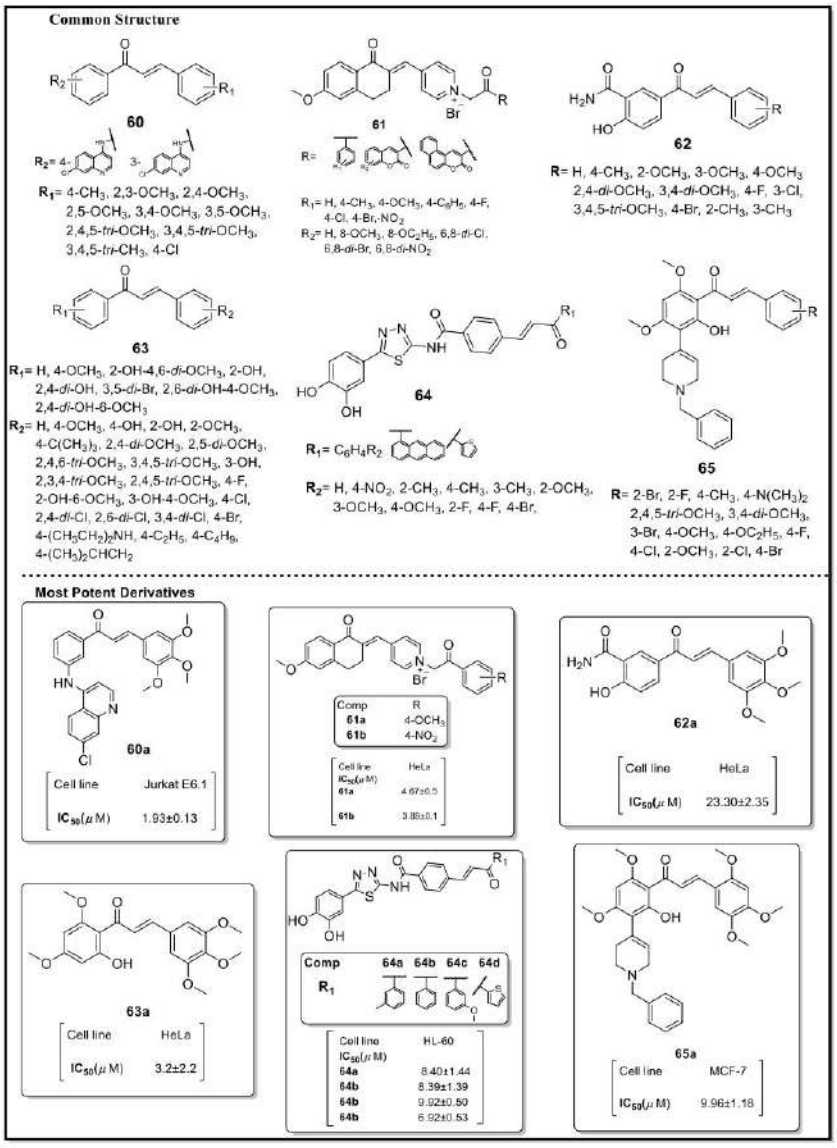

Fig. (21). Chalcone analogs (**60-65**) with potent anti-cancer activity.

MTT assay. SAR studies suggested the positive influence of methoxy groups on cytotoxicity. Hence, compound **60a** bearing methoxy groups at 3,4,5-position of phenyl ring exhibited comparable activity (IC_{50} = 1.93 μM) to standard drug Doxorubicin (IC_{50}= 1.03 μM). The plausible mechanism of action of these hybrids was reported as *in vivo* inhibition of β-hematin formation. Compound **60a** was also effective as an antimalarial agent.

Gondru *et al.* [114] developed chalcone-pyridinium hybrids (**61**, Fig. **21**) and screened for their anticancer potential using MCF-7, HeLa, U- 87MG cancer cell lines, and non-cancerous cell line, HEK293, in an MTT assay. Compounds **61a-b** showed the most potent inhibitory activity against the cancer cell lines without any toxicity against HEK293. *In vivo* studies of both active hybrids showed significant growth inhibition of Ehrlich ascites carcinoma (EAC) cells in mice.

Using Claisen Schmidt condensation of benzaldehyde and acetophenone, Hongtian *et al.* [115] synthesized some chalcone derivatives (**62**, Fig. **21**)and evaluated their cytotoxicity in an MTT assay against HeLa, A549, HepG2, HL-60, and WI-38 cell lines. Compound **62a** exhibited the most promising cytotoxicity profile against the cancer cells compared to the reference drug 5-FU. Mechanistic studies established that compound **62a** arrested the cell cycle at the G2/M phase and hindered the ROS-mitochondrial pathway to induce apoptosis in HepG2 cells. The compound also caused a down-regulation of Caspase-3 and PARP levels.

Based on the *in silico* docking studies, Kanyani *et al.* [59] accounted for the design and synthesis of chalcone derivatives (**63**, Fig. **21**) and evaluated their cytotoxicity *in vitro* against HT-1376, HeLa, and MCF-7 cell lines in an MTT assay. Compound **63a** displayed more favourable interaction energies towards the ATPase domain than salvicine and hTopoII-alpha inhibition. Further, compound **63a** emerged as the best cytotoxic agent against the tested cell lines with superior activity than the reference drug salvicine. Moreover, the biochemical and *in silico* data demonstrated that the methoxy substituent on ring B of chalcone plays an important role in anticancer activity.

Katarina *et al.* [116] synthesized 1,3,4-thiadiazole chalcone hybrids (**64**, Fig. **21**) and determined their antioxidant, cytotoxic, and DNA-binding activity. Compound **64a-d** displayed excellent cytotoxicity on HeLa and HL-60 cells but weaker activity against A549 cells. The mechanistic study showed that these molecular hybrids induced apoptosis in HeLa cells by arresting the cell cycle between Go/G1 phases. Further, the thiadiazole-chalcones hybrids have shown strong binding interaction,with DNA damaging capability. Moreover, these hybrids also exhibited excellent antioxidant activity (DPPH method) in the IC_{50} range of 9.76-18.04 μM compared to reference antioxidant, ascorbic acid (IC_{50}= 20.23 μM).

In vitro and *in vivo* studies of tetrahydropyridinyl-chalcones hybrids (**65**, Fig. **21**) as antiproliferative agents have been reported by Nigam *et al.* [117]. The preliminary *in vitro* studies revealed compound **65a** as the most potent against MCF-7, T-47D, MDA-MB-231, and HepG2. From the SAR study, it was elucidated that alkoxy substitution on chalcone nucleus improved anticancer activity. In mechanistic studies, tetrahydropyridinyl-chalcone hybrid induced apoptosis through cell cycle arrest at G0/G1 and G2/M phases. *In vivo* study further established the superior anticancer efficacy of compound **65a** against MCF-7 breast cancer cells in Sprague–Dawley female rats compared to standard drug doxorubicin. Moreover, compound **65a** was also found as a promising antioxidant agent against ABTS radical.

Park *et al.* [118] investigated the anticancer activity of indolizine-chalcone hybrids (**66**, Fig. **22**), among which compound **66a** showed the best inhibition of human lymphoma cells compared to cisplatin. The compound induced apoptotic cell death by activating caspase-3/7 in U932 cells. SAR studies concluded that methoxy and halo group substituents on aromatic ring B of chalcone nucleus favoured increased cytotoxicity.

The anticancer potential of synthesized chalcone hybrids (**67**, Fig. **22**) against human breast cell line MCF-7, TCDD, MDA-468, and MCF-10A was evaluated by Ruparelia *et al.* [119] using MTT assay. Compound s**67a-e** showed the highest antiproliferative activity overall. Further, these chalcone hybrids were found to exert their inhibitory potency on CYP1A1 and CYP1B1 enzyme expression in the MCF-7 breast cancer cell line. SAR studies revealed the positive impact of methoxy substituent on ring A on anti-cancer potency.

Stanojkovic *et al.* [120] evaluated the cytotoxic activity of anthraquinone-chalcone hybrids (**68**, Fig. **22**) against K562, Jurkat, and HL-60 leukemia cell lines and MRC-5 normal cell line. Compounds **68a-b** showed the most potent antiproliferative activity against the K562 cell line. Further, cell cycle analysis showed that active analogs caused cell cycle arrest in K562 cells at the subG1 phase. It was also observed that the angiogenesis inhibition in myeloid leukemia (ML) cells was accompanied by the down-regulated expression of MMP2, MMP9, and VEGFA gene. Further, molecular docking studies indicated that the apoptotic activity against caspase-3 is due to hydrophobic interactions with the target receptor.

Addila *et al.* [121] have reported the cytotoxic effects of flavokawain-B (FKB) chalcones (**69**, Fig. **22**) against MCF-7 and MDA-MB-231 breast cancer cell lines. Compounds **69a-c** exhibited potential cytotoxic effects on the MCF-7 and MDA-MB-231 cell lines

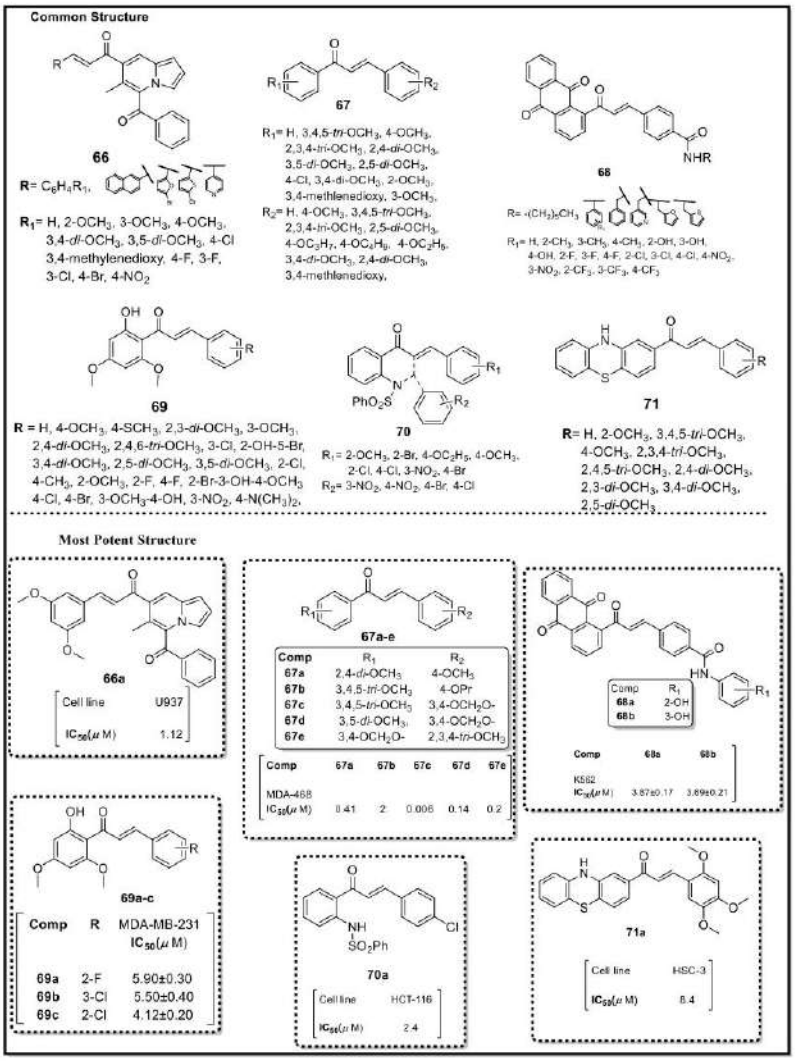

Fig. (22).Chalcone analogs (**66-71**) with potent anti-cancer activity.

with an IC_{50} value of 6.50 and 4.12 μM, 5.50 and 6.50 μM, and 7.12 and 4.04 μM, respectively. Their SAR studies concluded that FKB chalcones analogs with EWGs on ring B potentiated the cytotoxic effects on the breast cancer cells.

Oliveira *et al.* [122] have synthesized a library of chalcone-quinolinone hybrids (**70**, Fig. **22**) using Claisen-Schmidt condensation and evaluated their anti-proliferative activity against HCT-116 (colon) cancer cell lines in an MTT assay. It was observed that the antitumor potency of the chalcone-quinolinone hybrids was less than their chalcone intermediates.

Halise *et al.* [123] have also prepared some chalcone derivatives (**71**, Fig. **22**) as cytotoxic agents. Compounds **71a** showed good cytotoxicity with the highest selectivity index SI= 76.5 and potency-

selectivity expression (PSE) (PSE=>1285; > 1602) values. Western blot analysis demonstrated that compound **71a** cleaved the product of PARP and the activation of caspase-3 with 8–64 μM to induce apoptosis in HSC-2 cells. QSAR analysis revealed that compound **71a** with 2,4,5-trimethoxyphenyl was the most selective cytotoxic agent among the trimethoxylated derivatives.

Khan *et al.* [124] synthesized a series of thienopyrimidine-chalconehybrids(**72**, Fig. **23**) as Fas-activated serine/threonine kinase (FASTK) inhibitors. Compounds **72a-c** emerged as the most potent hybrids from enzyme inhibition assay. *In vitro* cytotoxicity evaluation also established that the compounds showed superior antiproliferative efficacy cytotoxicity against MCF-7 cells. Apoptosis assay also concluded that FASTK and reactive oxygen species production was inhibited by cell cycle arrest at the G0/G1 phase in MCF-7 cells.

Vongdeth *et al.* [125] reported the synthesis of polymethoxy-chalcones and polymethoxy-flavones (**73**, Fig. **23**) and screened for antiproliferative activity against HeLa, HCC1954, and SK-OV-3 by the cell counting kit-8 (CCK-8) assay. A preliminary *in vitro* study concluded that compounds **73a-d** exerted stronger antiproliferative efficacies compared to cisplatin.

Amar Djemoui *et al.* [126] have identified compound**74a** with excellent anticancer potential from a library of triazole-benzimidazole-chalcones (**74**, Fig. **23**). The compound displayed IC_{50} values of 6.23 μM, 5.89 μM, and 10.7 μM against T47-D, MDA-MB-231 and PC3 cancer cell lines. SAR studies demonstrated that chloro substituent on chalcone ring with 1-*N*-benzyl-1,2,3-triazole moiety enhanced the compounds' cytotoxic effect.

Olívia *et al.* [127] synthesized novel chalcones derivatives (**75**, Fig. **23**) and determined their anti-breast cancer potential using MCF-7, Hs578Tand MCF-10A cell lines. Compounds**75a-b** emerged as the most active with IC_{50}values of 5.07 and 3.98 μM, respectively, against the MCF-7 cell line. SAR studies revealed that bromo substituent on ring B is more effective than chloro substituent. Mechanistically chalcone analogs failed to arrest the cell cycle at the G2/M phase and tubulin polymerization in MCF-7 cells.

Adopting the concept of molecular hybridization, Yang *et al.* [128] synthesized a class of trimethoxyphenyl derived chalcone-benzimidazolium salts (**76**, Fig. **23**) and examined their anticancer potentials on leukemia (HL-60), myeloid liver carcinoma (SMMC-7721), lung carcinoma (A549), breast carcinoma (MCF-7), and colon carcinoma (SW480) in an MTT assay. Compound **76a** was more selective to HL-60, MCF-7, and SW-480 cell lines, howeverwith 8-, 11-, and 6-fold reduced potency compared to cisplatin (DDP). Further, mechanistic studies established that compound **76a** induced apoptosis in SMMC-7721 cells by cell cycle arrest at the G1 phase.

Two novel series of pyridoxine-azaheterocyclic hybrids of feruloyl methane (dehydrozingerone, DZG)were synthesized by Pavelyev *et al.* [129] and evaluated for their anticancer potential using MCF-7 (breast adenocarcinoma) and HEK293 cells (**77**, Fig. **23**). SAR study revealed the dependence of anticancer activity on the lipophilic substituents on acetal carbon ring. The most active compound **77a** exhibited excellent anticancer activity against MCF7 (IC_{50} = 1.1 μM) and toxicity profile against HEK293 superior to doxorubicin. Mechanistically, **77a** exhibited its activity by arresting the cell cycle at the G2/M phase.

A chalcone-sulfonamide hybrids (**78**, Fig. **24**) was discovered by Custodio *et al.* [130] as an anticancer drug candidate with IC_{50} values of 13.16, 5.39, and 10.84 μM against SF-295, HCT-116, and PC-3 cancer cell lines, respectively, in an MTT assay. Computational studies demonstrated that the carbonyl, nitro, and olefin groups formed a conjugate system with planer geometry that helps to bind the molecule with drug receptors. Moreover, the molecular electrostatic potential (MEP) map was used to find C-H···O and N-H···O (hydrogen bonding) intermolecular interaction at the molecular sites.

Dong *et al.* [131] investigated the anticancer activity of a chalcone derivative **79** (Fig. **24**) relative to reference drug 5-FU. The compound functioned by modulating caspase-3/8 and Bax/Bcl2 levels to induce apoptosis in HepG2 and H460 cancer cells. Compound **79** also inhibited the growth of tumour cells in a xenograft mouse model *via* suppression, invasion, and migration mechanism. The active hybrids possess good solubility than 5-FU in polar solvents. Molecular docking studies further suggested that the polar interaction between compound **79** and caspase-3 and -8 of the target cell favoured the induced apoptosis.

Agnieszka *et al.* [132] investigated the antiproliferative effect of six natural prenylated flavonoids (**80**, Fig. **24**) *viz.*, xanthohumol, α,β-dihydroxanthohumol isoxanthohumol, 8-prenylnaringenin and 6-prenylnaringenin alongside nonprenylated naringenin against MCF 10A, MDA-MB-231, T-47D cancer cell lines. Xanthohumol (**80**) emerged as the most active overall with superior cytotoxicity compared to cisplatin.

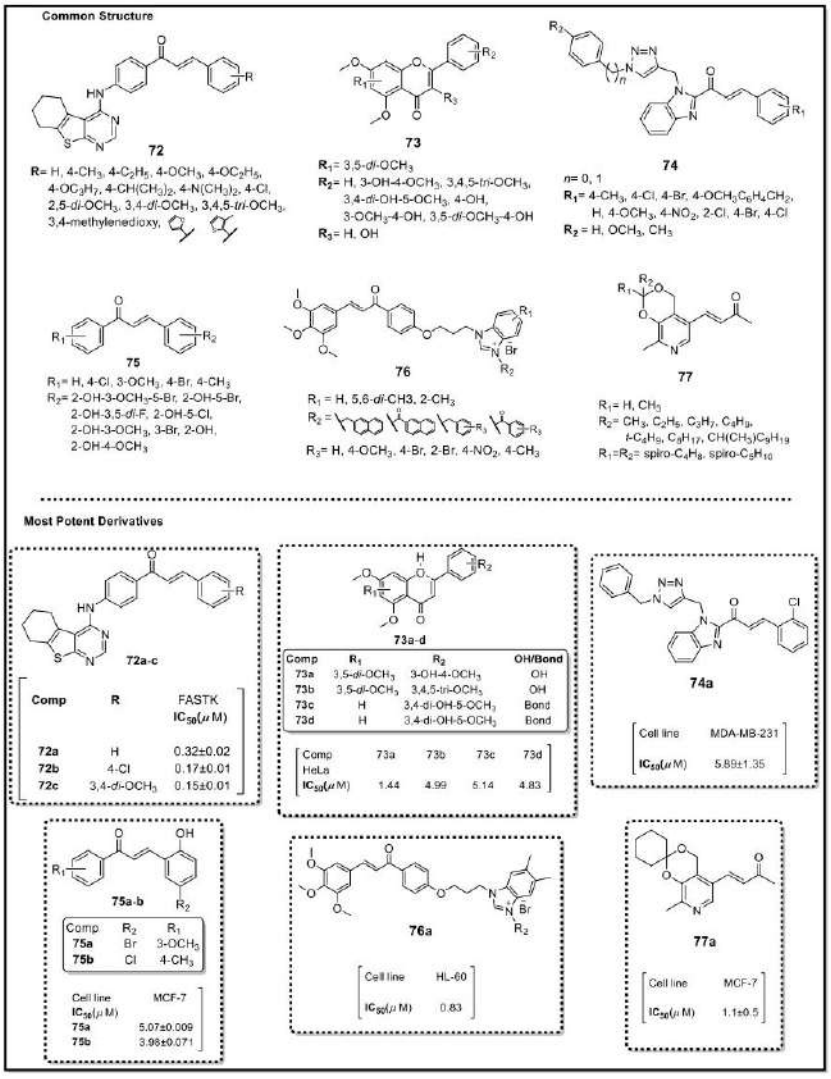

Fig. (23). Chalcone-hybrids (**72-77**) with active anticancer compounds.

Gil *et al*. [133] studied the mechanism of induced apoptosis in A549 lung cancer cells on treatment with 2-hydroxy-3′,5,5′-trimethoxychalcone analogs (**81**, Fig. **24**). It was confirmed that the treatment of cell line with DK-139 (**81**) increases expression of ER stress in A549 lung cancer cells which trigger caspase-mediated apoptosis through unfolded protein response (UPR) pathway.

The method to prevent tumour growth and metastasis by targeting TGF-β1- induced epithelial-mesenchymal transition was developed by Jeong *et al*. [134]. The chalcone analog **82** (Fig. **24**) was evaluated for anticancer activity against human A549 lung cancer cells through migration and invasion assays. It was demonstrated that compound **82** inhibited TGF-β1-induced smad2 phosphorylation, expression TGF-β1-

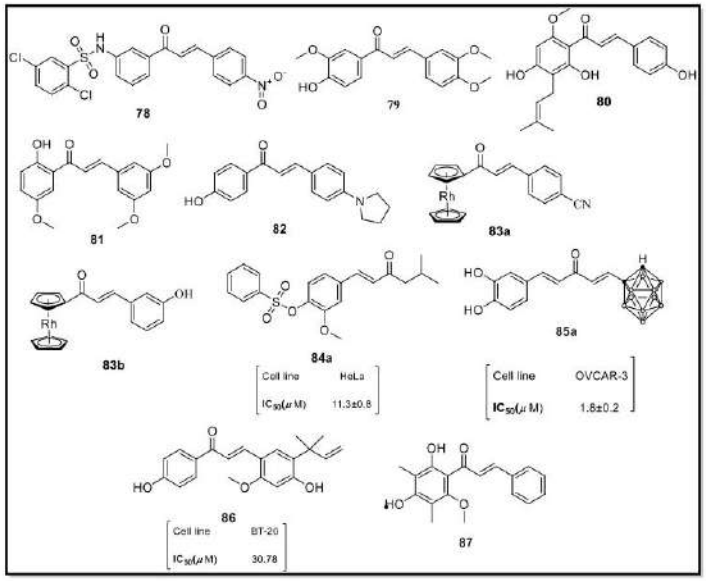

Fig. (24). Chalcone analogs (**78-87**) as anti-proliferative agents.

induced EMT markers, and suppressed the migration and invasion during TGF- β1- induced EMT.

Khanapure *et al.* [135] performed Claisen-Schmidt condensation of acetyl ruthenocene and aryl aldehydes to afford a series of ruthenocenyl chalcones (**83**, Fig. **24**). Cytotoxicity evaluation established that compound **83a-b** displayed 45% and 91% inhibition against NCI-lung cancer cell line and MDA-MB-435 respectively.

Cytotoxicity evaluation of chalcone-sulfonyl ester analogs (**84**, Fig. **24**) by Jovana *et al.* [136] has delivered compound **84a** as the most promising cytotoxic agent against HeLa and MCF-7 cell lines without any significant toxicity on non-cancerous MRC-5 cell lines. The compound effectively induced apoptosis by cell cycle arrest at G2/M in both HeLa and MCF-7 cell lines.

Curcumin has the potential to inhibit cell growth in different types of cancer. However, low *in vivo* bioavailability and metabolism are few limitations to the compound's efficacy as an ideal drug candidate; thus, encouraging synthetic chemists to make improvements in its structure. In this regard, Azzi *et al.* [137] prepared a series of boronated-monocarboxylic curcumin analogs (**85**, Fig. **24**) as cytotoxic agents against MCF-7 and OVCAR-3 cell lines. The majority of the compounds displayed significant improvement in their antiproliferative activity against both the cell lines and compound **85a** was identified as the most promising drug candidate with IC_{50} values of 2.6 and 1.8 μM against MCF-7 and OVCAR-3 cancer cells, respectively.

Komoto *et al.* [138] examined the ability of licochalcone A (**86**, Fig. **24**) to inhibit multiple drug-resistant MCF-7 and BT-20 breast cancer cells. Both *trans*-chalcone and Licochalcone A reduce cell viability in MCF-7 and BT-20 breast cancer cell lines, by inhibiting the expression of AURKA and MDR-1 at the mRNA and protein level.

Huynh *et al.* [139] studied the effect of 2',4'-dihydroxy-6'-methoxy-3',5'-dimethylchalcone (**87**, Fig. **24**) on two human pancreatic cancer cell lines. Compound **87** displayed IC_{50} values of 10.5 and 12.2 μM against PANC-1 and MIA PACA2 cells, respectively. The compound also induced apoptosis of PANC-1 cells *via* caspase-3 activation. From in vitro data, it was concluded that chalcone **87** exhibits significant anti-PANC-1 cancer cell activity.

9. LIST OF PATENTS

The chalcone hybrids from natural and synthetic origin have gained ample attention and focus due to their multifaceted pharmacological properties. Various

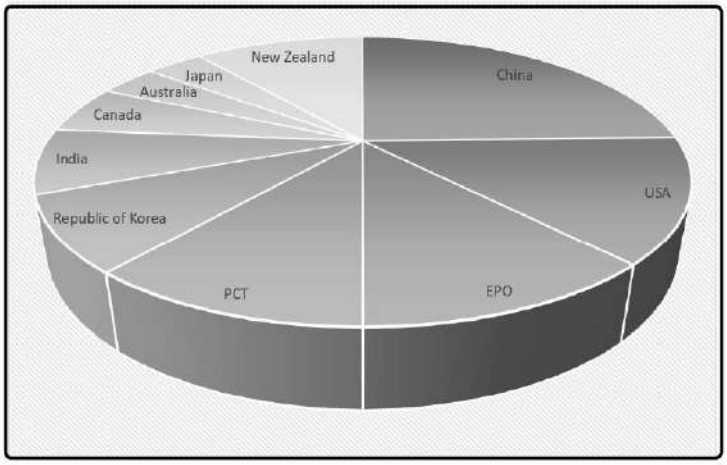

Fig. (25). Patent published in the last decade on chalcone as an anti-cancer agent.

Table 2. List of patents on chalcone as anti-cancer agents (2018-2019).

S. No	Patent Publication No.	Publication Date	Title	Cancer Type
1	CN 110590806	Dec 20, 2019	Chalcone analog containing thieno[2,3-d] pyrimid-2-yl and preparation method and application thereof as an antitumor drug	Neoplasm
2	CN 110563563	Dec 13, 2019	Chalcone-type compound, its preparation method from Spatholobus suberectus stems and application in the treatment and /or prevention of breast cancer	Human Mammary gland neoplasm
3	IN 201941046359	Nov 29, 2019	A process of synthesizing novel methyl-substituted chalcone molecules- the potential cancer inhibitors	Neoplasm
4	CN 110526809	Dec 3, 2019	Production method of chalcone compound from dried vines of Spatholobus suberectus by extracting and separating, and application thereof in treating and/or preventing lung cancer	Lung neoplasm
5	CN 110452162	Nov 15, 2019	Application of chalcone derivative as modulator of FLI-1 gene	Prostate gland neoplasm and Leukemia
6	CN 110143927	Aug 20, 2019	Benzimidazole chalcone derivative, its preparation method, and application as antitumor agents	Lung neoplasm, Homo sapiens, Liver neoplasm, and Prostate gland neoplasm
7	CN 110028421	Dec 11, 2018	Chalcone compound useful in the treatment of cancer and its preparation	Liver neoplasm, Homo sapiens Leukemia, Lung neoplasm, and Uterine cervical neoplasm
8	CN 109966275	Jul 5, 2019	Application of quinoid chalcone compound in preparing antitumor drug	Leukemia, Pancreatic adenocarcinoma, Lung, Mammary gland, Liver and Brain neoplasm

(Table 2) contd....

S. No	Patent Publication No.	Publication Date	Title	Cancer Type
9	CN 109985030	Jul 9, 2019	Quinoid chalcone compound application in the preparation of anti-tumor drugs	Neoplasm
10	CN 109879808	Jun 14, 2019	Preparation of chalcone derivatives as antitumor agents	Mammary gland, Lung adenocarcinoma, and Homo sapiens
11	CN 109824624	May 31, 2019	Preparation of chalcone compounds containing morpholine useful for the treatment of breast cancer	Homo sapiens and Neoplasm
12	KR 2019050074A	May 10, 2019	Preparation of chalcone derivative for protecting kidney	nephrotoxic
13	CN 109705017A	May 3, 2019	Preparation of chalcone indole derivative useful as antitumor drug	Neoplasm
14	BR 102016023358	May 2, 2018	Chalcones as anticancer agents for the treatment of breast cancer and their preparation	Homo sapiens neoplasm
15	CN 109651226	Apr 19, 2019	Chalcone indole derivatives useful in the treatment of colorectal cancer and their preparation	Colorectal neoplasm
16	BR 102016018123	Mar 6, 2018	Preparation of pyrazoles at antitumor agents for the treatment of breast cancer	Breast cancer
17	CN 109535068	Mar 29, 2019	Pyridine-chalcone compound or its pharmaceutically acceptable salt, preparation method, and application	Neoplasm
18	BR 102016018411 A2	Feb 27, 2018	Antitumor agent based on chalcones for treating bladder and urinary tract cancers in human and animals	Bladder neoplasm
19	CN 109467549	Mar 15, 2019	Preparation of quinoline substituted chalcone compounds useful as tubulin polymerization inhibitors for the treatment of cancer	Cell proliferation, Homo sapiens, and Microtubule-disrupting
20	CN 109456284	Mar 12, 2019	Chalcone containing substituted biphenyl and application thereof	Immunotherapy PD1/PD-L1 inhibitors and Homo sapiens
21	CN 109251189	Jan 22, 2019	Preparation of the 3-site piperazinyl chalcone derivative and their pharmaceutical composition and application	Neoplasm
22	CN 109232477	Jan 18, 2019	Chalcone-amino dithiocarbamate compound, its synthesis method and application as an active ingredient in preparing antineoplastic drug or catalase inhibitor	Homo sapiens Neoplasm
23	IN 302219	Oct 26, 2018	Chalcone linked pyrrolo[2,1-c][1,4] benzodiazepine hybrids as potential anticancer agents and their preparation, pharmaceutical compositions, and use in the treatment of cancers	Homo sapiens neoplasm

(Table 2) contd....

S. No	Patent Publication No.	Publication Date	Title	Cancer Type
24	IN 201811026442	Sep 28, 2018	Method for preparation of a composition for the treatment of breast cancer and skin cancer and gland tuberculosis (kanthmala)	Skin neoplasm, Homo sapiens, and Mallotus philippinensis Neoplasm,
25	CN 108558763	Sep 21, 2018	Indazole-containing chalcone and its application in the preparation of a drug for treating gastric cancer and lung cancer	Stomach neoplasm, Homo sapiens, and Lung neoplasm
26	EP 3562803	Nov 6, 2019	Preparation of substituted chalcones as notch inhibitors for use in the treatment of t-cell acute lymphoblastic leukemia	Acute T-cell leukemia
27	CN 108191898	Jun 22, 2018	4-(1-Hydroxy-1,3-dihydrobenzo[c][1,2] oxaborol-7-yl)chalcone derivative, and its preparation method and application in antitumor drug	Mammary gland neoplasm, Colon neoplasm, Ovary neoplasm, and Homo sapiens
28	CN 108191719	Jun 22, 2018	Chalcone analogue containing sulfone substitution useful in the treatment of cancer and its preparation	Homo sapiens and Liver neoplasm
29	CN 108047139	May 18, 2018	Preparation of chalcone-benzimidazole salts as antitumor agents	Homo sapiens Neoplasm
30	KR 2018015800	Feb 14, 2018	Resveratrol-chalcone derivative as an anticancer agent, and method for the preparation thereof	Bone marrow neoplasm, Mammary gland neoplasm, Pancreatic neoplasm, and Colorectal neoplasm
31	CN 107602367	Jan 19, 2018	Preparation of 4'-hydroxyl-3'-methoxychalcone derivatives as antitumor agents	Colon neoplasm, Homo sapiens, Lung neoplasm

patents on chalcone analogues as anti-cancer agents (Table **2**) have been substantially found from each database (Fig. **25**).

Another key feature of this review is that we have defined significant SAR parameters that coincide the chemical structure and the pharmacological activities of the molecules.

CONCLUSION AND FUTURE PERSPECTIVE

In this review, we have outlined the different drug targets of chalcone scaffolds used in the design of anticancer agents over the past two years. A broad variety of natural and synthetic chalcones with remarkable anti-cancer efficacy have been explicated together with their corresponding molecular targets *viz*., ABCG2, BCRP, P-glycoprotein, 5α-reductase, androgen receptor (AR), histone deacetylases (HDAC), sirtuin 1, proteasome, vascular endothelial growth factor (VEGF), cathepsin-K, tubulin, CDC25B phosphatase, topoisomerase, EBV, NF-κB, mTOR, BRAF and Wnt/β-catenin. Moreover, considerable focus has also been given to significant cellular processes and genetic pathways implicated in carcinogenesis. The majority of the chalcones presented herein have demonstrated excellent anticancer properties and are suitable drug candidates for chemotherapeutic intervention against different types of cancer. Although there are many products containing the chalcone nucleus in the market or under clinical trials, we hope that the evidence presented in this mini-review would not only provide researchers with the current developments on chalcones with interesting potencies but would also facilitate the recruitment of their structures as reliable templates for fast and successful development of novel molecules with enhanced chemotherapeutic benefits.

CONSENT FOR PUBLICATION

Not applicable.

FUNDING

Rajshekhar Karpoormath would like to thank the National Research Foundation-South Africa (NRF-SA) for funding this project (Grant Nos. 103728 and 112079).

CONFLICT OF INTEREST

The authors declare no conflict of interest, financial or otherwise.

ACKNOWLEDGEMENTS

The authors are thankful to the Discipline of Pharmaceutical Sciences, College of Health Sciences, University of Kwa-Zulu Natal (UKZN), Durban, South Africa, for providing all the necessary facilities. R.K. gratefully acknowledges National Research Foundation-South Africa (NRF-SA) for funding this project (Grant Nos. 103728 and 112079).

REFERENCES

[1] Bray, F; Ferlay, J; Soerjomataram, I. Global Cancer Statistics 2018 : GLOBOCAN Estimates of Incidence and Mortality Worldwide for 36 Cancers in 185 Countries. **2018**, 394-424.

[2] Dagogo-Jack, I.; Shaw, A.T. Tumour heterogeneity and resistance to cancer therapies. *Nat. Rev. Clin. Oncol.*, **2018**, *15*(2), 81-94. http://dx.doi.org/10.1038/nrclinonc.2017.166 PMID: 29115304

[3] Bozzuto, G.; Ruggieri, P.; Molinari, A. Molecular aspects of tumor cell migration and invasion. *Ann. Ist. Super. Sanita*, **2010**, *46*(1), 66-80. http://dx.doi.org/10.1590/S0021-25712010000100009 PMID: 20348621

[4] Mareel, M.; Leroy, A. Clinical, cellular, and molecular aspects of cancer invasion. *Physiol. Rev.*, **2003**, *83*(2), 337-376. http://dx.doi.org/10.1152/physrev.00024.2002 PMID: 12663862

[5] Lim, W.A.; June, C.H. The Principles of Engineering Immune Cells to Treat Cancer. *Cell*, **2017**, *168*(4), 724-740. http://dx.doi.org/10.1016/j.cell.2017.01.016 PMID: 28187291

[6] Lin, A.; Giuliano, C.J.; Palladino, A.; John, K.M.; Abramowicz, C.; Yuan, M.L.; Sausville, E.L.; Lukow, D.A.; Liu, L.; Chait, A.R.; Galluzzo, Z.C.; Tucker, C.; Sheltzer, J.M. Off-target toxicity is a common mechanism of action of cancer drugs undergoing clinical trials. *Sci. Transl. Med.*, **2019**, *11*(509), eaaw8412. http://dx.doi.org/10.1126/scitranslmed.aaw8412 PMID: 31511426

[7] Robey, R.W.; Pluchino, K.M.; Hall, M.D.; Fojo, A.T.; Bates, S.E.; Gottesman, M.M. Revisiting the role of ABC transporters in multidrug-resistant cancer. *Nat. Rev. Cancer*, **2018**, *18*(7), 452-464. http://dx.doi.org/10.1038/s41568-018-0005-8 PMID: 29643473

[8] Nevedomskaya, E.; Baumgart, S.J.; Haendler, B. Recent advances in prostate cancer treatment and drug discovery. *Int. J. Mol. Sci.*, **2018**, *19*(5), E1359. http://dx.doi.org/10.3390/ijms19051359 PMID: 29734647

[9] Toden, S.; Tran, H.M.; Tovar-Camargo, O.A.; Okugawa, Y.; Goel, A. Epigallocatechin-3-gallate targets cancer stem-like cells and enhances 5-fluorouracil chemosensitivity in colorectal cancer. *Oncotarget*, **2016**, *7*(13), 16158-16171. http://dx.doi.org/10.18632/oncotarget.7567 PMID: 26930714

[10] Bhanot, A.; Sharma, R.; Noolvi, M.N. Natural sources as potential anti-cancer agents: A review. *Int. J. Phytomed.*, **2011**.

[11] Karthikeyan, C.; Narayana Moorthy, N.S.H.; Ramasamy, S.; Vanam, U.; Manivannan, E.; Karunagaran, D. Advances in Chalcones with Anticancer Activities. *Recent Pat Anticancer Drug Discov.*, , **2014**. http://dx.doi.org/10.2174/1574892809666140819153902

[12] Gomes, M.N.; Muratov, E.N.; Pereira, M.; Peixoto, J.C.; Rosseto, L.P.; Cravo, P.V.L.; Andrade, C.H.; Neves, B.J. Chalcone derivatives: Promising starting points for drug design. *Molecules*, **2017**, *22*(8), E1210. http://dx.doi.org/10.3390/molecules22081210 PMID: 28757583

[13] Kurt, B.Z.; Ozten Kandas, N.; Dag, A.; Sonmez, F.; Kucukislamoglu, M. Synthesis and biological evaluation of novel coumarin-chalcone derivatives containing urea moiety as potential anticancer agents. *Arab. J. Chem.*, **2020**. http://dx.doi.org/10.1016/j.arabjc.2017.10.001

[14] Hampannavar, G.A.; Karpoormath, R.; Palkar, M.B.; Shaikh, M.S.; Chandrasekaran, B. Dehydrozingerone Inspired Styryl Hydrazine Thiazole Hybrids as Promising Class of Antimycobacterial Agents. *ACS Med. Chem. Lett.*, **2016**, *7*(7), 686-691. http://dx.doi.org/10.1021/acsmedchemlett.6b00088 PMID: 27437078

[15] Iwai, Y.; Hamanishi, J.; Chamoto, K.; Honjo, T. Cancer immunotherapies targeting the PD-1 signaling pathway. *J. Biomed. Sci.*, **2017**, *24*(1), 26. http://dx.doi.org/10.1186/s12929-017-0329-9 PMID: 28376884

[16] Chen, Z.; Shi, T.; Zhang, L.; Zhu, P.; Deng, M.; Huang, C.; Hu, T.; Jiang, L.; Li, J. Mammalian drug efflux transporters of the ATP binding cassette (ABC) family in multidrug resistance: A review of the past decade. *Cancer Lett.*, **2016**, *370*(1), 153-164. http://dx.doi.org/10.1016/j.canlet.2015.10.010 PMID: 26499806

[17] Lopes-Rodrigues, V.; Sousa, E.; Vasconcelos, M.H. Curcumin as a modulator of P-glycoprotein in cancer: Challenges and perspectives. *Pharmaceuticals (Basel)*, **2016**, *9*(4), E71. http://dx.doi.org/10.3390/ph9040071 PMID: 27834897

[18] Dai, C.; Ganesan, V.; Zabell, J.; Nyame, Y.A.; Almassi, N.; Greene, D.J. Impact of 5α-Reductase Inhibitors on Disease Reclassification among Men on Active Surveillance for Localized Prostate Cancer with Favorable Features. *J. Urol.*, **2018**. http://dx.doi.org/10.1016/j.juro.2017.08.006

[19] Guerrero, J.; Alfaro, I.E.; Gómez, F.; Protter, A.A.; Bernales, S. Enzalutamide, an androgen receptor signaling inhibitor, induces tumor regression in a mouse model of castration-resistant prostate cancer. *Prostate*, **2013**, *73*(12), 1291-1305. http://dx.doi.org/10.1002/pros.22674 PMID: 23765603

[20] Lasko, L.M.; Jakob, C.G.; Edalji, R.P.; Qiu, W.; Montgomery, D.; Digiammarino, E.L.; Hansen, T.M.; Risi, R.M.; Frey, R.; Manaves, V.; Shaw, B.; Algire, M.; Hessler, P.; Lam, L.T.; Uziel, T.; Faivre, E.; Ferguson, D.; Buchanan, F.G.; Martin, R.L.; Torrent, M.; Chiang, G.G.; Karukurichi, K.; Langston, J.W.; Weinert, B.T.; Choudhary, C.; de Vries, P.; Van Drie, J.H.; McElligott, D.; Kesicki, E.; Marmorstein, R.; Sun, C.; Cole, P.A.; Rosenberg, S.H.; Michaelides, M.R.; Lai, A.; Bromberg, K.D. Discovery of a selective catalytic p300/CBP inhibitor that targets lineage-specific tumours. *Nature*, **2017**, *550*(7674), 128-132.

http://dx.doi.org/10.1038/nature24028 PMID: 28953875

[21] Hsu, Y.J.; Hsu, S.C.; Hsu, C.P.; Chen, Y.H.; Chang, Y.L.; Sadoshima, J.; Huang, S.M.; Tsai, C.S.; Lin, C.Y. Sirtuin 1 protects the aging heart from contractile dysfunction mediated through the inhibition of endoplasmic reticulum stress-mediated apoptosis in cardiac-specific Sirtuin 1 knockout mouse model. *Int. J. Cardiol.*, **2017**, *228*, 543-552. http://dx.doi.org/10.1016/j.ijcard.2016.11.247 PMID: 27875732

[22] Wang, J.; Okkeri, J.; Pavic, K.; Wang, Z.; Kauko, O.; Halonen, T.; Sarek, G.; Ojala, P.M.; Rao, Z.; Xu, W.; Westermarck, J. Oncoprotein CIP2A is stabilized via interaction with tumor suppressor PP2A/B56. *EMBO Rep.*, **2017**, *18*(3), 437-450. http://dx.doi.org/10.15252/embr.201642788 PMID: 28174209

[23] Schrader, J; Henneberg, F; Mata, RA; Tittmann, K; Schneider, TR; Stark, H The inhibition mechanism of human 20S proteasomes enables next-generation inhibitor design. *Science (80-)*, **2016**.

[24] Liau, N.P.D.; Laktyushin, A.; Lucet, I.S.; Murphy, J.M.; Yao, S.; Whitlock, E.; Callaghan, K.; Nicola, N.A.; Kershaw, N.J.; Babon, J.J. The molecular basis of JAK/STAT inhibition by SOCS1. *Nat. Commun.*, **2018**, *9*(1), 1558. http://dx.doi.org/10.1038/s41467-018-04013-1 PMID: 29674694

[25] Johnson, K.E.; Wilgus, T.A. Vascular Endothelial Growth Factor and Angiogenesis in the Regulation of Cutaneous Wound Repair. *Adv. Wound Care (New Rochelle)*, **2014**, *3*(10), 647-661. http://dx.doi.org/10.1089/wound.2013.0517 PMID: 25302139

[26] Zhao, Y.; Adjei, A.A. Targeting Angiogenesis in Cancer Therapy: Moving Beyond Vascular Endothelial Growth Factor. *Oncologist*, **2015**, *20*(6), 660-673. http://dx.doi.org/10.1634/theoncologist.2014-0465 PMID: 26001391

[27] Pittayapruek, P.; Meephansan, J.; Prapapan, O.; Komine, M.; Ohtsuki, M. Role of matrix metalloproteinases in Photoaging and photocarcinogenesis. *Int. J. Mol. Sci.*, **2016**, *17*(6), E868. http://dx.doi.org/10.3390/ijms17060868 PMID: 27271600

[28] Duong, T.; Leung, A.T.; Langdahl, B.; Cathepsin, K. Cathepsin K Inhibition: A New Mechanism for the Treatment of Osteoporosis. *Calcif. Tissue Int.*, **2016**, *98*(4), 381-397. http://dx.doi.org/10.1007/s00223-015-0051-0 PMID: 26335104

[29] Chen, H.; Lin, Z.; Arnst, K.E.; Miller, D.D.; Li, W. Tubulin inhibitor-based antibody-drug conjugates for cancer therapy. *Molecules*, **2017**, *22*(8), E1281. http://dx.doi.org/10.3390/molecules22081281 PMID: 28763044

[30] George Rosenker, K.M.; Paquette, W.D.; Johnston, P.A.; Sharlow, E.R.; Vogt, A.; Bakan, A. *Synthesis and biological evaluation of 3-aminoisoquinolin-1(2H)-one based inhibitors of the dual-specificity phosphatase Cdc25B*; Bioorganic Med Chem, **2015**. http://dx.doi.org/10.1016/j.bmc.2015.01.043

[31] Panter, F.; Krug, D.; Baumann, S.; Müller, R. Self-resistance guided genome mining uncovers new topoisomerase inhibitors from myxobacteria. *Chem. Sci. (Camb.)*, **2018**, *9*(21), 4898-4908. http://dx.doi.org/10.1039/C8SC01325J PMID: 29910943

[32] Irwin, M.L.; Cartmel, B.; Gross, C.P.; Ercolano, E.; Li, F.; Yao, X.; Fiellin, M.; Capozza, S.; Rothbard, M.; Zhou, Y.; Harrigan, M.; Sanft, T.; Schmitz, K.; Neogi, T.; Hershman, D.; Ligibel, J. Randomized exercise trial of aromatase inhibitor-induced arthralgia in breast cancer survivors. *J. Clin. Oncol.*, **2015**, *33*(10), 1104-1111. http://dx.doi.org/10.1200/JCO.2014.57.1547 PMID: 25452437

[33] Krishnamurthy, N.; Kurzrock, R. Targeting the Wnt/beta-catenin pathway in cancer: Update on effectors and inhibitors. *Cancer Treat. Rev.*, **2018**, *62*, 50-60. http://dx.doi.org/10.1016/j.ctrv.2017.11.002 PMID: 29169144

[34] Wu, P.; Givskov, M.; Nielsen, T.E. Kinase Inhibitors. In: *Drug Selectivity: An Evolving Concept in Medicinal Chemistry*; , **2017**. http://dx.doi.org/10.1002/9783527674381.ch2

[35] Rodrik-Outmezguine, V.S.; Okaniwa, M.; Yao, Z.; Novotny, C.J.; McWhirter, C.; Banaji, A.; Won, H.; Wong, W.; Berger, M.; de Stanchina, E.; Barratt, D.G.; Cosulich, S.; Klinowska, T.; Rosen, N.; Shokat, K.M. Overcoming mTOR resistance mutations with a new-generation mTOR inhibitor. *Nature*, **2016**, *534*(7606), 272-276. http://dx.doi.org/10.1038/nature17963 PMID: 27279227

[36] Manzano, J.L.; Layos, L.; Bugés, C.; de Los Llanos Gil, M.; Vila, L.; Martínez-Balibrea, E.; Martínez-Cardús, A. Resistant mechanisms to BRAF inhibitors in melanoma. *Ann. Transl. Med.*, **2016**, *4*(12), 237. http://dx.doi.org/10.21037/atm.2016.06.07 PMID: 27429963

[37] Vogt, N.; Dai, B.; Erdmann, T.; Berdel, W.E.; Lenz, G. The molecular pathogenesis of mantle cell lymphoma. *Leuk. Lymphoma*, **2017**, *58*(7), 1530-1537. http://dx.doi.org/10.1080/10428194.2016.1248965 PMID: 27894215

[38] Vaidyanathan, A.; Sawers, L.; Gannon, A.L.; Chakravarty, P.; Scott, A.L.; Bray, S.E.; Ferguson, M.J.; Smith, G. ABCB1 (MDR1) induction defines a common resistance mechanism in paclitaxel- and olaparib-resistant ovarian cancer cells. *Br. J. Cancer*, **2016**, *115*(4), 431-441. http://dx.doi.org/10.1038/bjc.2016.203 PMID: 27415012

[39] Nanayakkara, A.K.; Follit, C.A.; Chen, G.; Williams, N.S.; Vogel, P.D.; Wise, J.G. Targeted inhibitors of P-glycoprotein increase chemotherapeutic-induced mortality of multidrug resistant tumor cells. *Sci. Rep.*, **2018**, *8*(1), 967. http://dx.doi.org/10.1038/s41598-018-19325-x PMID: 29343829

[40] Yin, H.; Dong, J.; Cai, Y.; Shi, X.; Wang, H.; Liu, G.; Tang, Y.; Liu, J.; Ma, L. Design, synthesis and biological evaluation of chalcones as reversers of P-glycoprotein-mediated multidrug resistance. *Eur. J. Med. Chem.*, **2019**, *180*, 350-366. http://dx.doi.org/10.1016/j.ejmech.2019.05.053 PMID: 31325783

[41] Riaz, S.; Iqbal, M.; Ullah, R.; Zahra, R.; Chotana, G.A.; Faisal, A.; Saleem, R.S.Z. Synthesis and evaluation of novel α-substituted chalcones with potent anti-cancer activities and ability to overcome multidrug resistance. *Bioorg. Chem.*, **2019**, *87*(March), 123-135. http://dx.doi.org/10.1016/j.bioorg.2019.03.014 PMID: 30884306

[42] Lu, S.; Obianom, O.N.; Ai, Y. Novel hybrids derived from aspirin and chalcones potently suppress colorectal cancer *in vitro* and *in vivo*. *MedChemComm*, **2018**, *9*(10), 1722-1732. http://dx.doi.org/10.1039/C8MD00284C PMID: 30429977

[43] Mu, J.; Wang, X.; Dong, L.; Sun, P. Curcumin derivative L6H4 inhibits proliferation and invasion of gastric cancer

cell line BGC-823. *J. Cell. Biochem.*, **2019**, *120*(1), 1011-1017.
http://dx.doi.org/10.1002/jcb.27542 PMID: 30242876

[44] Shang Y jing, Wei Q, Sun Z bin. Studying the cytotoxicity of coumarin–chalcone hybrids by a prooxidant strategy in A549 cells. *Monatsh. Chem.*, **2018**, *149*(12), 2287-2292.
http://dx.doi.org/10.1007/s00706-018-2273-0

[45] Wang, F.C.; Peng, B.; Cao, S.L.; Li, H.Y.; Yuan, X.L.; Zhang, T.T.; Shi, R.; Li, Z.; Liao, J.; Wang, H.; Li, J.; Xu, X. Synthesis and cytotoxic activity of chalcone analogues containing a thieno[2,3-d]pyrimidin-2-yl group as the A-ring or B-ring. *Bioorg. Chem.*, **2020**, *94*(September), 103346.
http://dx.doi.org/10.1016/j.bioorg.2019.103346 PMID: 31645277

[46] Hseu, Y.C.; Huang, Y.C.; Thiyagarajan, V.; Mathew, D.C.; Lin, K.Y.; Chen, S.C.; Liu, J.Y.; Hsu, L.S.; Li, M.L.; Yang, H.L. Anticancer activities of chalcone flavokawain B from Alpinia pricei Hayata in human lung adenocarcinoma (A549) cells via induction of reactive oxygen species-mediated apoptotic and autophagic cell death. *J. Cell. Physiol.*, **2019**, *234*(10), 17514-17526.
http://dx.doi.org/10.1002/jcp.28375 PMID: 30847898

[47] Culig, Z.; Santer, F.R. Androgen receptor signaling in prostate cancer. *Cancer Metastasis Rev.*, **2014**, *33*(2-3), 413-427.
http://dx.doi.org/10.1007/s10555-013-9474-0 PMID: 24384911

[48] Saito, Y; Mizokami, A; Tsurimoto, H; Izumi, K; Goto, M; Nakagawa-goto, K. European Journal of Medicinal Chemistry treatments for prostate cancer. **2018**, *157*, 1143-52.

[49] Burgess, A.; Chia, K.M.; Haupt, S.; Thomas, D.; Haupt, Y.; Lim, E. Clinical overview of MDM2/X-targeted therapies. *Front. Oncol.*, **2016**, *6*, 7.
http://dx.doi.org/10.3389/fonc.2016.00007 PMID: 26858935

[50] Zhao, T; Zhao, Y; Liu, X; Li, Z; Wang, B; Zhang, X European Journal of Medicinal Chemistry potent anti-gastric cancer agents: Design , synthesis and structural optimization. **2019**, *161*, 493-505.

[51] Alsaab, H.O.; Sau, S.; Alzhrani, R.; Tatiparti, K.; Bhise, K.; Kashaw, S.K.; Iyer, A.K. PD-1 and PD-L1 checkpoint signaling inhibition for cancer immunotherapy: mechanism, combinations, and clinical outcome. *Front. Pharmacol.*, **2017**, *8*, 561.
http://dx.doi.org/10.3389/fphar.2017.00561 PMID: 28878676

[52] Mohamed, M.F.; Hassaneen, H.M.; Abdelhamid, I.A. Cytotoxicity, molecular modeling, cell cycle arrest, and apoptotic induction induced by novel tetrahydro-[1,2,4]triazolo[3,4-a]isoquinoline chalcones. *Eur. J. Med. Chem.*, **2018**, *143*, 532-541. [Internet].
http://dx.doi.org/10.1016/j.ejmech.2017.11.045 PMID: 29207336

[53] Moraes, MO; De, ; Cláudia, F; Rodrigues, FWABTHS; Magalhães, HS Teixeira AMR. CHEMISTRY Synthesis , structural characterization , and cytotoxic evaluation of chalcone derivatives. *Med Chem Res.*

[54] Loureiro, JB; Carvalho, S; Hadjer, M; Brand, P; Cravo, S; Moreira, J European Journal of Medicinal Chemistry Targeting the MDM2-p53 protein-protein interaction with prenylchalcones: Synthesis of a small library and evaluation of potential antitumor activity. **2018**, *156*, 711-21.

[55] Salem, M.S.; Hussein, R.A.; El-Sayed, W.M. Substitution at Phenyl Rings of Chalcone and Schiff Base Moieties Accounts for their Antiproliferative Activity. *Anticancer. Agents Med. Chem.*, **2019**, *19*(5), 620-626.
http://dx.doi.org/10.2174/1871520619666190225122338 PMID: 30799796

[56] Villarino, A.V.; Kanno, Y.; O'Shea, J.J. Mechanisms and consequences of Jak-STAT signaling in the immune system. *Nat. Immunol.*, **2017**, *18*(4), 374-384.
http://dx.doi.org/10.1038/ni.3691 PMID: 28323260

[57] Harel, S.; Higgins, C.A.; Cerise, J.E.; Dai, Z.; Chen, J.C.; Clynes, R. Clinical Medicine: Pharmacologic inhibition of JAK-STAT signaling promotes hair growth. *Sci. Adv.*, **2015**.
http://dx.doi.org/10.1126/sciadv.1500973

[58] Sangpheak, K.; Tabtimmai, L.; Seetaha, S.; Rungnim, C.; Chavasiri, W.; Wolschann, P.; Choowongkomon, K.; Rungrotmongkol, T. Biological evaluation and molecular dynamics simulation of chalcone derivatives as epidermal growth factor-tyrosine kinase inhibitors. *Molecules*, **2019**, *24*(6), E1092.
http://dx.doi.org/10.3390/molecules24061092 PMID: 30897725

[59] Sangpheak, K.; Mueller, M.; Darai, N.; Wolschann, P.; Suwattanasophon, C.; Ruga, R.; Chavasiri, W.; Seetaha, S.; Choowongkomon, K.; Kungwan, N.; Rungnim, C.; Rungrotmongkol, T. Computational screening of chalcones acting against topoisomerase IIα and their cytotoxicity towards cancer cell lines. *J. Enzyme Inhib. Med. Chem.*, **2019**, *34*(1), 134-143.
http://dx.doi.org/10.1080/14756366.2018.1507029 PMID: 30394113

[60] Fathi, M.A.A.; Abd El-Hafeez, A.A.; Abdelhamid, D.; Abbas, S.H.; Montano, M.M.; Abdel-Aziz, M. 1,3,4-oxadiazole/chalcone hybrids: Design, synthesis, and inhibition of leukemia cell growth and EGFR, Src, IL-6 and STAT3 activities. *Bioorg. Chem.*, **2019**, *84*(84), 150-163.
http://dx.doi.org/10.1016/j.bioorg.2018.11.032 PMID: 30502626

[61] Yadav, L.; Puri, N.; Rastogi, V.; Satpute, P.; Sharma, V. Tumour angiogenesis and angiogenic inhibitors: A review. *J. Clin. Diagn. Res.*, **2015**, *9*(6), XE01-XE05.
http://dx.doi.org/10.7860/JCDR/2015/12016.6135 PMID: 26266204

[62] Wang, C; Li, L; Fu, D; Qin, T; Ran, Y; Xu, F European Journal of Medicinal Chemistry Discovery of chalcone-modi fi ed estradiol analogs as antitumour agents that Inhibit tumour angiogenesis and epithelial to mesenchymal transition. **2019**, *176*, 135-48.

[63] Elkhalifa, D.; Siddique, A.B.; Qusa, M.; Cyprian, F.S.; El Sayed, K.; Alali, F.; Al Moustafa, A.E.; Khalil, A. Design, synthesis, and validation of novel nitrogen-based chalcone analogs against triple negative breast cancer. *Eur. J. Med. Chem.*, **2020**, *187*, 111954.
http://dx.doi.org/10.1016/j.ejmech.2019.111954 PMID: 31838326

[64] Lamaa, D.; Lin, H.P.; Zig, L.; Bauvais, C.; Bollot, G.; Bignon, J.; Levaique, H.; Pamlard, O.; Dubois, J.; Ouaissi, M.; Souce, M.; Kasselouri, A.; Saller, F.; Borgel, D.; Jayat-Vignoles, C.; Al-Mouhammad, H.; Feuillard, J.; Benihoud, K.; Alami, M.; Hamze, A. Design and Synthesis of Tubulin and Histone Deacetylase Inhibitor Based on iso-Combretastatin A-4. *J. Med. Chem.*, **2018**, *61*(15), 6574-6591.
http://dx.doi.org/10.1021/acs.jmedchem.8b00050 PMID: 30004697

[65] Sultana, F; Reddy, S; Reddy, VG; Nayak, VL; Akunuri, R; Rani, S Bioorganic Chemistry Synthesis of benzo [d] im-

idazo [2 , 1- b] thiazole-chalcone conjugates as microtubule targeting and apoptosis inducing agents. **2018**, *76*, 1-12.

[66] Wang, G.; Peng, Z.; Li, Y. Synthesis, anticancer activity and molecular modeling studies of novel chalcone derivatives containing indole and naphthalene moieties as tubulin polymerization inhibitors. *Chem. Pharm. Bull. (Tokyo),* **2019**, *67*(7), 725-728. http://dx.doi.org/10.1248/cpb.c19-00217 PMID: 30982797

[67] Kim, H.G.; Oh, H.J.; Ko, J.H.; Song, H.S.; Lee, Y.G.; Kang, S.C.; Lee, D.Y.; Baek, N.I. Lanceoleins A-G, hydroxychalcones, from the flowers of Coreopsis lanceolata and their chemopreventive effects against human colon cancer cells. *Bioorg. Chem.,* **2019**, *85*, 274-281. http://dx.doi.org/10.1016/j.bioorg.2019.01.003 PMID: 30641321

[68] Huang, X; Huang, R; Wang, Z; Li, L; Gou, S; Liao, Z European Journal of Medicinal Chemistry Pt (IV) complexes conjugating with chalcone analogue as inhibitors of microtubule polymerization exhibited selective inhibition in human cancer cells. **2018**, 146.

[69] Pinto, P; Mariana, C; Moreira, J; Almeida, DP; Silva, PMA; Henriques, AC European Journal of Medicinal Chemistry Chalcone derivatives targeting mitosis : synthesis, evaluation of antitumor activity and lipophilicity. **2019**, 184.

[70] Bandyopadhyay, D.; Sanchez, J.L.; Guerrero, A.M.; Chang, F.M.; Granados, J.C.; Short, J.D.; Banik, B.K. Design, synthesis and biological evaluation of novel pyrenyl derivatives as anticancer agents. *Eur. J. Med. Chem.,* **2015**, *89*, 851-862. http://dx.doi.org/10.1016/j.ejmech.2014.09.072 PMID: 25462285

[71] Alswah, M.; Bayoumi, A.H.; Elgamal, K.; Elmorsy, A.; Ihmaid, S.; Ahmed, H.E.A. Design, Synthesis and Cytotoxic Evaluation of Novel Chalcone Derivatives Bearing Triazolo[4,3-a]-quinoxaline Moieties as Potent Anticancer Agents with Dual EGFR Kinase and Tubulin Polymerization Inhibitory Effects. *Molecules,* **2017**, *23*(1), E48. http://dx.doi.org/10.3390/molecules23010048 PMID: 29280968

[72] Li, W.; Xu, F.; Shuai, W.; Sun, H.; Yao, H.; Ma, C.; Xu, S.; Yao, H.; Zhu, Z.; Yang, D.H.; Chen, Z.S.; Xu, J. Discovery of Novel Quinoline-Chalcone Derivatives as Potent Antitumor Agents with Microtubule Polymerization Inhibitory Activity. *J. Med. Chem.,* **2019**, *62*(2), 993-1013. http://dx.doi.org/10.1021/acs.jmedchem.8b01755 PMID: 30525584

[73] Yan, W.; Xiangyu, C.; Ya, L.; Yu, W.; Feng, X. An orally antitumor chalcone hybrid inhibited HepG2 cells growth and migration as the tubulin binding agent. *Invest. New Drugs,* **2019**, *37*(4), 784-790. http://dx.doi.org/10.1007/s10637-019-00737-z PMID: 30740631

[74] Cong, H.; Zhao, X.; Castle, B.T.; Pomeroy, E.J.; Zhou, B.; Lee, J.; Wang, Y.; Bian, T.; Miao, Z.; Zhang, W.; Sham, Y.Y.; Odde, D.J.; Eckfeldt, C.E.; Xing, C.; Zhuang, C. An Indole-Chalcone Inhibits Multidrug-Resistant Cancer Cell Growth by Targeting Microtubules. *Mol. Pharm.,* **2018**, *15*(9), 3892-3900. http://dx.doi.org/10.1021/acs.molpharmaceut.8b00359 PMID: 30048137

[75] Du, S.; Sarver, J.G.; Trabbic, C.J.; Erhardt, P.W.; Schroering, A.; Maltese, W.A. 6-MOMIPP, a novel brain-penetrant anti-mitotic indolyl-chalcone, inhibits glioblastoma growth and viability. *Cancer Chemother. Pharmacol.,* **2019**, *83*(2), 237-254. http://dx.doi.org/10.1007/s00280-018-3726-1 PMID: 30426158

[76] Wang, B.; Chen, X.; Gao, J.; Su, L.; Zhang, L.; Xu, H. Anti-tumor activity evaluation of novel tubulin and HDAC dual-targeting inhibitors. *Bioorganic Med Chem Lett;* , **2019**. http://dx.doi.org/10.1016/j.bmcl.2019.07.045

[77] Takac, P.; Kello, M.; Pilatova, M.B.; Kudlickova, Z.; Vilkova, M.; Slepcikova, P.; Petik, P.; Mojzis, J. New chalcone derivative exhibits antiproliferative potential by inducing G2/M cell cycle arrest, mitochondrial-mediated apoptosis and modulation of MAPK signalling pathway. *Chem. Biol. Interact.,* **2018**, *292*(July), 37-49. http://dx.doi.org/10.1016/j.cbi.2018.07.005 PMID: 29981726

[78] Preti, D.; Romagnoli, R.; Rondanin, R.; Cacciari, B.; Hamel, E.; Balzarini, J.; Liekens, S.; Schols, D.; Estévez-Sarmiento, F.; Quintana, J.; Estévez, F. Design, synthesis, in vitro antiproliferative activity and apoptosis-inducing studies of 1-(3′,4′,5′-trimethoxyphenyl)-3-(2′-alkoxycarbonylindolyl)-2-propen-1-one derivatives obtained by a molecular hybridisation approach. *J. Enzyme Inhib. Med. Chem.,* **2018**, *33*(1), 1225-1238. http://dx.doi.org/10.1080/14756366.2018.1493473 PMID: 30141353

[79] Mphahlele, M.J.; Maluleka, M.M.; Parbhoo, N.; Malindisa, S.T. Synthesis, evaluation for cytotoxicity and molecular docking studies of Benzo[c]furan-chalcones for potential to inhibit Tubulin polymerization and/or EGFR-tyrosine kinase phosphorylation. *Int. J. Mol. Sci.,* **2018**, *19*(9), 1-18. http://dx.doi.org/10.3390/ijms19092552 PMID: 30154363

[80] Thomas, A.; Pommier, Y. Targeting topoisomerase I in the era of precision medicine. *Clin. Cancer Res.,* **2019**, *25*(22), 6581-6589. http://dx.doi.org/10.1158/1078-0432.CCR-19-1089 PMID: 31227499

[81] Duddukuri, NK; Thatikonda, S; Godugu, C Synthesis of Novel Thiophene-Chalcone Derivatives as Anticancer- and Apoptosis-Inducing Agents. **2018**, 6859-64.

[82] Li, P; Jiang, H; Zhang, W; Li, Y; Zhao, M; Zhou, W. European Journal of Medicinal Chemistry Synthesis of carbazole derivatives containing chalcone analogs as non-intercalative topoisomerase II catalytic inhibitors and apoptosis inducers. **2018**, *145*, 498-510.

[83] Elkins, J.M.; Fedele, V.; Szklarz, M.; Abdul Azeez, K.R.; Salah, E.; Mikolajczyk, J. Comprehensive characterization of the Published Kinase Inhibitor Set. *Eur J Med Chem;* , **2016**. http://dx.doi.org/10.1038/nbt.3374

[84] Richeldi, L.; Costabel, U.; Selman, M.; Kim, D.S.; Hansell, D.M.; Nicholson, A.G.; Brown, K.K.; Flaherty, K.R.; Noble, P.W.; Raghu, G.; Brun, M.; Gupta, A.; Juhel, N.; Klüglich, M.; du Bois, R.M. Efficacy of a tyrosine kinase inhibitor in idiopathic pulmonary fibrosis. *N. Engl. J. Med.,* **2011**, *365*(12), 1079-1087. http://dx.doi.org/10.1056/NEJMoa1103690 PMID: 21992121

[85] Castaño, L.F.; Cuartas, V.; Bernal, A.; Insuasty, A.; Guzman, J.; Vidal, O.; Rubio, V.; Puerto, G.; Lukáč, P.; Vinberg, V.; Baliková-Novtoná, G.; Vannucci, L.; Janata, J.; Quiroga, J.; Abonia, R.; Nogueras, M.; Cobo, J.; Insuasty, B. New chalcone-sulfonamide hybrids exhibiting anticancer and antituberculosis activity. *Eur. J. Med. Chem.,* **2019**, *176*, 50-60. http://dx.doi.org/10.1016/j.ejmech.2019.05.013 PMID: 31096118

[86] Abdelbaset, M.S.; Abdel-Aziz, M.; Ramadan, M.; Abdelrahman, M.H.; Abbas Bukhari, S.N.; Ali, T.F.S. *Discovery of novel thienoquinoline-2-carboxamide chalcone derivatives as antiproliferative EGFR tyrosine kinase inhibitors*; Bioorganic Med Chem, **2019**. http://dx.doi.org/10.1016/j.bmc.2019.02.012

[87] Abou-Zied, H.A.; Youssif, B.G.M.; Mohamed, M.F.A.; Hayallah, A.M.; Abdel-Aziz, M. EGFR inhibitors and apoptotic inducers: Design, synthesis, anticancer activity and docking studies of novel xanthine derivatives carrying chalcone moiety as hybrid molecules. *Bioorg. Chem.*, **2019**, *89*, 102997. http://dx.doi.org/10.1016/j.bioorg.2019.102997 PMID: 31136902

[88] Fu, D.J.; Li, J.H.; Yang, J.J.; Li, P.; Zhang, Y.B.; Liu, S.; Li, Z.R.; Zhang, S.Y. Discovery of novel chalcone-dithiocarbamates as ROS-mediated apoptosis inducers by inhibiting catalase. *Bioorg. Chem.*, **2019**, *86*, 375-385. http://dx.doi.org/10.1016/j.bioorg.2019.01.023 PMID: 30763884

[89] Khan, I; Rao, K; Setti, A; Basha, A; Vangara, N; Palbhadra, M European Journal of Medicinal Chemistry Design , synthesis , in silico pharmacokinetics prediction and biological evaluation of 1 , 4-dihydroindeno [1 , 2- c] pyrazole chalcone as EGFR / Akt pathway inhibitors. **2019**, *163*, 636-48.

[90] Zhou, Y.; Li, M.; Yu, X.; Liu, T.; Li, T.; Zhou, L.; Liu, W.; Li, W.; Gao, F. Butein suppresses hepatocellular carcinoma growth via modulating Aurora B kinase activity. *Int. J. Biol. Sci.*, **2018**, *14*(11), 1521-1534. http://dx.doi.org/10.7150/ijbs.25334 PMID: 30263005

[91] Suma, A.A.T.; Wahyuningsih, T.D. Mustofa. Efficient synthesis of chloro chalcones under ultrasound irradiation, their anticancer activities and molecular docking studies. *Rasayan J. Chem.*, **2019**, *12*(2), 502-510. http://dx.doi.org/10.31788/RJC.2019.1225020

[92] Kennedy, B.K.; Lamming, D.W. The Mechanistic Target of Rapamycin: The Grand ConducTOR of Metabolism and Aging. *Cell Metab.*, **2016**, *23*(6), 990-1003. http://dx.doi.org/10.1016/j.cmet.2016.05.009 PMID: 27304501

[93] Break, M.K.B.; Hossan, M.S.; Khoo, Y.; Qazzaz, M.E.; Al-Hayali, M.Z.K.; Chow, S.C.; Wiart, C.; Bradshaw, T.D.; Collins, H.; Khoo, T.J. Discovery of a highly active anticancer analogue of cardamonin that acts as an inducer of caspase-dependent apoptosis and modulator of the mTOR pathway. *Fitoterapia*, **2018**, *125*(January), 161-173. http://dx.doi.org/10.1016/j.fitote.2018.01.006 PMID: 29355749

[94] Zhang, Y.Q.; Wen, Z.H.; Wan, K.; Yuan, D.; Zeng, X.; Liang, G.; Zhu, J.; Xu, B.; Luo, H. A novel synthesized 3′, 5′-diprenylated chalcone mediates the proliferation of human leukemia cells by regulating apoptosis and autophagy pathways. *Biomed. Pharmacother.*, **2018**, *106*(April), 794-804. http://dx.doi.org/10.1016/j.biopha.2018.06.153 PMID: 29990873

[95] Zhou, X.; Zhou, R.; Li, Q.; Jie, X.; Hong, J.; Zong, Y.; Dong, X.; Zhang, S.; Li, Z.; Wu, G. Cardamonin inhibits the proliferation and metastasis of non-small-cell lung cancer cells by suppressing the PI3K/Akt/mTOR pathway. *Anticancer Drugs*, **2019**, *30*(3), 241-250. http://dx.doi.org/10.1097/CAD.0000000000000709 PMID: 30640793

[96] Jain, H.; Dhingra, N.; Narsinghani, T.; Sharma, R. Insights into the mechanism of natural terpenoids as NF-κB inhibitors: an overview on their anticancer potential. *Exp. Oncol.*, **2016**, *38*(3), 158-168. http://dx.doi.org/10.31768/2312-8852.2016.38(3):158-168 PMID: 27685522

[97] Yu, B.; Liu, H.; Kong, X.; Chen, X.; Wu, C. Synthesis of new chalcone-based homoserine lactones and their antiproliferative activity evaluation. *Eur. J. Med. Chem.*, **2019**, *163*, 500-511. http://dx.doi.org/10.1016/j.ejmech.2018.12.014 PMID: 30553142

[98] Han, X.; Peng, B.; Xiao, B.B.; Sheng-Li Cao, ; Yang, C.R.; Wang, W.Z.; Wang, F.C.; Li, H.Y.; Yuan, X.L.; Shi, R.; Liao, J.; Wang, H.; Li, J.; Xu, X. Synthesis and evaluation of chalcone analogues containing a 4-oxoquinazolin-2-yl group as potential anti-tumor agents. *Eur. J. Med. Chem.*, **2019**, *162*, 586-601. http://dx.doi.org/10.1016/j.ejmech.2018.11.034 PMID: 30472605

[99] Ortalli, M; Ilari, A; Colotti, G; Ionna, I; De, ; Battista, T; Bisi, A European Journal of Medicinal Chemistry Identi fi cation of chalcone-based antileishmanial agents targeting trypanothione reductase. **2018**, 152.

[100] Ahmed, FF; Ali, A; El-hafeez, A; Abbas, SH; Abdelhamid, D European Journal of Medicinal Chemistry New 1 , 2 , 4-triazole-Chalcone hybrids induce Caspase-3 dependent apoptosis in A549 human lung adenocarcinoma cells. **2018**, *151*, 705-22.

[101] Ocasio-Malavé, C.; Donate, M.J.; Sánchez, M.M.; Sosa-Rivera, J.M.; Mooney, J.W.; Pereles-De León, T.A.; Carballeira, N.M.; Zayas, B.; Vélez-Gerena, C.E.; Martínez-Ferrer, M.; Sanabria-Ríos, D.J. Synthesis of novel 4-Boc-piperidone chalcones and evaluation of their cytotoxic activity against highly-metastatic cancer cells. *Bioorg. Med. Chem. Lett.*, **2020**, *30*(1), 126760. http://dx.doi.org/10.1016/j.bmcl.2019.126760 PMID: 31767266

[102] Kocyigit, U.M.; Budak, Y.; Gürdere, M.B.; Ertürk, F.; Yencilek, B.; Taslimi, P.; Gülçin, İ.; Ceylan, M. Synthesis of chalcone-imide derivatives and investigation of their anticancer and antimicrobial activities, carbonic anhydrase and acetylcholinesterase enzymes inhibition profiles. *Arch. Physiol. Biochem.*, **2018**, *124*(1), 61-68. http://dx.doi.org/10.1080/13813455.2017.1360914 PMID: 28792233

[103] Liu, X.; An, L.J.; Li, Y.; Wang, Y.; Zhao, L.; Lv, X.; Guo, J.; Song, A.L. Xanthohumol chalcone acts as a powerful inhibitor of carcinogenesis in drug-resistant human colon carcinoma and these effects are mediated via G2/M phase cell cycle arrest, activation of apoptotic pathways, caspase activation and targeting Ras /MEK/ERK pathway. *J. BUON*, **2019**, *24*(6), 2442-2447. PMID: 31983118

[104] Saavedra, E.; Del Rosario, H.; Brouard, I.; Quintana, J.; Estévez, F. 6′-Benzyloxy-4-bromo-2′-hydroxychalcone is cytotoxic against human leukaemia cells and induces caspase-8- and reactive oxygen species-dependent apoptosis. *Chem. Biol. Interact.*, **2019**, *298*(298), 137-145. http://dx.doi.org/10.1016/j.cbi.2018.12.010 PMID: 30576621

[105] Engelsgjerd, S.; Kunnimalaiyaan, S.; Kandil, E.; Gamblin, T.C.; Kunnimalaiyaan, M. Xanthohumol increases death receptor 5 expression and enhances apoptosis with the TNF-related apoptosis-inducing ligand in neuroblastoma cell lines. *PLoS One*, **2019**, *14*(3), e0213776. http://dx.doi.org/10.1371/journal.pone.0213776 PMID: 30870485

[106] Gan, F.F.; Zhang, R.; Ng, H.L.; Karuppasamy, M.; Seah, W.; Yeap, W.H.; Ong, S.M.; Hadadi, E.; Wong, S.C.; Chui, W.K.; Chew, E.H. Novel dual-targeting anti-proliferative dihydrotriazine-chalcone derivatives display suppression of cancer cell invasion and inflammation by inhibiting the NF-κB signaling pathway. *Food Chem. Toxicol.*, **2018**, *116*(Pt B), 238-248. http://dx.doi.org/10.1016/j.fct.2018.04.003 PMID: 29630947

[107] Wang, Y; Xue, S; Li, R; Zheng, Z; Yi, H; Li, Z. Bioorganic & Medicinal Chemistry Synthesis and biological evaluation of novel synthetic chalcone derivatives as anti-tumor agents targeting Cat L and Cat K. **2018**, *26*, 8-16.

[108] Gupta, S; Maurya, P; Upadhyay, A; Kushwaha, P; Krishna, S; Imran, M European Journal of Medicinal Chemistry Synthesis and bio-evaluation of indole-chalcone based benzopyrans as promising antiligase and antiproliferative agents. **2018**, *143*, 1981-96.

[109] Burmaoglu, S; Ozean, S; Balcioglu, S; Gencel, M; Abbas, S; Noma, A. Bioorganic Chemistry Synthesis , biological evaluation and molecular docking studies of bis- chalcone derivatives as xanthine oxidase inhibitors and anticancer agents. **2019**, *91*(July), 1-8.

[110] Durgapal, S.D.; Soni, R.; Umar, S.; Suresh, B.; Soman, S.S. 3-Aminomethyl pyridine chalcone derivatives: Design, synthesis, DNA binding and cytotoxic studies. *Chem. Biol. Drug Des.*, **2018**, *92*(1), 1279-1287. http://dx.doi.org/10.1111/cbdd.13189 PMID: 29575807

[111] Ayati, A; Esmaeili, R; Moghimi, S; Oghabi, T. European Journal of Medicinal Chemistry Synthesis and biological evaluation of 4-amino-5-cinnamoylthiazoles as chalcone-like anticancer agents. **2018**, *145*, 404-12.

[112] Zhu, M.; Wang, J.; Xie, J.; Chen, L.; Wei, X.; Jiang, X.; Bao, M.; Qiu, Y.; Chen, Q.; Li, W.; Jiang, C.; Zhou, X.; Jiang, L.; Qiu, P.; Wu, J. Design, synthesis, and evaluation of chalcone analogues incorporate α,β-Unsaturated ketone functionality as anti-lung cancer agents via evoking ROS to induce pyroptosis. *Eur. J. Med. Chem.*, **2018**, *157*, 1395-1405. http://dx.doi.org/10.1016/j.ejmech.2018.08.072 PMID: 30196062

[113] Charris, J.E.; Monasterios, M.C.; Acosta, M.E.; Rodriguez, M.A.; Gamboa, N.D.; Martínez, G.P. Antimalarial, antiproliferative, and apoptotic activity of quinoline-chalcone and quinoline-pyrazoline hybrids. A dual action. *Med. Chem. Res.*, **2019**, *28*(11), 2050-2066. http://dx.doi.org/10.1007/s00044-019-02435-0

[114] Gondru, R.; Saini, R.; Vaarla, K.; Singh, S.; Sirassu, N.; Bavantula, R. Synthesis and Characterization of Chalcone-Pyridinium Hybrids as Potential Anti-Cancer and Anti-Microbial Agents. *ChemistrySelect*, **2018**, *3*(5), 1424-1431. http://dx.doi.org/10.1002/slct.201702971

[115] Zhu, H.; Tang, L.; Zhang, C.; Wei, B.; Yang, P.; He, D.; Zheng, L.; Zhang, Y. Synthesis of chalcone derivatives: Inducing apoptosis of HepG2 cells via regulating reactive oxygen species and mitochondrial pathway. *Front. Pharmacol.*, **2019**, *10*, 1341. http://dx.doi.org/10.3389/fphar.2019.01341 PMID: 31803052

[116] Jakovljević, K.; Joksović, M.D.; Matić, I.Z.; Petrović, N.; Stanojković, T.; Sladić, D.; Vujčić, M.; Janović, B.; Joksović, L.; Trifunović, S.; Marković, V. Novel 1,3,4-thiadiazole-chalcone hybrids containing catechol moiety: synthesis, antioxidant activity, cytotoxicity and DNA interaction studies. *MedChemComm*, **2018**, *9*(10), 1679-1697. http://dx.doi.org/10.1039/C8MD00316E PMID: 30429973

[117] Nigam, S.; Jayashree, B.S.; Pande, A.N.; Reddy, N.D.; Venkata Rao, J. Investigating the potential of tetrahydropyridinyl chalcones as useful agents against breast carcinoma: An in vitro and in vivo study. *Res. Chem. Intermed.*, **2018**, *44*(2), 901-924. http://dx.doi.org/10.1007/s11164-017-3143-9

[118] Park, S.; Kim, E.H.; Kim, J.; Kim, S.H.; Kim, I. Biological evaluation of indolizine-chalcone hybrids as new anticancer agents. *Eur. J. Med. Chem.*, **2018**, *144*, 435-443. http://dx.doi.org/10.1016/j.ejmech.2017.12.056 PMID: 29288944

[119] Ruparelia, K.C.; Zeka, K.; Ijaz, T.; Ankrett, D.N.; Wilsher, N.E.; Butler, P.C.; Tan, H.L.; Lodhi, S.; Bhambra, A.S.; Potter, G.A.; Arroo, R.R.J.; Beresford, K.J.M. The synthesis of chalcones as anticancer prodrugs and their bioactivation in CYP1 expressing breast cancer cells. *Med. Chem.*, **2018**, *14*(4), 322-332. http://dx.doi.org/10.2174/1573406414666180112120134 PMID: 29332599

[120] Stanojković, T.; Marković, V.; Matić, I.Z.; Mladenović, M.P.; Petrović, N.; Krivokuća, A.; Petković, M.; Joksović, M.D. Highly selective anthraquinone-chalcone hybrids as potential antileukemia agents. *Bioorg. Med. Chem. Lett.*, **2018**, *28*(15), 2593-2598. http://dx.doi.org/10.1016/j.bmcl.2018.06.048 PMID: 29970309

[121] Abu Bakar, A.; Akhtar, M.N.; Mohd Ali, N.; Yeap, S.K.; Quah, C.K.; Loh, W.S.; Alitheen, N.B.; Zareen, S.; Ul-Haq, Z.; Shah, S.A.A. Design, synthesis and docking studies of flavokawain B type chalcones and their cytotoxic effects on MCF-7 and MDA-MB-231 cell lines. *Molecules*, **2018**, *23*(3), 1-14. http://dx.doi.org/10.3390/molecules23030616 PMID: 29518053

[122] D'Oliveira, G.D.C.; Moura, A.F.; De Moraes, M.O.; Perez, C.N.; Lião, L.M. Synthesis, characterization and evaluation of in vitro antitumor activities of novel chalcone-quinolinone hybrid compounds. *J. Braz. Chem. Soc.*, **2018**. http://dx.doi.org/10.21577/0103-5053.20180108

[123] Gul, H.I.; Yamali, C.; Gunesacar, G.; Sakagami, H.; Okudaira, N.; Uesawa, Y. Cytotoxicity, apoptosis, and QSAR studies of phenothiazine derived methoxylated chalcones as anticancer drug candidates. *Med. Chem. Res.*, **2018**, *27*(10), 2366-2378. http://dx.doi.org/10.1007/s00044-018-2242-5

[124] Khan, N.S.; Khan, P.; Ansari, M.F.; Srivastava, S.; Hasan, G.M.; Husain, M.; Hassan, M.I. Thienopyrimidine-Chalcone Hybrid Molecules Inhibit Fas-Activated Serine/Threonine Kinase: An Approach To Ameliorate Anti-proliferation in Human Breast Cancer Cells. *Mol. Pharm.*, **2018**, *15*(9), 4173-4189. http://dx.doi.org/10.1021/acs.molpharmaceut.8b00566 PMID: 30040903

[125] Vongdeth, K.; Han, P.; Li, W.; Wang, Q.A. Synthesis and Antiproliferative Activity of Natural and Non-Natural Polymethoxychalcones and Polymethoxyflavones. *Chem. Nat. Compd.*, **2019**, *55*(1), 11-17. http://dx.doi.org/10.1007/s10600-019-02605-x

[126] Djemoui, A.; Naouri, A.; Ouahrani, M.R.; Djemoui, D.; Lahcene, S.; Lahrech, M.B. A step-by-step synthesis of triazole-benzimidazole-chalcone hybrids: Anticancer activity in human cells+. *J. Mol. Struct.*, **2020**, •••, 1204. http://dx.doi.org/10.1016/j.molstruc.2019.127487

[127] Pontes, O.; Costa, M.; Santos, F.; Sampaio-Marques, B.; Dias, T.; Ludovico, P.; Baltazar, F.; Proença, F. Exploita-

tion of new chalcones and 4H-chromenes as agents for cancer treatment. *Eur. J. Med. Chem.*, **2018**, *157*, 101-114. http://dx.doi.org/10.1016/j.ejmech.2018.07.058 PMID: 30081238

[128] Yang, J.L.; Ma, Y.H.; Li, Y.H.; Zhang, Y.P.; Tian, H.C.; Huang, Y.C.; Li, Y.; Chen, W.; Yang, L.J. Design, Synthesis, and Anticancer Activity of Novel Trimethoxyphenyl-Derived Chalcone-Benzimidazolium Salts. *ACS Omega*, **2019**, *4*(23), 20381-20393. http://dx.doi.org/10.1021/acsomega.9b03077 PMID: 31815242

[129] Pavelyev, RS; Bondar, O V; Nguyen, TNT; Ziganshina, AA; Al, M; Karwt, R Bioorganic & Medicinal Chemistry Synthesis and in vitro antitumor activity of novel alkenyl derivatives of pyridoxine, bioisosteric analogs of feruloyl methane. **2018**, *26*(August), 5824-37.

[130] Custodio, J.M.F.; Michelini, L.J.; De Castro, M.R.C.; Vaz, W.F.; Neves, B.J.; Cravo, P.V.L. Structural insights into a novel anticancer sulfonamide chalcone. *New J. Chem.*, **2018**, *42*(5), 3426-3434. http://dx.doi.org/10.1039/C7NJ03523C

[131] Dong, N.; Liu, X.; Zhao, T.; Wang, L.; Li, H.; Zhang, S.; Li, X.; Bai, X.; Zhang, Y.; Yang, B. Apoptosis-inducing effects and growth inhibitory of a novel chalcone, in human hepatic cancer cells and lung cancer cells. *Biomed. Pharmacother.*, **2018**, *105*(January), 195-203. http://dx.doi.org/10.1016/j.biopha.2018.05.126 PMID: 29857299

[132] Bartmańska, A.; Tronina, T.; Popłoński, J.; Milczarek, M.; Filip-Psurska, B.; Wietrzyk, J. Highly cancer selective antiproliferative activity of natural prenylated flavonoids. *Molecules*, **2018**, *23*(11), E2922. http://dx.doi.org/10.3390/molecules23112922 PMID: 30423918

[133] Gil, H.N.; Koh, D.; Lim, Y.; Lee, Y.H.; Shin, S.Y. The synthetic chalcone derivative 2-hydroxy-3′,5,5′-trimethoxychalcone induces unfolded protein response-mediated apoptosis in A549 lung cancer cells. *Bioorg. Med. Chem. Lett.*, **2018**, *28*(17), 2969-2975. http://dx.doi.org/10.1016/j.bmcl.2018.07.003 PMID: 30017320

[134] Jeong, J.H.; Jang, H.J.; Kwak, S.; Sung, G.J.; Park, S.H.; Song, J.H.; Kim, H.; Na, Y.; Choi, K.C. Novel TGF-β1 inhibitor antagonizes TGF-β1-induced epithelial-mesenchymal transition in human A549 lung cancer cells. *J. Cell. Biochem.*, **2019**, *120*(1), 977-987. http://dx.doi.org/10.1002/jcb.27460 PMID: 30216515

[135] Khanapure, S.; Jagadale, M.; Bansode, P.; Choudhari, P.; Rashinkar, G. Anticancer activity of ruthenocenyl chalcones and their molecular docking studies. *J. Mol. Struct.*, **2018**, *1173*, 142-147. http://dx.doi.org/10.1016/j.molstruc.2018.06.091

[136] Muškinja, J.M.; Burmudžija, A.Z.; Baskić, D.D.; Popović, S.L.; Todorović, D.V.; Zarić, M.M. Synthesis and anticancer activity of chalcone analogues with sulfonyl groups. *Med. Chem. Res.*, **2019**, *28*(3), 279-291. http://dx.doi.org/10.1007/s00044-018-02283-4

[137] Azzi, E.; Alberti, D.; Parisotto, S.; Oppedisano, A.; Protti, N.; Altieri, S.; Geninatti-Crich, S.; Deagostino, A. Design, synthesis and preliminary in-vitro studies of novel boronated monocarbonyl analogues of Curcumin (BMAC) for antitumor and β-amiloyd disaggregation activity. *Bioorg. Chem.*, **2019**, *93*, 103324. http://dx.doi.org/10.1016/j.bioorg.2019.103324 PMID: 31585269

[138] Komoto, T.T.; Bernardes, T.M.; Mesquita, T.B.; Bortolotto, L.F.B.; Silva, G.; Bitencourt, T.A.; Baek, S.J.; Marins, M.; Fachin, A.L. Chalcones repressed the AURKA and MDR proteins involved in metastasis and multiple drug resistance in breast cancer cell lines. *Molecules*, **2018**, *23*(8), E2018. http://dx.doi.org/10.3390/molecules23082018 PMID: 30104527

[139] Tuan, H.N.; Minh, B.H.; Tran, P.T.; Lee, J.H.; Oanh, H.V.; Ngo, Q.M.T.; Nguyen, Y.N.; Lien, P.T.K.; Tran, M.H. The Effects of 2′,4′-Dihydroxy-6′-methoxy-3′,5′- dimethylchalcone from *Cleistocalyx operculatus* Buds on Human Pancreatic Cancer Cell Lines. *Molecules*, **2019**, *24*(14), 1-11. http://dx.doi.org/10.3390/molecules24142538 PMID: 31336786

Tetrahedron 115 (2022) 132794

Contents lists available at ScienceDirect

Tetrahedron

journal homepage: www.elsevier.com/locate/tet

Metal-free direct annulation of 2-aminophenols and 2-aminothiophenols with unactivated amides through transamidation: Access to polysubstituted benzoxazole and benzothiazole derivatives

Vishal Kumar [a], Sanjeev Dhawan [a], Renu Bala [a], Pankaj Sanjay Girase [a], Parvesh Singh [b], Rajshekhar Karpoormath [a, *]

[a] Department of Pharmaceutical Chemistry, Discipline of Pharmaceutical Sciences, College of Health Sciences, University of KwaZulu-Natal (Westville), Durban, 4000, South Africa
[b] School of Chemistry and Physics, University of KwaZulu-Natal (Westville Campus), Private Bag X01, Scottsville, Durban, South Africa

ARTICLE INFO

Article history:
Received 8 February 2022
Received in revised form
1 April 2022
Accepted 22 April 2022
Available online 28 April 2022

Keywords:
Amine
Amide
Annulation
Transamidation

ABSTRACT

We herein report a simple yet novel oxidant, metal and solvent-free green protocol for synthesising differently 2-substituted 1,3-benzoxazoles and benzothiazoles from 2-aminophenol hydrochloride salt unactivated amide as *in situ* carbon source. Further, the hydrogen ion of hydrochloride played a crucial role in amide activation followed nucleophilic attack that through eliminations of amine as a side product, and de-hydrolysis step leads to final annulation. This versatile strategy is applicable to a wide variety of differently substituted *o*-aminophenols, unactivated aliphatic and aromatic amides, yielding the corresponding product in good to excellent yields in a single step.

1. Introduction

The development of convenient, economical and effective greener methods for benzoxazole synthesis is gaining significant interest. Benzoxazole is an important precursor or building block for the synthesis of more complex chemical structures [1], including pharmaceuticals [2], agrochemicals [3], and natural products [4]. Among these, the 2-substituted 1,3-benzoxazoles scaffold is of particular interest due to its wide range of applications [5]. Despite the usefulness of previously reported benzoxazole synthetic methods, they suffered from disadvantages such as expensive starting materials and reagents, specific or transition metal catalysts [6], environmentally hazardous chemicals [7] and solvents. As a result, there has been an ever-increasing demand for exploring new economical and greener methods for the synthesis of 2-substituted benzoxazole [8].

Recently, our research group reported on the reaction of diverse unactivated amides with widely substituted anilines to produce transamidation products [9] (Scheme 1). This protocol proceeds without any difficulty utilising hydrochloric acid in toluene under metal-free, radiation-free, and oxidant-free conditions.

Our success in transamidation reactions [10] of 2-aminothiophenols with a variety of amides encouraged us to explore the cyclisation reactions of 2-aminothiophenols with a variety of amides under similar reaction conditions except for solvent (Scheme 2). Thus, in our present work, we report the synthesis of benzoxazoles *via* cyclisation of 2-aminophenols with unactivated amides under neat conditions. Further, the hydrogen ion of hydrochloride initially activates the amide, and then the key compound amine attacks as a nucleophile in the reaction. After that, the elimination of side product amine and de-hydrolysis lead to the final annulated product.

To optimise the reaction conditions of benzoxazole synthesis (Table 1), we studied the effect of HCl salt mediated benzoxazole synthesis using 5-methyl-2-aminophenol **1a** as a model substrate and N,N-dimethylacetamide **2a**, in the presence of toluene at 150 °C for 15 h. This reaction yielded good results. Subsequently, we screened different solvents such as DMSO, xylene, and NMP

* Corresponding author.
E-mail address: karpoormath@ukzn.ac.za (R. Karpoormath).

https://doi.org/10.1016/j.tet.2022.132794
0040-4020/

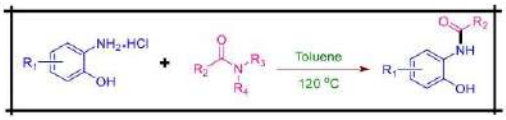

Scheme 1. Previously explored transamidation reaction of unactivated amide.

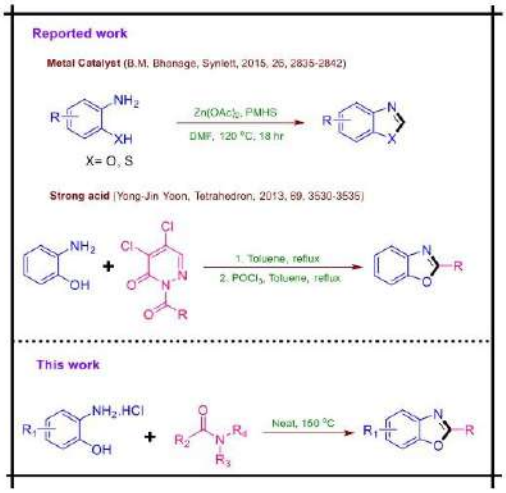

Scheme 2. 2-substituted benzoxazole synthesis from substituted 2-aminophenols.

(**entries 2–4**), but no improvement in the yield was observed. However, solvent-free reaction (**entry 5**) afforded a slightly improved yield as compared to that obtained in NMP solvent (**entry 1**). Further, the use of 4.0 equivalent (equiv.) of **2a** provided the best yield in the optimisation studies (**entries 6–9**). However, it was noted that excess of **2a** and longer duration of stirring resulted in no improvement in the yield, while shorter reaction time significantly decreased the reaction yield (**entries 11–13**). Subsequently, we investigated the effect of temperature on the reaction rate (**entries 15–17**) and observed that lower temperatures (**entries 15–16**) resulted in no formation of the desired product, whereas heating at 150 °C, resulted in excellent yields (**entry 17**). Finally, in terms of output, the optimal reaction condition was achieved when the reaction was carried out at 150 °C for 15.0 h with 5-methyl-2-aminophenol (**1a**) and N,N-dimethylacetamide (**2a**), both as a reactant and solvent (**entries 9, 14** and **17**).

Next, we explored the scope of different 2-aminophenols **1** with differently substituted tertiary amides **2** (Table 2). Initially, N,N-dimethylacetamide **2a** was reacted with several substituted 2-aminophenols (**1a-h**) (**entries 1–8**). Compounds **3a** and **3b** synthesised from 5-methyl (**1a**) and 4-methyl-2-aminophenol (**1b**) produced excellent yields (90 and 87% respectively), and when the reaction was carried out with 4-tertbutyl-2-aminophenol (**1c**), a similar result (91%) was obtained **3c**. To see the effect of electron-withdrawing groups, we included the chloro and nitro analogues (**entries 4–6**), which revealed that the yield of the desired product (**3d**) was higher for 4-chloro-2-aminophenol (**1d**) than those obtained from its 5-chloro-2-aminophenol (**1e**) and 5-nitro-2-aminophenol (**1f**) analogues. As a result of the electronic effect, the chloro on the meta position with respect to the amine of the 2-aminophenol produced an excellent yield. In addition, the heterocyclic compound (3-aminopyridin-3-ol, **1g**) provided a good yield of 2-methyloxazolo [5,4-*b*]pyridine (**3g**).

With the exception of N,N-dimethylacetamide (**2a**), a variety of derivatives of N,N-dimethylamide **2** bearing different R_1 groups such as butyramide (**2b**), valeramide (**2c**), 3,3-dimethylbutanamide (**2d**), isobutyramide (**2e**), pivalamide (**2f**), cyclopropanecarboxamide (**2g**), cyclohexanecarboxamide (**2h**), 2-phenylacetamide (**2i**), benzamide (**2j**), 2-phenoxyacetamide (**2k**), 2,2,2-trichloroacetamide (**2l**) and thiophene-2-carboxamide (**2m**) were reacted with 2-aminophenol (**1h**) employing optimised conditions (**entries 9–20**, Table 2). The steric hindrance of R_1 had a noticeable effect on this reaction, with the yield of **3** gradually reducing as the bulkiness of R_1 increased. (**entries 8–13**). The yields of benzoxazoles (**3n** and **3o**) obtained from the aliphatic cyclic amide (**2g** and **2h**) presented a similar trend suggesting steric hindrance affecting the product yields. Furthermore, aromatic amide derivatives (**entries 16–18**) resulted in a good yield (76–81%) of the desired products (**3p-3s**), respectively. Finally, trichloro substituted amide yielded the least of the corresponding product (**3t**), whereas heterocyclic amide (**2m**) yielded well under Standard conditions.

Subsequently explored the synthesis of 1,3-benzoxazoles from primary, secondary and tertiary amides as shown in Table 3. First, experiments were carried out using 5-methyl-2-aminophenol with

Table 1
Optimisation studies for 2,5-dimethyl-1,3-benzoxazole from 5-methyl-2-aminophenol hydrochloride and N,N-dimethylacetamide.

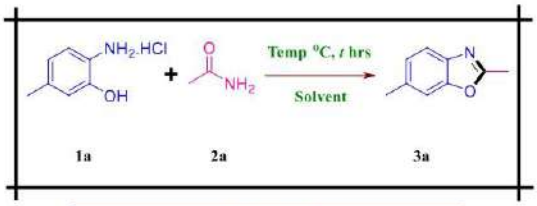

1a 2a 3a

Solvent study				
S.NO.	Solvent (5.0 Vol)	Temp (°C)	Time (hr)	% Yield[b]
1[a]	Toluene	150	15	85
2[a]	DMSO	150	15	15
3[a]	Xylene	150	15	80
4[a]	NMP	150	15	60
5	**2a**	**150**	**15**	**91**
Eq. study of acetamide				
S.NO.	Eq (2a)	Temp (°C)	Time (hr)	Yield[b]
6	1	150	15	45
7	2	150	15	72
8	3	150	15	85
9	**4**	**150**	**15**	**90**
10	5	150	15	91
Time study				
S.NO.	2a (4.0 eq)	Temp (°C)	Time (hr)	Yield[b]
11[a]	2a	150	4	10
12[a]	2a	150	8	60
13[a]	2a	150	12	80
14[a]	**2a**	**150**	**15**	**90**
Temperature study				
S.NO.	2a (4.0 eq)	Temp (°C)	Time (hr)	Yield[b]
15[a]	2a	100	15	0
16[a]	2a	120	15	0
17[a]	**2a**	**150**	**15**	**90**

[a]Conditions: 5-methyl-2-aminophenol **1a** (1.0 mmol), N,N-dimethylacetamide **2a** (4.0 mmol). All the reactions were conducted under air. [b]Isolated yields.

Table 2
The HCl-promoted direct cyclisation of 2-aminophenols with amides: scope of amines and tertiary amides[a].

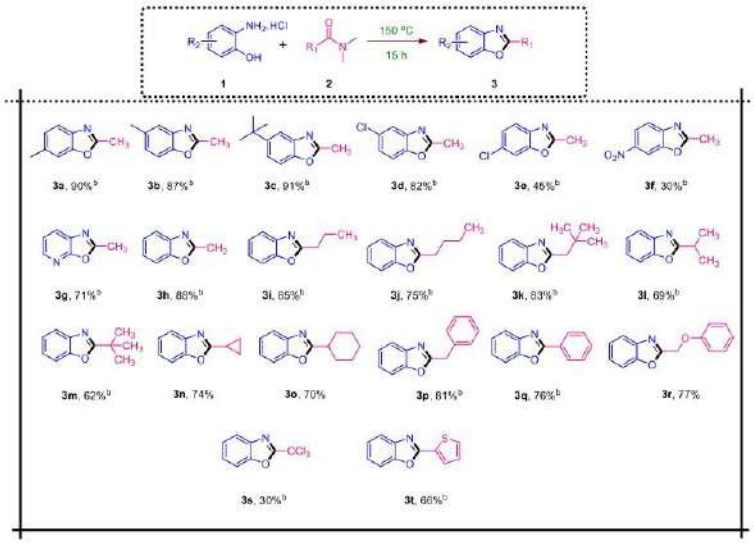

[a] Reaction conditions: A mixture of substituted 2-aminophenol hydrochloride salt **1** (1 mmol), amide **2** (4.0 mmol), 150 °C, 15 hr. [b] isolated yield.

various substitutions at nitrogen atoms in acetamide (Table 3, **entries 1–4**). It was observed that increasing the carbon chain length and the number of nitrogen atom substitutions reduced the yield of the corresponding oxazole compounds. Similar results were obtained when benzamides were reacted with the aminophenol **1h** (**entries 5–8**).

After establishing a suitable novel method for 2-substituted benzoxazole synthesis from *o*-aminophenol, we further explored the possibility of synthesising benzothiazole by replacing *o*-aminophenol with *o*-aminothiophenol. To our delight, it was observed that the two aminothiophenol presented a good yield of corresponding benzothiazoles (**5a** and **5b**) (Scheme 3).

However, the reaction of 2-aminophenol (**1h**) with formamide (**2v**) did not yield the desired product **3v** (Scheme 4) and only resulted in the formation of intermediate transamidation product **6a**.

Additionally, reactions performed at low temperatures did not result in the formation of the cyclised products, irrespective of the duration of stirring for 3 or 15 h (Scheme 5a), yielding only respective transamidation intermediate products. Thus, the annulation of the benzoxazole ring at a high temperature may correspond to the dehydration required temperature [9]. Subsequently,

Table 3
HCl-promoted 2-substituted 1,3-benzoxazole synthesis from 2-aminophenols and amides: scope of secondary and tertiary amides[a].

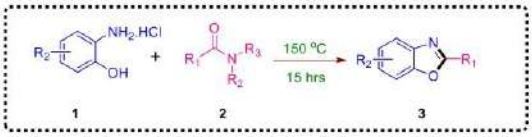

Entry	1	Amide 2	Benzoxzole 3	Yield[b]
1	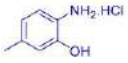 1a	 2n	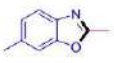 3a	93%
2	1a	 2o	3a	90%
3	1a	 2p	3a	79%
4	1a	 2q	3a	68%
5	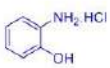 1h	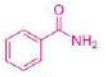 2r	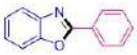 3o	87%
6	1h	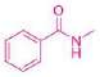 2s	3o	81%
7	1h	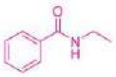 2t	3o	64%
8	1h	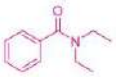 2u	3o	53%

[a] Reaction conditions: A mixture of substituted 2-aminophenol hydrochloride salt **1** (1 mmol), amide **2** (4.0 mmol), 150 °C, 15 hr.
[b] isolated yield.

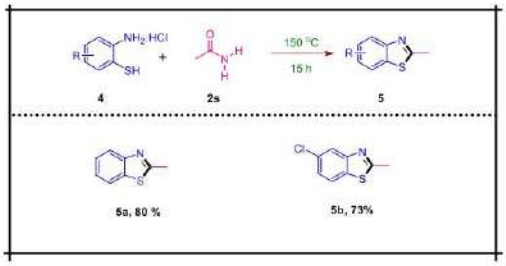

Scheme 3. Synthesis of 2-substituted benzothiazoles.

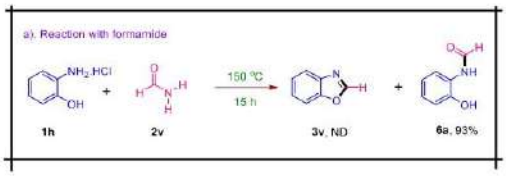

Scheme 4. The reaction between 2-aminophenol hydrochloride salt with formamide under optimised conditions.

we examined the importance of hydrochloride salt based on the cyclisation reaction of 5-methyl-2-aminophenol (**1a**) with acetamide (**2a**) in the absence of hydrochloride (Scheme 5b); however, no desired cyclised product [11] was obtained. Further, to determine whether a radical pathway was responsible for the annulation, an equivalent of TEMPO was introduced to the reaction mixture as a radical trap (Scheme 5c). The corresponding product, **3c**, was formed in 88% yield. As a result, no discernible difference in the outcome occurred, indicating that the reaction did not occur *via* a radical process. In continuation, we investigated the reactivity of the intermediate species **6d** in the presence or absence of hydrochloride under the annulation condition (Scheme 5d). To begin, we observed that **6d** cyclised independently and generated around 10% of **3c**. Subsequently, we performed an experiment in which the intermediate was annulated in the presence of hydrochloride, noting that hydrochloride boosted the production of the product to over 90%. Thus, we concluded that hydrochloride was a critical activator of the amide and intermediate in the reaction [12]. Finally, to verify whether the amide's oxygen participates in the cyclisation, we performed an annulation reaction between amine **7** and amide **2a** (Scheme 5e), resulting in no cyclised product **3h,** but only the formation of transamidation product **8**, confirming that the amide's oxygen did not participate in the annulation.

We proposed a probable mechanism based on the experimental data and published results [9] (Scheme 6). First, H ion activates the C–O bond of amide **2** to form cationic (highly electron-deficient centre) intermediate **a**, thereby promoting the nucleophilic attack of 2-aminophenol **1**, leading to a tetrahedral species **b**. The formation of transamidation compound **c** *via* elimination of the more basic amine of the amide with proton extraction from intermediate **b**. Eventually, an acidic proton activates the C–O bond (carbonyl) of compound **c**, creating an electron-deficient carbon again and in this instance, leading to intramolecular nucleophilic attack by phenol's oxygen resulting in a tetrahedral moiety **d**. Lastly, elimination of water from intermediate **e** to give the target compound **3**.

2. Conclusion

In summary, we have developed a very effective, base- and metal-free approach for synthesising a variety of benzoxazoles and benzothiazoles by employing unactivated amides as carbon sources. This methodology is versatile and applicable to a wide range of substrates to produce corresponding desired products. Furthermore, the protocol is simple and easy to handle, producing amines as by-products. Finally, this methodology is efficient and a more practical process as compared to previously reported methods.

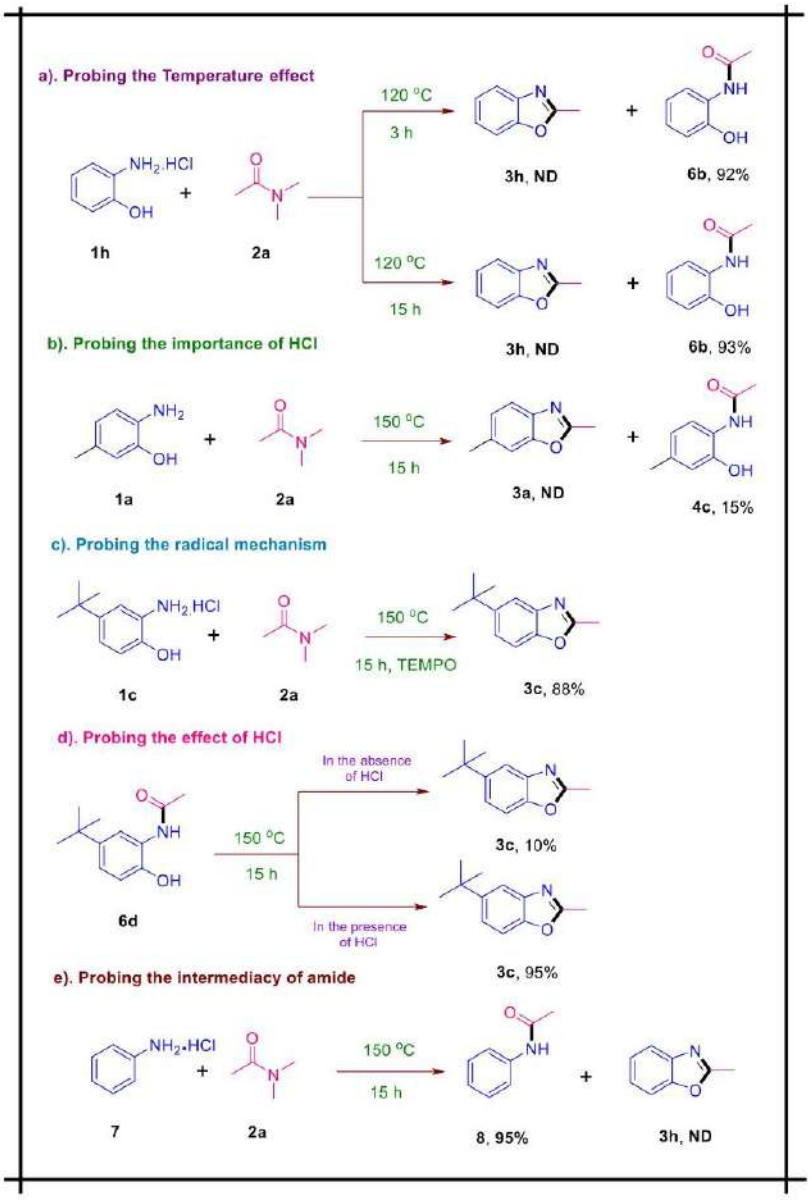

Scheme 5. Mechanistic Investigation Experiments.

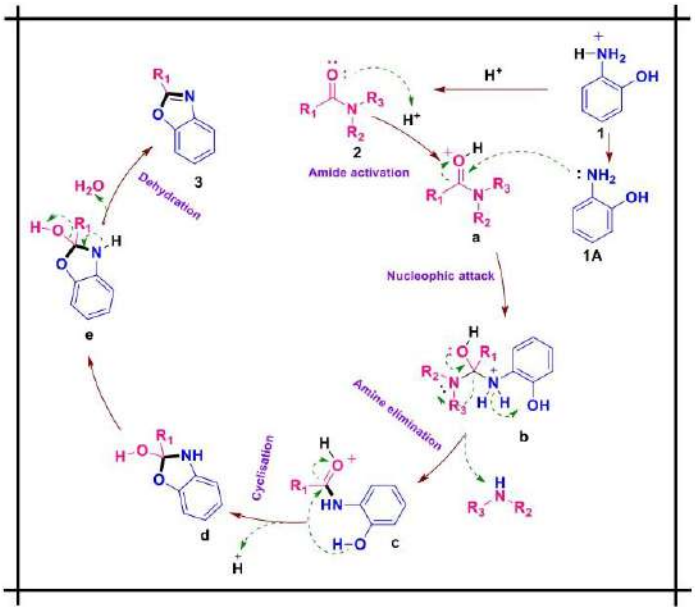

Scheme 6. The plausible mechanism.

Funding

Rajshekhar Karpoormath would like to thank College of Health Sciences, University of KwaZulu-Natal and the National Research Foundation-South Africa (NRF-SA) for funding this project (Grant Nos. 103,728 and 129,247).

Declaration of competing interest

The authors declare that they have no known competing financial interests or personal relationships that could have appeared to influence the work reported in this paper.

Acknowledgements

The authors are thankful to the Discipline of Pharmaceutical Sciences, College of Health Sciences (CHS), University of Kwa-Zulu Natal (UKZN), Durban, South Africa, for providing all the necessary facilities. R.K. gratefully acknowledges National Research Foundation-South Africa (NRF-SA) for funding this project (Grant Nos. 103728 and 129247).

References

[1] a) I.J. Turchi, Ind. Eng. Chem. Prod. Res. Dev. 20 (1) (1981) 32–76;
b) I.V. Smolyar, A.K. Yudin, V.G. Nenajdenko, Chem. Rev. 119 (17) (2019) 10032–10240;
c) J. Zhang, P.Y. Coqueron, M.A. Ciufolini, Heterocycles 82 (2) (2010) 949–980;
d) K. Passador, S. Thorimbert, C. Botuha, Synthesis 51 (2019) 384–398, 02.

[2] a) H.Z. Zhang, Z.L. Zhao, C.H. Zhou, Eur. J. Med. Chem. 144 (2018) 444–492;
b) S. Kakkar, B. Narasimhan, BMC Chem. 13 (2019) 16;
c) N.Y. Guerrero-Pepinosa, M.C. Cardona-Trujillo, S.C. Garzón-Castaño, L.A. Veloza, J.C. Sepúlveda-Arias, Biomed. Pharmacother. 138 (2021) 111495;
d) R. Kaur, K. Palta, M. Kumar, M. Bhargava, L. Dahiya, Expert Opin. Ther. Pat. 28 (11) (2018) 783–812.

[3] a) J.T. Mhlongo, E. Brasil, B.G. de la Torre, F. Albericio, Mar. Drugs 18 (2020) 4 203;
b) C. Lamberth, J. Heterocycl. Chem. 54 (2017) 2974.

[4] a) Z. Jin, Nat. Prod. Rep. 28 (2011) 1143–1191;
b) S. Tilvi, K.S. Singh, Curr. Org. Chem. 20 (8) (2016) 898–929;
c) Z. Jin, Nat. Prod. Rep. 30 (2013) 869–915;
d) Z. Jin, Nat. Prod. Rep. 26 (2009) 382–445;
e) Z. Jin, Z. Li, R. Huang, Nat. Prod. Rep. 19 (2002), 545-476;
f) Z. Jin, Nat. Prod. Rep. 23 (2006) 464–496.

[5] a) X.K. Wong, K.Y. Yeong, ChemMedChem 16 (21) (2021) 3237–3262;
b) R.V. Kumar, Asian J. Chem. 16 (3) (2004) 1241–1260;
c) C.S. Demmer, L. Bunch, Eur. J. Med. Chem. 97 (2015) 778–785.

[6] a) S. Bresciani, N.C.O. Tomkinson, Heterocycles 89 (11) (2014) 2479–2543;
b) S. Ueda, H. Nagasawa, Angew. Chem. 120 (34) (2008) 6511–6513;
c) A.R. Hajipour, Z. Khorsandi, New J. Chem. 40 (2016) 10474–10481;

d) F. Wu, J. Zhang, Q. Wei, P. Liu, J. Xie, H. Jiang, B. Dai, Org. Biomol. Chem. 12 (2014) 9696–9701;
e) M. Zhang, Adv. Synth. Catal. 351 (14–15) (2009) 2243–2270;
f) K. Oshimoto, H. Tsuji, M. Kawatsura, Org. Biomol. Chem. 17 (2019) 4225–4229;
g) L.A. Nguyen, T.T.T. Nguyen, Q.A. Ngo, T.B. Nguyen, Org. Biomol. Chem. 19 (2021) 6015–6020;
h) G. Chakraborty, R. Mondal, A.K. Guin, N.D. Paul, Org. Biomol. Chem. 19 (2021) 7217–7233;
i) D.B. Nale, B.M. Bhanage, Synlett 26 (20) (2015) 2835–2842.
[7] a) M.S. Rao, S. Hussain, Synth. Commun. 51 (17) (2021) 2684–2694;
b) J. Zhang, L. Hu, Y. Liu, Y. Zhang, X. Chen, Y. Luo, Y. Peng, S. Han, B. Pan, J. Org. Chem. 86 (21) (2021) 14485–14492;
c) G.H. Sung, I.H. Lee, B.R. Kim, D.S. Shin, J.J. Kim, S.G. Lee, Y.J. Yoon, Tetrahedron 69 (17) (2013) 3530–3535.
[8] a) S. Rajasekhar, B. Maiti, K. Chanda, Synlett 28 (2017) 521–541, 05;
b) X. Liu, Z.B. Dong, Eur. J. Org Chem. 4 (2020) 408–419;
c) S. Dhawan, V. Kumar, P.S. Girase, S. Mokoena, R. Karpoormath, ChemistrySelect 6 (4) (2021) 754–787;
d) S.R. Shinde, P. Girase, S. Dhawan, S.N. Inamdar, V. Kumar, C. Pawar, M.B. Palkar, M. Shinde, R. Karpoormath, Synth. Commun. 52 (1) (2021) 1–36.
[9] V. Kumar, S. Dhawan, P.S. Girase, P. Singh, R. Karpoormath, Eur. J. Org Chem. 41 (2021) 5627–5639.
[10] a) G. Li, M. Szostak, Synthesis 52 (18) (2020) 2579–2599;
b) G. Li, C. Ji, X. Hong, M. Szostak, J. Am. Chem. Soc. 141 (28) (2019) 11161–11172;
c) M. Rahman, G. Li, M. Szostak, J. Org. Chem. 84 (18) (2019) 12091–12100;
d) S. Dhawan, P.S. Girase, V. Kumar, R. Karpoormath, Synth. Commun. 51 (24) (2021) 3729–3739;
e) P.S. Girase, V. Kumar, S. Dhawan, R. Karpoormath, ChemistrySelect 7 (2022), e202103237.
[11] J. Yin, J. Zhang, C. Cai, G.J. Deng, H. Gong, Org. Lett. 21 (2) (2019) 387–392.
[12] a) L. Wang, X. Ren, J. Yu, Y. Jiang, J. Cheng, J. Org. Chem. 78 (23) (2013) 12076–12081;
b) K.L. Li, Z.B. Du, C.C. Guo, Q.Y. Chen, J. Org. Chem. 74 (9) (2009) 3286–3292;
c) V. Venkateswarlu, K.A.A. Kumar, S. Balgotra, G.L. Reddy, M. Srinivas, R.A. Vishwakarma, S.D. Sawant, Chem. Eur J. 20 (22) (2014) 6641–6645.